ACTA CHIMICA

ACADEMIAE SCIENTIARUM HUNGARICAE

ADIUVANTIBUS

V. BRUCKNER, GY. DEÁK, K. POLINSZKY,
E. PUNGOR, G. SCHAY, Z. G. SZABÓ

REDIGIT

B. LENGYEL

TOMUS 90 FASCICULUS 1

AKADÉMIAI KIADÓ, BUDAPEST

1976

ACTA CHIM. (BUDAPEST) ACASA 2 90 (1) 1—110 (1976)

ACTA CHIMICA

A MAGYAR TUDOMÁNYOS AKADÉMIA KÉMIAI TUDOMÁNYOK OSZTÁLYÁNAK IDEGEN NYELVŰ KÖZLEMÉNYEI

SZERKESZTI

LENGYEL BÉLA

TECHNIKAI SZERKESZTŐK

DEÁK GYULA és HARASZTHY-PAPP MELINDA

Az Acta Chimica német, angol, francia és orosz nyelven közöl értekezéseket a kémiai tudományok köréből.

Az Acta Chimica változó terjedelmű füzetekben jelenik meg, egy-egy kötet négy füzetből áll. Évente átlag négy kötet jelenik meg.

A közlésre szánt kéziratok a szerkesztőség címére (1521 Bp., Műegyetem) küldendők. Ugyanerre a címre küldendő minden szerkesztőségi levelezés. A szerkesztőség kéziratokat nem ad vissza.

Megrendelhető a belföld számára az Akadémiai Kiadónál (1363 Budapest, pf. 24. Bankszámla 215 11488), a külföld számára pedig a Kultúra Könyv és Hírlap Külkereskedelmi Vállalatnál (1389 Budapest 62, pf. 149. Bankszámla: 218 10990) vagy külföldi képviseleteinél és bizományosainál.

Die Acta Chimica veröffentlichen Abhandlungen aus dem Bereich der chemischen Wissenschaften in deutscher, englischer, französischer und russischer Sprache.

Die Acta Chimica erscheinen in Heften wechselnden Umfanges. Vier Hefte bilden einen Band. Jährlich erscheinen 4 Bände.

Die zur Veröffentlichung bestimmten Manuskripte sind an folgende Adresse zu senden:

Acta Chimica
H-1521 Budapest

An die gleiche Anschrift ist auch jede für die Redaktion bestimmte Korrespondenz zu richten. Abonnementspreis pro Band: $ 32.00.

Bestellbar bei dem Buch- und Zeitungs-Außenhandels-Unternehmen »*Kultúra*« (H-1389 Budapest 62, P. O. B. 149. Bankkonto Nr. 218 10990) oder bei seinen Auslandsvertretungen und Kommissionären.

ACTA CHIMICA

ACADEMIAE SCIENTIARUM HUNGARICAE

ADIUVANTIBUS

V. BRUCKNER, GY. DEÁK, K. POLINSZKY,
E. PUNGOR, G. SCHAY, Z. G. SZABÓ

REDIGIT

B. LENGYEL

TOMUS 90

AKADÉMIAI KIADÓ, BUDAPEST

1976

ACTA CHIM. (BUDAPEST)

ACTA CHIMICA

TOMUS 90

FASCICULUS 1: 1976
FASCICULUS 2: 1976
FASCICULUS 3: 1976
FASCICULUS 4: 1976

INDEX

ABOU-ZEID, N. Y., s. VALK, G.
ACKERMANN, I. s. SZEBÉNYI, I.
AKIMOV, V. K., BUSEV, A. I., KODUA, K. V., NENNING, P.: Analytical Use of Pt(II) Complexes with Pyrazolone Derivatives (in German) 375
ANTAL, E. S., SZABÓ, V.
ARSHINOVA, R., FAUCHER, J. P., GRAFFEUIL, M., LABARRE, J. F., LEIBOVICI, C.: Theoretical Conformational Analysis of Methoxydichlorophosphine CH_3O-PCl_2 207
BARCZA, L., GYEPES, L., KELEMEN, K.: Investigation of the Dimerization of Some Organic Acids in Non-aqueous Solvent 43
BARTÓK, M. s. FELFÖLDI, K.
BÁRCZAI-BEKE, M. s. DÖRNYEI, G.
BENKÓ, P., MESSMER, A., GELLÉRI, A., PALLOS, L.: Condensed *as*-Triazines, I. Synthesis of 3-Substituted Pyrido[3,4e]-*as*-Triazines 285
BENKÓ, P., BERÉNYI, E., MESSMER, A., HAJÓS, GY., PALLOS, L.: Condensed *as*-Triazines, V. Pyrido[4,3-e]-*as*-Triazines 405
BENKÓ, P. s. BERÉNYI, E.
BENKÓ, P. s. GELLÉRI, A.
BERÉNYI, E., BENKÓ, P., PALLOS, L.: Condensed *as*-Triazines, III. Synthesis of a New Heterocyclic System, the Derivatives of *as*-Triazino[6,5-c]Quinoline 395
BERÉNYI, E., BENKÓ, P., PALLOS, L.: Condensed *as*-Triazines, IV. Synthesis of *as*-Triazino[5,6-c]Quinoline and its Derivatives 399
BERÉNYI, E. s. BENKÓ, P.
BRUCK, P., TAMÁS, J., KÖRMENDY, K.: Rearrangement and Dissociation Processes in Tricyclic Phthalazinone Derivatives Upon Electron Impact 59
BUSEV, A. I. s. AKIMOV, V. K.
BUSEV, A. I., KARJAKINA, NENNING, P.: On the Extraction of Nb(V) with Polyphenols (in German) 365
CSÁKVÁRI, B., WAGNER, ZS., HARGITTAI, I.: On the Molecular Structure of Triethyl Silane as Studied by Electron Diffraction 141
CSÁKVÁRI, B., WAGNER, ZS., GÖMÖRY, P., HARGITTAI, I., ROZSONDAI, B., MIJLHOFF, F. C.: Electron Diffraction Study of the Molecular Structure of Trimethylysilane 149
CSÁKVÁRI, B., FÁBRY, L., GÖMÖRY, P., UJSZÁSZY, K.: Reactions of Chlorosilanes with Alkoxysilanes, I. Gas Chromatographic and Volumetric Study of the Catalytic Condensation. Connection Between Reactivity and Mass-Spectrometric Fragmentation 13
CSÁKVÁRI, B., FÁBRY, L., GÖMÖRY, P., UJSZÁSZY, K.: Reactions of Chlorosilanes with Alkoxysilanes, II. Mechanism of Catalysis in Chlorosilane + Alkoxysilane Type Condensations 233
CZIRA, G. s. SIMIG, GY.
DETREKŐY, E. s. KALLÓ, D.
DINYA, Z., REITER, J., TOLDY, L., ROCHLITZ, SZ.: Quantum-Chemical Study of Certain Imidazopyrimidone Derivatives 179
DOLESCHALL, G.: A Novel Aldehyde Synthesis Based on the Reduction of *s*-Triazolo [2,3-*c*] Quinazolin-4-ium Derivatives 419

DOMÁNY, GY., NYITRAI, J.: Thermally Induced Reactions of Imidazole Derivatives, VI. Rearrangement of 2,4,4,5-tetraphenyl-4*H*-imidazole (Short Communication) ... 109
DÖRNYEI, G., BÁRCZAI-BEKE, M., MAJOROS, B., SOHÁR, P., SZÁNTAY, CS.: Synthesis and Study of Monosubstituted α-Formylacetic Esters and Malondialdehydes 275
EL-BAYOUKI, KH. s. HAMMAD, M.
FÁBRY, L. s. CSÁKVÁRI, B.
FAUCHER, J. P. s. ARSHINOVA, R.
FELFÖLDI, K., MOLNÁR, Á., BARTÓK, M.: Chemistry of 1,3-Bifunctional Compounds, XVIII. Preparation of the Esters of Various 1,3-Amino Alcohols 75
GELLÉRI, A., MESSMER, A., BENKÓ, P., PALLOS, L.: Condensed *as*-Triazines, II. Synthesis of Pyrido[3,2-e]-*as*-Triazine 301
GELLÉRI, A. s. BENKÓ, P.
GÖBÖLÖS, S. s. SZEBÉNYI, I.
GÖMÖRY, É. s. CSÁKVÁRI, B.
GRAFFELI, M. s. ARSHINOVA, R.
GUCZI, L. s. SÁRKÁNY, A.
GYEPES, L. s. BARCZA, L.
HAJÓS, GY. s. BENKÓ, P.
HAMMAD, M., EL-BAYOUKI, KH.: Reactions of *o*-Phenylendiamine with α,β-Unsaturated Nitriles 193
HARGITTAI, I., SCHULTZ, GY., NAUMOV, V. A., KITAEV, YU. P.: Electron Diffraction Study of the Molecular Structure of Acetaldezine 165
HARGITTAI, I. s. CSÁKVÁRI, B.
HARGITTAI, I. s. ROZSONDAI, B.
HORNYÁK, I.: Spectrofluorometric Determination of 2,3-Benzfluorone (11H-Benzo(b) Fluorene) in Air Pollution 103
KAMEL, M. s. VALK, G.
KALLÓ, D., DETREKŐY, E., SCHAY, G.: Mechanistic Study of the Isomerization of *n*-Butene on Acid Catalysts, II. Evaluation of Kinetic Gases and Experimental Result 119
KARJAKINA, S. P. s. BUSEV, A. I.
KELEMEN, K. s. BARCZA, L.
KISS, Á. I., SZŐKE, J.: The Role of Molecular Conformation in π-Electron SCF-MO Calculations 131
KITAEV, YU. P. s. HARGITTAI, I.
KODUA, K. V. s. AKIMOV, V. K.
KÖRMENDY, K. s. BRUCK, P.
LABARRE, J. F. s. ARSHINOVA, R.
LEIBOVICI, C. s. ARSHINOVA, R.
LEMPERT, K. s. SIMIG, GY.
LISZI, J.: Static Dielectric Properties of Binary Liquid Mixtures Containing tri-*n*-Butylamin 21
MAJOROS, B. s. DÖRNYEI, G.
MALLÁT, T., PETRÓ, J., POLYÁNSZKY, É., MÁTHÉ, T.: Electrochemical Study of Palladium–Copper Catalysts 333
MARTIN, A.: Calculation of the π-Electronic Structure and Spectra of Halopyridines by the MIM and PPP Methods 1
MÁTHÉ, T. s. MALLÁT, T.
MESSMER, A. s. BENKÓ, P.
MESSMER, A. s. GELLÉRI, A.
MEZEY, P. s. NÁRAY-SZABÓ, G.
MICHAYLOVA, V.: Complex Formation Between Magnesium, Zinc, Cadmium and Arsenazo III 111
MIJLHOFF, F. C. s. CSÁKVÁRI, B.
MOLNÁR, Á. s. FELFÖLDI, K.
MOSTAFA, M. M. s. TAHA, F. I. M.
MOUSSA, M. N. H. s. TAHA, F. I. M.
NÁRAY-SZABÓ, G., PULAY, P., MEZEY, P.: Quantum Chemical Study of the Solvent Effect on the Isomerization of Cyanic Acid 199
NAUMOV, V. A. s. HARGITTAI, I.
NENNING, P. s. AKIMOV, V. K.
NENNING, P. s. BUSEV, A. I.
NOSZKÓ, L. s. SZAMMER, J.
NYITRAI, J. s. DOMÁNY GY.

Oszbach, Gy., Szabó, D., Vitai, M. E.: The Base-Catalyzed Dimerization of 2-Arylidene-cyclohexanones 51
Pallos, L. s. Benkó, P.
Pallos, L. s. Berényi, E.
Pallos, L. s. Gelléri, A.
Petró, J. s. Mallát, T.
Polyánszky, É. s. Mallát, T.
Pulay, P. s. Náray-Szabó, G.
Recensiones 203; 425
Reiter, J. s. Dinya, Z.
Rochlitz, Sz. S. Dinya, Z.
Rozsondai, B. s. Csákvári, B.
Rozsondai, B., Hargittai, I.: Electron Diffraction Study of the Molecular Structure of bis(Trimethylsilyl)Ketene 157
Sárkány, A., Guczi, L., Tétényi, P.: Catalytic Deuterium Exchange of Cyclopentane and Cyclohexane, and Dehydrogenation of Cyclohexane on Rh Black 345
Schay, G. s. Kalló, D.
Schultz, Gy. s. Hargittai, I.
Sebestyén, A. s. Vizi, B.
Shallaby, A. M. s. Taha, F. I. M.
Simig, Gy., Lempert, K., Tamás, J., Czira, G.: The Reaction of *N*-(*t*-Butyl)-α-Halo-α,α-Diarylacetamides with Cyanoamide and Monosubstituted Cyanoamide Salts 93
Singer, D.: Network-Thermodynamic Approach to Chemical Kinetics 255
Singh, V. P. s. Upadhyay, R. K.
Sohár, P. s. Dörnyei, G.
Srivastava, M. N. s. Tewari, R. C.
Szabó, D. s. Oszbach, Gy.
Szabó, V., Antal, E.: Reductive Conversions of Chromanoids, I. Catalytic Hydrogenation of Isoflavone(3-Phenylchromone) 381
Szammer, J., Noszkó, L.: Thermal Transcarboxylation Reactions, VII. The Relative Ability to Transfer of Aromatic Hydrogens 411
Szántay, Cs. s. Dörnyei, G.
Szebényi, I., Ackermann, I., Széchy, G., Göbölös, S.: Dehydrocyclization of *n*-Nonane and *n*-Decane Under the Conditions of Catalytic Gasoline Reforming 313
Széchy, G. s. Szebényi, I.
Szőke, J. s. Kiss, Á. I.
Taha, F. I. M., Moussa, M. N. H., Shallaby, A. M., Mostafa, M. M.: Studies on the Reaction Between Cu(II) Acetate and Sulphate and Some Acid Hydrazides 33
Tamás, J. s Bruck, P.
Tamás, J. s. Simig, Gy.
Tétényi, P. s. Sárkány, A.
Tewari, R. C., Srivastava, M. N.: Spectral and Magnetic Studies of Copper(II) Chelates of L-Asparagine and L-Glutamine (Short Communication) 371
Toldy, L. s. Dinya, Z.
Ujszászy, K. s. Csákvári, B.
Upadhyay, R. K., Singh, V. P.: Studies on Some Metal Complexes with Keto-Anils as Ligands, I (Short Communication) 325
Valk, G., Kamel, M., Abou-Zeid, N. Y.: Reactions of Hexahydro-1,3,5-Triacryloyl-*s*-Triazine 69
Vitai, M. E. s. Oszbach, Gy.
Vizi, B., Sebestyén, A.: Force Field Calculations for Malononitrile Molecules 355
Wagner, Zs. s. Csákvári, B.

Acta Chimica Academiae Scientiarum Hungaricae, Tomus 90(1), pp. 1—19 (1976)

CALCULATION OF THE π-ELECTRONIC STRUCTURE AND SPECTRA OF HALOPYRIDINES BY THE MIM AND PPP METHODS

A. MARTIN

(Department of Physical Chemistry, Technical University, Budapest)

Received May 20, 1975

The π-electronic structure and spectra of halopyridines were calculated by the Molecules in Molecules (MIM) and PARISER—PARR—POPLE (PPP) methods.

With the MIM method the charge transfer energies were calculated by the point charge, charged sphere and MATAGA—NISHIMOTO approximations. Different ionization potential and electron affinity values found in the literature were tested for the calculation of the one-center repulsion integrals and they were selected by comparison of the experimental and calculated data. The value of the carbon–halogen resonance integral (β_{CX}) was varied. On the basis of the results obtained for transition energies and wavefunctions, the MATAGA—NISHIMOTO approximation proved to be the most appropriate for the calculation of the two-center repulsion integrals.

In the PPP calculation only the MATAGA—NISHIMOTO approximation was used. The best value of the resonance integral was determined by β_{CX} variation. Singlet transition energies, charge density and bond order matrices, oscillator strengths and polarization directions were calculated.

1. Introduction

Several PARISER—PARR—POPLE (PPP) and Molecules in Molecules (MIM) calculations are to be found in the literature for pyridine derivatives [1, 2]. It seems that the halopyridines have not been treated in detail by the MIM method. In this work the π-electronic spectra of mono-halopyridines have been calculated by the MIM method and compared with the results obtained by the PPP method.

One of the purposes of the present work is to find a uniform parameter set for the substituents considered. For this reason, the applicability of the point charge, charged sphere and the MATAGA—NISHIMOTO (MN) approximations were investigated within the MIM method, and, by the MIM method, different one- and two-center repulsion integrals were tested. The results were compared with those for halobenzenes obtained earlier [3], which were used at the same time for a preliminary selection of the parameters tested. Our purpose was to check the applicability of the MATAGA—NISHIMOTO approximation, generally used in the PPP method, for the calculation of heterocyclic compounds by the MIM method.

2. MIM method

2.1. *Method of Calculation*

The principles of the MIM method used are given in Ref. [3]. The π-electron system of the molecules investigated was divided into two parts: the π-electrons of the pyridine ring and the non-bonding π-electrons of the substituent halogen atom. The pyridine ring was considered as an acceptor and the halogen atoms as donors. The interaction between the pyridine ring and the substituent atom was calculated by means of configuration interaction between the singly excited configurations. The interaction matrix was diagonalized by the JACOBI method. The locally excited configurations [4] and the experimental transition energies [5] of the pyridine molecule are given in Table I.

Table I

Wavefunctions of pyridine and values of experimental energy

Wavefunction	Energy (eV)
$\Gamma_\alpha = 0.8202\ \psi_{3\to4} - 0.5720\ \psi_{2\to5}$	4.90
$\Gamma_p = 0.8688\ \psi_{3\to5} + 0.4950\ \psi_{2\to4}$	6.38
$\Gamma_\beta = 0.5720\ \psi_{3\to4} + 0.8202\ \psi_{2\to5}$	7.07
$\Gamma_{\beta'} = 0.4950\ \psi_{3\to5} - 0.8688\ \psi_{2\to4}$	7.07

$$\psi_2 = 0.1815\,(\varphi_2 + \varphi_6) - 0.3610\,(\varphi_3 + \varphi_5) - 0.6113\,\varphi_4 + 0.5475\,\varphi_1$$

$$\psi_3 = 0.4970\,(\varphi_2 - \varphi_6) + 0.5030\,(\varphi_3 - \varphi_5)$$

$$\psi_4 = 0.3383\,(\varphi_2 + \varphi_6) + 0.2728\,(\varphi_3 + \varphi_5) - 0.5893\,\varphi_4 - 0.5244\,\varphi_1$$

$$\psi_5 = 0.5030\,(\varphi_2 - \varphi_6) + 0.4970\,(\varphi_5 - \varphi_3)$$

Three different methods were tested for the calculation of charge transfer (CT) energies: the point charge [6], the charged sphere [7] and the MATAGA—NISHIMOTO [4] approximations. Some different values found in the literature were used for the atomic valence state ionization potentials (I_μ) and electron affinities (A_μ), and thus for the one-center repulsion integrals ($\gamma_{\mu\mu}$).

The $\beta_{\mu\nu}$ resonance integral for bonds between the subsystems was taken as a variable parameter and its values between the non-bonded atoms were neglected.

2.2. *Starting Values*

The molecular geometry of the pyridine ring was taken from Ref. [9]. The carbon–halogen bond distances were: $r_{CF} = 1.30$ Å, $r_{CCl} = 1.70$ Å, $r_{CBr} = 1.86$ Å, $r_{CI} = 2.05$ Å [8].

The effective nuclear charges (Z_μ), valence state ionization potentials (I_μ) and electron affinities (A_μ) as well as the one-center repulsion integrals ($\gamma_{\mu\mu}$) used are collected in Table II. The I and γ values of bromine and iodine given in columns 1, 2 and 3 of the Table II were calculated by extrapolation from the $Ge^- \rightarrow As \rightarrow Se^+ \rightarrow Br^{++}$ and $Sn^- \rightarrow Sb \rightarrow Te^+ \rightarrow I^{++}$ isoelectronic series to be found in HINZE's tables [16]. In order to find the best starting data, we have performed the computation with all data series of Table II. Several further data can be found in the literature but, according to our experience [3], no additional information is to be expected from them.

The experimental first ionization potentials of the methyl compounds with the donor halogen substituents are: $I_{CH_3F} = 12.61$ eV [17], $I_{CH_3Cl} =$ $= 11.34$ eV [18], $I_{CH_3Br} = 10.50$ eV [17], $I_{CH_3I} = 9.55$ eV [17]. No experimental data can be found for the electron affinity of the pyridine ring, so it was calculated according to Ref. [5]. The experimental electron affinity of benzene (−1.10 eV [19]) and the energy difference of the ψ_4 and ψ_5 orbitals of pyridine [4], as well as the energy of the corresponding degenerate orbital of benzene [5] were used for the calculation. The values calculated are: $A_4 = -0.817$ eV, $A_5 = -0.530$ eV.

2.3. *Results*

2.3.1. *Charge Transfer Energies*

The charge transfer energies ($T^4(D_l)$, $T^5(D_i)$) as well as the interaction elements between CT states ($\gamma^{45}(D_i)$) of the *ortho-*, *meta-*, and *para*-halopyridines were calculated by means of the point charge, charged sphere and MATAGA–NISHIMOTO approximations, using the data of Table II and Sect. 2.2. The calculated values are listed in Table III, the heading of which has a serial number referring to Table II. As an example, we give the power series of the two-center repulsion integrals ($\gamma_{\mu\nu}$) calculated with data of the first column of Table II according to Ref. [7]:

$$\gamma_{CF} = 16.330 - 6.189 r_{CF} + 0.757 r_{CF}^2$$
$$\gamma_{CCl} = 12.080 - 3.509 r_{CCl} + 0.3440 r_{CCl}^2$$
$$\gamma_{CBr} = 11.660 - 3.2326 r_{CBr} + 0.3004 r_{CBr}^2$$
$$\gamma_{CI} = 11.065 - 2.8593 r_{CI} + 0.2429 r_{CI}^2$$
$$\gamma_{NF} = 16.935 - 6.5235 r_{NF} + 0.8050 r_{NF}^2$$

$$\gamma_{NCl} = 12.605 - 3.8420r_{NCl} + 0.3912r_{NCl}^2$$
$$\gamma_{NBr} = 12.265 - 3.5642r_{NBr} + 0.3473r_{NBr}^2$$
$$\gamma_{NI} = 11.670 - 3.1909r_{NI} + 0.2898r_{NI}^2$$

Table II

Atomic parameters used for MIM calculations

Z_μ, I_μ, A_μ, $\gamma_{\mu\mu}$ Reference	1 [10] [16] [16]	2 [10] [12] [16]	3 [11] [16] [16]	4 [10] [14] [14]	5 [11] [14] [14]	6 [10] [13]	7 [11] [13]	8 [10] [15]
Z_C	3.25	3.25	2.65	3.25	2.65	3.25	2.65	3.25
Z_N	3.90	3.90	3.30	3.90	3.30	3.90	3.30	3.90
Z_F	5.20	5.20	4.60	5.20	4.60	5.20	4.60	5.20
Z_{Cl}	6.10	6.10	5.20	6.10	5.20	6.10	5.20	6.10
Z_{Br}	7.60	7.60	8.20	7.60	8.20			
Z_I	7.60	7.60	8.20	7.60	8.20			
I_C^*	11.16	11.16	11.16	11.16	11.16			
I_N^*	14.12	14.12	14.12	14.12	14.12			
I_F	39.64	34.14	39.64	39.64	39.64			
I_{Cl}	26.36	24.37	26.36	26.37	26.37			
I_{Br}	24.26	22.69	24.26	19.10	19.10			
I_I	21.83	20.55	21.83	19.40	19.40			
A_C^*	0.03	0.03	0.03	0.03	0.03			
A_N^*	1.78	1.78	1.78	1.78	1.78			
A_F	18.11	12.61	18.11	18.11	18.11			
A_{Cl}	13.34	11.34	13.34	11.05	11.05			
A_{Br}	12.08	10.50	12.08	11.80	11.80			
A_I	10.83	9.55	10.83	10.60	10.60			
γ_{CC}^*	11.13	11.13	11.13	11.13	11.13	11.13	11.13	10.71
γ_{NN}^*	12.34	12.34	12.34	12.34	12.34	12.34	12.34	12.85
γ_{FF}	21.53	21.53	21.53	21.53	21.53	21.39	21.39	17.13
γ_{ClCl}	13.03	13.03	13.03	15.32	15.32	13.03	13.03	10.94
γ_{BrBr}	12.19	12.19	12.19	7.30	7.30			
γ_{II}	11.00	11.00	11.00	8.80	8.80			

* Values from Ref. [16]

Table III shows that there are no considerable differences between the calculated CT energies and the interaction elements evaluated with different starting atomic parameters within the same approximation, but essential differences are obtained, even for identical starting parameters, with dif-

ferent approximations. According to expectations [4, 13], the largest calculated CT energies were in each case obtained with the MATAGA—NISHIMOTO, and the smallest ones with the point charge approximation.

2.3.2. *Electron Transition Energies*

The π-electronic transition energies were calculated with the values of Table III. The $\beta_{\mu\nu}$ resonance integrals were taken as variable parameters and their optimum was found by variation. Figures 1, 2 and 3 represent the energy values calculated by the point charge, charged sphere and MATAGA—NISHIMOTO approximations from the data of the first column of Table II as an example. The experimental energies are indicated as horizontal lines. It can be seen that with the decrease of β the calculated energies decrease almost linearly in the interval examined. According to Table III, there is no significant difference between the CT energies calculated with the same approximation (less than 2%), thus Figs 1, 2 and 3 correctly represent the β variation diagrams calculated with other starting parameters.

In order to compare the starting parameters of Table II, the transition energies were calculated for each parameter set. This does not require a β optimization for each parameter set. Instead, for each approximation, a suitable value was chosen from Figs 1, 2 and 3 (point charge approximation: $\beta_{CX} = -1.5$ eV, charged sphere approximation: $\beta_{CX} = -1.5$ eV, MATAGA—NISHIMOTO approximation: $\beta_{CX} = -2.0$ eV) and the transition energies calculated with these β values are given in Table IV. It turned out that the

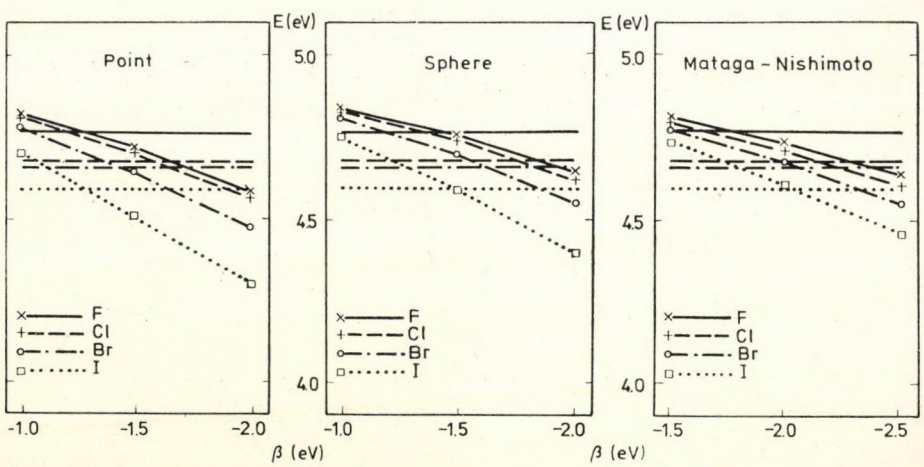

Fig. 1. First band energies of *ortho*-halopyridines as a function of the resonance integra β_{CX} calculated by the MIM method, using point charge, charged sphere and MATAGA—NISHIMOTO approximations. The horizontal lines denote the experimental energies; the curves are drawn from the calculated energy values. Symbols: ×——× fluoropyridine, +———+ chloropyridine, O - . - . - O bromopyridine, □ . . . . . □ iodopyridine

Table III

Charge transfer energies and their interaction elements

Approx.	Point	Charged sphere							Mataga–Nishimoto			
	0.	1.	3.	4.	5.	6.	7.	8.	1.	4.	6.	8.
T^4 (F_2)	7.805	8.062	8.114	8.062	8.114	8.066	8.119	8.209	9.344	9.344	9.349	9.509
T^5 (F_2)	6.864	7.331	7.391	7.331	7.391	7.339	7.398	7.582	8.793	8.793	8.799	9.004
γ^{45} (F_2)	0.819	0.592	0.595	0.592	0.595	0.589	0.591	0.471	0.346	0.346	0.345	0.308
T^4 (F_3)	7.951	8.175	8.235	8.175	8.235	8.179	8.238	8.304	9.405	9.405	9.410	9.570
T^5 (F_3)	6.953	7.410	7.468	7.410	7.468	7.417	7.476	7.654	8.842	8.842	8.848	9.049
$-\gamma^{45}$ (F_3)	0.522	0.345	0.350	0.345	0.350	0.342	0.347	0.256	0.198	0.198	0.198	0.173
T^4 (F_4)	6.786	7.372	7.426	7.372	7.426	7.381	7.435	7.685	8.936	8.936	8.942	9.158
T^5 (F_4)	8.078	8.207	8.271	8.207	8.271	8.209	8.273	8.278	9.307	9.307	9.311	9.460
γ^{45} (F_4)	0	0	0	0	0	0	0	0	0	0	0	0
T^4 (Cl_2)	7.333	7.597	7.645	7.561	7.609	7.597	7.645	7.633	8.762	8.676	8.762	8.858
T^5 (Cl_2)	6.638	7.072	7.129	7.007	7.063	7.072	7.129	7.145	8.330	8.231	8.330	8.455
γ^{45} (Cl_2)	0.511	0.318	0.317	0.357	0.356	0.318	0.317	0.274	0.202	0.215	0.202	0.185
T^4 (Cl_3)	7.416	7.646	7.702	7.623	7.678	7.646	7.702	7.672	8.797	8.713	8.797	8.898
T^5 (Cl_3)	6.706	7.129	7.185	7.066	7.122	7.129	7.185	7.199	8.365	8.268	8.365	8.488
$-\gamma^{45}$ (Cl_3)	0.302	0.156	0.158	0.187	0.189	0.156	0.158	0.122	0.103	0.111	0.103	0.093
T^4 (Cl_4)	6.713	7.245	7.299	7.159	7.213	7.245	7.299	7.340	8.537	8.433	8.537	8.662
T^5 (Cl_4)	7.398	7.542	7.599	7.537	7.593	7.542	7.599	7.549	8.630	8.551	8.630	8.730
γ^{45} (Cl_4)	0	0	0	0	0	0	0	0	0	0	0	0

T^4	(Br_2)	6.747	6.952	6.988	7.002	7.038				8.076	8.299
T^5	(Br_2)	6.115	6.452	6.499	6.556	6.602				7.664	7.917
γ^{45}	(Br_2)	0.434	0.284	0.282	0.214	0.212				0.176	0.146
T^4	(Br_3)	6.816	6.995	7.038	7.026	7.069				8.106	8.327
T^5	(Br_3)	6.177	6.506	6.552	6.607	6.652				7.697	7.945
$-\gamma^{45}$	(Br_3)	0.248	0.135	0.136	0.080	0.081				0.086	0.069
T^4	(Br_4)	6.228	6.641	6.685	6.783	6.827				7.883	8.145
T^5	(Br_4)	6.760	6.874	6.918	6.874	6.918				7.926	8.134
γ^{45}	(Br_4)	0	0	0	0	0				0	0
T^4	(I_2)	6.065	6.228	6.260	6.243	6.275				7.301	7.392
T^5	(I_2)	5.490	5.753	5.796	5.787	5.829				6.911	7.013
γ^{45}	(I_2)	0.362	0.251	0.247	0.228	0.225				0.149	0.138
T^4	(I_3)	6.120	6.265	6.303	6.275	6.313				7.327	7.417
T^5	(I_3)	5.546	5.803	5.845	5.835	5.877				6.940	7.041
$-\gamma^{45}$	(I_3)	0.199	0.116	0.115	0.098	0.097				0.070	0.064
T^4	(I_4)	5.637	5.956	5.997	6.001	6.043				7.141	7.247
T^5	(I_4)	6.029	6.127	6.165	6.127	6.165				7.133	7.219
γ^{45}	(I_4)	0	0	0	0	0				0	0

Acta Chim. (Budapest) 90, 1976

Table IV

Energies calculated by the MIM method

-pyridine	Point	Charged sphere							Mataga—Nishimoto			
	0.	1.	3.	4.	5.	6.	7.	8.	1.	4.	6.	8.
2-F-	−0.208	−0.202	−0.201	−0.202	−0.201	−0.202	−0.201	−0.200	−0.312	−0.312	−0.312	−0.307
	4.715	4.752	4.755	4.752	4.755	4.753	4.756	4.766	4.732	4.732	4.732	4.739
	5.879	6.045	6.057	6.045	6.057	6.047	6.059	6.097	6.105	6.105	6.105	6.122
3-F-	−0.190	−0.183	−0.182	−0.183	−0.182	−0.183	−0.182	−0.180	−0.280	−0.280	−0.280	−0.275
	4.691	4.727	4.730	4.727	4.730	4.727	4.730	4.741	4.693	4.693	4.694	4.702
	5.945	6.043	6.053	6.043	6.053	6.044	6.054	6.077	6.059	6.059	6.059	6.076
4-F-	−0.227	−0.209	−0.208	−0.209	−0.208	−0.209	−0.208	−0.201	−0.308	−0.308	−0.307	−0.300
	4.809	4.813	4.814	4.813	4.814	4.813	4.814	4.814	4.780	4.780	4.780	4.785
	5.969	6.130	6.140	6.130	6.140	6.131	6.142	6.182	6.189	6.189	6.189	6.205
2-Cl-	−0.223	−0.217	−0.215	−0.830	−0.216	−0.217	−0.215	−0 216	−0.334	−0.337	−0.334	−0.330
	4.705	4.741	4.744	4.293	4.740	4.741	4.744	4.746	4.712	4.707	4.712	4.717
	5.844	5.999	6.013	5.528	5.996	5.999	6.013	6.018	6.056	6.045	6.056	6.070
3-Cl-	−0.202	−0.195	−0.193	−0.195	−0.194	−0.195	−0.193	−0.194	−0.298	−0.301	−0.298	−0.295
	4.672	4.709	4.713	4.704	4.708	4.709	4.713	4.714	4.667	4.661	4.667	4.674
	5.866	5.969	5.982	5.957	5.971	5.969	5.982	5.981	5.997	5.985	5.997	6.011
4-Cl-	−0.229	−0.213	−0.211	−0.215	−0.214	−0.213	−0.211	−0.210	−0.321	−0.325	−0.321	−0.317
	4.784	4.790	4.792	4.790	4.792	4.790	4.792	4.790	4.758	4.755	4.758	4.762
	5.943	6.103	6.114	6.082	6.095	6.103	6.114	6.123	6.152	6.141	6.152	6.165

2-Br-	−0.242	−0.236	−0.235	−0.236	−0.234			−0.361	−0.352	
	4.644	4.692	4.696	4.703	4.707			4.674	4.689	
	5.613	5.796	5.815	5.842	5.859			5.961	6.001	
3-Br-	−0.219	−0.213	−0.211	−0.211	−0.210			−0.323	−0.314	
	4.606	4.652	4.657	4.664	4.668			4.620	4.639	
	5.654	5.776	5.793	5.802	5.818			5.889	5.931	
4-Br-	−0.246	−0.231	−0.230	−0.227	−0.225			−0.346	−0.336	
	4.745	4.753	4.757	4.753	4.757			4.724	4.735	
	5.719	5.914	5.932	5.968	5.984			6.063	6.104	
2-I-	−0.269	−0.263	−0.262	−0.263	−0.261			−0.398	−0.393	
	4.511	4.589	4.598	4.598	4.605			4.608	4.619	
	5.273	5.438	5.464	5.460	5.485			5.788	5.816	
3-I-	−0.243	−0.237	−0.235	−0.236	−0.235			−0.356	−0.352	
	4.472	4.541	4.549	4.548	4.556			4.540	4.552	
	5.319	5.439	5.462	5.452	5.474			5.704	5.732	
4-I-	−0.270	−0.256	−0.255	−0.255	−0.253			−0.380	−0.375	
	4.658	4.674	4.680	4.674	4.680			4.662	4.670	
	5.357	5.563	5.588	5.591	5.616			5.896	5.925	

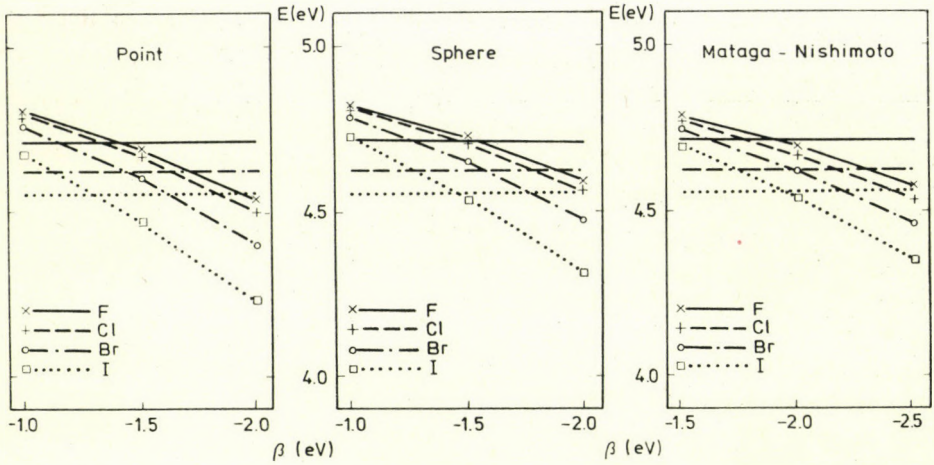

Fig. 2. First band energies of *meta*-halopyridines as a function of the resonance integral β_{CX} calculated by the MIM method, using point charge, charged sphere and MATAGA—NISHIMOTO approximations. Symbols as in Fig. 1

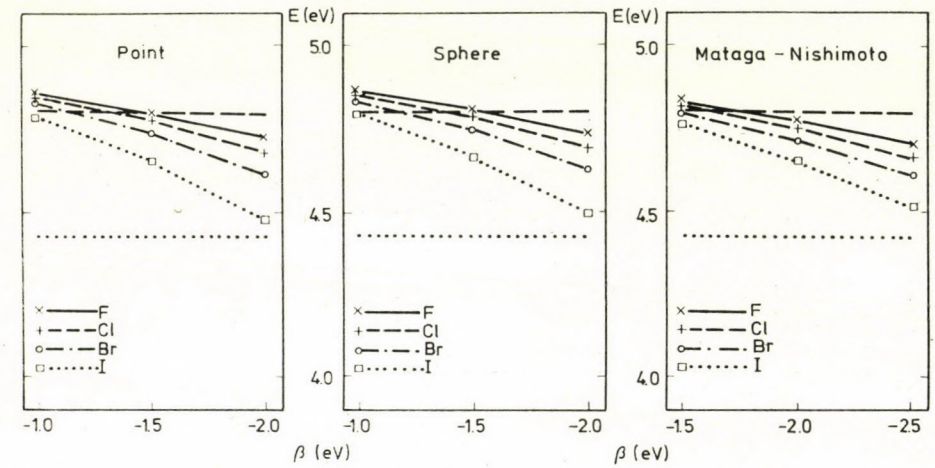

Fig. 3. First band energies of *para*-halopyridines as a function of β_{CX} calculated by the MIM method, using point charge, charged sphere and MATAGA—NISHIMOTO approximations. Symbols as in Fig. 1

results obtained by means of different starting values do not differ essentially. Their differences are less than 1%, which can be neglected compared with the uncertainty of the experimental data. This neglect is justified also by the error introduced by the use of the band maxima as experimental values instead of the 0.0 band. For this reason we shall use only the starting data given in the first column of Table II, as the trend in the values of the one-center repulsion integrals agrees with the expectations.

Thus the best values of resonance integrals were determined only for the data set of column 1 in Table II. The best β_{CX} values evaluated from Figs 1 and 2 are given in Table VII. The *para* isomers in Fig. 3 were not considered for the determination of the optimal β_{CX} values, because their experimental values are incomplete and unreliable. The best resonance integrals have the greatest absolute values with the MATAGA—NISHIMOTO approximation and the smallest ones with the point charge approximation.

The transition energies calculated with the β_{CX} values of Table VII and with the data of the first column of Tables II and III are given in Table V. It can be seen that the energies of the first bands are in good agreement with the experimental values for any of the three approximations. The greatest error occurs for *p*-iodopyridine: 6.5% of the experimental value. The calculated energies decrease in the orders F, Cl, Br, I and *ortho*, *meta*, in accordance with the order of experimental energies.

2.3.3. *Wavefunctions*

The calculated wavefunctions for some characteristic cases are given in Table VI. For the sake of brevity, only those contributions to the wavefunctions are given which correspond to the experimental band assignment and to the state giving the greatest contribution.

With fluoro- and chloropyridines, the CT states contribute only slightly to the wavefunctions belonging to the first four energies for all three approximations. The largest contribution to the configuration of the ground state ψ_0 is from the ground state of pyridine (Γ_0); to $\psi_1 - \psi_4$, the locally excited states contribute in the following order: Γ_α, Γ_p, Γ_β, $\Gamma_{\beta'}$. This is in accordance with the band assignment expected.

Using the point charge approximation, the second bands of iodopyridines and *o*-bromopyridine are CT bands and the higher excited states are mixed from pyridine and CT states, contrary to expectations. A strong mixing of the pyridine and CT states occurs in the excited states of *m*- and *p*-bromopyridines but this is not so strong that the order of the transitions of pyridine should be changed.

Using the charged sphere approximation, the Γ_p locally excited pyridine state gives the largest contribution to the second excited state of *o*-bromopyridine but a small mixing occurs in this case too. The second band of *o*-iodopyridine is given as a CT band by this approximation too.

The MATAGA—NISHIMOTO approximation produces better results: the above contradictions are not present and only a small mixing occurs with *o*-iodopyridine but this does not influence the order of the transitions of pyridine.

Table V

Energies calculated by the MIM method using the best β_{CX} resonance integrals

Compound	Calculated energies (eV)			Experimental energies (eV) [20]
	Point	Sphere	M.N.	
2-fluoropyridine	−0.182	−0.202	−0.282	
	4.738	4.752	4.748	4.769
	5.911	6.045	6.128	
3-fluoropyridine	−0.166	−0.183	−0.253	
	4.717	4.727	4.714	4.714
	5.982	6.043	6.087	
4-fluoropyridine	−0.198	−0.209	−0.278	
	4.821	4.813	4.793	
	6.009	6.130	6.210	
2-chloropyridine	−0.253	−0.310	−0.402	
	4.679	4.673	4.673	4.679
	5.812	5.898	6.003	
3-chloropyridine	−0.229	−0.279	−0.360	
	4.642	4.627	4.618	4.626
	5.827	5.851	5.932	
4-chloropyridine	−0.260	−0.305	−0.388	
	4.767	4.739	4.725	4.805
	5.904	5.996	6.100	
2-bromopyridine	−0.212	−0.268	−0.361	
	4.674	4.665	4.674	4.661
	5.638	5.762	5.961	
3-bromopyridine	−0.191	−0.241	−0.323	
	4.641	4.620	4.620	4.626
	5.690	5.735	5.889	
4-bromopyridine	−0.215	−0.263	−0.346	
	4.765	4.732	4.724	
	5.756	5.875	6.063	
2-iodopyridine	−0.203	−0.263	−0.398	
	4.589	4.589	4.608	4.592
	5.294	5.438	5.788	5.438
3-iodopyridine	−0.184	−0.237	−0.356	
	4.560	4.541	4.540	4.558
	5.367	5.439	5.704	5.438
4-iodopyridine	−0.204	−0.256	−0.380	
	4.717	4.674	4.662	4.428
	5.408	5.563	5.896	5.166

Table VI

Wavefunction contributions calculated by the MIM method

i	Point			Sphere		
	E (eV)	ψ_i		E (eV)	ψ_i	
	2-bromopyridine			2-bromopyridine		
Γ_0	−0.212	.985		−0.268	.981	
Γ_α	4.674	.922		4.665	.938	
Γ_p T_{D^4}	6.436	.592	−.601	5.762	.702	
Γ_β T_{D^4}	7.660	.576	.633	6.556	.422	−.592
$\Gamma_{\beta'}$	7.239	.901		7.397	.779	
T_{D^4} Γ_β	6.845	.257	−.744	7.844	.644	.519
T_{D^5} Γ_β	5.638	.726		6.869	.296	−.724
	3-bromopyridine			2-iodopyridine		
Γ_0	−0.191	.986		−0.263	.979	
Γ_α	4.641	.920		4.589	.882	
Γ_p T_{D^5}	5.690	.628	−.685	6.754	.694	
Γ_β T_{D^4}	7.751	.584	.632	7.428	.764	
$\Gamma_{\beta'}$	7.386	.804		7.234	.912	
T_{D^4} Γ_β	6.772	.222	−.708	6.221	.739	
T_{D^5} T_{D^4}	6.364	.250	.633	5.438	.764	
	2-iodopyridine			3-bromopyridine		
Γ_0	−0.203	.984		−0.241	.982	
Γ_α	4.589	.839		4.620	.929	
Γ_p	6.693	.753		5.735	.711	
Γ_β $\Gamma_{\beta'}$	7.312	.840		6.797	.739	
$\Gamma_{\beta'}$ Γ_β	7.165	.960		7.606	.709	
T_{D^4}	6.125	.750		7.947	.642	
T_{D^5} $\Gamma_{\beta'}$	5.294	.779		6.458	.258	−.645

i	Mataga—Nishimoto					
	E (eV)	ψ_i		E (eV)	ψ_i	
	4-bromopyridine			2-fluoropyridine		
Γ_0	−0.346	.979		−0.282	.985	
Γ_α	4.724	.964		4.748	.981	
Γ_p T_{D^4}	6.063	.791		6.128	.941	
Γ_β T_{D^4}	6.492	.846		6.982	.767	
$\Gamma_{\beta'}$	6.676	.762		6.924	.753	
T_{D^4} Γ_β	8.940	.841		10.001	.794	
T_{D^5} Γ_β	8.680	.839		9.056	.766	
	3-bromopyridine			2-chloropyridine		
Γ_0	−0.323	.980		−0.402	.977	
Γ_α	4.620	.952		4.673	.968	
Γ_p T_{D^5}	5.889	.840		6.003	.904	
Γ_β T_{D^4}	6.868	.823		6.852	.657	
$\Gamma_{\beta'}$	6.685	.827		6.954	.638	
T_{D^4} Γ_β	8.953	.715		9.566	.735	
T_{D^5} T_{D^4}	8.531	.682		8.867	.702	
	2-bromopyridine			2-iodopyridine		
Γ_0	−0.361	.978		−0.398	.974	
Γ_α	4.674	.962		4.608	.939	
Γ_p	5.961	.873		5.788	.790	
Γ_β $\Gamma_{\beta'}$	6.808	.620	−.661	6.658	.568	−.565
$\Gamma_{\beta'}$ Γ_β	6.938	.600	.700	6.898	.550	.668
T_{D^4}	8.863	.716		8.272	.637	
T_{D^5} $\Gamma_{\beta'}$	8.278	.663		7.806	.547	.576

It can be established that the CT contributions to the first four configurations increase in the order of decreasing electronegativity of halogen atoms, namely the mixing is the strongest with iodopyridine.

It can be concluded that the MATAGA—NISHIMOTO approximation is the most suitable for calculating the wavefunctions and the point charge approximation gives the least reliable results. This is in accordance with our earlier statements [21, 22].

Table VII

Best $-\beta_{CX}$ values for the calculations

	MIM calculation			PPP calculation
	Point	Sphere	M.N.	
F	1.4	1.5	1.9	2.6
Cl	1.6	1.8	2.2	2.8
Br	1.4	1.6	2.0	2.3
I	1.3	1.5	2.0	1.9

3. PPP Method

3.1. *Method of Calculation*

The PPP method was used in its original form [6, 7]. The $\gamma_{\mu\nu}$ two-center repulsion integrals were calculated by the MATAGA—NISHIMOTO approximation. The singlet transition energies, oscillator strengths, polarization directions, and charge density–bond order matrix were also calculated. The SCF convergence criterion was 10^{-3}.

3.2. *Starting Values*

The valence state ionization potentials and electron affinities can be found in Table II. Calculations were performed only with the data of the first two columns, found as most reliable previously. Results obtained with the data of the first column are not satisfactory because it was not possible to find a β_{CX} value attributable to a given halogen atom which would have resulted in a good agreement for all isomers, and the best β_{CX} was too large. The reason for this is that the values of valence state ionization potentials obtained from HINZE's tables are too high for substituent atoms having two π-electrons. Thus we give in the following only the results calculated with data of the second column. From these data the valence state ionization potentials of the halogen atoms were determined by KWIATKOWSKI's formula:

$$I_\mu = I_{CH_3X} + \gamma_{\mu\mu}$$

where the experimental ionization potential I_{CH_3X} (see Sect. 2.2.) was taken as the valence state electron affinity A_μ. This procedure has the advantage, that experimental data is used for starting value. The bond distances are given in Sect. 2.2. The resonance integrals of the pyridine ring are: $\beta_{CC} = -2.39$ eV and $\beta_{CN} = -2.58$ eV. The resonance integrals of carbon–halogen bonds were taken as variable parameters and the transition energies were calculated with different β_{CX} values to obtain their optimum. The calculated

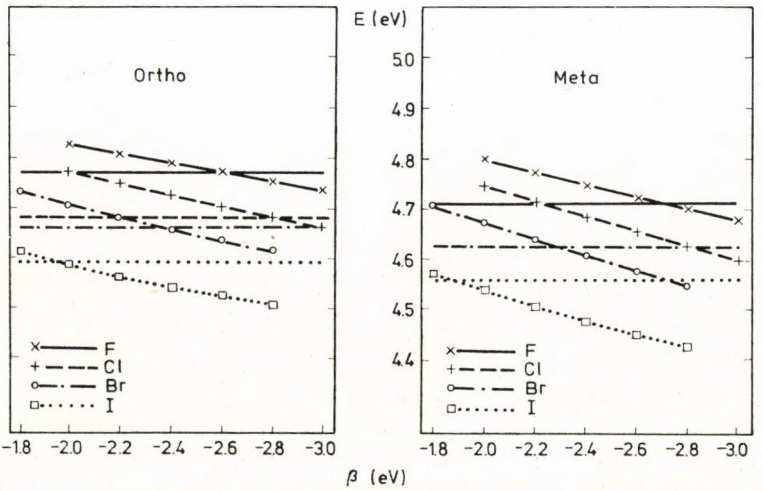

Fig. 4. First band energies of *ortho-* and *meta*-halopyridines as a function of β_{CX} calculated by the PPP method. Symbols as in Fig. 1

energies are given in Fig. 4 for the *o-* and *m*-halopyridines. The best β_{CX} resonance integral found from Fig. 4 are given in the last column of Table VII. In the following only results obtained with these β_{CX} values are given.

3.3. Results

3.3.1 *Transition Energies, Oscillator Strengths and Polarization Directions*

Spectral data for the four lowest singlet transitions calculated with the starting values given in Sect. 3.2. are presented in Table VIII together with the experimental data available. It can be seen that the results obtained for the energies of the first bands using the best β_{CX} are satisfactory, similarly to the results of the MIM method.

Table VIII contains the calculated oscillator strengths together with the experimental ones for which the values obtained by the equation $f = \varepsilon/41{,}700$ [23] were considered. The agreement is believed to be satisfactory.

The calculated polarization directions (α) are given in Table VIII too. The calculated α angles are measured from the $C_4 \rightarrow N$ bond axis having the

Table VIII

Spectral data calculated by the PPP method

Compound	Calculated			Experimental [20]		
	E (eV)	f	α	E (eV)	lg ε	f
1.	2.	3.	4.	5.	6.	7.
2-fluoropyridine	4.770	0.110	288.02	4.769	3.4	0.060
	6.024	0.183	29.14			
	7.061	1.059	46.60			
	7.156	0.913	135.63			
3-fluoropyridine	4.724	0.101	62.81	4.714	3.3	0.048
	5.901	0.174	309.83			
	6.933	0.953	162.34			
	7.064	0.965	76.63			
4-fluoropyridine	4.921	0.003	269.98			
	5.962	0.083	0.01			
	6.771	0.909	90.00			
	6.873	1.199	0.00			
2-chloropyridine	4.682	0.135	288.09	4.679	3.4	0.060
	5.866	0.319	36.57			
	6.972	1.007	57.20			
	7.104	0.774	147.24			
3-chloropyridine	4.627	0.119	240.08	4.626	3.3	0.048
	5.701	0.312	125.79			
	6.823	0.853	157.70			
	7.001	0.886	75.05			
4-chloropyridine	4.877	0.000	90.47	4.805	3.1	0.033
	5.759	0.255	0.00			
	6.630	0.821	270.00			
	6.758	1.126	0.00			
2-bromopyridine	4.667	0.130	283.46	4.661	3.4	0.060
	5.773	0.372	39.53			
	6.875	0.785	81.27			
	6.964	0.660	4.19			
3-bromopyridine	4.622	0.109	243.35	4.626	3.3	0.048
	5.621	0.356	124.96			
	6.693	0.641	168.26			
	6.911	0.830	88.03			
4-bromopyridine	4.856	0.001	269.95			
	5.653	0.335	0.00			
	6.531	0.721	90.00			
	6.683	0.992	0.00			

(Table VIII continued)

Compound	Calculated			Experimental [20]		
	E (eV)	f	α	E (eV)	lg ε	f
1.	2.	3.	4.	5.	6.	7.
2-iodopyridine	4.597	0.135	278.69	4.592	3.6	0.095
	5.547	0.450	43.49	5.438	3.8	0.151
	6.459	0.166	115.98			
	6.800	0.585	47.71			
3-iodopyridine	4.555	0.105	66.14	4.558	3.4	0.060
	5.410	0.417	303.81	5.438	3.8	0.151
	6.339	0.286	171.74			
	6.782	0.638	98.20			
4-iodopyridine	4.806	0.001	269.94	4.428	3.3	0.048
	5.389	0.448	180.00	5.166	3.9	0.191
	6.269	0.495	270.00			
	6.577	0.730	0.00			

origin at the N atom in clockwise direction. This choice of the polarization direction allows a direct comparison with the values obtained for halobenzenes. It seems that the polarization directions of the halopyridines differ considerably from the values obtained for the corresponding disubstituted benzenes [22] and are similar to those of monosubstituted benzenes [24].

3.3.2. *Charge Densities and Bond Orders*

The calculated charge densities on the ring nitrogen atom and on the halogen atoms (q_i) as well as the bond orders for the carbon–halogen bonds (p_{CX}) are given in Table IX. The charge density is the largest on the *m*- and

Table IX

Charge densities of halogen and ring nitrogen atoms, and bond orders of carbon–halogen bonds

X	2-X-pyridine			3-X-pyridine			4-X-pyridine		
	X		N	X		N	X		N
	q_X	p_{CX}	q_N	q_X	p_{CX}	q_N	q_X	p_{CX}	q_N
F	1.8891	0.3507	1.2692	1.9036	0.3118	1.2098	1.8947	0.3336	1.2417
Cl	1.8619	0.3917	1.2801	1.8790	0.3503	1.2103	1.8673	0.3750	1.2502
Br	1.8831	0.3581	1.2670	1.8988	0.3178	1.2118	1.8878	0.3424	1.2440
I	1.8963	0.3354	1.2580	1.9112	0.2957	1.2130	1.9002	0.3207	1.2402

the smallest on the *o*-halogen atom in each case. The order on the ring nitrogen is reversed.

The complete molecular diagrams of pyridine and the bromopyridines are shown in Fig. 5 as examples. On the basis of previous studies [3, 22], the expected order of charge densities related to the halogen atom is $2(ortho) > > 4(para) > 3(meta) > 1$. Taking this and the calculated charge density distribution of the pyridine ring into consideration, the calculated charge

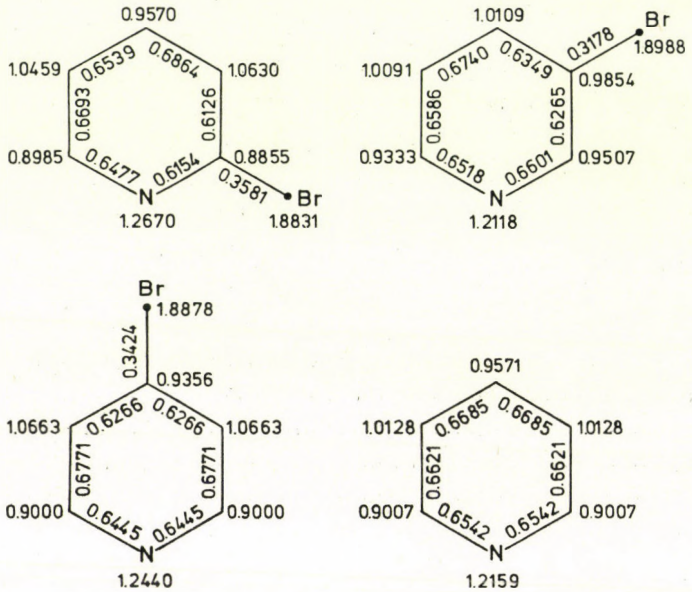

Fig. 5. Charge density and bond order molecular diagrams of pyridine and bromopyridine isomers

densities are in complete accordance with the expectation, *i.e.* the order of charge densities related to the halogen atom (X) and ring nitrogen is:

2-X-pyridines: N-*o* $>$ *m-o* $>$ *m-p* $>$ *p-m* $>$ *o-m* $>$ *o-i*
3-X-pyridines: N-*m* $>$ *p-o* $>$ *m-m* $>$ *m-i* $>$ *o-o* $>$ *o-p*
4-X-pyridines: N-*p* $>$ *m-o* $>$ *p-i* $>$ *o-m*

where *i* refers to the carbon atom bonded to the halogen atom.

REFERENCES

[1] Kwiatkowski, J. S.: Acta Phys. Polon., **30,** 963 (1966)
[2] Fischer-Hjalmars, I., Sundbom, M.: Acta Chem. Scand., **22,** 607 (1968)
[3] Kiss, Á. I., Martin, A.: Acta Chim. (Budapest), **77,** 179 (1973)
[4] Mataga, N., Nishimoto, K.: Z. Phys. Chem. N. F., **13,** 140 (1957)

[5] FAVINI, G., GAMBA, A., BELLOBONO, I. R.: Spectrochim. Acta, **23A**, 89 (1967)
[6] POPLE, J. A.: Trans. Faraday Soc., **49**, 1375 (1953)
[7] PARISER, R., PARR, R. G.: J. Chem. Phys., **21**, 466, 767 (1953)
[8] SUTTON, L. E.: Tables of Interatomic Distances, Spec. Publ. No. 11, Chem. Soc. London 1958; Supplement Spec. Publ. No. 18, Chem. Soc. London 1965.
[9] BAK, B., HANSEN-NYGAARD, L., RASTRUP-ANDERSEN, J.: J. Mol. Spectr., **2**, 361 (1958)
[10] SLATER, J. C.: Phys. Rev., **36**, 57 (1930)
[11] BURNS, G.: J. Chem. Phys., **41**, 1521 (1964)
[12] KWIATKOWSKI, J. S.: Acta Phys. Polon., **29**, 477 (1966); **30**, 529 (1966)
[13] FORD, B.: Theor. Chim. Acta, **10**, 342 (1968)
[14] KHETRAPAL, C. L., RAI, D. K.: Theor. Chim. Acta, **13**, 308 (1969)
[15] PAOLONI, L.: Nuovo Cimento, **4**, 410 (1956)
[16] HINZE, J., JAFFÉ, H. H.: J. Amer. Chem. Soc., **84**, 540 (1962)
HINZE, J.: PhD. Thesis, University of Cincinnati, USA, 1962.
[17] DIBELER, V. H., REESE, R. M.: J. Res. Nat. Bur. Stand., **54**, 127 (1955)
[18] DIBELER, V. H., REESE, R. M.: Anal. Chem., **30**, 604 (1958)
[19] BECKER, R. S., WENTWORTH, W. E.: J. Amer. Chem. Soc., **85**, 2210 (1963)
[20] Organic Electronic Spectral Data. Interscience Publ. New York, Vols I-VII.
[21] MARTIN, A., KISS, Á. I.: Acta Chim. (Budapest), **78**, 177 (1973)
[22] MARTIN, A., KISS, Á. I.: Acta Chim. (Budapest), **84**, 259 (1975)
[23] ALLINGER, N. L., STUART, T. W., TAI, J. C.: J. Amer. Chem. Soc., **90**, 2819 (1968)
[24] KISS, Á. I., SZŐKE, J.: Acta Chim. (Budapest), **74**, 33 (1972)

Antal MARTIN; H-1111 Budapest, Budafoki út 8.

Acta Chimica Academiae Scientiarum Hungaricae, Tomus 90(1), pp. 21—31 (1976)

STATIC DIELECTRIC PROPERTIES OF BINARY LIQUID MIXTURES CONTAINING TRI-*N*-BUTYLAMINE

J. Liszi

(Departmental Research Group on Electrochemistry of the Hungarian Academy of Sciences Department of Physical Chemistry, University of Chemical Industries, Veszprém)

Received 26 June, 1975

A study was made of the static dielectric properties of binary liquid mixtures of tri-*n*-butylamine with *n*-heptane, chloroform or acetone. The results show that the amine does not form associates either with itself or with *n*-heptane. In the mixtures containing chloroform or acetone, 'mixed' associates are formed from the amine and the polar component.

A study was made of the static dielectric properties and densities of three binary mixtures containing tri-*n*-butylamine as a function of the compositions of the mixtures at 20°. The components to be mixed with the amine were selected so that the polarities of the mixtures should be different. The three components were: *n*-heptane, chloroform and acetone. In the course of the investigations an answer was sought to the question of whether special intermolecular interactions leading to association occur between the amine and the second component.

Experimental

The static relative permittivities and conductances of the mixtures were determined at a frequency of 500 kHz with a Siemens Rel 3 R 277 impedance bridge. A thermostatable measuring cell with an empty capacity of 30 pF was used for the measurements. The densities of the mixtures were measured with a DMA OZC digital densimeter; the constant of the instrument was calculated from the densities of the pure substances, determined with a pycnometric method. Refractive indices referring to the NaD line were measured with a Carl Zeiss (Jena) Abbe refractometer. The chemicals employed were Fluka products of purum quality, and were used without purification from previously unopened bottles. The experimental results are listed in Tables I—VI.

Table I

Static relative permittivity (ε), density (ϱ) and conductance (G) of tri-n-butylamine–n-heptane mixtures as functions of the mole fraction of the amine (x_1)

x_1	ε	ϱ g · cm^{-3}	G μS
0	1.93	0.684	2.0
0.099	1.98	0.699	2.0
0.199	2.04	0.712	2.0
0.326	2.10	0.727	2.1
0.405	2.15	0.734	2.1
0.503	2.19	0.744	2.1
0.596	2.23	0.751	2.1
0.698	2.26	0.759	2.2
0.795	2.29	0.766	2.2
0.892	2.30	0.772	2.3
1	2.34	0.778	2.3

Table II

Static relative permittivity (ε), density (ϱ) and conductance (G) of tri-n-butylamine–chloroform mixtures as functions of the mole fraction of the amine (x_1)

x_1	ε	ϱ g · cm^{-3}	G μS
0	4.88	1.489	5.1
0.101	4.61	1.314	15.9
0.197	4.33	1.184	7.5
0.299	4.08	1.096	5.1
0.398	3.77	1.016	3.8
0.501	3.49	0.958	3.1
0.599	3.32	0.913	2.7
0.684	3.07	0.876	2.5
0.798	2.79	0.836	2.4
0.898	2.57	0.805	2.3
1	2.34	0.778	2.3

Table III

Static relative permittivity (ε), density (ϱ) and conductance (G) of tri-n-butylamine–acetone, mixtures as functions of the mole fraction of the amine (x_1)

x_1	ε	ϱ g · cm^{-3}	G μS
0	21.10	0.792	120.0
0.100	15.26	0.788	329.0
0.204	11.32	0.781	220.6
0.298	8.75	0.779	118.5
0.396	6.99	0.777	59.3
0.498	5.63	0.777	22.2
0.591	4.69	0.777	7.8
0.687	3.99	0.777	3.3
0.798	3.29	0.778	2.4
0.892	2.80	0.778	2.3
1	2.34	0.778	2.3

Table IV

Refractive index (n_D) referred to the NaD line for tri-n-butylamine–n-heptane mixtures as a function of the mole fraction of the amine (x_1)

x_1	n_D	x_1	n_D
0	1.3888	0.600	1.4170
0.101	1.3950	0.697	1.4196
0.206	1.4002	0.803	1.4227
0.316	1.4054	0.894	1.4261
0.399	1.4091	1	1.4298
0.496	1.4128		

Table V

Refractive index (n_D) referred to the NaD line for tri-n-butylamine–chloroform mixtures as a function of the mole fraction of the amine (x_1)

x_1	n_D	x_1	n_D
0	1.4430	0.507	1.4346
0.104	1.4400	0.599	1.4329
0.204	1.4389	0.701	1.4321
0.299	1.4369	0.802	1.4312
0.405	1.4357	0.907	1.4302

Table VI

Refractive index (n_D) referred to the NaD line for tri-n-butylamine–acetone mixtures as a function of the mole fraction of the amine (x_1)

x_1	n_D	x_1	n_D
0	1.3594	0.500	1.4229
0.103	1.3780	0.603	1.4249
0.197	1.3940	0.692	1.4265
0.303	1.4098	0.789	1.4276
0.402	1.4190	0.904	1.4289

Discussion

1. Molar volume

The molar volumes calculated from the density data for the three systems are shown in Fig. 1. The results demonstrate that mixing is not accompanied by either contraction or dilatation. Thus, even if special intermolecular interactions leading to association do occur in the liquid phase, these do not cause a change in volume on mixing.

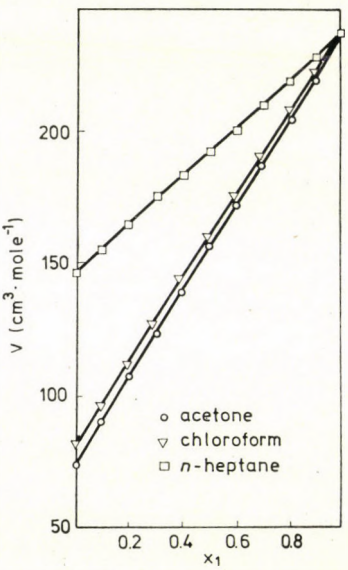

Fig. 1. Molar volume (V) of the mixtures as a function of the mole fraction of the amine (x_1)

2. Molar refraction

The molar refractions were calculated from the refractive indices relating to the NaD line and from the densities of the mixtures *via* the relation

$$R_D = \frac{n_D^2 - 1}{n_D^2 + 2} \frac{M}{\varrho} \tag{1}$$

where R_D is the molar refraction relating to the Na_D line, n_D is the refractive index relating to the NaD line, 9 is the density, and M is the average molar mass:

$$M = x_1 M_1 + x_2 M_2 \tag{2}$$

M_1 and M_2 are the molar masses of the pure components, and x_1 and x_2 their mole fractions; the index 1 denotes the amine, and 2 the second component. The molar refractions of the three systems are shown in Fig. 2 as a function of the mole fraction of the amine. The linear variation of the molar refractions with composition indicates that the mixtures do not involve any intermolecular interactions which would influence the electron polarizations of the components.

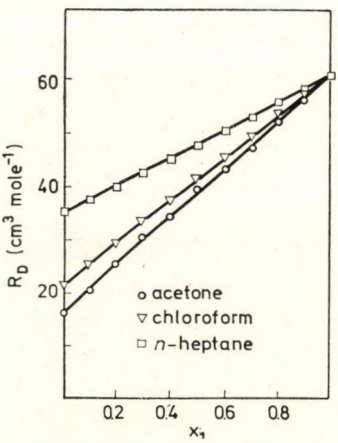

Fig. 2. Molar refraction (R_D) of the mixtures as a function of the mole fraction of the amine (x_1)

3. Molar polarization

The molar polarizations of the mixtures were calculated from the equation

$$P = \frac{\varepsilon - 1}{\varepsilon + 2} \frac{M}{\varrho} \tag{3}$$

where P is the molar polarization of the mixture, and ε is the static relative permittivity of the mixture. The molar polarizations of the three systems are shown in Fig. 3 as a function of the mole fraction of the amine.

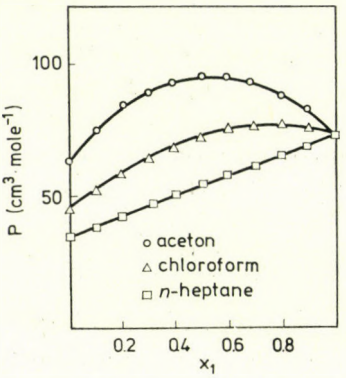

Fig. 3. Molar polarization (P) of the mixtures as a function of the mole fraction of the amine (x_1)

A. Tri-n-butylamine–n-heptane mixtures

The molar polarization of tri-*n*-butylamine–*n*-heptane mixtures is a linear function of the mole fraction of the amine. Such an additivity of the molar polarizations of the components shows that neither self-association of the amine, nor 'mixed' association between the amine and the *n*-heptane need be reckoned with. The molar polarization of the amine does not vary with the composition; in the whole concentration range its value is $\sim$73.6 $cm^3 . mole^{-1}$.

B. Tri-n-butylamine–acetone mixtures

The molar polarization of tri-*n*-butylamine–acetone mixtures exhibits a maximum as a function of composition. The excess molar polarization, P^E, calculated from the relation

$$P^E = P - (x_1P_1 + x_2P_2) \tag{4}$$

is symmetrical in form (Fig. 4, curve 3). The empirical relation describing the experimental values is

$$P = x_1P_1 + x_2P_2 + 96\, x_1x_2 \tag{5}$$

The interactions causing the non-linear behaviour of the molar polarization of the mixtures can be classified into two groups:

(a) The non-'special' interactions change the local electric field strength acting on the molecules of the liquid, and hence affect the molar polarization, but do not lead to association.

(b) The 'special' interactions cause association. In addition to monomer molecules, the liquid also contains associates of several monomer units. The dipole moments of the associates, in general, differ from those of the monomer molecules, and thus additivity of the molar polarizations is not to be expected either.

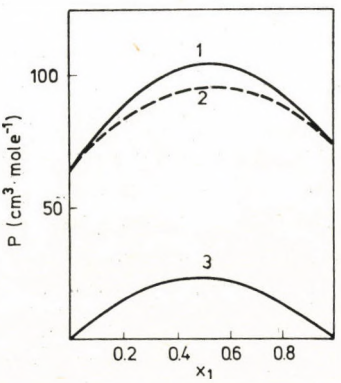

Fig. 4. Molar polarization (P) of the amine–acetone mixture as a function of the mole fraction of the amine (x_1). Curve 1: values calculated on the basis of the Onsager theory. Curve 2: experimental values. Curve 3: excess molar polarization

To decide whether intermolecular interactions leading to association occur in tri-*n*-butylamine–acetone mixtures, we calculated the molar polarization of the mixture on the basis of the ONSAGER theory [1]. The Onsager theory takes into consideration only the non-'special' intermolecular interactions not leading to association. According to the Onsager theory, the molar polarization of the binary mixture is

$$P = \frac{4\pi\varepsilon N_A}{\varepsilon + 2}\left[x_1 \frac{n_1^2 + 2}{2\varepsilon + n_1^2}\left\{\alpha_1 + \frac{(n_1^2 + 2)(2\varepsilon + 1)}{3\,(2\varepsilon + n_1^2)}\,\frac{\mu_1^2}{3kT}\right\} + x_2 \frac{n_2^2 + 2}{2\varepsilon + n_2^2}\left\{\alpha_2 + \frac{(n_2^2 + 2)(2\varepsilon + 1)}{3\,(2\varepsilon + n_2^2)}\,\frac{\mu_2^2}{3kT}\right\}\right] \tag{6}$$

where ε is the static relative permittivity, α is the polarizability, n is the internal refractive index, μ is the permanent dipole moment, N_A is Avogadro's number, k is the Boltzmann constant, T is the absolute temperature, and the other notations are the same as previously.

The permanent dipole moment of tri-*n*-butylamine is 0.78 D [2], and that of acetone is 3 D [2]. The displacement polarization of acetone, $P_{\text{disp.}} =$

$= 16.7$ cm^3 [3]. From this, with the aid of the equation

$$\frac{4\pi N_A}{3}\alpha = P_{\text{disp.}} \tag{7}$$

the polarizability of acetone, $\alpha_2 = 6.6\times10^{-24}$ cm^3. From the equation

$$\frac{n_D^2 - 1}{n_D^2 + 2}\,\frac{M_2}{\varrho_2} = \frac{4\pi N_A}{3}\alpha_2 \tag{8}$$

the refractive index relating to the NaD line leads to $\alpha_2 = 6.4\times10^{-24}$ cm^3. The two data approximate well to one another; to a first approximation the effect of atom polarization can be neglected. In our calculations the refractive index relating to the NaD line was used in place of the internal refractive index of acetone. Calculating the displacement polarizability of the tri-*n*-butylamine *via* equation (8) from the refractive index relating to the NaD line, $\alpha_1 = 23.4\times10^{-24}$ cm^3. With this datum, $P_1 = 73.9$ cm^3. mole^{-1}, while the molar polarization calculated from the relative permittivity and density *via* equation (3) is 73.6 cm^3. mole^{-1}. This agreement justified the use of the refractive index relating to the NaD line instead of the internal refractive index in the case of tri-*n*-butylamine too.

Curve 1 of Fig. 4 shows the molar polarization calculated from the above data *via* equation (6) as a function of the mole fraction of the amine. The Onsager theory gives a molar polarization larger by about 10% at most than the values calculated from the direct experimental data *via* equation (3) (Fig. 4, curve 2). Since the Onsager theory does not take into consideration the 'special' intermolecular interactions leading to association, it may be assumed that the difference between curves 1 and 2 of Fig. 4 is caused by just such interactions. The symmetrical form of the excess molar polarization curve indicates that amine and acetone molecules take part in identical numbers in the associates formed. (From steric considerations it may be presumed that 1 : 1 mixed associations develop.) The dipole moments of the associates formed are smaller than the sum of the absolute values of the dipole moments of the monomers comprising the associates.

C. Tri-n-butylamine–chloroform mixtures

The molar polarization of tri-*n*-butylamine–chloroform mixtures similarly exhibits an extreme value as a function of the mole fraction of the amine. The deviation from linear behaviour is of a lower extent than in the case of the acetone-containing mixtures. The maximum of the excess molar polarization, calculated from equation (4), is approximately at $x_1 = 0.55$ (Fig. 5, curve 1).

The square of the internal refractive index of chloroform is 2.2 [4], and from this its polarizability is 9.1×10^{-24} cm^3. The permanent dipole moment of chloroform is 1.01 D [4]. With the use of these data, the molar polarization of the mixture was calculated *via* equation (6), as a function of the mole fraction of the amine. The results are shown in curve 1 of Fig. 5. The molar polarization of the mixture is not a linear function of the composition according to the Onsager theory either. It is interesting that the Onsager theory gives a lower molar polarization than equation (3) (Fig. 5,

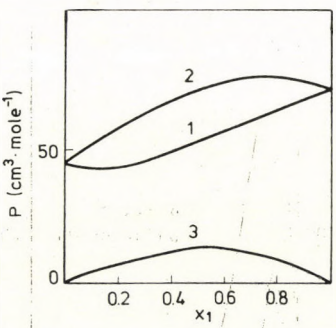

Fig. 5. Molar polarization (P) of the amine–chloroform mixture as a function of the mole fraction of the amine (x_1). Curve 1: values calculated on the basis of the Onsager theory. Curve 2: experimental values. Curve 3: excess molar polarization

curve 2). This indicates that the directional polarizability of the 'mixed' associates formed from chloroform and tri-*n*-butylamine is larger than the sum of the directional polarizabilities of the components forming the associate.

The results relating to the chloroform–tri-*n*-butylamine mixtures must be accepted with some reservation, as the action of light may convert the chloroform to hydrochloric acid, which forms a salt with the amine, thereby affecting perhaps the dielectric properties. In order to eliminate the error resulting from this, we always used freshly prepared solutions for the measurements. (We encountered a similar phenomenon with carbon tetrachloride–tri-*n*-butylamine mixtures too. The chlorine liberated from the carbon tetrachloride on the action of light extracted hydrogen from the alkyl groups of the amine to form hydrochloric acid. With the amine this yielded a salt, which separated in the form of colourless, needle-shaped crystals. The unsaturated bonds produced in the alkyl groups of the amine by the extraction of hydrogen gave a brown colour to the liquid phase. The crystals formed dissolve in polar solvents [including chloroform], and thus crystal separation can not be observed in the case of tri-*n*-butylamine–chloroform mixtures.)

4. Electric conductance

The conductance determined in μS units naturally depends on the dimensions of the measuring cell, but if an identical cell is employed, valuable information is obtained from the variation of G with the composition. The tri-*n*-butylamine–*n*-heptane system has a very low conductance, which varies practically linearly with composition (Table I). These data do not signify 'special' intermolecular interactions.

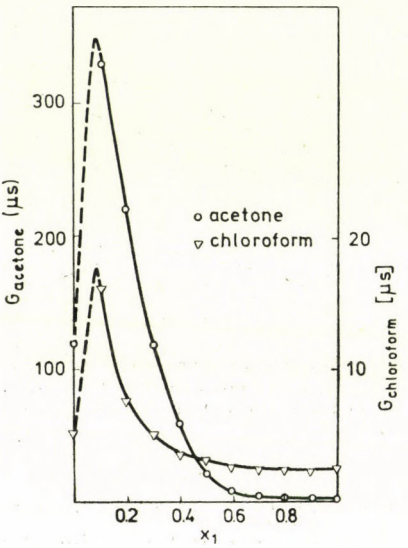

Fig. 6. Conductance (G) of mixtures containing acetone and chloroform as a function of the mole fraction of the amine (x_1). The dashed curve indicates uncertain values

The conductance data relating to the other two systems are more interesting; these are illustrated in Fig. 6. The left-hand ordinate refers to acetone, and the right-hand one to chloroform. Both curves exhibit a maximum in the vicinity of $x_1 = 0.1$. A similar phenomenon was observed in alcohol–amine mixtures [5]. For a qualitative interpretation of the phenomenon, use may be made of the finding [6] that the dipole moments of charge-transfer complexes depend on the environment of the complex: the larger the static relative permittivity of the environment, the larger is the dipole moment of the complex. In the systems containing chloroform and acetone, the concentrations of the 'mixed associates' are maximum at a composition $x_1 = 0.5$, whereas the static relative permittivities of the mixtures are greatest at $x_1 = 0$. In the range $x_1 = 0—0.5$ the concentration of the associate and the relative permittivity of the mixture have opposing effects on the conductance (which to a good approximation originates here from the dis-

placement current), and the maximum in the conductance curve may be caused by these two opposing effects.

To sum up, it may be stated that tri-*n*-butylamine does not form associates with either itself or *n*-heptane, whereas its intermolecular interactions with acetone and with chloroform do lead to association.

REFERENCES

[1] ONSAGER, L.: J. Amer. Chem. Soc., **58**, 1486 (1936)
[2] HILL, N. E., VAUGHAN, W. E., PRICE, A. H., DAVIES, M.: Dielectric Properties and Molecular Behaviour, Van Nostrand, Reinhold, London 1969
[3] STUART, H. A.: Die Struktur des Freien Moleküls, Springer Verlag, Berlin, Göttingen, Heidelberg 1952
[4] BÖTTCHER, C. J. F.: Theory of Electric Polarization, Revised by O. C. Van Belle, P. Bordewijk, A. Rip, Vol. I, Elsevier, Amsterdam, London, New York 1973
[5] LISZI, J., SALAMON, T., RATKOVICS, F.: Acta Chim. (Budapest), **81**, 467 (1974)
[6] JADZIN, J., MALECKI, J.: Acta Phys. Polon, **A41**, 599 (1972)

János LISZI; H-8201 Veszprém, Schönherz Z. u. 10.

Acta Chimica Academiae Scientiarum Hungaricae, Tomus 90(1), pp. 33–42 (1976)

STUDIES ON THE REACTION BETWEEN Cu(II) ACETATE AND SULPHATE AND SOME ACID HYDRAZIDES

F. I. M. TAHA, M. N. H. MOUSSA, A. M. SHALLABY and M. M. MOSTAFA
(Chemistry Department, El Mansoura University, Egypt)

Received June 30, 1975
In revised form January 20, 1976

Cu(II) acetate and sulphate react with all the hydrazides studied to give mono and/or bis-ligand complexes. In the case of the acetate complexes the ligand was shown by IR spectra to be monodentate coordinating through the NH_2 group. Spectral and magnetic measurements indicated that the acetate complexes have either octahedral or tetrahedral structures.

Introduction

In the last decades many studies have been carried out on carboxylic acid hydrazides as ligands [1–4]. Many conflicting views have been reported concerning stoichiometries, coordination sites and structures of the isolated hydrazide complexes. The aim of the present work is to ascertain by as much evidence as possible the nature and composition of some different hydrazide complexes with Cu(II) acetate and sulphate salts prepared in absolute ethanol.

Experimental

Acid hydrazides were prepared by refluxing methyl or ethyl esters of the acid with hydrazine [5]. 1 : 1 and 1 : 2 metal : ligand complexes were prepared by refluxing equimolar amounts of the hydrazide and the hydrated copper salts in absolute ethanol. BDH $CuSO_4 \cdot 5H_2O$ and Apolda $(CH_3COO)_2Cu \cdot H_2O$ were used.

Physical measurements

Spectrophotometric measurements in the visible and ultraviolet regions were carried out on Prolabo and Pye Unicam SP 1800 spectrophotometers using 1-cm matched silica and glass cells.

The IR spectra of solid materials were taken in KBr discs using a Pye Unicam SP 1000 infrared spectrophotometer.

The conductance values were measured using a conductivity cell of the G.M. type dipping in the solution to be titrated. The temperature was adjusted by placing the cell in an ultrathermostat. A Beckman conductance bridge was employed.

Magnetic moments for the acetate complexes were determined by the Gouy method at the Physics Department, Cairo University.

Results and Discussion

Isolation of pure compounds

On interacting formyl, acetyl, propionyl, butyryl, palmityl, benzoyl, salicyl and *p*-hydroxy benzoyl hydrazides with Cu(II) acetate or sulphate in absolute ethanol, both mono and bis-ligand complexes were frequently but not necessarily isolated. Results of elemental analysis are shown in Table I. The complexes were insoluble in most of the organic solvents tried. Accordingly molecular weights could not be determined.

Spectrophotometric studies

a) *Absorption Spectra of Cu^{2+}–Hydrazide Complexes:*

The absorption spectra of solutions formed from acetyl, benzoyl, *p*-methoxy benzoyl and salicyl hydrazides and Cu(II) acetate or sulphate were taken between 600 and 1000 nm. Sets of aqueous or ethanolic solutions were prepared in which Cu(II) concentration was kept constant at 10×10^{-2} *M* while the hydrazide concentration varied from 1.0 to 4.0×10^{-2} *M*.

The absorption curves obtained exhibited maxima in the visible region which shifted gradually to blue with increasing the concentration of hydrazides. These spectra are closely related to those of semicarbazide and Girard reagent cupric ion systems [6, 7]. Representative absorption spectra for Cu(II) sulphate–acetyl hydrazide mixtures are shown in Fig. 1.

Absorption spectra of the ligands and metal salts studied were also recorded in the ultraviolet region. Acetyl hydrazide did not show any absorption bands above 190 nm whereas benzoyl, salicyl and *p*-methoxy benzoyl hydrazides exhibited bands at 230; 200, 242 and 210, 238, 300 nm respectively.

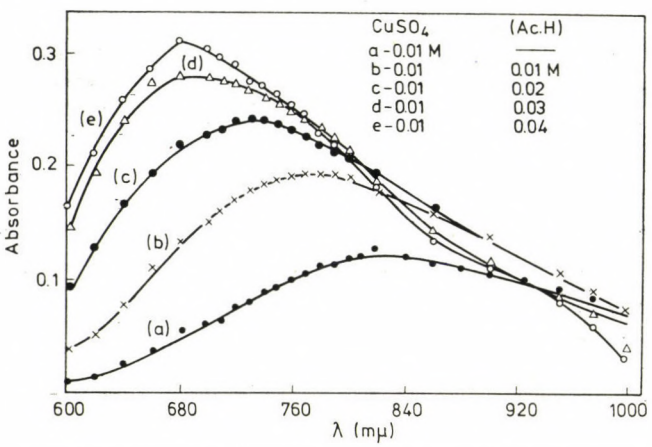

Fig. 1. Absorption spectra of $CuSO_4$—(Ac · H) mixtures

Table I

Elemental analysis of the ligands and Cu(II) complexes

Compound	% Calculated				% Found				Magnetic moment, μ eff.
	C	H	Cu	N	C	H	Cu	N	
Formyl hydrazide, CH_4N_2O	19.9	6.7	—	46.6	19.6	6.6	—	46.4	
$Cu(CH_4N_2O)Ac_2 \cdot H_2O$	23.1	4.6	24.6	10.7	22.6	3.9	25.1	10.1	1.52 BM
$Cu(CH_4N_2O)SO_4 \cdot 6H_2O$	3.6	4.9	19.3	8.5	3.2	4.6	18.9	7.9	
$Cu(CH_4N_2O)_2SO_4$	8.5	2.8	22.7	20.3	9.3	2.5	22.9	19.6	
Acetyl hydrazide, $C_2H_6N_2O$	32.4	8.1	—	37.8	32.3	8.1	—	37.3	
$Cu(C_2H_6N_2O)Ac_2$	29.1	5.5	19.2	16.9	28.6	4.9	18.9	16.5	
$Cu(C_2H_6N_2O)SO_4$	10.3	2.6	27.1	11.9	10.5	3.5	27.0	11.4	
$Cu(C_2H_6N_2O)_2SO_4$	15.6	3.9	20.6	18.2	15.1	3.4	20.3	18.6	
Propionyl hydrazide, $C_3H_8N_2O$	40.8	9.1	—	31.7	40.8	9.3	—	31.6	
$Cu(C_3H_8N_2O)_2Ac_2$	33.5	6.1	15.7	—	34.1	5.3	15.4	—	2.20 BM
$Cu(C_3H_8N_2O)_2SO_4$	21.4	4.8	18.9	—	21.5	5.0	18.3	—	
$Cu(C_3H_8N_2O)SO_4$	14.5	3.2	25.6	—	14.4	3.8	25.9	—	
Butyryl hydrazide, $C_4H_{10}N_2O$	47.0	9.8	—	27.0	47.0	9.3	—	27.1	
$Cu(C_4H_{10}N_2O)_2Ac_2 \cdot H_2O$	35.6	6.9	15.7	—	35.4	5.9	15.9	—	1.89 BM
$Cu(C_4H_{10}N_2O)SO_4 \cdot \cdot 5H_2O$	13.6	5.7	18.0	—	13.6	4.9	18.8	—	
Palmityl hydrazide, $C_{16}H_{34}N_2O$	71.5	12.6	—	10.3	71.4	12.4	—	10.2	
$Cu(C_{16}H_{34}N_2O)Ac_2 \cdot H_2O$	58.3	10.3	8.5	—	58.7	9.6	8.8	—	
$Cu(C_{16}H_{34}N_2O)SO_4 \cdot \cdot 2H_2O$	52.1	9.8	8.6	—	51.8	9.2	8.4	—	
Benzoyl hydrazide, $C_7H_8N_2O$	61.7	5.9	—	20.5	61.6	5.9	—	19.5	
$Cu(C_7H_8N_2O)Ac_2 \cdot H_2O$ $2H_2O$	35.6	5.1	25.9	11.3	35.1	4.8	26.4	11.7	2.09 BM
$Cu(C_7H_8N_2O)SO_4$	38.9	3.7	14.7	12.9	39.2	3.7	14.9	12.8	
Salicyl hydrazide, $C_7H_8N_2O_2$	55.2	5.3	—	18.4	56.0	5.3	—	18.2	
$Cu(C_7H_8N_2O_2)Ac_2 \cdot H_2O$	37.5	4.5	18.0	7.9	38.0	3.8	17.9	8.0	1.57 BM
$Cu(C_7H_8N_2O_2)SO_4$	26.9	2.5	20.4	8.9	26.7	2.1	20.3	9.3	
$Cu(C_7H_8N_2O_2)_2SO_4$	33.3	3.2	12.6	11.1	33.8	2.7	12.3	10.9	

Table I (continued)

Compound	% Calculated				% Found				Magnetic moment, μ eff.
	C	H	Cu	N	C	H	Cu	N	
p-hydroxy benzoyl hydrazide, $C_7H_8N_2O_2$	55.2	5.3	—	18.4	55.2	5.1	—	18.1	
$Cu(C_7H_8N_2O_2)_2Ac_2$	44.4	4.5	13.0	—	44.1	4.8	12.7	—	
$Cu(C_7H_8N_2O_2)Ac_2$	39.5	4.2	19.0	—	39.0	4.5	19.0	—	
$Cu(C_7H_8N_2O_2)SO_4$	29.9	2.5	20.4	—	29.6	2.2	20.1	—	
$Cu(C_7H_8N_2O_2)_2SO_4 \cdot H_2O$	34.8	3.7	13.1	—	35.0	3.8	13.3	—	
o-methyl benzoyl hydrazide, $C_8H_{10}N_2O$	63.9	6.7	—	18.6	63.4	6.2	—	18.2	
$Cu(C_8H_{10}N_2O)Ac_2$	42.4	4.8	19.1	—	42.9	4.2	19.1	—	
$Cu(C_8H_{10}N_2O)SO_4$	41.7	4.3	13.8	—	41.2	4.5	13.1	—	
p-methoxy benzoyl hydrazide, $C_8H_{10}N_2O_2$	57.8	6.0	—	16.8	58.7	5.8	—	16.7	
$Cu(C_8H_{10}N_2O_2)Ac_2 \cdot \cdot H_2O$	46.7	5.0	12.6	—	46.4	4.1	12.8	—	
$Cu(C_8H_{10}N_2O_2)SO_4 \cdot \cdot H_2O$	27.9	3.5	18.3	—	27.7	3.7	18.4	—	

Thus it is apparent that the complex compounds under investigation have characteristic absorption spectra different from those of the organic compounds and of Cu(II) alone. Although characteristic color is often a valuable tool in the detection and investigation of complex compounds, it is primarily a function of structure and bond type. The donation of electrons to the metal produces lower excited states and a shift of the absorption bands of the chelating agent to red.

b) *Stoichiometry of Cu(II) Hydrazide Complexes [8]:*

In order to determine the stoichiometry of complexes formed in aqueous solution between Cu(II) and the studied hydrazides making use of the molar ratio method, a series of solutions was prepared in which Cu(II) concentration was kept constant at 1.0×10^{-2} *M* while the ligand concentration was varied from 2.5×10^{-3} to 4×10^{-2} *M*. Monoligand complexes were detected in all systems studied except that involving acetyl hydrazide (Fig. 2) where a bis-ligand complex was shown to exist.

The composition of the Cu-hydrazide complexes was also determined by the application of the continuous variation method. A series of solutions was prepared in which varying proportions of Cu(II) and the ligand were mixed

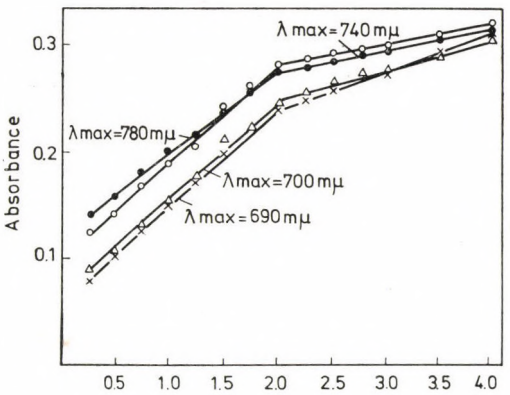

Fig. 2. Molar ratio plot of Ac · H—$CuSO_4$ system

keeping the total molar concentration constant at 1×10^{-2} *M*. The results obtained agreed with those determined by the molar ratio method. Representative curves for the Cu(II) *p*-methoxy benzoyl hydrazide system are shown in Fig. 3.

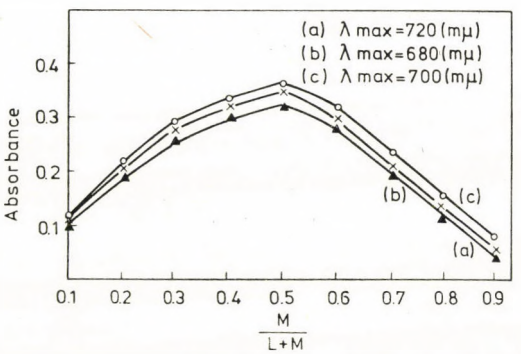

Fig. 3. Continuous variation plot of *p*-CH_3O—B.H.—$CuAc_2$ system

c) *Evaluation of the Apparent Formation Constants:*

Apparent formation constants were calculated from spectrophotometric measurements by the application of the molar ratio or continuous variation methods. Both methods gave concordant results. The average values obtained are shown in Table II.

Table II

Apparent formation constants of some Cu(II)-hydrazide complexes

Ligand	Type of complex	λ max (nm)	K
	Sulphate complexes		
Acetyl hydrazide	1 : 2	700	0.6×10^8
Benzoyl hydrazide	1 : 1	750	3.2×10^7
	Acetate complexes		
Benzoyl hydrazide	1 : 1	730	7.4×10^8
p-Methoxy benzoyl hydrazide	1 : 1	700	6.4×10^5

Electrical Conductance

The effect of dilution on the specific conductance of the complexes formed between formyl, acetyl, propionyl, butyryl, benzoyl and salicyl hydrazides and the studied Cu(II) salts was investigated. The large increase in electrical conductance of the mixtures for systems of formyl (Fig. 4), and propionyl hydrazides in aqueous solution or of salicyl hydrazide in ethanolic solution over that of Cu(II) salt and ligand alone is typical of strong complex formation. The increased conductance of the medium results from reactions producing conducting species in solution or through interaction of complex molecules having polar bonds with solvent molecules. The small increase in conductance values of the salicyl hydrazide system indicates poor solvation in ethanol. The same behaviour was exhibited when 10 ml 0.001 *M* solution of Cu(II) was titrated with 0.01 *M* ligand solution. Curves drawn between

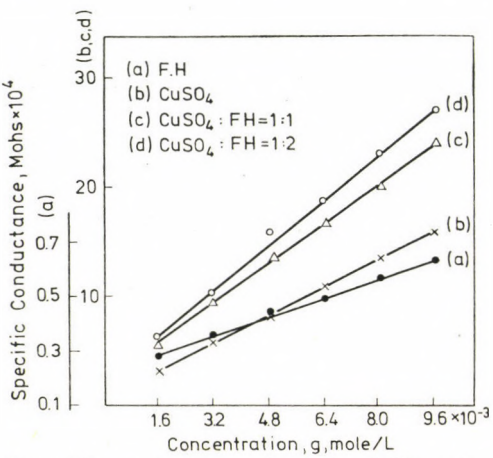

Fig. 4. Variation of specific conductance of $CuSO_4$—F.H mixtures with concentration

specific conductances of the solutions and the number of ml of formyl, propionyl (Fig. 5) and salicyl hydrazides showed continuous increase in specific conductance with increase in concentration. Moreover, the curves exhibited one or more breaks at certain molar ratios of ligand to metal. The position of the break denoted the composition of the complex formed.

In systems including acetyl, butyryl and benzoyl hydrazides and Cu(II) salts the reverse behaviour is observed. In this case interaction between the ligands and metal salts yields nonconducting complex species as evidenced by the lower specific conductance values of the mixtures than those of the

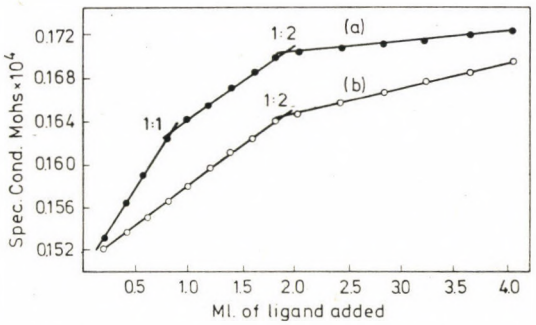

Fig. 5. Conductometric titration curve for $CuSO_4$ (a) and $CuAc_2$ (b) with propionyl hydrazide

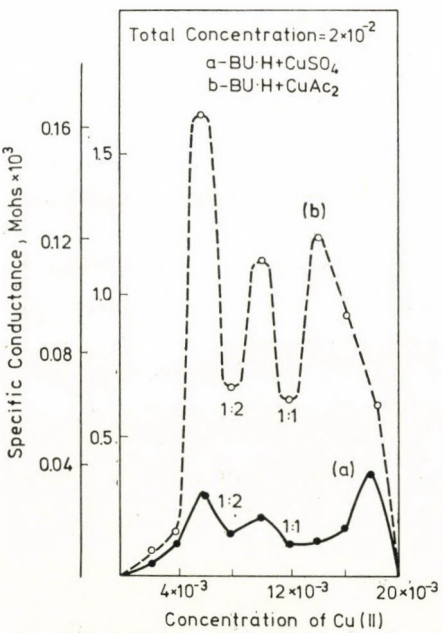

Fig. 6. Determination of composition of Cu(II) butyryl hydrazide complexes by continuous variation method

separate constituents alone. Also, conductometric titration curves showed continuous decrease in specific conductance on successive addition of the ligand. Curves for the butyryl hydrazide system (Fig. 6) showing the divergences from additivity [8] in the specific conductance of the mixtures were plotted against the molarity of the Cu(II) salt. The curves indicated minima. In all systems the existence in solution of complexes formed in simple stoichiometric ratios resembling those isolated in the solid state was ascertained.

Infrared Spectra

For the $Cu(HL)_2Ac_2$ complexes where HL = formyl, acetyl, propionyl, butyryl and benzoyl hydrazides a drastic change in the spectra occurred as compared with that of the ligand. Both the carbonyl stretching and NH_2 bending frequencies at 1675 and 1630 cm^{-1} respectively [9, 10] are displaced and the first strong band to appear at 1550 cm^{-1} in the spectra of the complexes is most probably due to the bending frequency of the NH_2 group which acts as the coordination site as shown by (**I**). It is suggested that the disappearance of the carbonyl stretching is due to

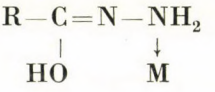

(I)

the enolization of the hydrogen of NH to the adjacent carbonyl group. The new C=N stretching frequency is probably overlapped by the strong 1550 cm^{-1} band. Next to this a strong band exists at 1535 cm^{-1} which can be attributed to the asymmetric C—O stretching vibration. The symmetric C—O stretching frequency is observed as a strong band at 1420 cm^{-1}. Since the difference between the asymmetric and symmetric C—O frequencies is only 115 cm^{-1}, it is believed that the carboxylato group in these complexes is bidentate [11]. In the formyl hydrazide complex the very strong asymmetric and symmetric C—O stretching frequencies occur at a higher wave number (1620, 1445 cm^{-1}) and the difference (175 cm^{-1}) between these two bands indicate that the carboxylato group is bidentate. The appearance of two bands at 1550 and 1535 cm^{-1} could be attributed to the displaced NH_2 bending frequency and ν(C=N), respectively.

Magnetic and Spectral Studies

The electronic spectrum of $Cu(HL)_2Ac_2$ in DMF (where HL = propionyl hydrazide) shows a broad band centered at 16.130 cm^{-1} with no shoulders.

The measured magnetic moment (Table I) indicates that no polymerization of any kind exists in this complex since it lies in the range of mononuclear Cu(II) complexes [12]. Magnetic and spectral data thus indicated that the complex has a distorted octahedral structure (structure **II**) with two acetate groups acting as bidentate ligands as evidenced from previously discussed IR spectra.

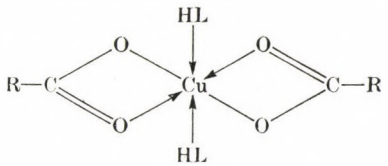

(II)

The room temperature magnetic moment of $Cu(HL)Ac_2 \cdot H_2O$ (where HL = butyryl hydrazide) indicates that it is a mononuclear complex having no major interaction between unpaired electrons on different copper ions. On the other hand $Cu(HL)Ac_2 \cdot H_2O$, HL = formyl hydrazide or salicyl hydrazide and $Cu(HL)Ac_2$ (HL = acetyl hydrazide) exhibit abnormally low magnetic moments which could be attributed to some sort of molecular association bringing the copper atoms closer together. It is suggested here that the acetate groups are bridging similar to the case of copper acetate [13]. This is in agreement with previously discussed IR spectra of these compounds in which the acetate was shown to be bidentate. The water molecule present in two of these complexes was proved to be a water of hydration and was removed on heating at 120 °C in the oven or under reduced pressure without any decomposition. Thes tructure of these complexes may be represented by (**III**).

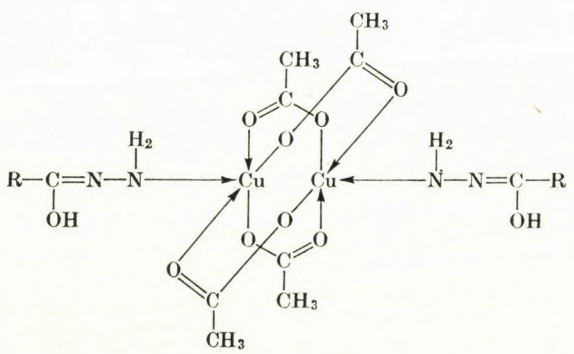

(III)

(III)

In the case of the complex $Cu(HL)Ac_2 \cdot 3H_2O$ where HL = benzoylhydrazide two of the water molecules were shown to be water of hydration since the complex loses them on heating at 120 °C in an electric oven or under vacuum. The magnetic moment of this compound is in the range normally accepted for monomeric d^9 configuration. The visible absorption of this complex in DMF shows a single band at 15.620 cm^{-1} with no shoulders. It is likely that the structure of this complex is similar to **(II)** except that one ligand is replaced by a water molecule.

REFERENCES

[1] DUTTA, A., RAY CHAUDHURI, N.: J. Inorg. Nucl. Chem., **33**, 189 (1971)
[2] DUTTA, A., MANDAL, P. K., RAY CHAUDHURI, N.: J. Inorg. Nucl. Chem., **28**, 2951 (1966)
[3] ISSA, R. M., ISKANDER, M. F., EL SHAZLY M. F.: Z. anorg. allg. Chem. **354** (1967)
[4] DUTTA, A., RAY CHAUDHURI, N.: J. Inorg. Nucl. Chem., **33**, 2556 (1969)
[5] VOGEL, A. I.: "Text Book of Practical Organic Chemistry." III ed. Longmans, London, 1957 p. 975
[6] EL KHADEM, H., ISKANDER, M. F., ZAYAN, S. E.: Z. anorg. allg. Chem., **325** (1963)
[7] MASUI, M., OHMORIE, H.: J. Chem. Soc., London, A, **153** (1969)
[8] HARVEY, A. E., MANNING, D.-L.: J. Am. Chem. Soc., **72**, 4488 (1950)
[9] MASHIMA, M.: Bull. Chem. Soc., Japan, **35**, 332 (1962)
[10] MASHIMA, M.: Bull. Chem. Soc., Japan, **35**, 1882 (1962)
[11] PERRY, C. L., WEBER, J. H.: J. Inorg. Nucl. Chem., **33**, 1017 (1971)
[12] MASSACESI, M., PONTICELLI: J. Inorg. Nucl. Chem., **36**, 2209 (1974)
[13] COTTON, F. A., WILKINSON, G.: "Advanced Inorganic Chemistry", I ed. Interscience Publishers, 1962 p. 197

F. I. M. TAHA
M. N. H. MOUSSA
A. M. SHALLABY
M. M. MOSTAFA

71, Mahmoud Sidki Street Sidi Bishr, Alexandria Egypt.
Chemistry Department, Mansoura University Faculty of Science, El Mansoura, Egypt.

Acta Chimica Academiae Scientiarum Hungaricae, Tomus 90(1), pp. 43–49 (1976)

INVESTIGATION OF THE DIMERIZATION OF SOME ORGANIC ACIDS IN NON-AQUEOUS SOLVENTS

L. BARCZA, L. GYEPES and K. KELEMEN

(Department of Inorganic and Analytical Chemistry, L. Eötvös University, Budapest)

Received October 15, 1975

In benzene, benzoic acid forms dimers of a stability essentially higher than that of aliphatic acid dimers, and a definite difference can be observed also between the dimerization of propionic acid, and of *n*- and isobutyric acid. The dimerization constants measured by cryoscopy (at 5.2 ± 0.4°C) of the mentioned acids were in the above order: 1700, 390, 239 and 453 kg/mole.

It can be detected by infrared spectrophotometry that the dimerization of benzoic acid is affected to a very great extent by the hydrogen bond forming abilities of the solvents. The examined solvents (and in parentheses the dimerization constants of benzoic acid measured at 42 ± 2°C) were: tetrachloromethane (1530); benzene (261); 1,4-dioxane (20.0) and chloroform (13.7).

It could be unequivocally proved in both series that in the investigated concentration range ($< 0.25\ M$) only dimerization occurs, the formation of higher polymers is negligible.

Of the compounds connected by hydrogen bonds, the dimerization of organic acids in non-aqueous media has been investigated mostly [1], and a number of equilibrium constants have been reported.

However, it is conspicuous that often very significant deviations occur between the values given by various authors. These deviations, particularly when different methods were applied for the determination of the stability constants, may attain and even exceed one order of magnitude [1].

As a consequence of this it is rather difficult to draw any conclusion concerning the degree to which the dimerization is affected by the structure of the basic compound (when the solvent is the same) or by the solvent (when the examined compound is the same). Therefore, in order to use uniform method for evaluation, it is reasonable to determine repeatedly the dimerization constants, and in addition to that, to select a reliably known system as reference basis.

Of the organic acids, the dimerization of benzoic acid in benzene solution has been investigated most thoroughly; this study still cannot be considered as a completed one even aside from the dispute concerning the effect of minor water content of benzene upon the process.

ALLEN et al. [2] summarized their measurements concerning the system: the values of lg K_D were plotted *versus* $1/T$, and thus they obtained a value very likely acceptable. This is the reason why we have chosen the dimeriza-

tion of benzoic acid in benzene solution as a basis in our series of measurements.

We investigated in benzene solution, besides the dimerization of benzoic acid, also that of three aliphatic carboxylic acids: propionic, *n*-butyric and isobutyric acids by cryoscopic measurements. The dimerization constant of benzoic acid was determined by infrared spectrophotometry not only in benzene but also in tetrachloromethane, dioxane and chloroform.

In the first series of experiments primarily the following problems were investigated: is there any deviation in the degree of dimerization (in a benzene solution) of two members of the homologous series of fatty acids (of propionic and *n*-butyric acids), and is this deviation significantly affected by the presence of a branched chain (in case of *n*- and isobutyric acid)?

In the second series of experiments, solvents differing from each other in hydrogen bond activity were chosen: tetrachloromethane is an almost inert solvent with minimum proton acceptor property, benzene is a stronger proton acceptor whereas dioxane is a definite proton acceptor, and chloroform has a molecule of definitely proton donor type.

As regards the technique of measurements, both methods are widely applied in the investigation of hydrogen bonded complexes. Measurement by cryoscopy though affording reliable results has been slightly overshadowed recently since infrared spectrophotometry is the method applied the most frequently and even almost exclusively in qualitative investigations. The selection of these diverse methods was supported also by our desire to collect data and experience also concerning the efficiency of the individual methods.

Experimental

Benzoic acid was recrystallized from water and subsequently dried over silica gel.
Propionic acid was purified by distillation, and only the main fraction was used.
n-Butyric acid and isobutyric acid (of analytical purity) were applied directly.
Though the applied solvents were of analytical and spectroscopical purity, respectively, they were subjected to purification in the following ways:
benzene was allowed to stand over phosphorus pentoxide and then distilled;
chloroform and tetrachloromethane were washed with water, traces of water removed with potassium carbonate, then freshly distilled from phosphorus pentoxide;
1,4-dioxane was heated with solid potassium hydroxide on a water bath, filtered, the filtrate boiled with sodium metal, and prior to use, freshly distilled from sodium.
The necessary solutions were prepared as follows:
the required amounts of acids were weighed-in directly with analytical accuracy;
the solvent was weighed similarly on a balance for the cryoscopic measurements;
solutions for infrared spectrophotometry were prepared in volumetric flasks, completing the volume with the solvent at 42°C.

Depression of the freezing point was measured in a cryoscope of the known Beckman type, under cooling with ice, using a thermometer suitable for attaining an accuracy of 10^{-3} °C at certain readings, and at readings repeated several times an accuracy of about $2 \cdot 10^{-4}$ °C.

It follows from the fundamental principle of the measurement that the temperature is not constant in that it varies between 5.5 and 4.8 °C, the average temperature being 5.2 ± ± 0.4 °C (though in general a value of 5.5 °C is given in literature).

The investigated concentration range was 0.02 to 0.25 mole/kg.

The applied infrared spectrophotometer was an instrument of Unicam SP 200 type, equipped with a NaCl prism and an automatic recording device. In case of the same substance the cell size was constant. In preliminary experiments the optimum layer thickness best suitable for recording a concentration change of about one order of magnitude was established. The (controlled) temperature of the cell housing and of the investigated solutions was 42 ± ± 2 °C.

The investigated concentration range was 0.005 to 0.05 mole/dm³.

Evaluation of the results of measurements

According to literature [1], too, the monomer–dimer equilibria are the decisive process in the investigated concentration range, in that

$$HA + HA \rightleftharpoons H_2A_2 \qquad K_D = \frac{[H_2A_2]}{[HA]^2} . \tag{1}$$

The results of the measurement of freezing point depression can be evaluated very simply since in the knowledge of the value of the molal freezing point depression (ΔT_m) the real molality of the solution is obtained directly:

$$\frac{\Delta T}{\Delta T_m} = m_m = [HA] + [H_2A_2] \tag{2}$$

(where ΔT is the measured freezing point depression).

The above value deviates from the molality calculated from the amount of substance weighed (on the basis of the molecular weight of the investigated substance), since it can be readily understood that

$$m_c = [HA] + 2[H_2A_2] \tag{3}$$

The concentrations of the monomer and dimer forms present, and at the same time also the value of K_D can be calculated directly on the basis of equations (2) and (3). This simple relationship is extremely sensitive to other polymerization processes eventually occurring in the solution. When, however, *e.g.* trimerization or tetramerization would occur, the values of the equilibrium constants calculated on the basis of Eqs (2) and (3) would exhibit a definite monotonous trend with the increase of concentration. (This is a very great advantage offered by the method of freezing point depression, and at the same time its probative force.) In our series of measurements we did not experience any changes of this monotonous type, and that confirms

that indeed only monomer–dimer equilibria are present in the examined systems.

The constants found in the various solutions are presented in Table I.

Table I

Dimerization constants of some organic acids in benzene, at 5.2 ± 0.4 °C

Organic acid	$K_D \pm 3\sigma$
Benzoic acid	1700 ± 90
Propionic acid	390 ± 48
n-Butyric acid	239 ± 42
Isobutyric acid	453 ± 56

The values given in Table I are obviously average values but also the values 3σ *i.e.* the threefold values of the mean errors of the mean values are listed.

The evaluation of the results of infrared spectrophotometry was greatly facilitated by the fact that, after a number of preliminary experiments, the spectra were recorded for the same solvent in all applied concentrations at the same cell thickness and slit width. Thus, at the adequately separating bands the band height could be used instead of the area below the band, as a characteristic parameter. (The constancy of the ratio of peak height to the area below the curve has been controlled in several cases in benzene and in tetrachloromethane. Also data of literature point out this constancy [3].)

On the effect of association the monomer O–H band undergoes the greatest change. However, this is at the same time the most sensitive to any external effects. That was one of the reasons why our results have not been evaluated on the basis of this band whereas another reason was that the dispersion of the given instrument was essentially worse in the wave number range over 2000 cm^{-1}.

It was more favourable to use the band characteristic of the monomer C=O which was found, in a fair accordance with data of literature, at the wave numbers 1725 (for tetrachloromethane, benzene), 1720 (dioxane) and 1695 (chloroform), respectively. The peak value of the band characteristic of the ('dimer') carbonyl group present in the hydrogen bridge C=O . . . H—O appeared in tetrachloromethane at the wave number 1685 cm^{-1} and in benzene at 1695 cm^{-1} whereas in case of both other solvents only changes in the band width and in the band shape of the band C=O of the monomer could be observed (at the given resolving power of the instrument).

Under experimental conditions kept strictly identically, the Bouguer—Lambert—Beer law can be applied. In two solutions of different concentrations (c_1 and c_2) *e.g.* for the quotient of the absorption measured at the monomer band it will be as follows

$$\frac{E_2}{E_1} = \frac{\varepsilon [HA]_2 d}{\varepsilon [HA]_1 d} = \frac{[HA]_2}{[HA]_1} = a \tag{4}$$

pointing out that the second solution contains the monomeric form in a concentration higher by a than the monomer concentration of the first solution.

However, in case of monomer–dimer equilibria, as indicated by Eqs (1) and (3), the concentrations of these two species are not independent of each other. It can be readily understood that

$$c_2 = [HA]_2 + 2[H_2A_2]_2 = a[HA]_1 + 2a^2[H_2A_2]_1 \tag{5}$$

In a similar way, on denoting by b the quotient of the extinctions measured at the maximum absorption of the dimer bands, we obtain that

$$c_2 = \sqrt{b}\,[HA]_1 + 2b[H_2A_2]_1 \tag{6}$$

The composition of the first solution is characterized obviously by the relationship

$$c_1 = [HA]_1 + 2[H_2A_2]_1 \tag{7}$$

Table II

Dimerization constants of benzoic acid in various solvents (at 42 ± 2 °C)

Solvent	$K_D \pm 3\sigma$
Tetrachloromethane	1530 ± 244
Benzene	261 ± 23.7
Dioxane	20.0 ± 2.7
Chloroform	13.7 ± 1.7

On solving Eqs (4) to (7) we find that our presumptions are unequivocally valid (or they prove their invalidity) and at the same time also that they are suitable for the calculation of the dimerization constants. (Otherwise

this task can be carried out even without using Eq. (6) which has been applied by us solely as a control.)

The calculated equilibrium constants, together with the values 3σ, are listed in Table II.

Discussion

The dimerization constant of benzoic acid measured by cryoscopy agrees well with the results of earlier measurements [4, 5].

On the basis of earlier data based on measurements of permittivity [6] and of recent values based on partition between water and benzene as solvents [7] it appears very likely that the dimerization constant of C_{1-6} fatty acids exhibits an almost identical monotonous increase to a small extent towards the fatty acids of higher carbon atom numbers. Problems exist concerning both methods of measurement — the present data show slightly differing results. A definite difference can be observed between 3- and 2-methylpropionic acid in that the dimerization constant of isobutyric acid is almost twice as high as that of *n*-butyric acid, and approximates that of propionic acid better.

Thus, it can be detected even in a non-aqueous medium that the hydrogen-bridged association of fatty acids, structurally closely related to each other, is a consequence of complex processes, and cannot be interpreted simply by alterations in the number of carbon atoms.

The data presented in Table I call attention to the fact that, though the carboxyl group is of decisive importance from the aspect of dimerization, the substituents exert their effect not only by influencing the properties of the carboxyl group.

Similarly few data are known concerning the dependence of the dimerization of benzoic acid on the solvent. The series: cyclohexane–tetrachloromethane–benzene has been investigated by ALLEN *et al.* [2] (our present results agree very well with both latter solvents). The benzoic acid dimer proved to be the most stable in cyclohexane, the value found in tetrachloromethane was about two-third of that value whereas the stability decreased by almost a whole order of magnitude on the effect of changing tetrachloromethane to benzene.

For chloroform as solvent only data measured by ligand–ligand partition are known, but the decrease is of a further order of magnitude [8]. Dimerization has not been measured in dioxane. However, on the basis of the partition between bis(3-methylbutyl)-ether and water the dimerization constant of benzoic acid is in a solvent deviating from dioxane to a not too great extent is even lower than that in chloroform [8].

The evaluation of the data in Table II is much easier than those in Table I.

According to our presumption, the dimerization of benzoic acid is inhibited in a competitive reaction by the interactions between solvent and solute. It is striking how definitely benzene participates in couplings by hydrogen bridge, due to its π-system. The effect of dioxane in great excess is still more definite: their oxygen atoms are possessing definite proton acceptor properties, and thus they obviously inhibit the formation of the structure

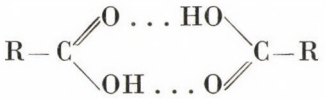

which is primarily characteristic of the dimer.

Chloroform, in turn, is definitely a proton donor: in that it inhibits dimerization by binding the carbonyl groups.

The measured data do not represent directly the stability of the benzoic acid complex of chloroform, dioxane or benzene. However, they indicate also the role and quality of solvatation, and thus they are indirectly suitable for the comparison of solvents.

*

The presented results are parts of the thesis of Mr. László Gyepes and of Miss Katalin Kelemen, respectively.

Thanks are expressed also here to Mr. György Milch (Chinoin Chemical and Pharmaceutical Works Ltd., Budapest) for his altruistic help in carrying out the measurements by infrared spectroscopy.

REFERENCES

[1] Pimentel, G. C., McClellan, A. L.: The Hydrogen Bond, W. H. Freeman and Co., 1960
[2] Allen, G., Watkinson, J. G., Webb, K. A.: Spectrochim. Acta **22,** 807 (1966)
[3] Glasoe, P. K., Hallock, St., Hove, M., Duke, J. M.: Spectrochim. Acta, Part A **27,** 2309 (1971)
[4] Barton, B. C., Kraus, C. A.: J. Amer. Chem. Soc. **73,** 4561 (1951)
[5] Izmailov, N. A., Partskhaladze, K. P.: Khim. Zh. **22,** 156, 167 (1956)
[6] Pohl, H. A., Hobbs, M. E., Gross, P. M.: J. Chem. Phys. **9,** 408 (1941)
[7] Korenman, I. M., Gurev, I. A., Gureva, Z. M.: Zh. Fiz. Khim. **47,** 1207 (1973)
[8] Davies, M., Griffiths, D. M. L.: Z. phys. Chem. (Frankfurt) **6,** 143 (1956)

Lajos Barcza; H-1443 Budapest, Pf. 123.

Acta Chimica Academiae Scientiarum Hungaricae, Tomus 90(1), pp. 51–57 (1976)

THE BASE-CATALYZED DIMERIZATION OF 2-ARYLIDENECYCLOHEXANONES

GY. OSZBACH, D. SZABÓ and M. E. VITAI
(Chemical Institute of the Medical University, Pécs)

Received February 8, 1975

2-Arylidenecyclohexanones dimerize in basic medium to 1,2,3,4,4a,5,6,7,8,9a-decahydro-5-arylidene-4a-hydroxyxanthenes (**IXa–e**). The structures are supported by IR, UV and NMR data. A reaction mechanism is proposed.

The mixed aldol condensation of ketones and aldehydes is, under vigorous conditions, often associated with further reactions [1]. In some cases, the isolated end-product is the dimer of the α,β-unsaturated ketone formed primarily (*in situ* dimerization). Naturally, the corresponding unsaturated ketone can also be dimerized by treatment with alkali.

NIELSEN *et al.* characterized the above reactions on the basis of data in the literature, supported also by their investigations, by the following reaction scheme (Fig. 1):

A: In the first step, the unsaturated ketone **I** is converted by Michael addition to the 1,5-diketone (**II**) [2, 3a–c, 4, 5].
B: **II** yields by intramolecular Michael reaction the cyclic diketone **III** [6–12].
C: The intramolecular aldol condensation of **II** gives the cyclic 1,3-ketol (**IV**), and from this compound the ketone **V** is formed by the loss of water [6, 7, 10, 13–17].

The dimer of 2-benzylidenecyclohexanone was obtained accidentally, when we allowed the monomer (**VI**) to react with NaCN in dimethyl sulfoxide (DMSO); **VI** was converted in a suprisingly quick reaction into another nitrogen-free substance. This product can also be prepared with sodium hydroxide or sodium ethoxide as catalyst; a 9 : 1 mixture of DMSO/EtOH proved to be the best solvent. The compound is identical with the substance characterized by TILICHENKO *et al.* [3a–c] by the structure **VIII** (Fig. 2). The mentioned authors established the structure on the basis of elementary analysis, molecular weight measurement and dioxime formation; later they converted the compound with $AcOH/NH_4OAc$ into the corresponding octahydroacridine derivative [3c].

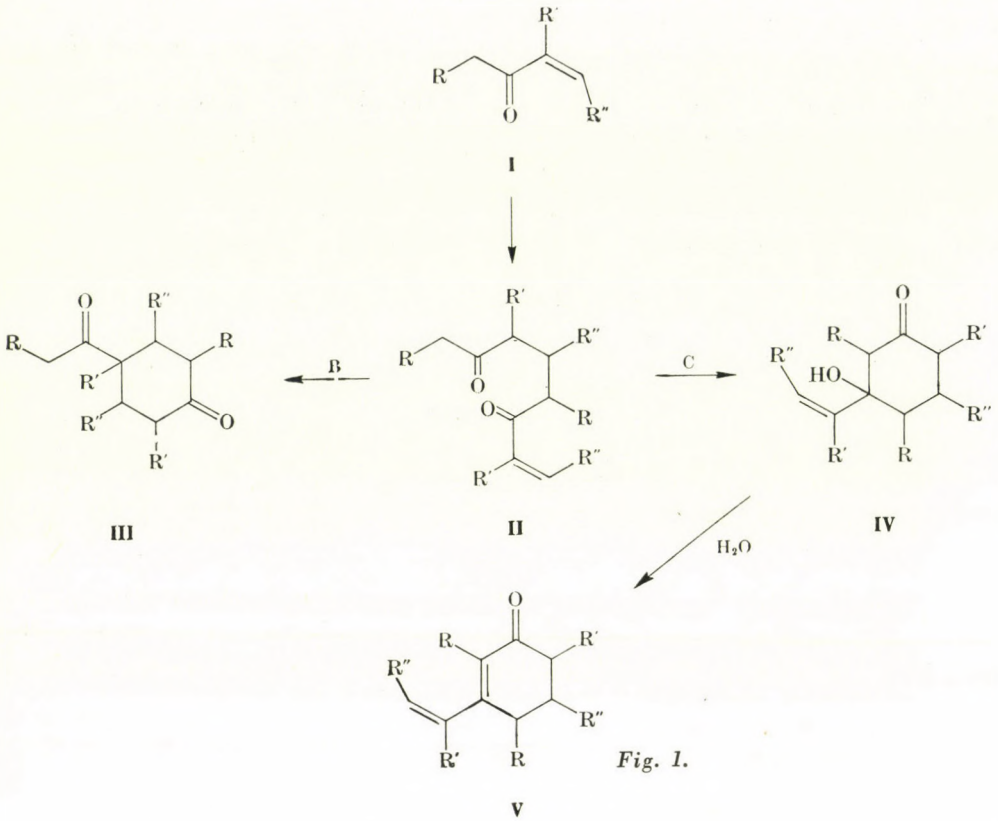

Fig. 1.

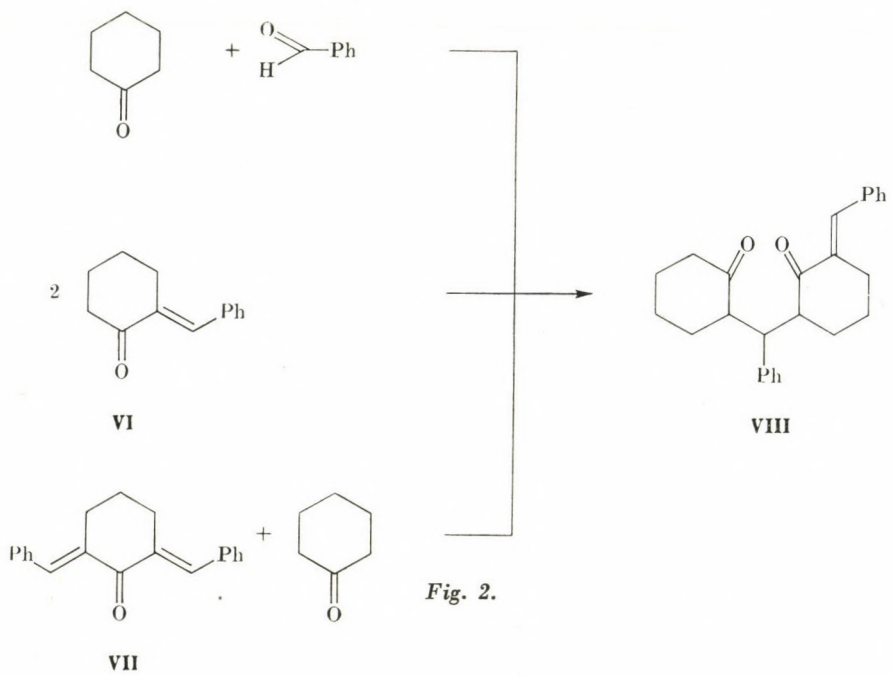

Fig. 2.

However, the IR spectrum of the compound has no carbonyl frequency; in fact, a hydroxyl stretching vibration can be observed at a wavenumber of 3470 cm^{-1} in the solid state, and at 3580 cm^{-1} in $CHCl_3$ solution. Accordingly, the compound does not belong to any of the four types of dimers (**II**, **III**, **IV**, **V**) known so far. The absorption occurring at 1640 cm^{-1} is indicative of a conjugated double bond.

The UV spectrum of the dimer is suggestive of a phenylbutadiene chromophore: $\lambda_{max} = 293$ nm, $\varepsilon = 25{,}300$.

In the NMR spectrum, two aromatic singlets, $\delta = 7.32$ and 7.28, a vinyl proton, $\delta = 7.05$, and an OH proton deuterizable with D_2O, $\delta = 2.45$, can be identified.

The hydroxyl group does not react with acylating agents, or more vigorous treatment results in a resinous substance.

When boiled with acetic anhydride, the dimer loses water (**XI**). In the IR spectrum, the disappearance of the OH vibration is accompanied by the appearance of a band at 1718 cm^{-1}, indicative of an isolated double bond. Similarly high binding frequencies have been reported by several authors for γ-pyrans and for octahydroxanthenes [18, 19, 23, 24].

The preparative and spectral data are consistent with structure **IX**. The agreement of the physical data with those of the aminoketals **X**, prepared by LEWIS *et al.* by another route, is remarkable. It is interesting that the hydrolysis product of **X** is not **IX**, but similarly a resin [19].

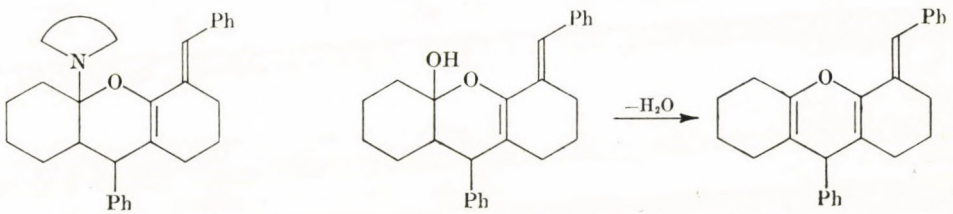

X **IX** **XI**

Fig. 3.

The formation of the hemiketal **IX** can be explained uniformly from the point or view of all three modes of preparation, as shown in Fig. 4.

In the dimerization of **VI**, the initial step is Michael addition. From the anion *K* no diketone **VIII** is formed by protonation, because the C-6' proton is strongly acidic; the product is the anion *L*, from which the further reaction route is evident. Compound **VII** gives the anion *L* immediately, the rest of the reaction sequence is the same. *In situ* dimerization is possible according to both reaction routes indicated.

It should be noted that no intermediate product could be detected in the reaction mixture by either chromatography or spectroscopy, thus it can

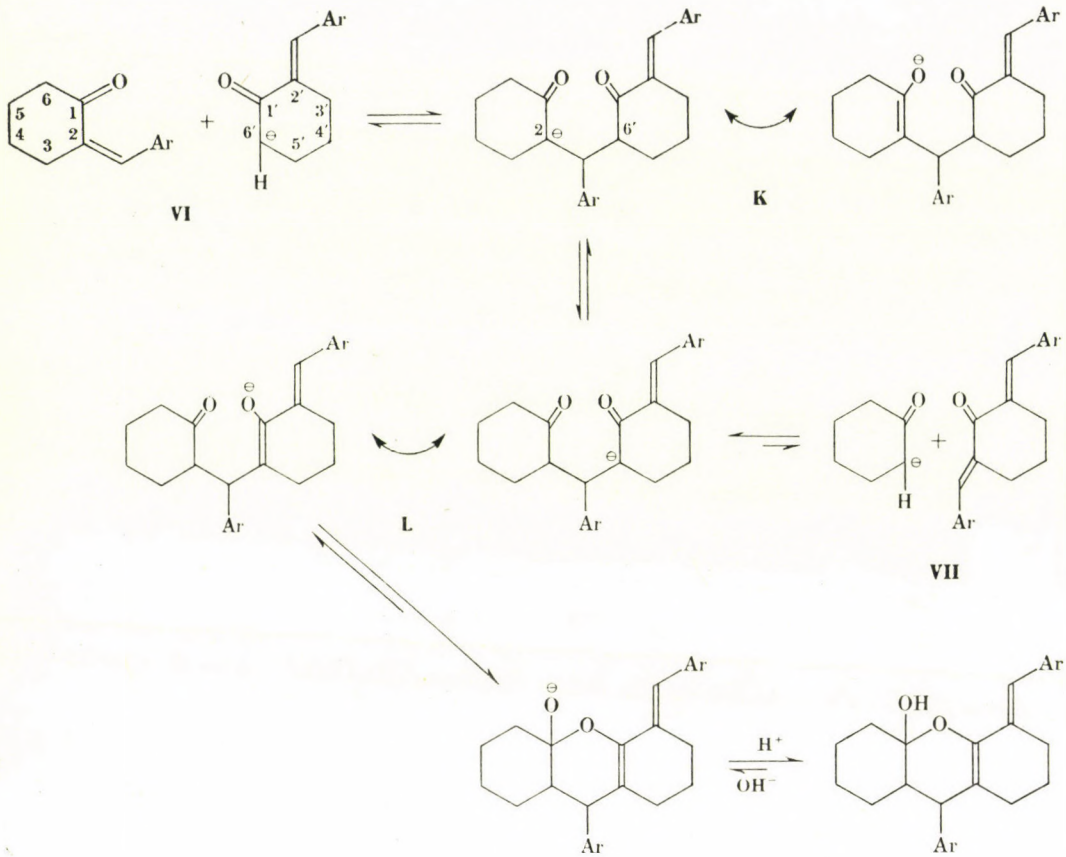

Fig. 4.

be presumed that the diketone **VIII** is not formed even transitorily, further, that the rate determining step is the initial Michael addition. Retro-Michael reaction cannot be observed even on increasing the temperature (as shown by TLC, the conversion is complete).

After the termination of our work, we obtained the communication of LYLE *et al.* [20], in which they report results identical with our findings:

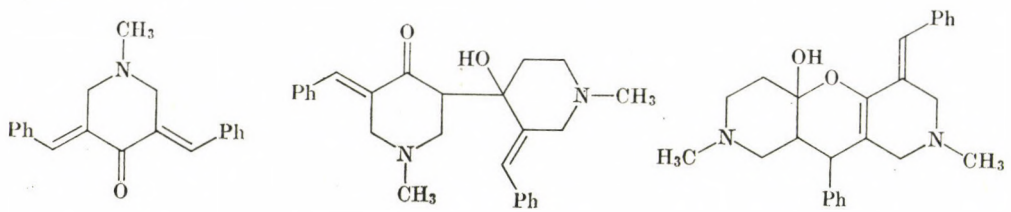

Fig. 5.

McElvain and Rorig [21] condensed 1-methyl-4-piperidone with benzaldehyde, and isolated two products; one of them was dibenzylidenepiperidone (**XII**), and the other was regarded later by McElvain and Parker [22] to be the aldol dimer **XIII**. Lyle *et al.* have proved beyond doubt that the compound has a hemiketal structure (**XIV**).

Identical structures were obtained also on changing the aromatic group (**IXb—e**).

Experimental

M.p.'s are uncorrected. IR spectra were obtained on a Zeiss UR-10 spectrophotometer in KBr pellets, the UV spectra with a Perkin–Elmer 402 instrument in ethanol solution; the NMR spectra were recorded with a Perkin–Elmer R-12 (60MHz) spectrometer in $CDCl_3$. TLC system: Kieselgel H_{254} (Merck); benzene–ethyl acetate (40 : 1).

1,2,3,4,4a,5,6,7,8,9a-Decahydro-5-benzylidene-9-phenyl-4a-hydroxyxanthene (IXa)

Direct method. To a solution of 18.6 g (0.1 mole) of 2-benzylidenecyclohexanone (**VI**) in 50 ml DMSO 4.5 ml of a 1*N* NaOH solution in ethanol was added, and the mixture was allowed to stand at room temperature for 1 hr. It was then poured into water acidified with acetic acid, and the semi-crystalline substance which separated was crystallized from ethanol (m.p. 85—91 °C), then from a 1 : 2 benzene–hexane mixture. 13.4 g (72%) of a colourless, crystalline substance was obtained, m.p. 135—136 °C (lit. [3a—b] m.p. 135—136 °C).

In situ dimerization. 10.6 g (0.1 mole) of benzaldehyde and 19.6 g (0.2 mole) of cyclohexanone, were dissolved in a mixture of 50 ml DMSO and 10 ml ethanol, and 6 ml of 50% aqueous NaOH was added to the solution, which was then stirred at room temperature, until TLC indicated that the conversion was complete (about 2.5 hrs). Processing was the same as described above.

The reaction of 2,6-dibenzylidenecyclohexanone (VII) and cyclohexanone. A suspension of 13.7 g (0.05 mole) of 2,6-dibenzylidenecyclohexanone and 5.9 g (0.06 mole) of cyclohexanone in 60 ml of a 9 : 1 DMSO/EtOH mixture was stirred first at 60 °C and, after the dissolution of the solid substance, at room temperature for 6 hrs with 6 ml of a 50% NaOH solution. The progress of the reaction was followed by TLC. The reaction mixture was worked up as described above. In all three experiments an identical substance was obtained.

The other compounds (**IX**b, c, d, e) were obtained in the same way. The progress of the reactions was checked by TLC. Detailed data are given in Table I.

Derivatives of IXa

Dioxime. A solution of 3.7 g (0.01 mole) of **IX**a in 50 ml ethanol was refluxed with 2.1 g (0.03 mole) of hydroxylamine hydrochloride and 10 g of K_2CO_3 for 3 hrs. The hot mixture was filtered and the solid washed with hot ethanol. The crystals obtained from the combined ethanol solutions were recrystallized from ethanol to obtain 1.5 g of the product, m.p. 210 °C (lit. [3a] m.p. 194—195 °C).

$C_{26}H_{30}N_2O_2$ (402.54). Calcd. C 77.60; H 7.46; N 6.96. Found C 77.22; H 7.77; N 6.87, 6.84%. IR: 3260 cm^{-1} (broad) (OH); 1670 cm^{-1} (=C=N—OH).

1,2,3,4,5,6,7,8-Octahydro-5-benzylidene-9-phenylxanthene (XI)

3.72 g (0.01) mole of **IX**a was refluxed in 8 ml of acetic anhydride for 7 hrs. The crystals which precipitating on cooling were filtered off, washed with water, and recrystallized three times from ethanol to obtain 1 g of **XI**, m.p. 107—108 °C.

$C_{26}H_{26}O$ (354.50). Calcd. C 88.09; H 7.39. Found C 87.84, H 7.13%.

IR: 1718 cm^{-1} C=C (pyran); 1645 cm^{-1} C=C (pyran, conjugated).

NMR ($CDCl_3$): δ = 7.32 s, 5H (Ar); 7.29 s, 5H (Ar); 7.00 s, 1H (=CH—; vinyl); 3.58 s, 1H (CH; benzyl); 1.4—2.8 m, 14H (cycloaliphatic).

Table I

Compound Ar-	Solvent m.p. (°C)	Formula Mol. weight Yield	Analysis, % Calcd.	Found	UV (ethanol) λ_{max} nm	ε	IR, cm^{-1} KBr	NMR, δ ppm $CDCl_3$
IXa[1] C_6H_5-	benzene/ hexane 135–6	$C_{26}H_{28}O_2$ 372.51 72%	C: 83.83 H: 7.57	83.68 7.49	209 293	21 000 25 300	3470 OH[2] 1640 C=C 1615 1605 C=C (Ar) 1400 760 =CH (Ar)	7.32 s 5H Ar 7.28 s 5H Ar 7.05 s 1H =CH– 0.9–3.3 m 16H 2.45 s 1H OH[3]
IXb 4–CH_3–C_6H_4–	ethanol 162–3.5	$C_{28}H_{32}O_2$ 400.57 90%	C: 83.96 H: 8.05	83.93 7.97	209 293.5	19 000 26 200	3570 OH 1630 C=C 1603 C=C (Ar) 1420 828 =CH (Ar)	7.2 s 4H Ar 7.1 s 4H Ar 7.0 s 1H =CH– 2.3 s 6H $-CH_3$ 1.0–3.3 m 17H[4]
IXc 4–CH_3O–C_6H_4–	benzene/ hexane 192–4	$C_{28}H_{32}O_4$ 432.57 85%	C: 77.75 H: 7.46	77.34 7.50	211 294	14 500 29 300	3470 OH 1638 C=C 1603 C=C (Ar) 1418 842 =CH (Ar) 1245 $-OCH_3$ 1040	6.4–7.0 m 8H Ar[5] 6.3 s 1H =CH– 3.0 s 6H $-CH_3$ 0.5–3.4 m 16H
IXd[6] 2-furyl	benzene/ hexane 131–4	$C_{22}H_{24}O_4$ 352.43 70%	C: 74.98 H: 6.86	74.88 6.90	211 296 308 323	9 800 shoulder 31 600 41 100 29 700	3470 OH 1640 C=C 1595 1550 C=C (Ar) 1410 1022 890 (furan) 740	6.1–7.5 m 6H Ar 6.75 s 1H =CH– 0.9–3.5 m 17H[7]
IXe 4–Cl–C_6H_4–	benzene/ hexane 148–50	$C_{26}H_{26}Cl_2O_2$ 441.41 62%	C: 70.75 H: 5.94 Cl: 16.06	70.55 6.00 16.00	210 299	16 100 26 200	3577 OH 1630 C=C 1605 C=C (Ar) 1395 832 =CH (Ar)	7.05–7.45 m 8H Ar 6.75 1H =CH– 1.0–3.3 m 17H[8]

1. [3a, b, c]
2. In $CHCl_3$ solution: 3580 cm^{-1}
3. Disappears in D_2O
4. D_2O decreases the integral by 1H
5. NMR spectrum recorded in C_5D_5N
6. [3a, b]
7. D_2O decreases the integral by 1H
8. D_2O decreases the integral by 1H

REFERENCES

[1] NIELSEN, A. T., HOULIHAN, W. J.: Org. Reactions, XVI. pp. 58—69. Wiley, London 1968
[2] BRIGHT, D. B.: J. Am. Chem. Soc. **79,** 3200 (1957)
[3] (a) TILICHENKO, M. N., KHARCHENKO, V. G.: Dokl. Akad. Nauk SSSR. **110,** 226 (1956)
(b) TILICHENKO, M. N., KHARCHENKO, V. G.: Zhurn. Obshch. Khim. **29,** 1909, 1911 (1959)
(c) TILICHENKO, M. N., KHARCHENKO, V. G., KRUPINA, T. I.: Zhurn. Obshch. Khim. **34,** 2721 (1964)
[4] ANET, R.: J. Org. Chem. **26,** 246 (1961)
[5] NIELSEN, A. T., MOORE, D. W., HIGHBERG, K.: J. Org. Chem. **26,** 3691 (1961)
[6] JONES, E. R. H., KOCH, H. P.: J. Chem. Soc. **1942,** 393
[7] BÜCHI, G., HANSEN, J. H., KNUTSON, D., KOLLER, E.: J. Am. Chem. Soc. **80,** 5517 (1958)
[8] NIELSEN, A. T., DUBIN, H. J.: J. Org. Chem. **28,** 2120 (1963)
[9] NIELSEN, A. T., DUBIN, H. J., HISE, K.: J. Org. Chem. **32,** 3407 (1967)
[10] NIELSEN, A. T., HASELTINE, S.: J. Org. Chem. **33,** 3264 (1968)
[11] NIELSEN, A. T., MOORE, D. W.: J. Org. Chem. **34,** 444 (1969)
[12] (a) NIELSEN, A. T., WEISS, R. C., MOORE, D. W.: J. Chem. Soc. (D) **1969,** 1281
(b) NIELSEN, A. T., WEISS, R. C., MOORE, D. W.: J. Org. Chem. **37,** 1086 (1972)
[13] DICKINSON, R., HEILBRON, I. M., IRWING, F.: J. Chem. Soc. **1927,** 1888
[14] IWANOW, D., IWANOW, T.: Ber. **77,** 173 (1944)
[15] MEERWEIN, H.: Ber. **77,** 227 (1944)
[16] AYER, W. A., TAYLOR, W. I.: J. Chem. Soc. **1955,** 2227
[17] BRAUDE, E. A., GOFTON, B. F., LOWE, G., WAIGHT, E. S.: J. Chem. Soc. **1956,** 4054
[18] BALABAN, A. T., MIHAI, G., NENITZESCU, C. D.: Tetrahedron **18,** 257 (1962)
[19] LEWIS, J. W., MYERS, P. L., READHEAD, M. J.: J. Chem. Soc. (C) **1970,** 771
[20] LYLE, G. G., DZIARK, J. J., CONNOR, J., SAUNDERSON HUBER, C.: Tetrahedron **29,** 4039 (1973)
[21] MCELVAIN, S. M., RORIG, K.: J. Am. Chem. Soc. **70,** 1820 (1948)
[22] MCELVAIN, S. M., PARKER, P. H., Jr.: J. Am. Chem. Soc. **77,** 492 (1955)
[23] KHARCHENKO, V. G., YARTSEWA, N. M., KOZHEWNIKOWA, N. I.: Zhurn. Org. Khim. **1973,** 189
[24] KHARCHENKO, V. G., YARTSEWA, N. M., KOZHEWNIKOWA, N. I., RASSUDOWA, A. A.: Zhurn. Org. Chim. **1974,** 99

György OSZBACH
Dezső SZABÓ
Mária E. VITAI
} H-7643 Pécs, Szigeti út 12.

Acta Chimica Academiae Scientiarum Hungaricae, Tomus 90(1), pp. 59—67 (1976)

REARRANGEMENT AND DISSOCIATION PROCESSES IN TRICYCLIC PHTHALAZINONE DERIVATIVES UPON ELECTRON IMPACT

P. BRUCK*, J. TAMÁS* and K. KÖRMENDY**

* *(Central Research Institute for Chemistry, Hungarian Academy of Sciences, and*
** *Research Group for Peptide Chemistry, Hungarian Academy of Sciences, Budapest)*

Received February 25, 1975

Dissociation and rearrangement processes of tricyclic phthalazinone derivatives (**I—IV**) upon electron impact have been studied using high- and low-resolution mass spectrometry. A method based on the determination of the activation energy of metastable decomposition processes has been applied to verify that some fragmentation processes involve methylene migration.

BOWIE *et al.* [1] were the first to study the fragmentation of phthalazinone derivatives upon electron impact. They have found that the substituents adjacent to the nitrogen atom interact with this atom ('proximity effect'). In an earlier work we used ^{15}N-labelling to prove that electron bombardment of 4-(ω-hydroxyalkylamino)phthalazinone derivatives produced a fragment ion that contained a four-membered ring formed by intramolecular ring closure [2].

This reaction is a consequence of the proneness to substitutions of the pyridine-type N atom present in the phthalazine ring.

Accordingly, intramolecular condenzation products of these compounds are easily obtained also by preparative methods from the above (ω-hydroxyalkylamino)-phthalazinones. However, condenzation due to electron bombardment occurs chiefly involving the carbon in β-position of the alkyl chain and the nitrogen in position 3, whereas in the preparative process, in the presence of a solvent, condenzation is achieved by bonding of the carbon in ω-position to the nitrogen mentioned.

In this paper we wish to report on a mass spectrometric study of the electron impact-induced fragmentation of the products of the later reaction (**I** to **IV**).

As a common characteristic of these compounds, the first step or steps of the electron impact-induced processes involve the fragmentation of the rings of imidazole (**I, II**) or pyrimidine (**III, IV**) type, formed by the condenzation reaction mentioned before.

In the course of the further decomposition of the fragment ions thus produced, a very interesting rearrangement takes place, proved by a novel method of ion structure identification [3].

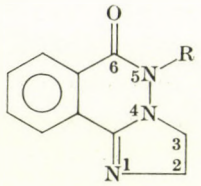

I: R = H
II: R = CH_3

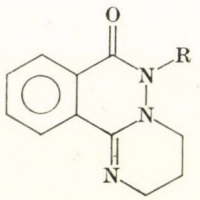

III: R = H
IV: R = CH_3

In the mass spectrum (Table I) of 2,3-*dihydroimidazo*[2,1-*a*]*phthalazin-6(5H)-one* (**I**), a characteristic fragment at mass number 130 and composition C_8H_4NO is the only abundant ion besides M^+ and $(M-1)^+$ (formed by the quaternization of the nitrogen atom is position 4). In contradistinction to the open-chain compounds where either of the two possible N atoms participates in the formation of the nitrile group with equal probability [2], in the case of **I** the *m/e* 130 type ion contains only the nitrogen atom in position 4.

The *m/e* 130 ion originates from the $(M-1)$ ion in two ways (Fig. 1, A and B). In both processes one of the σ bonds beside the sp^3 carbon atom of the imidazole-type ring is broken. (Only these two bonds do not participate in the conjugation extending over the entire skeleton.)

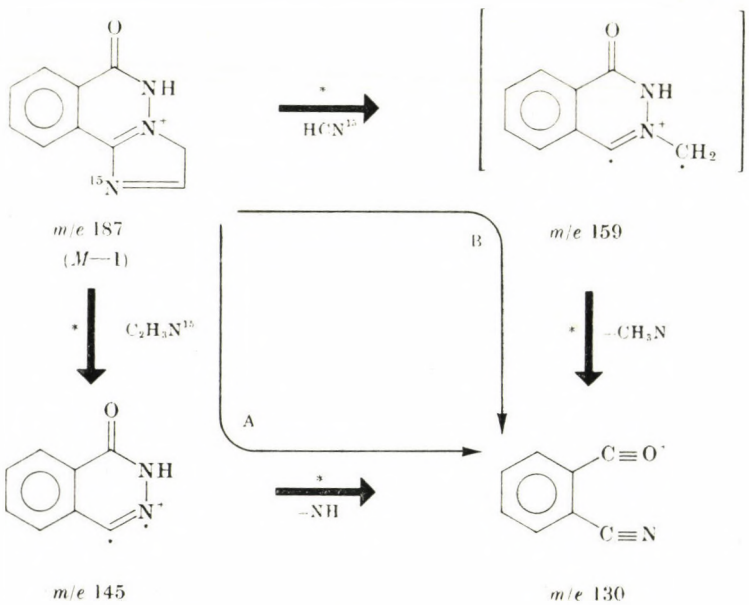

Fig. 1.

Table I

m/e	C	H	N	^{15}N	O	Abundance (%)					
						I	I*	II	III	III*	IV
215	12	13	3		1						100
214	12	12	3		1						28
202	11	11	2	1	1					100	
201	11	11	3		1			100	100		
	11	10	2	1	1					61	
200	11	10	3		1			28	66		
188	10	9	2	1	1		70				
187	11	11	2		1						8
	11	10	1	1	1					2	
	10	9	3		1	88					28
	10	8	2	1	1		100			6	
186	11	10	2		1				3		8
	11	9	1	1	1					2	
	10	8	3		1	100		5	7		48
185	11	10	2	1						1	
	11	9	2		1				3	1	9
184	11	10	3						1		
	11	7	1	1	1					1	
183	11	7	2		1				3	2	
174	10	9	1	1	1					2	
	9	7	2	1	1					3	
173	10	9	2		1			28	8	7	6
	9	7	3		1				4		
	9	6	2	1	1					18	
172	11	9		1	1					9	
	10	8	2		1						3
	10	7	1	1	1					5	
	9	6	3		1				23		
171	11	9	1		1				8		5
	10	7	2		1			10	5		3
160	9	8	2		1	3	3	3			3
	9	7	1	1	1		1				
159	9	7	2		1	5	4	9			6
158	9	8	3								1
148	8	7	1	1	1					4	
147	8	7	2		1				5	1	
	8	6	1	1	1					2	

Table I (Continued)

m/e	C	H	N	^{15}N	O	Abundance (%)					
						I	I*	II	III	III*	IV
146	8	6	2		1				28	21	
145	8	5	2		1	3	3				
143	9	7	2			4	4				
131	8	4		1	1		8			6	
130	8	5	1	1						4	
	8	4	1		1	68	65	45	42	28	24
129	8	5	2						9	6	

Following the fission of the C–N bond, C_2H_3N is eliminated (A) from the $(M - 1)^+$ ion; ^{15}N-labelling shows that the nitrogen removed originates from position 1, thus the 'lower part' of the imidazole-type ring is split off. From the *m/e* 145 ion thus produced, the abundant ion at mass number 130 is derived by loss of NH.

In the case of compound **I**, decomposition involving the cleavage of the C–C bond of the imidazole-type ring, *i.e.* pathway B is predominating; the $(M - 1)^+$ ion loses HCN by the elimination of the (labelled) nitrogen in position 1; the *m/e* 159 fragment thus formed gives then the *m/e* 130 ion by loss of CH_3N.

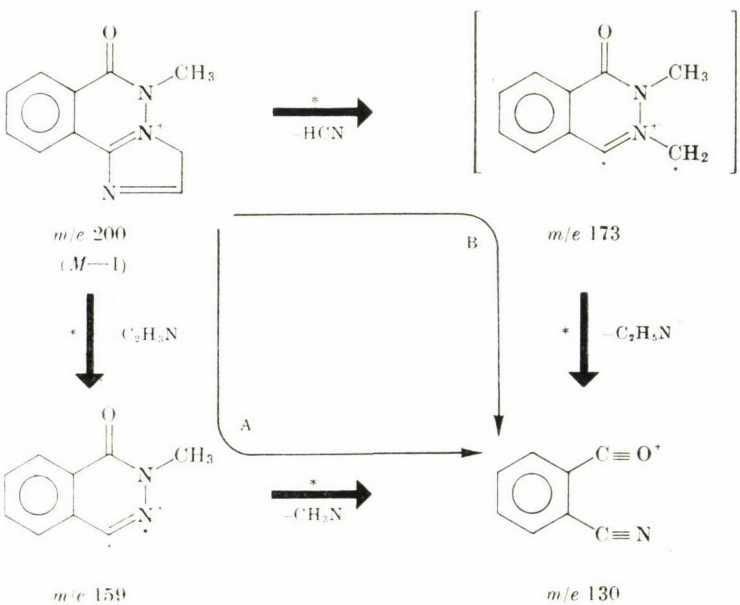

Fig. 2.

The loss of CH_3N from the *m/e* 159 ion cannot occur without rearrangement: most probably the methylene group in position 3 attaches first to the nitrogen in position 5, then the CO–N bond is broken.

In order to provide evidence for this rearrangement involving methylene group migration, it is helpful to compare the behaviour of **I** with that of its N-methyl derivative, 2,3-*dihydro*-5-*methylimidazo*[2,1-*a*]*phthalazin*-6-*one* (**II**) under electron bombardment (Fig. 2).

The decomposition scheme of the two compounds has the same structure: the *m/e* 130 ion is produced from the $(M - 1)^+$ ion in two ways (A and B). In the corresponding reactions either the eliminated neutral fragments are the same and the charged particles are homologues, or the neutral particles are homologues and the ions are the same. In the N-methyl derivative **II**, the two decomposition pathways A and B, leading to the *m/e* 130 ion, are almost equally important.

From the $(M - 1)^+$ ion (*m/e* 200) loss of HCN gives the *m/e* 173 fragment ion (pathway B), which is the homologue of the *m/e* 159 ion of **I**. If our suppositions concerning the rearrangement of *m/e* 159 ion of **I** are correct, then — in this analogous case — the N-methyl substitution will increase the mass of the neutral particle eliminated, while the charged fragment from the *m/e* 173 ion will be the same as in the case of the parent compound.

From the *m/e* 173 ion the known *m/e* 130 ion is produced by loss of C_2H_5N, as expected. This process supports, that both in the parent compound and in its N-methyl derivative, after the loss of HCN, the suggested rearrangement does occur.

At the same time, in the case of **II** the decomposition process A involving elimination of C_2H_3N from $(M - 1)^+$ is operating, as well. The charged particle produced agrees, at least as far as its empirical formula is concerned, with the ion produced from **I** by the loss of HCN. From this *m/e* 159 ion the *m/e* 130 fragment is formed by the elimination of CH_3N, in the same way as in the case of the parent compound. This suggests that the *m/e* 159 ions (X^+, *cf.* Fig. 3) originating from the two different sources, have the same structure; however, in the N-methyl derivative the 5 N–C bond has already been present in the neutral molecule, whereas in the parent compound the aforementioned rearrangement must occur to allow the formation of this bond.

In order to prove the occurrence of this migration of the methylene group, the structural identity of the two ions of *m/e* 159 must be confirmed by some quantitative mass spectroscopic method. For this purpose a mass spectroscopic method of ion structure identification, based upon the determination of the activation energies of metastable processes, ΔAP^*, has been elaborated [3]. Our results indicate (Fig. 3) that the ΔAP^* value, characteristic of the metastable process $159 \rightarrow 130$ is 0.96 eV in the case of the parent compound **I** and is 0.99 eV for the N-methyl derivative **II**. This proves that the

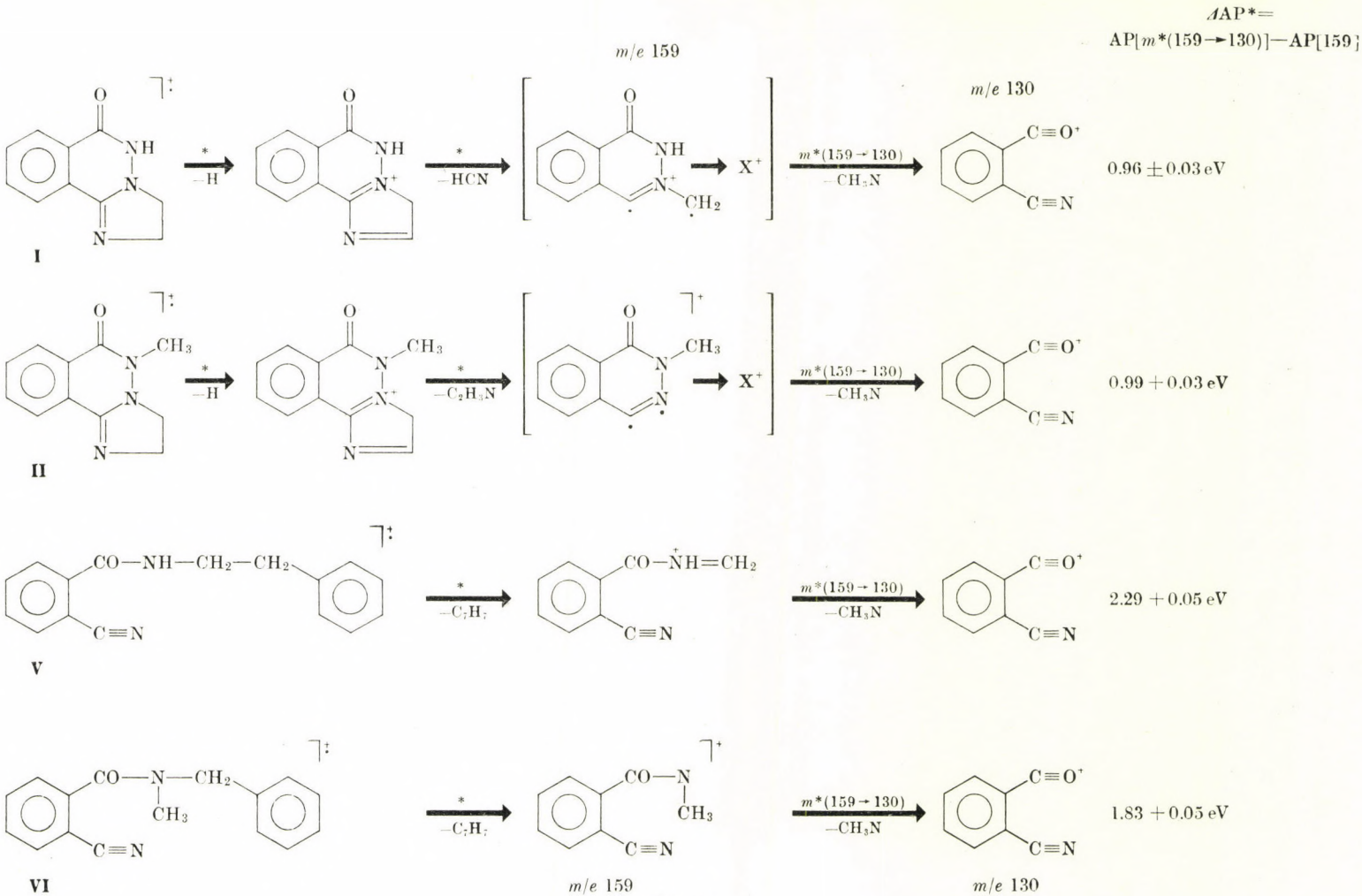
ΔAP*=
AP[m*(159→130)]—AP[159]
m/e 159
m/e 130
I
II
V
VI
m*(159→130)
—CH3N
—H
—HCN
—C2H3N
—C7H7
X+
0.96 ± 0.03 eV
0.99 + 0.03 eV
2.29 + 0.05 eV
1.83 + 0.05 eV

Fig. 3.

decomposing *m/e* 159 ions have the same structure in **I** and **II**, thus supporting the assumption about the migration of the methylene group.

The *m/e* 159 ions having certainly different structures, shown in Fig. 3 as counter-examples (compounds **V** and **VI**), reveal a very significant difference in the ΔAP* values.

Though the method applied does not give accurate information about either the exact structure of the ion produced or the mechanism of the rearrangement, it is probable that in the case of compound **I** this rearrangement is analogous to the methylene insertion reaction characteristic of the carbenes [4], resulting in a $N-CH_3$ group.

3,4-*Dihydro-2H-pyrimido*[2,1-*a*]*phthalazin-7(6H)-one* (**III**) is a homologue of **I** containing three vicinal CH_2 groups. The principal fragmentation process involves the fission of those two σ-bonds which are weakened due to their being in β-position to the C=N double bond (Fig. 4). The $M-C_2H_4$

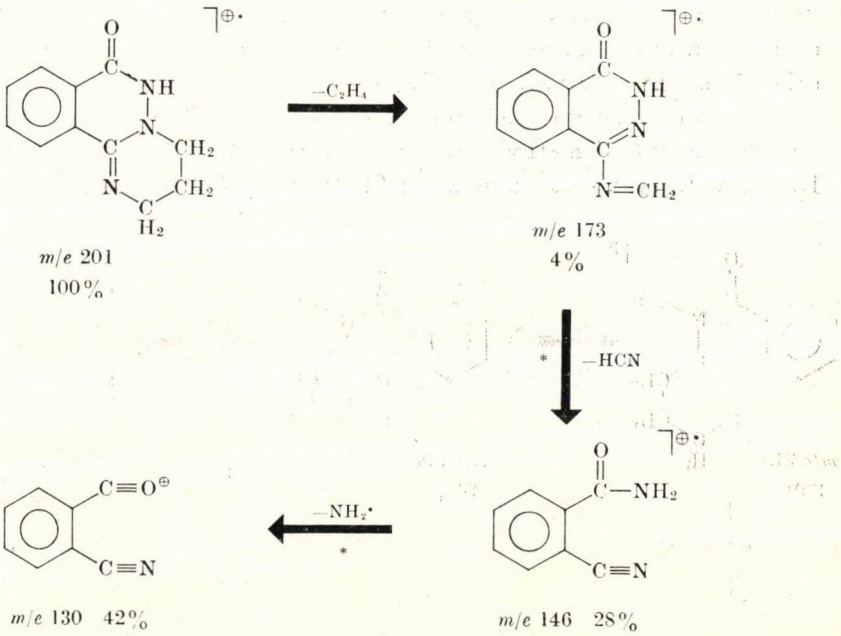

Fig. 4.

ion produced (*m/e* 173) contains conjugated double bonds; the delocalization energy in part compensates for the energy needed to the cleavage of the bonds (retro-Diels—Alder reaction). Retro-Diels—Alder reactions cannot occur in the case of five-membered rings (**I** and **II**); for these (*cf.* Figs 1 and 2), conjugation is achieved by the loss of H from the molecular ion and the quaternization of the N atom in position 4.

The *m/e* 173 ion loses HCN, and this HCN will contain the ^{15}N if the molecule has been labelled in position 1. The already known *m/e* 130 ion is produced from the *m/e* 146 ion thus formed, by cleavage of the amide bond.

It is evident that in contradistinction to the homologous open-chain phthalazinone derivatives, the fragmentation of the homologous condensed-ring parent compounds is essentially different from each other, since the 'lower part' of the pyrimidine-type ring can be eliminated as two stable, neutral molecules (C_2H_4 + HCN), while that of the imidazole-type ring cannot. In the latter case, the analogous process would involve the elimination of CH_2 from the *m/e* 159 fragment ion of **I**. This is greatly unfavoured from an energetical point of view, as the heat of formation of the CH_2 radical is extremely high. This is the main reason why the *migration* of CH_2, a process of comparatively low activation energy, is preferred.

3,4-*Dihydro*-6-*methyl*-2*H*-*pyrimido*[2,1-*a*]*phthalazinone* (**IV**) is the N-methyl derivative of compound **III**. The primary fragmentation processes of its molecular ion are analogous to those of the parent compound **III**, but the decomposition products of its fragments are the same as in the case of the other N-methyl derivative **II** (Table I).

Loss of ethylene from the molecular ion of **IV** gives rise to the *m/e* 187 ion; this is the N-methyl derivative of the $(M - 28)^+$ ion of **III** (Fig. 5). However, from *m/e* 187 now not HCN, but H_2CN is eliminated, and thus the

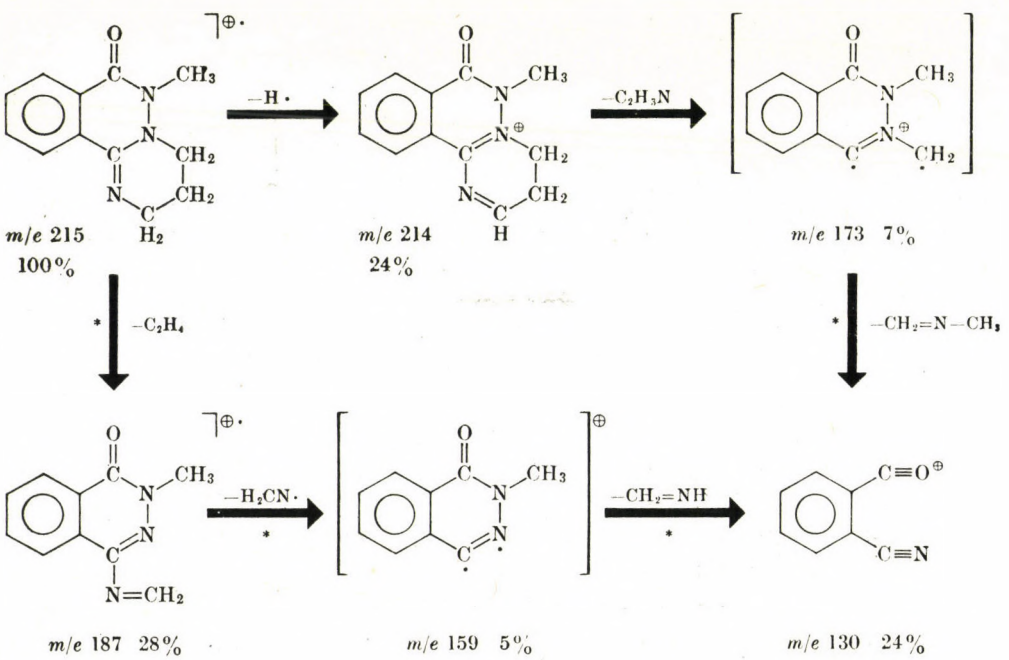

Fig. 5.

known *m/e* 159 ion is formed which decomposes to the *m/e* 130 ion by the loss of C_2H_5N.

The $(M - 1)^+$ ion of **IV** gives rise to an ion of *m/e* 173 having the empirical formula $C_{10}H_9N_2O$, which loses C_2H_5N to yield the ion of *m/e* 130.

The analogues of both steps of this decomposition pathway play a part in the case of the other N-methyl derivative (**II**): the five-membered ring of the $(M - 1)^+$ ion loses C_2H_3N; on the other hand, the *m/e* 173 ion formed by rearrangement gives the *m/e* 130 ion.

The corresponding decomposition route is of wholly subordinate importance in the case of parent compound **III**. This is probably due to the lower stability of the *m/e* 159 ion in comparison with that of the *m/e* 173 ion.

The $(M - 1)^+$ ions of both **III** and **IV** give rise to a relatively abundant, stable fragment by loss of ethylene; further decomposition does not produce ions of considerable intensity.

The molecular ions of both compounds can lose N_2HR (R = H or CH_3) to a small extent. This reaction, like decomposition pathway A of **I** and **II**, involves the fission of the weakened C–N bonds in position 4—5 of **III** and **IV** and is analogous to the loss of N_2H_2R from the (ω-hydroxypropylamino)-phthalazinone derivatives [2].

Experimental

An AEI MS-902 mass spectrometer with direct sample introduction was used. The temperature of the ion source was 150 °C. The empirical formulae of the ions discussed were determined by exact mass measurements. The decomposition pathways are supported by metastable ions. For the refocusing of the metastable ions, the voltage of the electrostatic analyzer was reduced.

The syntheses of the compounds studied will be described elsewhere.

REFERENCES

[1] Bowie, J. H., Cooks, R. G., Donaghue, P. F., Halleday, J. A., Rodda, H. J.: Australian J. Chem., **20**, 2677 (1967)
[2] Bruck, P., Tamás, J., Körmendy, K.: Org. Mass Spectrom., **9**, 335 (1974)
[3] Bruck, P., Tamás, J., Czira, G., Körmendy, K.: Advances in Mass Spectrometry **6**, 859 (1974)
[4] Kirmse, W.: Carbene Chemistry. Academic Press, London and New York 1964

Péter Bruck
József Tamás } H-1088 Budapest, Puskin u. 11—13.
Károly Körmendy; H-1088 Budapest, Múzeum krt. 4/b.

Acta Chimica Academiae Scientarium Hungaricae, Tomus 90(1), pp. 69—73 (1976)

REACTIONS OF HEXAHYDRO-1,3,5-TRIACRYLOYL-*s*-TRIAZINE

G. VALK,* M. KAMEL and N. Y. ABOU-ZEID
(National Research Centre, Dokki, Cairo, Egypt)

Received April 10, 1975

In revised form November 24, 1976

Some interesting results pertaining to the reactions of hexahydro-1,3,5-triacryloyl-*s*-triazine (**I**) with several reagents are described. Thin-layer chromatography proved to be very helpful in following the routes of bromination, addition of ethyl mercaptan, water, sodium bisulfite and/or sodium sulfite.

Hexahydro-1,3,5-triacryloyl-*s*-triazine (**I**) has for some time found several practical applications [1]. In the course of a research program carried out to create reactive centres on cellulose [2] using polyfunctional compounds, some interesting results pertaining to the reactions of **I** and its derivatives with different reagents were obtained. In the present communication these results are reported.

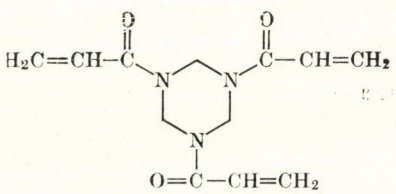

I

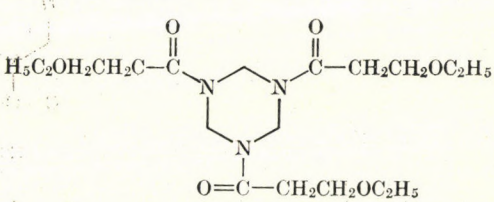

II

At variance with the statement of ZERNER and POLLOCK [3] that the addition of halogens to the three acryloyl groups of **I** is a stepwise process, it has now been found that this not the case. When a molar solution of **I** in chloroform was treated with 1—2 moles of bromine, it was possible by means of thin-layer chromatography (TLC) and preparative TLC to identify in the reaction mixtures unchanged **I**, the di- and hexabromo derivatives, as well as a fourth product believed to be the tetrabromo compound. Attempts at purifying the latter product from the contaminating hexabromo compound failed. Efforts to obtain solid mixtures from the solutions of the brominated compounds by evaporating the solvent in vacuum also remained unsuccessful because of the formation of polymeric products. On the other hand, addition

* Present address: Textilforschung Krefeld, 415 Krefeld, West Germany.

of the required amount of bromine to a chloroform solution of the partially brominated mixtures always afforded the hexabromo compound as the only reaction product.

Preliminary experiments on the addition of ethyl mercaptan to **I** indicated the dependence of the reaction on several factors, including the molar ratio, type of catalyst, temperature and time. If two or more moles of the thiol were added to a chloroform solution of **I** in the presence of triethylamine at 25 °C the di-adduct was formed, as confirmed titrimetrically and by TLC. When only one mole of the thiol was used under the same experimental conditions, a mixture of **I** and the di-adduct was obtained. When the di-adduct was treated with one mole (or when **I** was treated with 3 moles) of the thiol under reflux, the pure tri-adduct was quantitatively formed.

Previous investigations [4] on the addition of alcohols, *e.g.* EtOH, to **I** in the presence of a catalytic amount of potassium hydroxide indicated that the tri-adduct **II** was formed. Attempts to obtain this compound by treating an alcoholic solution of hexahydro-1,3,5-tris(3-chloropropionyl)-*s*-triazine (**III**) with sodium ethoxide gave **I** by β-elimination with E_2 mechanism. On the other hand, treatment of the compound with sodium mercaptide led to the thiol tri-adduct.

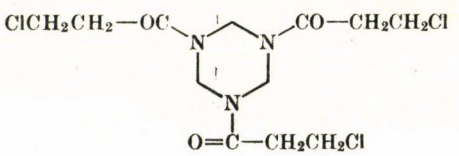

III

Very little is known about the behaviour of **I** in aqueous solutions of alkalis and acids. It was claimed [5] that it was possible to effect the addition of H_2O to two double bonds of **I**, leaving the third one intact, if **I** was treated with aqueous alkali at 100 °C and pH 11 for one hour. Now, a totally different picture was obtained when **I** was treated with aqueous sodium hydroxide solutions (0.08—4%) at temperatures between 20 and 50 °C. Using TLC it was possible to identify in the resulting complex mixture acrylamide **IV**, methylolacrylamide **V**, and methylenebisacrylamide **VI**. In addition, ammonia and formaldehyde were detected.

$CH_2=CHCONH_2$ $CH_2=CHCONHCH_2OH$ $CH_2=CHCONHCH_2NHCOCH=CH$

IV **V** **VI**

These results indicate that the hexahydro-1,3,5-triazine ring is unstable under these conditions. Along with **IV**—**VI**, unidentified high molecular weight oily

products were also formed. In fact, it was found that by prolonging the time of reaction **IV**, **V**, and **VI** disappeared completely, and only the oily products were obtained. On the other hand, treating **I** with HCl solutions (0.25—4%) at 80 to 100 °C gave **IV**, **V** and **VI**.

The addition of $NaHSO_3$ to **I** in aqueous solutions at pH 4 proceeds first at 60 °C. Addition of 1 or 2 moles of this reagent results in the formation of a mixture containing unchanged **I** and two other compounds, probably the mono- and di-adducts. If three moles are added, only one compound (the di-adduct) is formed. This has been confirmed by paper electrophoresis and iodimetric titration using the standard procedures. Here, too, attempts to distill off water caused polymerization, which rendered the separation of the addition compounds impossible.

However, the behaviour towards sodium sulfite is different because if **I** is treated with this reagent at 50 °C and pH 9, the tri-adduct is formed quantitatively within a very short time. This result confirms the findings of VANSHEIDT and GRUZ [6].

In comparison with the limited addition obtained in the case of $NaHSO_3$, the easiness of addition of Na_2SO_3 on **I** may be explained as follows:

(1) at pH 4 (HSO_3^- ion conc. = 94.7% [11]) the addition of the bisulfite ions on the acryloyl groups of **I** is much reduced due to the presence of the acidic medium;
(2) at pH 9, the sulfite ions present (SO_3^{--} conc. = 100% [11]) are just in equilibrium with the bisulfite ions:

$$SO_3^{--} + H_2O \rightleftharpoons HSO_3^- + OH^-$$

Since the reaction medium is alkaline (pH 9), the acryloyl groups of **I** are going to be activated, and hence the HSO_3^- ions add smoothly on the activated double bonds. So the attained equilibrium moves towards the right hand side of the equation leading to the formation of NaOH and the trisulfite adduct of **I**.

In view of this result, we tried to apply this simple procedure for the quantitative estimation of the double bonds in **IV**, **V** and **VI**. The results were satisfactory except in the case of methylolacrylamide **V** where a double amount of Na_2SO_3 was needed.

Experimental

Thin-layer chromatographic analysis

For the identification of **I**, its derivatives and its hydrolyzed products, TLC plates of cellulose or silica gel were used. The following mixtures were applied for development:

sec-BuOH–HCOOH–H_2O	75 : 13.5 : 11.5	For silica gel plates, slow development
$CHCl_3$–EtOH–H_2O	6 : 2 : 1	For silica gel plates, rapid development
$CHCl_3$–Pyridine–H_2O	8 : 17 : 3	For cellulose plates

For detection, the chlorine-*o*-toluidine method [7] was applied.

Hexahydro-1-3-5-tris(dibromopropionyl)-s-triazine

To a solution of **I** (12.45 g; 0.05 mole) in $CHCl_3$ (200 ml) bromine (24 g; 0.15 mole) was added dropwise, and the mixture was well stirred (1 1/2 hr) at room temperature. The white precipitate that formed was filtered off and washed with $CHCl_3$ (50 ml) and finally crystallized from the same solvent. Yield 80%, m.p. 180—181 °C (lit. [9] m.p. 175—177 °C).

$C_{12}H_{15}N_3O_3Br_6$. Calcd. Br 65.84. Found Br 66.25%.

Hexahydro-1,3,5-bisacryloyl-dibromopropionyl-s-triazine

A solution of **I** (12.45 g; 0.05 mole) in $CHCl_3$ (200 ml) was treated with bromine (16 g; 0.1 mole) as described above. After the colour of the bromine had disappeared, a small drop of the mixture was applied on a silica gel plate (F_{254}, Merck) along with **I** and the hexahydro-1,3,5-tris-(dibromopropionyl)-*s*-triazine, and then the chromatogram was developed with the *sec*-BuOH–HCOOH–H_2O solvent. It was found that the mixture contained unchanged **I**, the fully brominated compound, and at least one other component. The latter was isolated using preparative TLC and identified as hexahydro-1,3,5-bisacryloyl-dibromopropionyl-*s*-triazine, m.p. 110 °C.

$C_{12}H_{15}N_3O_3Br_2$. Calcd. Br 39.12. Found Br 39.62%.

Hexahydro-1,3,5-tris(3-chloropropionyl)-s-triazine III

Dry HCl gas was passed into a solution of **I** (12.45 g; 0.05 mole) in $CHCl_3$ (200 ml) until saturation. After standing for 2 hrs, the solution was concentrated in vacuum. The solid residue was recrystallized from EtOH to yield 85% of **III**, m.p. 173 °C (lit. [10] m.p. 164 °C).

$C_{12}H_{18}N_3O_3Cl_3$. Calcd. Cl 29.70. Found Cl 29.65%.

Hexahydro-1,3,5-tris(3-ethylmercaptopropionyl)-s-triazine

This substance can be prepared (a) directly from **I** and ethyl mercaptan, or (b) indirectly from **III** and sodium mercaptide using equimolecular mixtures.

(a) In a stoppered flask, 10 ml of Et_3N was mixed with a solution of **I** (0.01 mole; 2.49 g) in 50 ml $CHCl_3$ with good stirring, followed by a dropwise addition of ethyl mercaptan (2.21 ml; 0.03 mole) in about 30 min. This mixture was refluxed for 1 hr on a water bath. Concentration in vacuum left an oily product, which on treatment with diethyl ether gave a white precipitate; this was crystallized from aqueous EtOH (v/v = 1/1). Yield 90%, m.p. 59 °C.

$C_{18}H_{33}N_3O_3S_3$. Calcd. C 49.65; H 7.64; O 11.03; N 9.65; S 22.07. Found C 49.77; H 7.64; O 10.93; N 9.69; S 21.97%.

(b) To a solution of **III** (0.01 mole) in $CHCl_3$ (50 ml), sodium mercaptide (0.03 mole) in dry $CHCl_3$ (50 ml) (prepared by mixing equivalent amounts of ethyl mercaptan and metallic sodium in $CHCl_3$) was added, and the mixture was allowed to stand for 1 hr at room temperature. The white precipitate formed (NaCl) was filtered off and the filtrate concentrated in vacuum at 40 °C to yield a white residue, which on crystallization from aqueous EtOH (v/v = 1/1) gave white scales, m.p. 59 °C. Yield 95%.

Hexahydro-1,3,5-acryloyl-bis(3-ethylmercaptopropionyl)-s-triazine

To a solution of **I** (2.49 g; 0.01 mole) and Et_3N (10 ml) in $CHCl_3$ (50 ml) ethyl mercaptan (1.48 ml; 0.02 mole) was added dropwise (30 min) with good stirring. The reaction mixture was let to stand 3 hrs at room temperature. It was then concentrated in vacuum to leave an oily product. TLC and estimation of the acryloyl groups indicated that it was the di-adduct. Elemental analysis could not be carried out because of the unstable nature of the product.

Quantitative determination of the acryloyl groups in I

(a) *Ethyl mercaptan method.* A solution of **I** (0.01 mole) in $CHCl_3$ (50 ml) was mixed with triethylamine (10 ml). An excess of ethyl mercaptan (0.035 mole) was then added and the reaction mixture refluxed for 1 hr, after which the excess mercaptan was back-titrated with 1 *N* iodine solution [8]. Addition of 50 ml EtOH and 60 ml glacial AcOH was essential to give a one-phase solution.

(b) *Sodium sulfite method.* A solution of **I** (0.001 mole) in 20 ml H_2O (pH 9) was well stirred at constant temperature (50 °C). Sodium sulfite solution (5 ml, 2*N*) of pH 9 was then added where upon the pH rose to about 11.6. The liberated NaOH was then automatically back-titrated with 0.2 *N* HCl until pH 9 was attained.

REFERENCES

[1] LUETZEL, G.: J. Soc. Dyers and Colourists **82,** 293 (1966)
[2] VALK, G., KAMEL, M., ABOU-ZEID, N. Y.: Textile Res. J. **41,** 364 (1971)
[3] ZERNER, E., POLLOCK, M. W.: U. S. Pat. 2,615,887, 8, 9
[4] GRUZ, R. I., VANSHEIDT, A. A., KRYUCKKOV, F. A., POZIN, L. M., KANEVKAYA, N. V.: Zh. Prikl. Khim. **36,** 1307 (1963)
[5] BORODKIN, V. F., SEMENOVA, T. S., VOLKOVA, N. A.: Izv. Vysshikh. Uchebn. Zavdnii, Khim. i Khim. Tekhnol. **8,** 993 (1965)
[6] VANSHEIDT, A. A., GRUZ, R. I.: Zhur. Priklad. Khim. **34,** 895 (1961)
[7] SCHLIEFER, K., VALK, G.: Dtsch. Faerberkalender **70,** 517 (1971)
[8] BEESING, D. W., TYLER, W. P., KURTZ, D. M., HARRISON, S. A.: Ann. **21,** 1073 (1949)
[9] Chemische Werke Albert, Belg. Pat. 666,847
[10] WEGLER, R., BALLAUF, A.: Chem. Ber. **81,** 527 (1948)
[11] REINDERS, W., VLES, S. I.: Rec. Trav. Chim. **44,** 249 (1925)
RAHN, O., CONN, J. E.: Ind. Eng. Chem. **36,** 185 (1944)
v. SCHELHORN, M.: Dtsch. Lebensmittel-Rundschau **47,** 170 (1951)

G. VALK
M. KAMEL
N. Y. ABOU-ZEID

National Research Centre
El Tahrir street, Dokki, Cairo, U.A.R.

Acta Chimica Academiae Scientiarum Hungaricae, Tomus 90(1), pp. 75–91 (1976)

CHEMISTRY OF 1,3-BIFUNCTIONAL COMPOUNDS, XVIII*

PREPARATION OF THE ESTERS OF VARIOUS 1,3-AMINO ALCOHOLS

K. FELFÖLDI, Á. MOLNÁR and M. BARTÓK

(Department of Organic Chemistry, József Attila University, Szeged)

Received May 10, 1975

The synthesis of various aminoalkyl ester derivatives is reported. Depending on the structure of the compounds, various methods of synthesis have been developed and used. The majority of the compounds have a local anaesthetic effect, while the smaller part is efficient as peripheral vasodilator.

A great number of papers deal with the physiological properties of various amino alcohols and their esters. Particularly, many procaine homologues with local anaesthetic effect have been prepared by varying the substituents (amino and alkyl groups, and the esterifying carboxylic acid) bound to the basic skeleton. Relationships have been established between the structure of the compounds and their effect and potency. Two reviews report on the compounds prepared and their pharmacological properties [1, 2].

In the course of our work, piperidino-, morpholino- and heptamethyleneiminopropyl esters have been prepared. The local anaesthetic properties of the compounds and their effect on the cardiovascular system have been investigated by the Pharmacological Department of the Gedeon Richter Pharmaceutical Works [3].

Some of the compounds (**32**, **35**, **36**, **37**, **58**, **62**) have a very definite local anaesthetic action; they are suitable for both infiltration and conduction anaesthesia. Their therapeutic spectrum, established on the basis of efficiency, toxicity and local tolerance, is more favourable than that of the reference drugs used for comparison (lidocaine, procaine). They have a long duration of action, and do not produce hypersensitivity reactions. The members of the series in general, reduce the blood pressure, but the drop is not large and it is transitory. They enhance peripheral circulation. Some of the compounds (**53**, **57**, **70**) have peripheral vasodilating action.

* Part XVII: Acta Phys. et Chem. Szeged **17**, 55 (1971)

Method of synthesis

The synthesis of the aminoalkyl esters has been achieved by two methods. The majority of the compounds were prepared by the reaction of the appropriate amino alcohols and carboxylic acid chlorides. The addition was effected in anhydrous acetone or benzene, by adding the alcohol to the acid chloride employed in slight excess (Method D). In cases when the acid chloride could only be prepared with difficulty, the esters were obtained by allowing the corresponding aminopropyl chloride to react with the carboxylic acid in isopropyl alcohol [4] (Method E). The aminopropyl chlorides were made either from the amino alcohol with thionyl chloride [5], or by the reaction of the appropriate amine with 1-bromo-3-chloropropane [6]:

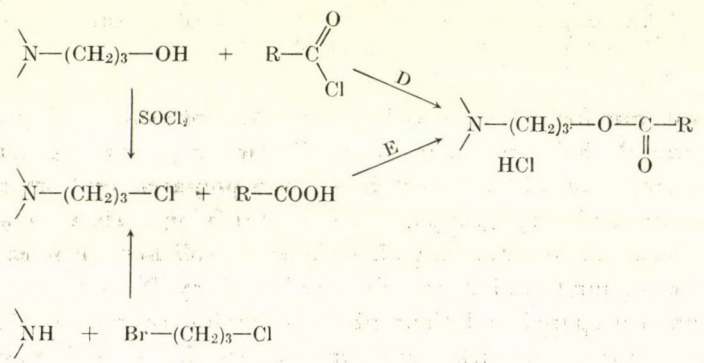

The quaternary products were prepared in acetone, in the usual way (Method F).

For the preparation of the amino alcohols three methods were used, depending on the position of the substituents and on the order of the hydroxyl group. Most frequently, chlorohydrins containing primary halogen atom [7—9] were made to react with the corresponding secondary amines [10] in ethyl alcohol or benzene. For binding the acid, an excess of amine or anhydrous potassium carbonate was used (Method A):

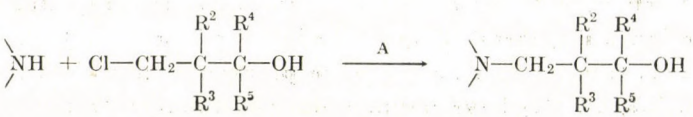

Substitution of a secondary halogen atom can only be effected under the given conditions in a low yield, owing to the elimination of hydrogen halide, which is the main reaction. Therefore, in the synthesis of amino alcohols of this type, acrylic acid esters were used as the starting materials. The amine addition [11, 12], which was carried out at the boiling point, with excess

amine acting also as solvent, was followed by reduction (Method B), or Grignard reaction (Method C):

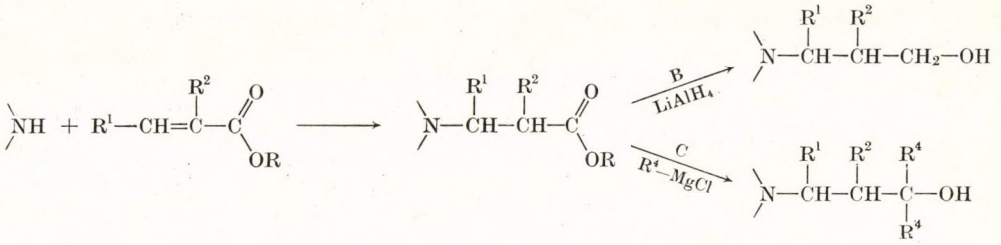

The physical constants and elementary analyses of the compounds prepared are listed in the Tables (temperature data are uncorrected).

Experimental

In addition to the characteristics given in the Tables, the purity of the compounds was checked by thin-layer chromatography. The chromatograms were prepared on Kieselgel (Merck) layer of 0.5 mm thickness, with a solvent mixture of ethyl alcohol–diethyl amine (95 : 5). The chromatograms were visualized by spraying with Draggendorff's reagent.

The IR spectra of the compounds were recorded. The carboxylic acid chlorides were prepared from the corresponding carboxylic acids with thionyl chloride, and purified by distillation or recrystallization.

For the purification of the aminoalkyl ester salts, recrystallization from acetone, ethyl alcohol or aqueous ethyl alcohol was used.

Method A:

2-Isopropyl-3-(piperidinyl-1)-propanol (6)

A mixture of 2-isopropyl-3-chloropropanol (**8**) (6.8 g; 0.05 mole) and piperidine (8.5 g; 0.1 mole) was refluxed in anhydrous benzene (50 ml) for 6 hrs. After cooling, the precipitated piperidine hydrochloride was filtered off, the filtrate evaporated and the residue distilled. The weight of the product (**6**) was 7.6 g (83%).

3-Heptamethyleneiminopropanol (12) [13]

A mixture of heptamethyleneimine (45.3 g; 0.4 mole) trimethylene chlorohydrin (39 g; 0.41 mole) and anhydrous potassium carbonate (55 g) was refluxed, with stirring, in ethyl alcohol (200 ml) for 20 hrs. After cooling, the inorganic salt was removed by filtration, the filtrate was evaporated, and the residue distilled to obtain 51 g (75%) of the product (**12**).

Method B:

3-Methyl-3-heptamethyleneiminopropanol (14)

A mixture of crotonic acid ethyl ester (26 g; 0.23 mole) and heptamethyleneimine (52 g; 0.46 mole) was refluxed for 8 hrs. The excess of the base was evaporated, and the resulting ethyl 3-heptamethyleneiminobutyrate was purified by distillation, to obtain 37 g (68%) of the product, b.p. 132—134 °C/12 torr, n_D^{20} 1.4635. The product (0.16 mole) was reduced with lithium aluminium hydride (6.5 g) in anhydrous ether (600 ml). The reaction mixture was decomposed with aqueous alkali, the ether phase was dried, the ether evaporated, and the residue distilled to obtain 21.2 g (71%) of the product (**14**).

Ethyl 2-methyl-3-heptamethyleneiminopropionate, obtained from the reaction of methyl methacrylate and heptamethyleneimine (65%, b.p. 110—112 °C/10 torr, n_D^{30} 1.4606), gave on reduction 2-methyl-3-heptamethyleneiminopropanol (**13**) (82%).

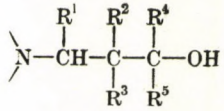

Table I

3-Aminopropyl alcohols

No.	>N—	R^1	R^2	R^3	R^4	R^5	B.p. °C Pressure, torr	n_D^{20}	Yield %	Empirical formula Molecular weight	Analysis, % Calcd./Found C	H	N	Method Ref.
1.	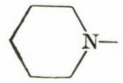	H	H	H	H	H	124—127 30	1.4735	78	$C_8H_{17}NO$ 143.20	67.25 67.20	11.90 11.85	9.78 9.52	A [10]
2.		H	H	H	H	C_2H_5	102—105 10	1.4652	80	$C_{10}H_{21}NO$ 171.28	70.12 70.35	12.36 12.50	8.18 7.88	A
3.	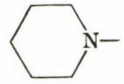	H	H	H	H	C_4H_9	115—117 10	1.4645	85	$C_{12}H_{25}NO$ 199.34	72.45 72.33	12.55 12.63	7.02 7.10	A
4.	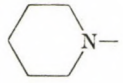	H	H	H	CH_3	C_3H_7	124—126 13	1.4630	81	$C_{12}H_{25}NO$ 199.34	72.45 72.50	12.55 12.35	7.02 7.28	A
5.	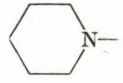	H	H	CH_3	H	H	66—68 5	1.4630	68	$C_9H_{19}NO$ 157.26	68.74 68.82	12.18 12.23	8.91 8.77	A [12]
6.	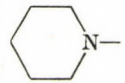	H	H	i-C_3H_7	H	H	88—91 5	1.4672	83	$C_{11}H_{23}NO$ 185.30	71.30 71.28	12.50 12.70	7.56 7.42	A

7.	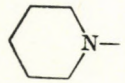	H	CH_3	CH_3	H	H	66—69 3	1.4653	75	$C_{10}H_{21}NO$ 171.28	70.12 69.95	12.36 12.45	8.18 8.11	A [14]
8.	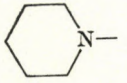	H	H	CH_3	CH_3	CH_3	120—122 25	1.4555	47	$C_{11}H_{23}NO$ 185.30	71.30 71.15	12.50 12.63	7.56 7.42	C
9.	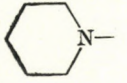	CH_3	H	H	H	H	106—108 10	1.4696	52	$C_9H_{19}NO$ 157.26	68.74 68.55	12.18 12.28	8.91 8.85	B
10.	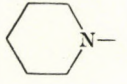	H	H	H	H	H	122—123 3	1.5393	51	$C_{14}H_{21}NO$ 219.33	76.75 76.65	9.58 9.37	6.40 6.52	B
11.	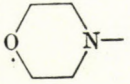	H	H	H	H	H	86—88 4	1.4728	90	$C_7H_{15}NO_2$ 145.22	57.85 57.78	10.31 10.35	9.65 9.48	A [10]
12.	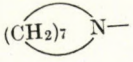	H	H	H	H	H	118—120 8	1.4830	75	$C_{10}H_{21}NO$ 171.28	70.12 70.28	12.36 12.31	8.18 8.11	A [13]
13.	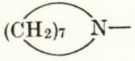	H	H	CH_3	H	H	93—95 3	1.4785	55	$C_{11}H_{23}NO$ 185.30	71.30 71.48	12.50 12.25	7.56 7.80	B
14.	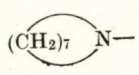	CH_3	H	H	H	H	98—101 3	1.4833	50	$C_{11}H_{23}NO$ 185.30	71.30 71.25	12.50 12.65	7.56 7.70	B

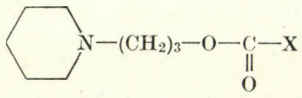

Table II

Derivatives of 3-(piridinyl-1)-propyl esters

No.	X	Derivative M.p. °C	Empirical formula Molecular weight	Analysis, % Calcd./Found			Method
				C	H	N	
15.	$-(CH_2)_2-CH_3$	HCl 157—158	$C_{12}H_{24}ClNO_2$ 249.60	57.24 57.43	10.40 9.95	5.56 5.86	D
16.	$-(CH_2)_4-CH_3$	HCl 131—132	$C_{14}H_{28}ClNO_2$ 277.84	60.52 60.20	10.16 9.80	5.04 5.38	D
17.	$-(CH_2)_6-CH_3$	HCl 140—141	$C_{16}H_{32}ClNO_2$ 305.90	62.82 62.60	10.54 10.35	4.58 4.89	D
18.	$-(CH_2)_8-CH=CH_2$	HCl 132—133	$C_{19}H_{36}ClNO_2$ 345.95	67.97 67.61	10.49 10.26	4.04 4.05	D
19.	$-(CH_2)_{14}-CH_3$	HCl 149—150	$C_{24}H_{48}ClNO_2$ 418.11	68.95 68.65	11.57 11.38	3.35 3.39	D
25.	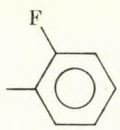	HCl 165—166	$C_{15}H_{21}ClFNO_2$ 301.80	59.70 59.41	7.01 6.98	4.64 4.56	D
26.	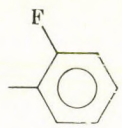	Methiodide 136—137	$C_{16}H_{23}FJNO_2$ 407.28	47.19 47.15	5.69 5.80	3.44 3.50	F
27.	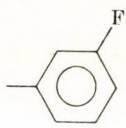	HCl 195—196	$C_{15}H_{21}ClFNO_2$ 301.80	59.70 60.00	7.01 6.71	4.64 4.84	D
28.	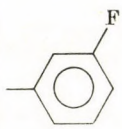	Methiodide 159—160	$C_{16}H_{23}FJNO_2$ 407.28	47.19 46.90	5.69 5.50	3.44 3.50	F
29.	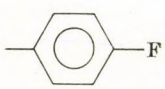	HCl 197—198	$C_{15}H_{21}ClFNO_2$ 301.80	59.70 59.89	7.01 7.12	4.64 4.39	D
30.	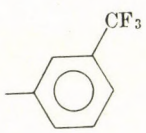	HCl 173—174	$C_{16}H_{21}ClF_3NO_2$ 351.80	54.63 54.36	6.00 6.16	3.98 4.15	D

Table II (continued)

No.	X	Derivative M.p. °C	Empirical formula Molecular weight	Analysis, % Calcd./Found			Method
				C	H	N	
31.	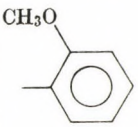	HCl 156—157	$C_{16}H_{24}ClNO_3$ 313.84	61.23 61.03	7.70 7.66	4.46 4.57	D
32.	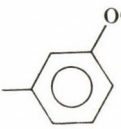	HCl 130—131	$C_{16}H_{24}ClNO_3$ 313.84	61.23 61.29	7.70 7.85	4.46 4.58	D
33.	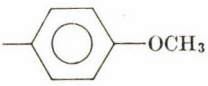	HCl 177—178	$C_{16}H_{24}ClNO_3$ 313.84	61.23 60.87	7.70 8.04	4.46 4.41	D
38.	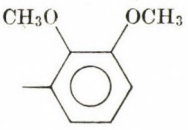	HCl 125—126	$C_{17}H_{26}ClNO_4$ 343.40	59.45 59.25	7.62 7.66	4.07 4.17	E
39.	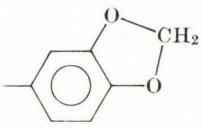	HCl 184—185	$C_{16}H_{22}ClNO_4$ 327.81	58.62 58.78	6.76 6.78	4.27 4.27	D
40.	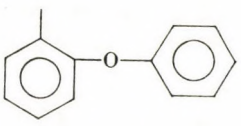	HCl 156—157	$C_{21}H_{26}ClNO_3$ 375.90	67.10 67.30	6.97 7.09	3.72 3.73	D
41.	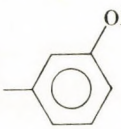	HCl 146—147	$C_{18}H_{28}ClNO_3$ 341.80	63.40 63.49	8.27 8.19	4.10 4.25	D
42.	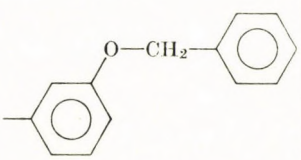	HCl 166—167	$C_{22}H_{28}ClNO_3$ 389.93	67.80 67.61	7.18 7.20	3.60 3.46	E
43.	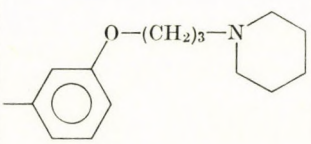	2HCl 236—237	$C_{23}H_{38}Cl_2N_2O_3$ 461.40	60.05 59.77	8.32 8.31	6.08 6.32	E

Table II (continued)

No.	X	Derivative M.p. °C	Empirical formula Molecular weight	Analysis, % Calcd./Found			Method
				C	H	N	
44.	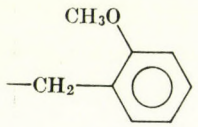	HCl 139—140	$C_{17}H_{26}ClNO_3$ 327.86	62.30 62.10	7.70 8.10	4.27 4.25	D
45.	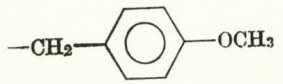	HCl 95—96	$C_{17}H_{26}ClNO_3$ 327.86	62.30 62.05	7.70 8.10	4.27 4.68	D
46.	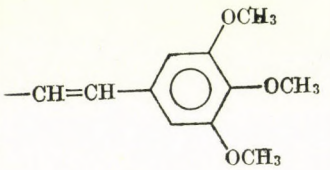	HCl 161—162	$C_{20}H_{34}ClNO_5$ 405.70	61.74 61.90	8.01 8.39	3.27 3.43	E
47.	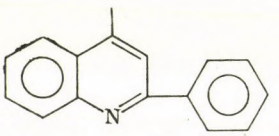	HCl 210—211	$C_{24}H_{27}ClN_2O_2$ 411.04	71.22 71.00	6.63 6.73	6.82 6.75	E
48.	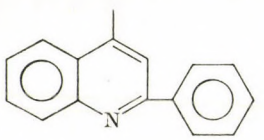	Methiodide 195—196	$C_{25}H_{29}JN_2O_2$ 516.40	58.20 58.44	5.65 5.28	5.43 5.53	E F

Method C:

1,1,2-Trimethyl-3-(piperidinyl-1)-propanol (8)

A solution of methyl 2-methyl-3-(piperidinyl-1)-propionate (**12**) (67.5 g; 0.36 mole) in anhydrous ether (100 ml) was added dropwise, with stirring and cooling, during 1 hr to a solution of methylmagnesium chloride (0.83 mole) in ether (500 ml), and the reaction mixture was stirred for further 5 hrs at roome temperature. The mixture was decomposed under cooling and stirring with dilute hydrochloric acid (280 ml), the aqueous phase was made alkaline and extracted with ether. The combined ethereal phases were dried, the ether evaporated, and the residue distilled to give 31 g (47%) of the product (**8**).

Method D:

3-(Piperidinyl-1)-propyl 3-methoxybenzoate hydrochloride (32)

A solution of 3-methoxybenzoyl chloride was prepared (3.4 g; 0.02 mole) in benzene (15 ml), and a solution of 3-(piperidinyl-1)-propanol (**1**) (2.8 g; 0.02 mole) was added to this dropwise, with stirring and cooling. After 30 min of boiling and subsequent cooling, the crystals which separated were filtered off (5.9 g) and recrystallized from ethyl alcohol (10 ml) to yield 5.1 g (80%) of the product (**32**).

Method E:

3-Heptamethyleneiminopropyl 2-phenylquinoline-4-carboxylate hydrochloride (92)

To a solution of 3-heptamethyleneiminopropanol (**12**) (45.4 g; 0.26 mole) in chloroform (150 ml), thionyl chloride (39 g; 0.47 mole) was added dropwise, under stirring and cooling. Stirring was continued at room temperature for one day. The solvent was then evaporated and the solid residue made alkaline with 30% cold sodium hydoxide solution (50 ml) and extracted with ether. The ethereal solution was dried, the solvent evaporated and the residue distilled to obtain 27 g (55%) of 3-heptamethyleneiminopropyl chloride, b.p. 90—93 °C/5 torr, n_D^{20} 1.4819.

A mixture of 3-heptamethyleneiminopropyl chloride (3.2 g; 0.017 mole) and 2-phenylquinoline-4-carboxylic acid (4 g; 0.016 mole) was boiled in isopropyl alcohol (30 ml) for 10 hrs. Acetone (15 ml) was added to the hot solution and, after cooling, the crystals which separated were filtered off and recrystallized from ethyl alcohol to yield 3.5 g (50%) of the product (**92**).

3-(Piperidinyl-1)-propyl 3-[3-(piperidinyl-1)-propyloxy]-benzoate dihydrochloride (43)

A solution of 3-hydroxybenzoic acid (3 g; 0.022 mole) and 3-(piperidinyl-1)-propyl chloride (7.2 g; 0.045 mole) (**6**) in ethyl alcohol (30 ml) was mixed with 10% potassium hydroxide solution in ethyl alcohol (25 ml) under stirring and boiling. The reaction mixture was refluxed for 5 hrs and, after cooling, the inorganic salt was removed by filtration. The filtrate was evaporated, the residue dissolved in ether, and the ethereal solution was extracted first with dilute aqueous NaOH solution, then with 15% HCl (20 ml). The acid solution was clarified and acetone (20 ml) was added. After cooling, the crystals which separated were filtered off, and recrystallized from aqueous ethyl alcohol to obtain 3.5 g (35%) of the product (**43**).

Method F:

3-Heptamethyleneiminopropyl 3,4,5-trimethoxybenzoate methiodide (83)

To a solution of 3,4,5-trimethoxybenzoyl chloride (6 g; 0.026 mole) in benzene (40 ml), a solution of 3-heptamethyleneiminopropanol (**12**) (4.3 g; 0.025 mole) in benzene was added dropwise, under stirring and cooling. After 30 min reflux and subsequent cooling, the mixture in benzene was extracted with dilute alkali solution. The organic phase was dried, and the solvent evaporated. The residue (7.4 g) was dissolved in acetone (25 ml), methyl iodide (4 g) was added, and the mixture was allowed to stand overnight. The crystals which separated were filtered off (9.2 g) and recrystallized from aqueous ethyl alcohol (60 ml) to obtain 6.4 g (50%) of the product (**83**).

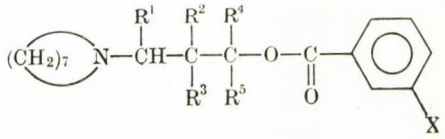

Table III

Derivatives of 3-aminopropyl benzoates

No.	n	R^1	R^2	R^3	R^4	R^5	X	Derivative M.p. °C	Empirical formula Molecular weight	Analysis, % Calcd./Found			Method
										C	H	N	
20.	5	H	H	H	H	C_2H_5	H	HCl 135—136	$C_{17}H_{26}ClNO_2$ 311.78	65.48 65.28	8.40 8.19	4.49 4.69	D
21.	5	H	H	H	H	C_4H_9	H	HCl 159—160	$C_{19}H_{30}ClNO_2$ 339.82	67.14 67.24	8.89 8.90	4.12 4.49	D
22.	5	H	H	H	CH_3	C_3H_7	H	HCl 123—124	$C_{19}H_{30}ClNO_2$ 339.82	67.14 67.31	8.89 8.79	4.12 3.95	D
23.	5	H	H	CH_3	CH_3	CH_3	H	HCl 156—157	$C_{18}H_{28}ClNO_2$ 325.81	66.34 66.27	8.66 8.41	4.28 4.40	D
24.	5	H	H	i-C_3H_7	H	H	H	HCl 154—155	$C_{18}H_{28}ClNO_2$ 325.81	66.34 66.56	8.66 8.52	4.28 4.49	D
34.	5	H	H	CH_3	H	H	OCH_3	HCl 141—142	$C_{17}H_{26}ClNO_3$ 327.80	62.28 62.09	7.99 7.97	4.27 4.21	D

35.	5	H	CH_3	CH_3	H	H	OCH_3	HCl 122—123	$C_{17}H_{26}ClNO_3$ 341.82	63.24 63.15	8.25 8.37	4.09 3.88	D
36.	5	CH_3	H	H	H	H	OCH_3	HCl 112—113	$C_{17}H_{26}ClNO_3$ 327.80	62.28 62.48	7.99 8.22	4.27 3.97	D
37.	5		H	H	H	H	OCH_3	HCl 121—122	$C_{22}H_{28}ClNO_3$ 389.91	67.77 67.50	7.24 7.35	3.59 3.27	D
79.	7	H	H	CH_3	H	H	OCH_3	HCl 104—105	$C_{19}H_{30}ClNO_3$ 355.89	64.12 63.94	8.50 8.62	3.94 4.08	D
80.	7	H	H	CH_3	H	H	OCH_3	Methiodide 172—173	$C_{20}H_{32}JNO_3$ 461.42	52.06 52.55	6.99 6.78	3.04 2.87	F
81.	7	CH_3	H	H	H	H	OCH_3	Methiodide 163—164	$C_{20}H_{32}JNO_3$ 416.42	52.06 52.11	6.99 7.11	3.04 3.00	F

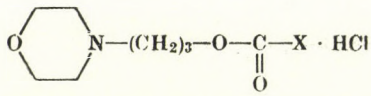

Table IV

Hydrochlorides of 3-(morpholinyl-4)-propyl esters

No.	X	Derivatives M.p. °C	Empirical formula Molecular weight	Analysis, % Calcd./Found			Method
				C	H	N	
49.	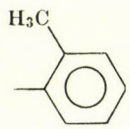	129—130	$C_{15}H_{22}ClNO_3$ 299.80	60.10 59.90	7.39 7.29	4.64 4.56	D
50.	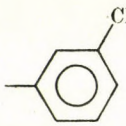	157—158	$C_{15}H_{22}ClNO_3$ 299.80	60.10 59.95	7.39 7.08	4.64 5.09	D
51.	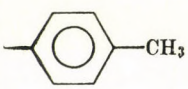	204 205	$C_{15}H_{22}ClNO_3$ 299.80	60.10 60.10	7.39 7.20	4.64 4.34	D
52.	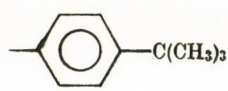	180—181	$C_{18}H_{28}ClNO_3$ 341.77	63.24 62.93	8.25 8.00	4.09 4.36	D
53.	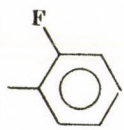	185—186	$C_{14}H_{19}ClFNO_3$ 303.77	55.35 55.17	6.30 6.49	4.60 4.95	D
54.	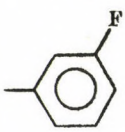	162—163	$C_{14}H_{19}ClFNO_3$ 303.77	55.35 55.42	6.30 6.19	4.60 4.75	D
55.	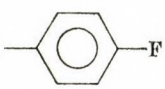	182—183	$C_{14}H_{19}ClFNO_3$ 303.77	55.35 55.13	6.30 6.59	4.60 4.80	D
56.	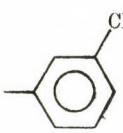	144—145	$C_{15}H_{19}ClF_3NO_3$ 353.75	50.93 50.68	5.41 5.75	3.96 3.93	D
57.	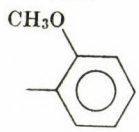	121—122	$C_{15}H_{22}ClNO_4$ 315.80	57.05 56.83	7.02 7.04	4.43 4.25	D

Table IV (continued)

No.	X	Derivatives M.p. °C	Empirical formula Molecular weight	Analysis, % Calcd./Found			Method
				C	H	N	
58.	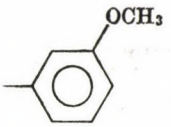	150—151	$C_{15}H_{22}ClNO_4$ 315.80	57.05 57.11	7.02 6.83	4.43 4.77	D
59.	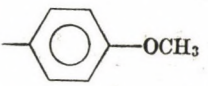	173—174	$C_{15}H_{22}ClNO_4$ 315.80	57.05 57.00	7.02 6.83	4.43 4.66	D
60.	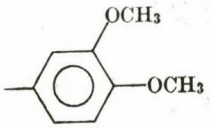	191—192	$C_{16}H_{24}ClNO_5$ 345.82	55.57 55.63	6.99 6.98	4.05 4.02	D
61.	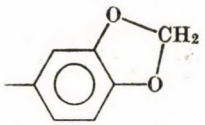	208—209	$C_{15}H_{20}ClNO_5$ 329.79	54.63 54.59	6.11 6.33	4.25 4.35	D
62.	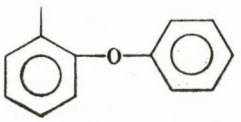	168—169	$C_{20}H_{24}ClNO_4$ 377.88	63.57 63.20	6.40 6.43	3.71 3.62	D
63.	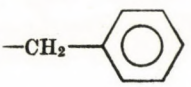	102—103	$C_{15}H_{22}ClNO_3$ 299.80	60.10 59.90	7.39 7.53	4.67 4.56	D
64.	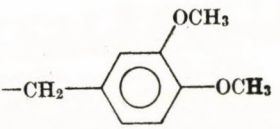	135—136	$C_{17}H_{26}ClNO_5$ 359.85	56.74 56.72	7.28 7.00	3.89 3.90	E
65.	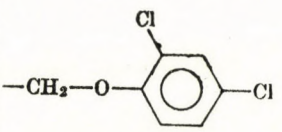	132—133	$C_{15}H_{20}Cl_3NO_4$ 384.70	46.83 46.60	5.24 5.45	3.64 3.97	D
66.	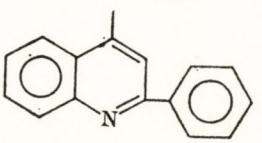	179—180	$C_{23}H_{25}ClN_2O_3$ 412.92	66.90 66.69	6.10 6.21	6.79 6.97	E

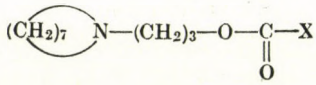

Table V

Derivatives of 3-heptamethyleneiminopropyl esters

No.	X	Derivatives M.p., °C	Empirical formula Molecular weight	Analysis, % Calcd./Found			Method Methiodide
				C	H	N	
67.	$-C(CH_3)_3$	HCl 155—156	$C_{15}H_{30}ClNO_2$ 291.87	61.73 61.92	10.36 10.20	4.50 4.97	D
68.	$-CH_3$	Methiodide 173—174	$C_{13}H_{26}JNO_2$ 355.26	43.95 44.09	7.37 6.93	3.94 3.67	F
69.	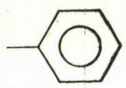	HCl 156—157	$C_{17}H_{26}ClNO_2$ 311.86	65.47 65.02	8.40 8.00	4.49 5.02	D
70.	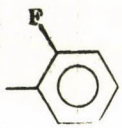	HCl 131—132	$C_{17}H_{25}ClFNO_2$ 329.85	61.90 61.63	7.64 7.40	4.24 4.15	D
71.	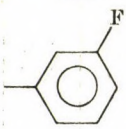	HCl 145—146	$C_{17}H_{25}ClFNO_2$ 329.85	61.90 61.75	7.64 7.44	4.24 3.90	D
72.		HCl 146—147	$C_{17}H_{25}ClFNO_2$ 329.85	61.90 62.07	7.64 7.64	4.24 4.35	D
73.	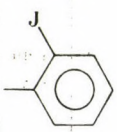	HCl 122—123	$C_{17}H_{25}ClJNO_2$ 437.76	46.64 46.48	5.76 5.40	3.20 3.27	D
74.	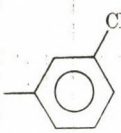	HCl 136—137	$C_{18}H_{25}ClF_3NO_2$ 379.85	56.92 56.88	6.63 6.90	3.68 3.69	D
75.	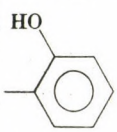	HCl 124—125	$C_{17}H_{26}ClNO_3$ 327.86	62.28 62.25	7.99 7.89	4.27 4.38	D
76.	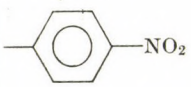	HCl 159—160	$C_{17}H_{25}ClN_2O_4$ 356.86	57.21 56.96	7.06 7.13	7.85 7.95	D

Table V (continued)

No.	X	Derivatives M.p., °C	Empirical formula Molecular weight	Analysis, % Calcd./Found			Method Methiodide
				C	H	N	
77.	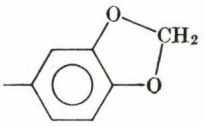	HCl 147—148	$C_{18}H_{26}ClNO_4$ 355.87	60.75 60.45	7.36 7.58	3.93 3.60	D
78.	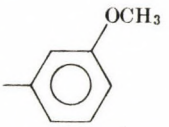	Methiodide 168—169	$C_{19}H_{30}JNO_3$ 447.30	49.90 50.25	6.61 6.69	3.06 2.90	F
82.	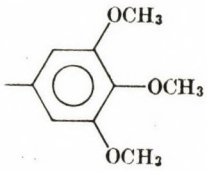	HCl 158—159	$C_{20}H_{32}ClNO_5$ 401.94	59.77 59.58	8.03 7.73	3.49 3.74	D
83.	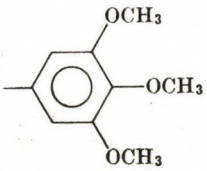	Methiodide 183—184	$C_{21}H_{34}JNO_5$ 513.42	49.13 49.34	6.67 6.64	2.72 2.52	F
84.	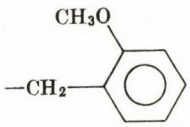	Methiodide 144—145	$C_{20}H_{32}JNO_3$ 355.91	52.10 51.80	7.00 6.85	3.04 3.26	F
85.	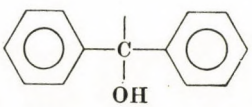	HCl 123—124	$C_{24}H_{32}ClNO_3$ 417.98	67.50 67.73	7.51 7.23	3.27 3.51	E
86.	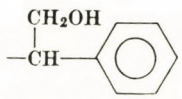	HCl 100—101	$C_{19}H_{30}ClNO_3$ 355.90	64.20 64.36	8.51 8.49	3.94 3.80	E
87.	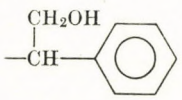	Methiodide 118—119	$C_{20}H_{32}JNO_3$ 461.40	52.10 51.90	7.00 6.71	3.04 3.50	E F
88.	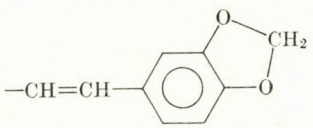	HCl 149—150	$C_{20}H_{28}ClNO_4$ 381.91	62.90 62.50	7.39 7.64	3.60 3.58	D

Table V (continued)

No.	X	Derivatives M.p,. °C	Empirical formula Molecular weight	Analysis, % Calcd./Found			Method Methiodide
				C	H	N	
89.	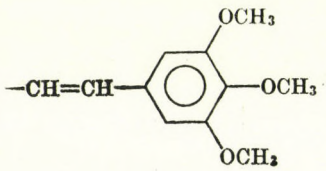	HCl 161—162	$C_{22}H_{34}ClNO_5$ 427.98	61.74 61.44	8.01 8.49	3.27 3.43	D
90.	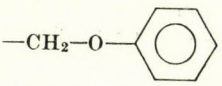	Methiodide 119—120	$C_{19}H_{30}JNO_3$ 457.36	49.90 50.00	6.61 6.78	3.06 2.99	F
91.	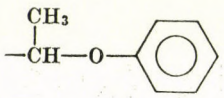	Methiodide 158—159	$C_{20}H_{32}JNO_3$ 461.40	52.10 51.85	7.00 6.87	3.40 3.48	F
92.	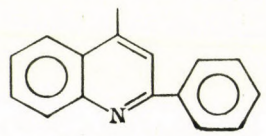	HCl 137—138	$C_{26}H_{31}ClN_2O_2$ 439.35	71.20 71.14	7.14 7.21	6.37 6.40	E
93.	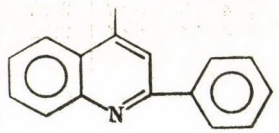	Methiodide 167—168	$C_{27}H_{33}JN_2O_2$ 544.50	59.60 59.58	6.11 6.24	5.15 5.37	E F

REFERENCES

[1] CHERKASOVA, E. M., BOGATKOV, S. V.: Uspekhi Khimii **31**, 963 (1962)
[2] CHERKASOVA, E. M., PRYANISNIKOVA, N. T., BOGATKOV, S. V.: Uspekhi Khimii **42**, 1892 (1973)
[3] SZPORNY, L., KÁRPÁTHY, E.: "Pharmacology of amino alcohol esters"; KÁRPÁTHY, E., SZPORNY, L.: "Pharmacological investigation of a new local anesthesic". First Congress of the Hungarian Pharmacological Society, Budapest 1971
[4] HORENSTEIN, H., PÄCHLIKE, H.: Ber. **71**, 1944 (1938)
[5] WRIGHT, J. B., KOLLOFF, H. G.: J. Am. Chem. Soc. **70**, 3098 (1948)
[6] LEONARD, F., SIMET, L.: J. Am. Chem. Soc. **77**, 2857 (1955)
[7] BARTÓK, M., GILDE, A. S.: Acta Phys. et Chem. Szeged **9**, 25 (1963)
[8] BARTÓK, M., KOZMA, B., GILDE, A. S.: Acta Phys. et Chem. Szeged **11**, 35 (1965)
[9] BARTÓK, M.: Acta Chim. Acad. Sci. Hung. **55**, 365 (1968)
[10] CLINTON, R. O., SALVADOR, U. J.: J. Am. Chem. Soc. **71**, 3366 (1949)
[11] POLLARD, C. B., MATTSON, G. C.: J. Am. Chem. Soc. **78**, 4089 (1965)
[12] BIEBER, P.: Compt. rend. **231**, 291 (1950)
[13] U. S. Pat. 2,748,113 (1956); C. A. **51**, P8816c (1957)
[14] WENNER, W.: J. Org. Chem. **15**, 301 (1950)

Károly FELFÖLDI
Árpád MOLNÁR
Mihály BARTÓK
H-6720 Szeged, Dóm tér 8.

Acta Chimica Academiae Scientiarum Hungaricae, Tomus 90(1), pp. 93—101 (1976)

THE REACTION OF *N*-(*t*-BUTYL)-α-HALO-α,α-DIARYLACETAMIDES WITH CYANOAMIDE AND MONOSUBSTITUTED CYANOAMIDE SALTS*

GY. SIMIG, K. LEMPERT

(Research Group for Alkaloid Chemistry of the Hungarian Academy of Sciences, Budapest,

and

J. TAMÁS, G. CZIRA

(Central Research Institute for Chemistry of the Hungarian Academy of Sciences, Budapest)

Received October 1, 1975

The *N*-(*t*-butyl)-α-halo-α,α-diphenylacetamides **1b** and **6a—c** furnish with monopotassium cyanoamide and its *N*-alkyl, *N*-aralkyl and *N*-aryl derivatives a variety of products, such as the *cine* substitution products **2b**, **2d—g**, the 3-(*t*-butyl)--glycocyamidines **3b—e**, **3j**, **5b** and **7** and the 1-(*t*-butyl)-glycocyamidines **3f—g** and **5a**. The latter are obviously formed through the intermediacy of the aziridinone **8a**. The relation between the types of the various cyanoamide anions and the types of products, as well as the spectral properties of the latter are discussed, in particular those which are of significance for their structure elucidations.

α-Chloro-α,α-diphenylacetamides (**1a—c**) yield *cine* substitution products (**2a—c**) with potassium *N*-cyano-anilide; 1,5,5-triphenyl- (**3a**) and 3-(*t*-butyl)--1,5,5-triphenylglycocyamidine (**3b**), respectively, were obtained (in addition to several minor products) as the by-products with **1a** and **1b** [2, 3]. The reactions of **1b** with potassium cyanoamide and several *N*-aryl and *N*-alkyl derivatives have now been studied.

1b and the potassium salts of *m*-chloro-*N*-cyano- and *N*-cyano-*p*--methoxyaniline and *N*-cyano-*p*-toluidine, respectively, furnished 37—68% of the *cine* substitution products **2d—f** and 5—15% of the glycocyamidines **3c—e**. The latter were identified by comparison with authentic samples [4], while the structures of the former were established on the basis of IR and NMR evidence (see Experimental). An important difference between the IR spectra of the *cine* products **2b** and **2d—f**, and the isomeric Type **4** α-substitution products (which are not formed under the conditions applied) is that the Amide I bands are at 1640—1635 cm^{-1} in the former case, whereas in the latter case they appear in the region 1685—1680 cm^{-1} [4].

No cine products were formed in the reactions of **1b** and potassium *N*-cyano-*N*-ethyl- and *N*-benzyl-*N*-cyanoamide, and the glycocyamidines **3f** and **3g**, obtained in 50 and 61% yield, differed from the glycocyamidines

* Hydantoins, thiohydantoins and glycocyamidines, Part 43. For Part 42, see Ref. [1].

3b—**e** prepared with potassium *N*-cyanoanilides in that the *t*-butyl group was attached to N(1) rather than to N(3). The structures of the glycocyamidines follow (1) from their non-identity with their known [4] isomers **3h** and **3i**, respectively, (2) from their conversion with HNO_2 into the corresponding hydantoins, proving that the exocyclic nitrogen atom is unsubstituted, and (3) from their IR, NMR and mass [1] spectra. In particular, the positions of the *t*-Bu signals in the NMR spectra of the glycocyamidines **3f** and **3g** (δ 1.28 ppm) clearly demonstrate [3] that these groups are attached to N(1) rather than to N(3).

Reaction of **1b** and potassium *N*-(*t*-butyl)-*N*-cyanoamide furnished two isomeric glycocyamidines (**5a** and **b**) (m.p.'s 150—1 °C and 120—1 °C, respectively); again, no *cine* substitution products were formed. The structure assignments of the glycocyamidines are based (1) on their non-identity with the known 1,3-di(*t*-butyl)-5,5-diphenylglycocyamidine [4], whence it follows that one of the *t*-butyl groups is attached to the exocyclic nitrogen atom, and (2) on their IR, NMR and mass [1] spectra. In the NMR spectrum of the lower melting isomer the signals of the *t*-butyl groups are at δ 1.60 and 1.55 ppm, respectively, whence attachment of either of them to N(1) is ruled out [3]. In the spectrum of the higher melting isomer, the *t*-butyl signals are at δ 1.67 and 1.25 ppm; the latter value is in agreement with the presence of a 1-(*t*-butyl) group [3]. The amide I and guanidine bands in the IR spectra (KBr) of **5a** and **5b** appear at identical wave numbers (1720 and 1635 cm^{-1}, respectively) which precludes that the C=O and C=N groups of **5**a are conjugated and proves that **5a** exists, in the crystalline state, as the tautomer containing a semicyclic C=N bond.

The reaction of **1b** with monopotassium *N*-cyanoamide furnished the glycocyamidine **3j**. The structure of the product follows from its IR, mass [1] and NMR spectra. The signal of the *t*-Bu group appears at δ 1.63 ppm, which precludes [3] that the *t*-Bu group is attached to N(1). Since *N*(2)-(*t*-butyl)-5,5-diphenylglycocyamidine could hardly be formed in the course of this reaction (*cf.* below), the *t*-butyl group must be attached to N(3).

In most of the above reactions *N*-(*t*-butyl)-benzilamide, resulting from the hydrolysis of **1b**, was obtained as a by-product.

Replacement of the α-chlorine of **1b** by bromine had no serious effect on the reactivity towards potassium *N*-cyanoanilide. When the latter was allowed to react with the bromo analogue **6a**, **2b** was formed as the only major product. The monochloro derivative **6b** furnished the *cine* product **2g**. Again, the position of the amide I band in the IR spectrum (1635 cm^{-1}) and the presence of the methine proton signal in the NMR spectrum were diagnostic for the type **2** structure. The formation of **6b** appears to indicate that the *N*-cyanoanilide anion is incapable of replacing a Cl atom in *para* position. In agreement with this, the *p,p'*-dichloro derivative **6c** did not furnish a *cine*

product with potassium *N*-cyanoanilide, but was converted into glycocyamidine **7**. The structure of the latter product is based on the mass and NMR spectra. The presence of an abundant M—56 ion in the mass spectrum and the position of the *t*-butyl signal (δ 1.80 ppm) prove that the *t*-butyl group is attached to N(3). The site of attachment of the phenyl group, too, follows from the mass spectrum, which exhibits abundant peaks at *m/e* 326 and 328, corresponding to the ions $(p\text{-}ClC_6H_4)_2C{=}\overset{\oplus}{N}HPh$. This type of ions was also observed as an abundant peak in the MS of 1,5,5-triphenylglycocyamidine [19]. The fragmentation pathway

$$m/e \quad 451 \xrightarrow{-C_4H_8} 395 \xrightarrow{-Ph\cdot} 318 \xrightarrow{-C_2N_2O} 250,$$

is also of diagnostic value for structure **7** (*cf.* Scheme 1 in Ref. [1]).

Formation of the glycocyamidines **3f** and **3g** requires migration of the *t*-butylamino group of **1b** from its original position to the vicinal carbon atom. This migration may easily be explained by assuming dehydrochlorination of **1b** by potassium *N*-cyano-*N*-ethyl- and *N*-benzyl-*N*-cyanoamide, respectively, to yield the aziridinone **8a**, and subsequent attack of the substituted nitrogen atom of the reagent at the carbonyl group of **8a**. Several examples of type **1** α-chloro-α,α-diphenylacetamides reacting with sufficiently basic nucleophiles through the intermediacy of type **8** aziridinones are known from the literature [5, 6], among which we wish to mention only the reaction of **1a** with sodium cyanamide furnishing *N*-benzhydryl-*N'*-cyanourea **9** [6], since this reaction is most closely related to those discussed here. (In contrast to the formation of **3f** and **3g**, that of **9** requires fission of the C–C bond of the intermediate aziridinone **8b**.)

While formation of the glycocyamidine **5a**, too, requires the intermediacy of **8a**, that of the isomeric **5b** does not. The attachment in both cases of one of the *t*-butyl groups to the exocyclic nitrogen atom shows that the reagent attacks both the carbonyl group of **8a** and the α-carbon atom of **1b** with its *un*substituted nitrogen atom which is apparently the result of steric inhibition by the bulky *t*-butyl group and, once again, demonstrates the ambident reactivity of cyanoamide anions (*cf.* Ref's [3] and [7]).

In contrast to the formation of **9** from **1a**, formation of **3j** from **1b**, effected by essentially the same reagent, does not require the intermediacy of an aziridinone.

Neither does the formation of the glycocyamidines **3a**—**e** and **7**, obtained by reacting type **1** amides with *N-aryl-N*-cyanoamides require the intermediacy of aziridinones and, as has been shown earlier [3], the *cine* substitution products of type **2** are not formed through aziridinones either (*cf.* Ref's [8] and [9]).

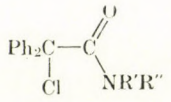

1

a: R′ = R″ = H
b: R′ = *t*-Bu, R″ = H
c: R′ = R″ = Me

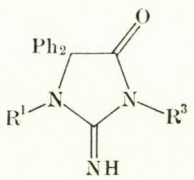

3

	R^1	R^3
a	Ph	H*
b	Ph	*t*-Bu
c	*m*-ClC_6H_4	*t*-Bu
d	*p*-$MeOC_6H_4$	*t*-Bu
e	*p*-MeC_6H_4	*t*-Bu
f	*t*-Bu	Et
g	*t*-Bu	$PhCH_2$
h	Et	*t*-Bu
i	$PhCH_2$	*t*-Bu
j	H	*t*-Bu*

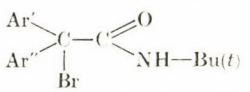

6

a: Ar′ = Ar″ = Ph
b: Ar′ = *p*-ClC_6H_4, Ar″ = Ph
c: Ar′ = Ar″ = *p*-ClC_6H_4

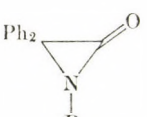

a: R = *t*-Bu
b: R = H

8

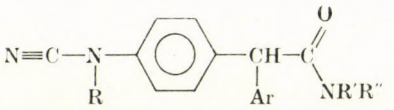

2

	R	Ar	R′	R″
a	Ph	Ph	H	H
b	Ph	Ph	*t*-Bu	H
c	Ph	Ph	Me	Me
d	*m*-ClC_6H_4	Ph	*t*-Bu	H
e	*p*-$MeOC_6H_4$	Ph	*t*-Bu	H
f	*p*-MeC_6H_4	Ph	*t*-Bu	H
g	Ph	*p*-ClC_6H_4	*t*-Bu	H

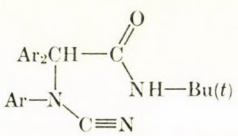

4

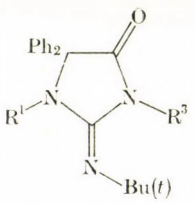

5*

a: R^1 = *t*-Bu, R^3 = H
b: R^1 = H, R^3 = *t*-Bu

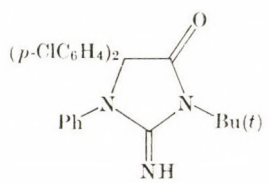

7

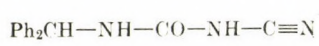

9

* Potentially tautomeric compound

The results obtained with the *N*-cyano-*N*-ethyl- and *N*-benzyl-*N*--cyanoamide anions and those obtained with *N*-aryl-*N*-cyanoamide anions as the reagents appear to be reasonable: while the type **1** chloroamides are rapidly converted into aziridinones (**8**) by the former, the less basic *N*-aryl-*N*-cyanoamide anions are, apparently, incapable of effecting such a transformation. As shown by the formation of **5a** and **9**, respectively, the *N*-(*t*-butyl)-*N*--cyanoamide and the unsubstituted cyanoamide anions are also capable of dehydrochlorinating type **1** chloroamides. The modes of formation, with the latter reagents, of compounds **5b** and **3j**, respectively, which, from a purely structural point of view, do not require the intermediacy of an aziridinone **8**, is less clear, because attack of nucleophiles at C(3) of the aziridinones* and direct α-attack on the corresponding chloroamides should lead to identical products. Although there is no conclusive evidence in favour of either of the two conceivable modes of formation of compounds **5b** and **3j**, we prefer the pathway leading through the intermediacy of the aziridinone **8a** since, if this were not the case, the absence of type **2** *cine* substitution products in these reactions could hardly be explained.

Experimental

Potassium N-cyanoamides

m-Chloro-*N*-cyanoaniline [10], *N*-cyano-*p*-anisidine [11], *N*-cyano-*p*-toluidine [4], *N*-cyanoethylamine [12], *N*-benzyl- [13] and *N*-(*t*-butyl)-*N*-cyanoamines [14] and *N*-cyanoaniline [15] were obtained as described in the literature and dissolved in an equivalent amount of 25% aqueous KOH. The solutions were evaporated to dryness, and the residues dissolved in MeOH. The small amounts of insoluble impurities occasionally present were filtered off, and the solutions were — if necessary, after treatment with charcoal — again evaporated to dryness. The crystalline residues were triturated with ether and filtered.

The monopotassium salt of cyanoamine was similarly obtained.

Reaction of 1b with potassium N-cyanoanilides

A solution of **1b** [3, 9] (1.0 g; 3.3 mmole) and potassium *m*-chloro-*N*-cyanoanilide, *N*-cyano-*p*-anisidide and *N*-cyano-*p*-toluidide, respectively, (9.9 mmoles, each) in anhydrous DMSO (10 ml) was allowed to stand 3 days at room temperature and poured into water (80 ml). The crystalline precipitates were taken up in dry benzene and dried by repeatedly distilling off the solvent to yield, in all three cases, oily residues.

The product of the *m*-chloro series was crystallized from EtOH to yield 41% of **2d**, m.p. 178—9 °C.

$C_{25}H_{24}ClN_3O$ (417.94). Calcd. Cl 8.48; N 10.05. Found Cl 8.94; N 9.84%.

NMR ($CDCl_3$): δ 7.5—7.1 m, 13H, ArH's; 4.88, s, 1H, Ar_2CHC  ; 1.36, s, 9H, *t*-Bu.

MS (70 eV, direct inlet, 160 °C): *m/e* 419 (1.6%); 417.1610 (5.0%, $C_{25}H_{24}N_3O^{35}Cl$, M); 320 (33%); 319 (36%), 318 (100%, M — *t*-BuNCO); 317 (66%, M — *t*-BuNHCO); 293 (31%); 291 (96%, 318—HCN); 283 (21%, 318—Cl); 166 (42%); 165 (66%); 57 (95%). Metastable transitions: 318 → 166; 318 → 291; 318 → 283; 166 → 165.

* For examples of such attacks see Ref. [4].

The ethanolic mother liquor of **2d** was evaporated to dryness and the resulting oil worked up by TLC (adsorbent: Kieselgel G, solvent: benzene–MeOH, 9 : 1) to yield 8% of **3c** [4].

The oily product of the *p*-methoxy series was crystallized from CCl_4 to yield 37% of **2e**, m.p. 104–5 °C (from CCl_4 or benzene–light petroleum).

$C_{26}H_{27}N_3O_2$ (413.52). Calcd. N 10.16. Found N 10.00%.

NMR ($CDCl_3$): δ 7.5–6.9, m, 13H, ArH's; 4.82, s, 1H, Ar_2CH-C(=O)–N<; 3.85, s, 3H, MeO; 1.33, s, 9H, *t*-Bu.

MS (70 eV, direct inlet, 150 °C): *m/e* 413.2108 (14%, $C_{26}H_{27}N_3O_2$, M); 314 (100%, M – *t*-BuNCO); 313 (66%, M – *t*-BuNHCO); 299 (1.5%, 314–CH_3); 298 (1.2%, 313–CH_3); 287 (68%, 314–HCN); 283 (4.5%, 314–CH_3O); 272 (11%, 287–CH_3); 166 (24%); 165 (36%); 57 (38%). Metastable transitions: 413 → 314; 314 → 287; 314 → 166.

The mother liquor of **2e** was worked up by TLC as above to yield 15% of **3d** [4].

The oily product obtained in the toluidine series was crystallized from benzene to yield 42% of **2f**, m.p. 148–9 °C.

$C_{26}H_{27}N_3O$ (397.52). Calcd. N 10.57. Found N 10.31%.

NMR ($CDCl_3$): δ 7.5–7.2, m, 13H, ArH's; 5.7, bs, 1H, NH; 4.87, s, 1H, Ar_2CH-C(=O)–N<; 2.4, s, 3H, (Ar)-Me; 1.33, s, 9H, *t*-Bu.

MS (70 eV, direct inlet, 150 °C): *m/e* 397.2150 (4.7%, $C_{26}H_{27}N_3O$, M); 298 (100%, M – *t*-BuNCO); 297 (57%, M – *t*-BuNHCO); 283 (3.7%, 298–CH_3), 271 (78%, 298–HCN); 166 (21%); 165 (34%); 57 (29%). Metastable transitions: 397 → 298; 298 → 271; 298 → 166.

The mother liquor of **2f** was worked up by TLC as above to yield an additional amount (26%) of **2f** and 5% of **3e** [4].

Reaction of 1b with potassium N-cyano-N-ethyl- and N-benzyl-N-cyanoamide

A solution of **1b** (1.0 g; 3.3 mmole) and the appropriate potassium *N*-cyanoamide (9.9 mmole) in anhydrous DMSO (10 ml) (heat was evolved during the preparation of the solution) was let to stand 3 days at room temperature, and poured into water (90 ml) to yield an oily precipitate in the ethyl, and a crystalline one in the benzyl series. The former was dried by azeotropic distillation with benzene and worked up by TLC (adsorbent: Kieselgel G, solvent: benzene–EtOAc, 8 : 2), while the latter was directly subjected to TLC (adsorbent as above, solvent: benzene–MeOH, 9 : 1).

0.56 g (50%) of **3f**, m.p. 139–40 °C (from gasoline) and 0.18 g (19%) of *N*-(*t*-butyl)-benzilamide [3], m.p. 134–5 °C, were obtained in the ethyl series, and 0.73 g (61%) of **3g**, m.p. 123–4 °C (from gasoline) was obtained in the benzyl series.

3f: $C_{21}H_{25}N_3O$ (335.45). Calcd. C 75.19; H 7.51; N 12.53. Found C 74.85; H 7.32; N 12.70%.

3g: $C_{26}H_{27}N_3O$ (397.52). Calcd. C 78.56; H 6.85; N 10.57. Found C 78.21; H 6.88; N 10.71%.

IR (KBr): **3f**, ν C=O 1715, ν C=N 1645; **3g**, ν C=O 1715, ν C=N 1645.

NMR ($CDCl_3$): **3f**, δ 7.7–7.3, m, 10H, ArH's; 6.15, q, 2H and 8.74, t, 3H, J = 7 Hz, Et; 1.28, s, 9H, *t*-Bu; **3g**, δ 7.7–7.1, m, 15H, ArH's; 4.79, s, 2H, $(Ph)CH_2$; 1.28, s, 9H, *t*-Bu.

Deimination of the glycocyamidines 3f and 3g

0.19 g (0.6 mmole) of **3f** and 0.20 g (0.5 mmole) of **3g**, respectively, were dissolved in AcOH (7 ml). An aqueous solution (4 ml) of $NaNO_2$ (1.0 g) was added at 60–80 °C by drops within about 20 min. The mixtures were boiled up, and hot water was added to yield, after cooling, 0.16 g (85%) of **1-(t-butyl)-3-ethyl-5,5-diphenylhydantoin,** m.p. 155–6 °C (from aqueous AcOH), and 0.17 g (85%) of **3-benzyl-1-(t-butyl)-5,5-diphenylhydantoin,** m.p. 121–2 C° (from aqueous AcOH).

1-(t-Butyl)-3-ethyl-5,5-diphenylhydantoin, $C_{21}H_{24}N_2O_2$ (336.44). Calcd. N 8.33. Found N 8.35%.

3-Benzyl-1-(t-butyl)-5,5-diphenylhydantoin, $C_{26}H_{26}N_2O_2$ (398.51). Calcd. N 7.03. Found N 7.07%.

IR (KBr): ν O=C–N–C=O 1750 + 1695, and 1750 + 1700 cm^{-1}, respectively.

For the mass spectra, see Ref. [1].

Reaction of 1b with potassium N-(t-butyl)-N-cyanoamide

1b (1.0 g; 3.3 mmole) and the potassium salt (1.35 g; 9.9 mmole) were dissolved in anhydrous DMSO (10 ml) (heat was evolved vigorously). The solution was kept for 3 days at room temperature and poured into water to yield a mixture of crystalline products. This was recrystallized from EtOH (10 ml) to obtain 0.31 g (26%) of **5a**, m.p. 150—1 °C.

The mother liquor was dried over $MgSO_4$ and evaporated to dryness. The oily residue was worked up by TLC (adsorbent: Kieselgel G, solvent; benzene–acetone, 9 : 1) to yield further 0.06 g (5%) of **5a**, 0.07 g (6%) of **5b**, m.p. 120—1 °C (from aqueous MeOH), and 0.29 g (31%) of *N*-(*t*-butyl)-benzilamide [3], m.p. 134—5 °C.

5a: $C_{23}H_{29}N_3O$ (363.51). Calcd. C 76.00; H 8.04; N 11.56. Found C 75.61; H 8.11; N 11.30%.

5b: $C_{23}H_{29}N_3O$ (363.51). Calcd. N 11.56. Found N 11.48%.

IR (KBr): ν C=O 1720, ν C=N 1635 cm^{-1} (for both **5a** and **5b**).

NMR ($CDCl_3$): **5a**: δ 7.8—7.3, m, 10H, ArH's; 1.67, s, 9H, *t*-Bu at exocyclic N; 1.25, s, 9H, 1-(*t*-Bu).

5b: δ 7.85—7.2, m, 10H, ArH's; 1.60 and 1.55, both s, 9H each, two *t*-Bu groups.

Reaction of 1b with monopotassium N-cyanoamide

A mixture of **1b** (2.0 g; 6.6 mmole), the potassium salt (1.6 g; 20 mmole) and anhydrous DMSO (10 ml) (heat was evolved during preparation of the solution) was allowed to stand 3 days at room temperature and poured into water (200 ml) to yield a crystalline product which was dried by repeated evaporations with dry benzene. The oily product resulting after the last evaporation was worked up by TLC (adsorbent: Kieselgel G, solvent: benzene–MeOH, 9 : 1) to yield 0.23 (12%) of **3j**, m.p. 149—50 °C (gasoline), and 0.19 g (10%) of *N*-(*t*-butyl)-benzilamide, m.p. 134—5 °C.

3j: $C_{19}H_{21}N_3O$ (307.40). Calcd. N 13.67. Found N 13.70%.

3j: IR (KBr): ν C=O 1730, ν C=N 1670 cm^{-1}.

NMR ($CDCl_3$): δ 7.5—7.25, m, 10H, ArH's; 4.55, bs, 2H, NH's; 1.63, s, 9H, 3-(*t*-Bu).

Synthesis of the bromoamides 6

(a) A mixture of diphenylacetyl chloride [16] (6.0 g; 26 mmole) and Br_2 (1.4 ml; 26 mmole) was heated at 120—130 °C. The colour of the Br_2 disappeared within about 15 min. Another portion of Br_2 (0.7 ml; 13 mmole) was added, and the mixture was again heated up and stirred for 1 hr at 130—140 °C. When triturated with light petroleum, the resulting oily α-bromodiphenylacetyl chloride turned crystalline (7.5 g).

4.5 g (14.5 mmole) of this product was dissolved in anhydrous CH_2Cl_2 (30 ml). At 0 °C a mixture of *t*-$BuNH_2$ (1.5 ml; 14.5 mmole), Et_3N (2.1 ml; 14.5 mmole) and anhydrous CH_2Cl_2 (20 ml) was added, under continuous stirring, within about 30 min. The solution was stirred for another hour and allowed to stand overnight. Next morning it was washed successively with water, 5% $NaHCO_3$, 1 *N* HCl and water, dried over $MgSO_4$ and evaporated to dryness. The residue was recrystallized from gasoline to yield 1.7 g of **6a**, heavily contaminated, according to the IR spectrum, with N-(*t*-butyl)-benzilamide. Evaporation of the filtrate to dryness furnished 1.3 g (24%) of oily **6a**.

(b) *p*-Chlorodiphenylacetic acid [17] (5.0 g; 20.4 mmole) was refluxed with $SOCl_2$ (15 ml) for 2 hrs. The excess reagent was distilled off, and the resulting oil was treated with Br_2 (1.09 + 0.5 ml; 20.4 + 9.1 mmole) at 140 °C as described under *(a)*. The crude α-bromoacid chloride was treated with charcoal in light petroleum. The solvent was distilled off and the resulting oil (5.6 g; 16.3 mmole) was treated in CH_2Cl_2 solution with *t*-$BuNH_2$ and Et_3N; the product was worked up as described under *(a)* to yield 3.4 g (44%) of **6b**.

(c) *p,p'*-Dichlorodiphenylacetic acid [18] was similarly converted into 54% of oily **6c**.

The α-bromoamides **6a—c** were used without further purification for the reaction with potassium N-cyanoanilide.

Reaction of the α-bromoamides 6 with potassium N-cyanoanilide

(a) A solution of **6a** (1.3 g; 3.7 mmole) and potassium N-cyanoanilide (1.7 g; 11 mmole) in anhydrous DMSO (15 ml) was allowed to stand for 3 days and poured into water to yield a viscous oil. The aqueous layer was decanted, and the oil was treated with Et_2O to yield 0.08 g of crystalline **2b**, identified by comparison with an authentic sample [2, 3]. Work-up of the filtrate by TLC furnished another 0.17g(total yield 17%) of **2b**, m.p. 141—2 °C.

(b) A solution of **6b** (1.0 g; 2.6 mmole) and potassium *N*-cyanoanilide (1.2 g; 7.8 mmole) in anhydrous DMSO (10 ml) was allowed to stand for 1 month and poured into water (90 ml) to yield a very fine precipitate which could not be separated by filtration and was therefore isolated by extraction with ether (2 portions, 50 ml, each). The ether solution was washed with water (3 portions, 50 ml, each), dried over $MgSO_4$ and evaporated to dryness to yield an oily residue which was triturated with light petroleum and recrystallized from light petroleum containing a few drops of benzene. Yield: 0.24 g (22%) **2g**, m.p. 173—4 °C.

$C_{25}H_{24}ClN_3O$ (417.94). Calcd. C 71.85; H 5.79; Cl 8.48; N 10.05. Found C 71.74; H 5.79; Cl 8.11; N 10.20 and 9.75%.

IR (KBr): ν C=O 1635 cm^{-1}.

NMR ($CDCl_3$): δ 7.5—7.2, m, 13H, ArH's; 4.74, s, 1H, $Ar_2CH-C(=O)-N<$; 1.34, s, 9H, *t*-Bu.

MS (70 eV, direct inlet, 150 °C): *m/e* 419 (0.9%); 417.1605 (3.1%, $C_{25}H_{24}N_3O^{35}Cl$, M); 320 (33%); 319 (36%); 318 (100%, M—*t*-BuNCO); 317 (57%, M—*t*-BuNHCO); 293 (23%); 291 (64%, 318—HCN); 283 (11%, 318—Cl); 282 (7.5%, 318—HCl); 257 (7.6%); 201 (2.5%); 200 (3.2%); 199 (4.1%); 165 (39%); 57 (68%). Metastable transitions: 318 → 291; 318 → 283; 318 → 200; 200 → 165.

(c) A solution of **6c** (1.3 g; 3.1 mmole) and potassium N-cyanoanilide (1.45 g; 9.3 mmole) in anhydrous DMSO (10 ml) was allowed to stand for 1 month and poured into water (90 ml). The crystalline precipitate was dried by repeatedly evaporating its benzene solutions. The oily residue (1.3 g) of the last evaporation was worked up by TLC (adsorbent: Kieselgel G, solvent: cyclohexane–EtOAc, 8 : 2) to yield 0.41 g (29%) of **7**, m.p. 192—3 °C (from EtOH).

$C_{25}H_{23}Cl_2N_3O$ (452.39). Calcd. C 66.38; H 5.12; N 9.29. Found C 66.71; H 5.32; N 9.28%.

IR (KBr): ν C=O 1725, ν C=N 1635 cm^{-1}.

NMR ($CDCl_3$): δ 3.3, s, 13H, ArH's; 1.80, s, 9H, 3-(*t*-Bu).

MS (70 eV, direct inlet, 170 °C): *m/e* 453 (3.8%); 451.1837 (5.9%, $C_{25}H_{23}N_3O^{35}Cl_2$, M); 397 (67%); 395 (100%, M—C_4H_8); 366 (1.4%, 395—CHO); 352 (1.2%, 395—CNOH); 328 (35%); 326 (53%, 395—C_2N_2OH); 320 (3.1%); 318 (5.4%, 395—Ph·); 292 (1.4%); 290 (4.2%, 326—HCl); 277 (2.1%); 275 (3.6%, 352—Ph·); 250 (1.1%, 318—C_2N_2O); 237 (4.2%); 236 (3.0%); 235 (8.5%, $[^{35}ClC_6H_4]_2C^+H$); 234 (3.8%); 216 (8.9%); 214 (25%, 250—HCl); 201 (8.2%); 199 (24%, 235—HCl); 164 (3.5%). Metastable transitions: 395 → 326; 395 → 318; 250 → 214; 235 → 199; 199 → 164.

*

The authors are indebted to Mrs. I. BALOGH-BATTA and staff for the microanalyses and to Dr. P. KOLONITS and staff for the IR and NMR spectra.

REFERENCES

[1] TAMÁS, J., CZIRA, G., SIMIG, GY., LEMPERT, K.: Organic Mass Spectrom. **10,** 390 (1975)
[2] LEMPERT, K., SIMIG, GY., VEZÉR, SZ.: Tetrahedron Letters **1972,** 805
[3] SIMIG, GY., LEMPERT, K.: Tetrahedron **31,** 983 (1975)
[4] SIMIG, GY., LEMPERT, K., TAMÁS, J., CZIRA, G.: Tetrahedron **31,** 1195 (1975)
[5] *(a)* BREUER, E., BERGER, T., SAREL, SH.: Chem. Communications **1968,** 1597; *(b)* LENGYEL, I., SHEEHAN, J. C.: Angew. Chem. **80,** 27 (1968); and earlier references cited.
[6] LEMPERT, K., PUSKÁS, J., VEZÉR, SZ.: Acta Chim. Acad. Sci. Hung. **67,** 369 (1971)
[7] LEMPERT, K., PUSKÁS, J.: Periodica Polytechn. Budapest, Ser. Chem. Engng. **12,** 123 (1968)
[8] NAGARAJAN, K., KULKARNI, C. L., VENKATESWARLU, A.: Tetrahedron Letters **1968,** 1387
[9] NAGARAJAN, K., KULKARNI, C. L.: Tetrahedron Letters **1968,** 2717
[10] SRINIVAS, K. S., GUPTA, R. D.: Current Sci. (India) **22,** 45 (1953); Chem. Abstr. **48,** 4456c (1954)
[11] HUNTER, L., REES, H. A.: J. Chem. Soc. **1945,** 617
[12] AINLEY, A. D., CURD, F. H. S., ROSE, F. L.: J. Chem. Soc. **1949,** 101
[13] KOVÁCS-NAGY, H., THOMSON, A. J., HORWITZ, J. P.: J. Am. Chem. Soc. **82,** 1609 (1960)

[14] MUKAIYAMA, T., OHISHI, SH., TAKAMURA, H.: Bull. Chem. Soc. Japan **27**, 416 (1954); Chem. Abstr. **49**, 10210h (1955)
[15] BAUM, F.: Ber. Dtsch. Chem. Ges. **41**, 524 (1908)
[16] STAUDINGER, H.: Ber. Dtsch. Chem. Ges. **44**, 1620 (1911)
[17] FORD MOOR, A. H.: J. Chem. Soc. **1947**, 952
[18] VOEGTLI, K., LÄNGER, P.: Helv. Chim. Acta **38**, 46 (1955)
[19] SIMIG, GY., LEMPERT, K., TAMÁS, J.: Tetrahedron **29**, 3571 (1973)

Gyula SIMIG
Károly LEMPERT } H-1521 Budapest, Gellért tér 4.

József TAMÁS
Gábor CZIRA } H-1525 Budapest, Pusztaszeri út 57—69.

Acta Chimica Academiae Scientiarum Hungaricae, Tomus 90(1), pp. 103—108 (1976)

SPECTROFLUOROMETRIC DETERMINATION OF 2,3-BENZFLUORENE (11H-BENZO/b/ FLUORENE) IN AIR POLLUTION

I. HORNYÁK

(Research Institute for Technical Physics of the Hungarian Academy of Sciences)

Received October 1, 1975

Fluorescence properties of 2,3-benzfluorene (BF) found in air-borne pollutants were studied in solutions and on Whatman paper. If 2,3-BF is dissolved in ethanol, the fluorescent emission occurs in the UV range; at 77 °K temperature the so-called 'blue shift' effect and the rearrangement of the band structure are observed. If 2,3-BF is adsorbed on Whatman paper the fluorescent emission is shifted towards the longer wavelengths. The concentration of 2,3-BF dissolved in ethanol was determined spectrofluorometrically in the 10^{-8}—10^{-5} M range. A method, based on the sensitized luminescence effect was developed to determine the quantity of 2,3-BF adsorbed on Whatman paper.

1. Introduction

There are a lot of aromatic hydrocarbons present in automobil and other exhaust gases polluting the atmosphere. In the polluted air several hard carcinogen agents were isolated and identified [1, 2]. For separation of these compounds chromatographic methods have been applied [3—6]. Qualitative investigations provide evidence that among these compounds 2,3-BF is frequently present, too. Upon UV illumination this compound emits a strong fluorescent light. The emission occurs in the UV range, therefore direct observation of the compound following the chromatographic separation is not possible. However, based on the characteristic fluorescent spectrum, there is an easy way to identify and determine this compound if a fluorescence spectrophotometer is employed [7—9].

2. Experimental

Analytical grade 2,3-benzfluorene and naphthacene of FERAK was used throughout the experiments. Analytical grade benzene and ethanol were purchased from REANAL (Hungary) and redistilled before use.

Measurements were carried out on a Hitachi MPF-2A spectrofluorimeter, equipped with a correction attachment. For measurements at the temperature of liquid nitrogen, the phosphorescence accessory was employed. The excitation source was a 150 W Xenon arc lamp and the detector an R 136 photomultiplier.

The fluorescence spectra were taken of 10^{-5} *M* 2,3-BF in ethanol. The excitation and fluorescence spectra of solutions were recorded both at room and 77 °K temperatures. A bandwidth of 1.5 nm was chosen for taking the spectra. The excitation wavelength was at room temperature 316 nm and at 77 °K 319 nm, while the emission was recorded at 359

nm and 339 nm, respectively. The calibration curve was obtained at constant slit widths with a 1 cm fluorescence-free cuvette, read off the 2,3-BF fluorescence intensity in the 10^{-8}—10^{-5} M range. The excitation and emission monochromators were set at 316 nm, and 342 nm respectively.

10^{-3} M 2,3-BF solution in benzene was prepared and a Whatman paper stripe was immersed into this solution. The solvent was evaporated and about 10—15 minutes later the excitation and the fluorescence spectra were recorded both at room temperature and the Dewar vessel of phosphorescence accessory was used.

The excitation wavelength selected was at 328 nm, the emission was recorded at 419 nm. For measurements of sensitized luminescence of naphthacene, $3 \cdot 10^{-5}$—10^{-3} M 2,3-BF solutions; containing $3 \cdot 10^{-8}$ M naphthacene, were prepared. Whatman 1 paper stripes were immersed into the solutions, the solvent was allowed to evaporate and 10 minutes later the fluorescence intensities of both the 2,3-BF and the naphthacene were measured. The excitation monochromator was set at 328 nm, the fluorescent intensities of 2,3-BF and naphthacene were read off at 396 nm and 491 nm, respectively.

3. Results

3.1. *Fluorescence spectra*

2,3-benzfluorene dissolved in ethanol emits a characteristic fluorescence spectrum of six bands in the UV range (Fig. 1). In fact, the character of the spectrum taken at 77 °K temperature is quite similar only the line structure of the bands is more apparent and the relative intensities of the bands are somewhat changed, as well as the peak maxima are shifted towards shorter wavelengths (Table I). The intensity values towards the lower frequencies strongly decrease.

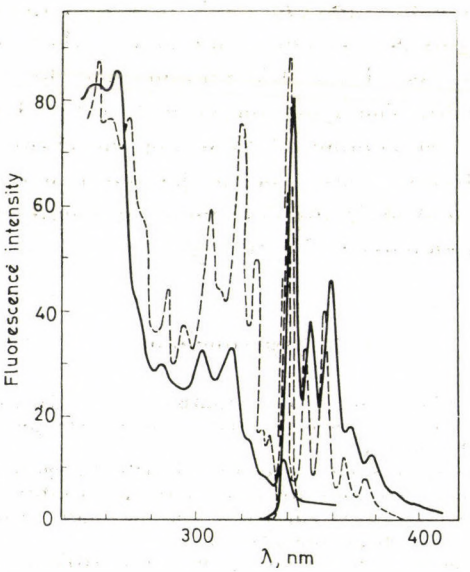

Fig. 1. Fluorescence excitation and emission spectra of 2,3-benzfluorene in ethanol solution; ———— at room temperature, — — — — at 77 K

Table I

Fluorescence excitation and emission maxima and peak intensities of the 2,3-benzofluorene

In ethanol at room temperature	Ex. maxima, nm	254	264	276	286	304	316.5	324	331	340				
	I.	96	100	46	35	38	39	30	10	14				
	Em. maxima, nm	342	350	359	368.5	378.5	390							
	I.	100	47	57	22	15	6							
In ethanol at 77 °K	Ex. maxima, nm	254	262	268	275	286	293	205	310	319	324	329	332	339
	I.	100	85	86	65	48	42	66	50	85	56	25	18	73
	Em. maxima, nm	339	348	356	366	376	388							
	I.	100	42	46	13	9	2							
On Whatman paper at room temperature	Ex. maxima, nm	282	300	313	328	342	355	369	390					
	I.	87	90	96	100	83	34	18	16					
	Em. maxima, nm	361	380	396	419	445	473							
	I.	21	16	100	84	33	10							
On Whatman paper at 77 °K	Ex. maxima, nm	280	300	314	330	337	343	357	370					
	I.	47	56	75	100	74	87	25	23					
	Em. maxima, nm	350	360	366	379.5	395	418	444	473					
	I.	12	98	39	47	100	68	27	10					

Ex.: excitation maxima, nm
Em.: emission maxima, nm
I.: intensity (in rel. units) and the values are normalized to the most intense peaks

However, comparing the excitation spectra, significant changes can be observed. The spectrum taken at 77 °K displays 13 bands compared with the 9 bands at room temperature; besides, a certain 'blue shift' can be noted,

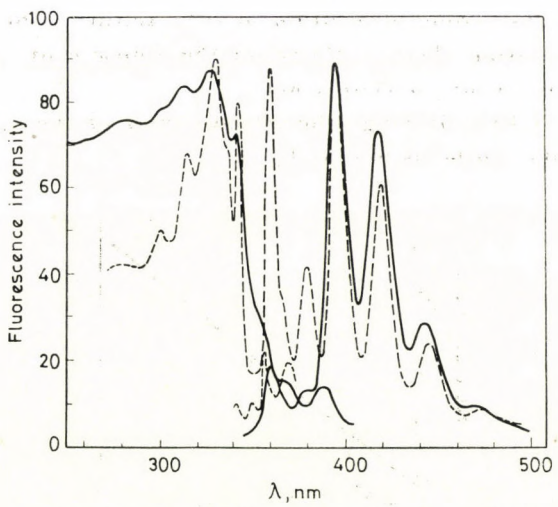

Fig. 2. Fluorescence excitation and emission spectra of 2,3-benzfluorene on Whatman paper; ——— at room temperature, — — — — at 77° K

too. With the appearance of the new bands the intensity ratios are significantly changed and there is a strong increase at the longer-wavelength side of the spectrum.

The 2,3-BF, adsorbed on Whatman paper, emits a fluorescence spectrum of six bands strongly shifted towards the red wavelengths. The appearance of the whole spectrum is quite different from the spectrum taken of solutions, the bands are more broad, the highes intensities are found at the 3rd and 4th peaks. The bands are partly in the UV, partly in the visible range.

Significant changes can be observed in the fluorescent spectrum taken at 77 °K. Bands in the UV range display an enormous increase and two new bands appear at 350 nm and 366 nm, respectively (Fig. 2). The excitation spectrum recorded at room temperature shows a broad, diffuse structure of eight peaks, while at 77 °K the bands are more separated. The intensities are strongly decreased at the lower side and strongly increased at the higher wavelength side of the spectrum (Table I).

3.2. *Determination of the* 2,3-*BF concentration in solution*

2,3-BF dissolved in ethanol emits a very intense fluorescent light. 10^{-8}—10^{-5} *M* 2,3-BF solutions were prepared to determine the calibration curve. The excitation monochromator was set at 317 nm and the fluorescence intensities were measured at 343 nm.

The fluorescence intensity is proportional to the concentration in the 10^{-8}—10^{-5} *M* range (Fig. 3). The lowest detectable concentration is 10^{-8} *M* corresponding to about a 2 ng/ml value. The fluorescence intensity strongly decreases with increasing concentrations above the 10^{-5} *M* value. This can be attributed to the strong absorption of the exciting light, as it is totally absorbed in the surface layers, therefore the fluorescent intensity rapidly decreases with increasing concentrations.

In the 10^{-8}—10^{-5} *M* range the relative error of the 2,3-BF concentration measurements can be as low as 1%.

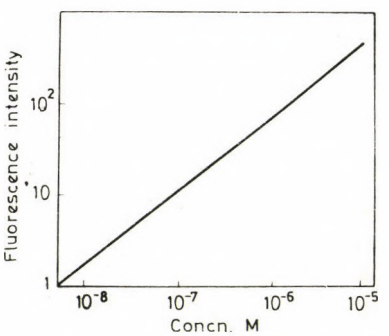

Fig. 3. Fluorescence analytical curve for 2,3-benzfluorene

3.3. *Determination of the* 2,3-*BF by sensitized luminescence*

The luminescence of naphthacene can be sensitized built into the 2,3-BF crystal lattice. If this mixed crystal is excited at the absorption band of the 2,3-BF, one part of the absorbed energy is transferred to the naphthacene molecule by radiationless transition. The system emits a complex spectrum consisting of the 2,3-BF and of the naphthacene characteristic spectra (Fig. 4). On the shorter wavelength side of the spectrum, the significant

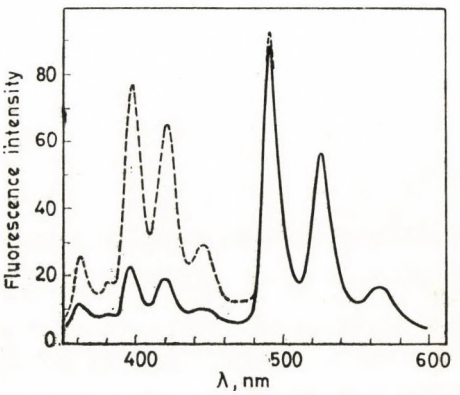

Fig. 4. Change in sensitized fluorescence intensity of 2,3-benzfluorene–naphthacene system on Whatman paper. Conc. of 2,3-benzfluorene ——— $3 \cdot 10^{-3}$ *M*, — — — — $5 \cdot 10^{-3}$

2,3-BF peaks — 361, 380, 396, 419 and 445 nm — can be seen. Due to its low intensity, the 2,3-BF band at 473 nm can not be seen separately from the naphthacene band. Bands on the longer wavelength side of the spectrum belong to the naphthacene fluorescence. The spectrum consisting of three maxima at 491, 527 and 566 nm represents the characteristic sensitized naphthacene fluorescence emission.

The radiationless energy transfer greatly reduces the intensity of the 2,3-BF fluorescence radiation and enhances that of the naphthacene. Due to the sensitized luminescence, the quantum efficiency of naphthacene is increased to unity from as low as 0.002.

Intensities of both of the 2,3-BF and of the naphthacene were found to change proportionaly with increasing 2,3-BF concentration. The intensity values were taken at 396 nm (I_{BF}^{396}) and 491 nm (I_{N}^{491}) for 2,3-BF and naphthacene, respectively. The rates of the intensity values of the components were plotted versus the 2,3-BF concentration (Fig. 5). From the calibration curve obtained it is possible to determine the 2,3-BF concentration in the $3 \cdot 10^{-5}$—10^{-3} *M* range. Above the $5 \cdot 10^{-4}$ *M* value, there is a deviation from the

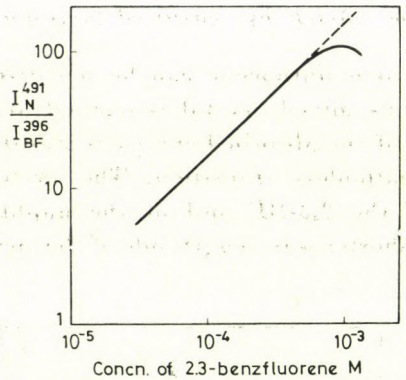

Fig. 5. Ratio of the fluorescence intensity of 2,3-benzfluorene–naphthacene versus 2,3-benzfluorene

linear relationship, due to the fact that the donor–acceptor concentration ratio results a change of the sensitized luminescence mechanism.

The relative deviation of the parallel measurements was always found to be about the 1—2 per cent.

REFERENCES

[1] Sawicki, E., Stanley, T. W., Elbert, W. C., Pfaff, J. D.: Anal. Chem. **36,** 497 (1964)
[2] Lane, D. A., Moe, H. K., Katz, M.: Anal. Chem. **45,** 1776 (1973)
[3] Sawicki, E.: Talanta **16,** 1231 (1969)
[4] Sawicki, E., Stanley, T. W., Elbert, W. C., Morgan, M.: Talanta **12,** 605 (1965)
[5] Sawicki, E., Stanley, T. W., Johnson, H.: Microchem. J. **8,** 257 (1964)
[6] Bergmann, E. D., Gruenwald, T.: J. Appl. Chem. **7,** 15 (1957)
[7] Porro, T. J., Anacreon, R. E., Flandreau, P. S., Fagerson, I. S.: J.A.O.A.C. **56,** 607 (1973)
[8] Matsushita, H.: Neutyo Kyokai-Shi **51,** 25 (1972)
[9] McKay, J. F., Latham, D. R.: Anal. Chem. **44,** 2132 (1972)
[10] Hornyák, I.: Anal. Chim. Acta **52,** 169 (1970)

István Hornyák; H-1325 Budapest, Újpest L., P.O. Box 76.

Acta Chimica Academiae Scientiarum Hungaricae, Tomus 90(1), pp. 109—110 (1976)

THERMALLY INDUCED REACTIONS OF IMIDAZOLE DERIVATIVES, VI*

REARRANGEMENT OF 2,4,4,5-TETRAPHENYL-4*H*-IMIDAZOLE

(SHORT COMMUNICATION)

GY. DOMÁNY** and J. NYITRAI

(Department of Organic Chemistry, Technical University, Budapest)

Received December 2, 1975

2,2,4,5-Tetraphenyl- (**1**) [2] and related 2,2-disubstituted 4,5-diphenyl--2*H*-imidazoles [2, 3] are thermally rearranged into their aromatic isomers, *viz.* the corresponding 1,2-disubstituted 4,5-diphenylimidazoles. Similarly to the related van Alphen rearrangements of 3,3-disubstituted 3*H*-pyrazoles [4], these reactions are thought to be concerted but not necessarily synchronous sigmatropic [1, 5] phenyl shifts [3].

We wish to report now that 2,4,4,5-tetraphenyl-4*H*-imidazole (**3**) [5] is similarly rearranged thermally into 1,2,4,5-tetraphenylimidazole (**2**) [6]. After heating for 1 hr at 300 °C the 4*H*-imidazole **3** was, according to TLC (Kieselgel $PF_{254+366}$, Merck; solvent: benzene; detection: UV light), completely converted into a single product which proved identical (m.p. and lit. [6] m.p.: 215 °C; mixed m.p., IR spectra) with an authentic sample of the imidazole **2**. The yield of recrystallized (*n*-BuOH) product was 60%.

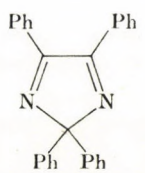

1

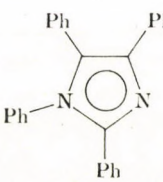

2

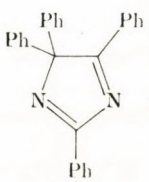

3

The mass spectra (AEI-MS-902, 70 eV, direct insertion, 170 °C) of the compounds **1**—**3** are shown in Table I. Those of the non-aromatic compounds **1** and **3** are rather similar, but differ considerably from that of the aromatic compound **2**, indicating that, under the mass spectroscopic conditions applied, rearrangement of compounds **1** and **3** into compound **2** does not take place.

*

The authors are grateful to Dr. J. TAMÁS for the mass spectra.

* For Part V, see Ref. [1]

** Chinoin Pharmaceutical and Chemical Works research fellow, 1973—1975

Table I

Mass spectra of compounds **1—3**
(AEI-MS-902, 70 eV, direct insertion, 170 °C)

m/e	I %			
	1	**2**	**3**	
372	10	*100*	13	$M^{+}\cdot$
371	2.0	34	3.3	$(M-H)^{+}$
295	0.26	0.4	0.08	$(M-Ph)^{+}$
294		0.75		
269	*100*	5.2	*100*	$(M-PhCN)^{+}$
268		4.0		
267		4.5		
241		0.8		
190	0.55	1.4	0.44	
186	2.3	6.2	1.0	M^{++}
176	0.5		0.38	
166	44	13	41	$(M-PhCN-PhCN)^{+}$
165	57	33	52	$C_{13}H_{9}^{+}$
139	1.1		1.0	
134.5	1.0		1.1	269^{++}
133.5		2.3		267^{++}
115	1.0		0.76	
103	2.0		2.5	$(PhCN)^{+}\cdot$
89	3.6	3.0	1.0	
77	0.9	7.2	0.9	Ph^{+}

REFERENCES

[1] KOLTAI, E., NYITRAI, J., LEMPERT, K., BURSICS, L.: Chem. Ber. **107,** 1649 (1974)
[2] WEISS, M.: J. Am. Chem. Soc. **74,** 5193 (1952)
[3] HILL, J. H. M., FOGG, T. R., GUTTMANN, H.: J. Org. Chem. **40,** 2562 (1975)
[4] LEMPERT-SRÉTER, M., LEMPERT, K.: Tetrahedron **31,** 1667 (1975) and earlier references cited therein.
[5] WHITE, D. M., SONNENBERG, J.: J. Org. Chem. **29,** 1926 (1964)
[6] EVEREST, A. E., MCCOMBIE, H.: J. Chem. Soc. **99,** 1762 (1911)

György DOMÁNY, H-1045 Budapest, Tó u. 1—5.
József NYITRAI, H-1521 Budapest, Gellért tér 4.

INDEX

PHYSICAL AND INORGANIC CHEMISTRY

Calculation of the π-Electronic Structure and Spectra of Halopyridines by the MIM and PPP Methods, A. MARTIN 1

Static Dielectric Properties of Binary Liquid Mixtures Containing tri-*n*-Butylamine, J. LISZI 21

Studies on the Reaction Between Cu(II) Acetate and Sulphate and Some Acid Hydrazides, F. I. M. TAHA, M. N. H. MOUSSA, A. M. SHALLABY, M. M. MOSTAFA 33

Investigation of the Dimerization of some Organic Acids in Non-aqueous Solvents, L. BARCZA, L. GYEPES, K. KELEMEN 43

ORGANIC CHEMISTRY

The Base-Catalyzed Dimerization of 2-Arylidenecyclohexanones, GY. OSZBACH, D. SZABÓ, M. E. VITAI 51

Rearrangement and Dissociation Processes in Tricyclic Phthalazinone Derivatives upon Electron Impact, P. BRUCK, J. TAMÁS, K. KÖRMENDY 59

Reactions of Hexahydro-1,3,5-Triacryloyl-*s*-Triazine, G. VALK, M. KAMEL, N. Y. ABOU-ZEID 69

Chemistry of 1,3-Bifunctional Compounds, XVIII. Preparation of the Esters of Various Amino Alcohols, K. FELFÖLDI, Á. MOLNÁR, M. BARTÓK 75

The Reaction of *N*-(*t*-Butyl)-α-Halo-α,α-Diarylacetamides with Cyanoamide and Mono-substituted Cyanoamide Salts, GY. SIMIG, K. LEMPERT, J. TAMÁS, G. CZIRA 93

Spectrofluorometric Determination of 2,3-Benzfluorene (11H-Benzo/b/ Fluorene) in Air Pollution, I. HORNYÁK 103

Thermally Induced Reactions of Imidazole Derivatives, VI. Rearrangement of 2,4,4,5-Tetraphenyl-4*H*-imidazole, (Short communication) GY. DOMÁNY, J. NYITRAI 109

Printed in Hungary

A kiadásért felel az Akadémiai Kiadó igazgatója — Műszaki szerkesztő: Zacsik Annamária

A kézirat nyomdába érkezett: 1976. IV. 1. — Terjedelem: 9,80 (A/5) ív, 61 ábra

76.3019 Akadémiai Nyomda, Budapest — Felelős vezető: Bernát György

ACTA CHIMICA

ТОМ 90 – ВЫП. 1

РЕЗЮМЕ

Расчет П-электронных спектров и электронной структуры галогенпиридинов с помощью методов MIM и PPP

А. МАРТИН

π-электронные спектры и электронная структура галогенпиридинов были рассчитаны с помощью методов Молекул в Молекулах (MIM) и Паризер—Парр—Попла (PPP).

При расчетах методом MIM для определения энергий переноса заряда были использованы приближения точечного заряда, шарового заряда и приближение Матага-Нишимото. Для расчета одноцентровых интегралов отталкивания были испробованы различные литературные значения ионизационных потенциалов и электроотрицательностей. Последние были выбраны на основе сравнения расчетных данных с экспериментальными. Резонансный интеграл связи углерод-галоген был принят в качестве изменяемого параметра. На основе результатов, полученных для энергии перехода и волновых функций, для расчета двухцентровых резонансных интегралов наиболее подходящим оказалось приближение Матага-Нишимото.

Для расчета методом PPP было использовано приближение Матага-Нишимото. Оптимум резонансного интеграла (β_{CX}) был определен с помощью изменения β_{CX}. Были рассчитаны энергии сингулетного возбуждения, матрицы плотности заряда — порядка связи, осцилляторные силы и направления поляризации.

Статические диэлектрические свойства бинарных жидких смесей, содержащих три-н-бутиламин

Й. ЛИСИ

Были исследованы статические диэлектрические свойства и плотность бинарных смесей, содержащих три-н-бутиламин. Исследования проводились при 20°C и в зависимости от состава смеси. Партнеры аминов в смесях были выбраны так, чтобы их полярность сильно различалась. Смесь состояла из следующих трех компонентов: н-гептан, хлороформ и ацетон. На основе проведенных исследований дается ответ на вопрос: возникают ли специальные интермолекулярные взаимодействия между амином и вторым компонентом, ведущие к ассоциации.

Исследование реакции ацетата и сульфата меди(II) с некоторыми гидразидами кислот

Ф. И. М. ТАХА, М. Н. Х. МОУСА, А. М. ШЕЛЕБАЙ и М. М. МОСТАФА

Ацетат и сульфат меди(II) реагируют со всеми исследованными гидразидами, давая моно- и/или бис-лигандные комплексы. В случае ацетатных комплексов с помощью ИК спектроскопии было обнаружено моноклешневое координирование лиганда через группу NH_2. Спектральные и магнитные измерения указывают на то, что ацетатные комплексы имеют либо октаэдрическую, либо тетраэдрическую структуру.

Димеризация некоторых органических кислот в неводных растворах

Л. БАРЦА, Л. ДЬЕПЕШ и К. КЕЛЕМЕН

В бензоле бензойная кислота образует гораздо более стабильные димеры, нежели алифатические кислоты. Особенно сильно проявляется это различие при сравнении с н- и изо-масляной кислотой. Криоскопические измерения (при $5{,}2 \pm 0{,}4°C$) димеризационных постоянных приводят к следующим значениям (величины даны в порядке согласно вышеперечисленным кислотам): 1700, 390, 239 и 453 кг/моль.

С помощью ИК спектроскопии было установлено, что способность растворителей к образованию водородных мостиков оказывает сильное влияние на димеризацию бензойной кислоты. Были исследованы следующие растворители (в скобках указаны димеризационные постоянные при $42 \pm 2°C$): четыреххлористый углерод (1530), бензол (261), 1,4-диоксан (20,0) и хлороформ (13,7).

В обоих рядах измерений однозначно было доказано, что в изученном интервале концентраций ($< 0{,}25$ М) протекает лишь димеризация и образованием более высоких полимеров можно пренебречь.

О димеризации 2-арилиденциклогексанонов, катализированной основаниями

ДЬ. ОСБАХ, Д. САБО и М. Э. ВИТАИ

2-Арилиденциклогексаноны в основных средах димеризуются до 1, 2, 3, 4, 4a, 5, 6, 7, 8, 9a-декагидро-5-арилиден-9-арил-4a-гидроксиксантена (IX*a—e*). Строение подтверждалось на основе ИК, УФ и ЯМР спектров. Приводится возможный механизм реакции.

Процессы перегруппировки и диссоциации в производных трициклических фталазинонов под влиянием электронной бомбардировки

П. БРУК, Й. ТАМАШ и К. КЁРМЕНДИ

С помощью масс-спектрометрического метода низкого и высокого разрешения были исследованы процессы диссоциации и перегруппировки, протекающие под влиянием электронной бомбардировки производных фталазинона (I—IV). Используя метод, основанный на определении энергии активации метастабильных процессов распада, было доказано, что в ходе отдельных процессов фрагментации происходит миграция метилена.

Исследование реакций гексагидро-1,3,5-триакрилоил-симм-триазина

Г. ВАЛЬК, М. КАМЕЛЬ и Н. Й. АБОУ-ЗЕЙД

Описываются некоторые интересные результаты, связанные с реакциями гексагидро-1,3,5-триакрилоил-*симм*-триазина с некоторыми реагентами. Весьма пригодной для выяснения пути бромирования, присоединения этилмеркаптана, воды, бисульфита натрия и/или сульфита натрия оказалась тонкослойная хроматография.

Химия 1,3-бифункциональных соединений, XVIII

Получение различных эфиров 1,3-аминоспиртов

К. ФЕЛЬФЛЬЁДИ, А. МОЛЬНАР и М. БАРТОК

Приводится получение производных различных аминоалкильных эфиров. В зависимости от строения соединения были разработаны и применены различные синтетические методы. Большинство соединений проявляет местноанестезирующее действие, а меньшая часть проявляет периферическое сосудорасширяющее действие.

Реакция N-(трет-бутил)-α-гало-α,α-диарилацетамидов с цианамидом и монозамещенными солями цианамида

ДЬ. ШИМИГ, К. ЛЕМПЕРТ, Й. ТАМАШ и Г. ЧИРА

При сплавлении N-(*трет*-бутил)-α-гало-α,α-дифенилацетамидов (*1b*) и *6a—c* с монокалийной солью цианамида и ее N-алкильными, N-аралкильными и N-арильными производными образуется большое число различных продуктов, таких как продукты *cine*-замещения *2b*, *2d—g*, 3-(*трет*-бутил)-гликоциамидины *3b—e*, *3j*, *5b* и *7* и *1*-(*трет*-бутил)-гликоциамидины *3f—g* и *5a*. Последние, очевидно, образуются через промежуточный азиридинон *8a*. Была обсуждена связь между типами различных цианамидных анионов и типами продуктов, а также спектральных свойств последних, в особенности тех, которые являются важными для определения структуры.

Спектрофлуорометрическое определение 2,3-бензфлуорена (11Н-бензо/b/флуорена) в воздушных загрязнениях

И. ХОРНЯК

Флуоресцентные свойства 2,3-бензфлуорена (2,3-БФ), обнаруженного в загязнениях воздушного происхождения, были исследованы в растворе и на ватмановской бумаге. Если 2,3-БФ растворен в этаноле, то флуоресцентная эмиссия наблюдается в УФ области; при температуре 77°К наблюдался эффект т. наз. «синего сдвига» и перегруппировка в структуре полос. Если 2,3-БФ адсорбирован на ватмановской бумаге, то флуоресцентная эмиссия сдвигается в область более длинных дволн. Концентрация 2,3-БФ, растворенного в этаноле, была определена спектрофлуорометрически в области $10^{-8} \div 10^{-5}$ моль/л. Метод, основанный на чувствительном эффекте люминесценции, был разработан для количественного определения 2,3-БФ, адсорбированного на ватмановской бумаге.

The Acta Chimica publish papers on chemistry in English, German, French and Russian.

The Acta Chimica appear in volumes consisting of four parts of varying size, 4 volumes being published a year.

Manuscripts should be addressed to

Acta Chimica
H-1521 Budapest, Hungary

Correspondence with the editors should be sent to the same address.

The rate of subscription in $ 32.00 a volume.

Orders may be placed with "*Kultúra*" Foreign Trade Company for Books and Newspapers (H-1389 Budapest 62, P. O. B. 149. Account No. 218 10990) or with representatives abroad.

Les Acta Chimica paraissent en français, allemand, anglais et russe et publient des mémoires du domaine des sciences chimiques.

Les Acta Chimica sont publiés sous forme de fascicules. Quatre fascicules seront réunis en un volume (4 volumes par an).

On est prié d'envoyer les manuscrits destinés à la rédaction à l'adresse suivante:

Acta Chimica
H-1521 Budapest, Hongrie

Toute correspondance doit être envoyée à cette même adresse.

Le prix de l'abonnement est de $ 32,00 par volume.

On peut s'abonner à l'Entreprise pour le Commerce Extérieur de Livres et Journaux «*Kultúra*» (H-1389 Budapest 62, P. O. B. 149 Compte-courant No. 218 10990) ou à l'étranger chez tous les représentants ou dépositaires.

«*Acta Chimica*» издают трактаты из области химической науки на русском, французском, английском и немецком языках.

«*Acta Chimica*» выходят отдельными выпусками разного объема. 4 выпуска составляют один том. 4 тома публикуются в год.

Предназначенные для публикации рукописи следует направлять по адресу:

Acta Chimica
H-1521 Budapest, ВНР

По этому же адресу направлять всякую корреспонденцию для редакции.

Подписная цена — $ 32,00 за том.

Заказы принимает предпринятие по внешней торговле книг и газет «*Kultúra*» H-1389 Budapest 62, P. O. B. 149. Текущий счет № 218 10990) или его заграничные представительства и уполномоченные.

Reviews of the Hungarian Academy of Sciences are obtainable at the following addresses:

AUSTRALIA

C. B. D. Library and Subscription Service
Box 4886, G. P. O.
Sydney N. S. W. 2001

Cosmos Bookshop
145 Acland St.
St. Kilda 3182

AUSTRIA

Globus
Höchstädtplatz 3
A—1200 Wien XX

BELGIUM

Office International de Librairie
30 Avenue Marnix
1050-Bruxelles

Du Minde Entier
162 Rue du Midi
1000—Bruxelles

BULGARIA

Hemus
Bulvar Ruszki 6
Sofia

CANADA

Pannonia Books
P. O. Box 1017
Postal Station "B"
Toronto, Ont. M5T 2T8

CHINA

C N P I C O R
Periodical Department
P. O. Box 50
Peking

CZECHOSLOVAKIA

Mad'arská Kultura
Národní třida 22
115 66 Praha

PNS Dovoz tisku
Vinohradská 46
Praha 2

PNS Dovoz tlače
Bratislava 2

DENMARK

Ejnar Munksgaard
Nörregade 6
DK—1165 Copenhagen K

FINLAND

Akateeminen Kirjakauppa
P. O. Box 128
SF-00101 Helsinki 10

FRANCE

Office International de Documentation et Librairie
48, Rue Gay-Lussac
Paris 5

Librairie Lavoisier
11 Rue Lavoisier
Paris 8

Europeriodiques S. A.
31 Avenue de Versailles
78170 La Celle St. Cloud

GERMAN DEMOCRATIC REPUBLIC

Haus der Ungarischen Kultur
Karl-Liebknecht-Strasse 9
DDR—102 Berlin

Deutsche Post
Zeitungsvertriebsamt
Strasse der Pariser Kommüne 3—4
DDR-104 Berlin

GERMAN FEDERAL REPUBLIC

Kunst und Wissen
Erich Bieber
Postfach 46
7 Stuttgart 5

GREAT BRITAIN

Blackwell's Periodicals
P. O. Box 40
Hythe Bridge Street
Oxford OX1 2EU

Collet's Holdings Ltd.
Denington Estate
London Road
Wellingborough Northants NN8 2QT

Bumpus Haldane and Maxwell Ltd.
5 Fitzroy Square
London W1P 5AH

Dawson and Sons Ltd.
Cannon House
Park Farm Road
Folkestone, Kent

HOLLAND

Swets and Zeitlinger
Heereweg 347b
Lisse

Martinus Nijhoff
Lange Voorhout 9
The Hague

INDIA

Hind Book House
66 Babar Road
New Delhi 1

India Book House
Subscription Agency
249 Dr. D. N. Road
Bombay 1

ITALY

Santo Vanasia
Via M. Macchi 71
20124 Milano

Libreria Commissionaria Sansoni
Via Lamarmora 45
50121 Firenze

JAPAN

Kinokuniya Book-Store Co. Ltd.
826 Tsunohazu 1-chome
Shinjuku-ku
Tokyo 160—91

Maruzen and Co. Ltd.
P. O. Box 5050
Tokyo International 100—31

Nauka Ltd.-Export Department
2—2 Kanda
Jinbocho
Chiyoda-ku
Tokyo 101

KOREA

Chulpanmul
Phenjan

NORWAY

Tanum-Cammermayer
Karl Johansgatan 41—43
Oslo 1

POLAND

Węgierski Instytut Kultury
Marszalkowska 80
Warszawa

BKWZ Ruch
ul. Wronia 23
00—840 Warszawa

ROUMANIA

D. E. P.
Bucureşti

Romlibri
Str. Biserica Amzei 7
Bucureşti

SOVIET UNION

Sojuzpechatj — Import
Moscow

and the post offices in each town
Mezdunarodnaya Kniga
Moscow G—200

SWEDEN

Almqvist and Wiksell
Gamla Brogatan 26
S—101 20 Stockholm

A. B. Nordiska Bokhandeln
Kunstgatan 4
101 10 Stockholm 1 Fack

SWITZERLAND

Karger Libri AG.
Arnold-Böcklin-Str. 25
4000 Basel 11

USA

F. W. Faxon Co. Inc.
15 Southwest Park
Westwood, Mass. 02090

Stechert-Hafner Inc.
Serials Fulfillment
P. O. Box 900
Riverside N. J. 08075

Fam Book Service
69 Fifth Avenue
New York N. Y. 1003

Maxwell Scientific International Inc.
Fairview Park
Elmsford N. Y. 10523

Read More Publications Inc.
140 Cedar Street
New York N. Y. 10006

VIETNAM

Xunhasaba
32, Hai Ba Trung
Hanoi

YUGOSLAVIA

Jugoslavenska Knjiga
Terazije 27
Beograd

Forum
Vojvode Mišića 1
21000 Novi Sad

ACTA CHIMICA

ACADEMIAE SCIENTIARUM HUNGARICAE

ADIUVANTIBUS

V. BRUCKNER, GY. DEÁK, K. POLINSZKY,
E. PUNGOR, G. SCHAY, Z. G. SZABÓ

REDIGIT

B. LENGYEL

TOMUS 90 FASCICULUS 2

AKADÉMIAI KIADÓ, BUDAPEST

1976

ACTA CHIM. (BUDAPEST) ACASA 2 90 (2) 111–205 (1976)

ACTA CHIMICA

A MAGYAR TUDOMÁNYOS AKADÉMIA KÉMIAI TUDOMÁNYOK OSZTÁLYÁNAK IDEGEN NYELVŰ KÖZLEMÉNYEI

SZERKESZTI

LENGYEL BÉLA

TECHNIKAI SZERKESZTŐK

DEÁK GYULA és HARASZTHY-PAPP MELINDA

Az Acta Chimica német, angol, francia és orosz nyelven közöl értekezéseket a kémiai udományok köréből.

Az Acta Chimica változó terjedelmű füzetekben jelenik meg, egy-egy kötet négy füzetből áll. Évente átlag négy kötet jelenik meg.

A közlésre szánt kéziratok a szerkesztőség címére (1521 Bp., Műegyetem) küldendők. Ugyanerre a címre küldendő minden szerkesztőségi levelezés. A szerkesztőség kéziratokat nem ad vissza.

Megrendelhető a belföld számára az Akadémiai Kiadónál (1363 Budapest, pf. 24. Bankszámla 215 11488), a külföld számára pedig a Kultúra Könyv- és Hírlap-Külkereskedelmi Vállalatnál (1389 Budapest 62, pf. 149. Bankszámla: 218 10990) vagy külföldi képviseleteinél és bizományosainál.

Die Acta Chimica veröffentlichen Abhandlungen aus dem Bereich der chemischen Wissenschaften in deutscher, englischer, französischer und russischer Sprache.

Die Acta Chimica erscheinen in Heften wechselnden Umfanges. Vier Hefte bilden einen Band. Jährlich erscheinen 4 Bände.

Die zur Veröffentlichung bestimmten Manuskripte sind an folgende Adresse zu senden:

Acta Chimica
H-1521 Budapest

An die gleiche Anschrift ist auch jede für die Redaktion bestimmte Korrespondenz zu richten. Abonnementpreis pro Band: $ 32.00.

Bestellbar bei dem Buch- und Zeitungs-Außenhandels-Unternehmen »*Kultúra*« (1389 Budapest 62, P. O. B. 149. Bankkonto Nr. 218 10990) oder bei seinen Auslandsvertretungen und Kommissionären.

Acta Chimica Academiae Scientiarum Hungaricae, Tomus 90(2), pp. 111–117 (1976)

COMPLEX FORMATION BETWEEN MAGNESIUM, ZINC, CADMIUM AND ARSENAZO III

V. MICHAYLOVA

(Department of Analytical Chemistry, University of Sofia, 1126 Sofia, Bulgaria)

Received January 10, 1975
In revised form November 24, 1975

Spectrophotometric studies of the reactions of magnesium, zinc and cadmium with Arsenazo III are described. Complex formation was studied by a method based on the relationship $A = f(\mathrm{pH})$. Equimolar solutions and solutions containing a slight metal ion excess were used. A single chelate equilibrium was considered for magnesium and zinc complexes, whereas in the case of cadmium two successive reactions were assumed. The equilibrium and stability constants were calculated. The relationship between the solubility products of the metal hydroxides and the pH of the half-reaction is also given.

Arsenazo III (1,8-dihydroxynaphthalene-3,6-disulfonic acid-2,7 bis/(azo-2)-phenylarsonic acid takes part in complexation reactions with different functional groups, depending on the nature of the metal ions and the reaction conditions [1].

In our previous work the analytical use of the reactions of Arsenazo III with Mg^{2+}, Zn^{2+} and Cd^{2+} has been shown only [2, 3]. A more detailed examination of these complexation processes is described in the present paper. It is of interest to establish the nature of the bonding groups of the reagent and the structure of the metal complexes. In this connection the number of protons released upon complexation and the equilibrium constants were determined.

Experimental

Reagents

A $10^{-4}M$ solution of Arsenazo III (Fluka) was standarized spectrophotometrically by titration with a thorium(IV) nitrate solution at 600 nm and pH 3. $10^{-2}M$ solutions of the metal ions were standarized by EDTA titration. Solutions of lower concentrations were obtained by dilution. An ionic strength of 0.1 was maintained with sodium nitrate.

The pH was adjusted with dilute sodium hydroxide.

Apparatus

Visible spectra of the solutions were recorded on a Specord UV — visible Spectrophotometer (Zeiss). Spectrophotometric measurements were performed with Universal Spectrophotometer VSU-1 (Zeiss). The pH of the solutions was measured with an LPU-01 (USSR) pH-meter, using a glass electrode.

Results and discussion

Absorption spectra of Arsenazo III and its complexes with magnesium, zinc and cadmium are presented in Fig. 1. Complex formation was investigated at metal to ligand mole ratios of 1 : 1 and in the presence of a slight metal ion

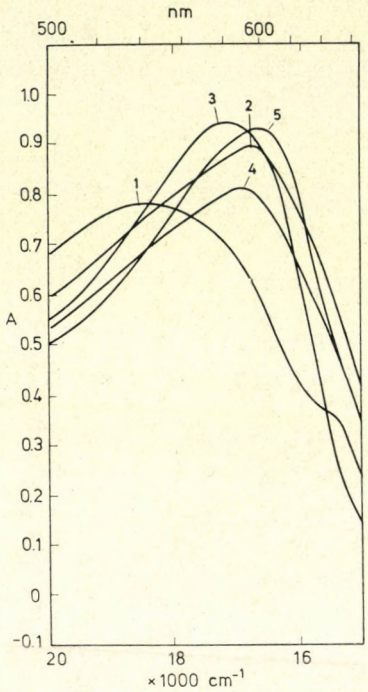

Fig. 1. Absorption spectres of arsenazo III and its complexes with magnesium, zinc and cadmium. $C_R = 2{,}17 \cdot 10^{-5}\ M$, pH 9,10 (borate buffer), 2-cm cells *vs.* water. (1) arsenazo III; (2) Mg complex, $C_{Mg} = 2{,}44 \cdot 10^{-5}\ M$; (3) Zn complex, $C_{Zn} = 2{,}34 \cdot 10^{-5}\ M$; (4) Cd complex, $C_{Cd} = 2{,}44 \cdot 10^{-5}\ M$; (5) Cd complex, pH 11,00.

excess. The method based on the relationship A = f(pH) was employed. On the S-shaped curves presented in Fig. 2 a single chelate equilibrium for magnesium and zinc is observed, whereas for the cadmium-Arsenazo III reaction two successive stages are evident. The different absorption spectra of cadmium complexes (Fig. 1) also show to this fact.

Equimolar solutions

The straight line portion of the S-shaped curves lies in the pH range of 6.2—8.5 for magnesium and zinc, and for the first stage of the cadmium-Arsenazo III reaction. Over this pH range, the H_3L^{5-} form predominates [4] and hence the following reaction should be considered:

$$M^{2+} + H_3L^{5-} \rightleftharpoons MH_{3-n}L^{2-(5+n)} + nH^+ \quad (1)$$

The number of protons released upon complexation and the equilibrium constant of this reaction were determined, using the expression

$$K_{eq} = \frac{(A-A_R)(A_0-A_R)[H^+]^n DF}{C(A_0-A)^2} \quad (2)$$

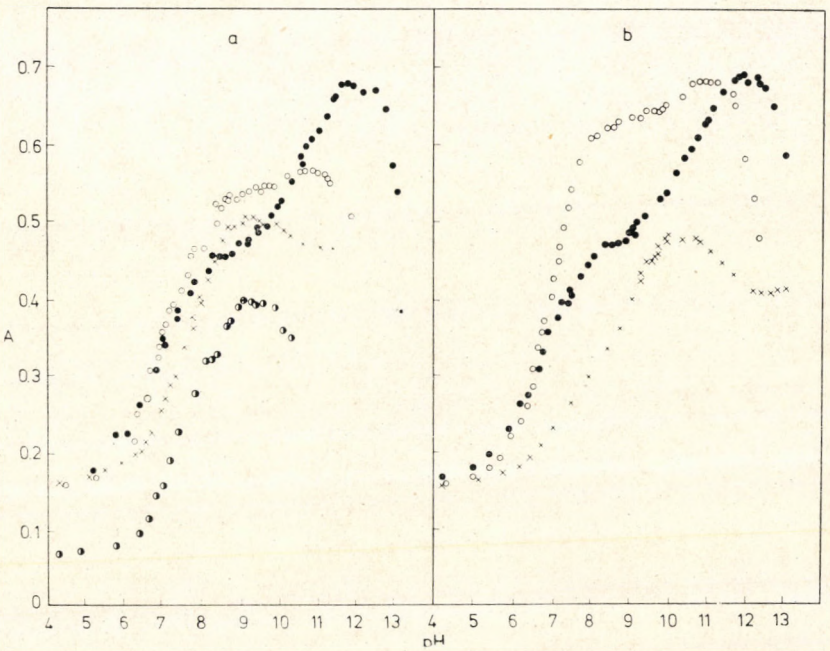

Fig. 2. pH-absorbance plots of arsenazo III complexes with magnesium, zinc and cadmium. a. ○ Zn complex $C_M = C_R = 2{,}17 \cdot 10^{-5}$ *M*, 610 nm; ● Cd complex $C_M = C_R = 2{,}49 \cdot 10^{-5}$ *M*, 610 nm; × Mg complex $C_M = 5{,}00 \cdot 10^{-5}$ *M*; $C_R = 2{,}49 \cdot 10^{-5}$ *M*, 610 nm; ◑ Mg complex $C_M = C_R = 2{,}17 \cdot 10^{-5}$ *M*, 650 nm. b. ○ Zn complex $C_M = 3{,}02 \cdot 10^{-5}$ *M*; $C_R = 2{,}49 \cdot 10^{-5}$ *M*, 610 nm; ● Cd complex $C_M = 2{,}99 \cdot 10^{-5}$ *M*; $C_R = 2{,}49 \cdot 10^{-5}$ *M*, 610 nm; × arsenazo III $C_R = 2{,}49 \cdot 10^{-5}$ *M*, 610 nm ionic strength 0,1 *M*, 1-cm cells *vs* water, pH adjust with sodium hydroxide.

where A is the absorbance at a given pH, A_R is the absorbance of the reagent solution, A_0 is the maximum absorbance, $C = C_R = C_M$ is the total metal and reagent concentration, D is the correction used for calculating the equilibrium concentration of the reagent, using its dissociation constants [5], F is the correction term for metal ion hydrolysis, and n is the number of protons. The logarithmic form of Eq. (2) corresponds to a straight line with a slope of n and an intercept including $K_{eq.}$:

$$\log B = \log K_{eq} C + np\text{H} \quad (3)$$

where

$$B = \frac{(A - A_R)(A_0 - A_R)\,BD}{(A_0 - A)^2} \,. \tag{4}$$

The results calculated from Eq (3) are given in Fig. 3a and Table I.

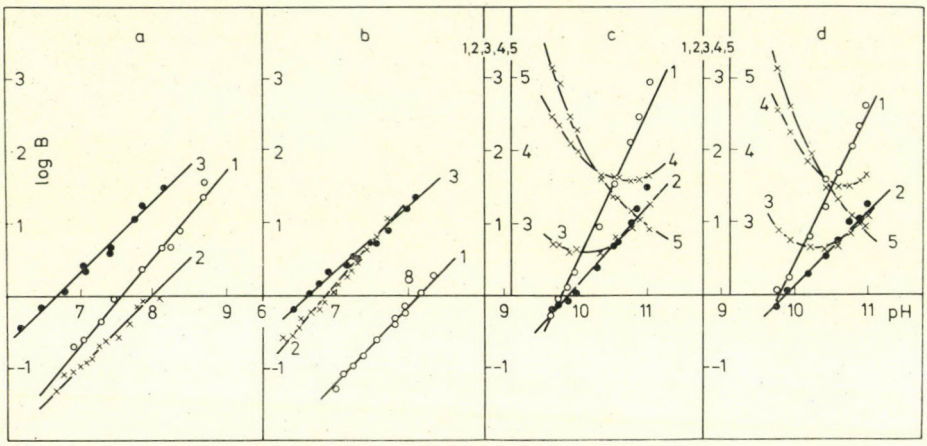

Fig. 3. Logarithmic plots according to eqs (3,6). a. equimolar solutions; b. solutions with a slight metal ions excess. (1) Mg complex; (2) Zn complex; (3) Cd complex, pH < 9. Cd complex at pH > 9; c. equimolar solutions; d. solutions with a slight metal ions excess. Reacting forms of cadmium: (1) as Cd^{2+}; (2) as $CdOH^+$; (3) as $Cd(OH)_2$; (4) as $Cd(OH)_3^-$; (5) as $Cd(OH_4)^{2-}$.

Solutions containing a slight metal ion excess

For calculations in the pH range of 6.2—8.3, the logarithmic form of the following equation was used:

Table I

Calculated data in the pH range of 6.2—8.5

Ion	$C_M \times 10^5$	$C_R \times 10^5$	$C_M : C_R$	n	$pK_{eq.}$
Mg	2.17	2.17	1	1.07	3.43±0.13
Zn	2.17	2.17	1	0.97	3.08±0.04
Cd	2.49	2.49	1	1.00	2.08±0.06
Cd*	2.17	2.17	1	0.96	1.91±0.08
Mg	5.00	2.49	2.01	0.98	3.40±0.04
Zn	3.02	2.49	1.21	1.12	3.09±0.04
Cd	2.99	2.49	1.20	0.94	1.66±0.09

* not given in Figs 2, 3.

$$K_{eq} = \frac{(A-A_R)(A_0-A_R)[H^+]^n DF}{C_R(A_0-A)[a(A_0-A_R)-(A-A_R)]} \quad (5)$$

i.e. $$\log B = \log K_{eq} C_R + n\text{pH} \quad (6)$$

where

$$a = \frac{C_M}{C_R} \quad \text{and}$$

$$B = \frac{(A-A_R)(A_0-A_R)DF}{(A_0-A)[a(A_0-A_R)-(A-A_R)]} . \quad (7)$$

The plots according to Eq. (6) are presented in Fig. 3b and the calculated data in Table I.

The good agreement of the results shown in Table I is evident.

Since one proton is liberated in all cases (the slopes of the straight lines *(n)* are always about unity), the following complex formation reaction is proposed:

$$M^{2+} + H_3L^{5-} \rightleftharpoons MH_2L^{4-} + H^+ \quad (8)$$

The spectrophotometric data for the reactions of Mg^{2+} Zn^{2+} and Cd^{2+} with Arsenazo III [2, 3] show that these systems can be described by the second type of reactions discussed by SAVVIN *et al.* [6—9]. It has been shown [10] that in reactions of the second type one proton is liberated and the peri-dihydroxy grouping of the reagent is engaged. The result is bond formation between the metal ion and one of the hydroxy groups of the naphthalene ring. Thus the complexes studied may be represented as MHH^*L^{4-}, where H is the proton of the arseno group of the reagent and H* is that of the second naphthalene ring hydroxy group. The stability constants of these complexes were not determined because the equilibrium concentration of the HH^*L^{5-} reagent form could not be calculated from the dissociation constant of the H_3L^{5-} form.

The cadmium-Arsenazo III reaction at pH $>$ **9**

In the pH range of 9.5—11.0, the H_3L^{6-} form predominates [4] and the following reaction proceeds:

$$M^2 + H_2L^{6-} \rightleftharpoons MH_{2-n}L^{2-(6+n)} + nH^+ \quad (9)$$

For the calculations, Eqs (3, 6) were used but the species Cd^{2+}, $CdOH^+$, $Cd(OH)_2$, $Cd(OH)_3^-$, $Cd(OH)_4^{2-}$ were considered [11, 12]. Correction F was calculated from the stability constants of the cadmium hydroxo complexes [13]. The results are presented in Figs. 3c, d and Table II.

The data obtained show that the reactions of Cd^{2+} and $CdOH^+$ with the species H_2L^{6-} are possible. For their comparison the values of the equilibrium

Table II

Data for the cadmium-Arsenazo III reaction at pH > 9

Reacting forms	$C_M \times 10^5$	$C_R \times 10^5$	$C_M : C_R$	n	$pK_{eq.}$	log βcompl.
Cd^{2+}	2.49	2.49	1	2.12	16.14±0.10	
*Cd^{2+}	2.17	2.17	1	2.08	15.48±0.12	
Cd^{2+}	2.99	2.49	1.20	2.10	15.92±0.13	
$CdOH^+$	2.49	2.49	1	1.10	6.24±0.13	5.74±0.13
*$CdOH^+$	2.17	2.17	1	1.09	5.86±0.09	6.12±0.09
$CdOH^+$	2.99	2.49	1.20	1.07	5.98±0.07	6.00±0.07

* not given in Fig. 2, 3.

constants were calculated, which show (Table II) that the following reaction of complex formation is predominating:

$$CdOH^+ + H_2L^{6-} \rightleftharpoons Cd(OH)HL^{6-} + H^+ \qquad (10)$$

The stability constant of the $Cd(OH)HL^{6-}$ complex was calculated using $K_7 = 1.05 \times 10^{-12}$ [5]. The results are given in Table II.

It is very likely that the mixed hydroxo complex of zinc and Arsenazo III forms too, but the straight line portion of the S-shaped curves presented in Fig. 2 is very short and therefore not suitable for calculations.

The data for the equilibrium and stability constants of the complexes obtained in the present paper, however, could not be compared with the data for the conditional stability constants of the complexes at pH 9 which were found earlier [2, 3].

Analytical use of the cadmium Arsenazo III complex in alkaline media

The reaction was studied at pH 12—13, adjusted with 2*N* NaOH and at an ionic strength of 0.1. The molar absorptivity of the cadmium complex at 610 nm is 2.75×10^4 l mol^{-1} cm^{-1} at pH 12, and 2.20×10^4 l mol^{-1} cm^{-1} at pH 13. The absorbance of the complex is stable for at least 24 hrs. Beer's law is obeyed up to 4.2 μg ml^{-1} at pH 12 and 1.6 μgml^{-1} at pH 13. The interference of zinc was studied at pH 13.39 μg of cadmium can be determined in the presence of 204 μg of zinc.

The curves $A = f(\text{pH})$ (Fig. 2) were also used to establish the relationship between the solubility products of the metal hydroxides pK_s [13] and the pH of the half-reaction, *i.e.* the pH at which the complex concentration is equal to one half of its maximum concentration [14]. The data for the alu-

minium-Arsenazo III complex [15] were also used. For this purpose the equilibrium concentrations of the complexes at a given pH were calculated. This dependence is shown graphically in Fig. 4, where α is the ratio between the equilibrium concentration of the complex and its maximum concentration. The pH value corresponding to $\alpha = 0.5$ defined as $pH_{1/2}$ was used for con-

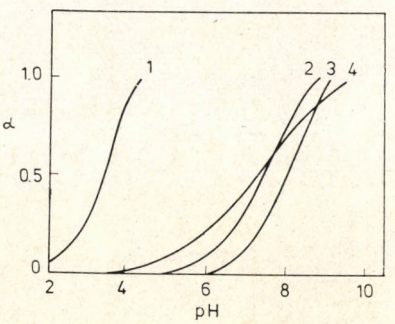

Fig. 4. Distribution diagram of arsenazo III complexes with (1) aluminium(III); (2) cadmium(II); (3) magnesium(II); (4) zinc(II). α-fraction of complexes at given pH. Equimolar solutions $C_M = C_R = 2{,}17 \cdot 10^{-5}\ M$.

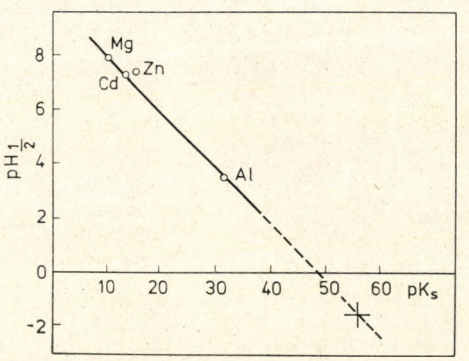

Fig. 5. Dependence between the pH of the half-reaction and the solubility products of the metal hydroxydes.

sideration of the relationship presented in Fig. 5. The straight line obtained (Fig. 5) passes through the point (56, −1.5), which have been established for the organic reagents of the Arsenazo III group [14], but has an intercept of 9.5 and a slope of −0.207, differing from those reported in Ref. [14]. This fact may be explained by the different types of the reactions used. The straight line obtained permits to establish conditions for complex formation of other metals with Arsenazo III and as well as the reaction selectivity.

REFERENCES

[1] SAVVIN, S. B.: Organic Reagents of the Arsenazo III group. Atomizdat, Moscow 1971.
[2] MICHAYLOVA, V., KOULEVA, N.: Annuaire Univ. Sofia "Cl. Ochridski", **66**, 21 (1971—2)
[3] MICHAYLOVA, V., YOUROUKOVA, L.: Anal. Chim. Acta, **68**, 73 (1974)
[4] MICHAYLOVA, V., KOULEVA, N.: Talanta, **20**, 453 (1973)
[5] BUDESINSKY, B.: Talanta, **16**, 1277 (1969)
[6] SAVVIN, S. B., PETROVA, T. V.: Zh. Anal. Khim., **24**, 177 (1969)
[7] PETROVA, T. V., SAVVIN, S. B.: Zh. Anal. Khim., **24**, 490 (1969)
[8] SAVVIN, S. B., KUZIN, E. L., PETROVA, T. V., KHAKIMKHODZAEV, N.: Zh. Anal. Khim. **24**, 1325 (1969)
[9] PETROVA, T. V., SAVVIN, S. B., DZHERAYAN, T. G.: Zh. Anal. Khim., **28**, 1888 (1973)
[10] PETROVA, T. V., SAVVIN, S. B., DZERAYAN, T. G.: Zh. Anal. Khim., **27**, 10 (1972)
[11] NAZARENKO, V. A., LEBEDEVA, N. V., BIRYUK, E. A., SHOUSTOVA, M. B.: Zh. Neorg. Khim., **7**, 2731 (1962)
[12] NAZARENKO, V. A., BIRYUK, E. A.: Zh. Anal. Khim., **22**, 57 (1967)
[13] SILLÉN, L. G. and MARTELL, A. E.: Stability Constants of Metal-Ion Complexes, 2nd Ed., Chem. Soc., London 1964.
[14] MUK, A., SAVVIN, S. B., PROPISTSOVA, R. F.: Zh. Anal. Khim., **23**, 1277 (1968)
[15] MICHAYLOVA, V.: J. Inorg. Nucl. Chem., **37**, 2317 (1975).

V. MICHAYLOVA; Department of Analytical Chemistry
University of Sofia, 1126 Sofia, Bulgaria.

Acta Chimica Academiae Scientiarum Hungaricae, Tomus 90(2), pp. 119—131 (1976)

MECHANISTIC STUDY OF THE ISOMERIZATION OF n-BUTENE ON ACID CATALYSTS, II

EVALUATION OF KINETIC CASES AND EXPERIMENTAL RESULTS

D. KALLÓ, E. DETREKŐY and G. SCHAY

(Central Research Institute for Chemistry of the Hungarian Academy of Sciences, Budapest)

Received May 22, 1975

The kinetic situations discussed in a previous paper have been extended to cases representing the simplest possibilities when one of the components reacts *via* a path different from those of the other two components. The initial rate of any $i \rightarrow j$ transformation can be written similarly to the previous cases as

$$r_{ij}^0 = \frac{a_{ij}\, p_i^0}{1 + b_i\, p_i^0} \,.$$

The meaning of constants a_{ij} and b_i was generalized for schemes of different structures, thus the above Langmuir-type rate equation could be generalized. On determining the constants a_{ij} and b_i for H-, Mg- and Ni-clinoptilolite at various temperatures, the only conclusion to be drawn was that the transformation involves a common surface intermediate on H-clinoptilolite whereas it does not on the Mg- and Ni-forms.

Introduction

The first paper of the present series has been devoted to the kinetic relations for catalytic transformations of three components into each other [1]. With the exception of Scheme IV, the discussion was based on reaction schemes with all three components regarded as equivalent with respect to the mechanism of their transformations; *i.e.* all of the macroscopic overall processes (i) $\rightleftarrows$ (j) were assumed to take place *via* identical numbers of elementary steps and intermediates, whose surface reactions are also, in fact, identical. Thus, the transformation schemes possessed 'trigonal' symmetries. In the meantime, further studies on the catalytic isomerization of *n*-butene have revealed some experimental facts [2—6] which seem to disprove the equivalence of the three isomers in question; in other words, the transformations pathway of two of the components may be different from that of the third one. Such a case is illustrated by Scheme IV in Part I [1], which has a plane of symmetry: the reactions of two components are identical, the transformation of the third component is, however, different. In order to include schemes of this type into our investigations, we shall discuss some simple cases of such schemes.

1. *Transformation schemes with mirror symmetry*

An overall catalytic transformation may involve a single surface intermediate if no surface reaction occurs [7, 8] (schematically: 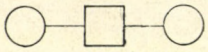
sign 1; hereafter ◯ denotes gas phase components and □ surface intermediates); it may involve two surface intermediates, in the latter case either two parallel processes take place with no surface reaction (sign 2 =: 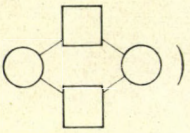
) or one surface reaction step occurs (sign 2 − −: 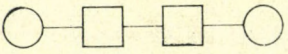
).

The simplest case of an essential difference between the mechanisms of two processes is when one of the processes involves only one, whereas the other involves two intermediates. Owing to its presumed complexity, no differentiation will be made between the two pathways involving two surface intermediates each (2= and 2− −). If the two components transforming *via* identical pathways are denoted by *j* and *k*, whereas the one whose reaction path is different by *i*, then the schemes with mirror symmetry will comprise the combinations corresponding to Columns 1 and 2 of Table I as shown in Column 3 of the same Table. These schemes become considerably simpler if common surface intermediates are assumed (Column 4, *cf. e.g.* [8]). It is obvious that a clear kinetic picture can be obtained for the latter cases since the three components transform into one another *via* as few intermediates and elementary steps as possible.

For the sake of completeness it should be mentioned that, based on the above selection principles, it is possible to construct a single asymmetric scheme (Table II), where all three components transform into each other *via* different pathways.

The simplifying assumptions included into the schemes (1 or 2 intermediates, common intermediates) do not influence the essential characteristics of the kinetic equations valid for each scheme, only convert them into more comprehensive forms. For example, schemes

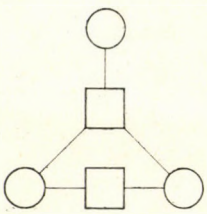
and
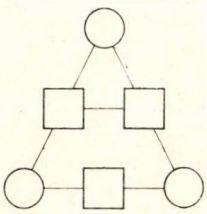

Table I

Simplest schemes with mirror symmetry

i ⇄ j i ⇄ k	j ⇄ k	Basic scheme	Simplified scheme	Symbol*
1.	2.	3.	4.	5.
1	2=	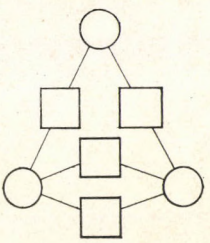	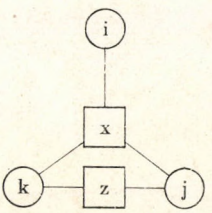	V+(2)
2=	1	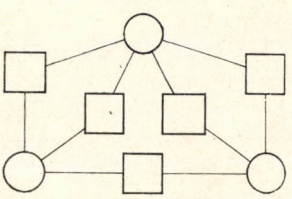	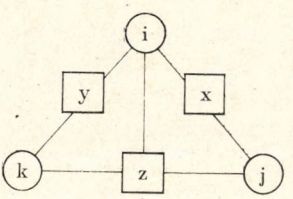	II+(1)
1	2– –	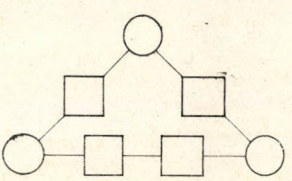	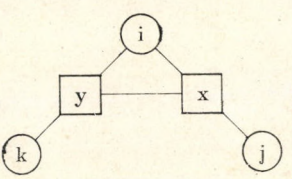	III–(1)
2– –	1	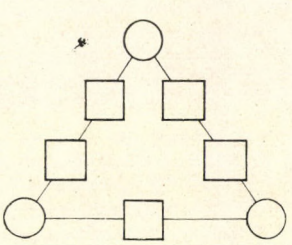	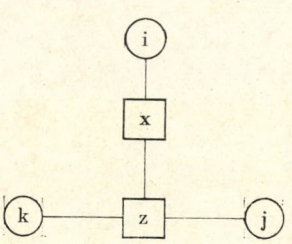	IV

* Schemes from Ref. [1] are shown also in the heading of Table IV, with addition or omission of one adsorption step each.

Table II

The asymmetrical reaction scheme

(i) ⇄ (j)	(j) ⇄ (k)	(k) ⇄ (i)	Basic scheme	Simplified scheme
1	2=	2– –	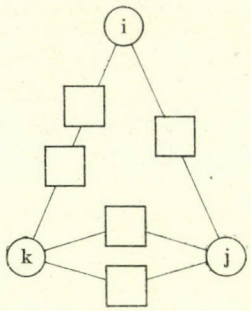	None

can be described by equations of the same form if the constants for the two cases are brought into correspondence (*cf.* Section 2).

2. *Derivation of kinetic equations*

Initial rate equations of so-called overall transformations observed macroscopically (*e.g.* (i) → (j)) have been derived for each scheme in the following way:

(1) the rate of transformation of any component in the gas phase has been given as the difference between its adsorption and desorption rates; for example, for i in Scheme III-(1):

$$r_i = k_{ix}p_i\Theta_0 - k_{xi}\Theta_x + k_{iy}p_i\Theta_0 - k_{yi}\Theta_y$$

where r_i is the rate of transformation of i;

k is the rate constant of the transformation denoted by the index;

p is the partial pressure of the component denoted by the index;

Θ_0, Θ_x, Θ_y are the fractions of active sites uncovered, covered by x and y, respectively.

(2) Corresponding to steady state, the variation of the concentration of individual surface species in time has been taken equal to zero, *i.e.* their formation rate was regarded as equal to their rate of decomposition. For example, in scheme III-(1) we obtain the following expression for x:

$$k_{ix}p_i\Theta_0 + k_{jx}p_j\Theta_0 + k_{yx}\Theta_y = k_{xi}\Theta_x + k_{xj}\Theta_x + k_{xy}\Theta_x$$

Thus, actual partial pressures are considered instead of values corresponding to the sorption equilibrium.

(3) A uniform surface with homogeneous activity is assumed, *i.e.*:

$$\Theta_0 + \Theta_x + \ldots = 1,$$
$$k \neq f(\Theta).$$

(4) When only one component is present in the gas phase, the Θ-values are expressed in terms of its partial pressure, using equations derived from (2) and (3).

(5) Values of Θ obtained for *e.g.* $p_i = p_i^0$, $p_j = p_k = 0$, are substituted into the rate equation of $-r_j$ and $-r_k$ derived according to (1), in order to be able to express initial rates such as

$$-r_j = r_{ij}^0 \quad \text{and} \quad -r_k = r_{ik}^0$$

as a function of partial pressure p_i^0, which is an experimental value. The value of r_j gives the rate of transformation of j according to (1), therefore $-r_j$ is the rate of formation of j; since at time zero i is the only reacting component, the value of $-r_j$ gives the initial rate of transformation of i into j, *i.e.* r_{ij}^0.

(6) Having performed the necessary rearrangements, let us examine the simplifications in the equations obtained for r_{ij}^0, permitted by the assumption of a rate-determining step; this, naturally has only to be performed with Schemes III-(1) and IV including also a surface reaction in addition to adsorption steps: for Scheme III-(1), the only case to be considered is the equilibration of the surface reaction; if the surface process were rate-determining, the sorption equilibria established would necessarily lead to an equilibrium of i, j, k with each other. On the other hand, both cases can be realized for Scheme IV, as has been demonstrated in Ref. [1].

The expression for the initial rate of formation of any component (*i*, *j* or *k*) from the remaining two will be an identical Langmuir-type equation for any of the schemes; the validity of the equation is, however, much more general in our case than that of the conventional Langmuir expression:

$$r_{ij}^0 = \frac{a_{ij} p_i^0}{1 + b_i p_i^0} \tag{1}$$

(i and j are arbitrary components; a_{ij} is a constant characteristic of transformation (i) → (j); b_i is a constant characteristic of component i; the interpretation of the constants will be given in Section 3.) Accordingly, the initial selectivity

$$S_{ik}^0 = \frac{r_{ij}^0}{r_{ik}^0} = \frac{dn_j}{dn_k} = \frac{dy_j}{dy_k} = \frac{a_{ij}}{a_{ik}} \tag{2}$$

(where n_j, n_k, y_j, y_k are the amounts and molar fractions of components j and k, respectively) will be independent of the partial pressure of the reacting component. We obtain a similar result if the differential equation of the selectivity function $y_k = f_i(y_j)$ is expressed by the ratio of general rate equations valid throughout the whole concentration range not only in the presence of the initial component. The selectivity will be independent of the pressure of the system and depends only on its composition in these cases as well as in the cases discussed in Ref. [1]. This statement has been confirmed by experiments, *cf. e.g.* Fig. 1 or Fig. 3 in [1].

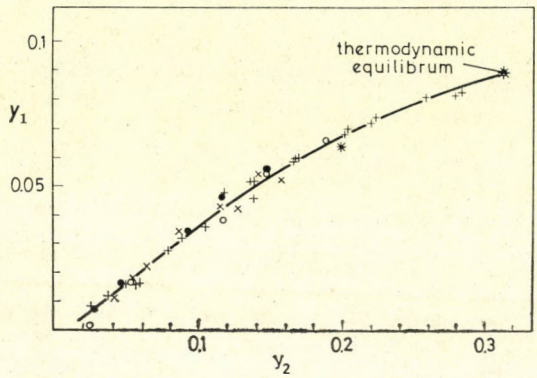

Fig. 1. Isomerization of *trans*-2-butene on Ni-clinoptilolite at 130 °C; ×: 50, +: 100, o: 200, ●: 300 Torr pressure; y_1: mole fraction of 1-butene; y_2: mole fraction of *cis*-2-butene

Table III summarizes the expressions for constants a and b in Eq. (1), for the simplified schemes of Table I. Since the transformation of j and k has a similar character, a_{ik}, a_{ki}, a_{kj} and b_k are not shown for the sake of simplicity. They can be obtained by simply changing the indexes in the expressions for a_{ij}, a_{ji}, a_{jk} and b_j. For the sake of better comparison, Table III shows only those expressions for Scheme IV (taken from Ref. [1]) which are valid for the case of sorption as the rate-determining step since this is regarded for the three remaining scheme, too.

In order to facilitate further discussion, the constants of Eq. (1) obtained for the schemes described in our previous paper [1] are also summarized. Since the individual transformations are equivalent there, only the expressions for a_{ij} and b_i are given for the cases of both surface equilibrium and sorption equilibrium (Table IV). Further constants can be obtained by the proper change of indices, according to the schemes.

3. *Interpretation of kinetic constants*

On evaluating the expressions in Tables III and IV the physical meaning of constants in the Langmuir-type rate equation (1) can be interpreted for the individual processes of these complex reactions. Direct visualization is also

Table III

Constants of Eq. (1) for simplest transformation schemes with mirror symmetry (k: rate constant; K: equilibrium constant)

	V+(2)	II+(1)
	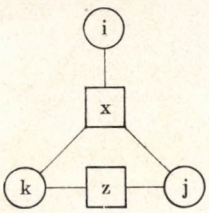	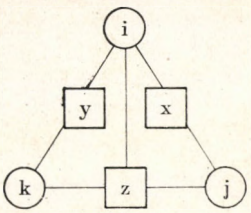
a_{ij}	$k_{xj}k_{ix}/X$	$k_{zj}k_{iz}/Z + k_{xj}k_{ix}/X$
a_{ji}	$k_{xi}k_{jx}/X$	$k_{zi}k_{jz}/Z + k_{xi}k_{jz}/X$
a_{jk}	$k_{xk}k_{jx}/X + k_{zk}k_{jz}/Z$	$k_{zk}k_{jz}/Z$
b_i	k_{ix}/X	$k_{iz}/Z + k_{ix}/X + k_{iy}/Y$
b_j	$k_{jx}/X + k_{jz}/Z$	$k_{jz}/Z + k_{jx}/X$
	$X \equiv k_{xi} + k_{xj} + k_{xk}$ $Z \equiv k_{zj} + k_{zk}$	$X = k_{xi} + k_{xj}$ $X \equiv k_{yi} + k_{yk}$ $Z \equiv k_{zi} + k_{zj} + k_{zk}$
	III−(1)	IV
	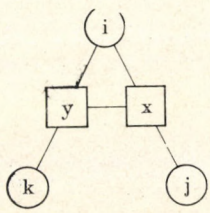	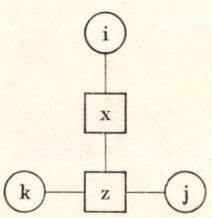
a_{ij}	$k_{xj}(k_{ix} + k_{iy})/XY$	$k_{zj}K_{xz}k_{ix}/XZ$
a_{ji}	$(k_{xi} + k_{yi}K_{xy})k_{jx}/XY$	$k_{xi}k_{jz}/XZ$
b_{jk}	$k_{yk}K_{xy}k_{jx}/XY$	$k_{zk}K_{xz}k_{jz}/XZ$
b_i	$(k_{ix} + k_{iy})(1 + K_{xy})/XY$	$k_{ix}(1 + K_{xz})/XZ$
b_j	$k_{jx}(1 + K_{xy})/XY$	$k_{jz}(1 + K_{xz})/XZ$
	$XY \equiv k_{xi} + k_{xj} + (k_{yi} + k_{yk})K_{xy}$	$XZ \equiv k_{xi} + (k_{zj} + k_{zk})K_{xz}$

possible for schemes without surface reaction (Table III: V+(2), II+(1), Table IV: II and V).

Constant a is a product for each term; it is the product of the "partial adsorption equilibrium constant" of the reactant and the desorption rate constant of the product. The former factor is the ratio of the rate constant of

Table IV

Constants of Eq. (1) for transformation schemes with trigonal symmetry [1]

Scheme I	Scheme III
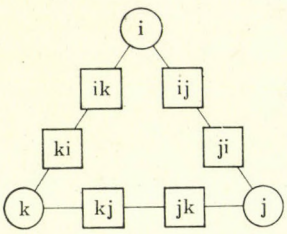	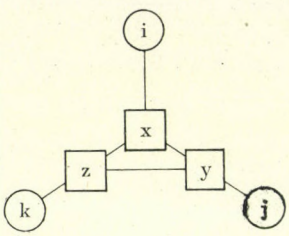
adsorption steps in equilibrium	
a_{ij} $k_{ij,ji}K_{i,ij}$ b_i $K_{i,ij} + K_{i,ik}$	$k_{xy}K_{ix}$ K_{ix}
surface reactions in equilibrium	
a_{ij} $k_{ji,i}K_{ij,ji}k_{i,ij}/X$ b_i $k_{i,ij}(1+K_{ij,ji})/X+k_{i,ik}(1+K_{ik,ki})/Y$	$k_{yj}K_{xy}k_{ix}/X$ $k_{ix}(1 + K_{xy} + K_{xz})/X$
$X \equiv k_{ij,i} + k_{ji,j}K_{ij,ji}$ $X \equiv k_{ik,i} + k_{ki.k}K_{ik,ki}$	$X \equiv k_{xi} + k_{yj}K_{xy} + k_{zk}K_{xz}$
Scheme II	Scheme V
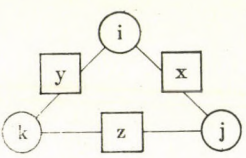	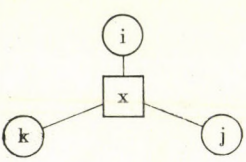
a_{ij} $k_{xj}k_{ix}/X$ b_i $k_{ix}/X + k_{iy}/Y$	$k_{xj}k_{ix}/X$ k_{ix}/X
$X \equiv k_{xi} + k_{xj}$ $Y \equiv k_{yi} + k_{yk}$	$X \equiv k_{xi} + k_{xj} + k_{xk}$

adsorption leading to a surface intermediate necessary for transforming the reactant into product and the sum of desorption rate constants of the given surface intermediate. Consequently, a contains as many terms as many intermediates are *necessary* for the reactant to give the product in question.

Constant b is a sum of the "partial equilibrium constants" of the reactant, consequently, it contains as many terms as many surface intermediates *may* form from it.

These statements are, in fact, valid in the case of an equilibrated surface reaction, too. The rate constants in the expressions are then modified by the equilibrium constant of the surface reaction, as demonstrated by a comparison of the constants for Schemes I and II as well as for Schemes V and III, III-(1) or IV.

The generalizations permit to give expressions by analogy for constants a and b in the so-called asymmetrical scheme (*cf.* Table II).

If the surface reaction is rate-determining in Schemes I or III (*cf.* upper part of Table IV), the constants of Eq. (1) have the same meaning as those of the classical Langmuir—Hinshelwood equation: a is the product of the effective adsorption equilibrium constant of the reactant and the rate constant of the surface reaction following this adsorption step; b is the total adsorption equilibrium constant of the reactant.

It is obvious from the above discussion that the physical meaning of the constants in the rate equations for initial, consequently, irreversible transformation is different depending on the structure and complexity of schemes assumed for catalytic transformations of three components into each other. Their common feature is that a consists of as many terms as many surface intermediates must be produced for the transformation in question; each term is a product of a quantity characteristic of the sorption constant of the reactant in the given system and the rate constant of the rate-determining step following this sorption process (regardless of whether this latter step is a surface reaction leading to an adsorbed product or a desorption step resulting in the final product); b consists of as many terms as many surface intermediates may be formed from the reactant; each term is a quantity characteristic of the equilibrium constant of adsorption leading to individual surface intermediates in the given system. Considering three-component systems, this is how the Langmuir-type rate equation can be generalized.

Another general feature of Eq. (1) is that

$$\frac{a_{ij}}{a_{ji}} = K_{ij} \tag{3}$$

for all schemes discussed here (*cf.* Tables I and II) and not only for the schemes presented in Ref. [1]; (i, j are any two of the components, K_{ij} is the equilibrium constant of the (i) $\rightleftarrows$ (j) overall process). This resembles very closely the traditional dynamic definition of the equilibrium constant according to which K is equal to the ratio of the rate constants of the forward and reverse elementary reactions. Since a similar conclusion has now been reached for systems of considerable complexity, one can attribute a meaning of a 'true rate constant' to a.

For the verification of Eq. (3) the following evidences are to be taken into account. The equilibrium constant of an elementary step $i \rightarrow x$ can be given as:

$$K_{ix} = k_{ix}/k_{xi} \; (= 1/K_{xi}).$$

It has also to be considered that the equilibrium can be established in parallel ways, too, as for example between j and k in Scheme V+(2) or between i and j in Scheme II+(1) (Table III); in the former case this means that

$$K_{jx}K_{xk} = K_{jz}K_{zk};$$

in the latter:

$$K_{ix}K_{xj} = K_{iz}K_{zj}.$$

This is essentially due to the fact that for a closed cycle of reactions the product of equilibrium constants for subsequent steps is equal to unity.

4. *Kinetic evaluation*

(a) Theoretical cases

The structures of kinetic equations obtained for different simplified transformations reflect their basic features; essentially nothing more can be seen from more complicated equations for more complex schemes, in other words, it is impossible to conclude to the existence of more complex schemes by kinetic methods. This becomes obvious on the basis of the comparison of schemes discussed here, *e. g.* on comparing the expressions obtained for Scheme I (surface reactions in equilibrium) with those for Scheme II (where no surface reactions are considered). Similarly, if an additional equilibrium adsorption step is considered, then its surface concentration should be included into the equation instead of the gas phase concentration (partial pressure) and this would only result in a formal but not essential complication.

The expressions for the constants of rate equation (1) reflect the characteristics of the basic schemes but the problem still has to be solved of how to decide on the basis of experimentally determined constants what the real kinetic case is [see next section (b)]; in other words, what characteristic features of these constants may be suitable as criteria for one or another kinetic case.

The most evident procedure would be to calculate 9 kinetic constants for the elementary steps based on independent experimental values of 3×2 a_{ij} and $3b_i$ constants, and evaluate their reality to make a decision. For the majority of schemes, however, even more unknown constants are involved, these would therefore be excluded from such investigations; in the case of surface reaction(s) in equilibrium its (their) equilibrium constant(s) is (are) inseparable from the desorption rate constants and cannot be calculated.

The only criterion characteristic of the experimental constants of the kinetic cases demonstrated (*cf.* Tables III and IV) can be that either

$$\frac{b_i}{a_{ij}} = \frac{b_k}{a_{kj}} \tag{4}$$

or

$$\frac{b_i}{a_{ij}} \neq \frac{b_k}{a_{kj}} . \tag{5}$$

Criterion (4) is always fulfilled for Schemes III-(1) and V and in the case of equilibrated surface reaction for Schemes III and IV.

Criterion (5) is fulfilled for all the remaining cases, *i.e.* for Schemes I, II, II+ (1), III (with adsorption equilibrium) and V+(2).

There is no criterion that would permit to decide from experimental kinetic results with certainty whether the transformation scheme has a mirror or trigonal symmetry.

The only thing that can be concluded on the basis of isothermal measurements is whether or not the process involves one or more surface intermediates being in equilibrium with each other.

(b) Experimental results

Initial transformation rates have been determined with all three *n*-butene isomers as the starting materials, over H-, Mg- and Ni-clinoptilolite, at various pressures and temperatures. (Catalysts will be described in a forthcoming publication which will conclude the present series.)

Parameter range of the experiments has been determined considering the following factors:

(1) The amount of catalyst was chosen so as to ensure a conversion degree of 10% within about 10 min in a closed circulation apparatus with a volume of 150 cm^3; thus the initial section of the conversion isotherms (to be regarded as linear) could be obtained from a proper number of chromatographic product analysis.

(2) The temperature range was chosen so that the following linear transformation (*cf. e.g.* Fig. 2b)

$$\frac{1}{r_{ij}^0} = \frac{1}{a_{ij}} \left(\frac{1}{p_i^0} + b_i \right) = m_{ij} \frac{1}{p_i^0} + b_{ij} \tag{6}$$

could be used in the pressure range between 20 and 760 Torr where the apparatus was operated for determining the values a_{ij} and b_i of Eq. (1) on the basis of pressure dependence of the reaction rate. In other words, the apparent kinetic order of the transformation should fall between zero and unity (see for example Fig. 2a). Thus, the kinetic measurements were carried out between

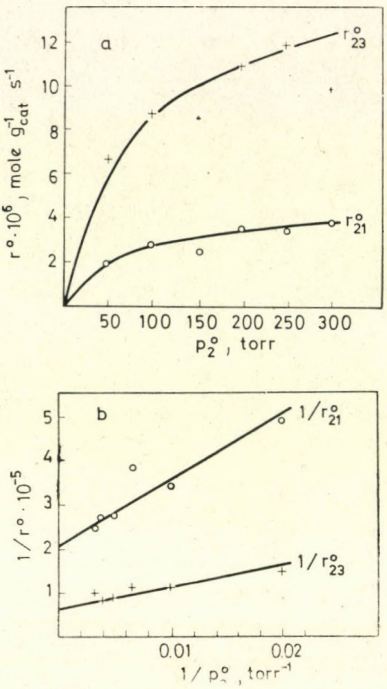

Fig. 2. Initital rate of isomerization of *cis*-2-butene on H-clinoptilolite at 100 °C at various pressures; r°_{21}: initital rate of transformation into 1-butene; r°_{23}: initital rate of transformation into *trans*-2-butene p°_2: initital pressure of *cis*-2-butene

100 and 160 °C on H- and Mg-clinoptilolite and between 70 and 130° on Ni-clinoptilolite.

Initial rates of transformations have been determined as a function of the pressure for all three *n*-butene isomers at identical temperatures; this allowed us to determine more exactly the constants of Eq. (6) taking Eqs (7) and (8) into account:

$$\frac{b_{ij}}{m_{ij}} = \frac{b_{ik}}{m_{ik}} = b_i \tag{7}$$

$$\frac{m_{ji}}{m_{ij}} = \frac{a_{ij}}{a_{ji}} = K_{ij} \,. \tag{8}$$

The other two isomers were never found to form in a ratio corresponding to thermodynamic equilibrium, regardless of the starting *n*-butene was; neither was an equilibrium established between the starting hydrocarbon and one of the products, thus Case IV-r of Ref. [1] could be excluded, *i.e.* a reaction corresponding to Scheme IV of the Table III with surface reaction as the rate-determining step.

On the other hand, it has been found that criterion (4), which can be written using the symbols of Eq. (6) as

$$b_{ij} = b_{kj} \tag{9}$$

is fulfilled for H-clinoptilolite at any temperature and for all three isomers, whereas this is not the case with Mg- and Ni-clinoptilolite. Thus, the isomerization of *n*-butenes involves a common surface intermediate on H-clinoptilolite (or a mixture of such intermediates in equilibrium with each other), but such a common species for all three butenes can be excluded for Mg- and Ni-clinoptilolite. There is no possibility to obtain a still deeper insight into this reaction by applying kinetic methods without considering the effect of temperature.

REFERENCES

[1] KALLÓ, D., DETREKŐY, E., SCHAY, G.: Acta Chim (Budapest) **72**, 189 (1972)
[2] SHANNON, I. R., KEMBALL, C., LEACH, H .F.: In "Chemisorption and Catalysis", p. 46. The Institute of Petroleum, London 1970
[3] CROSS, N. E., KEMBALL, C., LEACH, H. F.: J. Chem. Soc. (A), 3315 (1971)
[4] LOMBARDO, E. A., SILL, G. A., HALL, K. W.: J. Catal. **22**, 54 (1971)
[5] HATTORI, H., YOSHII, N., TANABE, K.: Proc. Vth Internatl. Congress on Catalysis (Ed.: J. W. HIGHTOWER), North-Holland, Amsterdam Am. Elsevier Co. New York, 1973. Vol. 1. p. 233.
[6] MICHEL, D., MEILER, W., PFEIFER, H.: III Intern. Katalyse-Konferenz der DDR, Schloss-Reinhardsbrunn, 1974, Paper 46
[7] KALLÓ, D., PRESZLER, I.: J. Catal. **12**, 1 (1968)
[8] KALLÓ, D., PRESZLER, I., SCHAY, G.: Acta Chim. Budapest **64**, 211 (1970)

Dénes KALLÓ
Emil DETREKŐY
Géza SCHAY

H-1025 Budapest, Pusztaszeri út 59—67.

Acta Chimica Academiae Scientiarum Hungaricae, Tomus 90(2), pp. 133—140 (1976)

THE ROLE OF MOLECULAR CONFORMATION IN *Π*-ELECTRON SCF-MO CALCULATIONS

Á. I. KISS and J. SZŐKE*

*(Department of Physical Chemistry, Technical University and *Department of Optical Spectroscopy, Central Research Institute for Physics, Budapest)*

Received August 5, 1975

The π-electronic structure and spectra of the planar conformations of disubstituted benzene derivatives containing a carbonyl group have been calculated by the Pariser–Parr–Pople method. The calculated total π-energy is not a reliable measure of the relative stability of the conformers. The calculation predicts that form to be more stable which has larger π-charges nearer to each other. The sensitivity of the calculated π-electron properties (charge density, dipole moment, spectral data) to conformational changes is demonstrated. The difference in the calculated properties of the two conformers is the largest for *o*-derivatives where the use of the experimentally most probable molecular structure is desirable. With *m*- and *p*-derivatives the difference is of the same magnitude as the error of computation.

It is well known that reliable results on conformational problems may be expected only from *ab initio* and some all-valence-electron calculations. The theoretical investigation of the π-electronic structure of molecules having more conformers raised the question of which molecular geometry would be the most appropriate for the calculation, *i.e.* which conformer would give the energies of the π-electronic transitions in best accordance with the experimental values. This kind of study may give information about the sensitivity of the π-electron approximation to conformational changes.

Aromatic carbonyl derivatives seem to be suitable model compounds. The investigation of different molecular properties has shown that *o*- and *m*-substituted benzaldehydes and benzoic acids exist in two planar (O-*cis* and O-*trans*) forms. Detailed experimental references will be given in the Discussion. Only a limited number of papers dealing with π-electron calculations has discussed the effect of conformation. MINKIN *et al.* [1] calculated the total π-energy and the π-dipole moment of the two conformers of *m*-methoxy and *m*-nitrobenzaldehyde. Recently, KLABUHN *et al.* [2] calculated the dipole moment of the conformers of benzene *m*- and *p*-dialdehyde. The π-charge distribution and the spectral data for the conformers of aromatic carbonyl compounds have not yet been reported.

The present paper deals with the calculation of the π-electron properties of conformers of some aromatic aldehydes and carboxylic acids by the PARISER–PARR–POPLE (PPP) method [3] for obtaining information on the role of conformations in the calculation. In order to obtain comparable results, the π-electronic structure and spectra of the conformers of all disubstituted

benzenes containing asymmetric substituents have been calculated with a single parameter system [4, 5] giving best results for the monosubstituted derivatives. The following substituents have been considered: F, Cl, OH, NH_2, CHO, COOH, NO_2. Only the planar conformations shown in Fig. 1 were studied. The computational method and the starting parameters were the same as in our previous work. [4, 5].

I

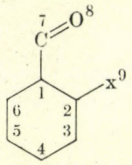

A

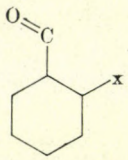

B

x = F, Cl, OH, NH_2, NO_2

II

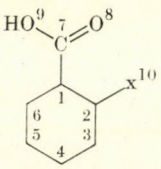

A

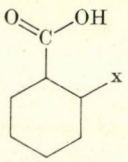

B

III

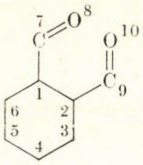

A

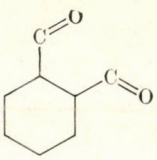

B

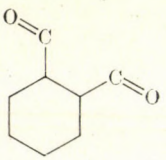

C

IV

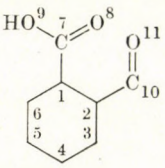

A

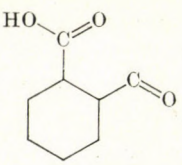

B

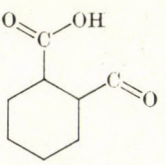

C

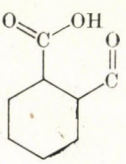

D

V

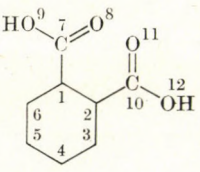

A

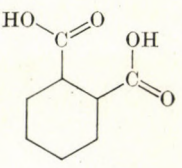

B

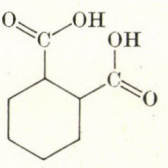

C

Table I

Calculated spectral data

Compound	E	f	α	E	f	α	E	f	α
	IA			**IB**					
o-fluoro-benzaldehyde	4.199	0.123	325.3	4.300	0.107	124.2			
	5.049	0.337	189.6	5.055	0.459	344.5			
	5.995	0.409	244.8	6.001	0.515	49.7			
	6.217	0.706	17.8	6.289	0.474	347.6			
m-fluoro-benzaldehyde	4.286	0.063	66.7	4.277	0.076	44.6			
	5.086	0.477	15.5	5.104	0.429	351.1			
	5.914	0.535	140.9	6.029	0.673	308.6			
	6.307	0.412	17.4	6.266	0.442	181.0			
o-hydroxy-benzaldehyde	3.938	0.173	146.9	4.092	0.102	130.0			
	4.998	0.188	6.2	5.007	0.334	339.7			
	5.833	0.436	232.6	5.823	0.678	38.5			
	5.988	0.703	25.0	6.096	0.284	351.9			
m-hydroxy-benzaldehyde	4.061	0.095	59.4	4.056	0.105	41.8			
	5.028	0.348	21.4	5.054	0.287	355.2			
	5.665	0.724	151.4	5.794	0.945	319.5			
	6.137	0.216	3.3	6.121	0.225	177.6			
	IIA			**IIB**					
o-hydroxy-benzoic acid	4.099	0.163	326.7	4.267	0.133	132.1			
	5.139	0.110	348.8	5.173	0.284	333.2			
	6.005	1.158	211.8	5.892	0.599	26.8			
	6.072	0.143	283.7	6.233	0.321	347.1			
m-hydroxy-benzoic acid	4.245	0.075	57.5	4.232	0.095	38.3			
	5.223	0.259	32.7	5.251	0.199	5.9			
	5.764	0.755	158.7	5.935	1.251	320.8			
	6.205	0.296	345.0	6.211	0.001	28.1			
	IIIA			**IIIB**			**IIIC**		
benzene-*o*-dialdehyde	4.281	0.024	30.0	4.253	0.060	236.5	4.222	0.080	210.0
	4.577	0.125	300.0	4.726	0.324	142.6	4.756	0.523	300.0
	5.841	1.371	210.0	5.650	1.156	221.4	5.554	0.883	30.0
	5.869	0.197	300.0	5.945	0.268	302.0	5.958	0.257	300.0
benzene-*m*-dialdehyde	4.307	0.036	150.0	4.319	0.017	161.1	4.324	0.002	150.0
	5.139	0.436	60.0	5.095	0.257	248.9	5.068	0.116	240.0
	5.342	0.889	330.0	5.345	1.149	156.3	5.379	1.496	150.0
	5.807	0.240	60.0	5.787	0.366	40.0	5.718	0.305	60.0
benzene-*p*-dialdehyde	4.236	0.052	270.0	4.230	0.060	297.0			
	4.734	0.880	0.0	4.741	0.920	14.2	Identical with **IIIA**		
	6.095	0.005	90.0	6.090	0.000	70.5			
	6.220	0.468	90.0	6.225	0.478	277.1			

Results

The calculated spectral data as defined in [4], for the two conformers of *o*- and *m*-fluoro- and hydroxybenzaldehyde and hydroxybenzoic acid as well as for the three conformations of the three benzene dialdehyde isomers are given in Table I. The total π-energy and π-dipole moment for the same conformers are collected in Table II. The calculated π-electronic properties of the conformers show differences which are larger with the *ortho*-isomers than with the *meta*-derivatives.

Table II

Total π-energies and π-dipole moments

Compound	$E_\pi(eV)$	$\mu_\pi(D)$	$E_\pi(eV)$	$\mu_\pi(D)$	$E_\pi(eV)$	$\mu_\pi(D)$
	IA		**IB**			
o-fluoro-benzaldehyde	−334.820	2.29	−331.929	3.45		
m-fluoro-benzaldehyde	−328.164	3.02	−327.401	3.89		
o-hydroxy-benzaldehyde	−327.426	1.96	−324.536	3.92		
m-hydroxy-benzaldehyde	−320.849	3.24	−320.094	4.54		
	IIA		**IIB**			
o-hydroxy-benzoic acid	−440.964	2.14	−443.837	4.95		
m-hydroxy-benzoic acid	−431.056	3.26	−431.651	5.40		
	IIIA		**IIIB**		**IIIC**	
benzene-*o*-dialdehyde	−315.996	4.96	−312.692	4.90	−310.530	2.15
benzene-*m*-dialdehyde	−308.555	5.34	−307.931	2.90	−307.344	0.84
benzene-*p*-dialdehyde	−306.896	3.55	−306.923	0	Identical with **IIIA**	

With the benzaldehyde derivatives containing a π-electron donor (fluoro, chloro, hydroxy or amino) and an acceptor (nitro or formyl) group, the O-*cis* form (IA, for the structural formulas, see Fig. 1) has a lower total π-energy, *i.e.* according to the calculation, this form is predicted to be the more stable. With the corresponding benzoic acids, the O-*trans* form (II B) has a smaller total energy. Of the benzene dialdehydes, the lowest total energy is obtained for the O-*cis*, O-*cis* form (IIIA), of the formylbenzoic acids for the aldehyde

Table III

Charge densities

Compund	IA			IB		
	q_8	q_9	q_5	q_8	q_9	q_5
o-fluoro-benzaldehyde	1.4092	1.9065	1.0232	1.3976	1.9170	1.0191
m-fluoro-benzaldehyde	1.3915	1.9236	0.9970	1.3902	1.9248	0.9939
o-hydroxy-benzaldehyde	1.3915	1.8384	1.0360	1.4035	1.8567	1.0317
m-hydroxy-benzaldehyde	1.4226	1.8689	0.9952	1.3908	1.8711	0.9922

	IIA				IIB			
	q_8	q_{10}	q_9	q_5	q_8	q_{10}	q_9	q_5
o-hydroxy benzoic acid	1.5260	1.8393	1.8142	1.0391	1.5052	1.8669	1.8232	1.0293
m-hydroxy-benzoic acid	1.5019	1.8682	1.8128	0.9964	1.4992	1.8721	1.8144	0.9902

	IIIA		IIIB			IIIC	
	q_8	q_5	q_8	q_{10}	q_5	q_8	q_5
benzene-*o*-dialdehyde	1.3444	0.9800	1.3854	1.3832	0.9781	1.3806	0.9724
benzene-*m*-dialdehyde	1.3818	1.0021	1.3873	1.3871	0.9989	1.3861	0.9956
benzene-*p*-dialdehyde	1.3804	0.9756	1.3818	1.3818	0.9538	1.3804	0.9756

O-*cis*, acid O-*trans* form (IVD) and of the dicarboxylic acids for the O-*trans*, O-*trans* form (VC).

The ground state charge densities of the conformers show considerable differences. Some examples are shown in Table III, complete data can be found in a separate Appendix [6].

The O-*cis* form of the donor substituted benzaldehydes and benzoic acids show a larger net π-charge separation: the charge density on the carbonyl oxygen atom is larger, on the donor atoms (as well as on the carboxy OH group) smaller than in the O-*trans* form. Accordingly, the differences in the charge densities of the ring carbon atoms are also larger in the O-*cis* form. With the acceptor substituted aldehydes the charge density on the carbonyl oxygen atom and on the nitro oxygen atom nearer to the carbonyl group is smaller and on the other nitro oxygen atom larger in the O-*cis* form than in the O-*trans* conformer. The differences in the charge densities of the ring carbon atoms are larger in the O-*trans* form. The O-*cis* form of nitrobenzoic acids shows larger charge densities on the carboxy oxygen atom and smaller ones

on the nitro oxygen atoms than does the O-*trans* form. With the dicarboxylic acids the conformer VB has the largest charge density on the carbonyl oxygen and smallest on the hydroxy oxygen atoms.

It can be concluded that the π-charge separation is determined by the relative position of the substituents: when groups of opposite directing character (net π-charges of opposite sign) are nearer to each other, the charge separation is larger within the molecule, for groups with identical directing character (net π-charges of the same sign), on the other hand, the separation is smaller.

The different conformers have considerably different π-dipole moment as can be seen from Table II. With derivatives containing substituents of different orienting character, the dipole moment of the O-*cis* conformer is smaller, with molecules having substituents of identical orienting character, it is, however, larger. In the former group of compounds the π-dipole moment of the O-*cis* form is smaller because the σ-dipole moment of opposite direction, belonging to the bond of the donor atom, is not considered in the present π electron approximation.

The spectral data of the different conformers also show considerable differences (Table I), especially with the *o*-isomers. The differences of the spectral data for the conformers of the *m*-derivatives are smaller, they are in general of the same magnitude as the difference between the calculated and experimental values. Since the agreement, between the calculated and experimental spectral data depend strongly on the parameterization of the calculation, it follows that this agreement cannot give reliable information regarding the really existing conformer.

The calculated total energy and dipole moment of *m*-nitro-benzaldehyde is in good accordance with the results given by MINKIN *et al.* [1]. The calculated π-dipole moment of benzene *m*- and *p*-dialdehyde is in close agreement with the PPP results by KLABUHN *et al.* [2] parameterized to experimental dipole moments.

Discussion

According to dipole moment [7—10], near infrared [10] and NMR [11—13] spectroscopic investigations the O-*trans* form of *o*- and *m*-substituted benzaldehydes is the preferred conformation except for the *o*-hydroxy and *o*-aminobenzaldehyde, the O-*cis* form of which is stabilized by intramolecular hydrogen bonding (*e.g.* [12]). Near IR [14] and far IR [15] spectroscopic studies of *m*-halogenobenzaldehydes favoured the O-*cis* form which may probably be a mis-assignment. With the *o*-halogenobenzoic acids, X-ray diffraction and IR spectroscopic measurements [16] show that O-*trans* is the favoured form of the *o*-fluoro derivative, and the proportion of the O-*cis* form increases

in the series F to I. The *o*-hydroxy and *o*-aminobenzoic acid are stabilized in the O-*cis* form by intramolecular hydrogen bonding (*e.g.* [17]).

Calculation of the total π-energy predicts the O-*trans* form of carboxylic acids as more stable in accordance with the experimental findings, with the aldehydes, on the other hand, the O-*cis* form is given by the calculation as more stable.

The results of the calculations are not satisfactory in each case.

The difference in computational results obtained by changing the conformation is a consequence of the different relative positions of the π-centres (*i.e.* of the atomic virtual π-charges) in the different conformers, which give rise to different two-center repulsion integrals. These quantities determine the differences in the F matrix of the conformers and, as a consequence, the differences in the calculated molecular properties.

In order to clarify this point, the effect of the two-center repulsion integrals ($\gamma_{\mu\nu}$) on the calculation was investigated. Using OHNO's approximation [18] instead of the MATAGA—NISHIMOTO approach [19], the same trend of results was obtained though the former produces smaller total energies (greater stability) and larger charge separations, owing to the larger values of $\gamma_{\mu\nu}$. The OHNO approximation gives rise to larger separations in the total energy of the conformers. It seems that considerable changes in the $\gamma_{\mu\nu}$ values do not alter the stability of conformers.

The decisive role of the relative position of the atomic virtual π-charges will be obvious from a comparison of the *o*-methyl and *o*-formylbenzaldehyde conformers. In order to demonstrate the effect of differently placed π-charges, the *o*-methylbenzaldehyde conformers were calculated both with one and two π-center methyl models [20] both in the MATAGA—NISHIMOTO [19] and OHNO [18] approximations. The one-center (conjugation) methyl model produces differences in the properties of the conformers in the same sense as do the other one-center substituents (contributing two electrons). The two-center (hyperconjugation) methyl model gives somewhat larger total energies but still that of the O-*cis* form remains smaller. In contrast to one-center model, the relative magnitude of the charge densities of the conformers are changed and become similar to that corresponding dialdehydes. For example, the charge density on the carbonyl oxygen atom is larger in the O-cis form with the one-center model (O-*cis* 1.4254, O-*trans* 1.4081) but becomes smaller with the two- center model (O-*cis* 1.3871, O-*trans* 1.3887) just as with the dialdehydes. The O-*trans* form has a smaller total energy only if two atoms contributing two electrons are close to each other. This means that the larger the neighbouring π-charges the more stable a conformation is shown to be by its calculated total π-energy.

It can be established that the π-electron approximation does not give the correct relative stability of the conformers; it is obvious, however, that the result of the calculation is strongly dependent on the choice of the confor-

mation. For the lowest energy transition, the energy difference of two conformers of *o*-disubstituted benzenes is 2.5—4%, which suggests to perform the calculation with the experimentally most probable structure. With *m*- and *p*-derivatives the difference between the spectral results for the different conformations is of the same magnitude as the error of computation. The detailed results for the different conformations is of the same magnitude as the error of computation. The detailed results of the calculations are collected in Ref. [6].

REFERENCES

[1] Minkin, V. I., Zhdanov, Yu. A., Malysheva, E. N.: Teor. Eksp. Khim., **7**, 180 (1971)
[2] Klabuhn, B., Clausen, E., Goetz, H.: Tetrahedron, **29**, 1153 (1973)
[3] Parr, R. G.: Quantum Theory of Molecular Electronic Structure. W. A. Benjamin, New York 1964
[4] Kiss A. I., Szőke, J.: Chem. Phys. Lett., **11**, 52 (1971); Acta Chim. (Budapest) **74**, 59 (1972)
[5] Kiss, A. I., Szőke, J.: J. Mol. Struct., **18**, 457 (1973)
[6] Kiss, A. I., Szőke, J.: KFKI-Report 75—13
[7] Bock, E., Tomchuck, E.: Can. J. Chem., **50**, 2890 (1972)
[8] Ritchie, G. L., Cheng, C. L., Le Fevre, R. J. W., Goodman, P. A., Gore, P. H.: J. Chem. Soc. B., 1198 (1971)
[9] Jones, G. A. Y., Katritzky, A. R., Ochkin, A. V.: J. Chem. Soc. **B, 1795** (1971)
[10] Aw, C. T., Huang, H. H., Tan, E. L. K.: J. Chem. Soc. Perkin Trans. I. 1638 (1972)
[11] Karabatsos, G. J., Vane, F. M.: J. Amer. Chem. Soc. **85**, 3886 (1963)
[12] Smith, W. B., Deavenport, D. L., Ihrig, A. M.: J. Amer. Chem. Soc., **94**, 1959 (1972)
[13] Wasylishen, R., Schaffer, T.: Can. J. Chem., **49**, 3216 (1971)
[14] Crowder, G. A., Northam, F.: J. Chem. Phys., **50**, 4865 (1969)
[15] Miller, F. A., Fateley, W. G., Witkowski, R. E.: Spectrochim. Acta, *23A*, 891 (1967)
[16] Eglinton, G., Ferguson, G., Islam, K. M. S., Glasby, J. S.: J. Chem. Soc. **B. 1141** (1967)
[17] Cochran, W.: Acta Cryst., **6**, 260 (1953)
[18] Ohno, K.: Theoret. Chim. Acta, **2**, 219 (1964)
[19] Mataga, N., Nishimoto, K.: Z. Phys. Chem (Frankfurt) **13**, 140 (1957)
[20] Kiss, A. I., Joó, F.: Int. J. Quant. Chem. **9**, 261 (1975)

Árpád Kiss
József Szőke } H-1525 Budapest 114, Pf. 49.

Acta Chimica Academiae Scientiarum Hungaricae, Tomus 90(2), pp. 141—148 (1976)

ON THE MOLECULAR STRUCTURE OF TRIETHYL SILANE AS STUDIED BY ELECTRON DIFFRACTION

B. CSÁKVÁRI*, ZS. WAGNER* and I. HARGITTAI**

*(*Department of General and Inorganic Chemistry, L. Eötvös University*
***Central Research Institute for Chemistry, Hungarian Academy of Sciences)*

Received, August 20, 1975

The electron diffraction data of triethyl silane are consistent with a C_3 symmetry model with rotational angle(s) between 105 and 145° around the Si–C bond (the *anti* position of the H–Si–C–C chain would correspond to 0°). The molecules are probably performing large amplitude twisting motion around the Si–C bonds. The Si–C bond length (r_g) and the Si–C–C bond angle were determined to be 1.887 ± 0.004 Å and 115.1 ± 1.1°, respectively.

Introduction

As part of our electron diffraction investigations of the vapour phase molecular structure of silicon compounds, *e.g.* $(CH_3)_3SiOSi(CH_3)_3$ [1], $(CH_3)_3SiOCH_3$ [2], $CH_3Si(OCH_3)_3$ [3], $(CH_3)_3SiC(CO)Si(CH_3)_3$ [4], the present study of triethyl silane, $HSi(C_2H_5)_3$, was initiated aiming at extending structural information for this compound.

Experimental

The sample of triethyl silane used in this study was a product of PCR (Peninsular ChemResearch).

The electron diffraction patterns were recorded on a modified EG-100A apparatus [5, 6] at room temperature. The ranges of intensity data corresponding to the 50 cm and 19 cm nozzle-to-plate distances were $2.50 \leq s \leq 13.50$ Å^{-1} and $6.50 \leq s \leq 33.00$ Å^{-1}, respectively. The procedure of data reduction including the determination and subsequent modifications of the experimental background was similar to that described elsewhere [7]. A composite molecular intensity distribution was used for further analysis (with $\Delta s = 0.25$ Å^{-1}) shown in Fig. 1.

Structure analysis

The experimental radial distribution shown in Fig. 2 directly provides us with a considerable amount of structural information. The first three maxima at 1.10, 1.55, and 1.89 Å can be assigned to the C–H, C–C, and Si–C bonds

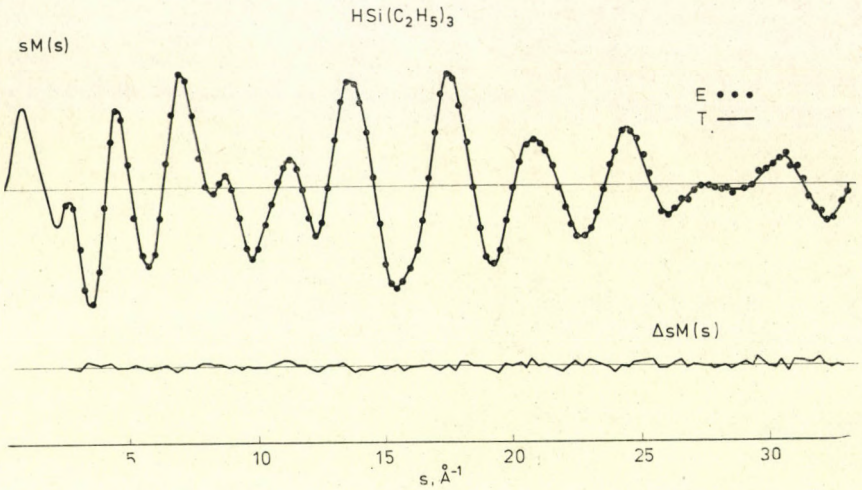

Fig. 1. Experimental (E) and theoretical (T) molecular intensities and the difference curve

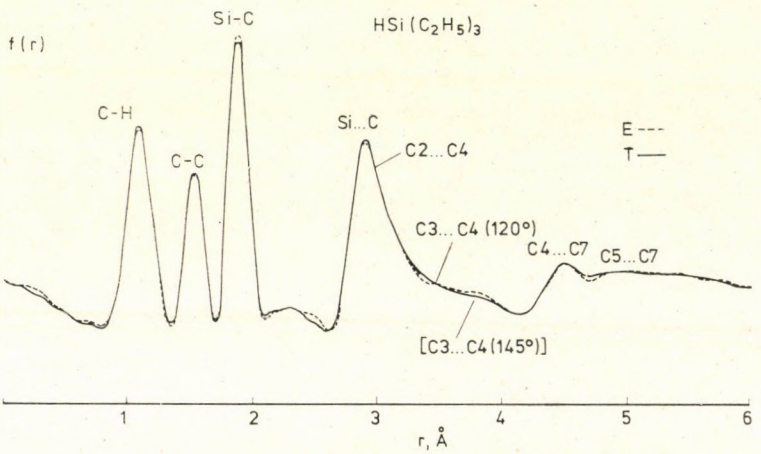

Fig. 2. Experimental (E) and theoretical (T) radial distributions. The theoretical curve was calculated for a model with $\varphi = 120°$. The position of the C3 . . . C4 distance that would correspond to $\varphi = 145°$ is also indicated. The numbering of atoms is presented in Fig. 4

in that order. The contribution of the Si–H bond is too small to be noticeable compared with that of C–C together with which it is expected to appear. In fact, the length and mean vibrational amplitude of the Si–H bond were assumed to be 1.48 Å and 0.08 Å and not varied in this analysis.

The position of the largest maximum in the region where the nonbond distances appear (at about 2.9 Å) may be a good indication of the Si . . .C nonbond distance. Thus it was possible to estimate the bond angle Si–C–C to be as large as 116° from the values of r(Si–C), r(C–C), and r(Si . . . C). The outer part of the radial distribution is determined mainly by the rotation-

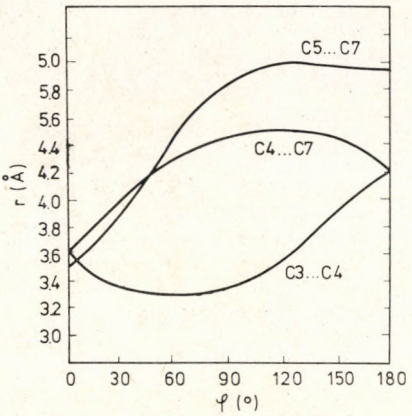

Fig. 3. The variations of the rotation-dependent C...C distances *vs.* the rotational angle around the Si–C bond. They were calculated from parameters similar to those presented in Table I. The numbering of atoms is presented in Fig. 4.

(around the Si–C bond)-dependent C . . . C distances and also by Si . . . H and C . . . H distances.

The most important assumption for the molecular model applied was that all three angles of rotation around the Si–C bonds (φ) were equal (C_3 symmetry). In addition, all C–H bonds were assumed to be of equal length, the C–H bonds of the methyl group staggered the bonds of the adjacent carbon atom, the threefold axis of the methyl group coincided with the C–C bond, the plane of the methylene group was perpendicular to the SiCC plane and bisected the Si–C–C angle. The following bond lengths and angles were chosen to describe the geometry: r(Si–C), r(C–C), r(C–H), r(Si–H), $<$C–Si–C, $<$Si–C–C, $<$C(H_2)–C–H and $<$Si–C(H_2)–H. The theoretical distributions have been seen to be so little sensitive to changes in the last two angles that they could not really be considered determined in this study.

The refinement* of the main geometric parameters and mean vibrational amplitudes of distances with relatively large contribution to the scattering has been performed employing fixed values for the angle of rotation around the Si–C bonds. The angle of rotation (φ) was put equal to zero when the threefold axis of the $HSiC_3$ fragment and the C–C bond were in the same plane and in *anti* position. The main geometric parameters, except perhaps $<$C–Si–C, were shown to be little sensitive to the angle of rotation used. This observation was later reinforced by refinement schemes in which the rotation-dependent C...C distances were allowed to vary without geometric constraint.

The variations of the rotation-dependent C...C distances are shown in Fig. 3. These curves were calculated from geometric parameters similar to those shown in Table I. The numbering of the atoms of the silicon–carbon

* The least squares refinement based on the molecular intensities was applied in a similar manner as described elsewhere [7]. For references of the scattering functions used see also [7].

Table I

Main molecular parameters of triethyl silane*

Parameters	(I) Model with $\varphi = 120°$	(II) Models with $\varphi =$ $= 105—145°$
r_a(Si—C)	1.886±0.004 Å	1.886±0.004 Å
l(Si—C)	0.046±0.002 Å	0.046±0.005 Å
r_a(C—C)	1.547±0.004 Å	1.548±0.004 Å
l(C—C)	0.043±0.002 Å	0.041±0.005 Å
r_a(C—H)	1.108±0.003 Å	1.109±0.003 Å
l(C—H)	0.066±0.002 Å	0.066±0.005 Å
<C—Si—C	108.7±1.9°	110.5±4.0°
<Si—C—C	114.4±0.2°	115.1±1.1°
l(Si...C)	0.085±0.005 Å	
l(C3...C4)	0.21 ±0.03 Å	
l(C2...C5)	0.101±0.010 Å	
l(C3...C5)	0.31 ±0.03 Å	

* For error estimates see comment in text.

skeleton is shown in Fig. 4. The results of the least squares refinements were judged in conjunction with an inspection of the experimental and theoretical radial distributions. Our efforts were aimed at finding at least the prevailing conformer under the assumption of C_3 symmetry, in addition to the determination of the main geometric parameters. As values of φ between 0 and 180° were tested with $\Delta\varphi$ steps of 5 to 30°, the changes of the generalized R-factor* showed the following features: A local minimum was found at about $\varphi = 30°$, and a deeper and shallow minimum in the interval of about $\varphi = 105$ to 145°. The model with $\varphi = 30°$ can be ruled out to be prevailing on the basis of the radial distributions. On the other hand, as the positions of the maxima at about 3.55, 3.85, 4.50, and 4.9 Å can be assigned to the rotation-dependent C...C distances, the models with rotational angles in the interval of $\varphi = 105$ to 145° seem to be probable indeed. The appearance of the double maximum at 3.55 and 3.85 Å may be an indication of the presence of two forms or one with an equilibrium angle in between and performing large amplitude twisting motion**. It is also possible that of the two features at 3.55 and 3.85 Å, only one corresponds to the C3...C4 distances and the other to Si...H and C...H interactions. The main geometric parameters and some important mean

* $R = \{\Sigma W(s)[sM^E(s) - sM^T(s)]^2/\Sigma W(s)[sM^E(s)]^2\}^{1/2}$, $W(s)$ are the weights of the observations.

** While C3...C4 varies between 3.55 and 3.85 Å, the other two distances (C4...C7 and C5...C7) change very little.

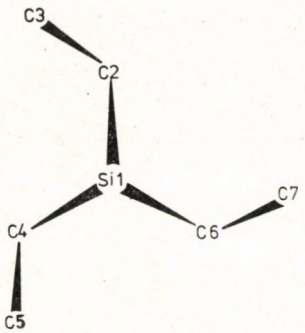

Fig. 4. The numbering of atoms of the silicon–carbon skeleton of triethyl silane

amplitudes of vibration are collected in Table I. Column (I) as determined for $\varphi = 120°$, and Column (II): as the average determined from the refinements with $\varphi = 105°$, $\varphi = 120°$, $\varphi = 145°$, and also with $\varphi = 120°$ and independently refining the rotation-dependent C...C distances. The errors indicated were estimated as usual [7], thus they include an 0.2 and 2 per cent experimental error for distances and amplitudes, respectively. Besides, the errors given in Column (II) are increased to cover the variations of the parameters obtained in the entire interval of $\varphi = 105$ to 145°. There is undeniably some arbitrariness in presenting these results and errors but it seems to us that these values provide a fair representation of what we learned about the structure of triethyl silane.

Discussion

The electron diffraction study of the triethyl silane vapour can provide a limited amount of structural information only. The most difficult and unsolved problem is posed by the presence of the three rotational axes. A complete determination is hindered also by strong correlations between the parameters that characterize bond configurations and the internal motion including rotation or twist

The length of the Si–C, C–C, and C–H bonds and the Si–C–C bond angle seem to be reliably determined and show no unusual features. The average length of the Si–C bond, r_g(Si–C) = 1.887 Å determined in this study is similar to those in tetramethyl silane and hexamethyl disilane, the mean for the two molecules being 1.878 ± 0.002 Å [8].

Discussing the conformational properties of triethyl silane, we would like to stress that neither mixtures of conformers, nor forms with unequal rotational angles have been considered in this structure analysis. On the other hand, the experimental data could be satisfactorily approximated with a C_3 symmetry model having angles of rotation around the Si–C bond $\varphi = 120°$, or rather, with C_3 models having rotational angles somewhere between 105 and 145° and, perhaps, performing large amplitude twisting motion.

From a chemical structural point of view the C_3 model with a rotational angle in the vicinity of 120° seems to be reasonable indeed since it represents an all-staggered conformation. It is also noteworthy that, as expected, the C2...C5 *anti* interaction has a much smaller mean vibrational amplitude than the C3...C4 *gauche* interaction.

We find it of interest to compare the conformational properties of triethyl silane and methyl trimethoxy silane considering the Si–C and Si–O bonds as rotation axes. As the lone pairs on the oxygen atom are also taken into account, similar rotation forms may be expected. The two molecules were indeed shown to have similar conformational properties under similar conditions of analysis.

Appendix

Reduced experimental molecular intensities

s	$sM^E(s)$	s	$sM^E(s)$
2.00	−57.4	8.00	18.8
.25	−101.6	.25	−15.6
.50	−65.1	.50	21.6
.75	−79.8	.75	38.8
3.00	−242.4	9.00	−1.9
.25	−395.2	.25	−137.0
.50	−454.4	.50	−236.9
.75	−324.9	.75	−285.6
4.00	−76.6	10.00	−245.8
.25	177.8	.25	−154.8
.50	300.9	.50	−60.1
.75	269.2	.75	27.6
5.00	92.8	11.00	92.6
.25	−117.9	.25	122.8
.50	−267.7	.50	74.6
.75	−315.7	.75	−14.8
6.00	−255.0	12.00	−147.7
.25	−116.3	.25	−217.0
.50	94.9	.50	−158.3
.75	281.8	.75	1.7
7.00	431.5	13.00	179.7
.25	417.6	.25	340.8
.50	278.1	.50	392.3
.75	127.9	.75	372.2

Appendix (Continued)

s	$sM^E(s)$	s	$sM^E(s)$
14.00	317.3	24.00	132.7
.25	188.1	.25	214.7
.50	27.0	.50	203.8
.75	−147.4	.75	182.6
15.00	−315.7	25.00	113.7
.25	−392.6	.25	38.1
.50	−398.4	.50	−25.1
.75	−396.5	.75	−108.0
16.00	−332.3	26.00	−122.3
.25	−258.3	.25	−96.0
.50	−136.7	.50	−64.9
.75	32.0	.75	−61.1
17.00	201.4	27.00	−19.8
.25	340.0	.25	−9.5
.50	432.8	.50	−1.3
.75	397.2	.75	−19.7
18.00	336.7	28.00	−18.4
.25	183.4	.25	−14.3
.50	−12.5	.50	−43.4
.75	−166.7	.75	35.9
19.00	−293.3	29.00	−19.9
.25	−335.3	.25	−15.9
.50	−290.2	.50	45.2
.75	−137.3	.75	55.5
20.00	−19.1	30.00	68.5
.25	102.1	.25	86.9
.50	139.7	.50	122.2
.75	198.2	.75	63.3
21.00	162.3	31.00	69.7
.25	134.1	.25	19.2
.50	57.9	.50	−47.3
.75	−27.5	.75	−94.4
22.00	−117.0	32.00	−105.2
.25	−154.8	.25	−148.5
.50	−176.7	.50	−134.2
.75	−212.0	.75	−76.8
23.00	−156.3	33.00	−28.4
.25	−102.3		
.50	−22.1		
.75	73.1		

REFERENCES

[1] CSÁKVÁRI, B., WAGNER, ZS., GÖMÖRY, P., MIJLHOFF, F. C., ROZSONDAI, B., HARGITTAI, I.: J. Organometal. Chem. **107**, 287 (1976)
[2] CSÁKVÁRI, B., WAGNER, ZS., GÖMÖRY, P., HARGITTAI, I., ROZSONDAI, B., MIJLHOFF, F. C.: Acta Chim. (Budapest), **90**, 149 (1976)
[3] GERGŐ, É., HARGITTAI, I., SCHULTZ, GY.: J. Organometal. Chem. **112**, 29 (1976)
[4] ROZSONDAI, B., HARGITTAI, I.: Acta Chim. (Budapest), **90**, 157 (1976)
[5] HARGITTAI, I., HERNÁDI, J., KOLONITS, M., SCHULTZ, GY.: Rev. Sci. Instrum. **42**, 546 (1971)
[6] HARGITTAI, I., HERNÁDI, J., KOLONITS, M.: Prib. Tekhn. Eksp. (Moscow) 239 (1972)
[7] HARGITTAI, M., HARGITTAI, I.: J. Chem. Phys. **59**, 2513 (1973)
[8] BEAGLEY, B., MONAGHAM, J. J., HEWITT, T. G.: J. Mol. Structure **8**, 401 (1971)

Béla CSÁKVÁRI
Zsófia WAGNER } H-1088 Budapest, Múzeum krt. 6—8.

István HARGITTAI H-1088 Budapest, Puskin u. 11—13.

Acta Chimica Academiae Scientiarum Hungaricae, Tomus 90(2), pp, 149—156 (1976)

ELECTRON DIFFRACTION STUDY OF THE MOLECULAR STRUCTURE OF TRIMETHYLMETHOXYSILANE

B. Csákvári*, Zs. Wagner*, P. Gömöry*,
I. Hargittai**, B. Rozsondai** and F. C. Mijlhoff***

(Department of General and Inorganic Chemistry, L. Eötvös University
** Central Research Institute for Chemistry, Hungarian Academy of Sciences
*** Gorlaeus Laboratoria der Rijksuniversiteit, Leiden)*

Received September 5, 1975

An electron diffraction study of trimethylmethoxysilane yielded, among others, the following geometrical parameters: r_a(Si–O) = 1.639 ± 0.004 Å, r_a(Si–C) = 1.864 ± ± 0.004 Å, r_a(C–O) = 1.423 ± 0.005 Å, r_a(C–H) = 1.114 ± 0.003 Å, <Si–O–C = = 122.5 ± 0.6°, and < O–Si–C = 108.6 ± 0.2°. The experimental data are interpreted in terms of a staggered conformation (C_s symmetry) and large amplitude twisting motion about the Si–O bond. A large (≈ 0.1 Å) shrinkage of the *anti* C . . . C distance is observed as compared with a strictly staggered geometry.

Introduction

Recently we have performed a structural study of the series of compounds $(CH_3)_{4-n}Si(OCH_3)_n$, $n = 1, 2, 3, 4$, by gas electron diffraction. Our primary interest is in the variation of the oxygen bond angle and the Si–O bond length in this series and also in the conformational properties of the individual compounds. So far the investigation of tetramethoxysilane [1] and methyltrimethoxysilane [2] has been completed. The present report deals with the results on trimethylmethoxysilane. The electron diffraction study of dimethyldimethoxysilane is in progress.

Experimental

The sample of trimethylmethoxysilane (b.p. 56.7 °C/760 Torr) was prepared by known methods [3] and purified by fractional distillation. A hexamethyldisiloxane impurity of somewhat less than 1% could not be eliminated, as was shown by gas chromatography.

The electron diffraction experiment and data treatment were carried out in the Leiden laboratory [4]. The following data ranges were used (Δs = = 0.25 Å^{-1}): $3.50 \leq s \leq 14.50$ Å^{-1}, $5.00 \leq s \leq 28.75$ Å^{-1}, and $15.75 \leq$ $\leq s \leq 33.00$ Å^{-1}.

The further analysis starting with the determination of the experimental background was performed in Budapest [4]. The composite electron

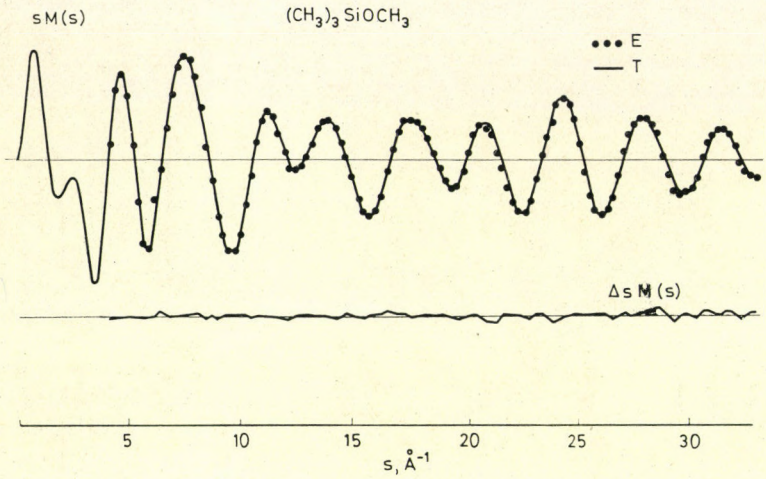

Fig. 1. Experimental (E, dots) and theoretical (T, full line) molecular intensities and difference curve ($\Delta\, sM(s)$). T and Δ refer to the model in Table I

diffraction molecular intensity distribution is shown in Fig. 1, corresponding to the expression $sM^E(s) = s[I(s) - B(s)]/B(s)$, where $I(s)$ and $B(s)$ are the total experimental intensities and the experimental backgrounds*.

Structure analysis

Direct information from the experimental radial distributions (Fig. 2) could be extracted for the bonds only. The values of 1.11, 1.42, 1.63, and 1.87 Å were estimated for r(C–H), r(C–O), r(Si–O), and r(Si–C), respectively,** and used in the trial structures.

The bond angles $<$Si–O–C and $<$O–Si–C have been varied in a wide range (especially the former, between 110 and 150°) and the calculated theoretical distributions were compared with the experimental ones to estimate good starting values for subsequent refinements. They turned out to be around 122—124° and 108°, respectively.

The first trial calculations and the least-squares refinements based on the molecular intensities*** were applied at the beginning to a model with C_s symmetry. The C7-Si1-O2-C3 plane (see Fig. 3) coincided with the plane of

* The numerical data are given in the Ph. D. Dissertation of (Miss) Zs. WAGNER, L. Eötvös University, Budapest, 1974.

** In fact, these estimates were obtained from an experimental radial distribution calculated without artificial damping, thus providing better resolution for the bond distances than the one seen in Fig. 2.

*** Some details and references can be found elsewhere concerning the procedure [5] and the scattering functions used [6].

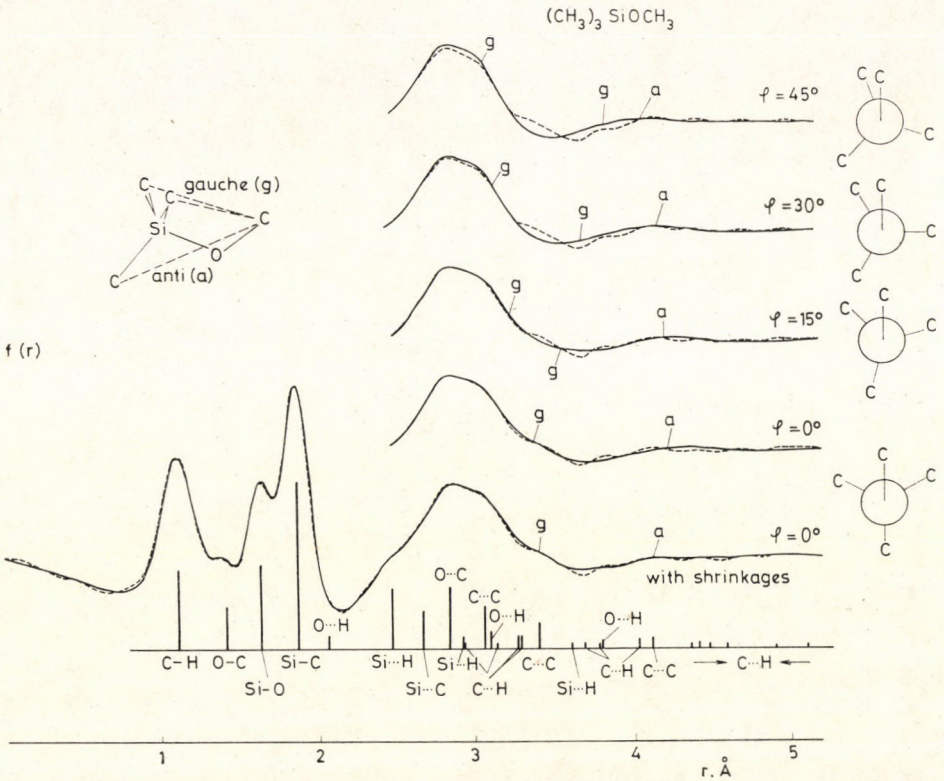

Fig. 2. Experimental (dotted line) and theoretical (full line) radial distributions, damping constant $a = 0.0018$ Å^2. The rods below represent contributions from pairs of atoms

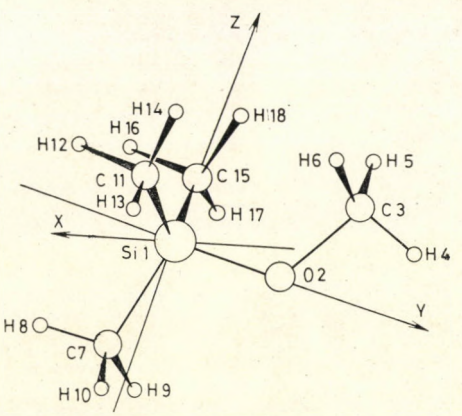

Fig. 3. Model of trimethylmethoxysilane with the numbering of atoms

symmetry in this case and, accordingly, the O–C bond staggered the Si–C bonds. This model is characterized by a zero twist angle ($\varphi = 0°$) about the Si–O bond. The Si–O bond coincided with a C_{3v} axis of the $(CH_3)_3SiO$ fragment (zero tilt). In some subsequent calculations these constraints were re-

moved. There were some other assumptions that remained in effect throughout this analysis. Thus all C–H bonds had the same length, the methyl groups had a staggered conformation with respect to the other bonds through one rotational axis, and the H...H distances were ignored except those within the same methyl group. All Si–C bonds and C–Si–C angles were the same even when tilt was introduced. In addition to the bond distances, the bond angles <Si–O–C, <O–Si–C, <O–C–H, and <Si–C–H were chosen to describe the geometry.

The molecular parameters determined by fixing the twist angle at zero were not appreciably different from those listed in Table I. The agreement with the experimental data achieved by means of this model is characterized by the generalized R factor (0.078, for definition of R see Table I) and the radial distributions ($\varphi = 0°$, upper curve, Fig. 2).

Table I

Results of refinement 'with shrinkages' for trimethylmethoxysilane

	r(Å) <(deg)	l(Å)
Independent distances		
Si–O	1.639±0.004	0.045±0.002
Si–C	1.864±0.004	0.062±0.002
C–O	1.423±0.005	0.082±0.004
C–H	1.114±0.003	0.079±0.002
C...C_{anti}	4.12[a]±0.03	0.12±0.03
C...C_{gauche}	3.40[a]±0.02	0.13±0.01
Independent angles		
Si–O–C	122.5±0.6	
O–Si–C	108.6±0.2	
O–C–H	108.5 (fixed)	
Si–C–H	110.5 (fixed)	
Dependent distances[b]		
Si...C	2.69	0.079±0.008
C7...C11	3.06	0.102±0.007
Si...H8	2.48	0.125±0.006
O...C	2.85	0.087±0.005
R[c]	0.065	

[a] If calculated from the geometry: 4.22 and 3.38 Å, resp.

[b] Only some of them are listed here.

[c] $R = \{\Sigma[sM^E(s) - sM^T(s)]^2/\Sigma[sM^E(s)]^2\}^{1/2}$, $sM^T(s)$ is the theoretical molecular intensity for the model.

In the next stage of the structure analysis twist angles different from zero have also been tested between 0 and 60° with $\Delta\varphi = 15°$ and later with $\Delta\varphi = 2.5$ to 5° for the interval between 0 and 15°. The radial distributions for some of the models with nonzero twist angles are shown in Fig. 2. The geometrical parameters showed little sensitivity to changes in the assumed values of the twist angle. Figure 4 demonstrates the variation of the R factor as a function of the twist angle applied. There is the same good agreement between the experimental and theoretical data for twist angles between 0 and 10°. This indicates a staggered conformation (C_s symmetry) indeed, with large amplitude twisting motion about the Si–O bond.

A closer examination of the radial distributions obtained experimentally and calculated for the staggered model, reveals, however, one interesting discrepancy. Namely, the *anti* C...C distance *(a)* appears at a somewhat larger value than would be expected by the features of the experimental distribution. Usually it is dangerous, of course, to assign such ill-defined maxima on the experimental radial distribution. However, this assignment is supported by the changes of the radial distributions calculated for different angles of rotation. Indeed, while the position of the *anti* C...C distance is shifted towards smaller values, the *gauche* C...C distances *(g)* split into two. By the time φ becomes 30°, the *anti* distance gets into its proper place but the disagreement observed for the *gauche* distances makes such a model obviously unacceptable.

Several approaches were considered of how to bring the *anti* distances to its 'right' place without disturbing the good position of the *gauche* interactions. The comparison of the radial distributions revealed that introducing a twist around the Si–O bond would not help.

A tilt of the threefold axis of the C_3Si fragment from the Si–O bond was introduced in some models while retaining the C_s symmetry of the molecular geometry. As is demonstrated by Fig. 5, however, the decrease of r(C3...C7) is accompanied by an increase of the *gauche* C...C distance by about the same amount.

The failure of these approaches to eliminate the discrepancy between the calculated and the experimental radial distributions does not mean that there is no twist or tilt in the actual structures, but merely that neither of these effects can be singled out to be the major source of the described phenomenon.

We feel that in any case it is the intramolecular vibrations, probably perpendicular vibrations, that provide the most reasonable explanation for the shortening of the *anti* C...C distance. While the average value for the *anti* r(C...C) decreases, due to these vibrations, as compared with the *anti* distance in the rigid molecule, it is more difficult to estimate the changes in the *gauche* C...C distance. We have found that the most proper approach, at least to eliminate the effect of the changes of the *anti* and *gauche* C...C

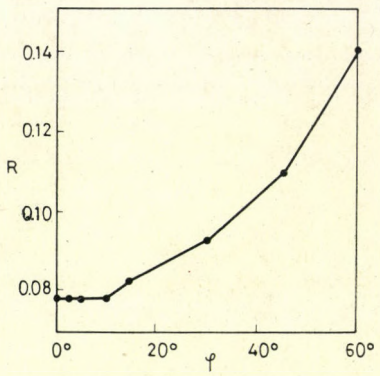

Fig. 4. R factor for models with different fixed twist angles φ

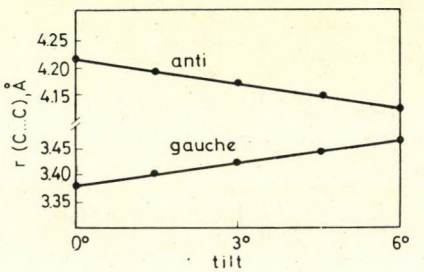

Fig. 5. Variation of the *anti* and *gauche* C...C distances with the tilt angle of the C_3Si group

distances on the other parameters refined, is to let these distances vary independently. This refinement scheme yielded an ever better agreement (R = = 0.065) and eliminated the above discussed discrepancy as is demonstrated by the 'with shrinkages' curves, $\varphi = 0°$, in Fig. 2. The geometrical parameters determined in this way, however, proved to be the same as for the constrained model*. The results of the least-squares refinement for trimethylmethoxysilane are compiled in Table I.

Discussion

According to the electron diffraction data, the trimethylmethoxysilane molecule takes a staggered conformation with C_s symmetry with large amplitude twisting motion around the Si–O bond. A large ($\approx$0.1 Å) shrinkage of the *anti* C...C distance is observed as compared with a strictly staggered equilibrium geometry. Large amplitude intramolecular motion has been found to be characteristic of other methoxysilanes [1, 2] and hexamethyldisiloxane [4] as well.

* However, this is not always necessarily so, as has been demonstrated for hexamethyldisiloxane [4].

All the geometrical and vibrational parameters determined seem to be reasonable with the exception of l(C–O), which is certainly too large.

The bond configurations found show no unusual features. The C–O bond length does not differ significantly from those observed in CH_3OCH_3 (1.416 ± 0.003 Å [7]) and in $Si(OCH_3)_4$ (1.416 ± 0.002 Å [1]). It is thus largely unaffected by the nature of the adjacent substituent, and keeps its value, which happens to be the same as the SCHOMAKER—STEVENSON estimate [8], *viz.* 1.42 Å [9].

More variation is displayed by the Si–O bonds in siloxanes and hexamethyldisiloxane. Some data are collected in Table II. First, all of them are shorter than the SCHOMAKER—STEVENSON estimate [8], *viz.* 1.76 Å [9]. This has been repeatedly interpreted as a consequence of $d\pi - p\pi$ interactions. The more subtle variations of the bond length in the compound series in Table II

Table II

Compound	r_a(Si–O) (Å)	<Si–O–C (deg)	<Si–O–Si (deg)	Ref.
H_3SiOCH_3	1.640 ± 0.003	120.6 ± 1.0		[10]
$(CH_3)_3SiOCH_3$	1.639 ± 0.004	122.5 ± 0.6		this work
F_3SiOCH_3	1.58	131.4 ± 3.2		[11]
$H_3SiOC_6H_5$	1.648 ± 0.007	121 ± 1		[12]
$CH_3Si(OCH_3)_3$	1.632 ± 0.004	123.6 ± 0.5		[2]
$Si(OCH_3)_4$	1.612 ± 0.003	120 ± 2		[1]
$H_3SiOSiH_3$	1.634 ± 0.002		144.1 ± 0.9	[13]
$(CH_3)_3SiOSi(CH_3)_3$	1.631 ± 0.003		148 ± 3	[4]
$Cl_3SiOSiCl_3$	1.592 ± 0.010		146 ± 4	[11]
$F_3SiOSiF_3$	1.580 ± 0.025		155 ± 2	[14]

also deserve attention. The Si–O bonds are of about the same length in H_3SiOCH_3, $(CH_3)_3SiOCH_3$, $C_6H_5OSiH_3$, $H_3SiOSiH_3$, $(CH_3)_3SiOSi(CH_3)_3$ if the experimental error is taken into consideration. Hopefully, more powerful studies will some day provide data accurate enough to make the interpretation of the differences among them possible. Comparison of the data on H_3SiOCH_3 and $(CH_3)_3SiOCH_3$ on the one hand and those on $H_3SiOSiH_3$ and $(CH_3)_3SiOSi(CH_3)_3$, on the other, reveals a slight shortening of the Si–O bond, which may be attributed to the introduction of a second silicon as a ligand of the oxygen atom*. A considerably shorter (1.613 Å) Si–O bond was found in tetramethoxysilane [1]. Probably an increasing number of electronegative ligands attached to the silicon atom shortens the Si–O distance.

* The molecules F_3SiOCH_3 and $F_3SiOSiF_3$ provide no information since the parameter r(Si–O) determined in the latter [14] has a very large uncertainty, while this very value was used as an assumed parameter in the analysis of the former [11] where the Si–O and Si–F distances are too close to each other to be determined separately.

Before commenting upon the bond angles, it should be stressed again that electron diffraction analysis provides some effective values that may be different from the equilibrium angles outside the experimental error especially if the molecules perform large amplitude motion. This warning aside, some interesting patterns seem to emerge from the data on the Si–O–C and Si–O–Si bond angles. It has been observed before that the shortening of the Si–O bond in the case of more electronegative ligands is accompanied by a considerable increase in the bond angles at the oxygen atom (see *e.g.* [9]). It is also remarkable that, though the introduction of the second silicon as a ligand of oxygen decreases r(Si–O) very slightly, the opening in the bond angle is substantial. We wish also to note that this additional opening is nearly the same for the three pairs of molecules studied so far:

		$\Delta(<\text{Si–O–X})$
H_3SiOCH_3,	$H_3SiOSiH_3$	23.5°
$(CH_3)_3SiOCH_3$,	$(CH_3)_3SiOSi(CH_3)_3$	25.5°
F_3SiOCH_3,	$F_3SiOSiF_3$	24.6°

REFERENCES

[1] BOONSTRA, L. H., MIJLHOFF, F. C., RENES, G., SPELBOS, A., HARGITTAI, I,: J. Mol. Struct., **28,** 129 (1975)
[2] GERGŐ, É., HARGITTAI, I., SCHULTZ, GY.: J. Organometal. Chem., **112,** 29 (1976)
[3] NOLL, W.: *Chemie und Technologie der Silicone.* Verlag Chemie, Weinheim/Bergstrasse 1968
[4] CSÁKVÁRI, B., WAGNER, ZS., GÖMÖRY, P., MIJLHOFF, F. C., ROZSONDAI, B., HARGITTAI, I.: J. Organometal. Chem., **107,** 287 (1976)
[5] HARGITTAI, M., HARGITTAI, I.: J. Chem. Phys., **59,** 2513 (1973)
[6] HARGITTAI, I., MIJLHOFF, F. C.: J. Mol. Struct., **16,** 69 (1973)
[7] KIMURA, K., KUBO, M.: J. Chem. Phys., **30,** 151 (1959).
[8] SCHOMAKER, V., STEVENSON, D. P.: J. Amer. Chem. Soc., **63,** 37 (1941)
[9] VILKOV, L. V., KHAIKIN, L. S.: *Topics in Current Chemistry*, Vol. 53. Springer, Berlin 1975
[10] GLIDEWELL, C., RANKIN, D. W. H., ROBIETTE, A. G., SHELDRICK, G. M., BEAGLEY, B., FREEMAN, J. M.: J. Mol. Struct., **5,** 417 (1970)
[11] AIREY, W., GLIDEWELL, C., ROBIETTE, A. G., SHELDRICK, G. M.: J. Mol. Struct., **8,** 413 (1971)
[12] GLIDEWELL, C., RANKIN, D. W. H., ROBIETTE, A. G., SHELDRICK, G. M., BEAGLEY, B., FREEMAN, J. M.: Trans. Faraday Soc., **65,** 2621 (1969)
[13] ALMENNINGEN, A., BASTIANSEN, O., EWING, V., HEDBERG, K., TRAETTEBERG, M.: Acta Chem. Scand., **17,** 2455 (1963)
[14] AIREY, W., GLIDEWELL, C., RANKIN, D. W. H., ROBIETTE, A. G., SHELDRICK, G. M., CRUICKSHANK, D. W. J.: Trans. Faraday Soc., **66,** 551 (1970)

Béla CSÁKVÁRI
Zsófia WAGNER
Pál GÖMÖRY — H-1088 Budapest, Múzeum krt. 6—8.

István HARGITTAI
Béla ROZSONDAI — H-1088 Budapest, Puskin u. 11—13.

Frans C. MIJLHOFF — Gorlaeus Laboratoria, Section X-ray and Electron Diffraction, P.O.Box 75, Leiden, The Netherlands.

Acta Chimica Academiae Scientiarum Hungaricae, Tomus 90(2), pp. 157—164 (1976)

ELECTRON DIFFRACTION STUDY OF THE MOLECULAR STRUCTURE OF BIS(TRIMETHYLSILYL)KETENE

B. ROZSONDAI and I. HARGITTAI

(Central Research Institute for Chemistry of the Hungarian Academy of Sciences, Budapest)

Received September 20, 1975

An electron diffraction study of bis(trimethylsilyl)ketene yielded a limited amount of structural information, including the molecular parameters $r_a(\text{Si–C})_{\text{av.}} = 1.886 \pm \pm 0.004$ Å, $l(\text{Si–C})_{\text{av.}} = 0.056 \pm 0.003$ Å and $<\text{Si–C–Si} = 129°$ (with error estimates of $+2°$ and $-4°$) for a model with C_{2v} symmetry. Bond angles at double-bonded carbon atoms and at N, O, *etc.* atoms bonded to C, Si or Ge are discussed.

The molecular geometry and dynamics, the electronic structure, energetics and the chemical behaviour of ketene and its organic derivatives have aroused much interest among theoretical chemists. Ketene itself has a relatively small dipole moment (1.414 ± 0.010 D [1], see also [2]), with the negative pole pointing towards the methylene carbon atom. Organometallic substituents like a silyl or germyl group, change the electronic structure of the $>C=C=O$ group substantially, as force constant calculations [2] and chemical properties of the derivatives (see *e.g.* [3]) show. It is highly challenging to test the influence of organometallic substituents on the geometrical parameters. This was the purpose of the present electron diffraction investigation of bis(trimethylsilyl)ketene, $[(CH_3)_3Si]_2C=C=O$, following a similar study of the corresponding germanium compound [4]. The main emphasis was on the determination of the bond angle at the $>C=$ atom. The Ge–C–Ge angle could be unambiguously determined as $127.6 \pm 1.3°$, whereas Si–C–Si angles in a wider range were found to be consistent with our electron diffraction experimental data.

Attempts to obtain electron diffraction patterns of bis(trimethylstannyl)-ketene vapours remained unsuccessful, probably because the sample decomposed before an appropriate vapour pressure was reached.

Structure analysis

The experimental procedure, data reduction and structure analysis were much the same as for bis(trimethylgermyl)ketene [4].

The sample of bis(trimethylsilyl)ketene (b.p. 69 °C/32 Torr, $n_D^{20} = 1.4410$ [6]) was provided by PONOMAREV and LEBEDEV [5] and contained

5—10% of hexamethyldisiloxane, according to a mass-spectrometric analysis [7]. The nozzle temperature was about 87 to 107 °C during the exposures. Two plates were used from the two camera distances each to obtain the experimental molecular intensities in ranges $1.875 \leq s \leq 12.25$ Å^{-1}, $\Delta s = 0.125$ Å^{-1} and $7.25 \leq s \leq 32.0$ Å^{-1}, $\Delta s = 0.25$ Å^{-1}, as described in Refs. [4] and [8]. The two ranges were treated separately in the refinements.

The molecular models used in the structure analysis were similar to those in Ref. [4]. The basic model (Fig. 1) has C_{2v} overall symmetry, the $(CH_3)_3Si$ and CH_3 groups have local symmetry C_{3v} around the Si–C(C) and Si–C(H) bonds, respectively. Bond lengths Si–C(C), Si–C(H), C=O, C=C and C–H, and bond angles Si–C–Si, (H)C–Si–C(H) and H–C–H define the geometry. Models with lower symmetry were also tried.

Bond distances (r) and mean amplitudes of vibration (l) for the C–H, C=O and C=C bonds, which constitute the peak at about 1.1 Å of the experimental radial distribution curve $f^E(r)$ (Fig. 2), were allowed to vary in some stages of the analysis, yet some of them had to be given assumed values in the end, because of large correlations with other parameters.

The Si–C(C) and Si–C(H) bonds dominate the peak at 1.88 Å. In most of the refinements, both were treated as independent parameters and usually the former proved to be shorter but the inverse order turned up too, depending on the conditions of the refinement. Therefore, they were confined then to be equal.*

As for the derivation of the Si–C–Si angle from the radial distribution, the correct assignment of the Si.Si distance is of vital importance, although other interatomic distances also help. The peak at 3.1 Å involves, among others, the C.C distances through one bond angle, and all our efforts to squeeze r(Si.Si) into the same range failed as discrepancies in other parts of the $f(r)$ emerged. Neither of the models with a twist of the trimethylsilyl groups about the Si–C(C) bonds (C_2 symmetry) or a tilt of their C_{3v} axes from the Si–C(C) bonds (C_{2v} symmetry) or a combination of twist and tilt (C_2) or even with a non-planar (!?) $Si_2C=C$ fragment (C_s) could be brought into satisfactory agreement with the experimental data. When r(Si.Si) was treated as an independent parameter (in addition to the bond lengths and angles), the Si–C–Si angle refined to about 127°, which would arise from an Si.Si distance of about 3.4 Å. In fact, it is the faint hump at 3.4 Å on the $f^E(r)$ curve, at the

* Stereochemical considerations do not help predict the relative magnitude of the Si–C bond lengths. On the one hand, comparisons of C–C bond lengths in *e.g.* propane and propene (1.532 ± 0.003 Å [9] and 1.506 ± 0.003 Å [10], respectively; r_g values) or Si–C bonds in ethylsilane and vinylsilane (1.866 ± 0.002 Å [11] and 1.853 ± 0.003 Å [13], respectively; microwave studies) would suggest shorter Si–C bonds adjacent to a C=C double bond. On the other hand, BAK *et al.* observed a lengthening of the C–C bond in methylketene (1.518 ± 0.002 Å [14], microwave study), as compared with propene or acetaldehyde. These authors pointed to "a possible effect of the cumulated double bonds". *Cf.* also r_0(C–C) = 1.514 ± 0.002 Å in 1,1-dimethylallene [15].

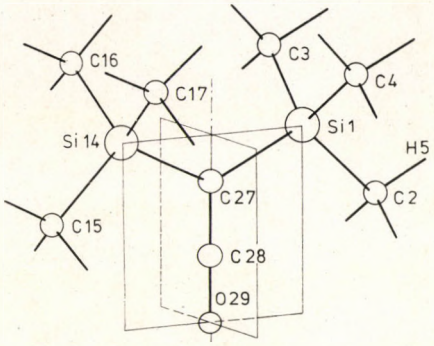

Fig. 1. C_{2v} model of bis(trimethylsilyl)ketene and numbering of atoms

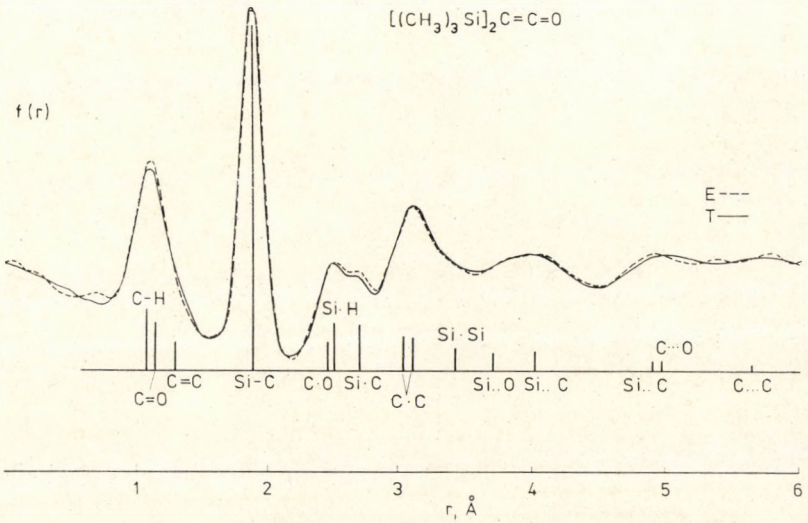

Fig. 2. Experimental (E, dashed line) and theoretical (T, full line) radial distribution. The range $2.0 \leq s \leq 32.0$ Å^{-1} and damping with $a = 0.002$ Å^2 were used. The vertical bars show contributions from some of the interatomic distances. The number of dots represents the number of bond angles separating the two atoms.

foot of the C.C peak, that must be recognized as the contribution from the Si.Si distance, in accordance with other non-bond distances. Correlations with other parameters have a large effect, and the structure analysis produces a rather uncertain value of the Si–C–Si angle. The (H)C-Si-C(H) angle was fixed at 111° for the model shown in Table I and Fig. 2, because it assumed ill-defined values in the previous refinements.

The feature at 1.6 Å of the $f^E(r)$ curve can be attributed to the Si–O bond distance in hexamethyldisiloxane. Corrections of the experimental molecular intensity for 5 or 10% of the admixture (the known structure of which [16] was used) did not change the parameters of bis(trimethylsilyl)-ketene appreciably.

Table I

Structural parameters of bis(trimethylsilyl)ketene, C_{2v} model[a]

	r_a, Å	l, Å
$(Si–C)_{av.}$	1.886±0.004	0.056±0.003
C–H	1.092±0.007	0.087±0.007[b]
C=C	1.318±0.013	0.050±0.007[b]
C=O	(1.16)	0.046±0.007[b]
Si–C–Si	129+2; −4°[c]	
(H)C–Si–C(H)	(111°)	
H–C–H	105.4±1.2[a]	
Si.Si	3.408±0.016	0.145±0.041
Si.H	2.526±0.008	0.110±0.009[d]
Si.C28	2.726±0.008	0.071±0.012
Si..O	3.703±0.011	0.210±0.041[e]
k_1	1.054±0.039	
k_2	1.046±0.026	
R	0.108	

[a] Error estimates include standard deviations obtained from the least-squares refinement, multiplied by $\sqrt{3}$ and, in case of distances (r_a) and amplitudes (l), an estimate for systematic errors of 0.2 and 2%, respectively. Assumed values are in parentheses (). For the definition of the scale factors k and of the R factor, see Ref. [4]. k_1 and k_2 apply to data for the short and long camera distance, respectively.

[b] l parameters coupled in the refinement

[c] The usual error estimate gives ±2°. The lower limit was extended on the basis of experience gained during the refinements.

[d] Coupled with l (C27.O) = 0.040 Å

[e] Coupled with other amplitudes (not listed here)

Discussion

Table I demonstrates the results for the C_{2v} model of bis(trimethylsilyl)-ketene. In addition to the error estimates given, further uncertainty arises as a consequence of possible large-amplitude intramolecular motions.

Similarly to the case of the germanium derivative [4], it was not possible to distinguish between the two types of silicon-carbon bond. On the other hand, the Si–C≡and Si–C(H) bonds were found to be 1.825±0.006 Å and 1.865± ±0.004 Å in $(CH_3)_3SiC{\equiv}CH$, and 1.825±0.008 Å and 1.855±0.006 Å in $(CH_3)_3SiC{\equiv}CCl$, respectively [17]. The average silicon-carbon bond length in the ketene derivative, $r_a(Si–C)_{av.}$ is in good agreement with, or seems to be slightly longer than the Si–C lengths in other molecules, *e.g.* 1.875±0.002 Å and 1.877±0.003 Å in tetramethylsilane and hexamethyldisilane, respectively ($r_g(1)$ values) [18].

Table II

Bond angles of double-bonded carbon atoms

Molecule	M–C(=)–M degrees	Reference
$H_2C=CH_2$	117.2±1.1	[19][a]
$F_2C=CH_2$[b]	109.1	[20]
$(H_3C)_2C=CH_2$[b]	115.6±0.3[c]	[21]
$(F_3C)_2C=CH_2$[b]	123.6±0.3	[22]
$F_2C=CF_2$	112.5[c]	[46]
$Cl_2C=CCl_2$	115.7±0.3	[23][a]
$Br_2C=CBr_2$	115.2±0.3	[23][a]
$I_2C=CI_2$	114.2±0.5	[23][a]
$(H_3C)_2C=C(CH_3)_2$	112.2±0.7[c]	[21]
$H_2C=O$	108.4[c]	[24][a]
$(H_3C)_2C=O$	116.7±0.3	[22]
$(F_3C)_2C=O$	121.4±0.4	[22]
$(Cl_3C)_2C=O$	122.2±1.0[c]	[25][a]
$(F_3C)_2C=NH$	121.6±0.4	[22]
$H_2C=C=CH_2$	118.4[c]	[26][a]
$(H_3C)_2C=C=CH_2$[b]	116.4±0.1	[15]
$H_2C=C=O$	122.5±0.5	[27]
$(H_3C)_2C=C=O$	117.4	[28]
$[(H_3C)_3Si]_2C=C=O$	129±2; −4	this work
$[(H_3C)_3Ge]_2C=C=O$	127.6±1.3	[4]

[a] Data and reference quoted from Ref. [29]
[b] The value given refers to the heavy atom skeleton.
[c] Angle and/or error estimate calculated from data given in the reference

The amount of structural data on ketene derivatives is rather limited. Table II lists some bond angles at double-bonded carbon atoms, for comparison with our Si–C–Si angle. The actual geometry is obviously a result of several effects. For instance, factors included in the valence shell electron pair repulsion (VSEPR) model [30] often compete with repulsive interactions between non-bonded pairs of atoms. It is difficult therefore to predict variations of bond angles in such compounds.

According to the VSEPR model, one expects an M–C(=)–M angle less than 120°. Indeed, in many of the molecules listed, this angle is considerably smaller than 120°. More accurate data will be required for the interpretation of more delicate trends.

Table III

Bond angles $M-X-M$ in molecules M_2X or M_3X

Group M	Atom X									
	O		S		Se		N		P	
H_3C	111.5±1.5	[31]	99.2±0.7	[35]	96.2±0.2	[37]	110.6±0.6	[39]	98.6±0.3	[42]
H_3Si	144.1±0.8$_6$	[32]	97.4±0.7	[36]	96.6±0.7	[36]	119.7±0.1	[40]	96.45±0.50	[43]
$(H_3C)_3Si$	148±3	[16]								
H_3Ge	126.5±0.3	[33]	98.9±0.1	[33]	94.6±0.5	[38]	(120)[a]	[41]	95.39±0.05	[44]
$(H_3C)_3Ge$	141±0.5	[34]								
$(H_3C)_3Sn$	141±0.5	[34]								

[a] Assumed value

It is instructive to compile some data on bond angles of atoms bonded to carbon, silicon, *etc.* (Table III). The observation that the Si–X–Si and C–X–C angles differ considerably when X has lone-pair electrons and belongs to the row of N, O, *etc.* of the periodic table [45], can be extended to Ge-X–Ge angles (as compared with C–X–C) and applies also to the ketene derivatives, although there are no lone-pair electrons on the carbon atom of ketene. The large Si–C–Si and Ge–C–Ge angle in the ketene derivatives may be due to non-bond interactions of bulky groups and to special interactions of silicon or germanium atoms with the electrons of the ketene group. Structural data on silyl and germyl ethylenes and ketones would throw more light on these phenomena.

Note added in proof. Both for bis(trimethylsilyl)ketene and bis(trimethylgermyl)ketene, small discrepancies at about 5 Å between the experimental and theoretical radial distribution curves (see Fig. 2 above and Fig. 4 in Ref. [4]) may be interpreted in terms of shrinkage effects. Therefore, some long distances with large contributions were treated as independent parameters in some additional calculations. Changes of the parameters in these refinements remained well within stated error limits.

*

The authors are indebted to Professor L. V. VILKOV (Moscow) for initiating this project and to Drs. S. V. PONOMAREV and S. A. LEBEDEV (Moscow) for the provision of the sample.

REFERENCES

[1] JOHNSON, H. R., STRANDBERG, M. W. P.: J. Chem. Phys., **20,** 687 (1952)
[2] LAZAREV, A. N., TENISHEVA, T. F., SHCHUKOVSKAYA, L. L., PAL'CHIK, R. I.: Dokl. Akad. Nauk SSSR, **190,** 1106 (1970)
[3] MAZEROLLES, P., LAPORTERIE, A., LESBRE, M.: C. R. Acad. Sci., **C268,** 361 (1969)
[4] ROZSONDAI, B., HARGITTAI, I.: J. Mol. Struct. **17,** 53 (1973)
[5] PONOMAREV, S. V., ERMAN, M. B., LEBEDEV, S. A., PECHURINA, S. YA., LUTSENKO, I. F.: Zh. Obshch. Khim., **41,** 127 (1971)
[6] PONOMAREV, S. V.: private communication, Moscow, 1971
[7] TAMÁS, J.: private communication, Budapest, 1971
[8] ROZSONDAI, B., KOLONITS, M., HARGITTAI, I.: Jenaer Rundschau, **19,** 285 (1974)
[9] IIJIMA, T.: Bull. Chem. Soc. Japan, **45,** 1291 (1972)
[10] TOKUE, I., FUKUYAMA, T., KUCHITSU, K.: J. Mol. Struct. **17,** 207 (1973)
[11] PETERSEN, D. H.: Dissertation, University of Notre Dame, Notre Dame, Indiana, 1961; quoted from Ref. [12]
[12] STARCK, B.: Bibliographie mikrowellenspektroskopischer Untersuchungen an Molekülen, Bd. I. 1945—1962; Bd. II. 1963—1965; STARCK, B., KETTESMANN, K.: as above, Bd. III. 1966—1970, Sektion für Strukturdokumentation der Universität Ulm
[13] O'REILLY, J. M., PIERCE, L.: J. Chem. Phys., **34,** 1176 (1961)
[14] BAK, B., CHRISTIANSEN, J. J., KUNSTMANN, K., NYGAARD, L., RASTRUP-ANDERSEN, J.: J. Chem. Phys., **45,** 883 (1966)
[15] DEMAISON, J., RUDOLPH, H. D.: J. Mol. Spectr., **40,** 445 (1971); quoted from Ref. [12]
[16] CSÁKVÁRI, B., WAGNER, ZS., GÖMÖRY, P., MIJLHOFF, F. C., ROZSONDAI, B., HARGITTAI, I.: J. Organometal. Chem., **107,** 287 (1976)
[17] ZEIL, W., HAASE, J., DAKKOURI, M.: Disc. Faraday Soc., **47,** 149 (1969)
[18] BEAGLEY, B., MONAGHAN, J. J., HEWITT, T. G.: J. Mol. Struct. **8,** 401 (1971)
[19] KUCHITSU, K.: J. Chem. Phys., **44,** 906 (1966)
[20] LAURIE, V. W., PENCE, D. T.: J. Chem. Phys., **38,** 2693 (1963)

[21] TOKUE, I., FUKUYAMA, T., KUCHITSU, K.: J. Mol. Struct., **23,** 33 (1974)
[22] HILDERBRANDT, R. L., ANDREASSEN, A. L., BAUER, S. H.: J. Phys. Chem., **74,** 1586 (1970)
[23] STRAND, T. G.: Acta Chem. Scand., **21,** 2111 (1967)
[24] KATO, C., KONAKA, S., IIJIMA, T., KIMURA, M.: Bull. Chem. Soc. Japan, **42,** 2148 (1969)
[25] ANDERSEN, P., ASTRUP, E. E., BORGAN, A.: Acta Chem. Scand., **A28,** 239 (1974)
[26] ALMENNINGEN, A., BASTIANSEN, O., TRAETTEBERG, M.: Acta Chem. Scand., **13,** 1699 (1959)
[27] BEAUDET, R. A.: Dissertation, Harvard University, 1961; Diss. Abstr., **23,** 2334 (1963); quoted from Ref. [12]
[28] SUTTER, D., CHARPENTIER, L., DREIZLER, H.: Z. Naturforsch., **27a,** 597 (1972)
[29] STARCK, B.: Electron Diffraction Catalogue, Sektion für Strukturdokumentation der Universität Ulm
[30] GILLESPIE, R. J.: Molecular Geometry. Van Nostrand Reinhold, London 1972
[31] KIMURA, K., KUBO, M.: J. Chem. Phys., **30,** 151 (1959)
[32] ALMENNINGEN, A., BASTIANSEN, O., EWING, V., HEDBERG, K., TRAETTEBERG, M.: Acta Chem. Scand., **17,** 2455 (1963)
[33] GLIDEWELL, C., RANKIN, D. W. H., ROBIETTE, A. G., SHELDRICK, G. M., BEAGLEY, B., CRADOCK, S.: J. Chem. Soc. (A), 315 (1970)
[34] VILKOV, L. V.: Kém. Közlemények, **35,** 375 (1971); VILKOV, L. V., TARASENKO, N. A.: Zh. Strukt. Khim., **10,** 1102 (1969)
[35] RADNAI, T., HARGITTAI, I., KOLONITS, M., GREGORY, D. C.: to be published
[36] ALMENNINGEN, A., FERNHOLT, L., SEIP, H. M.: Acta Chem. Scand., **22,** 51 (1968); ALMENNINGEN, A., HEDBERG, K., SEIP, R.: Acta Chem. Scand., **17,** 2264 (1963)
[37] BEECHER, J. F.: J. Mol. Spectr., **21,** 414 (1966); quoted from Ref. [12]
[38] MURDOCH, J. D., RANKIN, D. W. H., GLIDEWELL, C.: J. Mol. Struct. **9,** 17 (1971)
[39] BEAGLEY, B., HEWITT, T. G.: Trans. Faraday Soc., **64,** 2561 (1968)
[40] BEAGLEY, B., CONRAD, A. R.: Trans. Faraday Soc., **66,** 2740 (1970); *cf.* HEDBERG, K.: J. Amer. Chem. Soc., **77,** 6491 (1955)
[41] GLIDEWELL, C., RANKIN, D. W. H., ROBIETTE, A. G.: J. Chem. Soc. (A), 2935 (1970)
[42] BARTELL, L. S., BROCKWAY, L. O.: J. Chem. Phys., **32,** 512 (1960)
[43] BEAGLEY, B., ROBIETTE, A. G., SHELDRICK, G. M.: J. Chem. Soc. (A), 3002 (1968)
[44] RANKIN, D. W. H., ROBIETTE, A. G., SHELDRICK, G. M., BEAGLEY, B., HEWITT, T. G.: J. Inorg. Nucl. Chem., **31,** 2351 (1969)
[45] ALMENNINGEN, A., SEIP, H. M., SEIP, R.: Acta Chem. Scand., **24,** 1697 (1970)
[46] CARLOS, J. L., Jr., KARL, R. R., Jr., BAUER, S. H.: J. C. S. Faraday Trans. II, **70,** 177 (1974)

Béla ROZSONDAI
István HARGITTAI } H-1088 Budapest, Puskin utca 11—13.

Acta Chimica Academiae Scientarium Hungaricae, Tomus 90(2), pp. 165–178 (1976)

ELECTRON DIFFRACTION STUDY OF THE MOLECULAR STRUCTURE OF ACETALDAZINE

I. HARGITTAI*, Gy. SCHULTZ*, V. A. NAUMOV** and Yu. P. KITAEV**

*(*Central Research Institute for Chemistry, Hungarian Academy of Sciences, H-1088 Budapest, **Arbuzov Institute of Organic and Physical Chemistry, Kazan Branch of the U.S.S.R. Academy of Sciences, 420 083 Kazan)*

Received October 8, 1975

According to the electron diffraction data of acetaldazine, the *anti, trans-trans* conformer prevails in the vapour phase probably with a large amplitude twisting motion about the N–N bond. A smaller amount of the *gauche* form is also detected. The following molecular parameters characterize the structure of the heavy-atom skeleton: r_a(N–N) = 1.437±0.013 Å, r_a(N=C) = 1.277±0.003 Å, r_a(C–C) = 1.486±±0.008 Å, <N–N=C = 110.4±0.9°, and <N=C–C = 121.4±1.0°.

Introduction

The molecular structure of acetaldazine, $CH_3-CH=N-N=CH-CH_3$, has been studied by various physical techniques, *viz.* dipole moment measurements, Raman and infrared vibrational and ultraviolet spectroscopy, and nuclear magnetic resonance spectroscopy [1–5]. Of the following three isomers

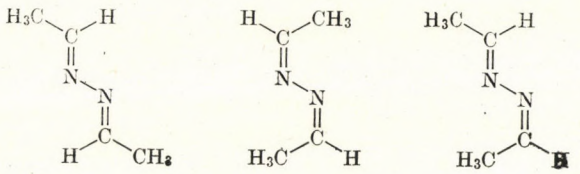

1 2 3

the one with the least steric interaction (*1*) was shown to be preferred in liquid solution by an NMR study [3]. The presence of other isomers in lesser amounts was also indicated. According to physical evidence and some theoretical calculations [1, 2, 4, 5] a nonplanar arrangement of the C=N—N=C chain was indicated.

The present electron diffraction study of acetaldazine was initiated with the aim of collecting direct structural information on the geometry of this molecule. The main features of our investigation have already been communicated in a short paper [6]. When our structure analysis was being completed, we learned from Prof. K. HEDBERG about an electron diffraction study of formaldazine performed at the CORVALLIS laboratory [7]. Thus it is possible to compare the results obtained for these two molecules.

Experimental

The electron diffraction patterns from a CH_3–CH=N–N=CH–CH_3 sample (bp. 95—96 °C/760 Torr) were taken with the EG-100A apparatus in Budapest during a visit of one of us (V.A.N.). The purity of the sample was confirmed by mass spectrometry. The so-called membrane nozzle system [8] and r^3 rotating sector [9] were used. The nozzle was at room temperature during the exposures. The experimental techniques and data reduction were essentially the same as described elsewhere [10, 11].

The ranges of intensity data used were $2.25 \leq s \leq 13.00$ Å^{-1} and $9.25 \leq s \leq 33.50$ Å^{-1} for the 50 cm and 19 cm camera ranges, respectively. The data intervals of $\Delta s = 0.125$ and 0.25 Å^{-1} were used. The molecular intensities are shown in Fig. 1.

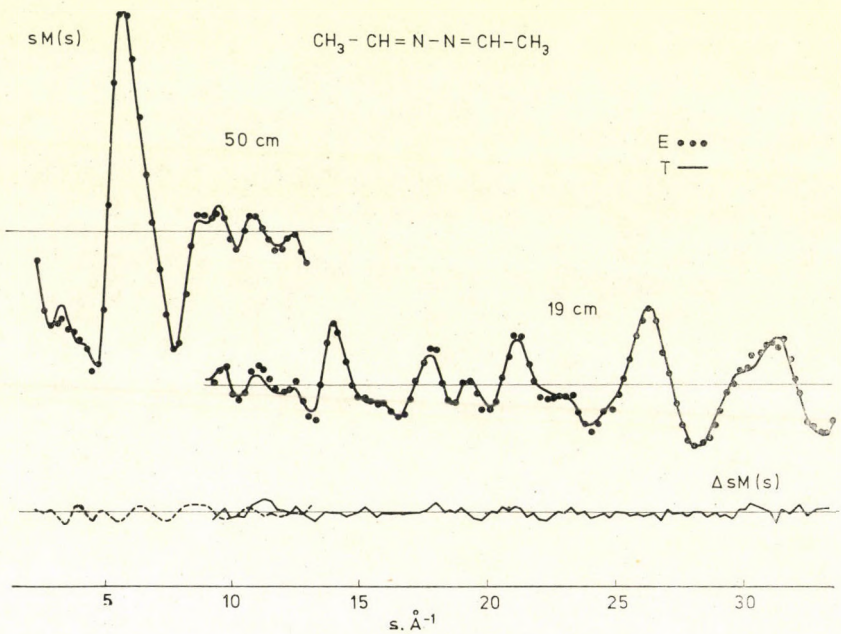

Fig. 1. The molecular intensities (E — experimental, T — theoretical) of acetaldazine

Structure analysis

The molecular model

As concerns the relative position of the =CH–CH_3 groups with respect to rotation about the N–N bond, the possible forms are *syn* ($\varphi = 0°$), *anti* ($\varphi = 180°$) and the forms corresponding to the rotational angles $0 < \varphi < 180°$ (see Fig. 2). If the C–C=N–N chains are assumed to have a planar structure,

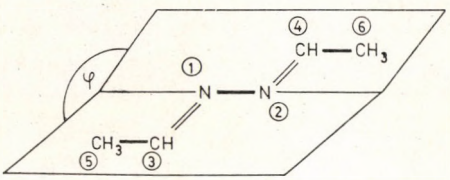

Fig. 2. The molecular model of acetaldazine

trans and *cis* isomers are possible with respect to the double bonds. Thus for each rotational form relative to the N–N bond, *trans-trans* (**1**), *cis-cis* (**2**) and *cis-trans* (**3**) isomers may exist. The only other assumptions are that the CH_3 group has a C_{3v} symmetry, the pyramidal axis coincides with the extension of the C–C bond, the configuration of the methyl group is such that the C=N bond staggers the C–H bond, and all C–H bonds are of equal length and have the same amplitude of vibration.

Experimental radial distribution

An experimental radial distribution is shown in Fig. 3. It was clear from the beginning of this structure analysis that the many features and the outstretched character of the experimental radial distribution reveals much about the geometry of this molecule. It also shows that a long chain molecule may be advantageous to study by electron diffraction.

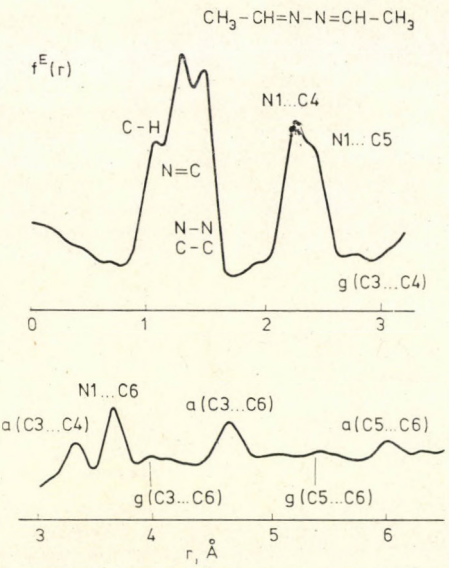

Fig. 3. Experimental radial distribution of acetaldazine with the assignment of its mos important features

The first three features on the experimental radial distribution between 0.9 and 1.7 Å correspond to the contributions from the four bonds, with the C–C and N–N bonds badly overlapping. Each of the well-expressed features at about 2.25, 2.40, 3.67, 4.64 and 6.01 Å represent the contribution from only one of the most important nonbond interactions that come from N...C or C...C atomic pairs. Of these, the C...C distances are dependent on the rotation about the N–N bond. The assignment of the maximum at 3.67 Å to the N...C distances through two bond angles unambiguously indicates the *trans* relative orientation of the N–N and C–C bonds in the CH_3–CH=N–N fragment. The assignment of the maximum at 6.01 Å to the largest C...C distance was especially instrumental in establishing that an *anti* or nearly *anti* form with *trans* isomers around the double bond is at least prevailing in the vapour phase.

Refinements and results

The least squares method was applied to the molecular intensities. The data corresponding to the two camera ranges were treated separately (*cf.* [10]). The major portion of these calculations was performed at the Department of Chemistry, University of Texas, during a visit of two of us (I. H. and Gy. Sch.).

As an *anti* or nearly *anti* form with *trans* isomers was seen to be prevailing on the experimental radial distribution, the structural analysis was first performed under the assumption of having this conformer only.

The bond distances, bond angles, mean amplitudes of vibration (l values) for the bonds and for the most important nonbond interactions have been refined in gradually larger groups for the *anti*, *trans-trans* form with $\varphi = 180°$ fixed. The refinements were then repeated for a series of other fixed values for the dihedral angle φ. The best agreements were obtained for values between $\varphi = 155$ and 160°. Later, the constraint for φ was removed and, as it turned out, all the bond distances, angles, and the l values for all the bonds, for the C...C and N...C distances plus for the shortest C...H interactions that had the multiplicity of 6, could be refined simultaneously. The results of such a refinement are given in Table I. Considering all the molecular parameters and the two scale factors corresponding to the two camera ranges a total of 253 correlation coefficients were calculated. Of these, in order to save space, only those are shown in Table II, whose absolute values are larger than 0.5. Note that 11 out of these 20 correlation coefficients refer to either r(N–N) or l(N–N). These parameters are very uncertain. The geometrical parameters show no unusual values except that both r(C–H) and l(C–H) are too small. Note, however, that no correlation coefficients in Table II refer to these parameters. The l values for the nonbond N...C and C...C interactions are relatively small and this indicates that the molecule is relatively rigid.

Table I

Results of least squares refinements for anti form only
N-multiplicity, σ-standard deviation from the least squares refinement

Bond (Å)	*N*	*r*	σ	*l*	σ
N–N	1	1.438	0.008	0.078	0.012
N=C	2	1.277	0.001_5	0.043	0.002
C–C	2	1.486	0.004	0.044	0.003
$(C–H)_{av.}$	8	1.068	0.002	0.066	0.002
Bond angle (°)		α	σ		
N–N=C		110.4	0.5		
N=C–C		121.8	0.4		
N–C–H		120.4	1.7		
C–C–H		106.6	0.6		
Dihedral angle (°)		φ			
		159.3	1.8		
Dependent N...C and C...C distances (Å)	*N*	*r*	σ	*l*	σ
N1...C4	2	2.231	0.002	0.048	0.002
N1...C5	2	2.416	0.003	0.057	0.002
N1...C6	2	3.657	0.002	0.055	0.003
C3...C4	1	3.312	0.004	0.062	00.07
C3...C6	2	4.617	0.004	0.087	0.007
C5...C6	1	6.006	0.005	0.066	0.012

It is very difficult, if possible at all, to evaluate the results concerning the dihedral angle in the prevailing rotational form. Although the deviation from the $\varphi = 180°$ *anti* conformation was indicated to be significant even on a 0.5% significance level* according to the Hamilton test [12] (*cf.* Fig. 4), the changes in the nonbond C...C distances that correspond to a decrease of about 25° in the dihedral angle φ are less than, say, 0.04 Å. Such shortenings then may well occur as a consequence of the intramolecular motion.

* Here the generalized R factors,
$R_1 = \{\Sigma W_s[M^E(s) - M^T(s)]^2\}/\{\Sigma W_s[M^E(s)]^2\}$, are used for comparison, as obtained in a refinement with φ being refined along with a series of other parameters, and in other refinements with φ fixed and the same series of parameters refined.

Table II

Correlation coefficients (associated with the results of Table I) whose absolute value is greater than 0.5

Parameters		Correlation coefficient	Parameters		Correlation coefficient
1	2		1	2	
r(N–N)	r(N–C)	0.618	r(C–C)	∠N–N–C	0.830
r(N–N)	r(C–C)	−0.840	r(C–C)	∠N–C–C	−0.745
r(N–N)	∠N–N–C	−0.967	r(C–C)	l(N–N)	−0.872
r(N–N)	∠N–C–C	0.681	∠N–N–C	∠N–C–C	−0.654
r(N–N)	l(N–N)	0.575	∠N–N–C	l(N–N)	−0.587
r(N–C)	r(C–C)	−0.741	∠N–C–C	l(N–N)	0.613
r(N–C)	∠N–N–C	−0.664	∠N–C–C	k'(*)	0.526
r(N–C)	l(N–N)	0.789	l(N–N)	l(N–C)	0.753
r(N–C)	l(N–C)	0.541	l(N–N)	l(C–C)	−0.684
r(N–C)	l(C–C)	−0.503	l(N–C)	l(C–C)	−0.688

(*) k' is the scale factor for the data from the long camera range

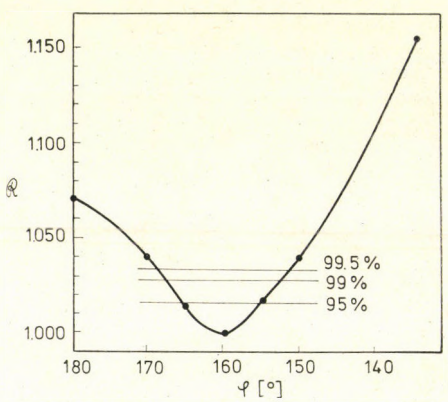

Fig. 4. R factor ratio *vs.* rotational angle φ (*cf.* [12])

As the experimental radial distribution is examined in detail, some additional features are observed in the regions where the contributions of rotation dependent C...C distances occur. These are most notably at about 4.0 and 5.4 Å, which would correspond to a *gauche* form with a dihedral angle of φ = = 60°. The third and shortest C...C distances should then be expected at about 2.6 Å and are not really well seen.

In order to estimate the relative abundance of the *anti* and *gauche* (φ = 60°)* conformers and to see the influence of taking the *gauche* content

* The value of 60° was assumed for the dihedral angle of the *gauche* form according to the experimental radial distribution and not refined in this analysis.

into account in the refinement of the geometrical parameters, the following scheme was set up. The *gauche* content was assumed to be 5, 10, 15, 20 etc. % and, fixing a given percentage, the refinement of the parameters for the *anti* form was repeated. In doing this the geometrical parameters of the *gauche* form were assumed to be the same as those of the *anti* form. The geometrical parameters from the refinement schemes with 0, 10, and 20% *gauche* content are given in Table III and show no considerable changes.

Table III

Bond lengths, bond angles and the values of φ as obtained from least squares refinements with 100%, 90%, and 80% anti form in the anti-gauche mixture (the σ values are parenthesized)

anti form content / parameters	100%	90%	80%
r(N–N) (Å)	1.438(8)	1.437(8)	1.438(9)
r(N=C) (Å)	1.2766(15)	1.2766(14)	1.2768(15)
r(C–C) (Å)	1.4857(44)	1.4864(49)	1.4860(51)
r(C–H) (Å)	1.0679(18)	1.0677(18)	1.0679(20)
<N–N=C (°)	110.45(53)	110.40(54)	110.26(58)
<N=C–C (°)	121.82(38)	121.45(38)	121.25(40)
<C–C–H (°)	106.56(63)	105.89(56)	105.46(60)
φ (°)	159.3(18)	161.5(19)	163.0(23)

The agreement between the experimental and theoretical intensity data improved, however, when 5% *gauche* form was introduced. A further improvement was achieved when using somewhat larger l values for the rotation dependent C...C distances of the *gauche* form than those of the *anti* form, *viz.* 0.0925, 0.1168, and 0.0970 Å for C3...C4, C3...C6, and C5...C6, respectively. As the experimental and theoretical radial distributions calculated for the *anti-gauche* mixtures were compared, it was seen that the *gauche* content may be higher than indicated by the least squares refinement based on the molecular intensities. A *gauche* content even as high as 15 to 20% cannot be excluded, considering the features at $r = 4.0$ and 5.4 Å assigned to r(C3...C6) and r(C5...C6) of the *gauche* form, respectively, while the contribution of the C3...C4 interaction from the *gauche* form was much less expressed. There is only the very small maximum at about 5.05 Å on the experimental radial distribution that remains unaccounted for by the *anti* and *gauche* forms described above.

It is interesting to note that the results obtained for the *gauche* content were invariant to geometries with $\varphi = 180°$ or $\varphi = 160°$ for the *anti* form.

Table IV

The bond lengths and angles of acetaldazine as determined by electron diffraction

r_a(N–N)	1.437±0.013 Å
r_a(N=C)	1.277±0.003 Å
r_a(C–C)	1.486±0.008 Å
r_a(C–H)$_{av}$	1.068±0.004 Å
<N–N=C	110.4±0.9°
<N=C–C	121.4±1.0°
<N–C–H	120.4±2.4°
<C–C–H	105.9±1.5°

The final geometrical parameters from this structure analysis referring to a model with 90% *anti* and 10% *gauche* forms are collected in Table IV. The total errors given include the estimated experimental scale error of 0.2%, the standard deviation from the least squares refinement and also the differences in the parameter values between two sets of results obtained for the models with 0% and 20% *gauche* form, in order to take also this uncertainty into account, with the exception of <N–C–H, which was kept constant in the calculations for determining the *gauche* content.

Discussion

According to the electron diffraction data, the majority of the acetaldazine molecules take an *anti trans-trans* form. About one fifth or less of the molecules assume a *gauche* form in which the two CH_3–CH=N– fragments are rotated to each other by 120° ($\varphi = 60°$) as compared with the *anti* form. The experimental data could be better approximated with a somewhat twisted ($\sim$20°) *anti* conformer than with a strictly coplanar form. This is thought to be a consequence of shrinkage effects. In fact, the rotation-dependent C...C distances decrease by only a few hundredths of an Å when a twist of 20° is introduced around the N–N bond. In spite of the somewhat better agreement with experimental data achieved for a twisted *anti* form, demonstrated even by the Hamilton test (Fig. 4), we prefer to interpret our findings in terms of a coplanar *anti* form performing large amplitude twisting motion about the N–N bond rather than by a twisted *anti* equilibrium structure.

The present findings are at variance with the conclusions made earlier concerning the prevailing rotational isomers (according to the definition of the dihedral angle φ used in the present work, the preferred conformer had $\varphi = 120°$, *i.e.* an angle of rotation of 60° from the *anti* form) [4]. Fortunately,

the experimental radial distribution of acetaldazine provides direct evidence for the *anti* conformer.

An electron diffraction study of formaldazine, $CH_2=N-N=CH_2$, by HAGEN, BONDYBEY and HEDBERG [7] performed at three different temperatures, has shown the *anti* form to be prevailing. The mole fractions of the *anti* conformer were found to be 0.911(0.077), 0.785(0.095), and 0.749(0.108) at −30, 60, and 225 °C, respectively, the parenthesized values being 2σ. The angle of rotation was around 120° relative to the *anti* form (according to the definition used in this study, φ was around 60°). The energy difference between the *gauche* and *anti* forms was found to be 1.2(0.5) kcal/mol. HAGEN, BONDYBEY and HEDBERG [7] determined also the root-mean-square torsional amplitude for the *anti* conformer: 15.8(3.7)°, indicating large amplitude torsional motion. In the structure refinement shrinkage corrections of 0.01—0.02 Å were applied to the C...C and C...H distances in the *anti* form. As demonstrated above, the more complete conformational analysis of formaldazine, utilizing experimental data at three different temperatures [7], is consistent with the findings of the present study concerning the conformational properties of acetaldazine.

The molecular parameters determined for acetaldazine display no unusual features except that the values determined for r(C–H) and l(C–H) are too small. The parameters that have analogs in formaldazine show a remarkable consistency indeed, HAGEN, BONDYBEY and HEDBERG determined the following molecular parameters of the C=N–N=C skeleton in formaldazine (the values of 2σ are parenthesized):

r(N–N)	1.418 (0.003) Å
l(N–N)	0.056 (0.003) Å
r(C=N)	1.277 (0.002) Å
l(C=N)	0.045 (0.002) Å
r(C...N)	2.229 (0.003) Å
l(C...N)	0.060 (0.003) Å
r(C...C)	3.309 (0.011) Å
l(C...C)	0.060 Å (assumed)
$<$C=N–N	111.4 (0.2)°
$<$H–C=N	120.7 (0.8)°

The only noteworthy differences occur in the length and mean vibrational amplitude of the N–N bond. Although some lengthening of the N–N bond in the molecule with more nonbond repulsions could be rationalized and although there is consistency in the longer bond associated with a larger l value, we wish to stress that the parameters for the N–N bond were determined much less accurately in acetaldazine than in formaldazine.

Appendix

The numerical values of the total experimental intensities, $I_t^E(s)$, and experimental backgrounds, $I_b^E(s)$

50 cm camera range

s(Å^{-1})	$I_t^E(s)$	$I_b^E(s)$	s(Å^{-1})	$I_t^E(s)$	$I_b^E(s)$
2.125	0.9928	0.9995	5.875	1.5117	1.3175
2.250	0.9555	1.0285	6.000	1.4891	1.3065
2.375	0.9389	1.0540	6.125	1.4606	1.2955
2.500	0.9361	1.0775	6.250	1.4262	1.2840
2.625	0.9478	1.0990	6.375	1.3867	1.2720
2.750	0.9731	1.1215	6.500	1.3505	1.2590
2.875	0.9987	1.1415	6.625	1.3116	1.2455
3.000	1.0235	1.1600	6.750	1.2758	1.2325
3.125	1.0493	1.1770	6.875	1.2392	1.2190
3.250	1.0693	1.1930	7.000	1.2091	1.2060
3.375	1.0828	1.2090	7.125	1.1825	1.1940
3.500	1.0949	1.2240	7.250	1.1545	1.1830
3.625	1.1078	1.2385	7.375	1.1291	1.1740
3.750	1.1221	1.2525	7.500	1.1100	1.1660
3.875	1.1336	1.2650	7.625	1.0917	1.1570
4.000	1.1461	1.2775	7.750	1.0795	1.1490
4.125	1.1544	1.2900	7.875	1.0760	1.1420
4.250	1.1598	1.3020	8.000	1.0774	1.1345
4.375	1.1599	1.3140	8.125	1.0852	1.1280
4.500	1.1610	1.3255	8.250	1.0956	1.1220
4.625	1.1724	1.3360	8.375	1.1052	1.1160
4.750	1.1952	1.3455	8.500	1.1137	1.1105
4.875	1.2287	1.3530	8.625	1.1157	1.1055
5.000	1.2746	1.3588	8.750	1.1133	1.1000
5.125	1.3299	1.3595	8.875	1.1075	1.0960
5.250	1.3863	1.3585	9.000	1.1017	1.0915
5.375	1.4379	1.3540	9.125	1.0953	1.0860
5.500	1.4807	1.3470	9.250	1.0907	1.0815
5.625	1.5062	1.3380	9.375	1.0877	1.0755
5.750	1.5161	1.3280	9.500	1.0819	1.0710

50 cm camera range (continued)

s(Å^{-1})	$I_t^E(s)$	$I_b^E(s)$	s(Å^{-1})	$I_t^E(s)$	$I_b^E(s)$
9.625	1.0755	1.0660	11.500	0.9885	0.9910
9.750	1.0682	1.0610	11.625	0.9811	0.9860
9.875	1.0593	1.0560	11.750	0.9752	0.9810
10.000	1.0505	1.0510	11.875	0.9699	0.9755
10.125	1.0433	1.0465	12.000	0.9652	0.9705
10.250	1.0377	1.0415	12.125	0.9619	0.9650
10.375	1.0355	1.0365	12.250	0.9577	0.9600
10.500	1.0335	1.0325	12.375	0.9529	0.9545
10.625	1.0301	1.0280	12.500	0.9483	0.9495
10.750	1.0288	1.0230	12.625	0.9418	0.9440
10.875	1.0236	1.0175	12.750	0.9334	0.9390
11.000	1.0172	1.0120	12.875	0.9253	0.9340
11.125	1.0102	1.0070	13.000	0.9203	0.9290
11.250	1.0020	1.0020	13.125	0.9158	0.9235
11.375	0.9954	0.9960			

19 cm camera range

s(Å^{-1})	$I_t^E(s)$	$I_b^E(s)$	s(Å^{-1})	$I_t^E(s)$	$I_b^E(s)$
8.00	0.9959	1.0446	15.50	0.6707	0.6732
8.25	0.9938	1.0190	15.75	0.6648	0.6679
8.50	0.9983	0.9953	16.00	0.6600	0.6627
8.75	0.9854	0.9736	16.25	0.6535	0.6577
9.00	0.9608	0.9537	16.50	0.6481	0.6527
9.25	0.9364	0.9353	16.75	0.6438	0.6481
9.50	0.9241	0.9181	17.00	0.6418	0.6437
9.75	0.9091	0.9022	17.25	0.6401	0.6394
10.00	0.8850	0.8872	17.50	0.6388	0.6353
10.25	0.8682	0.8728	17.75	0.6364	0.6314
10.50	0.8566	0.8588	18.00	0.6328	0.6277
10.75	0.8501	0.8453	18.25	0.6250	0.6244
11.00	0.8381	0.8322	18.50	0.6190	0.6208
11.25	0.8243	0.8192	18.75	0.6151	0.6173
11.50	0.8089	0.8066	19.00	0.6145	0.6140
11.75	0.7933	0.7945	19.25	0.6116	0.6108
12.00	0.7813	0.7826	19.50	0.6069	0.6078
12.25	0.7702	0.7713	19.75	0.6022	0.6048
12.50	0.7621	0.7608	20.00	0.5994	0.6020
12.75	0.7477	0.7508	20.25	0.5973	0.5993
13.00	0.7344	0.7413	20.50	0.5978	0.5968
13.25	0.7252	0.7323	20.75	0.5976	0.5943
13.50	0.7236	0.7236	21.00	0.5976	0.5918
13.75	0.7248	0.7159	21.25	0.5948	0.5994
14.00	0.7215	0.7087	21.50	0.5894	0.5871
14.25	0.7125	0.7021	21.75	0.5856	0.5850
14.50	0.7005	0.6959	22.00	0.5818	0.5828
14.75	0.6904	0.6901	22.25	0.5794	0.5808
15.00	0.6826	0.6843	22.50	0.5776	0.5788
15.25	0.6770	0.6787	22.75	0.5757	0.5768

19 cm camera range (continued)

s(Å^{-1})	$I_t^E(s)$	$I_b^E(s$	s(Å^{-1})	$I_t^E(s)$	$I_b^E(s)$
23.00	0.5739	0.5749	28.50	0.5405	0.5445
23.25	0.5723	0.5730	28.75	0.5408	0.5435
23.50	0.5685	0.5712	29.00	0.5407	0.5425
23.75	0.5661	0.5695	29.25	0.5412	0.5416
24.00	0.5637	0.5678	29.50	0.5408	0.5407
24.25	0.5630	0.5662	29.75	0.5410	0.5397
24.50	0.5623	0.5646	30.00	0.5401	0.5388
24.75	0.5610	0.5631	30.25	0.5399	0.5378
25.00	0.5611	0.5617	30.50	0.5391	0.5368
25.25	0.5610	0.5603	30.75	0.5385	0.5358
25.50	0.5611	0.5589	31.00	0.5377	0.5347
25.75	0.5616	0.5574	31.25	0.5363	0.5337
26.00	0.5618	0.5562	31.50	0.5356	0.5325
26.25	0.5612	0.5549	31.75	0.5331	0.5313
26.50	0.5590	0.5536	32.00	0.5305	0.5301
26.75	0.5549	0.5523	32.25	0.5284	0.5288
27.00	0.5521	0.5511	32.50	0.5253	0.5276
27.25	0.5485	0.5499	32.75	0.5239	0.5264
27.50	0.5458	0.5487	33.00	0.5225	0.5253
27.75	0.5434	0.5476	33.25	0.5216	0.5244
28.00	0.5421	0.5465	33.50	0.5206	0.5229
28.25	0.5412	0.5454			

*

We express our thanks to Dr. Z. S. Titova (Kazan) for synthesizing the sample and to Mrs. M. Kolonits for her experimental work. This study was supported in part by the Hungarian Institute for Cultural Relations and the U.S. National Science Foundation. Two of the authors (I. H. and Gy. Sch.) express their appreciation to Prof. J. E. Boggs (Austin, Texas) for provision of computational facilities, and to Prof. K. Hedberg for a discussion.

REFERENCES

[1] АРБУЗОВ, Б. А., САМИТОВ, Ю. Ю., КИТАЕВ, Ю. П.: Изв. АН СССР сер. хим., 56 (1966)
[2] КИТАЕВ, Ю. П., НИВОРОЖКИН, Л. Е., ФЛЕГОНТОВ, С. А., РАЕВСКИЙ, О. А., ТИТОВА, З. С.: Докл. АН СССР, **178,** 1328 (1968)
[3] Elguero, J., Jacquier, R., Marzin, C.: Bull. Soc. Chim. France, 1374 (1969)
[4] ТИТОВА, З. С., ФЛЕГОНТОВ, С. А., РАЕВСКИЙ, О. А., МИНКИН, В. И., КИТАЕВ, Ю. П.: Докл. АН СССР, **199,** 117 (1971)
[5] ЗВЕРЕВ, В. В. ЭЛЬМАН, М. С., СТОЛЯРОВ, А. П., ЕРМОЛАЕВА, А. В., КИТАЕВ, Ю. П.: Ж. общей химии, **XLIII,** 2019 (1973)
[6] ХАРГИТТАИ, И., ШУЛЬТЦ, Д., НАУМОВ, В. А., КИТАЕВ, Ю. П.: Докл. АН СССР, **227,** 1131 (1976)
[7] Hagen, K., Bondybey, V., Hedberg, K.: to be published

[8] HARGITTAI, I., HERNÁDI, J., KOLONITS, M., SCHULTZ, GY.: Rev. Sci. Instrum., **42**, 546 (1971)
[9] ХАРГИТТАИ, И., ХЕРНАДИ, Й., КОЛОНИЧ, М.: Приб. техн. эксп., 239 (1972)
[10] HARGITTAI, M., HARGITTAI, I.: J. Mol. Struct., **20**, 283 (1974)
[11] HARGITTAI, I., HARGITTAI, M.: J. Mol. Struct., **15**, 399 (1973)
[12] HAMILTON, W. C.: Acta Cryst., **18**, 502 (1965)

István HARGITTAI
György SCHULTZ
H-1088 Budapest, Puskin utca 11—13.

V. A. NAUMOV
Yu. P. KITAEV
Arbuzov Institute of Organic and Physical Chemistry, Kazan Branch of the U.S.S.R., Academy of Sciences, 420083 Kazan.

Acta Chimica Academiae Scientiarum Hungaricae, Tomus 90(2), pp. 179—191 (1976)

QUANTUM-CHEMICAL STUDY OF CERTAIN IMIDAZOPYRIMIDONE DERIVATIVES

Z. DINYA*, J. REITER**, L. TOLDY** and SZ. ROCHLITZ***

*(*Department of Organic Chemistry, Kossuth Lajos University, Debrecen
**Research Institute for Pharmaceutical Chemistry, Budapest
***Department of Computer Science, Kossuth Lajos University, Debrecen)*

Received February 19, 1973
in revised form August 30, 1975

Quantum-chemical methods (HMO, ω-SCF, PPP SCF MO CI) were used to study the electron-spectral properties of isomeric and tautomeric forms of certain imidazo(1,2-*a*)pyrimidinone derivatives, and the relative stability conditions of the forms.

With the aid of a selected model compound (**1a**, R = H), the empirical and semi-empirical β_{ij}^{core} values to be found in the literature were compared to the PPP SCF MO CI calculations of the transition energies $\Delta E^{s\to s}$ for the above compounds. Empirical β_{ij}^{core} values selected on the above basis were employed to determine the energies of the $s \to s$ ($\pi \to \pi^*$) electron transitions of these compounds, the directions of the transition moments, and the proportions of the most important configurations. HMO and ω-SCF methods were used to calculate the delocalization energies ED_π of the individual molecules **1a-2b**, R = H and CH_3; these follow very well our earlier observations on the structures and stability conditions of the compounds. The energy gain values $\Delta E\pi$ were also calculated with the PPP SCF MO CI method, but these do not provide essential information relating to the structures and stabilities of the compounds.

It was earlier reported [1—4] that, on heating, certain 2-(β-aryloxyethyl)-amino-5-methylpyrimidin-4(3*H*)-one type compounds undergo transformation, and two isomeric imidazo(1,2-*a*)pyrimidinone derivatives are produced (**A** = **1a**, R = H, and **B** = **2a**, R = H). The structures of A and B were proved in IR, UV, MS and NMR examinations, and by preparative means too, utilizing the corresponding spectra of the four possible isomeric N-methyl derivatives (**1a-2b**, R = CH_3), prepared for this purpose by structure-confirmatory methods.

It was desirable to confirm the correctness of these proved structures theoretically too. Accordingly, quantum-chemical calculations were carried out with the most frequently employed, simpler semi-empirical methods, with regard to the π-electron systems of the four possible isomeric or tautomeric imidazo(1,2-*a*)pyrimidone parent compounds (**1a-2b**, R = H), and the corresponding N-methyl derivatives (**1a-2b**, R = CH_3).

The aims of our calculations were as follows:

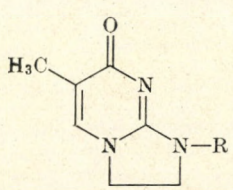

1a

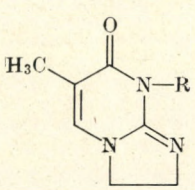

1b

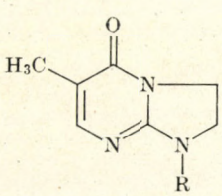

2a

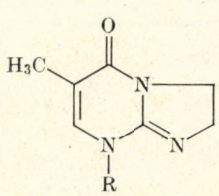

2b

1. With the aid of a selected model compound (**1a**, R = H), to compare the empirical β_{ij}^{core} values to be found in the literature, and the semi-empirical values calculated from various literature data, to the PPP SCF MO CI calculations of the transition energies $\Delta E^{s\to s}$ of the compounds studied (**1a-2b**, R = H, CH_3).

2. With the aid of the β_{ij}^{core} values selected on the basis of the above examination, to determine the energies of the $s \to s$ ($\pi - \pi^*$) electron transfer in the individual **1a-2b** isomeric and tautomeric forms, the directions of the transition moments referred to the first $s \to s$ ($\pi - \pi^*$) transition, and the proportions of the most important configurations.

3. To compare the π-energy conditions of the molecules **1a-2b** (R = H, CH_3) calculated with the HMO, ω-SCF and PPP SCF MO CI methods [5—7] with our earlier findings connected with the isomerism and tautomerism of the above compounds [1—4].

Calculations

Our calculations were performed with the simple HMO [8], ω-SCF [9—11] and PPP [12—15] methods. Figure 1 shows the co-ordinate system employed in the calculations on the molecules.

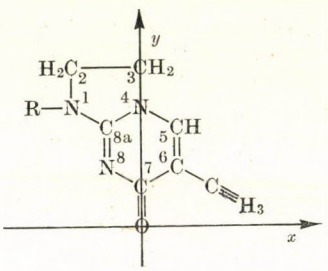

1a

Fig. 1. The numbering of the atoms, and the molecular axes

Table I contains the coulombic (h_i) and resonance (k_{ij}) integral parameters used for the HMO and ω-SCF calculations; these were selected from among the very varied parameters to be found in the literature [5, 7, 16, 17] involving calculations on other derivatives structurally closely related to the compounds under consideration in the present work (**1a-2b**). The parameters $\omega = 0.5$ and $\varepsilon = 10^{-4}$ were employed in the ω-SCF calculations, and the criterion of convergence were $\varepsilon = 10^{-3}$ in the PPP method*.

* The condition for attainment of the SCF state is

$$|P_{ij}^{(k+1)} - P_{ij}^{(k)}| < \varepsilon$$

where $P_{ij}^{(k)}$ is the charge-bond order matrix element in the k-th cycle.

Table I

Parameters used in the HMO and ω-SCF calculations

Atom	h_i	bond	k_{ij}	Ref.
$\dot{O}$	1.2	$\dot{C}=\dot{O}$	1.60	[16]
$\dot{N}$	0.8	$\dot{C}=\dot{N}$	1.10	[16]
$\ddot{N}$	1.5	$\dot{C}-\ddot{N}$	1.00	[16]
$\dot{C}H_3$	2.0	$\dot{C}-\ddot{C}H_3$	0.7	[18]

The same iteration criterion was also employed in our PPP calculations.

The effects of the $-CH_2-$ groups linked to the N atoms were taken into consideration with the customary [8] factor of -0.1 in the corresponding h_N value.

The π-delocalization energies of the molecules (ED_π) were calculated by the method of KRÜGER—THIEMER and HANSEN [19].

The PPP method [12, 13, 20] was used in the SCF MO-LCAO CI form with the ZDO (zero differential overlap) approximation. As regards the configuration interaction, all the singly excited configurations were taken into account.

The one-centre Coulomb repulsion integrals (γ_{ii}) (Table II) were approximated to, according to PARISER and PARR [13], as the difference between the ionization potential (I_i) and the electron affinity (A_i) of the valence states. The two-centre repulsion integrals (γ_{ij}) were calculated by the MATAGA—NISHIMOTO approximation [21].

The resonance integral values β_{ij}^{core}, which were considered only between directly adjacent atoms, were calculated by various means. Thus, empirical literature data [22—24] (Table III) were employed, or self-calculated β_{ij}^{core} values from the bond lengths R_{ij} (Å). These values were calculated for every bond under consideration *via* the following equations:

$$\beta_{ij}^{core} = -6442 \exp(-5.6864\ R_{ij}) \quad [13]$$

$$\beta_{ij}^{core} = -2.318 \exp[-2.3(R_{ij} - 1.397)] \quad [25]$$

$$\beta_{ij}^{core} = -2.39 \exp[3.2196(1.397 - R_{ij})] \quad [26]$$

$$\beta_{ij}^{core} = -1.403 \exp[-4.0(R_{ij} - 1.397)] \quad [27]$$

$$\beta_{ij}^{core} = -2524 \exp\left[-5.047\left(\frac{Z_i + Z_j}{Z_c} - 2\right) - 5\,R_{ij}\right] \quad [28]$$

where Z_i = the effective nuclear charge of the i-th atom;
and Z_c = the effective nuclear charge of the carbon atom

$$\beta_{ij}^{core} = k(I_i + I_j)S_{ij} \quad [29]$$

Table II

Atomic parameters used in the PPP SCF MO CI calculations

	Atom	I_i(eV)	γ_{ii}*(eV)	Ref.
	$\dot{C}$	11.16	11.13	[34, 22]
	$\dot{O}$	17.70	15.23	[34, 22]
	$\dot{C}$ (≡H_3)	11.16	11.13	[23]
	$\dot{H}_3$ (≡C)	9.50	9.50	[23]
**	$\dot{N}$ *(endo)*	14.12	12.34	[34, 22]
	$\dot{N}$ *(exo)*	12.71	11.11	
	$\ddot{N}$ (H, CO, C)	28.59	16.63	[34, 22]
model A	$\ddot{N}$ (H, CH_2, C)	25.73	14.97	
	$\ddot{N}$ (CH_2, C, C)	24.30	14.13	
	$\ddot{N}$ (CH_3, C, C)	24.30	14.13	
	$\ddot{N}$ (CH_3, CH_2, C)	22.87	13.30	
**	$\dot{N}$ *(endo)*	14.12	12.34	[34, 22]
	$\dot{N}$ *(exo)*	13.65	11.87	
	$\ddot{N}$ (H, CO, C)	28.59	16.63	
model B	$\ddot{N}$ (H, CH_2, C)	28.09	16.13	
	$\ddot{N}$ (CH_2, C, C)	27.59	15.63	
	$\ddot{N}$ (CH_3, C, C)	27.59	15.63	
	$\ddot{N}$ (CH_3, CH_2, C)	27.09	15.13	

* $\gamma_{ii} = I_i - A_i$ [13]; ** the effects of the alkyl groups attached to the N were taken into account starting from the values of [34, 22], on the basis of [32] for model A, and [17] for model B.

Table III

Bond parameters used in the PPP SCF MO CI calculations

Bond	$-\beta_{ij}$ (eV)	R_{ij} (Å)	Ref.
$\dot{C}=\dot{C}$	2.39	1.39	[22]
$\dot{C}-\ddot{C}H_3$	1.22	1.51	[23]
$\dot{C}\equiv\dot{C}H_3$	3.00	0.45	[23]
$\dot{C}=\dot{O}$	3.10	1.24	[24]
$\dot{C}-\dot{N}$ *(endo, exo)*	2.75	1.35	[22]
$\dot{C}-\ddot{N}H$	2.30	1.39	[22]
$\dot{C}(\dot{O})-\ddot{N}H$	2.75	1.32*	[22, 35]
$\dot{C}(\dot{O})-\dot{N}$	2.75	1.32*	[22, 35]
$\dot{C}-\ddot{N}$(C, C)	2.30	1.39	[22]
$\dot{C}(\dot{O})-\dot{C}$	2.39	1.44*	[24, 35]

* The data denoted by were taken from [35].

where $k = -0.5$; I_i = the valence state ionization potential; the overlap integral values S_{ij} were calculated according to MULLIKEN [30, 31].

The hyperconjugation model was used for the methyl group attached to C_6 (Fig. 1), with the parameters of LINDNER and MARTENSON [23]. (The value of $\beta^{core}_{C\equiv H_3}$ taken in account was the same in every calculation (Table II), as the formulas described for the calculation of β^{core}_{ij} gave irrealistically high values for the bond length ($R_{C\equiv H_3}$). The effects of the alkyl groups ($-CH_3$; $-CH_2$–R') attached to the nitrogen were taken into account with the method of Hoffmann and Ladik [17] for the HMO parameters (model A), or on the basis of the data of KATSUMATA and KIMURA [32] (model B). In the absence of experimental geometrical data relating to the molecules under consideration, all of them were assumed to be planar* and the bond angles were regarded as 120°. The bond lengths were taken on the basis of literature analogies [35].

The bond parameters used in the PPP calculations are shown in Tables II and III.

Examination of the electron spectra

In the course of our PPP SCF MO CI studies it was primarily desired to learn how the various resonance integral values β^{core}_{ij} used in the calculations affect the results obtained. Accordingly, models A and B were employed to calculate the singlet-singlet transition energies $\Delta E^{s\to s}$ of compound **1a** (R = H) referred to singly excited configurations, and also the oscillator strengths f in the case of various β^{core}_{ij} values (Table IV).

From the resulting $\Delta E^{s\to s}$ and f values it can be stated that the best agreement with the experimental values was obtained with the LONGUET—HIGGINS and SALEM [26] and the empirical β^{core}_{ij} (Table III) values. The agreement of the transition energies $\Delta E^{s\to s}$ is better than that of the oscillator strengths f (the cause of this is to be sought partly in the fact that the experimental oscillator strengths too were determined only approximately) [36].

The results for models A and B differ slightly, but definitely; in general, model B gives higher $s \to s$ transition energies, and lower oscillator strengths. The results of model A (*i.e.* those calculations in which the effects of the alkyl groups attached to the nitrogen were taken into account to a greater extent, and thus the decrease in the γ_{NN} values (Table II) was 1—3.5 eV compared to the parent compounds) exhibited a better agreement with the experimental values than did those calculated with model B (in this the decrease of γ_{NN} by 0.5—1 eV was taken into consideration). At the same time, however, it can be stated that there is no essential difference between the results obtained

* This assumption is in agreement with the finding of PAUDLER and BLEWITT [33] that the imidazo(1,2-a)pyridines, which are structurally very closely related to the imidazo(1,2-*a*)-pyrimidines, are nearly, if not completely planar.

Table IV

Comparison of the experimental spectra of compound

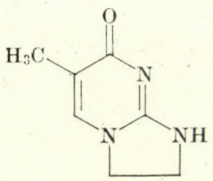

Model	Computed transitions*	β_{ij}^{core}		
		Empirical values [22—24]	[13]	[24]
	*	4.594 (0.057)	4.886 (0.136)	4.498 (0.105)
A	$\Delta E^{s\to s}(f)$			5.133 (0.261)
		5.105 (0.415)		5.888 (0.797)
		5.780 (0.231)	5.628 (0.175)	
	*	4.814 (0.071)	5.105 (0.110)	4.678 (0.103)
		5.208 (0.383)		5.240 (0.234)
B	$\Delta E^{s\to s}(f)$			
		5.829 (0.211)	5.794 (0.182)	5.943 (0.262)

* $\Delta E^{s\to s}$ is the singlet-singlet transition energy with singly excited configurations (in eV). Only transitions below 6 eV are shown. f is the oscillator strength.

** The experimental oscillator strengths were calculated on the basis of [36]. The experimental data refer to EtOH solution.

with the empirical β_{ij}^{core} values and the β_{ij}^{core} values calculated [26, 29] in the case of **1a** (R = H). Since the criterion of convergence (see above) can be attained substantially earlier with the empirical β_{ij}^{core} values, our calculations relating to the isomeric and tautomeric forms of the compounds examined were carried out with these β_{ij}^{core} values (Table III). The resulting and calculated „lower" singlet energies, oscillator strengths, directions of the transition moments, and proportions of the most important configurations (more than 10%) are listed in Table V.

The calculated results well support our earlier findings relating to the structures of the isomeric or tautomeric compounds **1a-2b** (R = H), according to which these compounds are present in the forms **1a** and **2a** (R = H).

A greater difference can be observed, however, between the calculated and measured $\Delta E^{s\to s}$ and f data for **1b** and **2b** ($R = CH_3$) containing an exo-

1a *(R = H) computed with various* β_{ij}^{core} *values*

β_{ij}^{core}				Experimental data**
[26]	[27]	[28]***	[29]	[4]
4.665 (0.118)	3.368 (0.091)	4.229 (0.215)	4.305 (0.116)	
	4.025 (0.017)	4.865 (0.028)	4.914 (0.196)	
	4.591 (0.401)			
	5.125 (0.561)	5.288 (0.674)	5.494 (0.553)	4.460 (0.108)
5.334 (0.258)	5.818 (0.138)	5.960 (0.149)	5.995 (0.670)	
4.860 (0.109)	3.383 (0.072)	4.327 (0.192)	4.441 (0.149)	
	4.256 (0.009)	5.148 (0.045)	5.060 (0.102)	5.368 (0.237)
	4.775 (0.330)	5.560 (0.596)	5.561 (0.518)	
	5.341 (0.772)			
5.4375 (0.247)	5.952 (0.026)			

*** Effective nuclear charges used: $Z_C = 2.095$, $Z_0 = 2.86$, $Z_N = 2.32$, $Z_N = 3.14$ [28]. (It should be noted that there is no essential difference in the calculated data if other effective nuclear charges are used (*e.g.* SLATER, J. C.: Phys. Rev., *36*, 57 (1970)).)

cyclic C=N bond. The difference is most marked for the band of lowest transition energy (*i.e.* the band with largest wavelength in the spectrum,) where it amounts to cca. 0.4e V. To a certain extent, however, this can be explained if it is assumed that the ring strain (which could not be taken into consideration because of the nature of our calculations) is greater in the compounds **1b** and **2b** (R = CH_3) containing an exocyclic C=N bond than in the compounds **1a** and **2a** (R = CH_3) containing an endocyclic C=N bond; accordingly, the geometrical data employed in the calculations here are of a more approximate nature. The above assumption is in agreement with our previous finding [37] that, in contrast with the stable and well isolable compounds **1a** and **2a** (R = CH_3), **1b** (R = CH_3) in particular, but **2b** (R = CH_3) as well, are extremely unstable, undergoing partial ring closure even in the course of simple recrystallization from isopropanol.

As regards the absorption maxima relating to the $\pi - \pi^*$ transitions in the spectra (with the exceptions of compounds **1a** (R = H, CH_3), in the first

Table V

*Observed and calculated singlet transition energies ($\Delta E^{s\to s}$ in eV), oscillator strengths (f), directions of transition moments, and proportions (in %) of most important configurations**

Compound	Calculated								Observed**	
	Model A				Model B					
	$\Delta E^{s\to s}$	f	Direction of transition moment	Proportion (in %) of most important configuration	$\Delta E^{s\to s}$	f	Direction of transition moment	Proportion (in %) of most important configuration	$\Delta E^{s\to s}$	f***
1a	4.594	0.057	x	6→8 (74.5)	4.814	0.071	x	6→8 (76.5)	4.460	0.108
	5.105	0.415	y	6→7 (69.3); 6→8 (11.5)	5.208	0.383	y	6→7 (48.6); 6→8 (19.9); 5→8 (18.2)	5.368	0.237
R=H	5.780	0.231	x	5→7 (56.0); 5→8 (10.7)	5.829	0.211	x	5→7 (61.1)		
1b	4.449	0.295	y	6→7 (65.5); 5→7 (10.2)	4.860	0.348	y	6→7 (64.6); 5→7 (15.1)		
	5.461	0.420	x	6→8 (44.2); 5→7 (33.8)	5.746	0.336	x	6→8 (45.0); 5→7 (28.2)	—	—
R=H	5.813	0.312	y	5→7 (74.3);						
2a	4.214	0.381	x	6→7 (77.5)	4.268	0.448	y	6→7 (79.0)	4.246	0.182
R=H	5.421	0.307	y	6→8 (64.4); 5→7 (11.8)	5.489	0.309	y	6→8 (71.0)	5.414	0.200
2b	4.547	0.200	y	6→7 (63.8); 5→7 (12.2)	4.869	0.343	y	6→7 (64.0); 5→7 (15.3)		
	5.467	0.478	y	5→7 (44.2); 6→8 (30.9)	5.748	0.335	x	6→8 (43.0); 5→7 (30.0)	—	—
R=H	5.757	0.327	x	6→8 (66.8)						
1a	4.630	0.044	x	6→8 (73.6); 5→7 (10.4)	4.795	0.759	x	6→8 (75.6)	4.460	0.092
	5.106	0.378	y	6→7 (57.8); 6→8 (15.6)	5.205	0.376	y	6→7 (50.0); 6→8 (23.4); 5→8 (18.9)	5.391	0.360
R=CH_3	5.508	0.312	x	5→7 (51.6); 5→8 (23.1)	5.834	0.229	x	5→7 (82.5)	5.904	0.401

1b	4.442	0.241	y	6→7 (67.2); 5→7 (10.6)	4.849	0.358	y	6→7 (64.7); 5→7 (15.0)	3.949	0.091
	5.408	0.444	x	5→7 (40.4); 6→8 (37.3)						
R=CH_3	5.712	0.305	y	6→8 (64.4);	5.748	0.323	x	6→8 (44.4); 5→7 (29.7)	5.322	0.341
2a	4.175	0.435	y	6→7 (76.8)	4.261	0.445	x	6→7 (82.6)	4.175	0.164
	5.372	0.312	y	6→8 (67.9); 4→7 (12.8)	5.491	0.306	y	6→8 (64.2)		
R=CH_3	5.989	0.279	x	5→7 (83.9)			x		5.414	0.214
2b	4.442	0.241	y	6→7 (67.2); 5→7 (10.6)	4.880	0.331	y	6→7 (64.0; 5→7 (16.1)	4.106	0.061
	5.408	0.444	x	5→7 (40.4); 6→8 (37.3)	5.752	0.350	x	6→8 (44.3); 5→7 (28.3)		
R=CH_3	5.712	0.305	y	6→8 (64.4)					5.462	0.341

* Calculated with empirical β_{ij}^{core} (Table III), $\Delta E^{s\to s}$ (3V).
** Experimental data relating to the compounds were reported earlier [4]. The data refer to EtOH solutions.
*** Calculated on the basis of [36].

singlet-singlet excitation the transition Φ_6^7 is the determining one (Table V), while for the second $s \rightarrow s$ excitation (at about 5—5.5 eV) the configurations Φ_6^8 and Φ_5^7 become predominant.

The directions of the transition moments (Table V), for which, unfortunately, experimental data are not available, proved to be almost the same for models A and B. The direction of the transition moments of compounds **1a** and **2a** is the x-direction in Fig. 1, while for the analogous derivatives **1b** and **2b** it is the y-direction.

Summary

The results of our PPP SCF MO CI calculations well follow the electron spectra of the compounds studied. The parameters employed in the above calculations (reported in Table III) were therefore also used to interpret the relative stability conditions of the individual isomeric and tautomeric forms.

Structural study of the compounds 1a—2b (R = H, CH_3)

In the literature, primarily the HMO [8] and ω-SCF [9, 10] calculations have been employed to investigate the various tautomeric structures [5, 7, 17, 38, 39].

The π-delocalization energies (EDπ) calculated with the above methods in general well follow other experimental findings relating to the tautomeric structures of the compounds.

Certain authors have recently attempted to use the PPP SCF MO CI method too to elucidate the tautomeric conditions of individual compounds [17, 38—42].

This method considers the degree of relative stability to be the energy gain $\Delta E\pi$ accumulating in the molecule as a result of the difference between the total π-energy (Eπ) of the molecule and the total π-energy of the free atoms in the corresponding valence states.

Using the above methods, we too calculated the delocalization energies (ED_π) and energy gains (ΔE_π) of compounds **1a-2b** (R = H, CH_3); these are given in Table VI.

The following conclusions may be drawn from the tabulated data:

1. The energies ED_π calculated with the HMO and ω-SCF methods well follow our earlier findings [1—4] relating to the isomeric and tautomeric structures of the compounds, according to which the two isolable imidazo-(1,2-*a*) pyrimidinone derivatives (A and B) have the structures **1a** (R = H) and **2a** (R = H). The energies ED_π of the compounds **1a** and **2a** (R = H) are

Table VI

Quantum-chemical data relating to the relative stabilities of the compounds

Compound		$ED_\pi(\beta^0)$*		ΔE_π (eV)** PPP SCF MO CI	
		HMO	ω-SCF	model A	model B
1a		3.423	4.574	−264 35	−265.97
1b	R = H	3.315	4.376	−258.42	−275.35
2a		3.435	4.606	−268.06	−270.57
2b		3.322	4.385	−258.48	−275.29
1a		3.428	4.575	−263.33	−265.23
1b		2.836	3.500	−271.85	−273.25
2a	$R=CH_3$	3.590	4.755	−267.06	−269.01
2b		3.380	4.429	−271.85	−273.28

* ED_π = π-delocalization energy; β_0 = standard value relating to carbon atoms of benzene

** ΔE_π = π-energy gain with respect to the free atoms in the appropriate valence state. Calculated with empirical β_{ij}^{core} (Table III).

almost the same in the case of the HMO and the ω-SCF calculations*, and substantially higher than those of the corresponding derivatives **1b** and **2b** (R = = H). In the case of the ED_π values obtained with both the HMO and the ω-SCF calculations, a surprising agreement was observed between the π-delocalization energies and stabilities of the compounds. The delocalization energies ED_π of the compounds **1a** and **2a** ($R = CH_3$) (earlier shown to be stable [37]) are almost the same as each other, and much larger than those of the analogous derivatives **2b** ($R = CH_3$), but particularly **1b** ($R = CH_3$), the extreme instability of which has already been mentioned.

2. Only for **1a-2b** (R = H), model A, do the energy gain values ΔE_π calculated with the PPP SCF MO CI method show agreement with our earlier experimental findings, according to which the ΔEf values for the more stable molecules **1a** and **2a** (R = H) are larger than those of the corresponding derivatives **1b** and **2b** (R = H). In all other cases, in contradiction with the experimental findings, the energy gains $\Delta E\pi$ for the derivatives **1b** and **2b** (R = H, CH_3) proved to be larger.

It may be stated, therefore, that the energies ED_π obtained with the HMO and ω-SCF methods well follow other spectroscopic and preparative findings relating to the structures and stability conditions of the compounds

* As a consequence of the differences in the two methods, the numerical values obtained with the HMO and ω-SCF methods are naturally not the same, but the natures of the changes obtained for the individual isomeric and tautomeric forms are identical in the two methods.

1a-2b (R = H, CH_3); indeed, a surprisingly good agreement is exhibited between the delocalization energies ED_π and the stabilities of the compounds.

In contrast, but in agreement with the findings of KWIATKOWSKI [43], the PPP SCF MO CI method can follow well only the electron spectra, and does not provide essential information on the structures and stabilities of the compounds. It must be noted, however, that the stability conditions of the various tautomeric and isomeric forms are not determined only by the properties of the π-electron system [17]. Hence, the semi-empirical quantum-chemical approximative methods employing the σ-π separation can provide only information of limited value for the interpretation of the stability conditions of the above compounds.*

*

The authors wish to express their thanks to the staff of the Computer Centre, Kossuth Lajos University, Debrecen, for technical assistance with the calculations.

REFERENCES

[1] REITER, J., SOHÁR, P., TOLDY, L.: Tetrahedron Lett., **1970,** 1411
[2] REITER, J., SOHÁR, P., LIPTÁK, J., TOLDY, L.: Tetrahedron Lett., **1970,** 1417
[3] SOHÁR, P., REITER, J., TOLDY, L.: Org. Magn. Res., **3,** 689 (1971)
[4] REITER, J., TOLDY, L.: Acta Chim. (Budapest), **82,** 107 (1974)
[5] PULLMAN, B., PULLMAN, A.: Quantum Biochemistry. Interscience Publ., New York, 196[3]
[6] PEACOCK, T. E.: Electronic Properties of Aromatic and Heterocyclic Molecules. Academi[c] Press, New York, 1965
[7] FERNANDEZ-ALONSO, J. I.: Structure of Biomolecules and Biological Systems (in Advances in Chemical Physics, Vol. 8, Ed. by DUCHNESE, J.). Academic Press, New York, 1967
[8] STREITWEISER, A., Jr.: Molecular Orbital Theory for Organic Chemists. Wiley, New York, 1961
[9] WHELAND, G. W., and MANN, D. E.: J. Chem. Phys., **17,** 264 (1949)
[10] BERGSON, G.: Arkiv för Kemi, **19,** 181 (1962)
[11] JANSSEN, M. J. and SANDSTRÖM, J.: Tetrahedron, **20,** 2339 (1964)
[12] POPLE, J. A.: Trans. Faraday Soc., **49,** 1375 (1953)
[13] PARISER, R., PARR, R. G.: J. Chem. Phys., **21,** 466, 767 (1953)
[14] POPLE, J. A., BEVERIDGE, D. L.: Approximate Molecular Orbital Theory, McGraw-Hill, New York, 1970
[15] MURRELL, J. N., HARGET, A. J.: Semi-empirical self-consistent-field molecular orbital theory of molecules. Wiley-Interscience, New York, 1972
[16] HÄFELINGER, G.: Chem. Ber., **103,** 2941 (1970)
[17] HOFFMANN, T. A., LADIK, J.: Advances in Chemical Physics (Ed. by Duchnese, J.), Vol. 7, Academic Press, New York, 1964
[18] MATSEN, F. A.: J. Amer. Chem. Soc., **72,** 5243 (1950)
[19] KRÜGER-THIEMER, E., HANSEN, R.: Arzneimittel-Forsch., **16,** 1453 (1966)
[20] PARR, R. G.: Quantum Theory of Molecular Electronic Structure. Benjamin, New York, 1963
[21] MATAGA, N., NISHIMOTO, K.: Z. physik. Chem. N. F., **13,** 140 (1957)
[22] FERRE, Y., VINCENT, E. J., LARIVE, H., METZGER, J.: Bull. Soc. Chim. Fr., **1972,** 3862
[23] LINDNER, P. and MARTENSSON, O.: Theoret. Chim. Acta (Berlin), **7,** 352 (1967)
[24] LADIK, J., BICZÓ, G.: Acta Chim. Acad. Sci. Hung., **62,** 401 (1969)
[25] FABIAN, I., GREGER, G.: Theor. i Exp. Khim., **7,** 170 (1971)
[26] LONGUET-HIGGINS, H. C., SALEM, L.: Proc. Roy. Soc. (London), **251A,** 172 (1959)
[27] GOLEBIEWSKI, A., NOWAKOWSKI, J.: Acta Phys. Polon., **25,** 647 (1964)
[28] FLURRY, R. L., Jr., STOUT, E. W., BELL, J. J.: Theoret. Chim. Acta (Berlin), **8,** 203 (1967)

* It must be noted that the total valence electron methods (CNDO/2, PCILO) do not give the total energy correctly in every case either!

[29] WOLFSBERG, M., HELMHOLZ, L.: J. Chem. Phys., **20,** 837 (1952)
[30] MULLIKEN, R. S.: J. Chem. Phys., **46,** 479, 497, 675 (1949)
[31] MULLIKEN, R. S., RIEKE, C. A., ORLOFF, D., ORLOFF, H.: J. Chem. Phys., **17,** 1248 (1949)
[32] KATSUMATA, S. and KIMURA, K.: Bull. Chem. Soc. Japan, **46,** 775 (1973)
[33] PAUDLER, W. W., BLEWITT, M. L.: J. Org. Chem., **31,** 1295 (1966)
[34] HINZE, J., JAFFE, H. H.: J. Amer. Chem. Soc., **84,** 540 (1962)
[35] SUTTON, L. E. (Ed.): Tables of Interatomic Distances and Configuration in Molecules and Ions. Spec. Publ. No. 11, Chem. Soc., London, 1958; Supplement, Spec. Publ. No. 18, Chem. Soc., London, 1965
[36] ALLINGER, N. L., STUART, T. W., TAI, J. C.: J. Amer. Chem. Soc., **90,** 2819 (1968)
[37] REITER, J.: unpublished data
[38] PULLMAN, A.: Quantum Aspects of Heterocyclic Compounds in Chemistry and Biochemistry (Proc. of International Symp. in Jerusalem, 1969. Ed. by BERGMAN, E. D., PULLMAN, B.). Jerusalem, 1970, pp. 1—31
[39] PULLMAN, B.: *ibid*, pp. 292—307
[40] KWIATKOWSKI, J. S.: Theoret. Chim. Acta (Berlin), **10,** 47 (1968)
[41] PAOLONI, L., CIGNITTI, M., TOSATO, M. L.: see ref. 38, pp. 324—337
[42] GUBANOV, V. A., PERELIAEVA, L. A., CHIRKOV, A. K., MATEVOSIAN, R. O.: Theoret. Chim. Acta (Berlin), **18,** 177 (1970)
[43] KWIATKOWSKI, J. S.: Bull. Acad. Polon. Ser. sci. chim., **29,** 405 (1973)

Zoltán DINYA
József REITER
Lajos TOLDY
H-4010 Debrecen 10.
H-1325 Budapest Pf. 82.

Szilveszter ROCHLITZ H-4010 Debrecen 10.

Acta Chimica Academiae Scientiarum Hungaricae, Tomus 90(2), pp. 193—197 (1976)

REACTIONS OF *o*-PHENYLENEDIAMINE WITH α,β-UNSATURATED NITRILES

M. HAMMAD and Kh. EL-BAYOUKI

(National Research Centre, Dokki, Cairo, Egypt)

Received July 7, 1975
in revised form January 20, 1976

The uncatalyzed reaction of *o*-phenylenediamine with α,β-unsaturated nitriles is described. *o*-Phenylenediamine reacts with fluoren-9-ylidenecyanoacetic ester (**1**) to give the cyanobenzimidazole (**2**) leaving the ethylenic double bond intact, whereas α-naphthylidenes (**5**) are cleaved with *o*-phenylenediamine to yield the unexpected 2-(1-naphthyl)benzimidazole (**6**). The unsaturated benzimidazoles **2** and **8** are reduced with sodium borohydride to give the saturated benzimidazoles **3** and **10**, respectively.

Cleavage of the acid group in the reaction of *o*-phenylenediamine with carbodithioic acid is well known [1]. The rupture of the C–C bond in some ketones when reacted with *o*-phenylenediamine under relative mild conditions to give benzimidazoles has been reported [2].

In the present work, we have found that when fluoren-9-ylidenecyanoacetic ester (**1**) is heated with *o*-phenylenediamine at 240°C, the unsaturated cyanobenzimidazole (**2**) is obtained in a good yield. In this reaction the diamine adds only on the ethoxycarbonyl group, leaving the ethylenic double bond intact.

The structure of **2** has been inferred from its correct analytical data; its IR spectrum has $\nu_{C\equiv N}$ at 2240 cm^{-1}, due to conjugated nitrile absorption, and ν_{N-H} at 2700—3100 cm^{-1} as a broad band [3, 4]. The UV spectrum also exhibits strong and broad bands with fine structure in the 255—285 nm region (alcohol), which is characteristic of a benzimidazole structure [3, 4]. Moreover, **2** is reduced with sodium borohydride to give the saturated analogue **3**, leaving the benzimidazole moiety intact. Compound **3** proved to be identical with the product obtained from the thermal reaction of *o*-phenylenediamine with the saturated ester [5] **4** at 240°C.

In contrast to the fluorenylidene analogue, the analogous α-naphthylidenes (**5**) are found to react with *o*-phenylenediamine in a different manner. Thus, when ethyl α-cyano-β-(1-naphthyl)-acrylate (**5a**), α-cyano-β-(1-naphthyl)acrylamide (**5b**), α-cyano-β-(1-naphthyl)acrylic acid (**5c**) or α-naphthylmethylidenemalononitrile (**5d**) is heated with the equimolecular amount of *o*-phenylenediamine at 180°C, the –C=C– bond is cleaved and, unexpectedly, 2-(1-naphthyl)benzimidazole (**6**) is obtained in each case, in a good yield.

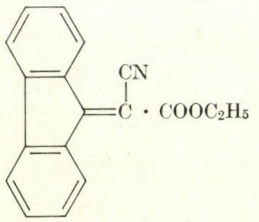

1

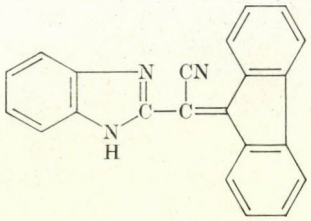

2

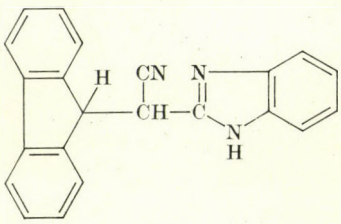

3

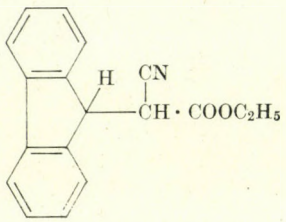

4

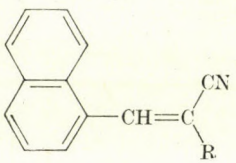

5

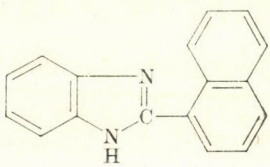

6

a R = $COOC_2H_5$
b R = $CONH_2$
c R = COOH
d R = CN

The same result is obtained when the reaction is effected in boiling methanol, or even at room temperature. Compound **6** proved to be identical with the product formed in the reaction of *o*-phenylenediamine and 1-naphthoic acid [6]. This compound is also obtained from the reaction of equimolecular proportions of *o*-phenylenediamine and 1-naphthaldehyde at 180 °C, or even when the reactants are allowed to stand overnight in ethanol at room temperature. In this reaction the monoanile **7** is not isolated as expected.

The unexpected production of 2(1-naphthyl)benzimidazole in the above reactions prompted us to attempt the indirect synthesis of benzimidazoles derived from naphthalene. It has been found that 2-cyanomethylbenzimidazole (**9**) is readily condensed with 1-naphthaldehyde in boiling benzene to give the unsaturated cyanobenzimidazole **8**. The structure of **8** is inferred from its analytical data, yellow colour and IR spectrum, which shows ν_{N-H} as a broad bend in the 2700—3100 cm^{-1} region, characteristic of imidazoles [3]. The UV spectrum also exhibits strong absorption bands with fine structure

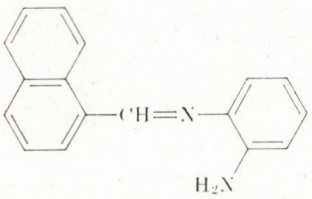

7

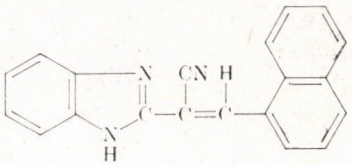

8

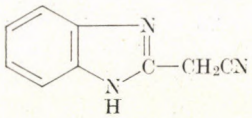

9

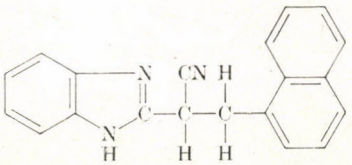

10

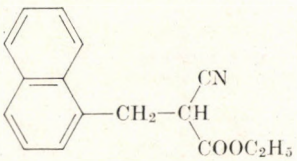

11

in the 220 and 285 nm region, similar to benzimidazole itself. When **8** is reduced with sodium borohydride in isopropanol, the saturated cyanobenzimidazole **10** is obtained in a good yield, which proved to be identical with the product obtained from the reaction of the saturated cyanoacetic ester (**11**) with *o*-phenylenediamine at 220 °C.

Cleavage of α, β-unsaturated nitriles derived from naphthalene has not been, to our knowledge, previously reported, so this reaction is first described in the present work.

Experimental

Microanalyses were performed by the Microanalytical Laboratory, National Research Centre, Cairo, A.R.E. M.p'.s are uncorrected. The IR spectra were recorded with a Zeiss Jena UR 10 spectrophotometer; the UV spectra were obtained on a Carl Zeiss PMQII spectrophotometer.

Reaction of 1 with o-phenylenediamine

Fluoren-9-ylidenecyanoacetic ester (**1**) (2.75 g) and *o*-phenylenediamine (1.1 g) were mixed and the mixture was heated at 240°C (bath temperature) for 1 hr., allowed to cool, then triturated with benzene. The solid was filtered off and recrystallized from methanol to give the unsaturated cyanobenzimidazole (**2**) (2.3 g) as yellow crystals, m. p. 252 °C.

$C_{22}H_{13}N_3$. Calcd. C 82.74; H 4.10; N 13.16. Found C 82.53; H 4.32; N 13.06%.

Reduction of (2) with sodium borohydride

A suspension of sodium borohydride (1.1 g) and the unsaturated cyanobenzimidazole (**2**) (3.05 g) in isopropanol was stirred for 6 hrs at room temperature, then decomposed with dilute acetic acid. The solid obtained was filtered off and recrystallized from ethanol to give the unsaturated cyanobenzimidazole (**3**) (2.35 g) as colourless crystals, m. p. 266 °C. (M. p. undepressed in admixture with an authentic sample prepared by the thermal reaction of *o*-phenylenediamine and the saturated cyano ester **4** [5]).

$C_{22}H_{15}N_3$. Calcd. C 82.22; H 4.71; N 13.08. Found C 81.82; H 4.84; N 13.29%.

General procedure for the thermal reaction of 1-naphthylidenes (5) with o-phenylenediamin methanol

The α-naphthylidene (**5**) (0.01 mole) and *o*-phenylenediamine (0.01 mole) were mixed, the mixture was heated at 180—190 °C for 1 hr., allowed to cool, then triturated with benzene. The solid obtained was filtered off and recrystallized from ethanol to give 2-(1-naphthyl)-benzimidazole (**6**) as colourless crystals. m. p. 266 °C. Detailed results are shown in Table I.

Table I

Reaction of α-naphthylidenes (**5**) *with o-phenylenediamine*

Type of reaction	α-Naphthylidene					
	5a*			**5b***		
	Time hr.	Temp. °C	Yield %	Time hr.	Temp. °C	Yield %
Thermal	1	180	70	1	185	60
In methanol	2	reflux	75	3	reflux	65
In methanol	24	room. temp. (25 °C)	60	24	room. temp. (25 °C)	50
Type of reaction	**5c***			**5d***		
	Time hr.	Temp. °C	Yield %	Time hr.	Temp. °C	Yield %
Thermal	1	190	60	1	190	70
In methanol	3	reflux	60	2	reflux	60
In methanol	24	room temp. (25 °C)	55	24	room temp. (25 °C)	57

* *Cf.* ref. [7]

General procedure for the reaction of α-naphthylidenes (5) o-phenylenediamine in boiling

The α-naphthylidene (**5**) (0.01 mole) and *o*-phenylenediamine (0.01 mole) were dissolved in methanol (40 ml). The reaction mixture was refluxed for 3 hrs. The solution was concentrated and allowed to cool. The solid was filtered off and recrystallized from ethanol to give 2-(1-naphthyl)benzimidazole (**6**), m. p. 266 °C. (M. p. undepressed with an authentic sample [6]). (Detailed results are shown in Table I.)

General procedure for the reaction of α-naphthylidenes (5) with o-phenylenediamine in methanol at room temperature

The reaction mixture was prepared as described above, stoppered, and allowed to stand overnight at room temperature. The crystalline solid product was filtered off and recrystallized from ethanol to give **6** (m. p. undepressed in admixture with an authentic sample [6]). (Detailed results are shown in Table I.)

Thermal reaction of α-naphthaldehyde with o-phenylenediamine

α-Naphthaldehyde (3.12 g) and *o*-phenylenediamine (2.16 g) were mixed, the reaction mixture was heated at 170—180 °C (bath temperature) for 1 hr., allowed to cool, then triturated with benzene. The solid was filtered off and recrystallized from ethanol to give **6**. (M. p. undepressed in admixture with an authentic sample [6]).

When the above reaction was made in boiling methanol for 3 hrs, or the mixture was kept overnight at room temperature, **6** was similarly obtained.

Condensation of α-naphthaldehyde with 2-cyanomethylbenzimidazole

A solution of α-naphthaldehyde (15.6 g) and 2-cyanomethylbenzimidazole (15.7 g) in dry benzene (75 ml) containing a few drops of morpholine was refluxed in a Dean—Stark moisture determination apparatus until no more water resulted from the reaction. The yellow precipitate was filtered off, washed with benzene, and crystallized from ethanol to obtain the unsaturated cyanobenzimidazole (**8**) as yellow crystals, m. p. 233—235 °C.

$C_{20}H_{13}N_3$. Calcd. C 81.34; H 4.44; N 14.23. Found C 81.39; H 4.50; N 14.86%.

Reduction of the unsaturated cyanobenzimidazole (8) with sodium borohydride

A suspension of sodium borohydride (1.1 g) and the unsaturated cyanobenzimidazole (**8**) (2.95 g) in isopropanol (30 ml) was stirred for 6 hrs at room temperature. The reaction mixture was decomposed with dilute acetic acid. The solid product was filtered off and recrystallized from ethanol to give the saturated cyanobenzimidazole (**10**) as colourless crystals, m. p. 196 °C.

$C_{20}H_{15}N_3$ Calcd. C 80.78; H 5.09; N 14.13. Found C 81.04; H 4.98; N 14.07%.

Thermal reaction of the saturated cyanoester (11) with o-phenylenediamine

The saturated cyanoester (**11**) (2.43 g) and *o*-phenylenediamine (1.1 g) were mixed, and the reaction mixture was heated at 220 °C (bath temperature) for 1 hr., allowed to cool, then triturated with benzene. The solid was filtered off and crystallized from ethanol to give the saturated cyanobenzimidazole (**10**) as colourless crystals, m.p. 196 °C.

REFERENCES

[1] Wuyts, H., Van Vaerenbergh, J.: Bull. Soc. Chim. Belg. **48,** 329 (1939); C. A. **34,** 1981 (1940)
[2] Elderfield, R., McCarthy, J. R.: J. Am. Chem. Soc. **73,** 975 (1951); C. A. **42,** 2975 (1948)
[3] Orgel, T. L., Cortnell, W. D., Sutton, L. W.: Trans Faraday Soc.; **47,** 113 (1951)
[4] Pazharshii, A. F., Ganovaskii, H. D., Siminov, A. M.: Russ. Chem. Rev. **35,** 122 (1966)
[5] Hammad, M. A.: Ph. D. Thesis ("Studies on Organic Cyanogen Compounds") Ain Shams University, 1974
[6] Poral-Koshits, B. A., Ginzburg, O. F., Efros, L. S.: J. Gen. Chem. USSR, **17,** 1768 (1947) C. A. **42,** 5903f (1948)
[7] James, E., Nakamichi, G. M., Liska, J. K.: J. Am. Pharm. Assoc. **48,** 61 (1959); C. A. **53,** 8082 (1959)

M. Hammad
Kh. El-Bayouki
National Research Centre,
Dokki, Cairo, Egypt.

Acta Chimica Academiae Scientiarum Hungaricae, Tomus 90(2), pp. 199–202 (1976)

QUANTUM CHEMICAL STUDY OF THE SOLVENT EFFECT ON THE ISOMERIZATION OF CYANIC ACID

(SHORT COMMUNICATION)

G. NÁRAY-SZABÓ*

(CHINOIN Pharmaceutical and Chemical Works)

P. PULAY**

*(**Central Research Institute for Chemistry, Hungarian Academy of Sciences, Budapest)*

P. MEZEY***

*(***Institute of Organic Chemistry, L. Eötvös University, Budapest)*

Received October 8, 1975

The results of CNDO force relaxation calculations are given for the two possible reaction paths of the S_Ni-type HOCN → HNCO isomerization. The catalytic effect of pyridine and dimethyl sulfoxide is investigated through modelling them by a H_2O molecule. The barrier height of the reaction is significantly lowered in the presence of solvent molecules.

Chemical catalysis can be treated as the lowering effect of a catalyst on the activation energy of a given reaction. The use of quantum chemically calculated potential barrier height in place of the activation energy is a commonly accepted approximation. The reaction path determining the barrier height can be calculated by minimizing the energy of the catalyst—reactant system with respect to all but the reaction co-ordinate. Such a minimization can be performed economically by the force relaxation procedure [1]. In a version adapted to the CNDO method [2], the forces on each atom of a reacting system are computed. The points of the reaction path are calculated by making all forces, but the one belonging to the reaction co-ordinate, approximately zero.

That CNDO yields qualitatively good reaction paths can be seen from the example of HCN → HNC isomerization. The isomerization energy and barrier height calculated by the *ab initio* CI method are 14.6 (53.0) and 34.9 (71.0) kcal/mole, respectively [3]. The values obtained by CNDO force calculations are given in parentheses. Upon subtracting 38.0 kcal/mole from the CNDO values, a very good agreement is obtained with the *ab initio* values. This means that the trends are reflected by CNDO correctly. In the case of interatomic distances, the agreement is better. A recent example of semiempirical quantum chemical calculations of a reaction path is the work of MARTIN *et al.* on the rearrangement of ethylcarbene [4].

* Guest at the Quantum Theory Group, Physical Institute, Polytechnical University, Budapest

This work is concerned with the S_N1-type isomerization of alkyl cyanates and cyanic acid in dimethyl formamide, dimethyl sulfoxide or pyridine. A possible mechanism suggested by MARTIN [5] *et al.* can be summarized as

$$\underset{\mathbf{1}}{\text{Solv}\ldots\text{ROCN}} \overset{\text{slow}}{\rightleftharpoons} \underset{\mathbf{2}}{[\text{Solv.R}^+.\text{OCN}^-]} \overset{\text{fast}}{\rightleftharpoons} \underset{\mathbf{3}}{[\text{Solv.R}^+] + \text{OCN}^-}$$

$$\mathbf{2} \xrightarrow{\text{slow}} \underset{\mathbf{4}}{\text{Solv. RNCO}} \xleftarrow{\text{fast}} \mathbf{3}$$

Cyanate is ionized through a slow solvation process. This polar aggregate dissociates rapidly to yield separated ions which can react further to give isocyanate. The isomerization of ionic aggregate **2** to isocyanate is a slow process. The presence of a solvent stabilized activated complex was indicated by NMR investigations, too [6].

The effect of dimethyl sulfoxide and related solvents was modelled by a water molecule. Thus the oxygen of the H_2O plays the role of the one in dimethyl sulfoxide or that of the nitrogen in pyridine. These atoms attract the proton or the alkyl carbonium ion to form the solvated transition state.

The reaction path of HOCN → HNCO isomerization (relative energy *vs.* NCO angle) is given in Fig. 1. Table I contains some numerical values. Figure 2

Table I

Characteristic parameters of the reactants and the transition complexes

Compound	Reaction co-ord. HCO ∢	r_{HC} (Å)	r_{NC} (Å)	r_{CO} (Å)	rel. energy (kcal/mole)	q(NCO)
HOCN	33	1.84	1.19	1.33	3	−0.176
NCO.H activated complex	78	1.18	1.23	1.32	96	−0.267
HNCO	152	1.90	1.26	1.24	0	−0.142
$HOCN.H_2O$	33	1.87	1.19	1.33	0	−0.281
$(NCO.H).H_2O$ activated complex	78	1.19	1.22	1.31	80	−0.532
$HNCO.H_2O$	154	1.94	1.25	1.24	1	−0.237

shows the variation of CO and NC bond lengths, as well as the O..H, distance in the hydrated complex against the reaction co-ordinate. The barrier height is 96 kcal/mole. The activated complex is T-shaped. The inversion barrier of the HOCN molecule was found to be 42 kcal/mole while in the case of HNCO it has a value of 9 kcal/mole. The barrier height was calculated as the difference between the energy of the linear and that of the bent (equilibrium shape) molecule. The effect of the solvent can be seen from the dashed curve in Fig. 1.

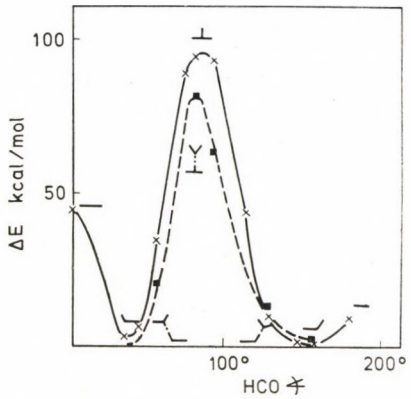

Fig. 1. Reaction paths for the HOCN → HNCO isomerization. Full line: HOCN, dashed line: $HOCN.H_2O$. The molecular shapes are indicated schematically.

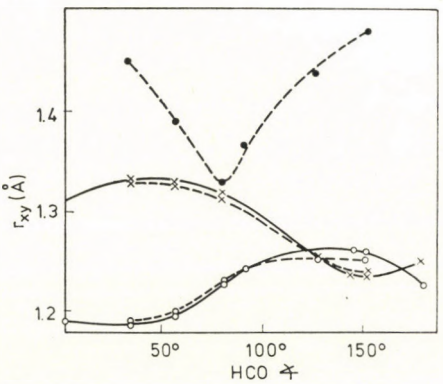

Fig. 2. Variation of different bond lengths *vs.* the reaction co-ordinate. ○—○ CN, x—x CO ●—● O...H distance. Full line: HOCN, dashed line: $HOCN.H_2O$.

A decrease by 16 kcal/mole of the barrier occurs when a water molecule is present. This is due to hydrogen bond formation between the solvent molecule and the activated complex. It is highly probable that solvents with strong proton binding power (*e.g.* dimethyl sulfoxide or pyridine) lower the barrier height to a greater extent. Thus, in these solvents, reaction step $\mathbf{2} \rightleftharpoons \mathbf{4}$ becomes faster than in non-polar medium.

The fast reaction step $\mathbf{2} \rightleftharpoons \mathbf{3}$ was followed by CNDO force calculations. The reaction paths (total energy against OH distance) for the dissociation of bare HOCN and $HOCN \cdot H_2O$ are given in Fig. 3. It is to be seen that the increase of the OH distance from the equilibrium value causes a monotonic increase in the energy. No maximum is observed on the reaction path. This would be necessary if the products **3** were stable intermediates. Thus it is indicated that reaction step $\mathbf{2} \rightarrow \mathbf{3}$ involves the formation of a solvate cloud around the reactant and this lowers the activation energy further. Indication

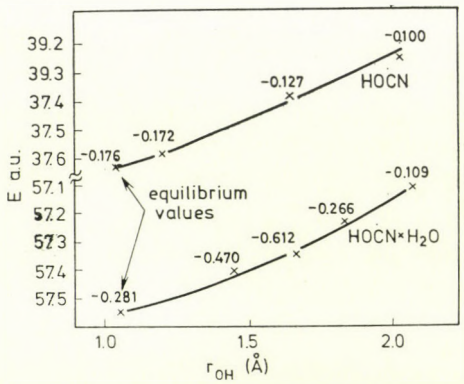

Fig. 3. Variation of the energy *vs.* the OH distance (dissociation). The net charge on the NCO moiety is given for each points.

for such a solvation can be gained from the calculated charges of the NCO moiety (Fig. 3). In the case of the HOCN molecule this is a rather low value and it decreases monotonically as the OH distance increases. If an H_2O molecule is present, the charge increases from the equilibrium value of 0.281 electrons to about 0.6 electrons at $R_{OH} \sim 1.65$ Å. When the OH distance increases further, the charge becomes smaller and the difference between the bare and solvated molecules diminishes. It cannot be excluded that this decrease of the charge is due to the failure of the CNDO method at large interatomic distances. The considerable negative charge of the NCO moiety makes solvation easy and, through this stabilizing effect, reaction step **2** → **3** becomes fast. A similar solvation process was investigated by CNDO calculations in the case of the Walden inversion of fluoromethane, too [7].

It is interesting to notice that the lowering effect on the barrier height, due to a water molecule, was indicated qualitatively by extended Hückel calculations, too. Here the NCO moiety and the H_2O molecule were fixed and the energy surface due to the displacement of the proton was calculated point by point. The barrier height was 65 kcal/mole for the free molecule and became 50 kcal/mole when a water molecule was present.

REFERENCES

[1] PULAY, P.: Mol. Phys., **17**, 197 (1969)
[2] PULAY, P., TÖRÖK, F.: Mol. Phys., **25**, 1153 (1973)
[3] PEARSON, P. K., SCHAEFER III, H. F., WAHLGREN, K.: J. Chem. Phys., **62**, 350 (1975)
[4] MARTIN, M., MENENDEZ, V., FIGUERA, J. M.: Chem. Phys. Lett., **27**, 292 (1974)
[5] MARTIN, D., NICLAS, H.-J., HABISCH, D.: Liebigs Ann. Chem., **10**, 727 (1969)
[6] NELSON, J., SPRATT, R., NELSON, S. M.: J. Chem. Soc. (A), 583 (1970)
[7] CREMASCHI, P., GAMBA, A., SIMONETTA, M.: Theor. Chim. Acta, **25**, 237 (1972)

Gábor NÁRAY-SZABÓ H-1045 Budapest, Tó u. 1.
Péter PULAY, Pál MEZEY } H-1088 Budapest, Múzeum krt. 4b.

RECENSIONES

R. BOYINGTON and W. L. MASTERTON: *Student's Guide to Masterton and Slowinski's Chemical Principles*

W. B. Saunders Co., Philadelphia, London, Toronto, 1975, 330 pages

The book has been written for university students of general chemistry, and serves primarily as a guide-book to *Chemical Principles* by W. L. MASTERTON and E. J. SLOWINSKI; it is also of assistance in providing an understanding of the material heard in the lectures and that contained in the earlier book, and in enhancing the ability of the student to employ this understanding. The sequence of the chapters and the selected topics run in parallel with the material in the text-book.

In effect, this guide-book does not report new knowledge, but in every case refers to the appropriate parts of the text-book, and to the Tables and Figures to be found in it.

Each chapter begins with a series of questions. These questions direct the student's attention to what parts of the lecture material and the text-book must be studied in order to be able to solve the problems posed in that chapter. Next follow references to the basic definitions and to the mathematical operations to be employed. The authors then give an extremely concise summary of the theoretical knowledge fundamentally necessary for an understanding of the chapter. The subsequent part always describes the methods for solving a number of problems, and illustrates these on one example each. The book also contains many calculation problems for solution, ranging from comparatively simple to quite complex ones. The solutions can be found in an appendix.

The following most important and most useful part of the chapters gives a possibility for the student to check his knowledge and understanding of the subject matter, and at the same time plays an important part in the active study, in the development of independent thinking, and in the discovery of correlations. The questions given here can be divided into two groups. In the first type the reader must establish whether a statement connected with that part of the material is true or false. In the second group of questions the student must select the correct answer from among several given possible answers. The correct answers are to be found in a separate part of the chapter, and finally each chapter is concluded by a list of recommended literature.

The first chapters deal with the fundamental knowledge relating to atoms, molecules and ions, and with chemical formulas and equations. The student may then become acquainted with thermochemistry and with the physical properties of gases. After the basic concepts on the structure of matter follow chapters connected with the properties of various states (liquids, solids, changes of state, and solutions). Three chapters present the reader with an account of chemical reactions (the spontaneity of reactions, the chemical equilibrium of gas reactions, and the rates of reactions). Separate chapters deal with precipitation reactions, acid–base theories, acid–base reactions, complex compounds, oxidation-reduction reactions, the basic concepts of electrochemistry, and nuclear reactions. The concluding chapter illustrates the manifestation of the fundamental correlations of general chemistry in the field of biochemistry.

The book provides extremely useful assistance to the student dealing with general chemistry, in broadening his knowledge, in an intelligible treatment of the subject matter, and in the constant checking of his grasp of the material. Although this guide-book is primarily intended to supplement the text-book referred to in the title, as a result of its posing questions demanding some thought and of the answers to the self-checking questions it is also of use to those students who have mastered their fundamental general chemical knowledge from books employing different systems and constructions. Thus, its translation into Hungarian (possibly together with the corresponding text-book) would be advantageous, as at the moment a book of such a nature is not available in Hungarian.

J. NAGY

E. WOLFRAM (editor): *Proceedings of the International Conference on Colloid and Surface Science.* Vol. 1. Preprints of contributed papers.

Akadémiai Kiadó, Budapest 1975, 776 pages

Results achieved in the last twenty years in colloid and surface chemistry have an increasing importance in science and from the economic point of view; in addition the interdisciplinary, and indeed, growingly multidisciplinary character of this branch of science has come more and more manifest.

A knowledge of disperse systems, of interfacial phases is required for solving many problems in several branches of industry and science, particularly in biology and medicine. Moreover, colloid and surface science is indispensable for dealing with some important problems of our days, such as the more efficient utilization of raw material sources and environmental protection.

The recognition of these facts motivated the six-day International Conference on Colloid and Surface Science, organized under the auspices of IUPAC in Budapest, September 1975.

The material presented in 95 contributed papers contained in this volume gives the reader a survey of the work of more than 200 researchers from 22 countries of four continents, carried out in numerous laboratories.

The editor had a difficult task in producing a well arranged grouping of the papers deeling with various topics in a multitude of heterogeneous fields. The principle that the basic common characteristic of the systems investigated was the large specific surface and/or the presence of supermolecular structure elements, made possible the arrangement of 85% of the material into the following three main chapters:

I. Surface chemistry,
II. Disperse systems,
III. Surfactants, monolayers and foams.

Chapter I is concerned with the following six branches of surface chemistry:

I/1 Surface structure and surface chemistry of solids (9 papers)
I/2 Adsorption at solid/gas and solid/liquid interfaces (7 papers).
I/3 Wetting (7 papers)
I/4 Thin liquid films (2 papers)
I/5 Adsorption of polymers (4 papers)
I/6 Adsorption of surfactants (3 papers)

Chapter II contains the papers which deal with the following problems of disperse systems:

II/1 Formation of disperse systems (3 papers)
II/2 Stability and structure of disperse systems (8 papers)
II/3 Electrical phenomena (6 papers)
II/4 Rheology (5 papers)
II/5 Gels (3 papers)

Chapter III comprises reports on researchw ork carried out in three different, independent fields:

III/1 Micellization and related phenomena (8 papers)
III/2 Monolayers and foams (9 papers)
III/3 Molecular interactions (7 papers)

The remaining material is reported in Chapter IV in two groups:

IV/1 The title "Applications" (8 papers) covers investigations on the practical solution of problems met with in some special fields, and

IV/2 "Methods" (6 papers) describes methods of testing applied recently in colloid and/or surface chemistry.

Orientation in the subject-matter is facilitated for the reader by a subject index at the end of the volume; it is a pity that several entries are incomplete (*e.g.* Rutile, p. 429, is missing; Surfactants, adsorption of, p. 231, missing; Suspensions, pp. 426, 695, missing, etc.).

The papers are complemented by a great number (a total of 989) references.

The typography of the book gives evidence of careful work; the text and the tables, with the exception of a few figures, are easy to read.

In summary, this publication will be of great value to colloid- and physical chemists, as well as to chemists, physicists and biologists, engaged in to most various theoretical or practical researches connected with colloid and surface science. The book is a good source of information on the present research trends in this branch of science, and on the results achieved in recent years.

Unfortunately, the compilation does not give the titles, the names and the working places of the authors of the contributed papers read at the conference, as this information did not arrive until the dead-line (June 15, 1975) of sending in the subject-matter intended for publication. It is hoped that Volume 2, to be published at a later date, which will present the discussions of the conference papers, will make up for this deficiency.

K. UDVARHELYI

INDEX

PHYSICAL AND INORGANIC CHEMISTRY

Complex Formation Between Magnesium, Zinc, Cadmium and Arsenazo III, V. Michaylova 111

Mechanistic Study of the Isomerization of *n*-Butene on Acid Catalysts, II. Evaluation of Kinetic Cases and Experimental Results, D. Kalló, E. Detrekőy, G. Schay 119

The Role of Molecular Conformation in π-Electron SCF-MO Calculations, Á. I. Kiss, J. Szőke 133

On the Molecular Structure of Triethyl Silane as Studied by Electron Diffraction, B. Csákvári, Zs. Wagner, I. Hargittai 141

Electron Diffraction Study of the Molecular Structure of Trimethylmethoxysilane, B. Csákvári, Zs. Wagner, P. Gömöry, I. Hargittai, B. Rozsondai, F. C. Mijlhoff 149

Electron Diffraction Study of the Molecular Structure of Bis-(Trimethylsilyl)Ketene, B. Rozsondai, I. Hargittai 157

Electron Diffraction Study of the Molecular Structure of Acetaldazine, I. Hargittai, Gy. Schultz, V. A. Naumov, Yu. P. Kitaev 165

ORGANIC CHEMISTRY

Quantum-Chemical Study of Certain Imidazopyrimidone Derivatives, Z. Dinya, J. Reiter L. Toldy, Sz. Rochlitz 179

Reactions of *o*-Phenylenediamine with α,β-Unsaturated Nitriles, H. Hammad, Kh. El-Bayouki 193

Quantum Chemical Study of the Solvent Effect on the Isomerization of Cyanic Acid. (Short Communication), G. Náray-Szabó, P. Pulay, P. Mezey 199

RECENSIONES 203

Printed in Hungary

A kiadásért felel az Akadémiai Kiadó igazgatója — Műszaki szerkesztő: Zacsik Annamária

A kézirat nyomdába érkezett: 1976. V. 12. — Terjedelem: 9,10 (A/5) ív, 66 ábra

76.3164 Akadémiai Nyomda, Budapest — Felelős vezető: Bernát György

ACTA CHIMICA
ТОМ 90—ВЫП. 2

РЕЗЮМЕ

Комплексообразование магния, цинка и кадмия с арсеназо III

В. МИХАЙЛОВА

Описываются спектрофотометрические исследования реакций магния, цинка и кадмия с арсеназо III. Комплексообразование было изучено методом, основанным на зависимости $A = f(\mathrm{pH})$. Были использованы растворы с эквимолярным составом и с содержанием небольшого избытка металла. Для магниевых и цинковых комплексов было найдено простое хелатное равновесие, в то время как для кадмия было найдено, что реакция протекает по двум ступеням. Были рассчитаны константы равновесия и константы устойчивости. Проводится зависимость между растворимостью продуктов гидроокисей металлов и pH полу-реакции.

Исследование механизма изомеризации н-бутена на кислых катализаторах, II. Кинетические примеры и оценка экспериментальных данных

Д. КАЛЛО, Э. ДЕТРЕКЁИ и Г. ШАЙ

Область кинетических примеров, изученных в предыдущем сообщении, была расширена такими схемами превращений, которые демонстрируют простейшие возможности, а именно, когда путь превращений одного компонента отличается от превращений двух других компонентов. Начальная скорость любого превращения $i \rightarrow j$ может быть выражена следующим уравнением

$$r_{ij}^{0} = a_{ij}\, p_i^0 / (1 + b_i\, p_i^0) \,.$$

Было установлено, что означают константы a_{ij} и b_i, с общей справедливостью, для случая схем различного строения и каким образом уравнение скорости типа Лангмюра может быть обобщено. Определяя постоянные a_{ij} и b_i на водородных, магниевых и никелевых клиноптилолитах при различных температурах, было выяснено, что в то время как на H-форме превращение протекает через образование общего поверхностного промежуточного продукта, на Mg- и Ni-формах наблюдается другое поведение.

Роль молекулярных конформаций в расчете π-электронной структуры методом ССП—МО

А. И. КИШ и Й. СЁКЕ

π-Электронная структура и спектры планарных конформаций дизамещенных бензолов, содержащих карбонильную группу, были рассчитаны с помощью метода Паризер—Парр—Попла. Рассчитанная общая π-энергия, однако, не является надежной мерой определения относительной стабильности конформеров. На основе расчета, однако, можно предсказать, что та форма будет более стабильной, в которой большие π-заряды находятся ближе друг к другу. Была продемонстрирована чувствительность расчетных π-электронных свойств (распределение заряда, дипольный момент, спектральные данные) на конформационные изменения. Различия в расчетных своействах двух конформеров являются наибольшими для о-производных, где желательно молекулярной структуры, наиболее вероятной экспериментально. В случае м и п-произвнодых различия являются того же порядка, как и погрешность расчета.

Электронографическое исследование строения молекулы триэтилсилана

Б. ЧАКВАРИ, Ж. ВАГНЕР и И. ХАРГИТТАИ

Электронографические данные триэтилсилана согласуются с моделью симметрии C_3 и углом вращения вокруг связи Si—C в интервале 105—145° (*анти*-положение цепи H—Si—C—C соответствует 0°). Молекулы вероятно претерпевают крутильные колебания с большой амплитудой вокруг связи Si—C. Длина связи Si—C (r_g) и валентный угол Si—C—C 1,887 ± 0,004 Å и 115,1 ± 1,1°, соответственно.

Электронографическое исследование строения молекул триметилметоксилана

Б. ЧАКВАРИ, Ж. ВАГНЕР, П. ГЁМЁРИ, И. ХАРГИТТАИ, Б. РОЖОНДАИ и Ф. С. МИЙЛХОФФ

Методом газовой электронографии изучено строение молекул триметилметоксилана. Некоторые из структурных параметров:

r_a(Si—O) = 1,639 ± 0,004 Å, r_a(Si—C) = 1,864 ± 0,004 Å, r_a(C—O = 1,423 ± 0,005 Å, r_a(C—H) = 1,114 ± 0,003 Å, < Si—O—C = 122,5 ± 0,6° и < O—Si—C = 108,6 ± 0,2°.

Найдена шахматная конформация (симметрия молекулы C_s) с вращательными колебаниями больших амплидут вокруг связи Si—O. Обнаружен большой эффект сокращения (≈ 0,1 Å) расстояний C. . .C *анти* по сравнению со строго шахматной конформацией.

Электронографическое исследование молекулярного строения бис (триметилсилил) кетена

Б. РОЖОНДАИ и И. ХАРГИТТАИ

Методом газовой электронографии были получены некоторые сведения относительно молекулярной структуры бис (триметилсилил) кетена. Для модели C_{2v} были найдены следующие структурные параметры: r_a(Si—C)$_{ср.}$ = 1,886 ± 0,004 Å, l(Si—C$_{ср.}$ = 0,056 ± ± 0,003 Å и < Si—C—Si = 129° (с погрешностью +2° и —4°). Сравниваются и обсуждаются валентные углы атома углерода при двойной связи, а также атомов N, O и т. п., связанных с атомами C, Si или Ge.

Электронографическое исследование строения молекулы ацеталдазина

И. ХАРГИТТАИ, Д. ШУЛЬЦ, В. А. НАУМОВ, Ю. П. КИТАЕВ

Согласно электронографическим данным, преобладающей конформацией ацеталдазина в газовой фазе является анти, транс-транс, вероятно с большими крутильными колебаниями вокруг связи N—N. Обнаружено также небольшое количество гош формы. Следующие молекулярные параметры характеризуют структуру скелета тяжёлых атомов: r_a(N—N) = 1,437 ± 0,013 Å, r_a(N=C) = 1,277 ± 0,003 Å, r_a(C—C) = 1,486 ± 0,008 Å, ∢ N—N=C = 110,4 ± 0,9°, и ∢ N = C—C = 121,4 ± 1,0°.

Квантово-химические исследования некоторых производных имидазопиримидона

З. ДЫНЯ, Й. РЕЙТЕР, Л. ТОЛЬДИ и С. РОХЛИЦ

С помощью различных квантово-химических методов (МО Хюккеля, ω—ССП, ССП—МО—КВ ППП) были исследованы некоторые производные имидазо (1,2-а) пиримидона, электронно-спектральные свойства их изомерных и таутомерных форм, а также их относительные условия стабильности.

На примере одного выбранного модельного соединения (1*а*, R = H) сравнивались эмпирические и полуэмпирические литературные величины β_{ij}^{core} для ССП—МО—КВ ППП расчета энергий перехода $\Delta E^{s\to s}$ вышеупомянутых соединений. С помощью эмпирических величин β_{ij}^{core}, выбранных таким образом, были определены энергии электронных переходов $S \to S(\pi—\pi^*)$, направления моментов переходов, а также количественные соотношения наиболее важных конфигураций. С помощью методов МО Хюккеля и ω—ССП были рассчитаны энергии делокализации ED_π молекул *1а—2б*, R = H и CH_3, которые хорошо согласуются с заключениями, сделанными ранее относительно строения соединений и их стабильности. С помощью метода ССП—МО—КВ—ППП были рассчитаны также величины «прироста энергии», которые, однако, не дают новой информации относительно структуры и стабильности.

Реакция о-фенилендиамина с α, β-ненасыщенными нитрилами

М. ХАММАД и К. ЭЛЬ-БАЙОКИ

Описывается некатализированная реакция о-фенилендиамина с α, β-ненасыщенными нитрилами. О-фенилендиамин реагирует с эфиром флуорен-9-илиденцианоуксусной кислоты, давая цианобензимидазоль (2), оставляя этиленовую двойную связь незатронутой. А α-нафтилидены (5) расщепляются о-фенилендиамином, давая неожиданные 2-(1-нафтил)-бензимидазоли (6). Ненасыщенные бензимидазоли (2) и (8) восстанавливаются боргидридом натрия, давая насыщенные бензимидазоли (3) и (10), соответственно.

Kristall und Technik

Zeitschrift für experimentelle und technische Kristallographie

Gegründet von WILL KLEBER/HERMANN NEELS

Herausgegeben von HERMANN NEELS

unter Mitwirkung eines internationalen Autorenkollektivs

Je Heft 128 Seiten — mit Abb. — 16,7 × 24 cm — jährlich erscheinen 12 Hefte — Preis je Heft M 20,—; Ausland M 25,—

Bestell-Nr. 1082

Die Zeitschrift berichtet über theoretische, experimentelle und technische Durchdringung aller mit dem kristallisierten Zustand verbundenen Zusammenhänge, in denen die Beziehungen zwischen dem inneren und äußeren Aufbau der Kristalle und den daraus resultierenden Eigenschaften und Verhaltensweisen der Klärung zugeführt werden. Dabei sollen die experimentellen und vor allem die technisch interessanten Aspekte im Vordergrund stehen. In den aufzunehmenden Themenkomplex gehören Arbeiten über Kristallisationsabläufe (Einkristallbildung und Fällungskristalle), Kristallkeimbildung und -wachstum, physikalisch-chemische Zusammenhänge der Kristallographie, ebenso kristallchemische und -physikalische, Kristallbau und Eigenschaften, Methoden der Untersuchung einschließlich der mathematischen, Gefüge, Textur, Bearbeitung, Verarbeitung und Verwendung von Kristallen und deren Verhalten unter verschiedenen äußeren Bedingungen.

Ihre Bestellungen richten Sie bitte an eine Buchhandlung für fremdsprachige Literatur oder an den Postzeitungsvertrieb.



AKADEMIE-VERLAG
DDR-108 Berlin
Leipziger Straße 3—4

Journal für Signalaufzeichnungsmaterialien

Herausgegeben von dem VEB Filmfabrik Wolfen Fotochemisches Kombinat unter der Chefredaktion von K. STOPPERKA

Je Heft 80 Seiten — mit Abb. — 16,7 × 24 cm — jährlich erscheinen 6 Hefte, je Heft M 15,—

Bestell-Nr. 1089

Mit dieser internationalen Fachzeitschrift, die Beiträge in deutscher, russischer und englischer Sprache aus dem Gebiet der Signalaufzeichnungsmaterialien publiziert, wird eine Lücke in der fachspezifischen Literatur der sozialistischen Länder geschlossen. Die Zeitschrift widmet sich sowohl theoretischen als auch anwendungstechnischen Problemen der wissenschaftlichen Fotografie, die magnetischen und andere Signalaufzeichnungsmaterialien, wobei es ihr Anliegen ist, ebenso Beiträge über die Theorie und Technologie der Fabrikation derartiger Signalaufzeichnungsmaterialien aufzunehmen.

Neben Originalarbeiten auf kurzen Originalmitteilungen werden auch Übersichtsartikel veröffentlicht, mit dem Ziel, den in Industrie, Forschung und Lehre tätigen Wissenschaftler über den erreichten Entwicklungsstand der genannten Fachgebiete zu informieren.

Ihre Bestellungen richten Sie bitte an eine Buchhandlung für fremdsprachige Literatur oder an den Postzeitungsvertrieb.



AKADEMIE-VERLAG
DDR-108 Berlin
Leipziger Straße 3—4

Wissenschaft und Fortschritt

Populärwissenschaftliche Monatszeitschrift für Naturwissenschaften und Mathematik

Je Heft 48 S. — mit Abb. — 21×29,7 cm — jährlich erscheinen 12 Hefte, je Heft M 1,— Ausland M 2,—
Bestell-Nr. 1087

»Wissenschaft und Fortschritt« ist eine populärwissenschaftliche Monatszeitschrift für Naturwissenschaften und Mathematik. Sie wendet sich an Oberschüler, Studenten, Lehrer, Wissenschaftler sowie alle an der Wissenschaft Interessierten.
Die Zeitschrift setzt bei ihren Lesern naturwissenschaftliche Grundkenntnisse voraus und regt das Interesse an mathematisch-naturwissenschaftlichen Problemen an.
Sie gibt eingehend Informationen über moderne Entwicklungsprobleme, neue Ergebnisse und Fragestellungen aller naturwissenschaftlichen Zweige, deren wichtigste Anwendungsgebiete sowie ihrer ökonomischen und weltanschaulichen Konsequenzen.
Das Hauptanliegen dieser Zeitschrift ist es, Anregungen und Informationen zu geben, sowohl für den Studenten aus naturwissenschaftlichen Disziplinen, die über den Lehrstoff hinausgehen, als auch für den Fachwissenschaftler zur Weiterbildung auf Nachbargebieten.
Durch die Stoffeinteilung mit Originalbeiträgen, mit Informationen über neue wissenschaftliche Forschungsergebnisse, durch interessante mathematische Aufgabenstellungen sowie ausgewählte Buchbesprechungen vermittelt sie den Lesern ein breites Spektrum der modernen Wissenschaft.

Ihre Bestellungen richten Sie bitte an eine Buchhandlung für fremdsprachige Literatur oder an den Postzeitungsvertrieb.



AKADEMIE-VERLAG
DDR-108 Berlin
Leipziger Straße 3—4

Faserforschung und Textiltechnik

Zeitschrift für Polymerforschung

Begründet von ERICH CORRENS und WALTER FRENZEL
Herausgegeben von WOLFGANG BOBETH, HERMANN KLARE, BURKART PHILIPP, CHRISTIAN RUSCHER

Je Heft 56 S. — mit Abb. — 21×29,7 cm — jährlich erscheinen 12 Hefte, Preis je Heft M 9,—; Ausland M 15,—

Bestell-Nr. 1014

Die Zeitschrift veröffentlicht theoretische und experimentelle Forschungsergebnisse aus Chemie, Physikalischer Chemie, Physik sowie Teilen der Werkstoffprüfung, Technologie und Applikation von Polymeren unter Betonung der Faserstoffe.

Neben Originalarbeiten und Kurzmitteilungen werden Fortschrittsberichte aufgenommen, um jeweils zu speziellen Gebieten einen Überblick über den wissenschaftlichen und wissenschaftlich-technischen Stand zu vermitteln. Der laufenden Literaturinformation dienen die Abschnitte »Neue Bücher«, »Patentschau« und »Literaturschau«.

Ihre Bestellungen richten Sie bitte an eine Buchhandlung für fremdsprachige Literatur oder an den Postzeitungsvertrieb.



AKADEMIE-VERLAG
DDR-108 Berlin
Leipziger Straße 3—4

The Acta Chimica publish papers on chemistry, in English, German, French and Russian.

The Acta Chimica appear in volumes consisting of four parts of varying size, 4 volumes being published a year.

Manuscripts should be addressed to

Acta Chimica
H-1521 Budapest, Hungary

Correspondence with the editors should be sent to the same address.

The rate of subscription in $ 32 00 a volume.

Orders may be placed with »*Kultúra*« Foreign Trade Company for Books and Newspapers (H-1389 Budapest 62, P. O. B. 149. Account No. 218 10990) or with representatives abroad.

Les Acta Chimica paraissent en français, allemand, anglais et russe et publient des mémoires du domaine des sciences chimiques.

Les Acta Chimica sont publiés sous forme de fascicules. Quatre fascicules seront réunis en un volume (4 volumes par an).

On est prié d'envoyer les manuscrits destinés à la rédaction à l'adresse suivante:

Acta Chimica
H-1521 Budapest, Hongrie

Toute correspondance doit être envoyée à cette même adresse.

Le prix de l'abonnement est de $ 32,00 par volume.

On peut s'abonner à l'Entreprise pour le Commerce Extérieur de Livres et Journaux «*Kultúra*» (1389 H-Budapest 62, P. O. B. 149 Compte-courant No. 218 10990) ou à l'étranger chez tous les représentants ou dépositaires.

«*Acta Chimica*» издают трактаты из области химической науки на русском, французском, английском и немецком языках.

«*Acta Chimica*» выходят отдельными выпусками разного объема, 4 выпуски составляют один том, 4 тома публикуются в год.

Предназначенные для публикации рукописи следует направлять по адресу:

Acta Chimica
H-1521 Budapest, ВНР

По этому же адресу направлять всякую корреспонденцию для редакции.

Подписная цена — $ 32,00 за том.

Заказы принимает предпринятие по внешней торговле книг и газет «*Kultúra*» (138 H-Budapest 62, P. O. B. 149. Текущий счет № 218 10990) или его заграничные представительства и уполномоченные.

Reviews of the Hungarian Academy of sciences are obtainable at the following addresses:

AUSTRALIA

C. B. D. Library and Subscription Service
Box 4876, G. P. O.
Sydney N. S. W. 2001

Cosmos Bookshop
145 Acland St.
St. Kilda 3182

AUSTRIA

Globus
Höchstädtplatz 3
A—1200 Wien XX

BELGIUM

Office International de Librairie
30 Avenue Marnix
1050-Buxelles

Du Monde Entier
162 Rue du Midi
1000—Bruxelles

BULGARIA

Hemus
Bulvar Ruszki 6
Sofia

CANADA

Pannonia Books
P. O. Box 1017
Postal Station "B"
Toronto, Ont. M5T 2T8

CHINA

C N P I C O R
Periodical Department
P. O. Box 50
Peking

CZECHOSLOVAKIA

Mad'arská Kultura
Národní třida 22
115 66 Praha

PNS Dovoz tisku
Vinohradská 46
Praha 2

PNS Dovoz tlače
Bratislava 2

DENMARK

Ejnar Munksgaard
Nörregade 6
DK—1165 Copenhagen K

FINLAND

Akateeminen Kirjakauppa
P. O. Box 128
SF-00101 Helsinki 10

FRANCE

Office International de Documentation et Librairie
48, Rue Gay-Lussac
Paris 5

Librairie Lavoisier
11 Rue Lavoisier
Paris 8

Europériodiques S. A.
31 Avenue de Versailles
78170 La Celle St.-Cloud

GERMAN DEMOCRATIC REPUBLIC

Haus der Ungarischen Kultur
Karl-Liebknecht-Strasse 9
DDR—102 Berlin

Deutsche Post
Zeitungsvertriebsamt
Strasse der Pariser Kommüne 3—4
DDR—104 Berlin

GERMAN FEDERAL REPUBLIC

Kunst und Wissen
Erich Bieber
Postfach 46
7 Stuttgart 5

GREAT BRITAIN

Blackwell's Periodicals
P. O. Box 40
Hythe Bridge Street
Oxford OX1 2EU

Collet's Holdings Ltd.
Denington Estate
London Road
Wellingrough Northants NN8 2QT

Bumpus Haldane and Maxwell Ltd.
5 Fitzroy Square
London W1P 5AH

Dawson and Sons Ltd.
Cannon House
Park Farm Road
Folkestone, Kent

HOLLAND

Swets and Zeitlinger
Heereweg 347b
Lisse

Martinus Nijhoff
Lange Voorhout 9
The Hague

INDIA

Hind Book House
66 Babar Road
New Delhi 1

India Book House
Subscription Agency
249 Dr. D. N. Road
Bombay 1

ITALY

Santo Vanasia
Via M. Macchi 71
20124 Milano

Libreria Commissionaria Sansoni
Via Lamarmora 45
50121 Firenze

JAPAN

Kinokuniya Book-Store Co. Ltd.
826 Tsunohazu 1-chome
Shinjuku-ku
Tokyo 160—91

Maruzen and Co. Ltd.
P. O. Box 5050
Tokyo International 100—31

Nauka Ltd.-Export Department
2—2 Kanda
Jinbocho
Chiyoda-ku
Tokyo 101

KOREA

Chulpanmul
Phenjan

NORWAY

Tanum-Cammermayer
Karl Johansgatan 41—43
Oslo 1

POLAND

Węgierski Instytut Kultury
Marszalkowska 80
Warszawa

BKWZ Ruch
ul. Wronia 23
00—840 Warszawa

ROUMANIA

D. E. P.
Bucureşti

Romlibri
Str. Biserica Amzei 7
Bucureşti

SOVIET UNION

Sojuzpechatj — Import
Moscow

and the post offices in each town
Mezhdunarodnaya Kniga
Moscow G—200

SWEDEN

Almaqvist and Wiksell
Gamla Brogatan 26
S—101 20 Stockholm

A. B. Nordiska Bokhandeln
Kunstgatan 4
101 10 Stockholm 1 Fack

SWITZERLAND

Karger Libri AG.
Arnold-Böcklin-Str. 25
4000 Basel 11

USA

F. W. Faxon Co. Inc.
15 Southwest Park
Westwood, Mass. 02090

Stechert-Hafner Inc.
Serials Fulfillment
P. O. Box 900
Riverside N. J. 08075

Fam Book Service
69 Filth Avenue
New York N. Y. 1003

Maxwell Scientific International Inc.
Fairview Park
Elmsford N. Y. 10523

Read More Publications Inc.
140 Cedar Street
New York N. Y. 10006

VIETNAM

Xunhasaba
32, Hai Ba Trung
Hanoi

YUGOSLAVIA

Jugoslavenska Knjiga
Terazije 27
Beograd
Forum
Vojvode Mišića 1
21000 Novi Sad

ACTA CHIMICA

ACADEMIAE SCIENTIARUM HUNGARICAE

ADIUVANTIBUS

V. BRUCKNER, GY. DEÁK, K. POLINSZKY,
E. PUNGOR, G. SCHAY, Z. G. SZABÓ

REDIGIT

B. LENGYEL

TOMUS 90 FASCICULUS 3

AKADÉMIAI KIADÓ, BUDAPEST

1976

ACTA CHIM. (BUDAPEST) ACASA 2 90 (3) 207–324 (1976)

ACTA CHIMICA

A MAGYAR TUDOMÁNYOS AKADÉMIA KÉMIAI TUDOMÁNYOK OSZTÁLYÁNAK IDEGEN NYELVŰ KÖZLEMÉNYEI

SZERKESZTI

LENGYEL BÉLA

TECHNIKAI SZERKESZTŐK

DEÁK GYULA és HARASZTHY-PAPP MELINDA

Az Acta Chimica német, angol, francia és orosz nyelven közöl értekezéseket a kémiai tudományok köréből.

Az Acta Chimica változó terjedelmű füzetekben jelenik meg, egy-egy kötet négy füzetből áll. Évente átlag négy kötet jelenik meg.

A közlésre szánt kéziratok a szerkesztőség címére ((1521 Bp., Műegyetem) küldendők.

Ugyanerre a címre küldendő minden szerkesztőségi levelezés. A szerkesztőség kéziratokat nem ad vissza.

Megrendelhető a belföld számára az „Akadémiai Kiadó"-nál (1363 Budapest, Pf 24. Bankszámla 215 11488), a külföld számára pedig a „Kultúra" Könyv- és Hírlap Külkereskedelmi Vállalatnál (1389 Budapest 62, P.O.B. 149. Bankszámla: 218 10990) vagy annak külföldi képviseleteinél és bizományosainál.

Die Acta Chimica veröffentlichen Abhandlungen aus dem Bereiche der chemischen Wissenschaften in deutscher, englischer, französischer und russischer Sprache.

Die Acta Chimica erscheinen in Heften wechselnden Umfanges. Vier Hefte bilden einen Band. Jährlich erscheinen 4 Bände.

Die zur Veröffentlichung bestimmten Manuskripte sind an folgende Adresse zu senden:

Acta Chimica
H-1521 Budapest

An die gleiche Anschrift ist auch jede für die Redaktion bestimmte Korrespondenz zu richten. Abonnementspreis pro Band: $ 32,00.

Bestellbar bei dem Buch- und Zeitungs-Außenhandels-Unternehmen »*Kultúra*« (1389 Budapest 62, P.O.B. 149 Bankkonto Nr. 218 10990) oder bei seinen Auslandsvertretungen und Kommissionären.

Acta Chimica Academiae Scientiarum Hungaricae, Tomus 90(3), pp. 207—212 (1976)

THEORETICAL CONFORMATIONAL ANALYSIS OF METHOXYDICHLOROPHOSPHINE CH_3O-PCl_2

R. ARSHINOVA,*

(A. E. Arbuzov Institute of Organic and Physical Chemistry Kazan Branch of the USSR Academy of Sciences),*

J. FAUCHER,** M. GRAFFEUIL,** J.-F. LABARRE**

*(** Laboratoire de Chimie de Coordination du CNRS, France),*

and

C. LEIBOVICI***

*(*** Société Nationale des Pétroles d'Aquitaine, Traitement de l'Information, France)*

Received July 11, 1975
In revised form January 31, 1976

The theoretical conformational analysis of methoxydichlorophosphine CH_3OPCl_2 using the CNDO/2 approximation, reveals the existence of two preferred equivalent *gauche* conformations, in agreement with electron diffraction data, and shows the molecule to be highly flexible around the corresponding potential wells. A comparison of calculated and experimental values of the dipole moment strongly supports the existence of *gauche* conformers.

Introduction

Recently, the geometric structure and conformation in the gas phase of some $X-PF_2$ compounds have been investigated by means of electron diffraction and microwave spectroscopy.

When X is a group linked by a first row element ($X = NH_2$, [1, 2], $N(CH_3)_2$, [1, 3], F_2PO [4]) to the phosphorus atom, it appears that — despite a few discrepancies in the literature — the preferred conformation of the corresponding XPF_2 molecules is *gauche*. This has been explained [5, 6] by quantum calculations performed with the CNDO/2 approximation.

Theoretical calculations point to a similar tendency for methoxydifluorophosphine, CH_3P-PF_2 [7]. Moreover, a recent microwave spectroscopic study by SCHWENDEMAN *et al.* [8] reveals the outstanding flexibility of this molecule oscillating between two *gauche* forms, symmetrical about the *cis* conformation.

It is worth pointing out that when X is a group linked by a second row atom (*e.g.* $X = PH_2$ [9]) to phosphorus, the $X-PF_2$ molecule adopts a *trans* conformation; CNDO/2 calculations allowed us to elucidate the origins of this peculiarity [9].

As this semi-empirical method allows to reproduce and to interpret the conformational characteristics experimentally observed for $X-PF_2$ molecules, we thought such an approach could help us to understand all the results — sometimes inconsistent — which have appeared in the literature concerning methoxydichlorophosphine CH_3O-PCl_2.

Experimental data

The molecular geometry of CH_3O-PCl_2 has been investigated by NAUMOV *et al.* [10] (Fig. 1) by means of electron diffraction.

In their study, the authors favour the existence of a preferred *gauche* conformation, which is characterized by a torsional angle $\Theta = (17.3 \pm 5)°$ (*Cf.* Fig. 1). Thus, the molecule studied conforms very well with the general tendency we described in the introduction.

However, two infrared spectroscopic studies, by DURIG and VIGORIO [11] and RAYEVSKII and HALITOV [12] respectively, roused these authors to favour a preferred conformation with a plane of symmetry to which the latter authors ascribed the *cis* conformation. (The chosen convention describing the relative positions of the O—C bond and the direction of the lone pair of phosphorus is depicted in Fig. 1.)

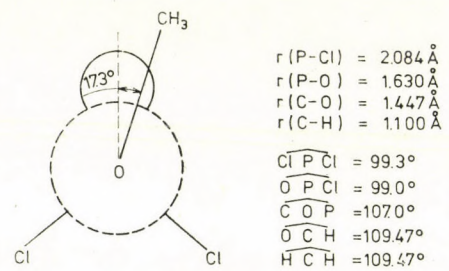

Naumov's conformation (10)

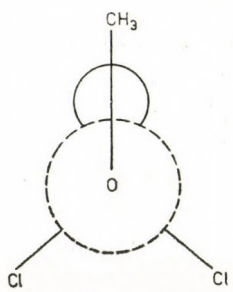

Rayevskii's cis conformation (12)

Fig. 1

Theoretical conformational analysis

All the calculations, using the CNDO/2 approximation [13], were performed on the IBM 370/168 computer of the CNRS (CIRCE, Orsay, France).

We used the geometrical model proposed by NAUMOV. The theoretical conformational analysis was performed on the basis of the now classical rigid rotor assumption.

The conformation at the outset of our calculations is represented in Fig. 2. Θ and Φ are the rotation angles around the P–O and O–C bonds, respectively, these rotations being anticlockwise for an observer located on O, and looking at P or C.

Isoenergy curves of the hypersurface $E(\Theta, \Phi)$ are shown in Fig. 3 (energy of — 42400 Kcal/mole).

This map shows that the molecule studied adopts two perferred equivalent *gauche* conformations, referred to as G (+53.60) and $\bar{G}$ (−53.60) (Fig. 4)- it is noteworthy that, in both conformations, one hydrogen from the methy;

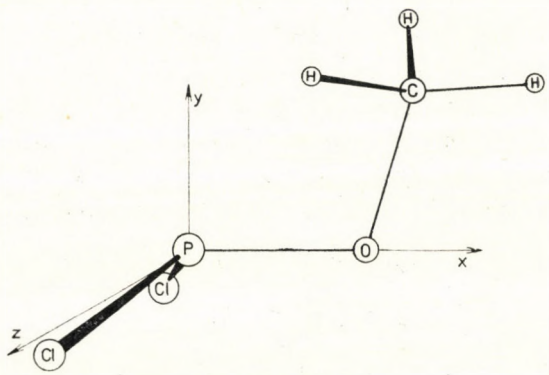

Fig. 2

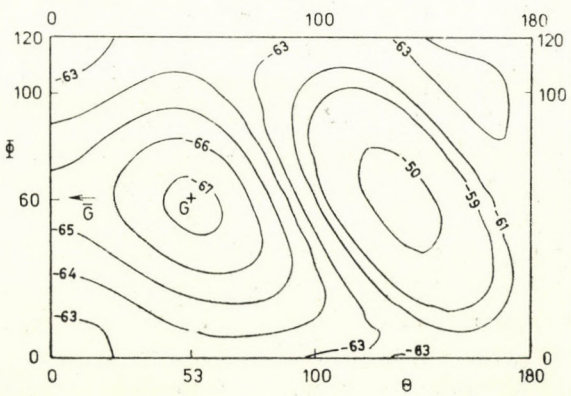

Fig. 3

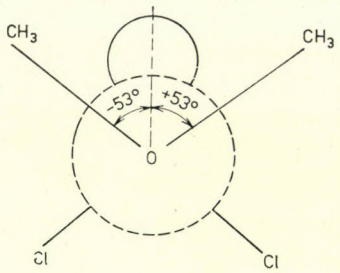

Fig. 4

group lies in the POC plane and eclipses the PO bond. This unusual position for a methyl group has been observed for CH_3O-PF_2 [7].

Although our calculations exaggerate the twist around the P—O bond, they are in good agreement with the conclusions of NAUMOV *et al.* [10] whose experimental observations favour a preferred *gauche* conformation. The quantitative disagreement is less important than it appears to be: the map $E(\Theta, \Phi)$ shows that, around the potential well corresponding to G, the radius of curvature of the hypersurface is large and is thus showing a high degree of flexibility of the molecule in this area. Thus, if we consider (taking into account molecular vibrations, zero point energy and thermal effects) that the actual energy of the molecule may be 1.5 Kcal/mole higher than the absolute minimum one, the area where preferred conformations may exist is found to be quite large (inside the — 66 curve in Fig. 3) and corresponds to:

$$25° < \Theta < 81°$$

$$34° < \Phi < 84°.$$

On the basis of this flexibility around the G well — especially noting that the angle Θ might easily differ $\pm 30°$ from its equilibrium value — the inconsistency with electron diffraction results seems to be removed.

In order to try to understand the experimental results obtained by infrared spectroscopy [11, 12], we can consider the interconversion between the two equivalent *gauche* forms, $G \rightleftarrows \bar{G}$. However, the CNDO/2 calculations show a barrier to internal rotation of 2.5 Kcal/mole. This barrier corresponds to the difference in energy between the *gauche* forms and the unstable *cis* form; such large value makes a hypothesis difficult, in which the molecule would be oscillating from G to $\bar{G}$ and would be observed in its intermediate *cis* state. We ought to add that calculations, performed by one of us (R.A.) using the extended Hückel method [14] with a (3s, 3p, 3d) basis set for the second row atoms, give results identical to the ones presented here, except for the barrier (0.8 Kcal/mole) between the G and the $\bar{G}$ forms. This low barrier would permit the interconversion $G \rightleftarrows \bar{G}$. However caution is advised

in using this value, as it is known that the generalized Hückel method — as usually used — often understimates rotational barriers.

We then approached the problem in a different way, noting that NAUMOV's experiments [10] correspond to a molecule in the gas phase, whilst the spectroscopic studies [11, 12] were made in solution.

We therefore repeated the conformational analysis of CH_3O-PCl_2, adding to the total energy calculated for the isolated molecule, the solvation energy as estimated by JANO [15]. Using the CNDO/2 approximation, JANO's formula may be written:

$$E_{\text{solv}} = -\frac{1}{2}\left(1-\frac{1}{D}\right)\sum_A \sum_B \Delta Q_A \cdot \Delta Q_B \cdot \gamma_{AB}$$

in which ΔQ = net atomic charges
γ = mono and bicentric bielectronic coulomb integrals
D = dielectric constant of the solvent.

This formalism which takes only into account the interactions between the point distribution of the atomic charges of the molecule and the solvent assumed as a perfect dielectric, has already allowed the interpretation of many solution phenomena (tautomeric equilibria [16], pK data [17, 18], solvatochromic effects [19, 20]) although it corresponds only to one of the terms involved in the true solvation energy. Nevertheless when we are interested only in *variations* of the solvation energy, we may consider the cavitation and saturation energies of the dielectric as constant [19].

The new map describing the variations of

$$E'(\Theta, \Phi) = E_{\text{tot}} + |E_{\text{solv}}|_{D=\infty}$$

proves that solvation has no influence upon the general features of the hypersurface. The flexibility of the molecule, as well as the barrier between G and $\bar{G}$, remain unchanged.

Hence if, the preferred conformation of CH_3O-PCl_2 is a *highly flexible gauche* one (as indicated by electron diffraction and quantum calculations), the IR results remain unexplained, if we use the simple approach of solvation effects outlined above. Finally, it should be mentioned that a *trans* form has never been experimentally observed; this is supported by the results of our calculation, the *trans* conformation being some 5 Kcal/mole above the G potential well.

Dipole moment

The dipole moment of methoxydichlorophosphine, in solutions in cyclohexane at 25°C, is found to be equal to 1.97 debyes.

The dipole moments of the *cis*, *gauche* and *trans* forms, calculated from atomic charge densities (μ_{at}) and hybridization contributions (μ_{sp} and μ_{pd}) are 0.64 D, 1.63 D and 3.67 D respectively. If we compare these calculated

values with the experimental ones, the only likely conformation for CH_3O-PCl_2 is again the *gauche* one.

At first sight it might seem surprising to find that the dipole moment of the *trans* form of CH_3O-PCl_2 be higher than that of the *cis* form. The reverse is the case in the difluoro derivative CH_3O-PF_2 [7]. We have shown, by an analysis of the various theoretical components of the dipole moment, that it is the predominant contribution of the lone pairs of electrons on the chlorine atoms, which causes this phenomenon in CH_3O-PCl_2.

*

We are grateful to Dr. István HARGITTAI for stimulating discussions during his visit to our Laboratory (Toulouse) regarding the approach in using electron diffraction and quantum calculations for solving geometrical and conformational problems in chemistry.

REFERENCES

[1] HOLYWELL, G. C., RANKIN, D. W. H., BEAGLEY, B., FREEMAN, J. M.: J. Chem. Soc. A, **1971**, 785
[2] BRITTAIN, A. H., SMITH, J. E., LEE, P. L., COHN, K., SCHWENDEMAN, R. H.: J. Amer. Chem. Soc., **93**, 6772 (1971)
[3] MORRIS, E. D., NORDMAN, C. E.: Inorg. Chem., **8**, 1673 (1969)
[4] ARNOLD, D. E. J., RANKIN, D. W. H.: J. Fluorine Chem., **2**, 405 (1972)
[5] BACH, M.-C., BRIAN, C., CRASNIER, F., LABARRE, J.-F., LEIBOVICI, C., DARGELOS, A.: J. Mol. Struct., **17**, 23 (1973)
[6] ROBINET, G., LABARRE, J.-F., LEIBOVICI, C.: Chem. Phys. Letters, **26**, 203 (1974)
[7] ROBINET, G., LABARRE, J.-F., LEIBOVICI, C.: Chem. Phys. Letters, **29**, 449 (1975)
[8] CODDING, E. G., JONES, C. E., SCHWENDEMAN, R. H.: Inorg. Chem., **13**, 178 (1974)
[9] BACH, M.-C., CRASNIER, F., LABARRE, J.-F., LEIBOVICI, C.: J. Mol. Struct., **13**, 171 (1972)
[10] NAUMOV, V. A., ZARIPOV, H. M., DASHEVSKII, V. G.: Zh. Strukt. Khim. **12**, 158 (1971)
[11] DURIG, J. R., VIGORIO, J. S.: J. Chem. Phys., **48**, 4154 (1968)
[12] RAYEVSKII, O. A., HALITOV, F. H.: Izvest. Akad. Nauk SSSR, 843 (1971)
[13] POPLE, J. A., SEGAL, G. A.: J. Chem. Phis., **43**, 5136 (1965); **44**, 3289 (1966); SANTRY, D. P., SEGAL, G. A.: J. Chem. Phys., **47**, 158 (1967)
[14] HOFFMANN, R.: J. Chem. Phys., **39**, 1397 (1963)
[15] JANO, I.: C. R. Acad. Sc. Paris, **261C**, 103 (1965)
[16] LEIBOVICI, C.: Theoret. Chim. Acta, **8**, 424 (1967)
[17] PERADEJORDI, F.: Thèse, Paris (1964)
[18] GRAFFEUIL, M., LABARRE, J.-F., LEIBOVICI, C.: J. Mol. Struct., **23**, 65 (1974)
[19] LEIBOVICI, C.: Thése, Bordeaux (1967)
[20] LEIBOVICI, C.: J. Mol. Struct., **20**, 429 (1974)
[21] ARBUZOV, B. A., ARSHINOVA, R. P., VUL'FSON, S. G.: Phosphorus (in press)

Rauza ARSHINOVA; A.E. Arbuzov Institute of Organic and Physical Chemistry Kazan, Branch of the USSR Academy of Sciences, 8, A.E. Arbuzov Street, 420083 Kazan (USSR)

Jean-Paul FAUCHER, Marcel GRAFFEUIL, Jean-François LABARRE: Laboratoire de Chimie de Coordination du CNRS, BP 4142, 31030 Toulouse Cedex (France)

Claude LEIBOVICI; Société Nationale des Pétroles d'Aquitaine, Traitment de l'Information, Avenue Jules Ferry, 64000 Pau (France)

Acta Chimica Academiae Scieniarum Hungaricae, Tomus 90(3), pp. 213–232 (1976)

REACTIONS OF CHLOROSILANES WITH ALKOXYSILANES, I

GAS CHROMATOGRAPHIC AND VOLUMETRIC STUDY OF THE CATALYTIC CONDENSATION. CONNECTION BETWEEN REACTIVITY AND MASS-SPECTROMETRIC FRAGMENTATION

B. CSÁKVÁRI,* L. FÁBRY,* P. GÖMÖRY* and K. UJSZÁSZY**

(Department of General and Inorganic Chemistry, Eötvös L. University, Budapest, ** Central Research Institute for Chemistry of the Hungarian Academy of Sciences, Budapest)*

Received September 5, 1975

The condensation of alkoxysilanes with chlorosilanes has been followed by gas volumetric and gas chromatographic techniques. The effect of the active and inactive ligands of the silicon moiety on the reactivity has been investigated.

As shown by the rate of gas evolution during the condensation of alkoxy- and chlorosilanes, the reactivity can be influenced by varying the substituents on both the oxygen and the silicon atom.

It has been established by mass spectrometry that there is a correlation between the reaction rate and the stability of the alkoxy group at the positively polarized silicon atom, which parallels the Hammett constants of the alkyl part of the alkoxy group, *i.e.* its electron donor ability. Conclusions can also be drawn on the effect of π-electron ligands in the silicon moiety on the Si–Cl and Si–O–C bonds, as well as on the steric effects.

The rate of condensation between alkoxysilanes and chlorosilanes increases when π-electron ligands (Vi, Ph) are attached to the Si atom; the same effect is observed upon increasing the electron donor ability of the alkyl part of the alkoxy group.

Introduction

In addition to hydrolytic methods, the siloxane bond may also be formed in certain non-hydrolytic condensation reactions of the type

$$\equiv Si - X + YO - Si \equiv \dashrightarrow \equiv Si - O - Si \equiv + XY \qquad (I)$$

Group X may be a halogen, H, $-OR$, $-OCOR$, whereas Y may be H, $-R$ or $-COR$; any combination of X and Y leads to the formation of siloxanes [1, 2]. Similar condensations occur if $X = -NH_2$, Y + H and X + halogen, $-OCOR$, Y = Na, K [3]. The common feature of condensations (I) is that one of the reactants carries a Si–O bond which, owing to the large difference between the electronegativities of silicon and oxygen, is extensively polarized so that the oxygen atom becomes strongly nucleophilic and the silicon strongly electrophilic. The reactivity of this bond is enhanced by the presence of empty silicon *d*-orbitals of favourable energy and symmetry, which permit the formation of pentacovalent silicon in donor–acceptor interactions. Although

the lone pairs of the oxygen in the $\equiv$Si–O bond may be shifted towards the silicon atom by a so-called $(p \rightarrow d)\pi$ interaction, which would tend to decrease the donor ability of oxygen and the acceptor ability of silicon, this delocalization is suppressed in the presence of a donor or acceptor reactant.

In the following we report on the investigation of one of the most important type of condensations (I), *viz.* on the combination of X = Cl and Y = = alkyl.

The first detailed description of the condensation between chlorosilanes and alkoxysilanes

$$\equiv \mathrm{Si} - \mathrm{Cl} + \mathrm{RO} - \mathrm{Si} \rightarrow \equiv \mathrm{Si} - \mathrm{O} - \mathrm{Si} \equiv + \mathrm{RCl} \qquad \text{(II)}$$

was given in 1946 in a patent by SERVAIS [1]. The reaction takes place above 50°C; the properties of the product siloxanes, in addition to the initial composition, can be influenced by the amount of $FeCl_3$ catalyst, the temperature and the reaction time. Inert solvent, *e.g.* toluene, slows down the reaction whereas a small amount of HCl brings about acceleration. The type of the alkoxy group determines the required amount of catalyst. According to the patent, di- and trifunctional chlorosilanes, alkoxysilanes and particularly alkoxychlorosilanes of the type $RSi(OR')_2Cl$ and $R_2Si(OR')Cl$ are suitable for the condensation. These mixed alkoxychlorosilanes may form *via* group exchange from the corresponding alkoxy- and chlorosilanes. The number of alkoxy groups in the starting silane mixture should be at least equal to the number of chloro substituents, thus no chloro function remains in the final product. There are both cyclic and linear siloxanes among the products. The alkyl chloride formed is of high purity and can thus be recycled in the production of organosilicon monomers [4].

The formation of alkoxychlorosilanes *via* group exchange is catalyzed by the HCl present already at the temperature of boiling [5]. In the case of alkyl hydrogen silanes, the exchange takes place upon mixing, the reaction being exothermic [6]. KUMADA [7] has also reported group exchange leading to the formation of alkoxychlorosilanes under more drastic conditions (bomb tube 200°C). The groups exchange of alkoxychlorosilanes affords dichlorosilanes also under milder conditions [8].

The application of the alkoxysilane–chlorosilane condensation extends the scope of laboratory syntheses too. Cyclic siloxanes have been prepared by ANDRIANOV *et al.* [9—12].

It should be noted that the strong decrease of conversion observed in the alcoholysis of chlorosilanes (40—50%) can be explained by the side reaction of condensation [13] as there is appreciable formation of alkyl chlorides [14].

On the basis of literature data we have selected model compounds and

reactant mixtures which permit to follow the course of the reaction in time. Special attention was directed to the reactions of bifunctional+bifunctional and bifunctional+tetrafunctional silanes, chloro- and alkoxysilanes because of their industrial importance but an explanation was also sought for the lack of reaction between certain monofunctional alkoxy- and chlorosilanes.

Under technological conditions (80—150°C, iron catalyst without a solvent) the alkoxysilane+chlorosilane condensation is carried out in such a manner that the number of functional groups per monomer unit be at least 2 (in exceptional cases 1); the sum of functional groups in the two kinds of monomer should be at least 3 and the average functionality *per* silane monomer 2 or greater.

In the experiments to be described we have studied, by gas volumetric and gas chromatographic techniques, the reactions of chlorosilane-alkoxysilane mixtures (in the presence of γ-Fe_2O_3 and $FeCl_3$) with various hydrocarbon and alkoxy groups attached to the silicon moiety.

Correlation between the reactivity and the number and type of the functional groups

Experimental

1) The reaction of the monochloro + monoalkoxy system

Mixtures of the following composition were reacted at 75°C under anhydrous conditions in a thermostated 3-necked flask equipped with a magnetic stirrer, a thermometer and a reflux condenser:

0.05 mol trimethylalkoxysilane (alkoxy = methoxy, ethoxy, *n*-propoxy or *t*-butoxy);
0.05 mol trimethylchlorosilane*;
0.1 mol cyclohexane;
1% (0.1385 g) γ-Fe_2O_3**

2) Reactions in the dichloro + monoalkoxy system

Dimethyldichlorosilane and trimethylalkoxysilanes (alkoxy = methoxy, ethoxy, *n*-propoxy and i-propoxy) were reacted in the same amounts and conditions as in 1), in the presence of 1% γ-Fe_2O_3 catalyst of the weight of the reactants. Gas evolution was only absent in the case of *n*-propoxysilane (*cf.* Table I, Fig. 1).

* The chlorosilanes were supplied by Wacker GmbH. These were the starting materials for the alkoxysilanes. The purities were checked by distillation through a 50 plate Büchi column with a rotary insert, followed by gas chromatography. Only those substances containing less than 5% impurities were used.

** The particle diameter of the γ-Fe_2O_3 used was 0.16—0.20 mm, unless stated otherwise.

Table I

Composition of product mixtures from the condensation of chlorosilanes

	Reactants		Ratio of reactants		System	
	A	B	mol A	mol B	Open	Closed
1	M		0.1			+
2	M	$+M_{OEt}$	0.05	0.05		+
3	M	$+M_{OEt}$	0.05	0.05	+	
4	M	$+M_{OEt}$	0.05	0.05	+	
5	M	$+M_{OnPr}$	0.001	0.001		+
6	M	$+M_{OiPr}$	0.001	0.001		+
7	M	$+O_{OtBu}$	0.05	0.05	+	
8	M_{OtBu}	+HCl		saturation at 0°C		+
9	M_{OEt}	+D	0.05	0.05	+	
10	M_{OEt}	+D	0.05	0.05	+	
11	$Me_2Si(OEt)Cl$	c	0.1		+	

[a] Determined by mass spectrometry
[b] Contains an oligosilane component too
[c] System studied by activation analysis

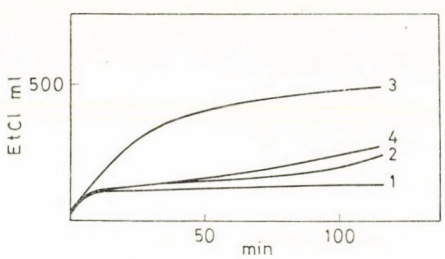

Fig. 1. Gas evolution curves for various dichloro + monoalkoxy and monochloro + dialkoxy systems. (1) $Me_2SiCl_2 + Me_3SiOMe$; (2) $Me_2SiCl_2 + Me_3SiOEt$; (3) $Me_2SiCl_2 + Me_3SiOiPr$; (4) $Me_3SiCl + Me_2Si(OEt)_2$

3) Reaction in the monochloro + dialkoxy system

Trimethylchlorosilane and dimethyldiethoxysilane were reacted in the presence of 1% γ-Fe_2O_3 catalyst in amounts, at mole ratios and under conditions described in 1). The shape of the curve obtained was similar to that observed for system 2).*

* The curves were in all cases drawn on the basis of the average of 3 parallel measurements (reproducible to within 1%) in which readings were taken at 1 min intervals.

with alkoxysilanes under various conditions

Conditions of the reaction					Components of product mixture	
Solvent cyclo-hexane (ml)	Mole ratio of catalyst		Time (hrs)	Temperature (°C)	Gas phase	Liquid phase (Other than the starting components)
	γ-Fe_2O_3 (A+B)	$FeCl_3$ (A+B)				
5.00	5		3	75		M_2 cyclohexane
5.00	5		3	75		EtCl, M_2 cyclohexane
0		1×10^{-2}	1	75	(EtCl), (Et_2O)	(Et_2O, M_2)
0		1×10^{-2}	1	65—75	(EtCl), (Et_2O)	Et_2O, (M_2)
0		5×10^{-2}	3	80		nPrCl, M_2r
0		5×10^{-2}	3	75		iPrCl, M_2r
0		1×10^{-2}	1	65—75		M_2, tBu_2O
	0	0	1/2	75		M_2, tBuCl, $t$$Bu_2O$
9.00		1×10^{-2}	3	75	EtCl, Bu_2O	(EtCl) (Et_2O)*b*
9.00	1×10^{-2}		3	75	EtCl, Et_2O	(EtCl) (Et_2O)*b*
9.00		2×10^{-2}	2	74	EtCl	2% EtOH

Symbols

M = Me_3SiCl
D = Me_2SiCl_2
M_{OEt} = Me_3SiOEt
M_{OnFr} = $Me_3SiOnPr$
M_{OiPr} = $Me_3SiOiPr$
M_{OtBu} = $Me_3SiOtBu$
M_2 = Me_3Si-O-$SiMe_3$
( ) = present at concentrations of less than 10%

4) Reactions in the dichloro + dialkoxy system

The bifunctional mixtures listed in Table I were reacted in the presence of 1% γ-Fe_2O_3 catalyst. The conditions, mole ratios and amounts were the same as in 1). The gas evolution curves are shown in Figs 2a and 2b.

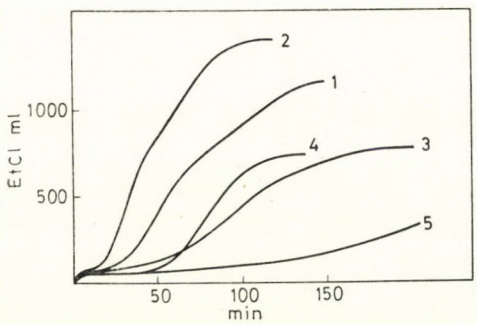

Fig. 2a. Gas evolution curves for various dichloro + diethoxy systems. (1) Me_2SiCl_2 + $Me_2Si(OEt)_2$; (2) $MeViSiCl_2$ + $Me_2Si(OEt)_2$; (3) $MeEtSiCl_2$ + $Me_2Si(OEt)_2$; (4) $MePhSiCl_2$ + $Me_2Si(OEt)_2$; (5) $MeChSiCl_2$ + $Me_2Si(OEt)_2$

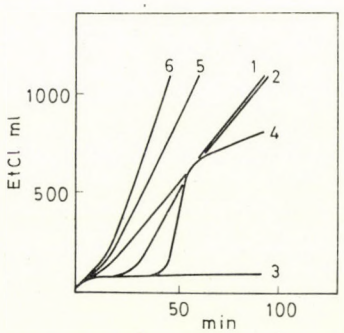

Fig. 2b. Dichloro + dialkoxy systems. (1) Me_2SiCl_2 + $Me_2Si(OMe)_2$; (2) Me_2SiCl_2 + + $Me_2Si(OEt)_2$; (3) Me_2SiCl_2 + $Me_2Si(OnPr)_2$; (4) Me_2SiCl_2 + $Me_2Si(OiPr)_2$; (5) Me_2SiCl_2 + +$MeViSi(OMe)_2$; (6) $MeViSiCl_2$+$Me_2Si(OMe)_2$

Table II

Relative rates and induction periods of reaction series 2—6 referred to the case of R=Me

	σ^*	E_s	v_{R}/v_{Me} *	lg v_{R}/v_{Me}	p	Induction period (min)
Series 2						
Me_2SiCl_2 + Me_3SiOMe			1/1			0
+ Me_3SiOEt			3/1			0
+ $Me_3SiOiPr$			11/1			0
Series 3						
Me_3SiCl + $Me_2Si(OEt)_2$			3.3/1			0
Series 4a						
Me_2SiCl_2 + $Me_2Si(OEt)_2$	0.00	0.00	17/17	0.00		22
$MeViSiCl_2$ +	—	−0.06	13/17	−0.287		12
$MeEtSiCl_2$ +	−0.100	−0.07	8/17	−0.328 ≳	0	28
$MePhSiCl_2$ +	+0.600	−0.90	14/17	−0.243 >	0	52
$MeChSiCl_2$ +	—	−0.79	2/17	−0.929		—
Series 4b						
Me_2SiCl_2 + $Me_2Si(OMe)_2$	0.00	0.00	12/12	0.00		13
+ $Me_2Si(OEt)_2$	−0.10	−0.07	16/12	0.125 ≪	0	28
+ $Me_2Si(OnPr)_2$	−0.12	−0.36	2/12	−0.779 >	0	—
+ $Me_2Si(OiPr)_2$	−0.20	−0.47	50/12	0.619 ≪	0	40
+ $MeViSi(OMe)_2$			50/12			13
$MeViSiCl_2$ + $Me_2Si(OMe)_2$			30/12			13
Series 5						
$Me_2Si(OEt)Cl$	0.00	−0.00	16/16	0.00		19
$MeViSi(OEt)Cl$ condensation	0.05	−0.23**	35/16	0.340	+2.19**	8
$MeEtSi(OEt)Cl$	−0.100	−0.07	8/16	−0.301	+2.31	20
$MePhSi(OEt)Cl$	+0.600	−0.90	35/16	0.340	+2.07	10
$MecSi(OEt)Cl$	—	−0.79	2/16	−0.903		—
Series 6a						
Me_2SiCl + $Me_2Si(OEt)Cl$	0.00	0.00	16/16	0.00		13
$MeViSiCl_2$ +	—	−0.06	40/16	0.397		9
$MeEtSiCl_2$ +	−0.100	−0.07	14/16	−0.059 >	0	18
$MePhSiCl_2$ +	+0.600	−0.90	26/16	0.211 >	0	11
$MecSiCl_2$ +	—	−0.79	2/16	−0.903		35
Series 6b						
Me_2SiCl_2 + $Me_2Si(OEt)Cl$	0.00	0.00	15/15	0.00		10
+ $MeViSi(OEt)Cl$	—	−0.06	18/15	0.079		8
+ $MeEtSi(OEt)Cl$	−0.100	−0.07	14/15	−0.068 ≳	0	19
+ $MePhSi(OEt)Cl$	+0.600	−0.90	19/15	0.103	0	9
+ $MechSi(OEt)Cl$	—	−0.79	2/15	—		—

* Assuming that on the steepest section of the gas evolution curve reaction (2) is the fastest, in the Taft equation

$$\lg (k_R/k_{Me}) = \sigma^* p + Ea$$

the ratio (k_R/k_{Me}) has been replaced by (v_R/v_{Me}). This substitution cannot be performed in the remaining series as the ratio of the rate constants for reactions proceeding at similar rates in complicated equilibrium systems will not be equal to the ratio of gas evolution rates even at identical conversions. It is only the sign of the p-value that can be estimated

** E_s may be obtained from Taft's equation if p is taken as the average of the values calculated for R = Et and R = Ph

5) Condensation of ethoxychlorosilanes

0.1 mol dimethylethoxychlorosilane, 0.1 mol anhydrous cyclohexane and 1% (0.1385 g) γ-Fe_2O_3 were reacted as in 1). The reaction was also carried out with other substituted ethoxychlorosilanes (*cf.* Table II). The results are listed in Table I and shown in Fig. 3.

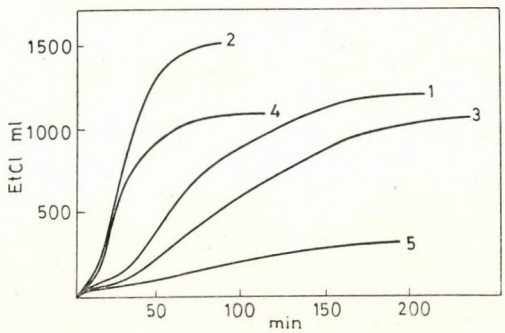

Fig. 3. Ethoxychloro systems. (1) $Me_2Si(OEt)Cl$; (2) $MeViSi(OEt)Cl$; (3) $MeEtSi(OEt)Cl$; (4) $MePhSi(OEt)Cl$; (5) $MeChSi(OEt)Cl$

6) The dichlorosilane + ethoxychlorosilane system

The mixtures shown in Table II were reacted in the presence of 1% γ-Fe_2O_3 under the same conditions as in 1). The results are shown in Figs 4a and 4b.

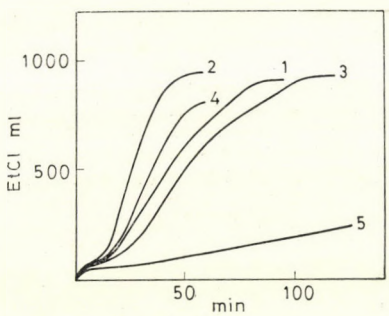

Fig. 4a. Dichloro + ethoxychloro systems. (1) Me_2SiCl_2 + $Me_2Si(OEt)Cl$; (2) $MeViSiCl_2$ + $Me_2Si(OEt)Cl$; (3) $MeEtSiCl_2$ + $Me_2Si(OEt)Cl$; (4) $MePhSiCl_2$ + $Me_2Si(OEt)Cl$; (5) $MeChSiCl_2$ + + $Me_2Si(OEt)Cl$

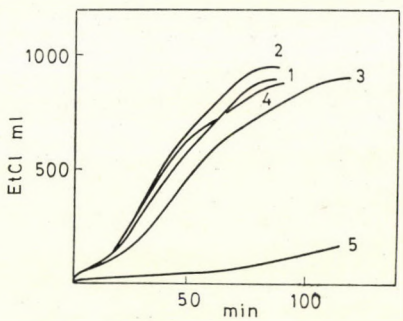

Fig. 4b. Dichloro + ethoxychloro systems. (1) Me_2SiCl_2 + $Me_2Si(OEt)Cl$; (2) Me_2SiCl_2 + $MeViSi(OEt)Cl$; (3) Me_2SiCl_2 + $MeEtSi(OEt)Cl$; (4) Me_2SiCl_2 + $MePhSi(OEt)Cl$; (5) Me_2SiCl_2 + + $MeChSi(OEt)Cl$

7) The ethoxychlorosilane + diethoxysilane system

The mixtures shown in Table II were reacted in the presence of 1% γ-Fe_2O_3 catalyst under the same conditions and in the same amounts as in 1). The results are given in Fig. 5.

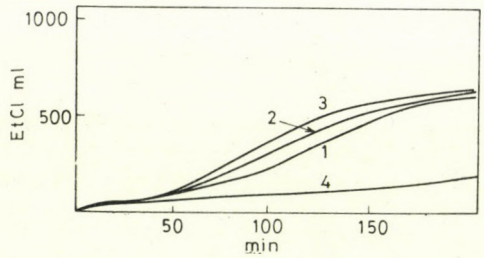

Fig. 5. Ethoxychloro + diethoxy systems. (1) $Me_2Si(OEt)Cl + Me_2Si(OEt)_2$; (2) $MeViSi(OEt)Cl + Me_2Si(OEt)_2$; (3) $MeEtSi(OEt)Cl + Me_2Si(OEt)_2$; (4) $MePhSi(OEt)Cl + Me_2Si(OEt)_2$

8) The mono(di)tetrachlorosilane + tetraethoxysilane system

0.1 mol tetraethoxysilane, an equivalent amount of chlorosilane and 0.5% $FeCl_3$ were charged into the vessel described in 1). The mixture was kept at 60°C and the amount of EtCl evolved was determined. The results are shown in Figs 6a and 6b. In another series of experiments tetraethoxysilane and trimethylchlorosilane were reacted in mole ratios of 1 : 1, 1 : 2 and 1 : 4 (total amount of reactants 0.1 mol) at 90°C, in the presence of 1% γ-Fe_2O_3 (grain size 0.10—0.08 mm) and 0.1 mol *n*-octane. The behaviour of the 1 : 1 mixture was followed gas-chromatographically (Fig. 7).

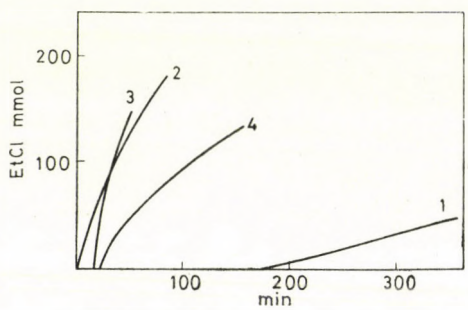

Fig. 6a. Gas evolution curves for mono-, di-, tri- and tetrachloro + tetraethoxy systems (60°C, no solvent, mol ratio given). (1) 4 Me_3SiCl + 1 $Si(OEt)_4$; (2) 2 Me_2SiCl_2 + 1 $Si(OEt)_4$; (3) 4/3 $MeSiCl_3$ + 1 $Si(OEt)_4$; (4) 1 $SiCl_4$ + 1 $Si(OEt)_4$

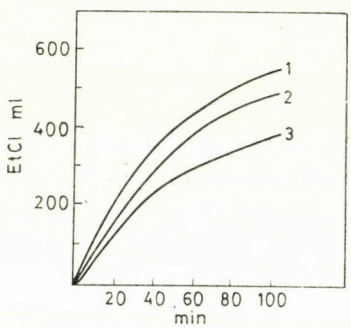

Fig. 6b. Gas evolution curves for trimethylchlorosilane + tetraethoxysilane systems at 90°C (n-octane solvent, mol ratio given). (1) 1 Me_3SiCl + 1 $Si(OEt)_4$; (2) 2 Me_3SiCl + 1 $Si(OEt)_4$; (3) 4 Me_3SiCl + 1 $Si(OEt)_4$

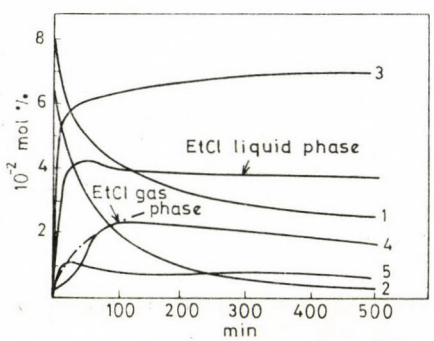

Fig. 7. Time-dependence of the concentrations of various components in the $Me_3SiCl + Si(OEt)_4$ system. (1) $Si(OEt)_4$; (2) Me_3SiCl; (3) $Me_3Si(OEt)$; (4) $Me_3Si-OSiMe_3$; (5) $(EtO)_3Si-O-Si(OEt)_3$

The gas volumetric curve of Fig. 6b shows that the reaction rate is the highest at the mole ratio of 1 : 1 and decreases gradually with decreasing amount of tetraethoxysilane. A characteristic feature is the absence of an induction period.

9) Behaviour of dimethylchloro(2-chloroethoxy)silane

0.1 mol dimethylchloro(2-chloroethoxy)silane was kept at 60°C in the presence of 0.5% (0.0871 g) $FeCl_3$, in the vessel described in 1). No reaction was observed even at boiling temperature.

10) The hexamethyldisiloxane + ethyl chloride system

We have examined whether the condensation step of the reaction is a reversible, equilibrium process. Hexamethyldisiloxane and ethyl chloride were used as model compounds. Hexamethyldisiloxane, ethyl chloride and $FeCl_3$ were mixed in a bomb tube and kept at 80°C for 6 hrs. No reaction was detected by gas chromatography. The mixture was kept at the temperature adjusted in previous experiments but no reaction could be observed.

Comparison and thermodynamic analysis of kinetic and structural parameters

Monofunctial monomers

In general there is no alkyl chloride formation in the reaction of monochloro and monoalkoxysilanes (Table I). In the case of methoxysilane, after refluxing for 3 hrs, hexamethyldisiloxane and dimethyl ether, corresponding to the methoxy group, can be detected by gas chromatography. However, the concentration of the chlorosilane does not change to an appreciable extent. With ethoxysilane, the evolution of ethyl chloride is observed when performing the reaction at 75°C in a bomb tube. (The alkyl chloride was detected by gas chromatography.) Among the propoxysilanes, only i-propoxysilane produces appreciable amounts of i-PrCl, although some *n*-PrCl can be detected in the case of *n*-propoxysilane, too.

t-Butoxysilane reacts also in the absence of a catalyst [15, 16]. With ethoxysilane, the course of the reaction did not change upon applying 2% $FeCl_3$ instead of 1% γ-Fe_2O_3. It should be noted that the formation of the $[FeCl_4^-]$ species can be detected in these systems by UV spectroscopy [17].

In the monoalkoxy + monochloro systems, the following two reactions can take place:

$$Me_3Si-OR + Cl-SiMe_3 \rightarrow Me_3Si-O-SiMe_3 + RCl \qquad (III)$$

$$2\,Me_3Si-OR \rightarrow Me_3Si-O-SiMe_3 + R-O-R. \qquad (IV)$$

If one compares the known heats of reactions and those calculated from the heats of formation derived from the bond additivity principle [18], an explanation emerges for the differences observed with the various compounds

Table III

Calculated heats of formation of gaseous trimethylalkoxysilanes and the enthalpies of reactions III and IV (reaction series 1)

	Me_3SiOMe	Me_3SiOEt	$Me_3SiOnPr$	$Me_3SiOiPr$
Heat of formation (gas phase) (kcal/mol)	−128.0	−132.4	−138.2	−138.2
H for reaction III (kcal/mol)	+ 7.1	+ 10.8	+ 5.6	+ 0.5
H for reaction IV (kcal/mol)	+ 26.1	+ 18.7	+ 23.3	+ 20.6

The data in the Table can be used only for comparison. Deviation from the measured value is ±3 kcal/mol [18]

(Table III). The endothermicity of reaction (III) shows a minimum for i-propoxysilane. The relative heats of reactions (III) and (IV) differ strongly from one another, the difference being the smallest for ethoxysilane.

Bifunctional monomers

From the series of reactions described under 1), it is apparent that the alkoxy group exerts a strong influence on the course of the process. In the bifunctional reactions listed under 2), the reactivity of a silane in the condensation reaction is primarily influenced by the inductive effect of the alkoxy group. The reactions in the bifunctional system (4—7) indicate that the suitable electron density on the oxygen atom of the Si–O–C bond is a necessary condition for the reaction to occur. However, the Si–Cl bond also plays an important part: the gas evolution will be accelerated if the Si–Me moiety is replaced by Si–Vi or Si–Ph both of them make the Si–Cl bond more polarizable. The Vi–Si–Cl bond system reacts faster than the Vi–Si–OEt system. The importanc of steric factors can be estimated from the behaviour of reactant mixtures containing Vi, Et, Ph and cyclohexyl groups.

The Hammett sigma values (σ^*) of the corresponding groups can be found in the literature [19, 20]. The logarithms of the relative rates of reactions (4—7) permit the following conclusions (Table II).

a) The values of parameter p defined by Eq. (V) and characteristic of the nucleophilic character of the reaction shows a pronounced change along the series;

$$p = \frac{B/D + \Delta c}{RTd^2} \qquad \text{(V)}$$

here B/D is characteristic of the solvolysis occurring in the system, Δc is the change in the charge of the reaction center during the reaction, relative to the

unsubstituted atom. R is the gas constant, T the absolute temperature and d the distance of the reaction center from the substituent. If one assumes that $\Delta c \ll RTd^2$, then d will be the smallest for the condensation of ethoxychlorosilane type compounds and the largest for the ethoxychlorosilane + dichlorosilane system.

b) Parameter p changes sign in the case of the dichloro + dialkoxy reactions; in this series, the substituents are varied on the oxygen atom. Thus the partial charge on the Si and O atoms differs significantly from the change in charge at the reaction center.

c) It is necessary to take into account the steric factor.

Tetrafunctional monomers

The gas chromatographic study of the tetraethoxysilane + monochlorosilane reaction indicates that the first step is group exchange which is then followed by condensation (Fig. 7).

$$Si(OEt)_4 + Me_3SiCl \rightleftarrows Me_3SiOEt + Si(OEt)_3Cl \qquad (VI)$$

$$Si(OEt)_3Cl + Si(OEt)_4 \xrightarrow{cond.} (EtO)_3Si-O-Si(OEt)_3 + EtCl \qquad (VII)$$

$$Me_3Si(OEt) + Me_3SiCl \longrightarrow Me_3Si-O-SiMe_3 + EtCl \qquad (VIII)$$

The above sequence is also consistent with the decreasing rate of gas evolution upon decreasing concentration of tetraethoxysilane. Experiments 1—9 permit conclusions on the role of the oxygen atom in the Si—O—C bond system as a nucleophilic center. It seems that the increasing partial negative charge on the oxygen atom accelerates or, in the case of other monofunctional species, permits the reaction to occur 1). As the reaction is influenced by the whole bond system, the studies were extended to cases when groups containing π-electron system are attached to the Si moiety.

Effect of π-electron systems on the reaction rate

Experimental

The following reactions were carried out at 70 and 90°C in 0.1 mol *n*-octane as solvent, in the presence of 1% γ-Fe_2O_3 catalyst (referred to the monomers), in the vessel described:

a) n $MePhSiCl_2$ + (1-n) Me_2SiCl_2 + $Si(OEt)_4$ at 70°C;
b) n $MeViSiCl_2$ + (1-n) Me_2SiCl_2 + $Si(OEt)_4$ at 70°C;
c) n $MeViSiCl_2$ + $Me_3Si(OEt)$ at 90°C;
d) n $MeViSi(OEt)_2$ + Me_3SiCl at 90°C;

where n = 0.0; 0.2; 0.5; 0.8; 1.0 mol.

The order of mixing the components was: alkoxysilane, solvent, chlorosilane, γ-Fe_2O_3 (grain diameter 0.100—0.008 mm).

The reaction of mixture a) shows that increasing amounts of the phenyl-substituted chlorosilane decrease the rate. Similarly, the rate decreases upon increasing the amount of Vi-substituted chlorosilane (Fig. 8a, b, c); *cf.* mixture b).

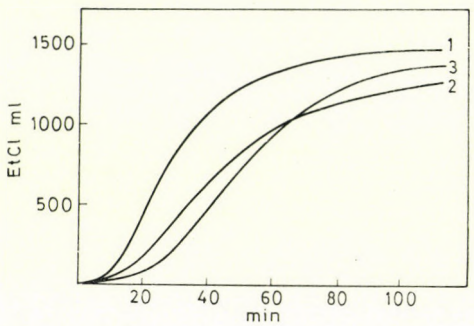

Fig. 8a. Effect of π-electron systems on the rate of gas evolution. (1) $Me_2SiCl_2 + Si(OEt)_4$; (2) $MeViSiCl_2 + Si(OEt)_4$; (3) $MePhSiCl_2 + Si(OEt)_4$

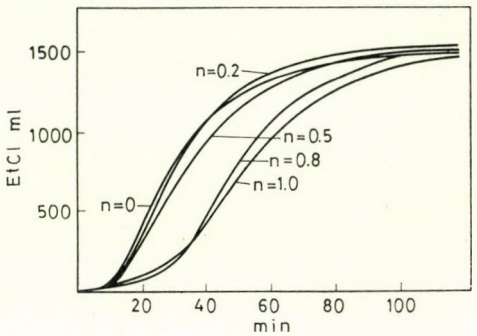

Fig. 8b. Effect of π-electron systems on the rate of gas evolution. $n$$MePhSiCl_2$ + $(1 - n)Me_2SiCl_2 + Si(OEt)_4$

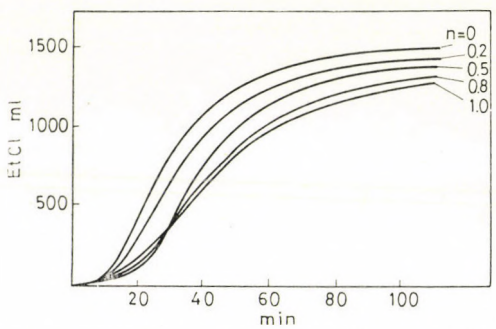

Fig. 8c. Effect of π-electron systems on the rate of gas evolution. $n$$MeViSiCl_2$ + $(1 - n)Me_2SiCl_2 + Si(OEt)_4$

Mixtures c) and d) show a totally different behaviour. A gas chromatographic monitoring of the faster reaction c) permits the following conclusions Fig. 9) concerning the mechanism:

$$MeViSiCl_2 + Me_3Si(OEt) \underset{}{\overset{\text{group exchange}}{\rightleftharpoons}} MeViSi(OEt)Cl + Me_3SiCl \qquad \text{(IX)}$$

$$\begin{array}{c} Me \\ | \\ EtOSi-Cl \\ | \\ Vi \end{array} + \begin{array}{c} Me \\ | \\ EtOSi-Cl \\ | \\ Vi \end{array} \longrightarrow \begin{array}{c} Me \\ | \\ EtO-Si-O-Si-Cl \\ | \\ Vi \end{array} + EtCl \qquad \text{(X)}$$

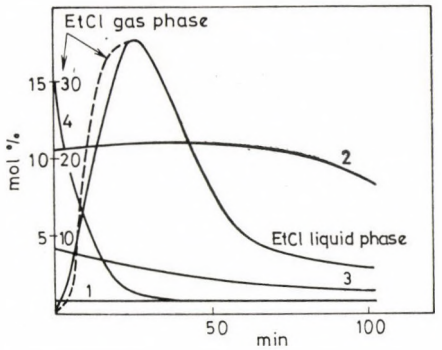

Fig. 9. Effect of π-electron systems on the reaction rate. Time-dependence of the concentrations of various components in the $MeViSiCl_2 + Me_3Si(OEt)$ system. (1) $MeViSiCl_2$; (2) Me_3SiCl; (3) $Me_3Si-O-SiMe_3$; (4) $MeViSi(OEt)Cl_2$. (Numbers in bold type indicate the concentration of ethyl chloride in the solution; normal type refers to the gas phase)

The initial steps of reaction a) may be the following (Fig. 10):

$$MeViSi(OEt)_2 + Me_3SiCl \overset{\text{group ecxhange}}{\rightleftharpoons} MeViSi(OEt)Cl + Me_3Si(OEt) \quad (XI)$$

$$MeViSi(OEt)Cl + Me_3SiCl \overset{\text{condensation}}{\rightleftharpoons} MeViSi(Cl)-O-SiMe_3 + EtCl \quad (XII)$$

$$2\ MeViSi(OEt)Cl \longrightarrow EtO-Si(Vi)(Me)-O-Si(Vi)(Me)-Cl + EtCl \quad (XIII)$$

The trimethylethoxysilane formed in group exchange (XI) is rather inert; by diluting the solution, it decreases the reaction rate.

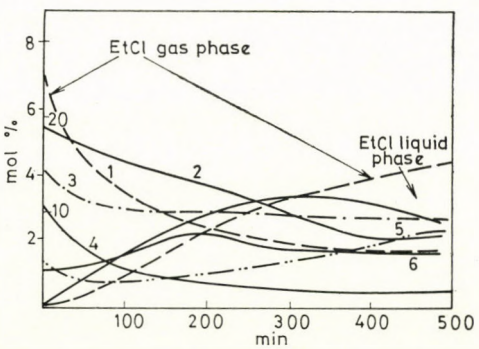

Fig. 10. Effect of π-electron systems on the rate of gas evolution. Time-dependence of the concentrations of various components in the $Me_3SiCl + MeViSi(OEt)_2$ system. (1) $MeViSi(OEt)_2$; (2) Me_3SiCl; (3) Me_3SiOEt); (4) $MeViSi(OEt)Cl$; (5) $Me_3Si-O-SiMe_3$; (6) $Me_3Si-O-Si-O-Si-Me_3$. (The scale and curve for ethyl chloride in the gas phase are marked by arrows)

The $(p-d)\pi$ effect and the reaction rate

Compounds containing atoms with unoccupied *d*-orbitals of suitable energy, especially organometallic derivatives, undergo redistribution type group exchange processes [7, 8, 21], which are characterized by thermodynamic rather than kinetic control. This feature is generally observed in the reactions of substituted silanes.

The condensation processes are reversible, leading to an equilibrium. The condensation between an alkoxysilane and a chlorosilane is influenced not only by the equilibrium between the siloxane and ethyl chloride formed but also by the equilibria between the starting silane and the product oligosilanes. The thermodynamic control is important in all such reactions.

According to the experimental results, the reactivity of both the chloro- and the alkoxysilane increases if the nucleophilic character of the O and Cl atoms increases and if the π-bonding in the Si–O and Si–Cl bond is enhanced. The formation of a $(p-d)\pi$ bond is possible in both the Si–O–C and the Si–Cl bond system. This increases the polarizability of the bonds and, consequently, the molecular geometry will deviate from the tetrahedral, *i.e.* the C–Si–Cl and Si–O–C bond angles will increase, thus facilitating the formation of a pentacovalent transition state. The asymmetrically substituted derivatives are more reactive than the symmetrical species, and the trisubstituted compounds are more reactive than the tetrasubstituted ones.

The reactions are nucleophilic substitutions (S_N); the correlation between the reaction rate and the stability of the Si–O–C bond follows the tendency expected from the Hammett constants.

The gas volumetric and gas chromatographic measurements were completed with mass spectrometric studies with the objective of a possible comparison of the reactivity order and the stabilities of the individual bonds.

Mass spectrometric studies

Mass spectrometric measurements were performed in order to find a correlation between the features observed in the condensation of substituted mono- and bifunctional alkoxychlorosilanes and their fragmentation patterns.

The compounds used were purified by preparative gas chromatography before the measurement performed on a type AEI MS-902 instrument. The mass spectra were recorded at an ionization voltage of 70 eV.

Mass spectra of $MeRSiCl_2$ and $MeRSi(OEt)Cl$ type bifunctional silanes

(i) *$MeRSiCl_2$ type silanes* (Table IV)

The relative intensities of the various primary fragment ions permit

Table IV

Intensity data for the main MS peaks of the $MeRSiCl_2$ type compounds

	Me_2SiCl_2	$MeEtSiCl_2$	$MeViSiCl_2$	$MecHSiCl_2$	$MePhSiCl_2$
M	7	13	20	27	24
M–Me		18	100	1	100
	100				
M–R	100	100	29	51	6
M–Cl	8	2	5	—	2
SiCl	13	11	17	9	12
R	—	—	—	100	8

conclusions on the role of the $(p-d)\pi$ bond and the relative strength of the SiC and SiCl bonds. The mass spectrometric results show that:

a) the frequency of Si–C bond fission decreases in the following order* for various R groups

$$R = Et > c\text{-hexyl} > Vi > Ph$$

b) The fission frequency of the Si–Cl bond is much lower than that of the Si–C bond. The influence of substituents on the fission probability is reflected by the following order:

$$R = Me > Vi > Ph = Et > c\text{-hexyl}.$$

The order of rates shown in Table II, as a function of the nature of group R (reaction series 4 and 6), is

$$R = Vi > Ph > Et > c\text{-hexyl}.$$

The above two orders show the same tendency. Thus the weaker is the Si–Cl bond in the given compound, the faster is its condensation reaction. (In the case of R = Me, the reaction rate is determined by the composition of the other partner.)

c) The intesity of molecular ion decreases in the order

$$R = c\text{-hexyl} > Ph > Vi > Et > Me.$$

* In the case of R = Me, the point of fission is uncertain, therefore, these data have been omitted

The above order, *i.e.* the frequency of appearance of the siliconium ion, does not seem to correlate with the relative rates. The $(p - d)\pi$ bond strengthens both the Si–R and the Si–Cl bond. The $(p-d)\pi$ character is more pronounced for the Si–Cl than for the Si–Vi bond. This observation is in agreement with the results reported by EGOROCHKIN *et al.* [22, 23].

(ii) *MeRSi(OEt)Cl type compounds*

Table V

Intensity data for the main MS peaks of the MeRSi(OEt)Cl type compounds

	$Me_2Si(OEt)Cl$	MeEtSi(OEt)Cl	MeViSi(OEt)Cl	MecHSi(OEt)Cl	MePhSi(OEt)Cl
M	3	—	—	13	40
M–Et (OEt)	-	—	—	—	—
M–Me	—	2	100	4	100
M–R	100	100	14	76	5
M–Cl	11	—	13	1	—
M–OEt	—	—	—	—	—
SiCl	6	4	13	—	28
R	—	—	—	100	—
M–Me–28	49	62	51	1	80
M–Me–28–2	37	33	39	19	40

The analysis of the mass spectra (Table V) has been performed as described. The following conclusions have been reached:

a) the fission frequency of the Si–C bond changes in the same order as observed for the diorganodichlorosilanes, *i.e.*

$$R = Et > c\text{-hexyl} > Vi > Ph.$$

b) The loss of Cl occurs only for R = Vi and Me, in agreement with the strong tendency of these compounds to condensation. The mass spectrum does not reveal any effect of the phenyl group.

c) The peaks of molecular ions are of low intensity, being completely absent is the case of Vi and Et. The intensity order of the observed molecular ions is

$$R = Ph > c\text{-hexyl} > Me.$$

d) Neither ethyl nor ethoxyl radicals are released from the ethoxy group. The characteristic fragmentation pattern involves olefin elimination which is energetically more favourable.

Study of the Si—O—C bond in Me_3SiOR type silanes

The energy of olefin elimination, which can be determined by mass spectrometry, provides characteristic data on the electron donor ability of the alkyl part of the alkoxy group, the stability of the Si–O–R bond and on the amount of excess electrons on the O atom.

Measurements have been performed in the R = Me, Et, Pr and i-Pr systems; the olefin elimination energies are given relative to the R = Me case [24].

The basis of the measurements and the evaluation is the following set of reactions occurring in the mass spectrometer [25]:

$$Me_3SiOR + IP \longrightarrow Me_3\overset{+}{S}iOR^{\cdot}$$

$$Me_3\overset{+}{S}iOR^{\cdot} + E_R \longrightarrow Me_2\overset{+}{S}iOR + Me^{\cdot}$$

$$Me_2\overset{+}{S}iOR + E'_R \longrightarrow Me_2\overset{+}{S}iOH + Ro$$

$$Me_3SiOR + IP + E_R + E'_R \longrightarrow Me_2\overset{+}{S}iOH + Me^{\cdot} + Ro \qquad \text{(XIV)}$$

In order to calculate E'_R, we have measured the appearance potentials of the M-15 and of the $m/e = 75$ ions; the deviations in the corresponding differences are due to the olefin elimination energies

$$AP(Me_2\overset{+}{S}iOH) = AP(Me_2\overset{+}{S}iOR) + E'_R \qquad \text{(XV)}$$

The appearance potential of the theoretical $m/e = 75$ peak of trimethylmethoxysilane has been calculated and the remaining E'_R values are given relative to this. (The IP was assumed to be nearly constant along the series.)

The results thus obtained run in parallel with the corresponding Hammett constants (Tables II and VI). Actually, these data refer to the stability of the alkoxy substituent on the Si atom carrying a partial positive charge. If this value exerts a noticeable influence on the reaction rate, then the Arrhenius equation requires that the tendency of reaction rates apparent from Table VII should be observed. It is clear that the tendency to electron donation follows the trend of olefin elimination energies and relative rates.

Table VI

Mass-spectrometric olefin elimination energies of Me_3SiOR type compounds

	Me_3SiOMe	Me_3SiOEt	$Me_3SiOnPr$	$Me_3SiOiPr$	$Me_2\overset{+}{S}iOH$	Me·	C_nH_{2n}		
							$n=1$	2	3
H_f (kcal/mol)	−128*	−132.4*	−132.4*	−138.2*	315.7 R=iPr 329.7 *n*Pr 328.1 Et 329** Me	33.2	93.7	12.49	4.88
AP (M-15) eV/mol kcal/mol	10.02/231	9.86/228	9.86/228	9.77/225					
AP (75) eV/mol kcal/mol	15.5 /357**	12.05/278	12.05/278	11.53/267					
E_R eV/mol kcal/mol	5.5 /126**	2.19/ 50.3	2.19/ 50.3	1.76/40.5					
Hammett constant (σ^*)	0	−0.10	−0.12	−0.20					
Taft's steric factor (E_s)	0	−0.07	−0.36	−0.47					

* Calculated from the bond additivity values of O'NEAL and RING [18] (error ±3 kcal/mol, less than the experimental error)
** Calculated from the mean values for the cases of R=*n*Pr and R=Et

Table VII

Comparison of the experimental relative reaction rates with those calculated from the olefin elimination energies referred to the case of R=Me

R	$v_{OR}/v_{OMe} = k_{OR}/k_{OMe}$*	Measured v_{OR}/v_{OMe}	v_{OR}
Me	1.00	1.00	$10^{5.5} = 3.162\times10^5$
Et	2.02×10^3	1.33	$10^{2.18} = 1.549\times10^2$
*n*Pr	2.02×10^3	—	$10^{2.19} = 1.549\times10^2$
iPr	5.49×10^3	4.17	$10^{1.76} = 5.755\times10^1$

From the Arrhenius equation

$$\frac{\lg k_{Me}}{\lg k_R} = \frac{-E_{Me}}{-E_R};$$

$$\frac{v_{OMe}}{v_R} = \frac{k_{Me}}{k_R} = \frac{10-E_{Me}}{10-E_R};$$

where: v_{OR}/v_{OMe} is the ratio of the maximum rates in series 4,
k is the rate constant,
B is a constant,
T is the temperature,
R is the universal gas constant, and
the E_R values are those in Table VI

* Assuming a type I reaction at identical conversion

REFERENCES

[1] SERVAIS, PH. C.: US P 2.485.928 (1949), Br P 655.003 (1951)
[2] SMITH, B.: Svensk Kem. Tid. **67,** 421 (1955), *ibid* **65,** 101 (1953)
[3] CHUGUNOV, V. S.: Zh. Obshch. Khim. **27,** 494 (1957)
[4] REED, CH. E., TOME, J. M.: US P 2.741.630 (1956)
[5] Dow Corming Corp. Br. 653238 (1951)
[6] HUNTER, M. J., SERVAIS, PH. C.: US P 2.626.273 (1953)
[7] MAKOTO KUMADA: J. Inst. Polytechnics Osaka City Univ. C. 2. (1952) 139
[8] ANDRIANOV, K. A., GOLUBTSOV, S. A., LOBUSEICH, N. P.: Zh. Obshch. Khim. **27,** 918 (1957), *ibid.* **26,** 197 (1956)
[9] ANDRIANOV, K. A., ZACHERNYUK, A. B., DANIELOV, S. A.: Khim. Geterotsikl. Soedin, **1972** (7) 893
[10] ANDRIANOV, K. A., VASILIEVA, T. V., DYASCHENKO, R. A., DYASCHENKO, B. I., YASTREBOV, V. V., RAIFELD, YU.: Zh. Obshch. Khim. **41,** (5) 1090 (1971), *ibid.* **40,** 1565 (1970)
[11] ANDRIANOV, K. A.: Metody Elementoorg. Khim. Nauka, Moscow, 1968
[12] ANDRIANOV, K. A., DYASCHENKO, N. I., VASILIEVA, T. V., YASTREBOV, V. V., RAIFELD, YU. E.: C. A. **81,** (11) 063716f (1974)
[13] Gmelins Handbuch der Chem. 190 p. Verlag Chem. Weinheim (Bergstr. 1958)
[14] EMELEUS, H. J., ROBINSON, S. R.: J. Chem. Soc. (London) **1947** (1952)
[15] DOYLE, C. D.: US P 2.542.641 (1951)
[16] BRITTON, E. C., BERHENKE, L. F.: US P 2.521.673 (1950)
[17] CSÁKVÁRI, B., FÁBRY, L., GÖMÖRY, P., UJSZÁSZY, K. (Second part of this publication)
[18] O'NEAL, H. E., RING, M. A.: Inorg. Chem. **5,** (3) (1966)
[19] NEWMAN, M. S.: Steric Eff. in Org. Chem. J. Wiley and Sons, Inc. New York 1956
[20] TAFT, R. W., PRICE, E., FOX, I. R., LEWIS, L. C., ANDERSEN, K. K., DAVIES, G. TA.: J. Am. Chem. Soc. **85,** 709 (1963)

[21] MOEDRITZER, K.: Organometallic Chem. Rev. **1,** 179 (1966)
[22] EGOROCHKIN, A. N., VZYANKIN, N. S., KHORSHEV, S. YA.: Izv. Akad. Nauk SSSR, Ser. Khim. **1971** (9) 2074
[23] EGOROCHKIN, A. N., VZYANKIN, N. S., SKOBELEVA, S. E., KHORSHEV, S. YA., ZUEBA, G. YA.: Izv. Akad. Nauk SSSR Ser. Khim. **1971** (10) 2329
[24] LOSSING, T. P., TICKER, A. W., BRYCE, W. A.: J. Chem. Phys. **19,** 1254 (1951)
[25] TAMÁS, J., UJSZÁSZY, K., BUJTÁS, GY.: Adv. in M. S. 5. vol. 703 p. The Inst. of Petr. (London) (1971)

Béla CSÁKVÁRI
László FÁBRY
Pál GÖMÖRY
Kálmán UJSZÁSZY
H–1088 Budapest, Múzeum krt. 6–8.

Acta Chimica Academiae Scientiarum Hungaricae, Tomus 90(3), pp. 233–253 (1976)

REACTIONS OF CHLOROSILANES WITH ALKOXYSILANES, II

MECHANISM OF CATALYSIS IN CHLOROSILANE + ALKOXYSILANE TYPE CONDENSATIONS

B. CSÁKVÁRY,* L. FÁBRY,* P. GÖMÖRY* and K. UJSZÁSZY**

(Department of General and Inorganic Chemistry, Eötvös L. University, Budapest*
*** Central Research Institute for Chemistry of the Hungarian Academy of Sciences, Budapest)*

Received September 5, 1975

We have performed a study of the compounds that can be used as catalysts of the condensation between chlorosilanes and alkoxysilanes. Generally, the catalysts are Lewis acids. According to UV spectrophotometric and X-ray diffraction measurements in the presence of γ-Fe_2O_3 and $FeCl_3$ catalysts, the γ-$Fe_2O_3 \rightarrow FeCl_3$ transformation starts in the solid phase. Iron can be detected in the solution even if γ-Fe_2O_3 is applied as catalyst, which means that the catalysis is homogeneous and the iron is dissolved in the form of $FeCl_4^-$ in both cases.

Introduction

The condensation of alkoxysilanes with chlorosilanes ("heterofunctional condensation") offers a favourable route for the preparation of polysiloxanes. The industrial application of this reaction is probably impeded by the lack of data concerning its mechanism.

The reaction has been patented with the application of Friedel-Crafts type catalysts; in the absence of a catalyst, group exchange processes take place [1—7].

The preparation of silicone oils of the formula R_nSiX_m and $R'Si(OR'')_m$ with controlled chain length (R = H, alkyl, aryl or cycloalkyl groups containing a maximum of 10 carbon atoms; *m* and *n* are 1 and 3, or 3 and 1) has been patented by GUILLISSEN and GANCBERG [2, 7, 8] using $AlCl_3$, $ZnCl_2$ and $FeCl_3$ as catalysts. In the presence of mixed catalysts ($FeCl_3$ + $AlCl_3$) and by changing the number of functional groups, resins may also be obtained [9]. Catalytic activity was observed with BCl_3 [10], $GaCl_3$ [11], $Fe_2(SO_4)_3$ [12], $CaCl_2$, $SnCl_2$ [3], hydrated $FeCl_3$, $FeCl_2$, $SnCl_4$ and $CuSO_4$ [12]; in the case of the latter the bound water apparently also plays a role. The assortment of catalysts was later extended; the iron content of the product was decreased by applying Fe_2O_3 [14] and pyrophoric iron [15] as catalysts.

The nature of the alkoxy group profoundly changes the course of the reaction: *tert*-butoxysilanes can be condensed with chlorosilanes even in the absence of a catalyst [1, 5, 16]. The fact that the ethoxy-fluorosilanes react

with alcohol much slower than the corresponding chlorosilanes (*e.g.* triethoxyfluorosilane cannot be alcoholyzed with *n*-BuOH in pyridine, whereas the corresponding chlorosilane readily undergoes alcoholysis [17]) indicates that the reaction may probably be influenced also by changing the halogen atom.

The results concerning the condensation between alkoxysilanes and chlorosilanes have been reported in detail [18]. We have established that in addition to thermodynamic factors, the rate of the reaction is controlled by the electron distribution within the Si–Cl and Si–O–C bonds. The reaction is of the nucleophilic type: the rate increases with increasing electron density on the Cl and O atoms and with the enhancement of the π-character of the Si–Cl and Si–O–C bonds.

In this paper studies will be described concerning the mechanism of the catalytic condensation reaction.

Study of the catalytic process

Catalytically active compounds

Although numerous catalysts have been described in the literature, it was necessary to undertake a systematic study of the catalytic systems.

Experimental

In a 3-necked, 80 ml, thermostated (85°C) flask equipped with a thermometer and connected to a reflux condenser thermostated at 18°C (Fig. 1), 0.2 mol (27.7 g, 30 ml) dimethylethoxychlorosilane and 0.2800 g (1%) of the catalyst were reacted under anhydrous conditions. Under magnetic stirring, the amount of gaseous ethyl chloride relased in the reaction

$$n\ Me_2Si(OEt)Cl \longrightarrow Cl-\left[\begin{array}{c} Me \\ -Si-O- \\ Me \end{array}\right]_m -Et + \begin{array}{c} Me\ \ Me \\ \diagdown\ \diagup \\ Si-O \\ \bigcirc \end{array} + (n-1)EtCl \qquad (1)$$

was measured volumetrically.

The results are summarized in Table I. (According to gas-chromatographic measurements, after a treatment with Mg powder to remove metal impurities which may act as catalysts, $Me_2Si(OEt)Cl$ remains unchanged after refluxing for 6 hrs in the absence of a catalyst.)

The condensation of the model compounds used are catalyzed by Group III and VIII metal compounds; the catalytic activity depends on the nature of the ligands ($NiCl_2 - Ni(NO_3)_2$) and on the oxidation state of the metal

($FeCl_3$—$FeCl_2$). The active compounds are usually halides but $Fe_2(SO_4)_3$ [11, 12] and Fe_2O_3 [14] are also active, as well as $CaCl_2$ [3], $ZnCl_2$ [2, 4, 7] and $SnCl_2$ [3]. A very active catalyst is iron(III) triethoxide [17]. The compounds of iron with strong complexing agents (*e.g.* cyanide) are inactive. Other inactive compounds are *e.g.* MgO, B_2O_3, Co_2O_3, etc.; a slow reaction and a low yield are observed with V_2O_5, Cr_2O_3, CdO and MoO_3.

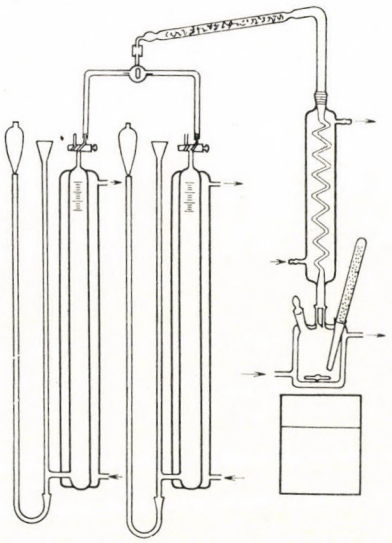

Fig. 1. Apparatus for measuring gas evolution

Analysis of the catalytic action in the system catalyzed by γ-Fe_2O_3/$FeCl_3$

The reaction takes place in a heterogeneous system in the presence of solid, liquid and gaseous phases. If the catalyst is introduced as a solid, in spite of a heterogenous dissolution process, the catalysis seems to be homogenous, associated with the liquid phase. To prove this, the following experiments have been performed.

a) Evidence for the homogenous character of catalysis

Experimental

To 0.1 mol (13.85 g, 15.0 ml) dimethylethoxychlorosilane and 0.1 mol (8.4 g) cyclohexane was added 0.1385 g (1%) γ-Fe_2O_3 in the flask shown in Fig. 1 and the mixture was reacted at 75°C. The specific surface area of the catalyst was varied (grain size 0.250—0.315, 0.250—0.160 or $<$0.100 mm). The amount of gas evolved was measured volumetrically. The measurements were reproducible to within 1—2%.

Table I

Compounds tested as catalysts for the condensation of $Me_2Si(OEt)Cl$

	I	II	III	IV	V
1	H				
2	**Li** LiCl	**Be** $BeCl_2$ BeO	**B** B_2O_3	**C**	**N**
3	**Na** $Na_2B_4O_7 \times aq$	**Mg** $MgCl_2 \times aq$	**Al** $AlCl_3$	**Si**	**P** PCl_3 P_2O_5
4	**K** K_2SiF_6; $Al_2(SO_4)_3 \times aq$ $K_2Cr(SO_4)_2 \times aq$ $K_4Fe(CN)_6 \times aq$ $K_3Fe(CN)_6 \times aq$	**Ca** $CaCl_2$ $CaCl_2 \times aq$	**Sc**	**Ti** $TiCl_4$	**V** V_2O_5
	Cu CuCl $CuCl_2$ $CuSO_4 \times$ aq $CuSO_4$	**Zn** $ZnCl_2$ $ZnCl_2 \times$ aq	**Ga** $GaCl_3$* $GaBr_3$*	**Ge** $GeCl_4$	**As** $AsCl_3$
5	**Rb**	**Sr** $SrCl_2 \times$ aq	**Y**	**Zr** $ZrOCl_2 \times$ aq	**Nb**
	Ag $AgNO_3$	**Cd** $CdCl_2$ CdO**	**In** InCl* InBr*	**Sn** $SnCl_2$ $SnCl_4 \times$ aq $SnCl_4$	**Sb** $SbCl_3$
6	**Cs**	**Ba** $BaCl_2 \times$ aq	**La**	**Hf**	**Ta**
	Au	**Hg** $HgCl_2$ HgCl HgO	**Tl**	**Pb** $PbCl_2$	**Bi** $BiCl_3$

* Active under the conditions described in a) Experimental
** Active in a 50- l volume under industrial conditions

	VI	VII	VIII		
1					
2	**O**	**F**			
3	**S** SCl_2 $SOCl_2$	**Cl**			
4	**Cr** $CrCl_3 \times$ aq Cr_2O_3**	**Mn** $MnCl_2$ $MnCl_2 \times$ aq	**Fe** $FeFe_3$* $FeCl_3$* Fe_2O_3* $FeCl_3 \times$ aq* Mohr' salt Prussian blue $Fe(SCN)_3$ $FePO_4$ $FeBr_3$* aq* $FeSO_4$* $Fe_2(SO_4)_3$*	**Co** Co_2O_3	**Ni** NiCl* NiO $Ni(NO_3)_2$
	Se	**Br**			
5	**Mo** MoO_3**	**Tc**	**Ru**	**Rh**	**Pd** $PdCl_2$
	Te	**I**			
6	**W**	**Re**	**Os**	**Ir**	**Pt** $PtCl^-$
	Po	**At**			

In two flasks identical with that shown in Fig. 1, the following two systems were introduced:

Mixture 1: 0.1 mol $Me_2SiOEtCl$
0.1 mol cyclohexane
2% (0.2770 g) γ-Fe_2O_3 (⌀ 0.250—0.160 mm)

Mixture 2: 0.05 mol $Me_2SiOEtCl$
0.05 mol cyclohexane

Both mixtures were kept at 75°C, and 5 ml aliquots of mixture 1 was transferred into mixture 2, 20, 40 and 60 min after starting the reaction.

Table II

Rate of EtCl evolution as a function of the specific surface area of γ-Fe_2O_3 in the condensation of $Me_2Si(OEt)Cl$

Grain diameter (mm)	Specific surface[a] (m^2/g)	v[b] (ml/min)	Relative rate	
			measured	calculated[c]
0.250—0.315	11.02	12	1	1
0.160—0.250	13.02	15	1.25	1.15
< 0.100	23.74	16	1.33	3.56

[a] Determined by the BET method
[b] Rate measured at the steepest section (EtCl evolution)
[c] Calculated from the formula $v = kF(c_s - c)$

where k — constant
F — surface area
c_s — concentration of the saturated solution
c — actual concentration

The data in Table II show that the length of the induction period and the conversion varies with the grain size of the catalyst, but the differences at the steepest sections are insignificant (Fig. 2). To prove the homogenous nature of the reaction, we injected an aliquot of the reacting mixture into a catalyst-free system: the process has started without an induction period (Fig. 3).

The experimental fact that the reaction can be started in an intact, catalyst-free mixture by injecting the reacting mixture shows that the catalysis is homogenous presumably even in the case of γ-Fe_2O_3. At the same time, it is necessary to assume the chemical dissolution of γ-Fe_2O_3 in the chlorosilane, which probably occurs according to Eq. (2):

$$Fe_2O_3 + 6 \gtrless Si{-}Cl \longrightarrow 2\ FeCl_3 + 3 \gtrless Si{-}O{-}Si \lessgtr \qquad (2)$$

b) Variation of iron concentration in the mixture

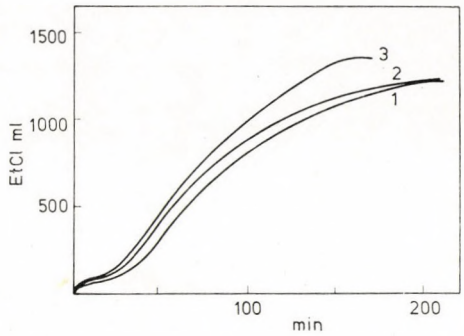

Fig. 2. Effect of the grain size of γ-Fe_2O_3 on the rate of gas evolution; experiment according to section a); 1) Φ 0.250—0.315 mm; 2) Φ 0.160—0.200 mm; 3) Φ < 0.100 mm

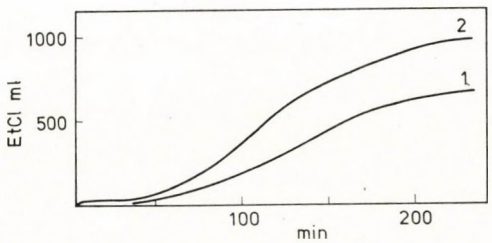

Fig. 3. Gas evolution for the reaction started with an injection after 20 min; experiment according to section a); 1) in toluene as solvent; 2) in cyclohexane as solvent

The variation of the catalyst concentration with time is expected to correlate with the rate of gas evolution, therefore, the iron concentration was measured parallel with the gas evolution.

Experimental

The reaction was performed with the compositions and conditions described in chapter a), using ∅ 0.250—0.160 mm γ-Fe_2O_3 grains. From the stirred reacting mixture, 0.02 ml samples were periodically taken out using a Teflon syringe. The reaction was also carried out with anhydrous $FeCl_3$ as catalyst, too, at the same Si to Fe ratio as above.

The iron content was determined spectrophotometrically [19]. 0.02 ml of the sample was dissolved in 2 ml analytical grade carbon tetrachloride. In a separating funnel, 1 ml 10% aqueous hydroxylamine, 4 ml 10% aqueous sodium acetate were added to the above sample, then after shaking 6 ml 0.25% *o*-phenanthroline in 1 : 1 water–alcohol was added. Iron(III) forms a 1 : 1 red complex with phenanthroline, which can be measured spectrophotometrically at 510 nm (ε = 11,100). The variation of the iron concentration with time was followed by this method in mixtures containing 1% γ-Fe_2O_3 and 2% $FeCl_3$ catalysts. The composition of the mixture and the

Table III

Variation of the iron concentration with time during the condensation of $Me_2Si(OEt)Cl$, in the presence of γ-Fe_2O_3 or $FeCl_3$ catalyst

Fe_2O_3	t (min)	EtCl (ml)	Fe*		Density (g/ml)	Volume of solution (ml)	Fe** 10^{-2} (gatw/l)
			(g)	10^{-2} (gatw/l)			
1	10	50	0.13	4.58	0.892	26.1	4.52
2	20	80		4.62		25.7	4.47
3	30	140		5.44		25.3	5.18
4	40	260		5.46		24.9	5.13
5	50	380		5.70		24.5	5.26
6	60	520	1.42	6.10		24.1	5.54
7	70	600		6.74		23.7	6.03
8	80	670		7.42		23.3	6.52
9	90	720		7.62		22.9	6.57
10	100	760		7.86		22.5	6.67
11	110	810		7.86		22.1	6.56
12	120	830		7.86		21.7	7.45
13	130	840	2.26		0.903	21.3	
$FeCl_3$							
1	10	200	0.54	11.16	0.892	25.7	10.82
2	15	400		11.68		25.3	11.11
3	20	570		11.84		24.9	11.11
4	25	700		12.20		24.5	11.25
5	30	800		13.66		24.1	12.41
6	40	980		13.94		23.3	12.25
7	50	1130		15.32		22.5	13.05
8	60	1240		16.30		21.7	13.30
9	70	1340		16.44		20.9	12.90
10	76	1380	3.71	18.30	0.919	20.1	13.80

* Measured directly
** Values calculated from linearized variation of the solution volume

conditions were identical with those described in chapter a). The results are shown in Table III and Fig. 4. The reproducibility of the measurements was within 1—2% [20].

In the solution iron is present as $FeCl_4^-$ even if γ-Fe_2O_3 is applied, as evidenced by the results to be described here. The reaction is not accelerated in spite of the gradual increase of the iron content in the mixture. This may

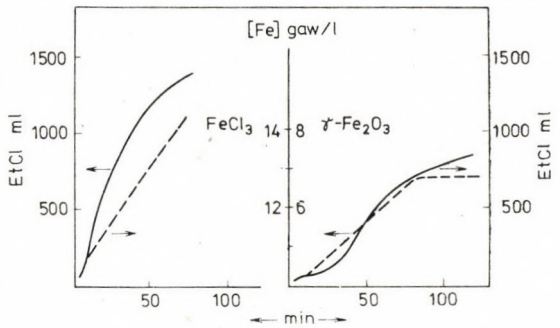

Fig. 4. Variation of the iron content of the mixture (broken line) in time for γ-Fe_2O_3 and $FeCl_3$ catalysts; experiment according to section b)

be explained either by its incorporation into the siloxane framework, or by the increasing molecular weight of the reactants, which strongly decreases the concentration of the active terminals. As the amount of non-bonded iron in the product siloxanes can be minimized by treatment with activated carbon, the latter case seems to be more likely. The rate of gas evolution and the dissolution of iron show similar tendencies.

c) Correlation between the rate and the catalyst concentration

Experimental

Under the conditions and at the compositions given in chapter b), the reactions were carried out at various concentrations of the catalysts γ-Fe_2O_3 and $FeCl_3$. In each pair of experiments with γ-Fe_2O_3—$FeCl_3$, the Fe/Si ratios were equal.

The experimental results are shown in Figs 5 and 6. At low iron contents, the rate of gas evolution depends only on the iron concentration. Irrespective of whether iron is introduced as oxide or chloride, the gas evolution rate from mixtures with Fe/Si ratios of about 10^{-2} is the same. According to X-ray diffraction data, in mixtures containing γ-Fe_2O_3, the reaction described by stoichiometric equation (2) occurs gradually. At the beginning, probably owing to the combined effect of the less active FeOCl and the slower diffusion process, the kinetic order with respect to iron (v)

$$v = (\lg v_{0,\,II} - \lg v_{0,\,I}\, v)/\lg r \qquad (3)$$

(where $v_{0,\,I}$ and $v_{0,\,II}$ are the initial gas evolution rates (at a conversion of 2.5%) for reactions I and II, respectively, and r is the ratio of iron concentrations in reactions I and II) is 2.08 for $FeCl_3$ and 0.48 for γ-Fe_2O_3, the latter indicating heterogeneous reaction steps.

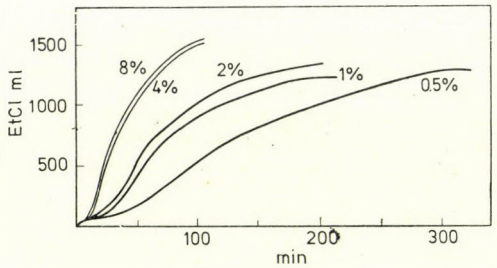

Fig. 5. Effect of γ-Fe_2O_3 concentration on the rate of gas evolution; experiment according to section c)

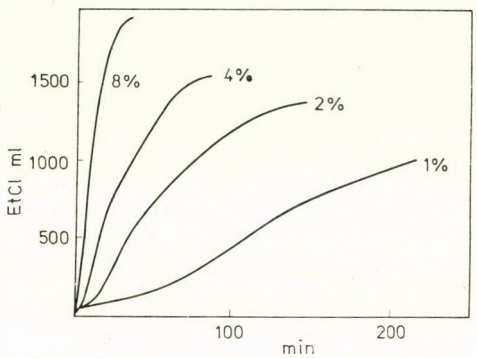

Fig. 6. Effect of the $FeCl_3$ concentration on the rate of gas evolution; experiment according to section c)

d) Effect of the nature of catalyst on the reaction

The intermediates and products have been studied by mass spectrometry in the case of the reactions of bifunctional silanes catalyzed by γ-Fe_2O_3 and $FeCl_3$. The experiments were performed in a bomb tube or in an open system so that the effect of conditions could be elucidated.

Experimental

Dimethyldiethoxysilane and dimethyldichlorosilane were reacted at a mole ratio of 1 : 1 in a bomb tube at 80°C, in the presence of $FeCl_3$ or γ-Fe_2O_3 (the reaction did not start at 75°C). The mixtures were analyzed by mass spectrometry, using the intensities of the basis peaks and the molecular ions.

The catalyst and the conditions affect the formation of cyclosiloxanes. The product mixtures are different in the case of $FeCl_3$ and γ-Fe_2O_3 catalysts (Table IV). Characteristically, the concentration of the tetrasiloxane corresponding to the condensation of the starting compounds is higher than that of cyclopentasiloxane. On the other hand, a higher amount of cyclotrisiloxane is formed in the bomb tube reaction catalyzed by γ-Fe_2O_3. This can be explained by the lower initial iron chloride concentration due to the slow heterogeneous dissolution process; consequently, group exchange reactions predominate

Table IV

Relative amounts of the oligocyclosiloxane products from the condensation of $Me_2Si(OEt)_2$ with Me_2SiCl_2 as a function of the conditions (mass-spectrometric data)

Composition*	$D + D_{(OEt)_2}$	$D + D_{(OEt)_2}$	$D + D_{(OEt)_2}$
Conditions of reaction	closed space (bomb tube) Initial state 20°C, 2% $FeCl_3$	2 hrs 80°C, 1% Fe_2O_3	2 hrs 80°C, 2% $FeCl_3$
Relative amount of components	$D_4 > D_5$	$D_3 > D_4 \gg D_5$	$D_4 \gg D_5$

Composition*	$D + D_{(OEt)_2}$	$D + D_{(OEt)_2}$		
Conditions of reaction	2 hrs 75°C, 2% $FeCl_3$	open space Initial state 68°C, 2% $FeCl_3$	3 hrs 68°C, 2% $FeCl_3$	4 hrs 68°C, 2% $FeCl_3$
Relative amount of components	$D_4 > D_5$	$D_4 > D_5$	$D_4 > D_5$	$D_4 \gg D_5$

* Symbols:

$D = Me_2SiCl_2$

$D_{(OEt)_2} = Me_2Si(OEt)_2$

$D_3 = \left[\begin{smallmatrix} Me & Me \\ & SiO \end{smallmatrix}\right]_3$

$D_4 = \left[\begin{smallmatrix} Me & Me \\ & SiO \end{smallmatrix}\right]_4$

$D_5 = \left[\begin{smallmatrix} Me & Me \\ & SiO \end{smallmatrix}\right]_5$

and the formation of odd-numbered rings becomes characteristic because of the presence of the ethoxychlorosilane formed.

e) Effect of the temperature

The effect of temperature on the mixture described under b) is shown in Fig. 7. With increasing temperature, the induction period becomes shorter and the yield increases.

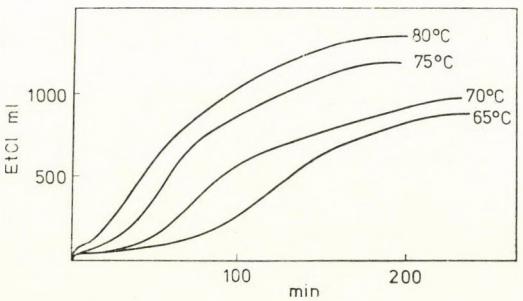

Fig. 7. Effect of the temperature on the rate of gas evolution; experiment according to section e)

f) Effect of the solvent

Experimental

The reactions were carried out in 0.1 ml of an anhydrous solvent under the conditions given under b). The results are shown in Fig. 8.

The solvent effect is insignificant in the cases studied. It is remarkable that with n-heptane, the induction period becomes much longer and the yield decreases. In the case of the strongly polar methyl ethyl ketone, the lower conversion is probably due to side-reactions involving the enol form [21, 22].

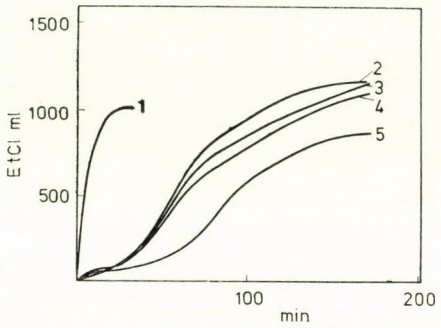

Fig. 8. Effect of the solvent; experiment according to section f); 1) methyl ethyl ketone; 2) toluene; 3) cyclohexane; 4) carbon tetrachloride; 5) *n*-heptane

Transformation of the γ-Fe_2O_3 catalyst during the reaction

We have performed experiments aimed at determining the composition of the iron-containing intermediate in order to elucidate the differences between the application of γ-Fe_2O_3 and $FeCl_3$ catalysts.

UV absorption spectra

According to ZEMANY and PRICE [23], trimethylchlorosilane reacts with $AlCl_3$, a Lewis acid, to form a halogen-bridged complex $\geqslant SiCl-AlCl_3$.

Mössbauer spectra indicate [24] that the reacting mixture contains iron(III) as a molecular complex. We have studied this complex by UV spectroscopy.

Experimental

The spectra were recorded on a Carl Zeiss Jena SPECORD UV-VIS instrument. The organosilicon compounds were of gas chromatographic purity; the solvents used (cyclohexane, carbon tetrachloride, di-i-propyl ether) were spectropure, anhydrous substances. The composition of γ-Fe_2O_3 was 97.88% Fe_2O_3 and 1.85% FeO in a magnetite lattice. $FeCl_3$ contained 33.45% Fe^{3+} and 65.21% Cl (calcd. 34.28 and 65.72%).

Table V

UV spectra of γ-Fe_2O_3 and $FeCl_3$ dissolved in $Me_2Si(OEt)Cl$ and Me_2SiCl_2 (from the evaluation of the spectra in Fig. 9)

Sample and solvent	Iron(III) concentration (mol'l)		Absorption maxima (cm^{-1}) shoulder			
	solution saturated at 20°C	concn. in sample solution				
a) Me_2SiCl_2/γ-Fe_2O_3 cyclohexane	0.72×10^{-2}	3×10^{-3}	27 500	25 600		(40 000)
$Me_2SiCl_2/FeCl_3$ cyclohexane	0.90×10^{-2}	3×10^{-3}				
		1×10^{-3}	27 500			(40 000)
b) $Me_3SiOEt/FeCl_3$ diisopropyl ether	15.71×10^{-2}	1.462×10^{-4}	27 500		30 700	(40 000)
c) $Me_2Si(OEt)Cl/\gamma$-Fe_2O_3 diisopropyl ether	2.671×10^{-2}	1.461×10^{-4} (1)	26 700	25 600	30 700	(40 000)
		0.487×10^{-4} (2)	26 700		30 650	(40 000)
		0.325×10^{-4} (3)	26 700		30 500	(40 000)
d) $Me_2Si(OEt)Cl/FeCl_3$ diisopropyl ether	7.87×10^{-2}	4.32×10^{-4} (1)	27 500	25 600	30 700	(40 000)
		0.481×10^{-4} (2)	26 700		30 650	(40 000)
e) Separating slurry $Me_2Si(OEt)Cl/\gamma$-Fe_2O_3 diisopropyl ether	55.3×10	5.5×10^{-4}	27 800	25 600	(31 000)	(40 000)
		4.9×10^{-4}	28 500		31 000	(40 000)
f) Me_3SiCl/γ-Fe_2O_3		(1)	27 500		30 600	(40 000)
$Me_3SiCl/FeCl_3$		(2)	26 700		31 000	(40 000)

The solutions to be studied were prepared by dilution from saturated solutions of the iron compounds in organosilicon solvents or from samples of the reacting solutions. Iron was analyzed when necessary. The wavelengths of the absorbance maxima and their shift upon dilution were measured. The results are shown in Tables V and VI, and in Figs 9 and 10. The spectra recorded under the conditions described in the literature (Fig. 9) and the shifts of the maxima upon dilution are in agreement with those reported for the $FeCl_4^-$ complex. It is remarkable that the break characteristic of $FeCl_4^-$ was reproducibly present on the spectra. According to quantumchemical calculations [24, 31], the absorbance maxima obtained corresponds to the charge-transfer (redox) band of $FeCl_4^-$. A brown, heterogenous phase separates from the mixture after the reaction which, according to gas chromatographic measurements, consists of concentrated cyclic polysiloxanes. The iron concentration

Table VI

UV spectra of γ-Fe_2O_3 and $FeCl_3$ dissolved in Me_3SiCl and $Me_3Si(OEt)$, and the spectra after the condensation of $Me_2Si(OEt)Cl$*

	Fe(III) content (mol/l)	Absorption maxima (cm^{-1})					
M/Fe_2O_3 CCl_4 (Fig. 9f)	Saturated solution, 20°C	27 500 —	30 600 —	(40 000) —			
$M/FeCl_3$ CCl_4 (Fig. 9f)	Saturated solution	26 700 —	31 000 —	(40 000) —			
$M_{OEt}/FeCl_3$ CCl_4	Saturated solution	— —	29 000 —	(40 000) —			
$M + M_{OEt}/\gamma$-Fe_2O_3 CCl_4	Saturated solution	27 500 —	31 000 —	(40 000) —			
$M + M_{OEt}/FeCl_3$ CCl_4	Saturated solution	27 500 — 26 700 —	31 000 — 31 800 —	(40 000) — (40 000) —			
$D_{(OEt)2}/FeCl_3$	Saturated solution	— —	29 000 —	(40 000) —			
D_{Vi}/γ-Fe_2O_3 CCl_4	Saturated solution	27 500 —	— —	(40 000) —			
$E/FeCl_3$ cyclohexane after reaction, 2% $FeCl_3$ (Fig. 10, (1))	6.5×10^{-2}	20 500	19 300	18 700	16 700	14 800	13 200
E/Fe_2O_3 cyclohexane after reaction (Fig. 10 (2))	2.4×10^{-2}	20 500	19 300	18 700	17 000	14 800	13 200
Ref [26] measured values diisopropyl ether	3×10^{-1}	21 000	19 700	18 900	16 400	16 000	12 950
calculated values [30]		—	18 800	16 300	15 600	13 000	—

* Symbols
Me = Me_3SiCl; D_{Vi} = $MeViSiCl_2$; E = $Me_2Si(OEt)Cl$; M_{OEt} = Me_3SiOEt; $D_{(OEt)2}$ = = $Me_2Si(OEt)_2$

in this phase is appreciably higher than that in the homogenous residual phase; its UV spectrum corresponds to that of $FeCl_4^-$. The results point to the formation of a $\geqslant Si-Cl-FeCl_3$ type complex from both γ-Fe_2O_3 and $FeCl_3$.

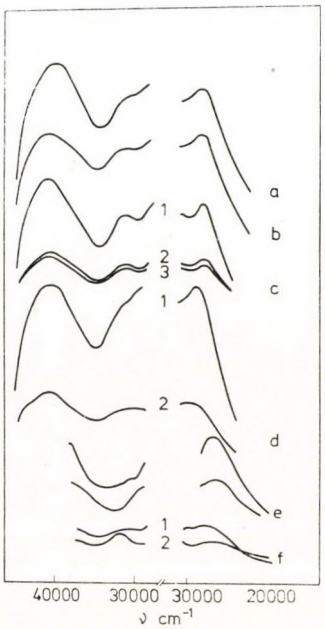

Fig. 9. UV spectrophotometric measurements. a) Me_3SiCl/γ-Fe_2O_3; b) $Me_3Si(OEt)/FeCl_3$; c) $Me_2Si(OEt)Cl/\gamma$-Fe_2O_3; d) $Me_2Si(OEt)Cl/FeCl_3$; e) $Me_2Si(OEt)Cl/\gamma$-Fe_2O_3; the phase separated; f) Me_3SiCl/γ-Fe_2O_3 (1), $Me_3SiCl/FeCl_3$ (2). (The symbols and concentrations are the same as in Table V)

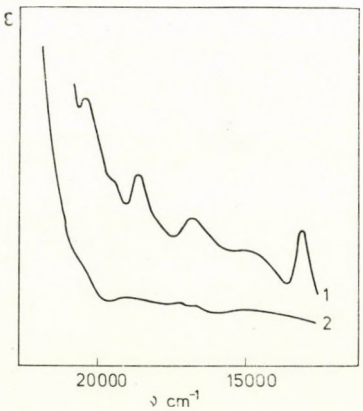

Fig. 10. Visible spectrum of the product mixture from the condensation of $Me_2Si(OEt)Cl$ in cyclohexane; experiment according to section d). 1) 2% $FeCl_3$ as catalyst; 2) 1% γ-Fe_2O_3 as catalyst

X-ray diffraction analysis of the transformation of the γ-Fe_2O_3 catalyst

Experimental

The experiments were performed with the substances described above, under the conditions and at the compositions given in Table VII using bomb

Table VII

X-ray diffraction analysis of the transformation of solid γ-Fe_2O_3 under the action of chlorosilanes
(First figure is d/hkl and second is the intensity)

I. 1 g γ-Fe_2O_3, 5 ml $Me_2Si(OEt)Cl$, 5 ml cyclohexane, 1 week at 21°C then 3 hrs at 70°C					
γ-Fe_2O_3 and $FeCl_3$	5.900/5 2.683/6 1.642/1	*FeOCl*	3.399/6 2.634/1 1.642/1		
II. 1 g γ-Fe_2O_3, 5 ml $Me_2Si(OEt)Cl$, 5 ml cyclohexane, 1 week at 21°C					
γ-Fe_2O_3 and Fe_2SiO_3 orthorhombic		$FeCl_3 \times 6H_2O$	5.965/8 4.400/2 3.547/2 2.768/3 2.579/2 1.919/2	$2FeCl_3 \times 7H_2O$	6.367/5 5.510/2 4.360/2 3.882/2 3.063/2 2.870/2 2.430/2
FeOCl	3.410/7 2.637/5 1.672/2 1.640/2 1.527/3	$FeCl_2 \times 4H_2O$	5.510/4 5.371/4 3.946/4 3.063/3 2.768/2 2.173/2	$FeSiO_3$ monoclinic	3.260/3 3.260/3 3.063/4 2.870/2 2.637/5
III. 1 g γ-Fe_2O_3, 0.5 ml HCl, 5 ml cyclohexane, 1 week at 21°C then 3 hrs at 70°C					
γ-Fe_2O_3 and *FeO*	1.516/1 2.166/2	$FeCl_3$	5.900/9 2.690/1 1.784/1 1.626/3	*FeOCl*	3.451/3 2.641/2 1.784/2 1.516/2
IV. 1 g γ-Fe_2O_3, 5 ml Me_3SiCl, 5 ml cyclohexane, 1 week at 21°C then 3 hrs at 70°C					
$FeCl_3 \times 6H_2O$	6.021/ 2 4.400/ 1 3.500/ 1 3.162/ 2 2.746/23 2.421/ 2	$FeCl_2 \times H_2O$	5.447/25 4.237/20 2.863/10 2.746/25 2.384/ 1 2.318/ 5 2.128/10 2.680/15	$FeCl_3$	5.782/5 1.756/2 1.652/5 1.460/1
		FeOCl	2.630/ 4 1.833/ 2 1.523/ 2		

V. 1 g γ-Fe_2O_3, 2.5 ml Me_3SiCl, 2.5 ml $Me_3Si(OEt)$, 5 ml cyclohexane, 1 week at 21°C then 3 hrs at 70°C

γ-Fe_2O_3 and $FeCl_3 \times 2H_2O$	4.716/2 3.517/2 2.511/2	*FeO(OH)*	3.277/8 2.569/8	$FeCl_3$	2.682/ 6 2.085/20 1.767/ 6 1.630/ 6

VI. 1 g γ-Fe_2O_3, 5 ml Me_3SiCl, 5 ml cyclohexane, 1 week at 21°C then 3 hrs at 70°C

$FeCl_3 \times 6H_2O$	5.893/14 3.497/5 2.757/20 2.423/6	$FeCl_3 \times 2H_2O$	5.511/37 4.255/21 2.872/12 2.318/9 2.135/9 2.085/22	$FeCl_2 \times 4H_2O$	5.511/37 3.940/6 2.757/10 2.179/4 2.135/9
$FeCl_3 \times 2H_2O$	5.893/14 4.831/10 3.940/6 3.497/5 2.511/10	*Philosilicate*	14.290/10 12.020/3 11.210/4 10.660/4 9.501/5 8.972/4 1.875/5 1.822/6 1.796/6		

VII. 1 g γ-Fe_2O_3, 2.5 ml Me_2SiCl_2, 2.5 ml $Me_3Si(OEt)$, 5 ml cyclohexane, 1 week at 21°C then 3 hrs at 70°C

$FeCl_3$	1.754/6	$2FeCl_3 \times 7H_2O$	6.320/16 5.511/37 3.827/7 2.873/12 2.423/6

VIII. 1 g γ-Fe_2O_3, 5 ml Me_2SiCl_2, 5 ml cyclohexane, 1 week at 21°C then 3 hrs at 70°C

γ-Fe_2O_3 $FeCl_2$	3.048/30 2.526/90 1.945/25 1.792/100 1.714/40 1.466/21	$FeCl_2 \times 2H_2O$	5.400/62 4.247/36 2.862/20 2.740/40 2.384/30 2.328/40 2.073/22

tubes. Parameters: Siemens Crystalloflex instrument, iron cathode, 35 kV, Mn filter. In Table VII, the data of the evaluated X-ray diffractograms are shown. A chlorine-containing phase is detectable in all samples as are, in some cases, the intermediates of the desctruction of the maghemite lattice having loose spinel structure, *e.g.* FeOCl. This is due to the reaction between chlorosilanes and iron(III) oxide

$$Fe_2O_3 + 6 \geqslant Si-Cl \longrightarrow 2\ FeCl_3 + 3 \geqslant Si-O-Si \leqslant \qquad (2)$$

which has been described [32], but has not yet been followed by X-ray diffraction analysis.

According to Table VII,

a) a treatment with concentrated hydrochloric acid (36 wt%) does not decrease the FeO content of the sample, but no FeO can be detected in the system after treatment with chlorosilanes (Samples I, II and III);

b) the alkoxy group suppresses the effect of chlorosilanes unless both functional groups are attached to the same silicon atom;

c) the presence of surface phases cannot be excluded (unidentified doublet lines of low intensity with philosilicate character);

d) the γ-$Fe_2O_3 \longrightarrow FeCl_3$ transformation takes place gradually in the solid phase.

IR spectroscopic study of the condensation between alkoxy- and chlorosilanes

Experimental

The IR spectra of dimethylethoxychlorosilane (gas chromatographic purity) have been recorded in the pure state and upon treatment with 1% γ-Fe_2O_3 or 2% $FeCl_3$ using a UR 10 instrument (0.02 mm NaCl cell). The spectrum of the untreated substance was recorded several times in succession. The treatment was performed in bomb tubes for 1 week at room temperature and for 3 hrs at 75°C. The slurry that separated from the reacting mixture under the conditions given in b), containing a high concentration of iron, has also been investigated in carbon disulfide solution. The IR spectrum of the mixture was compared with that of a mixture kept at room temperature for 1 week.

The changes in the band intensities (Table VIII, Fig. 11) indicate the formation of siloxanes. After treatment with γ-Fe_2O_3, the reaction goes to completion in the bomb tube. The broad band corresponding to the asymmetric Si–O–Si stretching vibration shows absorption maxima at 1087 and 1020 cm^{-1}, characteristic of the siloxane polymers [33]. The Si–Cl bonds probably disappear in a process corresponding to reaction (2). In the sample treated with $FeCl_3$, no reaction can be detected and the siloxane band maximum (1045 cm^{-1}) points rather to the formation of cyclosiloxanes. It should be noted that in an open system, $FeCl_3$ is a more efficient catalyst than γ-Fe_2O_3.

The spectrum of the slurry indicates the presence of water, probably formed in the process

$$Fe_2O_3 + 6\ HCl \longrightarrow 2\ FeCl_3 + 3\ H_2O \qquad (4)$$

Table VIII

Variation in time of some IR bands of mixtures containing γ-Fe_2O_3 in $Me_2Si(OEt)Cl$

(cm^{-1})	480	537	560	665	850	960	1020	1090	1110	1160	1295	1395	1440
(4) $Me_2Si(OEt)Cl$	s	m	o	s	s	s	o	s	s	s	m	s	m
(3) $Me_2Si(OEt)Cl/\gamma$-Fe_2O_3 $Me_2Si(OEt)Cl/FeCl_3$	vw	vw	o	vw	w	vw	s	s	o	o	o	vw	o
(2) t = 0 min	s	w	w	s	s	s	?	s	s	m	(1285)	s	m
t = 15 min	s	w	w	s	s	s	s	s	s	m	o	m	m
							(1040)				(1285)		
(1) t = 30 min	s	w	w	w	(1040)	s	s	s	s	m	o	m	m
											(1285)		
	Si | Cl	Si / \ Cl Cl	Si | O	Si | Cl	Si | O / C_2H_5	Si | O / C_2H_5	Si | O | Si	Si | O | Si	Si | O | C	Si | O | C	Si | CH_3	C | H	C | CH_3
	νs	νas	νs	νas	νs		νas	νas	ϱ	νas	δ	δs	δas

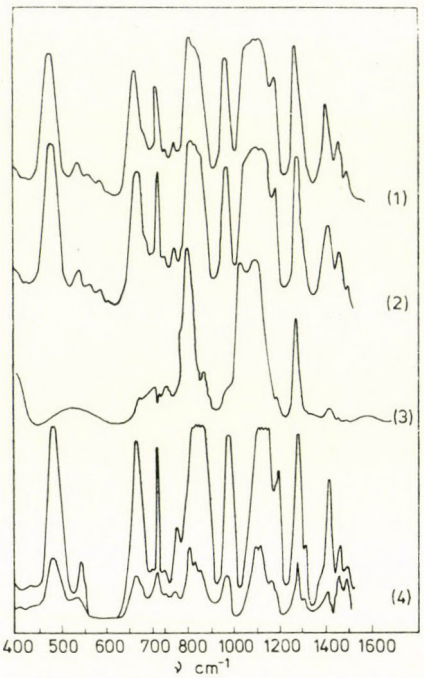

Fig. 11. Stages of the condensation of $Me_2Si(OEt)Cl$; IR spectra: 1) and 2) 2% $FeCl_3$, $t = 30$ min (1), $t = 0$ min (2); 3) Product mixture from $Me_2Si(OEt)Cl$ containing 1% γ-Fe_2O_3; 4) $Me_2Si(OEt)Cl$

involving the HCl always present in small amounts. The formation of a hydroxy compound (≥Si—OH) can also be observed. The C–O stretching vibration at 1100 cm^{-1} decreases in intensity, whereas the asymmetric Si–O–Si stretching at 1060 cm^{-1} shows an increase.

REFERENCES

[1] Servais US P 2.485.928 (1949), Br P 655.003 (1951)
[2] Guilliessen, C. J., Gancberg, A.: US P 2.695.307 (1954)
[3] Monsanto Chem. Br. P 657.704 (1951)
[4] Reed, Ch. E., Tome, J. M.: US P 2.741.630 (1956)
[5] Doyle, C. D.: US P 2.542.641 (1951)
[6] Moedritzer, K.: Organometallic Chem. Rev. **1**, 179 (1966)
[7] Emblem, M. G., Meadowcraft, A. E.: Br P 698.866 (1953)
[8] Guillissen, C. J., Gancberg, A.: Belg. P 496.045 (1950)
[9] Guillissen, C. J., Gancberg, A.: US P 2.768.152 (1956)
[10] Wagner, G. H., Erickson, Ch. E.: US P 2.731.485 (1956)
[11] Un. Chem. Belge Belg. P 491.765, 576.174 (1950)
[12] Un. Chem. Belge Belg. P 491.799 (1950)
[13] Wright, J. G. E., Marsden, J.: US P 2.389.744 (1945)
[14] Gömöry, P.: Hung. P 155.811 (1967)
[15] Lengyel, B., Székely, T., Szepes, L.: Hung. P 130.571 (1973)
[16] Britton, E. C., Berhenké, L. F.: US P 2.521.673 (1950)

[17] PEPPARD, D. F., BROWN, W. G., JOHNSON, W. C.: J. Am. Chem. Soc. **68,** 77 (1946)
[18] CSÁKVÁRI, B., FÁBRY, L., GÖMÖRY, P., UJSZÁSZY, K. (first part of these publications)
[19] BRANDT, W. W., SMITH, G. F.: Anal. Chem. **21,** 1313 (1949)
[20] ZIMMERMANN, M.: Photometrische Metall- und Wasseranalysen 2nd ed. Stuttgart, Wissenschaftlische Verlagsges. 1961.
[21] TOSHIO TAKIGUCHI: J. Org. Chem. **23,** 1216 (1958)
[22] CALES, R., DUNOGUES, J., DIFFAUT, N., BIRON, C.: C. R. Acad. Sci. Paris Ser. C. **1968,** 267 (6) 494
[23] ZEMANY, P. D., PRICE, F. D.: J. Am. Chem. Soc. **70,** 4222 (1948)
[24] VÉRTES, A., CSÁKVÁRI, B., GÖMÖRY, P., KOMOR, M.: Radiochem. Radional. Lett. 1972, 9 (4) 303
[25] KISS, A., ÁBRAHÁM, J., HEGEDÜS, I.: Z. allg. anorg. Chem. **244,** 98 (1940)
[26] ANTIPOVA-KARATAEVA, I. I., ZOLOTOV, YU. A., SERYAKOVA, U. V.: Zh. Neirg. Khim. **9,** (7) 1712 (1964)
[27] METZLER, D. E., MYERS, R. J.: J. Am. Chem. Soc. **72,** 3776 (1950)
[28] NACHTRIEB, N. H., CONWAY, J. G.: J. Am. Chem. Soc. **70,** 3547 (1948)
[29] FRIEDMAN, H. L.: J. Am. Chem. Soc. **74,** 5 (1952)
[30] ZASLOW, B., RUNDLE, R. E.: J. Phys. Chem. **61,** 490 (1957)
[31] KLEBANSKI, A. K., DOROFEENKO, L. P., FIKHTENGOL, V. S., GRIDINA, V. E.: Zh. Obshch. Khim. **43,** (10) 2250 (1973)
[32] TOSHIO TAKIGUCHI, MASARU SAKURAI, TAKESHI KISHI, JUNEI ICHIMURA, YASUCHI IIZIKA: J. Org. Chem. **25,** 310 (1960)
[33] YOUNG, C. W., SERVAIS, PH. C., CURIE, C. C., HUNTER, M. J.: J. Am. Chem. Soc. **70,** 3758 (1948)

Béla CSÁKVÁRI
László FÁBRY
Pál GÖMÖRY
H-1088 Budapest, Múzeum krt. 6—8.

Kálmán UJSZÁSZY; H-1025 Budapest, Pusztaszeri út 57—69.

Acta Chimica Academiae Scientiarum Hungaricae, Tomus 90(3), pp. 255—273 (1976)

NETWORK-THERMODYNAMIC APPROACH TO CHEMICAL KINETICS

D. SINGER

(Computer and Automation Institute, Hungarian Academy of Sciences, Budapest)

Received October 15, 1975

Earlier attempts to describe chemical kinetics in terms of chemical resistances were from a thermodynamic viewpoint not fully adequate. A correct network model of the reaction mechanism must give the same entropy production as the pure thermodynamic theory. It is shown that the entropy production can be interpreted as that of a physical network. In general, this consists of galvanically separated parts belonging to the chemical, transport and thermal processes, respectively. It is shown that the matrix of the phenomenological coefficients of the original system can be interpreted as the loop-impedance matrix of the network. An appropriate network model permits also to separate conceptually the partial processes with and without entropy production, as pointed out by OSTER, DESOER *et al.* Using the loop representation, it is shown how network models of complex chemical reactions with and without reversible reactions can be constructed, including cases where also transport processes are relevant.

Introduction

The theory of physical networks offers some methodological advantages originating from the fact that the problem is divided in the analysis of the topological structure and of the algebraic relations of the system. An extension of physical network theory can be given on the basis of some recent ideas concerning the thermodynamic aspects of the problem [1, 2]. The combination of network and non-equilibrium thermodynamic methods permits to replace the pure kinetic models of reaction mechanisms by dynamic ones giving deeper insight into the behaviour of complicated chemical reaction systems.

Physical networks

Physical network theory is based on the following assumptions.

a) The physical system has a structure representable by a graph.

b) The system can be characterized by some "through" and "across" variables isomorphic with electric current and potential, respetively.

c) "Through" and "across" variables can be related to the branches and nodes of the graph in such a way that Kirchhoff's current law and Kirchhoff's voltage law are valid.

d) There exist real or conceptual discrete elements, whose terminal equations represent the "constitutive" relationships between through and across variables.

Through variables are hydraulic flow, power flow in a frame, heat flow, chemical reaction rate. The appropriate across variable are hydraulic pressure, longitudinal deformation of the frame, temperature, chemical affinity. We denote the generalized through variables, the "generalized flows" and the across variables, the "generalized potentials" by i and e isomorphic with the electric intensity and potential, respectively. Beside i and e also their integrals

$$q(t) = q(o) + \int_0^t i(t)\, \mathrm{d}t \qquad 1)$$

the "generalized charge", and

$$p(t) = p(o) + \int_0^t e(t)\, \mathrm{d}t$$

the "generalized" flux have physical meanings.

The elements of the physical network are:

a) "capacitive" and "inductive" energy stores,

b) dissipative elements (resistors),

c) sources (sinks),

d) transducers.

Capacitive energy stores can be characterized by relationships of the form:

$$q = \Psi(e)$$

$$\frac{\mathrm{d}q}{\mathrm{d}t} = \frac{\mathrm{d}\Psi}{\mathrm{d}e}\frac{\mathrm{d}e}{\mathrm{d}t}\,; \quad C(e)\,\frac{\mathrm{d}e}{\mathrm{d}t} = i \qquad (3)$$

(*cf.* Eg. (1) where $d\Psi/\mathrm{d}e = C(e)$ is, by definition, the generalized capacitance which is not a constant as in the case of simple electric capacitors but a function of e. For an inductive energy store the constitutive relation is

$$p = \Phi(i) \qquad (4$$

$$\frac{\mathrm{d}p}{\mathrm{d}t} = \frac{\mathrm{d}\Phi}{\mathrm{d}i}\frac{\mathrm{d}i}{\mathrm{d}t}\,; \quad L(i)\frac{\mathrm{d}i}{\mathrm{d}t} = e$$

(*cf.* Eq. (2)) where $\mathrm{d}\Phi/\mathrm{d}i = L(i)$ is the generalized inductance.

Dissipative elements can be characterized by the relation

$$e = \Omega(i) \qquad (5)$$

The derivative $d\Omega/di$ is the resistance $R(i)$ of the element. For other generalized network elements, see Refs [3, 4].

Kirchhoff's laws and the constitutive relationships of the elements permit to write the interdependence of network variables and the network equations in different forms according to the need of further use. Applying the tree-technique and matrix notation, this can be made in compact form. A symbolic representation of the relationships of network variables is given

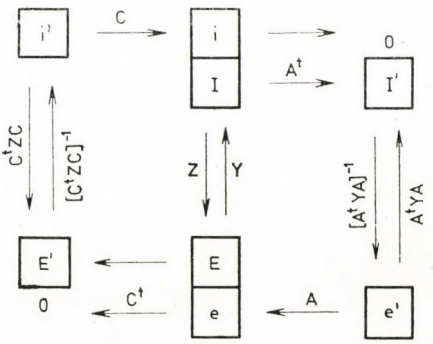

Fig. 1

in Fig. 1 [5, 6]. For the notation, see the list of symbols. **Y** and **Z** are differential operators representing relationships between e and i according to Eqs (3) and (5), (6), respectively. **Y** and **Z** are the primitive admittance and impedance operator matrices of the network, respectively. **A** and **C** are the node and loop incidence matrices characterizing the topology of the network.

The various forms of network equations can be directly obtained from Fig. 1. As can be seen further, for the purpose of analysis of reaction systems, the loop form

$$i' = [\mathbf{C}^t\,\mathbf{ZC}]^{-1}\,\mathbf{C}^t[-\mathbf{ZI}] \tag{6}$$

s the most convenient.

Non-equilibrium thermodynamics and its relation to network theory

The main result of classical thermodynamics is the recognition that spontaneous processes in the nature can take place only if the entropy of the system

$$S = \int \frac{dQ}{T}$$

increases. More precisely, the entropy change S of a system consists of two parts S_e and S_i

$$S = S_e + S_i$$

where S_i can have only positive values, $S_i > 0$. In spite of the entropy production, spontaneous processes are always irreversible.

The development leading to non-equilibrium thermodynamics has made it possible to replace the inequality relations of classical thermodynamics, as the entropy principle mentioned, by equality relations. Introduction of the concept of generalized flows J and generalized forces X permits to express quantitatively the entropy production S_i of the process and to determine its dynamics. Investigations concerning the dependence of flows on forces are therefore one of the main goals of non-equilibrium thermodynamics [7—9].

Generalized flows in non-equilibrium thermodynamics are the amount of internal entropy, energy, mass, mole numbers of chemical components, etc., passing through unit area and unit time in a given direction

$$J_u = \frac{1}{a}\frac{\mathrm{d}u}{\mathrm{d}t}; \; J_s = \frac{1}{a}\frac{\mathrm{d}s}{\mathrm{d}t}; \; J_v = \frac{1}{a}\frac{\mathrm{d}v}{\mathrm{d}t}; \; J_{ni} = \frac{1}{a}\frac{\mathrm{d}n_i}{\mathrm{d}t} \tag{7}$$

where s, u, v and n_i are the entropy, internal energy, volume and mole number of the ith component, respectively. The generalized forces are appropriate potentials μ and their gradients

$$X = -\mathrm{grad}\,\mu \tag{8}$$

Flows and forces are interrelated by relations of the form

$$J = LX \tag{9}$$

where L is a phenomenological coefficient. Flows and forces are generally interrelated. This means that flow J_i is influenced not only by its own force X_i, but also by all others. Instead of a set of independent equations (9), for small deviations the relations

$$\begin{aligned} J_i &= L_{11}X_1 + \ldots + L_{1n}X_n \\ &\ldots\ldots\ldots\ldots\ldots\ldots\ldots \\ J_n &= L_{n1}X_1 + \ldots + L_{nn}X_n \end{aligned} \tag{10}$$

are valid. The coefficient matrix **L** is symmetric (Onsager's principle).

The formal framework of non-equilibrium thermodynamics is based on the assumption that the Gibbs equation of chemical thermodynamics is also valid for non-equilibrium conditions. (This assumption is limited to cases not too far from equilibrium.) Thus

$$T\mathrm{d}s = \mathrm{d}u + P\mathrm{d}v - \sum_{i=1}^{n} \mu_i \,\mathrm{d}n_i \tag{11}$$

where T, P and μ_i are the temperature, pressure and the chemical potentials. By introducing local concentrations

$$s_v = \frac{s}{v}; \; u_v = \frac{u}{v}; \; c_i = \frac{n_i}{v} \tag{12}$$

it can be shown that Eq. (11) is equivalent to the expression

$$T\mathrm{d}s_v = \mathrm{d}q_v - \sum_{i=1}^{n} \mu_i \, \mathrm{d}c_i \tag{13}$$

where $\mathrm{d}q_v$ is the total heat increment per unit volume [8]. Thus for the change of local entropy with time we have

$$\frac{T\partial s_i}{\partial t} \frac{\partial q_v}{\partial t} - \sum_{i=1}^{n} \mu_i \frac{\partial c_i}{\partial t} \tag{14}$$

The derivatives in this expression are closely related to the appropriate thermodynamic flows J_s, J_q and J_i

$$\begin{aligned} \frac{\partial s_v}{\partial t} &= -\operatorname{div} J_s + \sigma \\ \frac{\partial q_v}{\partial t} &= -\operatorname{div} J_q \\ \frac{\partial c_i}{\partial t} &= -\operatorname{div} J_i + \nu_i J_{ch} \end{aligned} \tag{15}$$

The derivatives consist of a divergence and a source term (except for the second, having no source term); σ is the entropy production, $\nu_i J_{ch}$ the concentration change due to the chemical reaction; J_{ch} is the rate of the chemical reaction and ν_i is the stoichiometric number.

Upon inserting Eq. (15) into (14) and making use of the general relation

$$\operatorname{div} ab = \mathrm{q} \operatorname{div} b + b \operatorname{grad} \mathrm{a} \tag{16}$$

after rearrangement, for the local entropy production one obtains

$$\sigma = J_q \operatorname{grad} \frac{1}{T} + \sum_{i=1}^{n} J_i \operatorname{grad} \left(-\frac{\mu_i}{T} \right) + J_{ch} \frac{A_r}{T} \tag{17}$$

where A_r denotes the sum $-\Sigma \nu_i \mu_i$ called the *affinity* of the chemical reaction.

Equation (17) shows that the entropy production is a sum of products of the flows J_k with the conjugated forces X_k

$$\sigma = \sum_k J_k X_k \qquad 18)$$

From Eq. (17) it is obvious that the true thermodynamic driving forces of heat, diffusion and chemical flow are

$$X_q = \text{grad}\,\frac{1}{T}; X_i = \text{grad}\left(-\frac{\mu_i}{T}\right); \; X_{ch} = \frac{A_r}{T} \qquad 19)$$

According to Eq. (10), the flows are functions of the thermodynamic forces. Upon inserting Eq. (10) into (18) and using matrix notation, we get for the entropy production

$$\sigma = X^t \mathbf{L} X \qquad (20)$$

A relation similar to Eq. (20) can be written for a complex system consisting of several systems with entropy production σ_1, $\sigma_2 \ldots \sigma_m$. In this case X and $\mathbf{L}$ are hypervectors and hypermatrices, respectively. For simplicity we assume that interrelations exist only between flows of the *same* type of the individual systems. This means that *e.g.* J_q from the kth system does not *directly* influence J_i from the $(k+1)$th system. In this case $\mathbf{L}$ can be transformed into a diagonal hypermatrix and Eq. (20) can be written in the form

$$\sigma = X_q^t \mathbf{L}_q X_q + X_d^t \mathbf{L}_d X_d + X_{ch}^t \mathbf{L}_{ch} X_{ch} \qquad (21)$$

where X_q, X_d and X_{ch} are vectors of forces conjugated to J_q, J_d and J_{ch}. (The components of the vectors belong to *several* systems.) $\mathbf{L}_q$, $\mathbf{L}_d$ and $\mathbf{L}_{ch}$ are matrices of the appropriate phenomenological coefficients. According to Eq. (10), expression (21) can also be written in the form

$$\sigma = J_q^t \mathbf{L}_q^{-1} J_q + J_d^t \mathbf{L}_d^{-1} J_d + J_{ch}^t \mathbf{L}_{ch}^{-1} J_{ch} \qquad (22)$$

The three terms of Eq. (21) can be considered as contributions of independent subsystems. If the subsystems have defined structures, then they can be characterized by networks having, roughly speaking, the ability to conduct and to store thermodynamic flows. Further, as a consequence of the conservation character of flows and the uniqueness of potentials, Kirchoff's laws are valid. Therefore the terms of Eq. (21) belong to partial networks which model the system considered.

The matrices $\mathbf{L}_q$, $\mathbf{L}_d$, $\mathbf{L}_{ch}$ are nothing else than the loop-impedence matrices of the partial networks, if X and Y are considered as loop quantities [10]. This can be shown in the following manner. The dissipated energy W in a thermodynamic system under isothermal condition is

$$W = T\sigma \tag{23}$$

The dissipated energy due to transport phenomena is

$$W_d = T\sigma_d \tag{24}$$

where σ- is the entropy production of the transport process.

The free energy losses in a single branch of the partial network modelling the transport phenomena are

$$W_d = TX_dJ_d = TL_{pd}^{-1}J_d^2 \tag{25}$$

where L_{pd} is the phenomenological coefficient of the single branch. Therefore, according to strict additivity, for the whole transport network the dissipated energy is

$$W_d = TJ_d^t\,\mathbf{L}_{pd}^{-1}J_d \tag{26}$$

where L_{pd} is the *primitive* admittance matrix of the network. The relation between branch and mesh current i and i' is

$$i = Ci' \tag{27}$$

(see Fig. 1). Upon writing instead of Eq. (27)

$$J_d = CJ_d' \tag{28}$$

and inserting into Eq. (26), one obtains

$$W_d = TJ_d'^t[\mathbf{C}^t\mathbf{L}_{pd}^{-1}\mathbf{C}]\,J' = TJ_d'^t\,\mathbf{Z}_{Ld}\,J_d' \tag{29}$$

where $\mathbf{Z}_{Ld}$ is the loop impedance matrix. Similar expressions can be obtained for the energies W_q and W_{ch} dissipated by the networks of heat and chemical processes.

As a conclusion we can say that the first condition for the validity of the network model is the equality of W's calculated from the original system and the model. The model must further give a right description of the reversible energy transformations in the system and that of the energy losses.

For this purpose the network technique is extraordinarily suitable, especially the loop method permitting an easy separation and localization of dissipative and non-dissipative processes in the system [1].

Network theory and kinetics

For a general chemical reaction

$$\nu_A A + \nu_B B = \ldots \rightleftarrows \nu_M M + \nu_N N + \ldots \tag{30}$$

one can write

$$\mathrm{d}n_A = -\nu_A \mathrm{d}\xi \; ; \; \mathrm{d}n_B = -\nu_B \mathrm{d}\xi \; ; \; \mathrm{d}n_M = \nu_M \mathrm{d}\xi \ldots \tag{31}$$

where A, $B \ldots$ are the masses of the original, and N, M, . . ., those of the product components, respectively, n and μ are the mole and stoichiometric numbers, respectively, μ is the reaction coordinate. The reaction rate w can be defined by any of the relations (31),

$$w = \frac{\mathrm{d}\xi}{\mathrm{d}t} = -\frac{1}{\nu_A}\frac{\mathrm{d}n_A}{\mathrm{d}t} = -\frac{1}{\nu_B}\frac{\mathrm{d}n_B}{\mathrm{d}t} = \frac{1}{\nu_M}\frac{\mathrm{d}n_M}{\mathrm{d}t} \ldots \tag{32}$$

From a kinetic point of view, the necessary condition for the formation of a new species is that collisions between the molecules of the original components occur. The kinetic equation of the reaction has therefore the form

$$w = k_1 c_A^{\nu_A} c_B^{\nu_B} \ldots - k_{-1} c_M^{\nu_M} c_N^{\nu_N} \ldots \tag{33}$$

where k_1 and k_{-1} are the rate constants of the forward and reverse reactions. Generally, higher than ternary collisions are considered as improbable. Real reactions occur, therefore, as consecutive uni-, bi- and trimolecular steps. In reality, complex rection systems are often encountered.

An example of an elementary reaction is the well-known process

$$\mathrm{H_2} + \mathrm{J_2} \rightleftharpoons 2\mathrm{HJ}$$

The overall reaction rate is the difference between the rates in the forward and reverse direction

$$w = w_1 - w_{-1} = \frac{1}{2}\frac{\mathrm{d}c_{HI}}{\mathrm{d}t} = k_1 c_{H2} c_{I2} - k_{-1} c_{HI}^2 \tag{34}$$

Instead of Eq. (24) we may write

$$w = k_1 c_{H2} c_{I2} \left(1 - \frac{k_{-1}}{k_1}\frac{c_{HI}^2}{c_{H2} c_{I2}}\right) \tag{35}$$

According to Eq. (9), (35) can be written in the form

$$J = LX \tag{36}$$

where L and X are

$$L = k_1 c_{H2} c_{I2} \tag{36'}$$

$$X = \left(1 - k_{-1}/k_1 \frac{c_{HI}^2}{c_{H2} c_{I2}}\right) \tag{36''}$$

In the case of ideal gases or dilute solutions, the following relation between thermodynamic potentials of the reaction components and their concentration is valid

$$\mu_k = R_g T \ln c_k + \mu_{ok} \tag{37}$$

μ_{ok} are constants dependent on the temperature. By definition the *affinity* of the rection A_R according to (37) is

$$A_r = -(2\mu_{HI} - \mu_{H2} - \mu_{I2}) = -R_g T \ln \frac{c_{HI}}{c_{H2} c_{I2}} - \\ -(2\mu_{0HI} - \mu_{0H2} - \mu_{0I2}) \tag{38}$$

The constant terms in parentheses can be expressed with the equilibrium constant of the raction K. In equilibrium $A_r = 0$ and therefore

$$2\mu_{0HI} - \mu_{0H2} - \mu_{I2} = -R_g T \ln \frac{c_{HI}^2}{c_{H2} c_{I2}} = -R_g T \ln K \tag{39}$$

substitution into Eq. (38) yields

$$A_r = R_g T \ln \frac{K}{c_{H2}^{-1} c_{I2}^{-1} c_{HI}^2} \tag{40}$$

In the vicinity of the equilibrium it can be assumed that

$$z = \frac{A_r}{RT} \ll 1\,;\; 1 - e^{-z} \simeq z\,;\; \frac{k_{-1}}{k_1} = K \tag{41}$$

According to Eqs (36'') and (40), the driving force of the overall reaction can be written as

$$X = \frac{A_r}{R_g T} \tag{42}$$

Thus according to Eq. (36')

$$w = J_{ch} = \frac{k_1 c_{H2} c_{I2}}{R_g T} A_r$$

Considering now A_r as the true driving force (instead of A_r/R_gT), the phenomenological coefficient, or, in network terminology, the admittance of the reversible reaction will be

$$L = \frac{k_1 c_{H2} c_{I2}}{R_g T} \tag{43}$$

This result can be generalized to any single reversible reaction. The numerator in Eq. (43) is the rate of the *forward* reaction w_1. The admittance of reversible reactions, near equilibrium becomes

$$L = \frac{w_1}{R_g T} \tag{44}$$

According to the foregoing chapter, a simple chemical reactions can be modelled by single loop network. The driving force of the reaction will be equal to the potential drop on a dissipative element (resistor) inserted into the link branch. To each reaction component, there belongs a true branch with a capacitor representing the reversible changes in components energies. As the reaction proceeds, the irreversible energy dissipation will be equal to the difference between the free energy supplied by reversible discharge of the reactant capacitors and that stored by the capacitors of the products. The potentials of the individual capacitors correspond to the chemical potentials of the appropriate components. The flow through the capacitors equals the decrease or increase of component quantities per unit time.

In the case of ideal gases and dilute solutions the capacity modelling of the kth chemical component is, according to Eqs (3) and (37),

$$C_k = \frac{\mathrm{d}\xi}{\mathrm{d}t} \Big/ \frac{\mathrm{d}\mu_k}{\mathrm{d}t} = \frac{\mathrm{d}n_k}{\mathrm{d}\mu_k} \frac{\mathrm{d}c_k}{\mathrm{d}\mu_k} \tag{45}$$

The incremental resistance representing the dissipative process in the link branch is,

$$R = \frac{\mathrm{d}A_r}{\mathrm{d}w} \tag{46}$$

According to Eq. (43), R is not a constant, but a function of the actual reactant concentrations.

Reaction systems

In the case of a complex reaction system, each reaction corresponds to individual loops having some common capacitor branches belonging to common components. The system of reactions

$$\begin{aligned} &\nu_A A + \nu_B B \longrightarrow \nu_C C + \nu_B D \\ &\nu_C C + \nu_E E \longrightarrow \nu_F F \\ &\cdots\cdots\cdots\cdots\cdots\cdots\cdots \\ &\nu_S U + \nu_U V \longrightarrow \nu_Z Z \end{aligned}$$

can be characterized by the matrix of the stoichiometric coefficients

$$\boldsymbol{\nu} = \begin{array}{c} \\ \text{reactions} \end{array} \begin{array}{c} \text{components} \\ \begin{bmatrix} -\nu_A & -\nu_B & \nu_C & \nu_D & & \\ & & -\nu_C & -\nu_E & \nu_F & \\ \cdots & \cdots & \cdots & \cdots & \cdots & \cdots \\ & & & & -\nu_S & -\nu_U & \nu_Z \end{bmatrix} \end{array} \tag{47}$$

The rate of consumption and production of the kth component in all reactions is

$$\sum_i \frac{\mathrm{d}n_k}{\mathrm{d}t} = \sum_i \mu_k J_k \tag{48}$$

Introducing a matrix $\mathbf{C}^t$ of identical structure as (47) with elements 1, −1 and 0, one obtains

$$\begin{array}{c} \\ \text{reactions} \end{array} \begin{array}{c} \text{components} \\ \begin{bmatrix} -1 & -1 & 1 & . & . & & & & & & \\ . & . & -1 & . & -1 & 1 & . & . & . & & \\ . & . & . & . & . & . & . & . & . & & \\ . & . & . & . & . & . & . & . & . & -1 & -1 & 1 \end{bmatrix} \end{array} = \mathbf{C}_T^t \tag{49}$$

Matrix (49) can be interpreted, according to the foregoing considerations, as the tree-component of a loop-matrix belonging to a network with loops modelling the individual reactions of the recation system. The link component of the loop matrix belongs to the branches with "dissipative e ements" of the individual reactions.

Assuming the capacitor potentials to be equal to the chemical potentials, the loop currents will be equal to the reaction rates of the individual reactions. According to the Kirchhoff voltage law, the driving forces of the individual reactions are the appropriate affinites. The affinities are equal to the potential drops across the link resistors modelling the irreversible dissipations. Therefore, for the whole system the affinity is

$$A_r = \nu\mu \tag{50}$$

where A_r and μ are the vector of the affinities and that of the thermodynamic potentials of the individual reactions, respectively.

Relations between reaction rates w and affinities A_r are given by the loop equation of the reaction network (see Fig. 1).

$$w = J_{ch} = [\mathbf{C}^t\,\mathbf{Z}\mathbf{C}]^{-1}\,A_r \tag{51}$$

or in more detail

$$w = \left[\begin{array}{c|c} \mathbf{C}_T^t & \mathbf{U} \end{array}\right] \left[\begin{array}{c|c} \mathbf{Z} & \mathbf{0} \\ \hline \mathbf{0} & \mathbf{R} \end{array}\right] \left[\begin{array}{c} \mathbf{C}_T \\ \hline \mathbf{U} \end{array}\right] A_r \tag{52}$$

where $\mathbf{C}_T$ and $C_L = U$ are the three and link components of $\mathbf{C}$, respectively, $\mathbf{Z}$ is the matrix of the differential operators defined by Eq. (3) (with $e = A_r$, and $i = w$), $\mathbf{R}$ is the matrix of the link resistors. For reaction systems near equilibrium, it can be assumed that $\mathbf{Z}$ and $\mathbf{R}$ are diagonal matrices and the single capacities and resistances are, as in the case of a single reaction

$$C_k = \frac{\mathrm{d}n_k}{\mathrm{d}\mu_k};\quad R_i = \frac{\mathrm{d}A_{ri}}{\mathrm{d}w_i} \tag{53}$$

where k and i are serial numbers of the components and reactions, respectively.

For illustration we shall give the network interpretation of a reaction studied by PRIGOGINE and applied by MARTINEZ for the morphogenesis of some biological structure [1, 12]. The reaction scheme is

$$\begin{aligned} A &\underset{k_{-1}}{\overset{k_1}{\rightleftharpoons}} E \\ 2X + Y &\underset{k_{-2}}{\overset{k_2}{\rightleftharpoons}} 3X \\ B + X &\underset{k_{-3}}{\overset{k_3}{\rightleftharpoons}} Y + D \\ X &\underset{k_{-4}}{\overset{k_4}{\rightleftharpoons}} E \end{aligned} \tag{54}$$

where A, B, D and E are components in constant amounts, and X and Y are intermedials. The overall reaction system is

$$A + B \rightleftarrows E + D$$

The reaction is somewhat unrealistic because it includes also a trimolecular step, but this could be eliminated by a more detailed structure.

The appropriate kinetic equations are

$$\begin{aligned} \frac{dn_X}{dt} &= k_1 n_A = k_2 n_X^2 n_Y - k_3 n_B n_X - k_4 n_X) - \\ &- k_{-1} n_X - k_{-2} n_X^3 + k_{-3} n_Y n_D + k_{-4} n_D \\ \frac{dn_Y}{dt} &= k_3 n_B n_X - k_2 n_X^2 n_Y + k_{-2} n_X^3 - k_{-3} n_Y n_D \end{aligned} \tag{55}$$

Omitting the reverse reactions, the network model in Fig. 2a can be constructed. The appropriate graph is shown in Fig. 2b. The network has 6 capacitor (tree) and 4 resistor (link) branches, as well as 4 independent loops. The loop incidence matrix C is

$$\mathbf{C}^t = \begin{array}{c|cccc} & \multicolumn{4}{c}{\text{reactions}} \\ \text{components} & 1 & 2 & 3 & 4 \\ \hline A & -1 & & & \\ B & & & -1 & \\ D & & & 1 & \\ E & & & & 1 \\ X & 1 & -1 & -1 & -1 \\ Y & & 1 & 1 & \\ \hline R_1 & 1 & & & \\ R_2 & & 1 & & \\ R_3 & & & 1 & \\ R_4 & & & & 1 \end{array} \begin{array}{l} \left.\vphantom{\begin{array}{c}1\\1\\1\\1\\1\\1\end{array}}\right\} \mathbf{C}_t \\ \left.\vphantom{\begin{array}{c}1\\1\\1\\1\end{array}}\right\} \mathbf{C}_L = U \end{array} \tag{56}$$

As can be seen, instead of the second reaction in (54),

$$2X + Y \longrightarrow 3X \tag{57}$$

the network models, the net reaction

$$Y \longrightarrow X \tag{58}$$

This is admissible because the differences between (57) and (58) are *not* in the topology, *but* in the *order* of the reaction. In our network-thermodynamic treatment, the kinetic notion "reaction order" is concealed in the expression of the component capacities and of the reaction resistances.

The loop equation of reaction system (54) can be written according to Eq. (52). For the numerical integration of these equations, it is convenient to use a special network-analysis program.

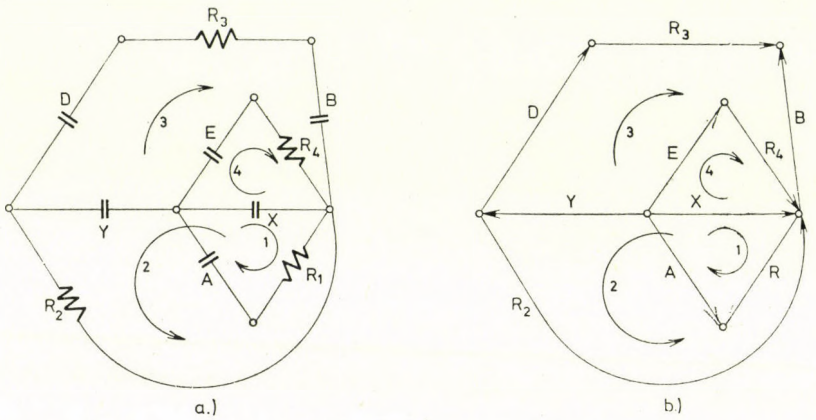

Fig. 2

Reversible reactions

In the foregoing, reaction system (54) was treated as unidirectional. If we consider also the reverse reaction, the system can be written in the form

$$\begin{aligned} A &\longrightarrow X \\ X &\longrightarrow A \\ 2X + Y &\longrightarrow 3X \\ 3X &\longrightarrow 2X + Y \\ B + X &\longrightarrow Y + D \\ Y + D &\longrightarrow B + X \\ X &\longrightarrow E \\ E &\longrightarrow X \end{aligned} \tag{59}$$

This is formally a unidirectional system which can be treated by the network model in a similar manner as in the foregoing example. Each reaction

of Eq. (59) represents a loop, with the same capacitive elements, but because of the different rates of the forward and reverse reactions, the link resistors R_i and R_{-i} are different — The loop incidence matrix of the network is

$$\mathbf{C} = \begin{array}{c|cccccccc} & \multicolumn{8}{c}{\text{reactions}} \\ \text{components} & 1 & 2 & 3 & 4 & 5 & 6 & 7 & 8 \\ \hline A & -1 & -1 & & & & & & \\ B & & & & & -1 & -1 & & \\ D & & & & & 1 & 1 & & \\ E & & & & & & & 1 & 1 \\ X & 1 & 1 & -1 & -1 & -1 & -1 & -1 & -1 \\ Y & & & 1 & 1 & 1 & 1 & & \\ \hline R_1 & 1 & & & & & & & \\ R_{-1} & & 1 & & & & & & \\ R_2 & & & 1 & & & & & \\ R_{-2} & & & & 1 & & & & \\ R_3 & & & & & 1 & & & \\ R_{-3} & & & & & & 1 & & \\ R_4 & & & & & & & 1 & \\ R_{-4} & & & & & & & & 1 \end{array} \quad \begin{array}{l} \} \mathbf{C}_T \\ \\ \\ \\ \\ \\ \} \mathbf{C}_L = U \\ \\ \\ \\ \\ \\ \\ \end{array} \tag{60}$$

The appropriate network is shown in Fig. 3.

To avoid short circuits between resistors belonging to the forward and reverse reactions, the link branches contain ideal diodes. Diodes allow

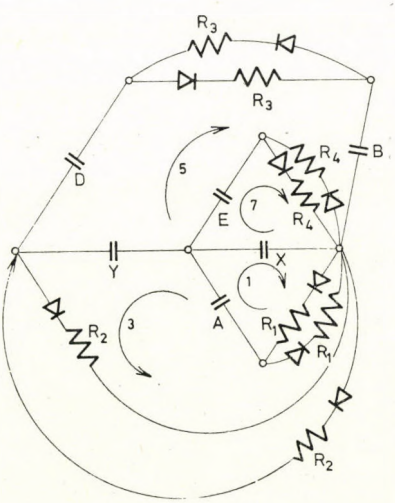

Fig. 3

only flows in one direction, thus the chemical flow can pass only in the loop direction as in the case of unidirectional reactions. In this manner also the network model of the reversible reaction can be tretaed numerically by network analysis programs.

Reaction-diffusion systems

In most cases the behaviour in time of the reaction system is determined by elementary diffusion processes. This is always the case if the transport velocity is of the same order as, or less than, the chemical reaction rate. We consider a one-dimensional idealized case in Fig. 4.

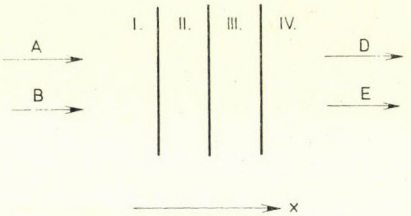

Fig. 4

The reaction components are transported from compartment I (surroundings) into reaction zone II and from here into reaction zone III. Finally the end-product is conveyed to compartment IV.

We consider again the reaction scheme in (54) and assume that only the forward reactions take place. Assuming further that all transport rates are significantly greater than those of the chemical reaction (except for the transport rate of component X between zones II and III) the kinetic equations of the system will be

$$\frac{\partial n_X}{\partial t} = k_1 n_A + k_2 n_X^2 n_Y - k_3 n_B n_X - k_4 n_X + D_X \frac{\partial^2 n_X}{\partial x^2}$$

$$\frac{\partial n_Y}{\partial t} = k_3 n_B n_X - k_2 n_X^2 n_Y \tag{61}$$

For simplicity the transport direction was identified with the x axis. D_X is the diffusion coefficient of component X. Assuming that the diffusional flows between zones II and III are stationary, we may write

$$D_X \frac{\partial^2 n_X}{\partial x^2} k_X (n_{X(II)} - n_{X(III)}) \tag{62}$$

where $n_{X(II)}$ and $n_{X(III)}$ of X are moles in zones II and III, respectively. Thus, instead of Eq. (61),

$$\begin{aligned} \frac{dn_X}{dt} &= k_1 n_A + k_2 n_X^2 n_Y - k_3 n_B n_X + k_X n_{X(II)} - k_X n_{X(III)} \\ \frac{dn_Y}{dt} &= k_3 n_B n_X - k_2 n_X^2 n_Y \end{aligned} \tag{63}$$

Formally, $n_{X(II)}$ and $X_{(III)}$ can be considered as the amounts of two *different* components, *viz.* of X_{II} and X_{III}. In other words, the rate of transport of X and Y from compartment II to III can be regarded as the rate of isomorphus change

$$X_{II} \xrightarrow{k_X} X_{III}$$

Equation (63) can therefore be treated in first approach as a kinetic equation *without* a diffusion component. The scheme of the reaction system will be:

$$\begin{aligned} A &\xrightarrow{k_1} X_{III} \\ X_{II} &\xrightarrow{k_X} X_{III} \\ 2X_{III} + Y &\xrightarrow{k_2} 3X_{III} \\ B + X_{III} &\xrightarrow{k_3} Y + D \\ X_{III} &\xrightarrow{k_4} E \end{aligned} \tag{64}$$

The network model of reaction system (64) constructed according to the method mentioned above is shown in Fig. 5.

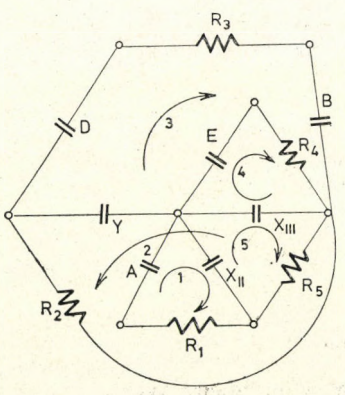

Fig. 5

REFERENCES

[1] OSTER, G. F., DESOER, C. A.: J. Theor. Biol., **32**, 219–241 (1971)
[2] OSTER, G., PERELSON, A., KATCHALSKY, A.: Nature, **234** (1971)
[3] DESOER, G. A., KUH, E.: Basic Circuit Theory. McGraw-Hill, New York 1969
[4] KOENIG, H., TOKAD, Y., KESAVAN, H.: Analysis of Discrete Physical Systems. McGraw-Hill, New York 1969
[5] ROTH, J. P.: Quart. Appl. Math., **17**, 1 (1959)
[6] BRANIN, F. H.: Proc. Symp. Generalized Networks, 453. Polytechnic Press, New York 1966
[7] DE GROOT, S. R., MAZUR, P.: Non-equilibrium Thermodynamics. North-Holland Publ. Co., Amsterdam 1962
[8] KATCHALSKY, A., CURRAN, P. F.: Non-equilibrium Thermodynamics in Biophysics. Harvard Univ. Press, Cambridge 1965
[9] MEIXNER, I.: Proc. Symp. Generalized Networks, p. 13. Polytechnic Press, New York 1966
[10] SINGER, D.: D. Sc. Thesis, Budapest 1973
[11] GLANSDORFF, P., PRIGOGINE, I.: Thermodynamic Theory of Structure, Stability and Fluctuations. J. Wiley-Interscience, London 1971
[12] MARTINEZ, H. M.: J. Theor. Bull., **36**, 479 (1972)

List of symbols

a	area
$\mathbf{A}$	branch node incidence matrix
A_r	affinity of a chemical reaction
c_k	concentration of chemical component k
$\mathbf{C}$	loop incidence matrix
$C(e)$	generalized capacitance
D	diffusion coefficient
e	branch 'across' variable; electric branch potential loop
e'	node 'across' variable; electric node potential
E	branch source 'across' variable; electric branch source potential
E'	loop 'across' variable; electric loop potential
F	free energy
i	branch 'through' variable; electric branch current
i'	loop 'through' variable; electric loop current
I	branch 'through' source; electric branch source current
I'	node 'through' source; electric node source current
J	thermodynamic flow
k	reaction rate constant
K	chemical equilibrium constant
$L(i)$	generalized inductance
L_i	phenomenological coefficient of species i
n_i	number of moles of species i
p	generalized flux
P	pressure
q	generalized charge
Q, q	heat quantity
R	generalized resistance
R_g	universal gas constant
S, s	entropy
t	time
T	temperature
u	internal energy
U	unit matrix
v	volume
w	chemical reaction rate
W	dissipated energy
Z	differential operator of impedance type
X	thermodynamic force

Y	differential operator of admittance type
μ	thermodynamic potential
ν	stoichiometric coefficient
σ	entropy production
ξ	reaction coordinate

D. SINGER, H–1021 Budapest, Nyéki u. 9.

Acta Chimica Academiae Scientiarum Hungaricae, Tomus 90(3), pp. 275—285 (1976)

SYNTHESIS AND STUDY OF MONOSUBSTITUTED α-FORMYLACETIC ESTERS AND MALONDIALDEHYDES

G. Dörnyei, M. Bárczai-Beke, B. Majoros, P. Sohár* and Cs. Szántay

(Department of Organic Chemistry, Technical University Budapest)

(Research Institute for Pharmaceutical Chemistry, Budapest)*

Received April 12, 1975

A new method has been developed for the synthesis of monosubstituted α-formylacetic esters (**4**) and malondialdehydes (**5**), by the selective lithium aluminium hydride reduction of the appropriately substituted malonic ester derivative (**3**). The solvent-dependent tautomerism of these compounds has been investigated by means of ^{1}H-NMR spectroscopy and the presence of the (E)-enol ester form (**4c**) was detected for the first time.

Previously we reported the stereoselective total synthesis of (—)-corynantheidine (**1**) [1], a representative of alkaloids having indolo (2,3-a) quinolizidine skeleton; as a model compound, dimethoxydespyrrolo-corynantheidine (**2**) was also prepared [2]. In synthesizing these compounds, the α-formylacetic ester group, or the tautomeric β-hydroxyacrylic ester function, was developed by means of a new method not reported up to then in the literature.

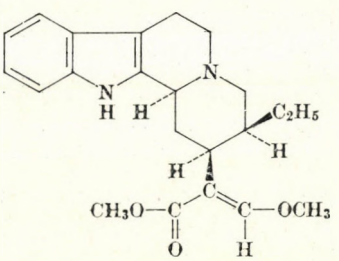

1

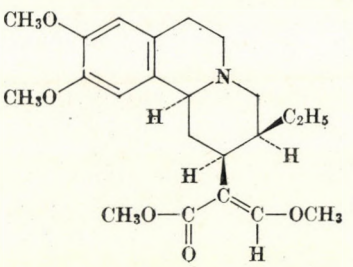

2

The appropriate malonic ester derivative (**3a, b**) was partially reduced in absolute ether at —70°C, with a calculated amount of lithium aluminium hydride, stopping at the malonaldehyde ester (**4a, b**) stage.

Since substituted α-formyl esters are reactive bifunctional compounds and thus eminently suitable for the synthesis of many non-cyclic, cyclic and heterocyclic compounds, we have investigated whether the reduction **3** → **4** is a general reaction, or practicable only in the case of compounds **3a, b**, owing to some special structural factor.

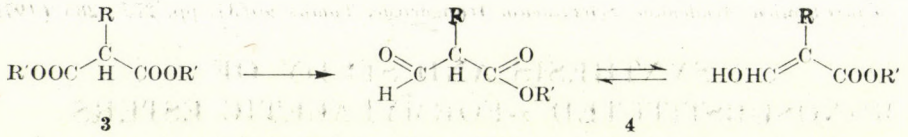

3 4

3, 4	R	R′
a	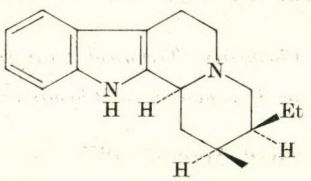	$-CH_3$
b	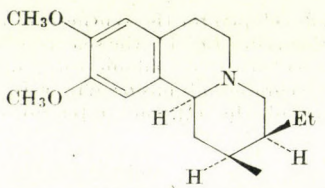	$-CH_3$
c	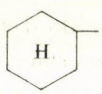	$-CH_3$
d	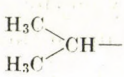	$-CH_3$
e	CH_3-CH_2-	$-C_2H_5$

It has been found that the reaction is generally applicable for the synthesis of α-formylacetic esters, and by optimization of the reaction conditions, we obtained the appropriate α-formylacetic esters (**4c—e**) from cyclohexyl-, isopropyl- and ethylmalonic esters (**3c—e**) in about 60—69% yields. Thus for the preparation of compounds of type **4**, a new procedure has been developed, which is often more convenient and gives better yields, than the methods [3, 4, 5, 7] used so far.

The tautomeric equilibria [7] of compounds **4c—e** were investigated in different solvents by means of ^1H—NMR [6] and IR spectroscopy. In accordance with the results of JOFFE *et al.* [6, 7], we observed that nonpolar solvents, in general, favour the presence of the (Z)-enolic form (*B*), whereas in more polar solvents the ratio of the oxo-form (*A*) gradually increases. Using solvents prone to form intermolecular hydrogen bonds, and depending on the nature of group R, we succeeded for the first time in detecting also the (E)-enolic form (*C*) in the equilibrium mixture.

Table I

Solvent-dependent ^{1}H-NMR spectra of 4c-e *(δ ppm)*

Solvent		*A*			*B*		*C*		Isomeric ratio A : B : C
		$-C\overset{O}{\underset{H}{<}}$	μ C–H		=CH	–OH	=CH	–OH	
CCl_4	**4c**	9.5 d J=4	2.88 J=4	2×d J=8	6.85d J=13	11.30d J=13	—	—	2 : 3 : 0
	4d	9.7 d J=4	2.98 J=8	2×d J=4	7.08d J=13	11.55d J=13	—	—	3 : 2 : 0
	4e	9.05d J=2.5	3.00 J_d=2	2×t Jt=7	6.68d J=12	10.6 d J=12	—	—	1 : 1 : 0
$CDCl_3$	**4c**	9.74d J=4	3.05 J=4	2×d J=8	7.03d J=13	11.5 d J=13	—	—	2 : 1 : 0
	4d	9.75d J=4	3.65 J=8	2×d J=4	7.12d J=13	11.6 d J=13	—	—	3 : 2 : 0
	4e	9.75d J=2.5	3.15 J_d=2.5	2×t Jt=7	7.0 d J=12	10.9 d J=12	—	—	3 : 2 : 0
CD_3CN	**4e**	9.6 d J=2	3.24 J_d=2	2×t Jt=7	7.05 d J=12	11.3 d J=12	—	—	4 : 3 : 0
$(CD_3)_2CO$	**4d**	9.72d J=4	3.12 J=8	2×d J=4	7.23d J=13	11.6 d J=13	—	—	3 : 1 : 0
	4e	9.65d J=2	3.30 J_d=2	2×t Jt=7	7.1 d J=12	11.37d J=12	~7.1s	~7.7s	4 : 3 : 1
CF_3COOH	**4e**	~9.7s	3.45 J_d=3	2×t Jt=7	Only the quantity of the form *A* is measurable, but from the intensity of the μH signal the combined ratio of *B* and *C* estimated to be 40%.				
$(CD_3)_2SO$	**4c**	9.80d J=3	3.20 J=3	2×d J=8	8.40s	10.48s diff.	—	—	2 : 3 : 0
	4d	9.78d J=4	3.23 J=8	2×d J=4	7.25d J=13	11.48d J=13	7.65s	10.4 s	2 : 2 : 3
	4e	9.65d J=2			7.12d J=12	11.25d J=12	7.6 s	~10.25s	1 : 5 : 10
$(CD_3)_2SO$ + D_2O	**4e**	9.65s	3.2 J_d=2	2×t Jt=6	7.12s	— —	7.6 s	—	1 : 2 : 7

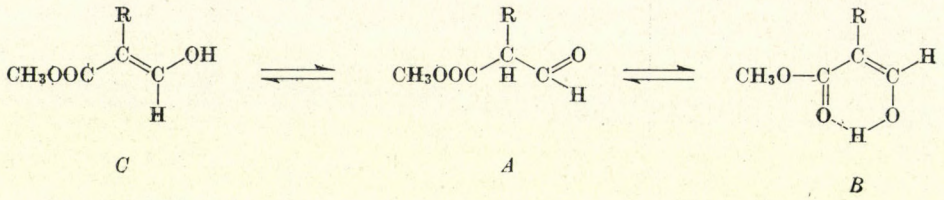

C *A* *B*

4

The experiences obtained for the tautomeric equilibria of compounds **4c—e** are summarized in Table I.

As seen from Table I, in the case of the cyclohexyl derivative (**4c**), the (*Z*)-enolic form (*B*) is in equilibrium with the oxo-form (*A*) in the different solvents, and the ratio of the oxo-form increases with the solvent polarity.

The results of the solvent dependent ^{1}H—NMR investigation of the isopropyl- aldehyde ester derivative (**4d**) are in good agreement with the data reported by other authors (6a, 7]; like in the case of compound **4c**, the *A* : *B* ratio increases in function of the polarity of the solvent. In the ^{1}H—NMR spectrum of the compound in DMSO-d_6 as solvent, which has not been investigated up to now, the (E)-enol ester form (*C*) was also detected. Similarly, in compound **4e** the signal of the (E)-enol form (*C*) equally appears in acetone-d_6, TFA or DMSO-d_6. When D_2O is added to the DMSO-d_6 solution, the ratio of the (E)-enol form (*C*) increases as expected, in the other solvents, however, only the (Z)-enol (*B*) and aldehyde (*A*) forms appear in the equilibrium mixture.

Assigment of the signals to the various tautomeric forms is facilitated by the appearance in some cases of all the three tautomeric forms. As an example, the ^{1}H-NMR spectrum of ethylmalonaldehyde ester (**4e**) in DMSO-d_6 is given (Fig. 1).

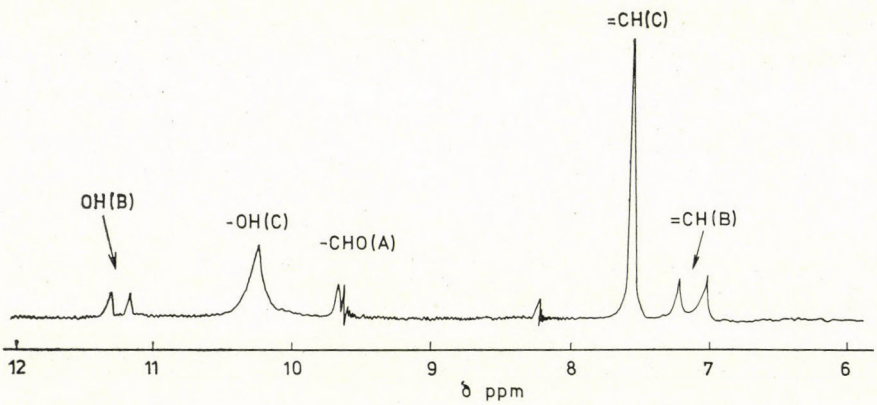

Fig. 1

The chemical shifts of the olefinic protons present in the tautomers (Z) and (E), as well as the differences in the shifts are in accordance with the data in the literature [8]. The assignment of the signals to the appropriate tautomeric forms is also facilitated by the fact that — owing to the rapid proton exchange — no splitting is caused by the spin–spin interaction of the olefinic and enolic hydroxyl protons in the more acidic (E)-enol form (*C*), whereas the coupling constant of these protons can be measured in the (Z)-enolic form (*B*) having a chelate ring.

Based on the study of the tautomeric equilibria of the above monosubstituted malonaldehyde esters, it is assumed, that the tautomeric equilibrium is influenced by the relative bulk of the nonpolar part (R) of the molecule too. The solvation of the molecule in polar solvents is promoted by the decrease of the bulk of the nonpolar moiety, thus giving rise to an increase in the ratio of the more polar forms (*trans* enolic and oxo forms). This assumption is substantiated by the increase of the quantity of the (E)-enolic form (*C*), found in a given solvent, according to the following order: **4c** → **4d** → **4e** (R = cyclohexyl → isopropyl → ethyl).

In the course of the lithium aluminium hydride reduction of malonic ester derivatives, described previously, the malondialdehyde derivative is a by-product, which can be readily separated by chromatography. When the ratio of the reducing agent is higher, the yield of malondialdehyde may come up to 54—57%; this method is therefore suitable for the synthesis of malondialdehydes (**5c**—**e**), which are also valuable compounds in organic preparative work.

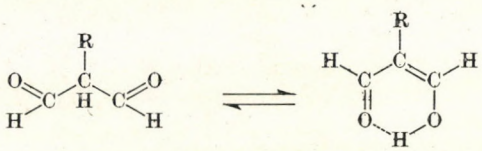

5c—e

5	R
c	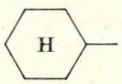
d	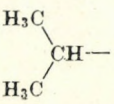
e	$CH_3—CH_2—$

It is of interest to mention that in the course of the synthesis of (—)-corynantheidine (**1***) and dimethoxydespyrrolo-corynantheidine (**2**), the methylation of the sodium salt of the enol esters **3a** and **3b** with an equivalent amount of dimethyl sulfate in benzene was a most highly stereoselective reaction, *i.e.* only *trans*[$CH_3O/COOCH_3$]-β-methoxyacrylic ester derivatives with E-geometry (**1** and **2**) were formed. In contrast, similar methylation of the sodium compounds of **4c—e** yielded the isomers (Z)-**6c—e** and (E)-**6c—e** in a ratio of ~1 : 1.

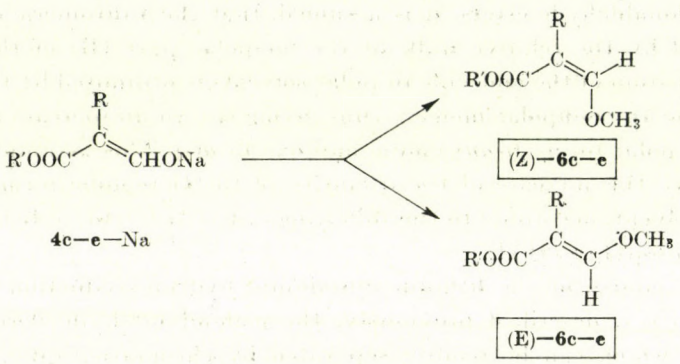

4, 6	R	R'
c		—CH_3
d		—CH_3
e	CH_3—CH_2—	CH_3—CH_2—

Isomers (E) and (Z) are readily separated by chromatography, and their steric structures can be unambiguously established on the basis of their ^{1}H—NMR data [6c, 9]. The ratio of the isomers remains constant throughout the reaction (TLC). The thermoanalytical investigation (DSC) of compound **6e** has shown that below 160°C, no transisomerization takes place either with the pure E or the Z geometric isomer.

The difference found in stereoselectivity in the course of the methylation of the desmethyl derivatives of indolo(2,3-a)quinolizidine (**4a**) and benzo(a)-quinolizidine (**4b**) and of compound **4c—e** is probably due to electronic and steric reasons. Investigation of the mechanism of the methylation reaction is in progress.

Experimental

The IR spectra were recorded with a Perkin-Elmer 211 and 457, as well as a Spectromom 2000 spectrophotometer; the ^{1}H-NMR spectra were taken with a Perkin-Elmer R12 (60 Mc) and JEOL C 60 HL instrument; for obtaining the mass spectra a MS 902 (70 eV) spectrometer was used.

The ^{1}H-NMR spectra were recorded at room temperature, with TMS internal standard; the chemical shifts (δ) are given in ppm. The thermoanalytical (DSC) investigations, as well as the melting point determinations of the alkali metal salts were made on a Perkin-Elmer DSC 1B instrument.

Qualitative TLC was effected on layers of 0.25 mm of inactive Kieselgel GF_{254} (Merck) on 4×7.5 cm plates. The spots were visualized by means of iodine, iron(III) chloride, or using a Desaga-Univ UV lamp (254 and 366 nm). The relative R_f values are given. Column chromatography was achieved on hundred-fold amounts of silicagel (0.05—0.2 mm; Merck). The developing solvent systems were: *A* $CHCl_3$–CH_3OH 25 : 1; *B* CH_2Cl_2–CH_3OH 100 : 1; *C* $CHCl_3$–CH_3OH 50 : 1; *D* $CH_3COOC_2H_5$–*n*-hexane 1:10.

1. Synthesis of monosubstituted α-formylacetic esters

1.1. (±)-α-*Formylcyclohexylacetic acid methyl ester* (**4c**)

Cyclohexylmalonic acid dimethyl ester (**3c**) (20 mmoles; 4.3 g) was dissolved in freshly dried ether (80 ml) in a flask which had been carefully dried in a nitrogen or argon atmosphere. The solution was cooled to —70°C and 1.75 equivalent of lithium aluminium hydride in ether (0.24 mmole/ml; 37 ml = 8.75 mmoles) was added drop by drop with stirring, during 50 min. After stirring at —70°C for 20 min, the reaction mixture was decomposed by the cautious addition of saturated aqueous sodium sulfate solution (16 ml), while maintaining the same temperature. After careful shaking, the mixture was let to stand in a refrigerator overnight. Next day the ether layer was decanted and the aqueous slurry cautiously washed with three portions of ether. After filtration the combined ether phases were extracted with 2*N* NaOH solution (3×50 ml). According to TLC, the residual ether solution contained unchanged diester (**3c**). The ether part was washed with saturated NaCl solution until neutral, dried ($MgSO_4$), and evaporated to dryness in vacuum (1.67 g; 38.9%).

The alkaline solution was neutralized with 2*N* HCl while cooling with ice. A white precipitate separated. The neutral aqueous suspension was extracted with $CHCl_3$ (4×26 ml), the combined chloroform solutions washed with saturated sodium chloride solution, dried ($MgSO_4$), and evaporated in vacuum. As shown by TLC, the extract contained the aldehyde ester (**4c**), as well as a small amount of cyclohexylmalondialdehyde (**5c**) as an impurity. The oil obtained was purified from the small amount of dialdehyde by means of column chromatography (System A). TLC (System A): **3c**, $R_f = 0.9$; **4c**, $R_f = 0.7$; **5c**, $R_f = 0.42$. The phases containing the aldehyde ester **4c** were evaporated again to dryness. The yield was 1.54 g, *i.e.* 69% estimated on the non-recovered diester (**3c**). It should be mentioned that additional malondialdehyde (**5c**) was obtainable by acidifying the aqueous phase (*cf.* Paragraph 2.1).

IR (CCl_4): 1740, 1720, 1670, (ν C=O), 1610 cm^{-1} (ν C=C).

^{1}H-NMR: *cf.* Table I.

MS (*m/e*, %): 184 (M^+, 8), 156 (32), 153 (9), 125 (7), 124 (7), 123 (15), 113 (37), 103 (81), 95 (19), 90 (12), 83 (71), 82 (48), 81 (29), 75 (35), 74 (100), 71 (32), 67 (58), 55 (74), 43 (30), 41 (55), 39 (23).

$C_{10}H_{16}O_3$. Calcd. mol. wt. 184.1099. Found mol. wt. 184.1098 (MS).

2,4-Dinitrophenylhydrazone of **4c**: m. p. 150—151°C (from methanol).

Calcd. C 52.70; H 5.49; N 15.58. Found C 52.96; H 5.57; N 15.64%.

IR (KBr): 1740 (ν C=O), 1620 cm^{-1} (ν C=N).

1.2. (±)-α-*Formyl-β-methylbutyric acid methyl ester* (**4d**)

The reduction was effected as described in 1.1, using isopropylmalonic ester (**3d**) as the starting material. 33% of the starting diester (**3d**) was recovered. The yield of aldehyde ester **4d**, estimated on the non-recovered diester, was 66%. TLC (System A): **3d**, $R_f = 0.9$; **4d**, $R_f = 0.75$; **5d**, $R_f = 0.4$. The chromatogram on the column was developed with chloroform.

IR (CCl_4): 1750, 1735, 1720, 1660 (ν C=O), 1605 cm^{-1} (ν C=C).

^{1}H-NMR: *cf.* Table I.

MS (*m/e*, %): 144 (M^+, 7), 129 (14), 116 (26), 113 (30), 101 (100), 97 (39), 84 (15), 83 (11), 71 (51), 69 (88), 44 (26), 43 (42), 41 (58), 39 (27).

$C_7H_{12}O_3$. Calcd. mol. wt. 144.0786. Found mol. wt. 144.0804 (MS).

1.3. (±)-α-*Formylbutyric acid ethyl ester* (**4e**)

The reduction was effected as described in 1.1, but at −45°C, using ethylmalonic ester (**3e**) as the starting material. The yield of the recovered diester (**3e**) was 31.5%. The ethylmalondialdehyde (**5e**), formed as a by-product, was separated from the aldehyde ester (**4e**) by means of column chromatography. TLC (System C): **3e**, $R_f = 0.9$; **4e**, $R_f = 0.75$; **5e**, $R_f = 0.45$. IR (film): 1735, 1720, 1680 (ν C=O), 1610 cm^{-1} (ν C=C).

^{1}H-NMR: *cf.* Table I.

MS (*m/e*, %): 144 (M^+ 10), 129 (8), 116 (33), 101 (33), 99 (44), 98 (11), 97 (4), 73 (73), 70 (60), 59 (29), 57 (100).

$C_7H_{12}O_3$. Calcd. mol. wt. 144.0786. Found mol. wt. 144.0804 (MS).

2,4-Dinitrophenylhydrazone of **4e**: m. p. 111°C (from ethyl acetate).

Calcd. C 48.14; H 4.79; N 17.27. Found C 48.13; H 4.89; N 17.11%.

IR (KBr): 1730 (ν C=O), 1615 cm^{-1} (ν C=N).

2. Synthesis of monosubstituted malondialdehydes

2.1. *Cyclohexylmalondialdehyde* (**5c**)

As described in 1.1, cyclohexylmalonic acid dimethyl ester (**3c**) (4.3 g; 20 mmoles) was reduced with 2.25 equivalent of lithium aluminium hydride (11.25 mmoles) to yield cyclohexylmalondialdehyde (**5c**) as the main product. The decomposed reaction mixture was extracted with ether and the aqueous phase acidified with 5*N* HCl. The acidic solution was extracted with $CHCl_3$ (4×25 ml). The combined organic phases were washed with saturated NaCl solution until neutral, dried, and evaporated to dryness in vacuum. The residual oil contained a small amount of aldehyde ester (**4c**) impurity. The components were separated by means of column chromatography (System A). The combined fractions containing dialdehyde **5c** were evaporated to dryness in vacuum (1.06 g; 54%). The product was purified by means of vacuum sublimation (0.5 Hgmm, 60°C); m. p. 119—120°C (lit. [11] m. p. 119—121°C).

IR and ^{1}H-NMR: *cf.* Ref. [11].

MS (*m/e*; %): 154 (M^+, 100), 136 (67), 135 (13), 125 (13), 121 (20), 111 (19), 108 (81), 107 (85), 79 (90), 67 (73), 57 (52), 55 (71), 41 (71), 39 (48).

$C_9H_{11}O_2$. Calcd. mol. wt. 154.0994. Found mol. wt. 154.0984 (MS).

2,4-Dinitrophenylhydrazone of **5c**: m. p. 176—179°C (from ethyl acetate).

Calcd. C 58.40; H 3.27; N 16.51. Found C 58.52; H 3.54; N 16.60%.

IR (KBr): 3400 (ν NH), 1620 cm^{-1} (ν C=N).

2.2. *Isopropylmalondialdehyde* (**5d**)

The preparation of compound **5d** was effected as described in 2.1. The yield was 55%, m. p. 62—63°C (lit. [10] m. p. 62°C).

3. Synthesis of 2-substituted-3-methoxyacrylic acid esters [(E)- and (Z)-6c—e]

3.1. 2-*Cyclohexyl*-3-*methoxyacrylic acid methyl ester* [*(E)- and (Z)*-**6c**]

An equivalent amount of 1*N* $NaOCH_3$ in methanol was added to the α-formyl ester **4c** (0.92; 5 mmoles) in abs. benzene (10 ml), under nitrogen atmosphere during magnetic stirring. A precipitate separated in about 10 min. After an hour the solution was evaporated to dryness. The residual solid was digerated with ether and filtered off (1.0 g; 97%); m. p. 163.2°C.

IR (KBr): 1670 (ν C=O), 1610 cm^{-1} (ν C=C).

To a suspension of the sodium compound (**4c**) (0.206 g; 1.0 mmole) in abs. benzene an equivalent amount of dimethyl sulfate in benzene was added, during magnetic stirring under nitrogen atmosphere, at room temperature. After stirring for 6 hrs at room temperature the suspension, which first cleared up, then contained a white precipitate, was extracted with 2*N* NaOH solution (3×25 ml). The benzene phase was washed to neutral with saturated NaCl solution, dried ($MgSO_4$), and evaporated to dryness in vacuum. The residual oil contained two components. (System B: $R_f = 0.8$ for isomer E, and $R_f = 0.6$ for isomer Z.)

The isomers and the starting sodium compound (**4c**) can be well separated in System D, therefore the reaction can be followed by means of TLC (compound **4c** and sodium salt of **4c**: $R_f = 0.65$; (E)-**6c**: $R_f = 0.45$; (Z)-**6c**: $R_f = 0.2$). The oil of two components contained 58% and 42% of the enolic ethers having *trans-* and *cis* geometry, respectively. The two components were separated by means of column chromatography (System *B*).

MS (Z)-**6c**: 198 (M^+, 38), 183 (16), 167 (28), 166 (31), 139 (51), 111 (36), 95 (30), 83 (100).
(E)-**6c**: 198 (M^+, 46), 183 (37), 167 (34), 166 (48), 139 (65), 111 (40), 95 (100), 83 (95).
$C_{11}H_{18}O_3$. Calcd. mol. wt. 198.1256. Found mol. wt. 198.1256.
IR (film) (Z)-**6c**: 1700 (ν C=O), 1640 cm^{-1} (ν C=C)
(E)-**6c**: 1715 (ν C=O), 1635 cm^{-1} (ν C=C).
IR ($CHCl_3$) (Z)-**6c**: 1690 (ν C=O), 1640 cm^{-1} (ν C=C).
(E)-**6c**: 1690 (ν C=O), 1640 cm^{-1} (ν C=C).
^{1}H-NMR (CCl_4) (Z)-**6c**: C=CH 6.25 ppm; (E)-**6c**: C=CH 7.05 ppm.

3.2. 2-*Isopropyl*-3-*methoxyacrylic acid methyl ester* [*(E)- and (Z)*-**6d**]

The preparation of the enolic ester was effected as in 3.1. The yield was 68%. The oil consisted of two components, the (E)-enolic ether (58%) and (Z)-enolic ether (42%). TLC (System B): (E)-**6d**, $R_f = 0.8$; (Z)-**6d**, $R_f = 0.55$; System D: **4d** and sodium salt of **4d**, $R_f = 0.6$; (Z)-**6d**, $R_f = 0.2$ (E)-**6d**, $R_f = 0.45$.

MS (*m/e*, %) (Z)-**6d**: 158 (M^+, 28), 143 (45), 129 (7), 127 (45), 126 (12, 111 (64), 99 (44), 85 (14), 83 (16), 75 (100) 59 (15).
(E)-**6d**: 158 (M^+, 31), 143 (55), 129 (5), 127 (33), 126 (14), 111 (67), 99 (50), 85 (12), 83 (11), 75 (100), 59 (17).
$C_8H_{14}O_3$. Calcd. mol. wt. 158.0943. Found mol. wt. 158. 0950 (MS).
IR (KBr) (Z)-**6d**: 1700(ν C=O), 1640 cm^{-1} (ν C=C)
(E)-**6d**: 1700 (ν C=O), 1635 cm^{-1} (ν C=C)
^{1}H-NMR (CCl_4):

	CH_3	CH	OCH_3	=CH
(Z)-**6d**	1.05 d $J = 7$	2.62 sp	3.70 s 3.73 s	6.25 d $J = 1$
(E)-**6d**	1.10 d $J = 7$	2.95 sp	3.68 s 3.80 s	7.10 s

3.3. 2-*Ethyl*-3-*methoxyacrylic acid ethyl ester* [*(E)- and (Z)*-**6e**]

The sodium salt of **4e** was prepared as described in 3.1 (95%); m. p. 299.4°C.
IR (KBr) 1660 cm^{-1} (ν C=C).

According to the method described in 3.1, the enol ethers (Z)- and -E)-**6e** were prepared in a yield of 62%. According to the TLC investigations (System B: (E)-**6e**: $R_f = 0.85$; (Z)-**6e**, $R_f = 0.65$; System D: **4e** and sodium salt of **4e**, $R_f = 0.7$; (Z)-**6e**, $R_f = 0.2$; (E)-**6e**, $R_f = 0.5$) the product contained 45% and 55% of the enol ethers with (Z) and (E) geometry, respectively.

MS (*m/e*, %): (Z)-**6e**, 158 (M^+, 22), 143 (15), 129 (34), 127 (3), 115 (18), 113 (100), 97 (52), 89 (9), 85 (34), 83 (23), 75 (87).
(E)-**6e**, 158 (M^+, 30), 143 (24), 129 (43), 127 (6), 115 (27), 113 (100), 97 (66), 89 (9), 85 (46), 83 (30), 75 (69).
$C_8H_{14}O_3$. Calcd. mol. wt. 158.0943. Found mol. wt. 158.0952 (MS).
IR (film): (Z)-**6e** 1690 (ν C=O), 1640 cm^{-1} (ν C=C)
IR (film): (E)-**6e** 1700 (ν C=O), 1640 cm^{-1} (ν C=C).
IR ($CHCl_3$): (Z)-**6e** 1690 (ν C=O), 1635 cm^{-1} (ν C=C)
IR ($CHCl_3$): (E)-**6e** 1690 (ν C=O), 1635 cm^{-1} (ν C=C).
^{1}H-NMR (CCl_4):

	$C-CH_2-CH_3$	$O-CH_2-CH_3$	$C-CH_2-CH_3$	$O-CH_2-CH_3$	OCH_3	$=CH$
(Z)-**6e**	1.03 t	1.30 t	2.15 qa	4.22 qa	3.80 s	6.40 s
(E)-**6e**	0.96 t	1.25 t	2.22 qa	4.12 qa	3.78 s	7.20 s

Every coupling constant was 7 cps

*

The authors are thankful to Dr. J. TAMÁS for recording and evaluating the mass spectra, to (Mrs.) Dr. B. LENGYEL for the thermoanalytical investigations, and to Mrs. S. KRAKOVICZER for her precious technical assistance.

REFERENCES

[1] SZÁNTAY, Cs., BÁRCZAI-BEKE, M.: Tetrahedron Letters **1968,** 1405; Chem. Ber. **102,** 3963 (1969); Magyar Kém. Foly. **77,** 160 (1971)
[2] BÁRCZAI-BEKE, M., DÖRNYEI, G., TAMÁS, J., SZÁNTAY, Cs.: Chem. Ber. **105,** 3244 (1972); Magyar Kém. Foly. **79,** 4 (1973)
[3] HOUBEN-WEYL: Methoden der Organischen Chemie, IV. Ed. Vol. 7/1; (a) p. 44; (b) p. 61; (c) p. 55
[4] STEENBERGEN, G. F.: U. S. Pat. 3,658,883 (1972)
[5] MYAZAKI, M.: Yakugaku Zasshi **77,** 415 (1957); C. A. **51,** 12068 (1957)
[6] (a) JOFFE, S. T., PETROVSKII, P. V., GORGUNOV, E. I., ERSHOVA, T. V., KABACHNIK, M. I.: Tetrahedron **28,** 2783 (1972)
(b) JOFFE, S. T., VATSURO, K. V., PETROVSKII, P. V., FEDIN, E. I., KABACHNIK, M. I.: Izvest. Akad. Nauk SSSR, Ser. Khim. **1960,** 1650; **1970,** 1504.
(c) JOFFE, S. T., FEDIN, E. I., PETROVSKII, P. V., KABACHNIK, M. I.: Tetrahedron Letters **1966,** 2661
(d) JOFFE, S. T., VATSURO, K. V., PETROVSKII, P. V., KABACHNIK, M. I.: Izvest. Akad. Nauk SSSR, Ser. Khim. **1971,** 731
(e) KOL'TSOV, A. I., KHEIFETS, G. M.: Usp. Khim. **40,** 1646 (1971)
[7] NIERLICH, F., POLANSKY, O. E.: Monatshefte, **99,** 1351 (1968)
[8] NOI, R. S., ERSHOV, B. A., KOL'TSOV, A. I.: Zh. Org. Khim. **9,** 426 (1973)
[9] (a) EISTERT, B., ARNDT, F., LOEWE, L., AYCA, E.: Chem. Ber. **84,** 156 (1951)
(b) WINTERFELDT, E., PREUSS, H.: Chem. Ber. **99,** 450 (1966)
(c) LEGUAN, R. M., SIMONNIN, M. P.: Bull. Soc. Chim. France **1970,** 4419
(d) EFFENBERGER, F., HARUNAUN, W.: Chem. Ber. **102,** 3260 (1969)
[10] ARNOLD, Z., SORM, F.: Chem. listy **51,** 1082 (1957)
[11] FERWANAK, A., PRESSLER, W., REICHARDT, C.: Tetrahedron Letters **1973,** 3979

Gábor DÖRNYEI
Marietta BÁRCZAI-BEKE
Béla MAJOROS
Csaba SZÁNTAY
} H-1111 Budapest, Gellért tér 4.
Pál SOHÁR; H-1045 Budapest, Szabadságharcosok útja 47/49.

Acta Chimica Academiae Scientiarum Hungaricae, Tomus 90(3), pp. 285–299 (1976)

CONDENSED *as*-TRIAZINES, I

SYNTHESIS OF 3-SUBSTITUTED PYRIDO[3,4-e]-*as*-TRIAZINES

P. BENKÓ, A. MESSMER,* A. GELLÉRI* and L. PALLOS

(EGyT Pharmacochemical Works, Budapest, and

** Central Research Institute for Chemistry of the Hungarian Academy of Sciences, Budapest)*

Received July 7, 1975

The Bischler method for synthetizing benzo-*as*-triazines [6] has been extended to pyrido[3,4-e]-*as*-triazines. The starting material, 4-chloro-3-nitropyridine is converted with acylhydrazines into 4-acylhydrazino-3-nitropyridines, which yield dihydropyrido[3,4-e]-*as*-triazines on reduction and subsequent cyclodehydration of the resulting amino compounds. The aromatic end-products are obtained after a final oxidation step.

Recently, several papers [1–5] have dealt with the chemistry of *as*-triazines condensed with various heterocyclic ring structures. The synthesis methods employed in constructing the condensed *as*-triazine skeletons can usually be regarded as modifications of one of the following three fundamental methods.

(*a*) *Bischler reaction* [6], which is essentially an acid-catalyzed cyclodehydration taking place between an amino group and acylhydrazino group attached to the aromatic skeleton in *ortho* position:

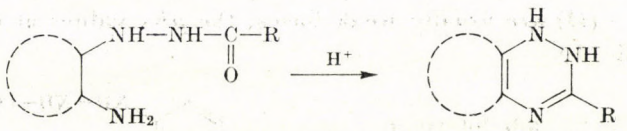

(*b*) *Arndt synthesis* [7], consisting in the alkali-catalyzed reaction of *o*-nitrophenylguanidines:

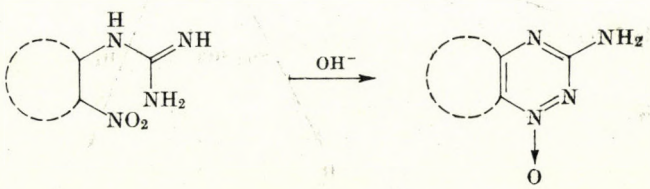

(*c*) *Method of reductive cyclization* [8], which yields the *as*-triazine ring through intramolecular condensation of amino compounds obtained by the reduction of imino ethers carrying a nitro group in *ortho* position:

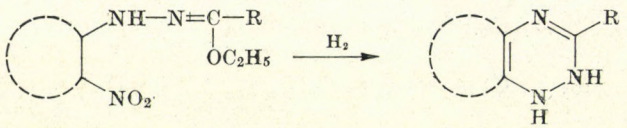

In the present work, the applicability of these synthesis methods to nitrogen-containing heterocyclic compounds has been investigated. In this paper, the preparation of pyrido [3,4-e]-*as*-triazine derivatives by the Bischler method is described. POLYA and SHANKS [9] have prepared a single dihydro derivative of pyrido[3,4-e]-*as*-triazine isomer, but the final aromatization step was not solved.

In the reaction of 4-chloro-3-nitropyridine (**Ia**) with acylhydrazines, hydrochlorides of acylhydrazino-nitropyridines (**II**) were obtained in 80—90% yield. The reaction of 4-hydrazino-3-nitropyridine and the appropriate acid chlorides also yielded the intermediates **II**.

In a modification of the procedure, an acid-binding agent was also employed in the above-mentioned reactions, however, the yield was then usually lower.

In the reaction which proved to be the most favourable, the starting material was 4-methoxy-3-nitropyridine (**Ib**) or its salt; the intermediates **II** were obtained under well controlled conditions in 80—90% yield.

The chemical properties of these compounds correspond to those expected in view of their structures. Thus, for example, 4-*o*- and *p*-hydroxybenzoyl-hydrazino-3-nitropyridine (**IIk** and **IIl**), as well as 4-isonicotinoyl-hydrazino-3-nitropyridine (**IIr**) show reversible acid-base indicator properties. When dissolved in bases, the colour is deep blue, while in acids it is pale yellow. The transition colour is brick red in the pH range 5.5—6.5. The 4-acylhydrazino-3-nitropyridines (**II**) are usually weak bases, the pK_b values at the *isoelectric* point being 8.5—10.

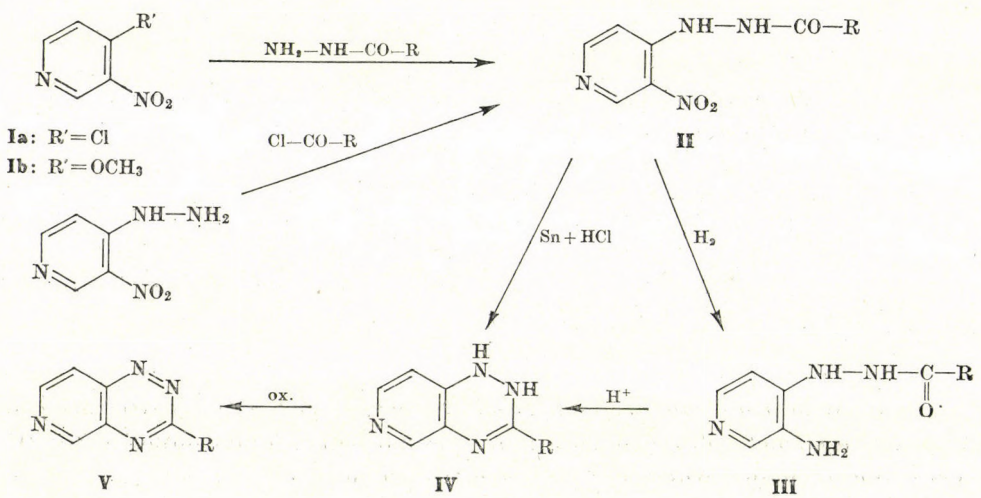

In the subsequent reaction step, the 4-acylhydrazino-3-amino compounds (**III**) are usually obtained in higher yield and purity, when the bases **II** are reduced by catalytic hydrogenation, and the amino compounds (**III**) are isolated as salts. It has been found that the 3-amino-4-acylhydrazinopyridine bases are rather unstable compounds, sensitive to air and sometimes also to light. Thus their purification is often impossible. An interesting exception is the group of 4-benzoylhydrazino-3-nitropyridines carrying alkoxy substituents (**IIm, n, o**); these are stable and can be crystallized without decomposition.

In the essential cyclization step, the 1,2-dihydropyrido[3,4-e]-*as*-triazines (**IV**) can be prepared by acid-catalyzed dehydration of the appropriate precursors (**III**). In the shortened variation of the cyclization step, the nitro compounds (**II**) are reduced with stannous chloride in concentrated hydrochloric acid. This latter procedure is less favourable, since the intermediate dihydro-*as*-triazines give tin complexes which must be decomposed in alkaline medium resulting in a low — usually about 50% — yield. Further, the dihydro compounds (**IV**) are preferably aromatized immediately, in order to avoid the formation of oxidative by-products appearing in a larger amount in alkaline medium.

Dihydropyrido[3,4-e]-*as*-triazines (**IV**) are stable in the salt form only, otherwise they undergo oxidation under the effect of atmospheric oxygen rather rapidly, even in the solid state. This tendency to aromatization is the highest in the case of the non-substituted substance (**IVa**): it transforms into the aromatic product (**Va**) during 1—2 hrs in the solid state and within minutes when in solution. The tendency to oxidation is significant in the case of the C-3-alkyl derivatives, too (**IVb**—f), while the hydrochloride of 3-phenyl-1,2-dihydropyrido[3,4-e]-*as*-triazine, in the solid state undergoes hydrolysis and aromatization only when stored at 25°C for 3 months.

The aromatic end-products **V** can be obtained by the oxidation of the dihydro compounds **IV**. This reaction can be accomplished by means of atmospheric oxygen, or with potassium ferricyanide in alkaline medium, or in a solution of ferric chloride providing acidic medium. The products are very weak bases, they form salts with acids, but also these undergo hydrolysis very rapidly.

In view of the present studies, aromatization can be accomplished easily and in high yield in the case of these compounds. The assumption forwarded by POLYA and SHANKS that — like in 1,2-dihydropyrimido [5,4-e]-*as*-triazines — the formation of the corresponding aromatic product cannot be expected in this group of compounds, proved to be faulty.

Acta Chim. (Budapest) 90, 1976

Table I

4-Acylhydrazino-3-nitropyridines **(II)**

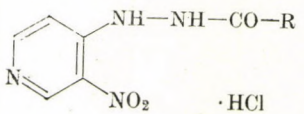

	R	Method	Yield, %	M. p., °C	Solvent	Formula (M.W.)	Analysis Calculated/Found C	H	N	Cl
a	H	A	54	204—205*	MeCN	$C_6H_6N_4O_3$ (182.15)	39.58 40.25	3.20 3.02	30.75 30.46	—
b	methyl	B	92	274—275	EtOH	$C_7H_9ClN_4O_3$ (232.64)	36.10 36.19	3.90 3.79	24.10 24.16	15.25 15.47
c	octyl	C	79	188—189	EtOH	$C_{14}H_{23}ClN_4O_3$ (330.83)	50.80 50.70	7.03 7.00	16.95 16.79	10.38 10.19
d	nonyl	B	54	119—120*	EtOH	$C_{15}H_{24}N_4O_3$ (308.38)	58.40 58.62	7.84 7.69	18.18 18.11	—
e	undecyl	B	76	180—181	EtOH	$C_{17}H_{29}ClN_4O_3$ (372.91)	58.40 54.75	7.82 7.80	15.05 15.08	9.52 9.49
f	tridecyl	B	67	211—212*	EtOH	$C_{19}H_{32}N_4O_3$ (364.50)	64.25 64.20	8.84 8.90	15.38 15.40	—
g	phenyl	C	89	266—267	EtOH	$C_{12}H_{11}ClN_4O_3$ (294.71)	48.70 48.66	3.76 3.80	19.00 18.85	12.03 12.15

h	benzyl	C	90	229—230	EtOH	$C_{13}H_{13}ClN_4O_3$ (308.73)	50.55 50.59	4.23 4.30	18.15 18.23	11.50 11.52
i	2-phenylethyl	C	92	244—245	Me-cello-solve	$C_{14}H_{15}ClN_4O_3$ (322.76)	52.15 52.10	4.72 4.70	17.30 17.19	10.09 10.15
k	*o*-hydroxyphenyl	B	95	279—280	EtOH	$C_{12}H_{11}ClN_4O_4$ (310.71)	46.42 46.11	3.57 3.49	18.05 17.95	11.45 11.37
l	*p*-hydroxyphenyl	C	84	280—281	EtOH	$C_{12}H_{11}ClN_4O_4$ (310.71)	46.42 46.28	3.57 3.48	18.05 18.00	11.46 11.25
m	*p*-anisyl	C	89	280—281	EtOH	$C_{13}H_{13}ClN_4O_4$ (342.74)	48.15 48.00	3.76 3.70	17.25 17.40	10.91 10.70
n	3,5-dimethoxyphenyl	B	88	252—253	i-PrOH	$C_{14}H_{15}ClN_4O_5$ (354.83)	47.40 47.74	4.28 4.26	15.82 15.73	10.00 9.98
o	3,4,5-trimethoxyphenyl	C	97	240—241	EtOH	$C_{15}H_{17}ClN_4O_6$ (384.78)	46.70 46.21	4.44 4.43	14.55 14.45	9.22 9.17
p	2-hydroxy-3-naphthyl	B	89	261—262*	DMF	$C_{16}H_{12}N_4O_4$ (324.31)	59.25 59.20	3.73 3.39	17.29 17.19	— —
r	4-pyridyl	C	91	272—273	EtOH	$C_{11}H_{10}ClN_5O_3$ (209.69)	44.70 44.59	3.66 3.62	23.65 23.60	12.00 11.91

* Base

Experimental

The IR spectra were recorded in KBr pellets with a UR-10 spectrophotometer, and UV spectra with a UNICAM SP 800 spectrophotometer. M.p.'s (measured in capillaries) are uncorrected.

4-Acylhydrazino-3-nitropyridines (II)

Method A

4-Hydrazino-3-nitropyridine (0.015 mole) was dissolved in 96—100% acylating agent (aliphatic carboxylic acid, acid anhydride, or acid halide) (10—15 ml) applying slight heating when necessary. The solution was allowed to stand for 24 hrs, and evaporated to dryness. The residue was suspended in water and neutralized with potassium carbonate. The precipitate was filtered off and crystallized.

Method B

4-Methoxy-3-nitropyridine (**Ib**) (0.1 mole) or its hydrochloride was refluxed together with the appropriate acid hydrazide (0.1 mole) in ethanol (250—350 ml) for 3—5 hrs. The precipitate formed was crystallized after filtration and drying. The base was liberated from the hydrochloride of the product with sodium carbonate.

Method C

4-Chloro-3-nitropyridine (**Ia**) (0.02 mole) and the appropriate acid hydrazide (0.02 mole) were allowed to react in anhydrous ethanol (80—150 ml). Evolution of some heat could be observed after the addition of the chloronitropyridine. The evolution of reaction heat ceased after stirring for 4—6 hrs. The precipitate was filtered off or, if it did not separate spontaneously, the solution was evaporated to dryness and the residue crystallized.

4-Acylhydrazino-3-aminopyridines (III)

4-Acylhydrazino-3-nitropyridine (0.067 mole) was dissolved in ethanol (or isopropanol or methanol) (800 ml). (When the substance was insoluble, hydrogenation could also be accomplished in suspension.) The solution was shaken in hydrogen atmosphere in the presence of Pd/C catalyst (1 g) until the calculated amount of hydrogen (5.3 litres) had been absorbed. When a solution was obtained, the catalyst was filtered off and the solvent removed by evaporation; in the other case, the suspension was heated to 50—60°C before filtering off the catalyst. The precipitate that separated on cooling was filtered off, or the product was obtained by evaporating the solution.

1,2-Dihydropyrido[3,4-e]-as-triazines (IV)

3-(o-Hydroxyphenyl)-1,2-dihydropyrido[3,4-e]-as-triazine (IVk)

4-(*o*-Hydroxybenzoylhydrazino)-3-aminopyridine hydrochloride (4.3 g; 0.015 mole) was refluxed in isopropanol containing three equivalents of hydrochloric acid (100 ml) for 1.5 hrs. When boiling starts, bright red crystals appear (2.8 g; 69.3%), m.p. 298—299°C from DMF.

$C_{12}H_{11}ClN_4O$ (262.71). Calcd. C 54.75; H 4.22; Cl 13.51; N 21.27. Found C 54.69; H 4.20; Cl 13.44; N 21.17%.

UV (EtOH): λ_{max} nm (log ε): 260 (5.43), 323 (4.95).

3-Phenyl-1,2-dihydropyrido[3,4-e]-as-triazine hydrochloride (IVg) [9]

3-Amino-4-benzoylhydrazinopyridine (**III g**) (3.3 g; 0.015 mole) was refluxed in 10% hydrochloric acid-ethanol (300 ml) for 1 hr. The deep red solution was clarified while hot, and filtered. After cooling, brick red plates (3.2 g; 89.6%) were obtained, m.p. 229—230°C (from water).

$C_{12}H_{11}Cl_4 \cdot 2H_2O$ (282.74). Calcd. C 50.85; H 3.92; Cl 12.55; N 19.85. Found C 50.70; H 3.89; Cl 12.54; N 19.94%.

The base liberated from its salt had m.p. 120—121°C; brown, cotton-like crystals.

$C_{12}H_{10}N_4$ (210.24). Calcd. C 68.65; H 5.13; N 26.70. Found C 68.62; H 5.10; N 26.59%.

UV (0.1*N* HCl): λ_{max} (nm log ε): 226 (4.18), 257 (4.11), 400 (2.79).

Table II

Spectral data of 4-acylhydrazino-3-nitropyridines **(II)**

	R	UVmax. nm (log ε)	solvent	IR (KBr), cm^{-1}
b	methyl	350 (3.54) 264 (4.03) 231 (4.23)	0.1*N* HCl	3200—3300 (aromatic CH) 1620—1640 (amide I) 1530, 1260 (NO_2)
c	octyl	350 (3.61)	EtOH	3290, 3240, 1655 (amide) 2850, 2900, 1480 (methylene) 1530, 1260 (NO_2)
d	nonyl	336 (3.60) 260 (4.10)	EtOH	3350, 3250, 1655 (amide) 1530, 1265 (nitro)
e	undecyl	342 (3.58) 227 (4.23)	EtOH	3350, 3290, 1650 (amide) 1540, 1265 (nitro)
f	tridecyl	327 (3.57) 259 (4.06) 225 (4.23)	0.1*N* HCl	
g	phenyl	330 (3.63) 266 (4.16)	0.1*N* HCl	
h	benzyl	352 (3.56) 232 (4.25)	EtOH	1365, 1550 (NO_2) 3300—3000 (aromatic CH) 2950 (methylene)
i	2-phenylethyl	350 (3.58) 234 (4.19)	EtOH	1570, 1380 (NO_2)
k	*o*-hydroxyphenyl	306 (3.83) 265 (4.17) 233 (4.33)	0.1*N* HCl	3300—2700 (NH) 1640 (CO) 1570, 1350 (NO_2)
l	*p*-hydroxyphenyl	327 (3.61) 270 (4.34) 234 (4.26)	0.1*N* HCl	3350, 1650 (OH) 3200—2800, 1620 (amide) 1580, 1380 (NO_2)
m	*p*-anisyl	349 (4.45) 260 (4.46) 237 (4.45)	i-PrOH	3350, 3150, 1660 (amide) 2845 (methoxy) 1370, 1535 (nitro)
n	3,5-dimethoxyphenyl	327 (3.74) 258 (4.23)	EtOH	3355, 3200, 1660 (amide) 2850 (methoxy) 1370, 1540 (nitro)
o	3,4,5-trimethoxy-phenyl	345 (3.75) 260 (4.20)	EtOH	3300—2400 (NH) 2845 (methoxy) 1370, 1540 (nitro) 1650 (CO)

Acta Chim. (Budapest) 90, 1976

Table III

4-Acylhydrazino-3-aminopyridines **(III)**

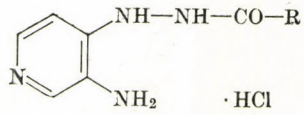

	R	Yield, %	M. p., °C	Solvent	Formula (M. W.)	Analysis Calculated/Found C	H	N	Cl
a	H	92	265—266	MeOH	$C_6H_{10}Cl_2N_4O$ (225.09)	32.05 32.00	4.7 4.75	24.90 25.23	31.55 31.58
b	methyl	86	286—287	EtOH	$C_7H_{11}ClN_4O$ (202.66)	41.60 41.46	5.48 5.45	27.70 27.55	17.50 17.44
c	octyl	56	217—218	EtOH	$C_{14}H_{25}ClN_4O$ (300.84)	55.95 55.70	8.39 8.30	18.65 18.42	11.82 11.71
d	nonyl	97	186—187	EtOH	$C_{15}H_{27}ClN_4O$ (314.87)	57.25 57.10	8.64 8.49	17.80 17.49	11.25 11.02
	undecyl	86	210—211	EtOH	$C_{17}H_{31}ClN_4O$ (342.93)	59.40 59.53	9.12 9.15	16.35 16.30	10.35 10.19
g	phenyl	78	252—253	i-PrOH	$C_{12}H_{13}ClN_4O$ (264.72)	54.30 54.68	4.94 5.00	21.15 21.02	13.41 13.40
h	benzyl	88	208—209	EtOH	$C_{13}H_{15}ClN_4O$ (278.75)	55.40 55.41	5.42 5.39	20.10 20.03	12.73 12.70

i	2-phenylethyl	74	176—177	EtOH	$C_{14}H_{17}ClN_4O$ (292.78)	57.45 57.40	5.92 5.79	19.25 19.31	12.15 12.05
k	*o*-hydroxyphenyl	94	223—224	EtOH	$C_{12}H_{13}ClN_4O_2$ (280.72)	51.40 51.35	4.67 4.63	20.00 20.05	12.70 12.65
l	*p*-hydroxyphenyl	54	250—251	EtOH	$C_{12}H_{13}ClN_4O_2$ (280.72)	51.40 51.29	4.67 4.62	20.00 19.97	12.70 12.63
n	3,5-dimethoxyphenyl	79	280—281	DMF	$C_{14}H_{17}ClN_4O_3$ (324.78)	51.70 51.49	5.32 5.30	17.25 17.38	10.92 10.79
o	3,4,5-trimethoxyphenyl	84	265—266	DMF	$C_{15}H_{19}ClN_4O_4$ (354.80)	50.70 50.70	5.38 5.28	15.77 15.70	9.99 9.92
r	4-pyridyl	58	233—234	EtOH	$C_{11}H_{12}ClN_5O$ (265.72)	49.70 49.19	4.56 4.48	26.35 26.35	13.35 13.25

Table IV

Spectral data of 4-acylhydrazino-3-aminopyridines (III)

	R	UV max. nm (log ε)	Solvent	IR (KBr), cm^{-1}
c	octyl	415 (3.20) 340 (3.50) 247 (4.25)	EtOH	3400, 3250 (NH) 1640 (CO) 2900, 2820, 1460 (methylene)
e	undecyl	445 (3.14) 340 (3.59)	EtOH	
g	phenyl	350 (3.62) 232 (4.34)	EtOH	3400, 3300, 1625 (NH) 1640 (CO)
h	benzyl	450 (4.03) 339 (3.45) 245 (4.26)	EtOH	3400—3200 (NH- and NH_2) 1620 (CO) 2920 (methylene)
i	2-phenylethyl	280 (3.73) 228 (4.04)	0.1*N* HCl	
k	*o*-hydroxyphenyl	311 (4.14) 233 (4.39)	EtOH	3400—3300, 2700—2300 (OH, NH) 1650 (OH def.), 1620 (CO)
n	3,5-dimethoxyphenyl	290 (4.03) 249 (4.28)	0.1*N* HCl	
o	3,4,5-trimethoxyphenyl	455 (3.10) 258 (4.21)	0.1*N* HCl	3350, 1630 (NH_2), 1640 (CO), 2960, 2860, 1460, 1125, 900 (trimethoxyphenyl)

Pyrido[3,4-e]-as-triazines (V)

Method A

Pyrido[3,4-e]-as-triazine (Va) [2]

IVa (5.1 g; 0.03 mole) was dissolved in water (120 ml) and the solution was basified (pH 9) with ammonium hydroxide; a solution of potassium ferricyanide (19.8 g; 0.06 mole) in water (120 ml) was then added and the mixture kept at 4—8°C for 30 min. The solution was subjected to continuous extraction with chloroform (1.2 l) for 5 hrs. The $CHCl_3$ extract was dried over Na_2SO_4, filtered and evaporated to dryness, to obtain brick-red crystals (3.5 g; 88.3%), m.p. 90—91°C.

$C_6H_4N_4$ (132.13). Calcd. C 54.60; H 3.05; N 42.40; Found C 54.54; H 3.00; N 42.35%.

UV (EtOH): λ_{max} nm (log ε): 225 (4.29); 332 (3.42), 475 (2.37).

Method B

3-Methylpyrido[3,4-e]-as-triazine (Vb)

The nitro compound **IIb** (13.9 g; 0.06 mole) was refluxed with granulated tin (39 g) in 18% hydrochloric acid (225 ml) for 1 hr. The metal which remained was removed by filtration and the solution was cooled to obtain a yellow precipitate. This was filtered off (17.4 g; m.p. 193—195°C) and dissolved in saturated sodium carbonate solution (70 ml) without previous drying. The solution became dark-coloured on heating. The solid particles were removed by filtration, and the solution was continuously extracted with chloroform for 78 hrs. The solvent was evaporated and the product crystallized from ethanol to obtain bright crystals (1 g; 11.9%), m.p. 115—116°C.

Table V

1,2-Dihydropyrido[3,4-e]-as-triazines (IV)

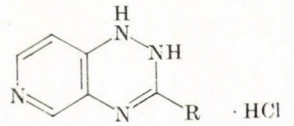

	R	Yield, %	M. p., °C	Solvent	Formula (M. W.)	Analysis Calculated/Found C	H	N	Cl
a	H	76	238—240	EtOAc	$C_6H_7ClN_4$ (170.61)	42.20 42.25	4.16 4.13	20.85 20.77	32.80 32.69
b	methyl	63	296	EtOH	$C_7H_9ClN_4$ (184.64)	45.62 45.48	4.90 4.84	30.35 29.98	19.15 19.05
h	benzyl	89	278—280	EtOH	$C_{13}H_{13}ClN_4$ (260.73)	59.95 59.29	5.04 5.00	21.55 21.41	13.65 13.49
k	*o*-hydroxyphenyl	69	298—299	DMF	$C_{12}H_{11}ClN_4O$ (262.71)	54.75 54.69	4.22 4.20	21.27 21.17	13.51 13.44
l	*p*-hydroxyphenyl	92	317—318*	DMF	$C_{12}H_{12}Cl_2N_4O$ (299.218)	48.20 48.10	4.04 4.00	18.75 18.68	23.70 23.32
n	3,5-dimethoxyphenyl	86	272—273	i-PrOH	$C_{14}H_{15}ClN_4O_2$ (306.76)	54.70 54.59	4.92 4.90	18.25 18.40	11.55 11.43
o	3,4,5-trimethoxyphenyl	98	266—267	H_2O	$C_{15}H_{17}ClN_4O_3$ (336.79)	53.40 53.35	5.08 5.06	16.65 16.69	10.06 10.00
p	2-hydroxy-3-naphthyl	97	246—247	i-PrOH	$C_{16}H_{13}ClN_4O$ (312.77)	61.20 61.07	4.18 4.12	17.90 17.71	11.35 11.10
r	4-pyridyl	95	287—288**	DMF	$C_{11}H_{12}Cl_3N_5$ (320.62)	41.25 41.30	3.78 3.69	21.92 22.00	33.10 33.35

* dihydrochloride
** trihidrocchloride

Acta Chim. (Budapest) 90, 1976

Table VI

3-substituted pyrido[3,4-e]-as-triazines

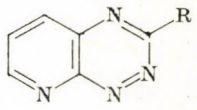

	R	Method	Yield, %	M. p., °C	Solvent	Formula (M.W.)	Analysis Calculated/Found C	H	N
c	octyl	B	50	46—47	EtOH	$C_{14}H_{20}N_4$ (244.35)	68.80 68.49	8.26 8.19	22.95 22.90
d	nonyl	B	65	45—46	EtOH	$C_{15}H_{24}N_4$ (260.38)	69.20 69.03	9.30 10.09	21.50 21.25
f	tridecyl	B	62	65—66	EtOH	$C_{19}H_{30}N_4$ (314.48)	72.50 72.45	9.59 9.50	17.82 17.75
g	phenyl	A	96	127—128	EtOH	$C_{12}H_8N_4$ (208.23)	69.20 69.14	3.87 3.86	26.85 26.99
h	benzyl	A	89	167—168	EtOH	$C_{13}H_{10}N_4$ (222.26)	70.20 70.00	4.54 4.50	25.25 25.12
i	2-phenylethyl	B	52	76—77	EtOH	$C_{14}H_{12}N_4$ (236.28)	71.20 71.05	5.12 5.06	23.72 23.64
k	*o*-hydroxyphenyl	A	95	182—183	EtOH	$C_{12}H_8N_4O$ (224.23)	64.25 64.20	3.58 3.52	25.00 24.97
l	*p*-hydroxyphenyl	A	92	288—289	EtOH	$C_{12}H_8N_4O$ (224.23)	64.25 64.25	3.58 3.68	25.00 24.98

m	*p*-anisyl	B	58	198—199	$CHCl_3$	$C_{13}H_{10}N_4O$ (238.25)	65.40 65.21	4.23 4.45	23.52 23.39
n	3,5-dimethoxyphenyl	A	93	158—159	DMF	$C_{14}H_{12}N_4O_2$ (268.28)	62.60 62.45	4.47 4.40	20.85 20.60
o	3,4,5-trimethoxyphenyl	A	68	204—205	$CHCl_3$	$C_{15}H_{14}N_4O_3$ (298.31)	60.30 60.52	4.73 4.75	18.80 18.71
p	2-hydroxy-3-naphthyl	A	38	256—257	DMF	$C_{16}H_{10}N_4O$ (274.29)	70.00 69.55	3.67 3.90	20.45 20.23
r	4-pyridyl	A	44	169—170	$CHCl_3$	$C_{11}H_7N_5$ (210.09)	62.80 62.70	3.36 3.29	33.85 33.19

Table VII

*Spectral data of 3-substituted pyrido[3,4-e]-as-triazines**

	R	UV max. nm (log ε)	IR (KBr), cm^{-1}
a	H	475 (2.37); 332 (3.43); 226 (4.29)	3030, 3060, 3080 (aromatic CH) 1600, 1560, 1520, 1450 (aromatic skeletal vibrations)
b	methyl	475 (2.38); 342 (4.30); 230 (5.10)	3040, 3060 (aromatic CH) 2960 (methyl); 1620, 1525, 1440 (aromatic skeletal vibrations)
c	octyl	341 (3.48); 233 (4.33)	—
d	nonyl	341 (3.45); 233 (4.32)	3040 (aromatic CH) 2960, 2930, 2850 (methylene)
f	tridecyl	341(3.47); 234 (4.31)	—
g	phenyl	490 (2.34); 285 (4.38) 253 (4.28)	—
h	benzyl	335 (4.32); 234 (4.27)	3300—3000 (aromatic CH), 2950, 2850, 1440, 1320 (methylene)
i	2-phenylethyl	341 (3.48); 233 (4.41)	3300—3020 (aromatic CH), 2960, 2840, 1445, 1320 (methylene)
k	*o*-hydroxyphenyl	390 (3.62); 287 (4.31)	3200—2600 (bound OH), 1620, 1585, 1520, 1475, 1440 (sh), 1380 (aromatic skeletal vibrations)
l	*p*-hydroxyphenyl	390 (3.74); 305 (4.30); 280 (4.43)	3200—2400 (OH, bound) 1610, 1590, 1510, 1480, 1440, 1395 (aromatic skeletal vibrations)
m	*p*-anisyl	400 (3.59); 313 (4.45); 270 (4.09)	—
n	3,5-dimethoxyphenyl	370 (3.60); 296 (4.28); 243 (4.29)	—
o	3,4,5-trimethoxyphenyl	384 (3.75); 282 (4.33)	2960, 2850, 1120, 840 (trimethoxyphenyl)
p	2-hydroxy-3-naphthyl	388 (3.62); 324 (4.30); 266 (4.37); 226 (4.36)	—

* in ethanol solutions

$C_7H_6N_4$ (146.16). Calcd. C 57.60; H 4.14; N 38.35. Found C 57.06; H 4.20; N 37.98%.
IR (KBr): 3040, 3060 cm^{-1} (aromatic CH); 2960 cm^{-1} (methyl); 1620, 1525, 1440 cm^{-1} (aromatic skeletal vibrations).
UV (EtOH): λ_{max} nm (log ε): 230 (5.10), 342 (4.30), 475 (2.38).
NMR ($CDCl_3$, TMS): 3.25 (s) 3H, methyl; 9.50 (s) 1H, 5-*H*; 8.25 (d) 1H; 7-*H*; 8.94 (d 1H, 8-H; $J = 6.3$ Hz.

*

The authors' thanks are due to Dr. L. RADICS and Dr. L. BUDA for the instrumental and microanalytical measurements.

REFERENCES

[1] TEMPLE, C., KUSSNER, G. L., MONTGOMERY, J. A.: J. Org. Chem. **36,** 3502 (1971)
[2] LEWIS, A., SHEPHERD, R. G.: J. Heterocycl. Chem. **8,** 41 and 47 (1971)
[3] MESSMER, A., HAJÓS, GY., BENKÓ, P., PALLOS, L.: J. Heterocycl. Chem. **10,** 575 (1973)
[4] DOLESCHALL, G., LEMPERT, K.: Tetrahedron **30,** 3997 (1974)
[5] WRIGHT, G. C., GRAY, J. E., CHIA-NIEN YU.: J. Med. Chem. **17,** 244 (1974)
[6] BISCHLER, A.: Ber. **22,** 2801 (1889)
[7] ARNDT, F.: Ber. **46,** 3522 (1913)
[8] BIFFIN, M. E. C., BROWN, D. J.: Tetrahedron Letters **1968,** 2505
[9] POLYA, J. B., SHANKS, G. F.: J. Chem. Soc. **1964,** 4986

Pál BENKÓ; H-1106 Budapest 10. Pf. 100.

András MESSMER, András GELLÉRI } H-1025 Budapest, Pusztaszeri út 57—69.

László PALLOS; H-1106 Budapest 10. Pf. 100.

Acta Chimica Academiae Scientiarum Hungaricae, Tomus 90(3), pp. 301—311 (1976)

CONDENSED *as*-TRIAZINES, II*

SYNTHESIS OF PYRIDO[3,2-e]-*as*-TRIAZINE DERIVATIVES

A. GELLÉRI, A. MESSMER, P. BENKÓ* and L. PALLOS*

*(Central Research Institute for Chemistry of the Hungarian Academy of Sciences, Budapest, and * EGyT Pharmacochemical Works, Budapest)*

Received August 22, 1975

The Bishler synthesis [4] of benzo-*as*-triazines has been extended to the preparation of pyrido[3,2-e]-*as*-triazines. The procedure proposed can generally be applied in the case of derivatives not accessible by the method suggested by LEWIS and SHEPHERD [2]. Dimorphism in the crystals of some 2-acylhydrazino-3-nitropyridine intermediates was also studied.

Experimental work has shown that the reaction of 2-chloro-3-nitropyridine (**I**) with aliphatic and aromatic acid hydrazides can be controlled by the use of suitable acid-binding agents. For example, 2-acylhydrazino-3-nitropyridines (**II**) can be obtained in high yields if an excess of the starting material is used. However, in order to achieve more favourable conditions for the purification of the intermediates (**II**), triethylamine is preferred as the acid-binding agent.

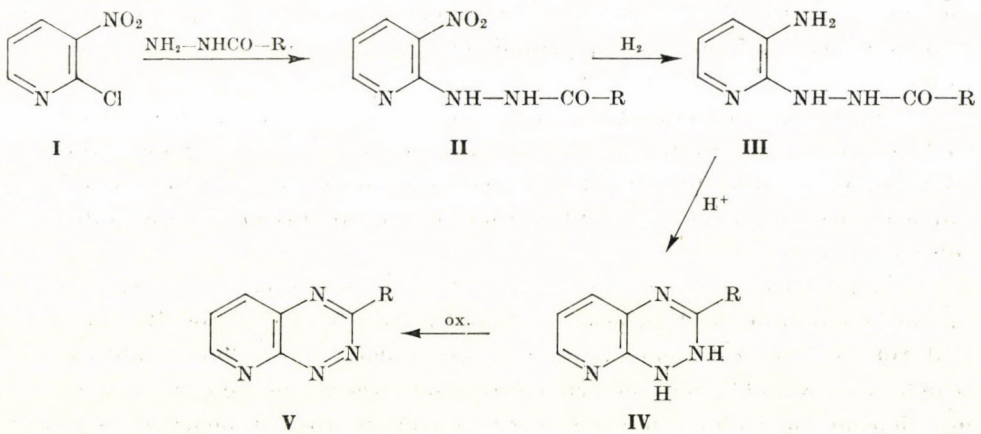

I **II** **III** **IV** **V**

In the absence of such an agent, particularly in the preparation of compounds **IIa** (R = methyl) and **IIc** (R = phenyl), side reactions take place yielding 3-substituted 8-nitro-*s*-triazolo[4,3-a]-pyridine (**VI**). The yields of the desired main products **IIa** and **IIc** may thus decrease to as low as 50%.

* Part I: P. BENKÓ, A. MESSMER, A. GELLÉRI, L. PALLOS: Acta Chim. (Budapest) *90* (**3**), 285 (1976)

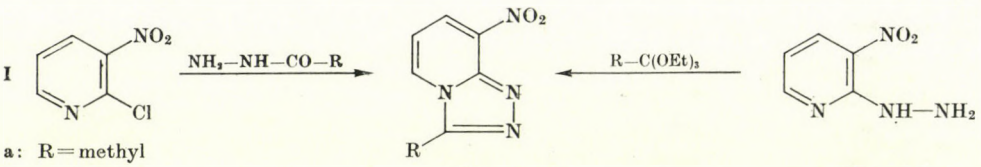

a: R = methyl
b: R = benzyl

VI VII

Compounds with structure **VI** have already been synthesized by POTTS an SURAPANENI [1], by the reaction of 2-hydrazino-3-nitropyridine (**VII**) and appropriate ortho acid esters.

The reaction of 2-chloro-3-nitropyridine (**I**) with acid hydrazides is significantly slower and proceeds at higher temperatures than that of 4-chloro-3-nitropyridine. Accordingly, the reaction time is 10—18 hrs in DMF, DMSO or in *t*-butanol, at about 90—110°C. The reduction of the resulting 2-acylhydrazino-3-nitropyridines (**II**) is accomplished rapidly, particularly in the presence of Pd/C catalyst. Hydrogenation is usually carried out at atmospheric pressure and room temperature. The amino compounds formed (**III**) are white, crystalline substances and — unlike the analogous derivatives of pyrido [3,4-e]-*as*-triazine — are stable as free bases; they are mostly insensitive to atmospheric oxygen and can be readily crystallized.

In the subsequent step of the synthesis, cyclization of 2-acylhydrazino-3-aminopyridines (**III**) is carried out in anhydrous acidic medium; usually heating for 1—2 hrs is applied. The dihydropyrido [3,2-e]-*as*-triazines formed in about 90% yield can be stabilized as their hydrochlorides. The free bases undergo oxidation very rapidly under the effect of atmospheric oxygen; also in respect of their physical properties they are similar to the analogous [3,4-e]-isomers.

The dihydro compounds (**IV**) were converted into C-3 substituted pyrido-[3,2-e]-*as*-triazines (**V**) by oxidation with potassium ferricyanide. Products with different shades of red colour were obtained in yields higher than 75%. Some of the derivatives — unlike other pyrido-*as*-triazine — are quite well soluble in water.

Some derivatives of the 2-acylhydrazino-3-nitropyridines (**II**) formed in the first step of the synthesis, such as **IIa** (R = methyl), **IIc** (R = phenyl) and **IId** (R = benzyl), may appear in dimorphous crystalline modifications which can reversibly be converted into each other. The colour change does not depend on cooling, but on recrystallization from a polar or nonpolar solvent. As usual with polymorphous substances, the IR and UV spectra of both forms are identical in solution, whereas the IR spectra recorded in KBr pellets are different. In the case of 2-acetylhydrazino-3-nitropyridine (**IIa**) -- in contrast with the suggestion of LEWIS and SHEPHERD [2] supposing irreversible polymorphism — the appearance of the red modification was observed, but this have a yellow product when recrystallized from isopropa-

nol. On the other hand, the yellow modification became red when recrystallized from benzene or toluene. The red modification contains firm intermolecular hydrogen bonds. (A similar opinion was expressed by SKULSKI [3] in connection with *o*-nitroacetanilides.) The IR spectrum has bands characteristic of bound NH (3240 cm^{-1}) and carbonyl groups involved in hydrogen bonds (1630 cm^{-1}). The IR spectrum of the orange yellow modification recorded in KBr pellet is similar to that obtained in solution, and the characteristic bands appear at different frequencies. The NH vibration gives rise to a band at 3245 cm^{-1}, while the vibration of the non-bonded carbonyl group may be responsible for the band at 1700 cm^{-1}. This indicates that in the yellow modification the two hdyrogen atoms attached to the nitrogen atoms of acetylhydrazine form an intramolecular bond with the nitro group and the nitrogen atom in pyridine, thus the intermolecular hydrogen bond involving the carbonyl group characteristic of the red modification cannot develop.

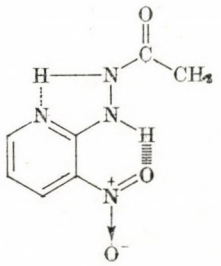

IIa

orange modification

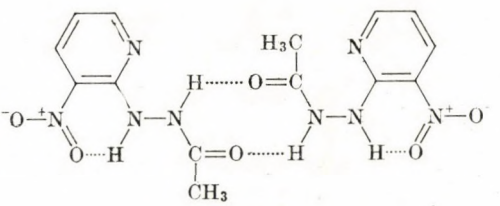

red modification

In the case of **IIc**, the lighter yellow modification melts at 122—125°C, and can be recrystallized from toluene, while that with darker shade (greenish-yellow) appears as needle-shaped crystals melting at 115—116°C when crystallized from isopropanol. The greatest difference in melting points was observed for the two modifications of **IId** (R = *o*-hydroxyphenyl). The red crystals melting at 217—218°C as obtained from acetic acid, transform into the yellow modification, m.p. 133—134°C, on recrystallization from toluene, and this transformation is reversible. The isobestic points observed in the UV spectra of the latter two compounds recorded in various solvents also indicate the presence of structures with different hydrogen bridges.

Experimental

The spectra were recorded with spectrophotomers UR 10 (IR), UNICAM SP 800 (UV) and HA-60 VARIAN (NMR). M.p.'s were determined in capillaries and are uncorrected.

2-Acetylhydrazino-3-nitropyridine (IIa)

(*a*) A solution of 2-chloro-3-nitropyridine (**I**) (4.75 g; 0.03 mole) and acetyl-hydrazine (4,43g; 0,06 mole) in *t*-butanol (60ml) was refluxed for 20 hrs. The yellowish red crystalline

Acta Chim. (Budapest) 90, 1976

Table I

2-Acylhydrazino-3-nitropyridines (**II**)

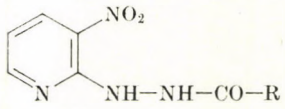

	R	Yield, %	M. p., °C	Solvent	Formula (M.W.)	Analysis Calculated/Found C	H	N
a	methyl	60	153—154	i-PrOH	$C_7H_8N_4O_3$ (196.17)	42.85 42.60	4.12 4.11	28.62 28.57
b	nonyl	63	88—89	Cyclohexane	$C_{15}H_{24}N_4O_3$ (308.39)	58.80 58.35	7.84 7.59	18.18 17.98
c	phenyl	65	142—143	70% EtOH	$C_{12}H_{10}N_4O_3$ (258.25)	55.75 55.49	3.93 3.90	21.70 21.55
d	benzyl	47	122—123	toluene	$C_{13}H_{12}N_4O_3$ (272.27)	57.35 57.30	4.42 4.29	20.65 20.45
e	*o*-hydroxyphenyl	60	217—218	acetic acid	$C_{12}H_{10}N_4O_4$ (274.25)	52.40 52.29	3.69 3.67	20.45 20.40
f	*p*-hydroxyphenyl	55	216—217	*t*-BuOH	$C_{12}H_{10}N_4O_4$ (274.25)	52.40 52.30	3.69 3.63	20.45 20.50
g	3,4,5-trimethoxyphenyl	50	164—165	EtOH	$C_{15}H_{16}N_4O_6$ (348.33)	51.70 51.63	4.67 4.64	16.10 16.14

Table II

Spectral data of 2-acylhydrazino-3-nitropyridines **(II)**

	R	UV max. nm (log ε) Solvent	IR (KBr), cm^{-1}
a	methyl	— —	3200—2900 (NH), 1620—1640 (amide I)
b	nonyl	376 (3.69) EtOH 256 (3.70)	3350, 3250, 1655 (amide), 2850, 2930, 1480, 1220 (methylene), 1530, 1260 (nitro)
c	phenyl	376 (3.23) EtOH 262 (3.74) 222 (4.08)	3300—2700 (NH), 1660 (CO), 1530 (nitro)
d	benzyl	— —	3300—3200 (NH), 2860 (methylene), 1640 (CO), 1570, 1380 (nitro)
e	*o*-hydroxyphenyl	— —	3300—2700 (NH), 1640 (CO), 1570, 1350 (nitro)
f	*p*-hydroxyphenyl	— —	3350, 1650 (OH), 3200—2800 (amide), 1620 (amide), 1580—1380 (nitro)
g	3,4,5-trimethoxyphenyl	377 (3.43) EtOH 265 (3.98) 219 (4.53)	3300—2500 (NH), 1630 (amide), 1530, 1340 (nitro)

precipitate was filtered off and washed with hot methanol. After recrystallization from dioxan, 3-methyl-8-nitro-s-triazolo[4,3-a]-pyridine **(VI a)** was obtained (1.6 g); m. p. 288°C.

$C_7H_6N_4O_2$ (178.15). Calcd. C 47.20; H 3.37; N 31.47. Found C 47.18; H 3.40; N 31.38%.

UV (MeOH): λ_{max} nm (log ε): 225 (4.18), 360 (3.68).

The combined filtrates were evaporated to dryness in vacuum and the residue rubbed with water to obtain a solid substance (3.9 g). Recrystallization from isopropanol gave a mixture of red and yellow crystal **(IIa)** (3.2 g; 51%); m.p. 153—154°C (lit. [2] m.p. 157—158°C).

$C_7H_8N_4O_3$ (196.17). Calcd. C 42.85; H 4.12; N 28.62. Found C 42.60; H 4.11; N 28.57%.

IR (KBr): 3200—2900 cm^{-1} (ν NH), 1620—40 cm^{-1} (Amide I).

The mixture was twice recrystallized from about a 50-fold volume of benzene. The red product was obtained without the yellow modification.

IR (KBr): 3240 cm^{-1} (bound NH), 1630 cm^{-1} (bound CO).

Recrystallization of the mixture from isopropanol, repeated four times, yielded the yellow modification as a pure, homogeneous substance.

IR (KBr): 3260 cm^{-1} (non-bound NH), 1700 cm^{-1} (non-bound CO).

(b) When using the same amounts of reactants as in Method *(a)*, in the presence of triethylamine (0.04 mole) the formation of the by-product 3-methyl-8-nitro-*s*-triazolo[4,3-a]-pyridine **(VIa)** was practically negligible, while the product **IIa** was obtained in 60% yield. This greatly facilitated the recrystallization procedure.

2-Decanoylhydrazino-3-nitropyridine (IIb)

2-Chloro-3-nitropyridine **(I)** (0.78 g; 0.0048 mole) and decanoic acid hydrazide (0.88 g; 0.0051 mole) were allowed to react in a mixture of anhydrous DMF (10 ml) and triethylamine (1.5 ml; 0.0015 mole) for 24 hrs at 85°C. The solution was evaporated to dryness and the residue rubbed with water. The crystals obtained were then dissolved in chloroform and chromatographed on a column packed with aluminium oxide (30 cm long). 1.25 g (80%) of the product was obtained. Dissolution in ether and precipitation with petroleum ether resulted in the separation of yellow plates (1.15 g; 74%), m.p. 88—89°C.

Table III

2-Acylhydrazino-3-aminopyridines **(III)**

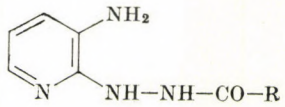

	R	Yield, %	M. p., °C	Solvent	Formula (M.W.)	Analysis Calculated/Found C	H	N
a	methyl	80	154	MeOH–ether	$C_7H_{10}N_4O$ (166.19)	50.55 50.49	6.12 6.10	33.70 33.55
b	nonyl	90	78	ether–petroleum ether	$C_{15}H_{26}N_4O$ (278.41)	64.80 64.69	9.42 9.50	20.15 20.22
c	phenyl	65	185	i-PrOH	$C_{12}H_{12}N_4O$ (228.26)	63.12 62.92	5.17 5.27	24.55 24.25
d	benzyl	62	117—118	ethylene-chloride	$C_{13}H_{14}N_4O$ (242.29)	66.95 66.87	5.82 5.79	23.15 23.25
e	*o*-hydroxyphenyl	72	196	EtOH	$C_{12}H_{12}N_4O_2$ (244.26)	58.98 59.12	4.84 4.94	22.94 22.65
f	*p*-hydroxyphenyl	94	186	EtOH–ether	$C_{12}H_{12}N_4O_2$ (244.26)	58.98 59.14	4.84 4.75	22.94 22.58
g	3,4,5-trimethoxyphenyl	90	199	i-PrOH	$C_{15}H_{18}N_4O_4$ (318.34)	56.58 56.49	5.76 5.70	17.62 17.58

Table IV

Spectral data of 2-acylhydrazino-3-aminopyridines

	R	UV max. nm (log ε)	Solvent	IR (KBr), cm^{-1}
b	nonyl	288 (3.56)	MeOH	3400, 3250 (NH), 1640 (CO), 2900, 2820, 1460 (methylene), 1600, 760 (pyridine)
c	phenyl	307 (3.57)	EtOH	3400, 3300, 1620 (amino), 1640 (CO), 690 (pyridine), 750 (phenyl)
d	benzyl	—	—	3400—3200 (NH and NH_2), 2920 (methylene), 1650, 1580 (amide)
e	*o*-hydroxyphenyl	303 (3.45) 242 (3.54) 210 (3.79)	EtOH	3400—3300, 2700—2300 (OH, NH), 1650 (OH-def.), 1620 (CO)
f	*p*-hydroxyphenyl	318 (3.90) 260 (4.28)	0.1*N* HCl	3300—3110 (NH and OH), 1640 (OH def.), 1625 (CO)
g	3,4,5-trimethoxyphenyl	295 (3.18) 252 (3.35) 214 (3.72)	EtOH	3350, 1630 (NH_2), 1640 (CO), 2960, 2860, 1460, 1125, 900 (trimethoxyphenyl)

$C_{15}H_{24}N_4O_3$ (308.39). Calcd. C 58.80; H 7.84; N 18.18. Found C 58.35; H 7.59; N 17.98%.
UV (EtOH): λ_{max} nm (log ε): 256 (3.70), 376 (3.69).
IR (KBr): 3350, 3250, 1655 cm^{-1} (amide); 2850, 2930, 1480, 1220 cm^{-1} (methylene); 1600, 1400, 765 cm^{-1} (pyridine); 1530, 1260 cm^{-1} (nitro).

Preparation of 2-acylhydrazino-3-aminopyridines (III)

2-Acylhydrazino-3-nitropyridine (**II**) (0.1 mole) was shaken in alcohol solution (ethanol, isopropanol, etc.) (200 ml) in the presence of Pd/C catalyst, until the calculated amount of hydrogen (7.2 l) had been absorbed. The catalyst was filtered off and the solution was evaporated to dryness to yield the crude product, which was recrystallized.

Preparation of C-3 substituted 1,2-dihydropyrido[3,2-e]-as-triazines (IV)

2-Acylhydrazino-3-aminopyridine (**III**) (0.01 mole) was dissolved in anhydrous alcohol (20 ml). Conc. hydrochloric acid (5 ml) was added, and the solution was allowed to stand overnight, then evaporated to dryness. The residue was recrystallized.

Preparation of C-3 substituted pyrido[3,2-e]-as-triazines (V)

Method A

A solution of **IV** (0.0012 mole) in water (15 ml) was allowed to react with a mixture of 20% potassium ferricyanide (5 ml) and 10% potassium carbonate (12 ml) at 30—40°C. In most cases a crystalline mass with red colour separated (several times the dihydro compound was insoluble, too). It was filtered off, and recrystallized to obtain reddish-brown plates.

Method B

Compound **III** (0.01 mole) was refluxed with polyphosphoric ester in chloroform (40 ml) for 30—45 min, and the mixture was then evaporated to dryness in vacuum. The residue was mixed with ice and the solution obtained was continuously extracted with chloroform or stirred together with 36% potassium ferricyanide solution (30 ml) for 30 min, at 30—40°C. The product was recrystallized.

Table V

C-3 substituted 1,2-dihydropyrido[3,2-e]-as-triazines **(IV)**

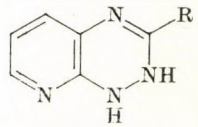

	R	Yield, %	M. p., °C	Solvent	Formula (M.W.)	Analysis Calculated/Found C	H	N	Cl
a	methyl	67	218—219*	EtOH	$C_7H_{10}Cl_2N_4$ (221.10)	38.10 38.02	4.62 4.60	25.35 25.12	32.11 32.00
b	nonyl	71	247—249	EtOH	$C_{15}H_{25}ClN_4$ (332.92)	54.15 54.02	7.56 7.40	16.82 17.02	21.32 21.38
d	benzyl	71	156*	MeOH–ether	$C_{13}H_{16}Cl_2N_4$ (315.22)	49.42 49.29	5.12 5.10	17.57 17.61	22.55 22.49
f	*p*-hydroxyphenyl	69	281*	MeOH–ether	$C_{12}H_{12}Cl_2N_4O$ (299.27)	48.20 47.95	4.02 4.00	18.72 18.85	23.70 23.78
g	3,4,5-trimethoxyphenyl	75	227—228 (d.)	EtOH	$C_{15}H_{17}ClN_4O_3$ (336.79)	53.35 53.29	5.08 5.00	16.62 16.66	10.51 10.45

* dihydrochloride

Table VI

Spectral data of C-3 substituted 1,2-dihydropyrido[3,2-e]-as-triazines (IV)

	R	UV max. nm (log ε)	Solvent	IR (KBr), cm^{-1}
b	nonyl	383 (3.39) 397 shoulder	MeOH	3500—2400 (NH^+), 2900, 2800 (methylene), 1640 (C=N)
d	benzyl	383 (3.70)	EtOH	3300—2800 (NH), 1620—1600 (diffuse NH, aromatic)
f	*p*-hydroxyphenyl	394 (3.93) 269 (4.13) 434 shoulder	EtOH	—
g	3,4,5-trimethoxyphenyl	376 (3.70) 269 (3.95) 220 (4.13)	MeOH	3300—2600 (NH), 1600 (C=N), 1130 (OCH_3)

Acta Chim. (Budapest) 90, 1976

Table VII

C-3 substituted pyrido[3,2-e]-as-triazines (V)

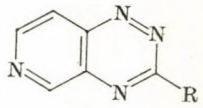

	R	Method	Yield, %	M. p., °C	Solvent	Formula (M.W.)	Analysis Calculated/Found C	H	N
a	methyl	A	54	171	EtOH	$C_7H_7N_4$ (147.16)	57.25 57.20	4.78 4.70	38.20 38.00
b	nonyl	A	93	83—84	petroleum ether	$C_{15}H_{22}N_4$ (258.38)	69.90 69.59	8.58 8.65	21.62 21.43
c	phenyl	B	43	225	i-PrOH	$C_{12}H_8N_4$ (208.23)	69.19 69.00	4.37 4.27	26.95 26.90
d	benzyl	A	69	125	50% EtOH	$C_{13}H_{10}N_4$ (222.26)	70.31 70.51	4.57 4.60	25.20 25.32
e	*o*-hydroxyphenyl	B	53	247—248	BuOH	$C_{12}H_8N_4O$ (224.23)	64.25 64.20	3.60 3.51	24.99 24.95
f	*p*-hydroxyphenyl	A	95	315	EtOH–MeC.*	$C_{12}H_8N_4O$ (224.23)	64.25 64.32	3.60 3.65	24.99 24.95
g	3,4,5-trimethoxyphenyl	B A	42 60	207—208	i-PrOH	$C_{15}H_{14}N_4O_3$ (298.31)	60.25 60.17	4.73 4.70	18.75 18.54

* MeC. = methylcellosolve

Table VIII

Spectral data of C-3 substituted pyrido[3,2-e]-as-triazines (V)

	R	UV max. nm (log ε)	Solvent	IR (KBr), cm^{-1}
a	methyl	312 (3.48) 330 (3.94) 476 (2.27)	EtOH	—
b	nonyl	263 (3.19) 311 (3.53) 323 (3.45) 498 (2.29)	cyclohexane	3050 (aromatic CH), 2970, 2850 (methylene), no NH band
c	phenyl	210 (4.43) 269 (4.54) 352 (3.91)	EtOH	—
d	benzyl	265 (3.63) 317 (3.90) 489 (2.33)	dioxan	3300—3000 (aromatic CH), 2950, 2850, 1440, 1330 (methylene), 1600, 1560, 1550, 1500, 1480, 1460, 1450 (aromatic skeletal vibrations)
e	*o*-hydroxyphenyl	262 (4.40) 309 (4.05) 385 (3.65)	dioxan	3200—2600 (bound OH), 1620, 1580, 1550, 1520, 1480 (aromatic skeletal vibrations), 750 (*o*-substituted phenyl)
f	*p*-hydroxyphenyl	275 (3.60) 380 (3.25)	dioxan	3400—3000 (OH, strongly bound), 1610—1400 (aromatic skeletal vibrations)
g	3,4,5-trimethoxyphenyl	222 (4.46) 277 (4.44) 370 (3.82)	EtOH	2960, 2850, 1120, 840 (trimethoxyphenyl), 1610, 1580, 1550, 1500 (aromatic skeletal vibrations)
h	*p*-acetoxyphenyl	263 (4.57) 353 (4.12) 484 (2.49)	dioxan	3010 (aromatic CH), 2950, 1760, 1470, 1365, 1200 (O-acetyl)

*

The authors' thanks are due to Dr. L. RADICS and Dr. S. HOLLY for the instrumental analyses.

REFERENCES

[1] POTTS, K. T., SURAPANENI, C. R.: J. Heterocycl. Chem. **7,** 1019 (1970)
[2] LEWIS, A., SHEPHERD, R. G.: J. Heterocycl. Chem. **8,** 41 (1971)
[3] SKULSKI, L.: J. Org. Chem. **28,** 3565 (1963)
[4] BISCHLER, A.: Ber. **22,** 2801 (1889)

András GELLÉRI
András MESSMER
H-1025 Budapest, Pusztaszeri út 57—69.

Pál BENKÓ
László PALLOS
H-1106 Budapest 10. Pf. 100.

Acta Chimica Academiae Scientiarum Hungaricae, Tomus 90(3), pp. 313—324 (1976)

DEHYDROCYCLIZATION OF *N*-NONANE AND *N*-DECANE UNDER THE CONDITIONS OF CATALYTIC GASOLINE REFORMING

I. SZEBÉNYI, L. ACKERMANN, G. SZÉCHY and S. GÖBÖLÖS

(Department of Chemical Technology, Technical University, Budapest)

Received June 12, 1975

The conversion of *n*-nonane and *n*-decane was investigated on an industrial gasoline reforming catalyst containing platinum, at temperatures from 480 to 530°C, in the range of 3 to 10 ml/ml · hr space velocity. The experiments were carried out at a pressure of 30 kp/cm² in a microreactor. Though only a few per cent of aromatic compounds were obtained from either of the starting compounds, the conversion to aromatics increased significantly with the increase of temperature and decrease of space velocity. At 530°C the maximum amounts of 1,2,4-trimethylbenzene formed from *n*-nonane and *n*-decane were 3.7% and 2.1% (w/w), respectively. *n*-Nonane gave mostly 1,2,4-trimethylbenzene whereas from *n*-decane relatively significant amounts of xylenes, *n*-butylbenzene and 1,3-diethylbenzene were also obtained. Formation of aromatic compounds having a lower number of C-atoms than that of the starting compounds was observed both from *n*-nonane and *n*-decane, but this was more characteristic of the conversion of *n*-decane. The conversion of both starting compounds was increased by raising the temperature, whereas the decrease of space velocity affected mainly the conversion of *n*-decane.

Introduction

The dehydrocyclization of paraffins is, besides the dehydrogenation and dehydroisomerisation of naphthenes, one of the important reactions of catalytic gasoline reforming. This reaction, involving several steps, eventually results in the formation of aromatic compounds. The mechanism of dehydrocyclization has been studied by several authors. In the earlier researches mainly catalysts of oxide nature ($Cr_2O_3—Al_2O_3$, $MoO_3—Al_2O_3$) were used, and it was suggested that dehydrocyclization takes place *via* the formation of six-membered rings (C_6-dehydrocyclization). According to HERRINGTON and RIDEAL [1], paraffins are first dehydrogenated to olefins, and the latter are adsorbed on the surface of the catalyst. The next step is the formation of a six-membered ring (provided that the position of the double bond and the geometry of adsorption are favourable); finally the ring is quickly dehydrogenated to the aromatic compound.

Using an oxide catalyst, ROZENGART, et al. [2, 3] showed that prior to ring closure a stepwise dehydrogenation takes place, *i.e.* olefines, then aliphatic dienes and lastly aliphatic trienes are formed from the initial paraffin, and the ring closure of triene to cyclohexadiene occurs only subsequently. It was proved by PAÁL and TÉTÉNYI [4, 5] that the C_6-dehydrocyclization follows

the above mechanism also on metal catalysts and thus also on platinum. Later on, the same conclusion was attained also by KAZANSKY *et al.* [6, 7].

In 1954 KAZANSKY *et al.* discovered that paraffins can be converted on metal catalysts (mainly platinum) not only to six-membered but also into five-membered compounds (C_5-dehydrocyclization) [8]. Several suggestions have been published in the literature about the mechanism of C_5-dehydrocyclization [9, 10, 11, 12], but none of them is generally accepted. It has not been decided whether unsaturated compounds are necessary intermediates in the C_5-dehdyrocyclization of paraffins. The partial pressure of hydrogen and the hydrogen coverage of the catalyst certainly play a significant role in the course of C_5-dehydrocyclization [13].

GAULT *et al.* [10] observed considerable C_5-dehydrocyclization activity in the case of a bifunctional $Pt-Al_2O_3$ catalyst, whose platinum content was less than 1%. Since most of the industrial reforming catalysts are of this type, under the conditions of reforming one must reckon with the occurrence of C_5-dehydrocyclization along with C_6-dehydrocyclization. This has been pointed out as early as 1955 in a paper of HETTINGER *et al.* [14], who detected 1.0—1.5% alkylcyclopentanes in the reforming products of *n*-heptane. On converting *n*-hexane, *n*-heptane and *n*-octane in the presence of a $Pt-\gamma-Al_2O_3$ catalyst containing 0.6% platinum, KAZANSKY *et al.* [15] found significant amounts of alkylcyclopentanes in the products. The results obtained with bifunctional catalysts indicate that the acidic centres of the catalyst play a significant part in C_5-dehydrocyclization. This is suggested also by DAVIS and VENUTO [16] who examined the dehydrocyclization of C_8-C_9 paraffins on non-acidic $Pt-Al_2O_3$ catalysts; in their opinion, on the basis of product distribution, the C_6-dehydrocyclization appeared to predominate.

During reforming C_5-dehydrocyclization also contributes to the formation of aromatic compounds, or plays a role as an intermediate step of the aromatization process, since the acidic function of the catalyst causes the alkyl-cyclopentanes produced by C_5-dehydrocyclization to undergo dehydroisomerization yielding aromatic compounds.

Thus, dehydrocyclization processes leading to the formation of both six-membered and five-membered rings have an important role in reforming. SINFELT and ROHRER [17] carried out dehydrocyclization experiments on a $Pt-Al_2O_3$ catalyst containing 0.3% platinum, using C_6, C_7 and C_8 paraffins. In their opinion, the first step of the reaction is dehydrogenation resulting in olefins (this takes place on the platinum surface), followed by the formation of carbonium ions as a result of the interaction of the olefins and the acidic sites. The relative stability of the carbonium ions will determine whether C_5- or a C_6-dehydrocyclization will occur. Since secondary carbonium ions are much more stable than the primary ones, *n*-hexane gives a five-membered ring; C_6-dehydrocyclization could only take place through a primary carbo-

nium ion. With *n*-octane, in turn, and obviously also in the cases of *n*-nonane and *n*-decane a C_6-dehydrocyclization is expected to be the dominating process.

Nearly all the above-mentioned investigations were carried out at atmospheric pressure with C_6, C_7 and C_8 hydrocarbons. The catalysts applied were prepared in the laboratory mostly by the authors themselves. It is known that the way of preparation of the catalyst affects the catalytic activity in several ways [18]. It appears from a survey of the literature that the dehydrocyclization of paraffins containing more than eight carbon atoms has been only scarcely studied, and, even the few investigations reported were carried out under conditions greatly differing from those of industrial gasoline reforming.

The aim of the present work was to establish the extent of the dehydrocyclization of *n*-nonane and *n*-decane under the conditions of gasoline reforming, *i.e.* with an industrial catalyst of the $Pt-Al_2O_3$ type, at a pressure of 30 kp/cm^2.

Our primary object was to study the formation of C_9- and C_{10}-aromatics, and within these groups mainly that of trimethylbenzenes, whose industrial utilization is increasing [19], and may arouse interest in Hungary when the utilization of these compounds as starting materials of the petrochemical industry advances.

Investigation of the thermodynamic equilibrium of dehydrocyclization does not afford practical information for the given purpose; according to the calculations, the thermodynamic equilibrium of the formation of C_9- and C_{10}-aromatics from paraffins with an identical number of C-atoms is shifted, even at higher pressures, towards the formation of aromatics.

Besides dehydrocyclization, however, also hydrocracking, isomerization and dealkylation reactions also take place on the catalyst. This fact causes the product distributions to be very complex and makes the determination of the total equilibrium product distributions by way of calculations unreasonable. The main reason being that the "equilibrium" of the hydrocracking reactions is shifted towards the cracking products to such an extent that the reaction can be considered practically irreversible. Therefore, the practical yields and distributions of aromatics can only be determined by experiments.

Experimental

The model compounds applied in our work were in each case the 'purum' quality products of the Swiss firm Fluka. Our experiments were carried out in a pressure-tight, flow-type, isothermal microreactor of 6 ml volume, constructed in the High Pressure Research Institute, and described in our earlier paper [20]. In the experiments an industrial platinum catalyst of type RD-150C was applied which is used all over the world in many reforming plants and also applied in our country. This is a $Pt-\gamma-Al_2O_3$ bifunctional catalyst containing 0.35% platinum whose detailed, mainly electron optical, investigation has been reported

by VAJTA *et al.* [21, 22]. Since the inner diameter of the microreactor was 6.8 mm, the catalyst was crushed and the fraction with the grain size 0.6—0.8 mm was used in the reactor. The catalyst packed into the reactor was then subjected to the treatment specified by the manufacturer firm, and subsequently the actual experiments were started.

To investigate the dehydrocyclization of both *n*-paraffins as a function of temperature, the measurements were carried out at 480, 500, 515 and 530°C, keeping the space velocity at 3 ml/ml · hr. when investigating the effect of space velocity, in turn, the measurements were carried out at space velocities of 3, 5, 7 and 10 ml/ml · hr maintaining the temperature at 500°C. The pressure was held at 30 kp/cm² and the gas–liquid ratio at 1300 ml H_2/ml hydrocarbon in all experiments. This value of the gas–liquid ratio corresponds to a H_2 : *n*-nonane mole ratio of 9.7 : 1 and H_2 : *n*-decane mole ratio of 10.6 : 1.

The experimental parameters were in agreement with the values usually applied in industrial gasoline reforming plants using platinum catalysts.

According to an experiment with *n*-heptane, the activity of the catalyst was stable, after some initial fluctuations, for at least 48 hours of continuous operation. Therefore, the periods of our measurements, were selected to last no longer than 48 hours, and the reactor was packed with fresh catalyst at the beginning of each period. In the course of the experiments the liquid yield was measured (in per cent by weight), and the amount of alkylbenzenes present in the reformate was determined by a gas chromatographic method developed specially for this purpose at our Department [23]. The method is based on the relationship according to which, on an Apiezon phase, the logarithmic value of the relative retention of the individual alkylaromatic compounds plotted against the boiling point of the compounds affords straight lines for compounds having in their alkyl chains an identical number of C atoms [24]. It was found in our investigations that this relationship also holds for a polar packing and polyethyleneglycol adipate (PEGA) is the most suitable partition phase for the separation of alkylbenzenes. The analyses were performed with a CHROM 31 gas chromatograph, under the conditions given below:

Column length:	360 mm
Column diameter:	6 mm
Packing:	10% PEGA on Rysorb C support of 0.2—0.3 mm grain size
Carrier gas:	50 ml N_2/min
Temperature of thermostat:	40—120°C

Results and their evaluation

The results of our experiments carried out at different temperatures are summarized in Table I, and those of runs made with various space velocities are shown in Table II.

The experimental results concerning the temperature dependence are also shown in Figs 1, 2, 3 and 4, and those with different space velocities in Figs 5, 6, 7 and 8.

It appears from the data in Table I that a significant part of *n*-nonane remained unchanged, and that the degree of conversion markedly depended on the temperature. This is mentioned here because in the reforming of naphthenes a very high degree of conversion can be observed already at 480°C, in fact, some compounds are almost completely converted at this temperature. In the reforming of *n*-nonane, the quantity of unconverted initial substance in the product amounted to 53.2% at 480°C and 19.4% at 530°C. On raising the temperature, the liquid yield appreciably decreased as a result of increased hydrocracking. In the reforming of naphthene-containing hydrocarbon mixtures or of pure naphtenes, the liquid yield does not decrease so much at temper-

Table I

Effect of temperature on the formation of aromatic compounds in the reforming of n-nonane and n-decane

Space velocity: 3 ml/ml·hr pressure: 30 kp/cm² gas–liquid ratio: 1300 ml/ml

Starting compound	*n*-Nonane				*n*-Decane			
Reforming temperature, °C	480	500	515	530	480	500	515	530
Aromatics yield, % (w/w) of the starting compound								
Toluene	0.5	0.9	2.0	2.2	2.3	3.7	3.2	2.8
m- and *p*-Xylene	0.4	1.2	1.6	1.8	1.6	3.0	3.6	4.1
o-Xylene	0.2	0.4	0.4	0.7	0.8	1.4	1.5	1.9
n-Propylbenzene	0.3	0.4	0.4	0.6	—	—	—	—
1,3,5-Trimethylbenzene	0.1	0.7	0.8	0.9	0.3	0.7	0.7	0.6
1,2,4-Trimethylbenzene	0.6	1.8	2.9	3.7	1.1	1.1	1.6	2.1
1,2,3-Trimethylbenzene	0.2	0.6	0.8	0.8	1.2	0.8	0.8	0.8
n-Butyl- and 1,3-diethylbenzene	—	—	—	—	2.4	2.1	1.6	1.1
1,2,4,5-Tetramethylbenzene	—	—	—	—	0.5	0.7	0.7	0.7
Unconverted *n*-nonane	48.0	44.0	19.6	11.0	—	—	—	—
Unconverted *n*-decane	—	—	—	—	36.1	11.7	8.1	4.3
Liquid product, %, (w/w)	90.0	86.0	71.0	56.6	81.2	65.6	58.7	50.5

Table II

Effect of space velocity on the formation of aromatic compounds in the reforming of n-nonane and n-decane

Temperature: 500°C pressure: 30 kp/cm² gas–liquid ratio: 1300 ml/ml

Starting compound	*n*-Nonane				*n*-Decane			
Space velocity of reforming ml/ml·hr	3	5	7	10	3	5	7	10
Aromatics yield, % (w/w) of the starting compound								
Toluene	0.9	0.9	0.9	0.8	3.7	3.1	2.1	1.3
m- and *p*-Xylene	1.2	0.7	0.6	0.5	3.0	2.4	1.7	0.3
o-Xylene	0.4	0.3	0.3	0.2	—	—	—	—
n-Propylbenzene	0.4	0.4	0.5	0.4	—	—	—	—
1,3,5-Trimethylbenzene	0.7	0.5	0.4	0.2	0.7	0.6	0.4	0.2
1,2,4-Trimethylbenzene	1.8	1.7	1.8	1.0	1.1	1.1	0.7	0.6
1,2,3-Trimethylbenzene	0.6	0.6	0.7	0.6	0.8	0.9	0.7	0.4
n-Butyl- and 1,3-diethylbenzene	—	—	—	—	2.1	1.9	1.5	0.9
1,2,4,5-Tetramethylbenzene	—	—	—	—	0.7	0.4	0.4	0.1
Unconverted *n*-nonane	44.0	46.4	47.1	50.1	—	—	—	—
Unconverted *n*-decane	—	—	—	—	11.7	26.2	33.4	40.7
Liquid product, % (w/w)	86.0	86.5	87.2	87.3	65.6	69.2	73.5	79.6

atures above 500°C; hydrocracking played such a great part in our case because the applied initial substance was a pure paraffin.

As expected, the degree of conversion of *n*-decane was higher than that of *n*-nonane over the whole temperature range examined. At 530°C the conversion was nearly complete. The rise of temperature resulted in an even greater decrease of the liquid yield than observed in the case of *n*-nonane, which may be explained by the higher proneness of *n*-decane to cracking. At 530°C very low liquid yields were obtained with both initial substances, indicating that this temperature corresponds to extremely severe reforming. This is quite in accordance with the industrial experience.

The amounts of xylenes formed from *n*-nonane and *n*-decane are shown in Fig. 1. Essentially greater amounts of xylene are formed from *n*-decane than from *n*-nonane. Thus, *n*-decane is inclined more than *n*-nonane to form aromatics which contain less carbon atoms than the starting material. This is also shown by Figs 2 and 3, in which the amounts of trimethylbenzenes

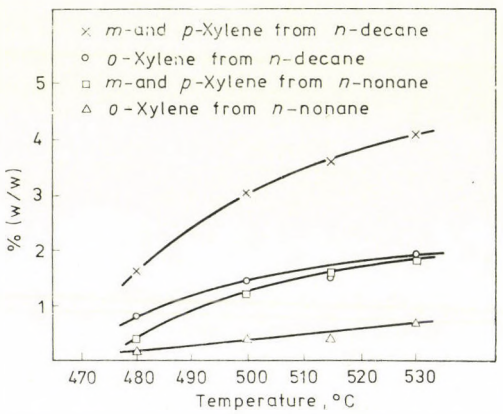

Fig. 1. Xylenes formed at different reforming temperatures

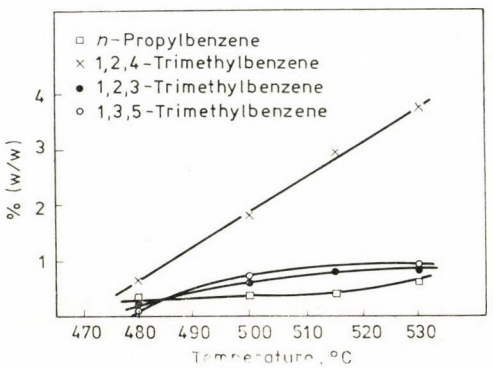

Fig. 2. Trimethylbenzenes formed at different reforming temperatures from *n*-nonane

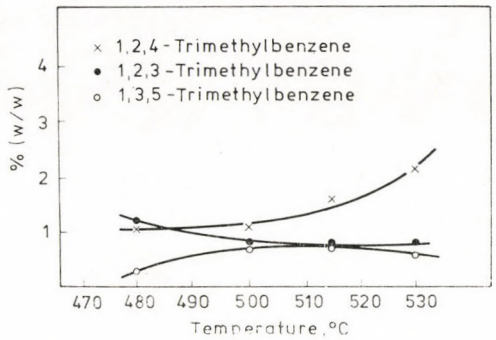

Fig. 3. Trimethylbenzenes formed at different reforming temperatures from *n*-decane

obtained from both initial model compounds are plotted. It can be seen that a considerable amount of trimethylbenzenes is formed from *n*-decane. Higher temperatures enhance mainly the formation of 1,2,4-trimethylbenzene, as it was also experienced in the reforming of gasoline fractions [20]. This is due to a better approach of the thermodynamic equilibrium of the various trimethylbenzenes at high temperatures, corresponding to a higher proportion of 1,2,4-trimethylbenzene.

In Tables III and IV the values of xylenes and trimethylbenzenes obtained at 530°C are compared with the thermodynamical equilibrium values.

Table III

Distribution of xylenes (%, w/w) formed from n-nonane and n-decane at 530°C

Starting compound	*n*-Nonane		*n*-Decane	
Product	Experimental value	Calculated equilibrium value	Experimental value	Calculated equilibrium value
m- and *p*-Xylene	71.0	74.3	68.6	74.3
o-Xylene	29.0	25.7	31.4	25.7

Table IV

Distribution of trimethylbenzenes (%, w/w) formed from n-nonane and n-decane at 530°C

Starting compound	*n*-Nonane		*n*-Decane	
Product	Experimental value	Calculated equilibrium value	Experimental value	Calculated equilibrium value
1,2,4-Trimethylbenzene	67.8	62.3	60.9	62.3
1,3,5-Trimethylbenzene	16.7	20.9	16.0	20.9
1,2,3-Trimethylbenzene	15.5	16.8	23.1	16.8

The obtained amount of *o*-xylene was in the case of both starting compounds higher than the equilibrium value. The ratio of *o*-xylene formed from *n*-nonane was closer to the equilibrium distribution. In the case of the trimethylbenzenes it is interesting to note that the experimental ratio of the 1,3,5-isomer was in both cases lower than the equilibrium value. When starting from *n*-decane, the experimental value of the 1,3,5-isomer approached the equilibrium value of the 1,2,3-isomer and *vice versa*. This phenomenon was also observed in the reforming of gasoline fractions [20] and in industrial reformates [23].

Fig. 2 also shows the amounts of *n*-propylbenzene formed from *n*-nonane. The quantity of this compound in the product does not exceed 1% (w/w) even at 530°C. This experience and the appreciable quantity of trimethylbenzenes in the reformate point to the importance of the isomerizing capability of the RD-150C catalyts and of industrial reforming catalysts, in general. In the reforming experiments of DAVIS and VENUTO [16] with definitely non-acidic $Pt-Al_2O_3-K$ catalysts at atmospheric pressure, the products did not contain trimethylbenzenes at all, whereas the quantity of *n*-propylbenzene amounted to 25 mole % of the C_9-aromatic fraction.

n-Nonane above 500°C gave 1,2,4-trimethylbenzene as the individual aromatic compound which formed in the greatest amount. From *n*-decane, in turn, at higher temperatures toluene, *meta*- and *para*-xylene were formed in the greatest amounts, whereas below 500°C the main products were *n*-butylbenzene and 1,3-diethylbenzene. The quantitities of the two latter compounds and also that of 1,2,4,5-tetramethylbenzene (durene), produced from *n*-decane, are shown in Fig. 4. At temperatures higher than 500°C, the longer side chains of the resulting alkylaromatic compounds are readily split off the aromatic ring. Consequently, raising the temperature above 500°C causes a decrease of the amounts of *n*-butylbenzene and 1,3-diethylbenzene formed, and aromatics with a smaller number of C-atoms (*e.g.* xylenes) are obtained.

The quantity of durene in the liquid product is small, and above 500°C it does not depend on the temperature. The amounts of the 1,2,3,4-isomer and the 1,2,3,5-isomer also remained always below 1% (these values are not shown in Fig. 4). The small amount of tetramethylbenzenes formed from *n*-decane and the relatively appreciable quantities of trimethylbenzenes indicate that dealkylation is much more an accompanying reaction of the isomerization and dehydrocyclization of *n*-decane than of *n*-nonane.

In the experiments carried out for determining the influence of space velocity, within the range investigated, low space velocities hardly decreased the yield of the liquid products and the amount of unchanged *n*-nonane (Table II). Obviously the rate of conversion of *n*-nonane starts to increase rapidly below a space velocity of 3 ml/ml · hr; this value corresponds only to a mild reforming which leaves *n*-nonane largely unchanged.

No experiments were however, carried out at space velocities below

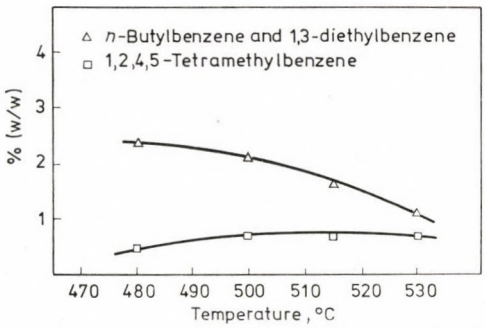

Fig. 4. Some C_{10}-aromatic compounds formed at different reforming temperatures from *n*-decane

3 ml/ml·hr, because the accuracy of measurements would have been poor, owing to difficulties in manipulation with extremely small amounts of material.

The conversion of *n*-decane and the amount of liquid products are affected by space velocity stronger than experienced in the case of *n*-nonane. This can be readily understood by considering that the larger molecule of *n*-decane is less stable and more inclined to cracking than *n*-nonane.

The quantities of xylenes formed from *n*-nonane and *n*-decane in the experiments at various space velocities are shown in Fig. 5. It can be seen that the amount of xylenes formed from *n*-decane is more affected by the space velocity than in case of *n*-nonane as the starting material. The quantity of xylenes in the latter case is practically the same within the range of 5—10 ml/ml·hr space velocities.

Fig. 6 shows the unconverted quantities of *n*-nonane and the amounts of trimethylbenzenes and *n*-propylbenzene formed from this starting material. (It must be noted concerning Fig. 6 that the ordinate on the right-hand side indicates the quantity of *n*-nonane, and the ordinate on the left shows the yield of the C_9 aromatic products in per cent by weight.) The question of un-

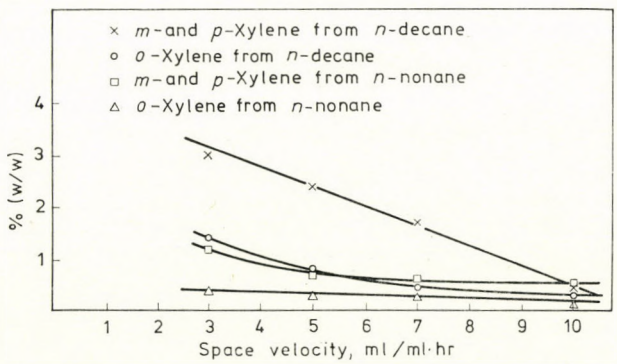

Fig. 5. Xylenes formed at different reforming space velocities

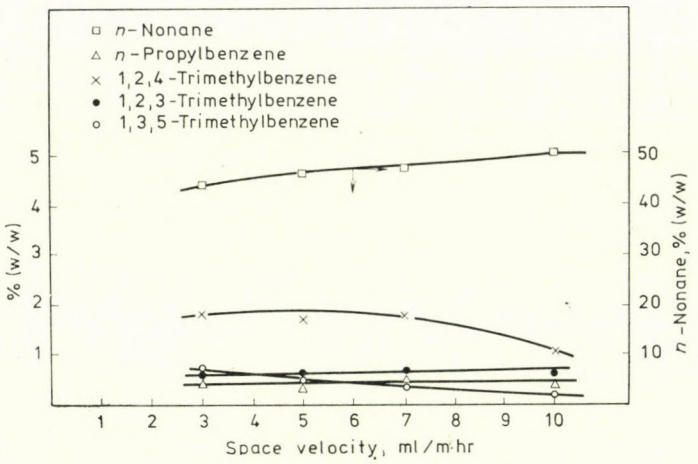

Fig. 6. Amounts of unconverted *n*-nonane and some C_9 aromatic compounds formed at different space velocities at the reforming of *n*-nonane

changed *n*-nonane has been discussed above. The yields of *n*-propylbenzene and 1,2,3-trimethylbenzene are not affected by the variation of space velocity. Since *n*-propylbenzene can be produced without isomerization by the dehydrocyclization of *n*-nonane, its formation is obviously rapid. The formation of 1,2,4-trimethylbenzene is similarly affected only by space velocities in the range of 7—10 ml/ml·hr, thus also the production of this isomer must be rather fast.

The amounts of unconverted *n*-decane and of the three trimethylbenzene isomers formed from this compounds are given in Fig. 7. The conversion of *n*-decane has been discussed above. With this starting material, lower space velocity has a greater influence on the formation of 1,2,3-trimethylbenzene than when *n*-nonane is used. In the case of the other two isomers, the effect of space velocity is very similar to that observed in the reforming of *n*-nonane;

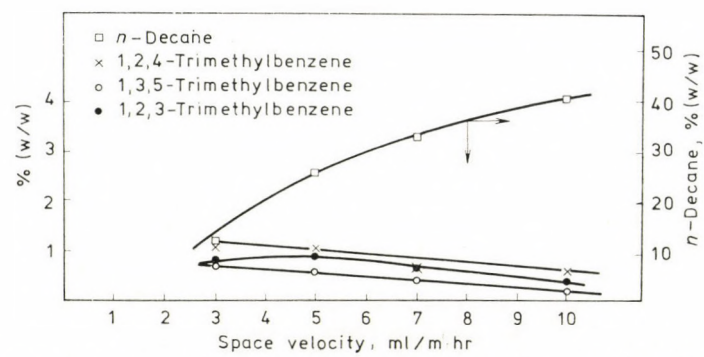

Fig. 7. Amounts of unconverted *n*-decane and the trimethylbenzenes formed at different space velocities at the reforming of *n*-decane

i.e., the quantity of the 1,2,4-isomer increases by 1.8-times, while that of the 1,3,5-isomer by about 3.5-times at the space velocities investigated. Interestingly, the amounts of trimethylbenzenes formed from *n*-decane are commensurable with those formed from *n*-nonane already at a space velocity as high as 10 ml/ml·hr, despite the fact that with *n*-decane as the starting compound dehydrocyclization must be accompanied by dealkylation to give rise to the above products. This fact suggests that dealkylation occurs relatively quickly, and the cyclization has a rate-determining role also in the formation of the aromatics having a smaller number of C-atoms than the initial compound.

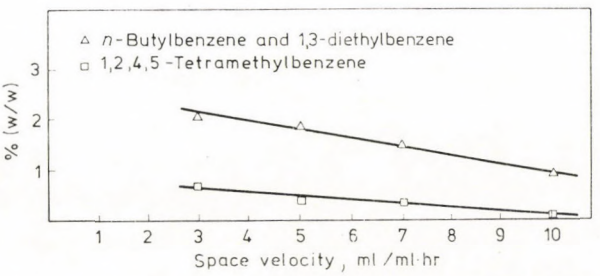

Fig. 8. Some C_{10} aromatic compounds formed at different reforming space velocities from *n*-decane

It can be seen in Fig. 8 that on reducing the space velocity, the amounts of *n*-butylbenzene, 1,3-diethylbenzene and 1,2,4,5-tetramethylbenzene increase. The enhanced formation of *n*-butylbenzene and 1,3-diethylbenzene may presumably be due to the fact that the conversion of *n*-decane is significantly affected by increased residence time. The quantity of 1,2,4,5-tetramethylbenzene increases more slowly and rather in the range of lower space velocities, since the formation of this latter compound requires significant isomerization besides dehydrocyclization.

Our experiments have shown that under the conditions of the reforming of *n*-nonane and *n*-decane on a platinum catalyst, aromatic compounds are formed in rather small quantities. However, when the conditions of reforming are more severe *i.e.* either the temperature is raised or the space velocity decreased, the formation of aromatic compounds is significantly enhanced. Some of the aromatic products have a lower number of carbon atoms than the feedstock.

REFERENCES

[1] HERRINGTON, E. F. G., RIDEAL, E. K.: Proc. Roy. Soc. **184,** 447 (1945)
[2] ROZENGART, M. I., MORTIKOV, E. S., KAZANSKY, B. A.: Dokl. Akad. Nauk SSSR **158,** 911 (1964)
[3] ROZENGART, M. I., MORTIKOV, E. S., KAZANSKY, B. A.: Dokl. Akad. Nauk SSSR **166,** 619 (1966)

[4] PAÁL, Z., TÉTÉNYI, P.: Acta Chim. Acad. Sci. Hung. **53,** 193 (1967)
[5] PAÁL, Z., TÉTÉNYI, P.: Acta Chim. Acad. Sci. Hung. **54,** 175 (1967)
[6] KAZANSKY, B. A., FADEEV, V. S., GOSTUNSKAYA, I. V.: Izv. Akad. Nauk SSSR Ser. Khim. **1971,** 677
[7] FADEEV, V. S., GOSTUNSKAYA, I. V., KAZANSKY, B. A.: Dokl. Akad. Nauk SSSR **199,** 622 (1971)
[8] KAZANSKY, B. A., LIBERMAN, A. L., BULANOVA, T. E., ALEXANYAN, V. T., STERIN, KH. E.: Dokl. Akad. Nauk SSSR **95,** 77 (1954)
[9] KAZANSKY, B. A., LIBERMAN, A. L.: Proc. VIIIth World Petroleum Congress, Moscow, 1971. Vol. 4, 395. Applied Science Publishers, London 1971.
[10] BARRON, Y., MAIRE, G., MULLER, J. M., GAULT, F. G.: J. Catal. **5,** 428 (1966)
[11] MULLER, J. M., GAULT, F. G.: J. Catal. **24,** 361 (1972)
[12] SHEPHARD, F. E., ROONEY, J. J.: J. Catal. **3,** 129 (1964)
[13] PAÁL, Z., TÉTÉNYI, P.: Kémiai Közl. **37,** 129 (1972)
[14] HETTINGER, W. P., KEITH, C. D., GRING, J. L., TETER, J. W.: Ind. Eng. Chem. **47,** 719 (1955)
[15] FOMICHOV, YU. V., GOSTUNSKAYA, I. V., KAZANSKY, B. A.: Izv. Akad. Nauk SSSR Ser. Khim. **1968,** 142
[16] DAVIS, B. H., VENUTO, P. B.: J. Catal. **15,** 363 (1969)
[17] SINFELT, J. H., ROHRER, J. C.: J. Chem. Eng. Data **8,** 109 (1963)
[18] TÉTÉNYI, P., PAÁL, Z., GUCZI, L., BABERNICS, L.: A kémia újabb eredményei (Recent Advances in Chemistry). (in Hungarian) Vol. 19, p. 19. Akadémiai Kiadó, Budapest 1974.
[19] OCKERBLOOM, N. E.: Hydrocarbon Processing **51,** No. 4, 114 (1972)
[20] SZEBÉNYI, I., SZÉCHY, G., PAP, G.: Kőolaj és Földgáz **8,** 193 (1975)
[21] MOSER, M., VAJTA, L., SZEBÉNYI, I.: Periodica Polytechnica, Chem. Eng. **15,** No. 1—2, 129 (1971)
[22] VAJTA, L.: Periodica Polytechnica, Chem. Eng. **19,** No. 1—2, 3 (1975)
[23] ACKERMANN, L., SZEBÉNYI, I., VERMES, E.: Periodica Polytechnica, Chem. Eng. **16,** 279 (1972)
[24] TA-CHUANG LO CHANG, KARR, C.: Anal. Chim. Acta **21,** 474 (1959)

Imre SZEBÉNYI
László ACKERMANN
Gábor SZÉCHY
Sándor GÖBÖLÖS

H-1521 Budapest.

INDEX

PHYSICAL AND INORGANIC CHEMISTRY

Theoretical Conformational Analysis of Methoxydichlorophosphine CH_3O-PCl_2, R. ARSHINOVA, J. P. FAUCHER, M. GRAFFEUIL, J. F. LABARRE, C. LEIBOVICI 207

Reactions of Chlorosilanes with Alkoxysilanes, I. Gas Chromatographic and Volumetric Study of the Catalytic Condensation. Connection between Reactivity and Mass-Spectrometric Fragmentation, B. CSÁKVÁRI, L. FÁBRY, P. GÖMÖRY, K. UJSZÁSZY 213

Reactions of Chlorosilanes with Alkoxysilanes, II. Mechanism of Catalysis in Chlorosilane + Alkoxysilane Type Condensations, B. CSÁKVÁRY, L. FÁBRY, P. GÖMÖRY, K. UJSZÁSZY 233

Network-Thermodynamic Approach to Chemical Kinetics, D. SINGER 255

ORGANIC CHEMISTRY

Synthesis and Study of Monosubstituted α-Formyl-Acetic Esters and Malondialdehydes, G. DÖRNYEI, M. BÁRCZAI-BEKE, B. MAJOROS, P. SOHÁR, CS. SZÁNTAY 275

Condensed *as*-Triazines, I. Synthesis of 3-Substituted Pyrido[3,4-e]-*as*-Triazines, P. BENKÓ, A. MESSMER, A. GELLÉRI, L. PALLOS 285

Condensed *as*-Triazines, II. Synthesis of Pyrido[3,2-e]-*as*-Triazine Derivatives, A. GELLÉRI, A. MESSMER, P. BENKÓ, L. PALLOS 301

CHEMICAL TECHNOLOGY

Dehydrocyclization of *n*-Nonane and *n*-Decane under the Conditions of Catalytic Gasoline Reforming, I. SZEBÉNYI, I. ACKERMANN, G. SZÉCHY, S. GÖBÖLÖS 313

Printed in Hungary

A kiadásért felel az Akadémiai Kiadó igazgatója. Műszaki szerkesztő: Zacsik Annamária

A kézirat nyomdába érkezett: 1976. V. 27. — Terjedelem: 10,50 (A/5) ív 65 ábra

76.3226 Akadémiai Nyomda, Budapest — Felelős vezető: Bernát György

ACTA CHIMICA
ТОМ 90—ВЫП. 3

РЕЗЮМЕ

Теоретический конформационный анализ метоксидихлорфосфина

Р. АРШИНОВА, Ж—П. ФОШЕ, М. ГРАФФЕИ, Ж.-Ф. ЛАБАРР и К. ЛЕЙБОВИЧИ

На основе теоретического конформационного анализа метоксихлорфосфина CH_3OPCl_2, проведенного в рамках приближения CNDO/2, было обнаружено существованиедвух предпочитаемых эквивалентных «гош» конформаций, что находится в согласии с дан ными электронной диффракции. Молекула весьма эластична около соответствующих потенциальных седловин. Сравнение расчетных и экспериментальных величин дипольных моментов решительно подтверждает существование конформаций «гош».

Реакции хлорсиланов с алкоксисиланами, I

Газово-хроматографическое и волюметрическое исследование каталитической конденсации. Связь между реактивностью и масс-спектрометрической фрагментацией

Б. БАКВАРИ, П. ГЁМЁРИ и К. УЙСАСИ

За процессом конденсации алкоксиланов с хлорсиланами следили с помощью газово-волюметрической и газово-хроматографической техник. Был исследован эффект активных и неактивных лигандов кремниевых частиц на реакционность.

Как можно заключить из скорости выделения газа при конденсации алкокси- и хлоросиланов, реактивность изменяется в зависимости от заместителей как на кислороде, так и на кремнии.

С помощью масс-спектрометрических исследований было установлено, что существует корреляция между скоростью реакции и стабильностью алкокси-группы при положительно поляризованном атоме крешния, которая изменяется параллельно с константами Гаммета алкильной части группы алкокси, т. е. с ее электронодонорной способностью. Были сделаны заключения относительно эффекта П-электронных лигандов в силикатной части на связи Si—C и Si—O—C, а также и на стерические эффекты.

Скорость конденсации алкоксиланов с хлорсиланами увеличивается в случае, если П-электронные лиганды (Vi, Ph) присоединены к атому кремния; тот же самый эффект наблюдается при увеличении электроно-донорных свойств алкильной части алкокси группы.

Реакции хлорсиланов с алкоксисиланами, II

Механизм катализа конденсации хлорсиланов с алкоксиламином

Б. ЧАКВАРИ, Л. ФАБРИ, П. ГЁМЁРИ

Были проведены исследования соединений, которые могут быть использованы как катализаторы конденсации хлорсиланов с алкоксисиланами. Обычно это кислоты Льюиса Согласно УФ спектрометрическим и рентгено-диффракционным измерениям, в присут-

ствии катализаторов γ-Fe_2O_3 и $FeCl_3$ превращение γ-$Fe_2O_3 \rightarrow FeCl_3$ начинается в твердой фазе. Железо было детектировано в растворе даже и в том случае, когда в качестве катализатора был использован γ-Fe_2O_3. Это же означает, что катализ является гомогенным, и железо растворяется в виде $[FeCl_4]^-$ в обоих случаях.

Узловой термодинамический подход к химической кинетике

Д. ЗИНГЕР

Более ранние попытки описать химическую кинетику в понятиях «химического сопротивления» с термодинамической точки зрения были не совсем адекватными. Действительная узловая модель механизма реакции должна давать ту же самую продукцию энтропии, как и чисто термодинамическая теория. Показано, что выражение для продукции энтропии можно рассматривать как продукцию энтропии физических узлов. Она состоит в основном из «гальванически» разделенных частей, относящихся к химическим, транспортным и термическим процессам, соответственно. Было показано, что матрица феноменологических коэффициентов исходной системы может быть интерпретирована как матрица импеданса контуров узлов. Правильно выбранная узловая модель, в принципе, позволяет разделить частичные процессы, протекающие с выигрышем и без выигрыша энтропии, как это указано Остером, Дезором и сотр. Было показано, каким образом, используя контурную репрезентацию, можно конструировать узловую модель сложных химических реакций — с обратимыми и необратимыми реакциями — включая также и транспортные процессы. Транспортный процесс можно рассматривать как химическую реакцию между транспортированным и нетранспортированным питанием. Это предположение позволяет рассматривать транспортные явления на основе узловой модели таким же образом, как и химические реакции.

Синтез и исследование эфиров монозамещенной γ-формилуксусной кислоты и малондиальдегидов

Г. ДЁРНЕИ, М. БАРЦАИ-БЕКЕ, Б. МАЙОРОШ, П. ШОХАР и Ч. САНТАИ

Был разработан новый метод синтеза эфиров монозамещенной α-формилуксусной кислоты (*4*) ималондиальдегидов (*5*). Соответственно замещенные производные малонового эфира (*3*) подвергались селективному восстановлению с помощью алюмогидрида лития. Была исследована таутомерия этих соединений, зависящая от растворителя, и впервые, с помощью ЯМР—H^1, была выявлена форма (E)-энол—эфира (*4c*).

Конденсированные асим-триазины, I

Синтез 3-замещенных пиридо[3,4-e]-асим-триазинов

П. БЕНКО, А. МЕССМЕР, А. ГЕЛЛЕРИ и Л. ПАЛЛОШ

Синтез Бишлера для бензо-*асим*-триазинов был распространен на получение пиридо-[3,4-e]-*асим*-триазинов. Исходный 4-хлор-3-нитропиридин был превращен с помощью ацилгидразиноов в 4-ацилгидразино-3-нитропиридины. Амины, полученные восстановлением последних, подвергались циклодегидратации, в результате чего были получены дигидропиридо[3,4-e]-*асим*-триазины. Окисление последних приводит к ароматическим конечным продуктам.

Конденсированные асим-триазины, II

Синтез производных пиридо[3,2-3]-асим-триазина

А. ГЕЛЛЕРИ, А. МЕССМЕР, П. БЕНКО и Л. ПАЛЛОШ

Синтез Бишлера для бензо-*асим*-триазина был распространен на получение пиридо-[3,2-е]-*асим*-триазинов. Данный метод в общем случае применим и для таких производных, которые не могут быть получены методом Льюиса и Шеферда. Была исследована кристаллическая диморфия некоторых представителей промежуточных 2-ацилгидразино-3-нитропиридинов.

Исследование дегидроциклизации н-нонана и н-декана в условиях каталитического риформинга бензина

И. СЕБЕНИ, Л. АҚЕРМАН, Г. СЕЧИ и Ш. ГЁБЁЛЁШ

Превращения н-нонана и н-декана были исследованы в условиях промышленного риформинга бензина на катализаторе, содержащем платину, в интервале температур 480—530°С и при объемной скорости 3—10 мл/мл/час. Исследования проводились в микрореакторе при давлении 30 кГ/см². Из обоих исходных продуктов образовалось лишь несколько %-ов ароматических соединений; однако, содержание ароматики значительно повышалось с увеличением температуры и уменьшением объемной скорости. При 530°С из н-нонана и н-декана образуется 1,2,4-триметилбензол с выходами 3,7 и 2,1 вес%, соответственно. Из н-нонана с наибольшим выходом образуется единственное ароматическое соединение 1,2,4-триметилбензол, а из н-декана с относительно высоким выходом обрезуется также ксилол, н-бутил- и 1,3-диэтилбензол. Образование ароматических соединений с числом углеродных атомов, меньшим чем в исходном соединении, наблюдалось как в случае н-нонана, так и в случае н-декана, что, однако, более характерно для превращений н-декана. Повышение температуры оказывало влияние на протекающие процессы для обоих исходных соединений, а уменьшение объемной скорости в изученном интервале скорее лишь на превращения н-декана.

The Acta Chimica publish papers on chemistry, in English, German, French and Russian.

The Acta Chimica appear in volumes consisting of four parts of varying size, 4 volumes being published a year.

Manuscripts should be addressed to

Acta Chimica
H-1521 Budapest, Hungary

Correspondence with the editors should be sent to the same address.

The rate of subscription is $ 32,00 a volume.

Orders may be placed with "*Kultúra*" Foreign Trade Company for Books and Newspapers (1389 Budapest 62, P.O.B. 149 Account No. 218 10990) or with representatives abroad.

Les Acta Chimica paraissent en français, allemand, anglais et russe et publient des mémoires du domaine des sciences chimiques.

Les Acta Chimica sont publiés sous forme de fascicules. Quatre fascicules seront réunis en un volume (4 volumes par an).

On est prié d'envoyer les manuscrits destinés à la rédaction à l'adresse suivante:

Acta Chimica
H-1521 Budapest, Hungary

Toute correspondance doit être envoyée à cette même adresse.

Le prix de l'abonnement est de $ 32,00 par volume.

On peut s'abonner à l'Entreprise pour le Commerce Extérieur de Livres et Journaux «*Kultúra*» (1389 Budapest 62, P.O.B. 149 Compte-courant No. 218 10990) ou à l'étranger chez tous les représentants ou dépositaires.

«*Acta Chimica*» издают трактаты из области химической науки на русском, французском, английском и немецком языках.

«*Acta Chimica*» выходят отдельными выпусками разного объема. 4 выпуска составляют один том. 4 тома публикуются в год.

Предназначенные для публикации рукописи следует направлять по адресу:

Acta Chimica
H-1521 Budapest, BHP

По этому же адресу направлять всякую корреспонденцию для редакции.

Подписная цена — $ 32,00 за том.

Заказы принимает предприятие по внешней торговле книг и газет «*Kultúra*» (1389 Budapest 62, P.O.B. 149 Текущий счет № 218 10990) или его заграничные представительства и уполномоченные.

Reviews of the Hungarian Academy of Sciences are obtainable at the following addresses:

AUSTRALIA

C. B. D. Library and Subscription Service
Box 4886, G. P. O.
Sydney N. S. W. 2001

Cosmos Bookshop
145 Acland St.
St. Kilda 3182

AUSTRIA

Globus
Höchstädtplatz 3
A—1200 Wien XX

BELGIUM

Office International de Librairie
30 Avenue Marnix
1050-Buxelles

Du Monde Entier
162 Rue du Midi
1000—Bruxelles

BULGARIA

Hemus
Bulvar Ruszki 6
Sofia

CANADA

Pannonia Books
P. O. Box 1017
Postal Station "B"
Toronto, Ont. M5T 2T8

CHINA

C N P I C O R
Periodical Department
P. O. Box 50
Peking

CZECHOSLOVAKIA

Mad'arská Kultura
Národní třida 22
115 66 Praha

PNS Dovoz tisku
Vinohradská 46
Praha 2

PNS Dovoz tlače
Bratislava 2

DENMARK

Ejnar Munksgaard
Nörregade 6
DK—1165 Copenhagen K

FINLAND

Akateeminen Kirjakauppa
P. O. Box 128
SF-00101 Helsinki 10

FRANCE

Office International de Documentation et Librairie
48, Rue Gay-Lussac
Paris 5

Librairie Lavoisier
11 Rue Lavoisier
Paris 8

Europeriodiques S. A.
31 Avenue de Versailles
78170 La Celle St. Cloud

GERMAN DEMOCRATIC REPUBLIC

Haus der Ungarischen Kultur
Karl-Liebknecht-Strasse 9
DDR—102 Berlin

Deutsche Post
Zeitungsvertriebsamt
Strasse der Pariser Kommüne 3—4
DDR—104 Berlin

GERMAN FEDERAL REPUBLIC

Kunst und Wissen
Erich Bieber
Postfach 46
7 Stuttgart 5

GREAT BRITAIN

Blackwell's Periodicals
P. O. Box 40
Hythe Bridge Street
Oxford OX1 2EU

Collet's Holdings Ltd.
Denington Estate
London Road
Wellingborough Northants NN8 2QT

Bumpus Haldane and Maxwell Ltd.
5 Fitzroy Square
London W1P 5AH

Dawson and Sons Ltd.
Cannon House
Park Farm Road
Folkestone, Kent

HOLLAND

Swets and Zeitlinger
Heereweg 347b
Lisse

Martinus Nijhoff
Lange Voorhout 9
The Hague

INDIA

Hind Book House
66 Babar Road
New Delhi 1

India Book House
Subscription Agency
249 Dr. D. N. Road
Bombay 1

ITALY

Santo Vanasia
Via M. Macchi 71
20124 Milano

Libreria Commissionaria Sansoni
Via Lamarmora 45
50121 Firenze

JAPAN

Kinokuniya Book-Store Co. Ltd.
826 Tsunohazu 1-chome
Shinjuku-ku
Tokyo 160—91

Maruzen and Co. Ltd.
P. O. Box 5050
Tokyo International 100—31

Nauka Ltd.-Export Department
2—2 Kanda
Jinbocho
Chiyoda-ku
Tokyo 101

KOREA

Chulpanmul
Phenjan

NORWAY

Tanum-Cammermayer
Karl Johansgatan 41—43
Oslo 1

POLAND

Węgierski Instytut Kultury
Marszalkowska 80
Warszawa

BKWZ Ruch
ul. Wronia 23
00—840 Warszawa

ROUMANIA

D. E. P.
Bucureşti

Romlibri
Str. Biserica Amzei 7
Bucureşti

SOVIET UNION

Sojuzpechatj — Import
Moscow

and the post offices in each town
Mezhdunarodnaya Kniga
Moscow G—200

SWEDEN

Almaqvist and Wiksell
Gamla Brogatan 26
S—101 20 Stockholm

A. B. Nordiska Bokhandeln
Kunstgatan 4
101 10 Stockholm 1 Fack

SWITZERLAND

Karger Libri AG.
Arnold-Böcklin-Str. 25
4000 Basel 11

USA

F. W. Faxon Co. Inc.
15 Southwest Park
Westwood, Mass. 02090

Stechert-Hafner Inc.
Serials Fulfillment
P. O. Box 900
Riverside N. J. 08075

Fam Book Service
69 Filth Avenue
New York N. Y. 1003

Maxwell Scientific International Inc.
Fairview Park
Elmsford N. Y. 10523

Read More Publications Inc.
140 Cedar Street
New York N. Y. 10006

VIETNAM

Xunhasaba
32, Hai Ba Trung
Hanoi

YUGOSLAVIA

Jugoslavenska Knjiga
Terazije 27
Beograd

Forum
Vojvode Mišića 1
21000 Novi Sad

6. XII. 1976

Index: 26.007

ACTA CHIMICA

ACADEMIAE SCIENTIARUM HUNGARICAE

ADIUVANTIBUS

V. BRUCKNER, GY. DEÁK, K. POLINSZKY,
E. PUNGOR, G. SCHAY, Z. G. SZABÓ

REDIGIT

B. LENGYEL

TOMUS 90 FASCICULUS 4

AKADÉMIAI KIADÓ, BUDAPEST

1976

ACTA CHIM. (BUDAPEST) ACASA 2 90 (4) 325–432 (1976)

ACTA CHIMICA

A MAGYAR TUDOMÁNYOS AKADÉMIA KÉMIAI TUDOMÁNYOK OSZTÁLYÁNAK IDEGEN NYELVŰ KÖZLEMÉNYEI

SZERKESZTI

LENGYEL BÉLA

TECHNIKAI SZERKESZTŐK

DEÁK GYULA és HARASZTHY-PAPP MELINDA

Az Acta Chimica német, angol, francia és orosz nyelven közöl értekezéseket a kémiai tudományok köréből.

Az Acta Chimica változó terjedelmű füzetekben jelenik meg, egy-egy kötet négy füzetből áll. Évente átlag négy kötet jelenik meg.

A közlésre szánt kéziratok a szerkesztőség címére (1521 Bp., Műegyetem) küldendők. Ugyanerre a címre küldendő minden szerkesztőségi levelezés. A szerkesztőség kéziratokat nem ad vissza.

Megrendelhető a belföld számára az Akadémiai Kiadónál (1363 Budapest, pf. 24. Bankszámla 215 11488), a külföld számára pedig a Kultúra Könyv- és Hírlap-Külkereskedelmi Vállalatnál (1389 Budapest 62, pf. 149. Bankszámla: 218 10990) vagy külföldi képviseleteinél és bizományosainál.

Die Acta Chimica veröffentlichen Abhandlungen aus dem Bereich der chemischen Wissenschaften in deutscher, englischer, französischer und russischer Sprache.

Die Acta Chimica erscheinen in Heften wechselnden Umfanges. Vier Hefte bilden einen Band. Jährlich erscheinen 4 Bände.

Die zur Veröffentlichung bestimmten Manuskripte sind an folgende Adresse zu senden:

Acta Chimica
H-1521 Budapest

An die gleiche Anschrift ist auch jede für die Redaktion bestimmte Korrespondenz zu richten. Abonnementpreis pro Band: $ 32.00.

Bestellbar bei dem Buch- und Zeitungs-Außenhandels-Unternehmen "*Kultúra*" (1389 Budapest 62, P. O. B. 149. Bankkonto Nr. 218 10990) oder bei seinen Auslandsvertretungen und Kommissionären.

Acta Chimica Academiae Scientiarum Hungaricae, Tomus 90 (4), pp. 325—332 (1976)

STUDIES ON SOME METAL COMPLEXES WITH KETO-ANILS AS LIGANDS, I

(SHORT COMMUNICATION)

R. K. UPADHYAY* and V. P. SINGH

(Department of Chemistry N. R. E. C. College, Khurja **203131** *India)*

Received April 8, 1975

In revised from January 2, 1976

Introduction

UPADHYAY *et. al.* [1—4] recently studied the interaction of *p*-dimethylaminoanils of, 3-phenanthryl glyoxal and 4-hydroxyl 1-naphthyl glyoxal with some transition metal ions in the solution. The complexes were isolated and characterized by analysis, conductometrically and spectrophotometrically. In the present communication various aspects not investigated to date as magnetic, infrared spectral and electronic spectral of few transition metal complexes are reported. Based on these studies an octahedral stereochemistry may be assigned to Cr(III), Mn(II), Fe(III) and Pt(IV) complexes whereas the complexes of Pd(II) and Cu(II) are typical square-planar. However, the Co(II) complex is tetrahedral.

Infrared spectral studies show that both the ligands offer carbonyl oxygen and azomethine nitrogen atoms for coordination, whereas hydroxyl group of *p*-dimethyl aminoanil of 4-hydroxyl 1-naphthyl, being at a more remote position than that of former adjacent groups, does not participate in chelation. Furthermore, this group would not involve in coordination even in meta position owing to comparatively lower donor ability of its oxygen than that of a carbonyl group.

Experimental

Both the ligands, *p*-dimethylaminoanil of 3-phenanthryl glyoxal (A) and *p*-dimethylaminoanil of 4-hydroxyl 1-naphthyl glyoxal (B) and their complexes were prepared [1—3,5] by using B. D. H. or J. M. (London) reagents.

Magnetic measurements were made on the solid products with GOUY's balance. Electronic spectral observations (optical density) were recorded with Beckmann D. U. spectrophotometer at 293 °K. All infrared spectra were recordded in Nujol mulls. Some spectra were recorded between 4000 cm^{-1} and 200

Table I

Magnetic and electronic spectral characteristics of complexes

Complex	Medium	Observed bands cm^{-1}	Assignments	10 Dq cm^{-1}	Racah's parameters cm^{-1}	Nephel-auxetic ratio β	LFSE K. cals/mole	μeff. B. M.
CrB_2Cl_3	Dioxane	12 658		17 094	$B = 697.7$	0.68	58.60	3.71
		15 152			$C = 2581.5$			
		17 094	$^4A_{2g}(F) \rightarrow {}^4T_{2g}(F)$					
		18 519	$\rightarrow {}^4T_{1g}(F)$					
		25 641	$\rightarrow {}^4T_{1g}(P)$					
MnA_2Cl_2	Acetone	12 500	$^6A_{1g} \rightarrow {}^4T_{1g}(G)$	5 730	$B = 521$	0.54	—	5.74
		12 988	$\rightarrow {}^4T_{2g}(G)$		$C = 1824$			
		13 333	$\rightarrow {}^4E_g(G)$					
		14 707	$\rightarrow {}^4T_{2g}(D)$					
		16 129	$\rightarrow {}^4E_g(D)$					
		17 544	$\rightarrow {}^4T_{1g}(P)$					
MnB_2Cl_2	Dioxane	10 417	$^6A_{1g} \rightarrow {}^4T_{1g}(G)$	4 774	$B = 434.0$	0.45	34.72	5.77
		11 364	$\rightarrow {}^4T_{2g}(G)$		$C = 1519.14$			
		12 121	$\rightarrow {}^4E_g(G)$					
		15 267	$\rightarrow {}^4A_{2g}(F)$					
		19 231 }	Charge transfer					
		21 739 }	$L \rightarrow M$					
FeB_2Cl_3	Dioxane	14 706	$^6A_{1g} \rightarrow {}^4T_{1g}(G)$	6 741	$B = 612.8$	0.47	—	5.79
		17 241	$\rightarrow {}^4T_{2g}(G)$					
		18 519	$\rightarrow {}^4E_g(G)$					
		21 739	$\rightarrow {}^4T_{2g}(D)$					

$CoBCl_2$	Dioxane	17 241 18 519 21 739	$^4A_2(F) \rightarrow {}^4T_1(P)$	—	—	—	—	4.70
$CuACl_2$	Acetone	11 364 12 410 27 027	$^2B_{1g} \rightarrow {}^2A_{1g}$ $\rightarrow {}^2E_g$ Charge transfer $L \rightarrow M$	—	—	—	—	1.84
$CuBCl_2$	Dioxane	14 706 17 241 20 000 22 727 26 316 29 412	$^2B_{1g} \rightarrow {}^2A_{1g}$ $\rightarrow {}^2E_g$ Charge transfer $L \rightarrow M$	—	—	—	—	1.89
$PdACl_2$	Acetone	14 925 16 529 24 096 27 778	$^1A_{1g} \rightarrow {}^1B_{1g}$ $\rightarrow {}^1E_g$ $\rightarrow {}^1A_{2u}$ Charge transfer $\rightarrow {}^1E_u$ L $\rightarrow M$	—	—	—	—	Diamagnetic
PtA_2Cl_4	Ethanol	12 625 16 129 17 241	$^1A_{1g} \quad {}^3T_{1g}$ $\rightarrow {}^1T_{1g}$ $\rightarrow {}^1T_{2g}$	16 976	$B = 424$	—	—	Diamagnetic

Table II

I. R. Frequencies with their tentative

A	MnA_2Cl_2	$CuACl_2$	$PdACl_2$	$PtACl_4$	B	CrB_2Cl_3
3219 m	3333 s	3333 s	3448 s	3521 s	3333 m	3350 m
2857 w	—	—	2907 s	2841 s	3030 m	3080 m
—	—	—	—	—	2899 m	2800 m
—	—	—	—	—	2778 m	—
1653 s	1608 s	1595 s	1595 s	1608 s	1668 s	1625 m
1613 s	1511 s	1505 s	1508 s	1502 s	1612 s	1600 m
1575 s	—	—	—	—	1575 s	1540 m
1515 s	1537 w	1435 s	1437 s	1449 s	1527 s	1490 m
1439 m	—	—	—	—	—	—
—	—	—	—	—	1450 s	1440 m
1342 s	1351 m	—	1346 s	—	1360 s	1380 m
1282 s	—	1299 s	—	1299 s	—	—
—	—	—	—	—	1275 s	1270 w
1227 s	1235 w	—	1235 s	1235 s	1235 s	1230 m
1170 s	1188 w	1176 m	1179 s	1178 s	1190 s	1170 w
1103 w	1096 w	1095 m	1092 s	—	—	—
1081 w	1062 w	—	1062 m	—	1070 m	1060 w
1034 w	—	1035 m	—	1018 w	1012 m	1005 m
948 m	945 w	—	943 s	—	922 m	—
905 w	901 w	897 m	—	899 w	900 m	—
870 w	—	—	867 w	—	—	—
820 s	816 w, b	817 s	813 s, b	817 w	821 s	800 w
752 w	746 w	746 s	746 s, b	752 w, b	772 s	—
738 m	—	—	—	—	—	—
719 w	702 w	704 w	703 w	714 w	—	—
					—	500 m
					—	350 s
					—	265 s, b

cm^{-1} on a Beckmann infrared spectrophotometer 621 and some with infracord. Magnetic and electronic spectral data are given in Table I and i. r. data is noted in Table II.

Results and discussion

Analytical results show 1 : 1 metal-to-ligand stoichiometry in Co(II)-B, Cu(II)-A, Cu(II)-B, Pd(II)-A and Pt(IV)-A systems while in Cr(III)-B, Mn(II)-A, Mn(II)-B and Fe(III)-B complexes it is 1 : 2. Molar conductance measurements show that Cr(III) and Fe(III) chelates are 1 : 1 electrolytes and all the other chelates are non-electrolytes.

The magnetic moment value 3.71 BM of the Cr(III) complex is very close to the spin-only value 3.88 BM. The agreement in experimental and spin-only values infers d^3 octahedral stereochemistry of the Cr(III) complex. Five bands at 12 658 cm^{-1}, 15 152 cm^{-1}, 17 094 cm^{-1}, 18 519 cm^{-1} and 25 641 cm^{-1} have been observed in the electronic spectrum of the complex. First two bands at 12 658 cm^{-1} and 15 152 cm^{-1} which are weak and may

assignment for ligands and complexes

MnB_2Cl_2	FeB_2Cl_3	$CoBCl_4$	$CuBCl_2$	Assignment
3350 m	3350 s	3440 s	3330 s	C—H str. (alkylene) and/or O—H str. (phenolic)
3020 m	3100 m	2900 m	—	C—H str. (aromatic)
2840 s	2860 m	—	2910 m	
—	—	—	—	
1630 w	1640 m	1650 m	1650 s	C = O str.
1590 m	1595 s	1595 s	1600 s	C = N str.
1550 m	1550 m	—	—	
1480 m	—	1490 s	1490 s	C = C str.
—	—	—	—	
1440 w	1440 m	1450 m	1450 s	O—H bending + C—O str.
1380 w	1360 m	—	—	CH_3 symm. bending
—	—	—	—	
1270 w	1260 w	1270 w	1265 w	O—H bending + C—O str.
1225 w	1230 m	1230 m	1230 m	
1150 m	1160 m	1155 m	1175 m	
—	—	—	—	C—N str. (aliphatic)
—	—	1050 m	1060 w	Benzene ring breathing
—	1000 w	1000 w	—	
—	—	—	—	
—	—	—	—	
805 w	810 w	800 w	800 w	C—H bending (two adjacent H atoms) + 1,4 disubstitution
760 w	770 m	750 s	760 s	C—H bending (four adjacent H atoms)
—	—	—	—	
—	—	—	—	C—H out of plane bending
470 m	500 m	480 m	500 m	M—N str.
342 s	345 s	348 s	320 s	M—Cl str.
280 s, b	295 s, b	270 s, b	280 s, b	M—O str.

s, strong; m, medium; w, weak; b, broad; M, metal

be best fitted to spin-forbidden transitions. Comparatively strong bands observed at 17 094 cm^{-1} and 18 519 cm^{-1}, on the basis of TANABE and SUGANO. [6] diagram predictions may be assigned to one-electron jumps from ground term $^4A_{2g}$ (F) to excited quartet terms $^4T_{2g}$ (F) and $^4T_{1g}$ (F), respectively. The band appeared at 25 641 cm^{-1} only as a shoulder on large charge transfer band has also been assigned to ligand field transition $^4T_{1g}$ (P). The ligand field splitting energy (10 Dq) similar to the energy of $^4A_{2g}$ $(F) \rightarrow {}^4T_{2g}$ (F) transition comes out to be 17 094 cm^{-1}. 'B' has been calculated from the ratio Dq/B (2.45) and its value is noted in Table I. C, B and LFSE have also been evaluated.

The magnetic moment values of spin-free d^5 octahedral Mn(II) and Fe(III) complexes reported [7—9] are 5.70—6.05 BM, very close to the spin-only value 5.92 BM. The magnetic moments 5.74 BM, 5.77 BM and 5.79 BM of all the three Mn(II) and Fe(III) complexes under study, respectively, are in fair agreement with the values reported earlier and therefore suggest

d^5 spin-free octahedral metal ion configuration in the complexes. In the electronic spectrum of each product all the bands have been observed in the visible region. The first two bands may only be fitted best to the quartet excited terms $^4T_{1g}$ (*G*) and $^4T_{2g}$ (*G*), respectively. Other bands with appropriate assignments are noted in Table I. 10 *Dq* and *B* for the complexes have been calculated from the equations $^4T_{1g}$ (*G*)/*B* = 24.0 and *Dq*/*B* = 1.1. Other ligand field parameters like *C*, β and *LFSE* have also been calculated by usual methods.

The observed magnetic moment of Co(II) complex 4.70 BM, not very different from the reported [9] values 4.30—5.20 BM for d^7 tetrahedral complexes suggests it spin-free d^7 tetrahedral stereochemistry. In the electronic spectrum only three peaks have been observed although only the first has been identified with certainty and assigned to transition $^4A_2$ (*F*) → $^4T_1$ (*P*). The remaining bands obtained at 18 519 cm^{-1} and 21 739 cm^{-1} may only be spinforbidden.

Cu(II) generally forms square-planar paramagnetic complexes. The magnetic moments of the Cu(II) complexes are 1.84 BM and 1.89 BM, respectively, very close to spin-only value 1.73 BM. These results reveal that experimental products are square-planar involving spinfree d^9 metal ion configuration in the electronic spectra of the products bands at 11 364 cm^{-1}, 12 410 cm^{-1} (Cu(II)-*A* and at 14 706 cm^{-1}, 17 241 cm^{-1} Cu(II)-*B* have been assigned to the *d–d* transition $^2A_{1g}$, ^2E_g, respectively, from the ground term $^2B_{1g}$. The last high-energy band at 27 027 cm^{-1} in Cu(II)-*A* complex accompanied with two shoulders separated by 2400 cm^{-1} and the last high-energy two bands separated by 3096 cm^{-1} in Cu(II)-*B* complex, on the basis of GREY and BALHAUSEN discussion [10] on charge transfer bands these are ligand → metal charge transfer bands.

Pd(II) generally forms square-planar diamagnetic complexes. The complex studied is also diamagnetic and square-planar involving spin-paired d^8 metal ion configuration. Four bands have been observed at 14 925 cm^{-1}, 16 529 cm^{-1}, 24 096 cm^{-1} and 27 778 cm^{-1} in the electronic spectrum of the complex. The first two bands are spin-allowed *d–d* transitions corresponding to one-electron jumps $^1A_{1g} \rightarrow {}^1B_{1g}$ (14 925 cm^{-1}), $^1A_{1g} \rightarrow {}^1E_g$ (16 529 cm^{-1}). On the basis of the GREY and BALHAUSEN discussion [10] on charge transfer bands, the latter two bands 3682 cm^{-1} apart are ligand → metal charge transfer bands and be assigned to transitions $^1A_{1g} \rightarrow {}^2A_{2u}$ (24 096 cm^{-1}) and $^1A_{1g} \rightarrow {}^1E_u$ (27 778 cm^{-1}).

Magnetic moment 0.53 BM of the Pt(IV) complex corresponding to spin-only value 0.00 BM is fairly attributable to its diamagnetic nature and d^6 octahedral stereochemistry. In the electronic spectrum of the complex three bands have been observed which on the basis of TABANE and SUGANO [6] diagram predictions may be assigned to ligand field transitions $^3T_{1g}$, $^1T_{1g}$ $^1T_{2g}$, respectively, from the found term $^1A_{1g}$. 10 *Dq* and *B* were calculated by using equations $^1T_{1g}/B = 38$ and $Dq/B = 4$.

I. R. Studies

The infrared frequencies with tentative assignment [11—14] for the ligands and complexes are given in Table II. A comparison of i. r. data of each ligand with that of its complexes reveals that some of the stretching bands of the ligands are perturbed on complexation. A number of important structural informations about the ligands and complexes are obtained from the study of these shifts in frequencies.

In the i. r. spectra of ligands, strong absorption bands at 1653 cm^{-1} and 1613 cm^{-1} (*A*), and at 1668 cm^{-1} and 1612 cm^{-1} (*B*) corresponding to stretching vibrations of C = O (carbonyl) and C = N (azomethine) groups, respectively, of the ligands have been observed at lower values in the complexes. The lowering of these frequencies shows that carbonyl and azomethine groups, are participating in complexation. New bands appeared in the *B* ligand complexes at 265—295 cm^{-1} and at 470—500 cm^{-1}, fairly attributable to metal–oxygen and metal–nitrogen stretching vibrations, respectively, support the above conclusion and also show with certainty that oxygen and nitrogen atoms are the coordination centres. The bands observed in the range from 1439 cm^{-1} to 1575 cm^{-1} in the spectra of free ligands, assigned to the C = C stretching vibrations (aromatic) have been perturbed on complexation. This perturbation in frequency of C = C stretching vibrations, (aromatic) indicates conjugation in the ligand during interaction with metal ions. The shift in the frequency for 1,4 disubstitution (*p*- substitution) from 820 cm^{-1} in ligand *A* and from 821 cm^{-1} in ligand *B* to lower values in their respective complexes indicates only the possibility of change of benzenoid structure of ligands to quinonoid on chelation.

Very little disturbance in the ligand bands observed at 3333 cm^{-1}, 1450 cm^{-1} and 1275 cm^{-1} corresponding to O–H stretching and O–H bending vibrations, respectively, attributable only to the structural change during complexation, suggests that phenolic group does not particpate in the ligand–metal interaction.

On the basis of above studies the possible structures of the ligand and complexes assigned are as follows:

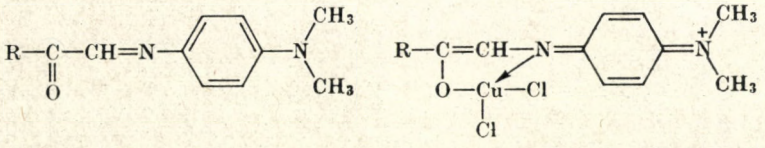

Ligand (Benzenoid) Complex (Quinonoid)

where R = Phenanthrene or (hydroxyl) naphthylene nucleus

*

We owe deep sense of gratitute to Prof. J. P. VAJPAI, D. S. College, Aligarh and to friends who have helped in the work. Authors are also indebted to the Principal, Dr. P. C. GUPTA, N. R. E. C. College, Khurja, 203131 (India) for providing the adequate facilities.

REFERENCES

[1] UPADHYAY, R. K., SINGH, V. P., SHARMA, S. C.: J. Indian Chem. Soc. **51,** 781 (1974)
[2] UPADHYAY, R. K. SAXENA, R. C.: Indian J. Chem. **11,** 697 (1973)
[3] UPADHYAY, R. K., BANSAL, R. R.: J. Indian Chem. Soc. (in press)
[4] UPADHYAY, R. K., SINGH, V. P.: J. Indian Chem. Soc. **51,** 832 (1974)
[5] UPADHYAY, R. K., SINGH, V. P., VAJPAI, U.: J. Chromatogr. **93,** 494 (1974)
[6] TANABE, Y., SUGANO, S.: J. Phys. Soc., Japan 4, 293 (1949)
[7] FIGGIS, B. N.: Introduction to Ligand Fields, Interscience, London (1966)
[8] RASTOGI, D. K.: Ph. D. Thesis, Agra University, Agra (1970)
[9] EARNSHAW, A.: Introduction to Magnetochemistry, Academic Press, London (1968)
[10] GREY, H. B., BALHAUSEN, C. J.: J. Amer. Chem. Soc. **85,** 260 (1963)
[11] DYER, J. R.: Applications of Absorption Spectrosocopy of Organic Compounds, Prentice-Hall of India Pvt. Ltd., New Delhi (1969)
[12] SAXENA, R. N., PANDAY, K. K.: J. Indian Chem. Soc. **49,** 782 (1972)
[13] NAKAMOTO, K.: Infrared Spectra of Inorganic and Coordination Compounds, John Wiley, New York (1968)
[14] UPADHYAY, R. K., SINGHAL, M. L., SAXENA, A. K., PRASAD, R.: Acta Chim. (Budapest) **83,** 299 (1974)

R. K. UPADHYAY
V. P. SINGH
57 Chhatta Street, Khurja 203131, India

Acta Chimica Academiae Scientiarum Hungaricae, Tomus 90 (4), pp. 333—344 (1976)

ELECTROCHEMICAL STUDY OF PALLADIUM–COPPER CATALYSTS

T. MALLÁT, J. PETRÓ, É. POLYÁNSZKY and T. MÁTHÉ

(Research Group of Organic Chemical Technology, Hungarian Academy of Sciences, Technical University, Budapest)

Received July 28, 1975

A study was made of the correlations between the composition, hydrogen sorption and catalytic activity of Pd–Cu powder catalysts containing 0, 10, 20, 30 or 40 at. % copper, prepared from alkaline medium by hydrogenation.

Galvanostatic measurements were made in 1 *N* sodium hydroxide, and potentiodynamic measurements in 1 *N* sulfuric acid, at room temperature. The activities of the catalysts were measured in liquid-phase hydrogenation at 25° and 1 atm.

It was found that as a result of the incorporation of copper the sorbed hydrogen became more homogeneous and its bond energy decreased. For Cu contents of 0—20 at. % there was also a considerable decrease in the quantity of dissolved hydrogen, while for 20—40 at. % Cu the decrease was primarily in the adsorbed hydrogen. Study of hydrogen sorption indicates that 20 at. % Cu is probably the concentration above which the alloy no longer dissolves, but only adsorbs hydrogen.

Copper brought about a change in the activity of the palladium catalyst in the hydrogenation of the double bond and the carbonyl group.

No-homogeneous solid solution was formed on the surface of the Pd–Cu catalyst grains, but the copper partially dissolved in the palladium, and partially produced new, intermetallic phases with the palladium.

Introduction

Alloys of the elements of column 3 of group VIII and of the metals of group I/B are equally important theoretically and practically in catalytic hydrogenation. The changes arising in the catalytic properties as a result of alloying can be explained in accordance with the electron theory by the interaction of the *s* electrons of Cu, Ag or Au and the partially filled *d* bands of Ni, Pd or Pt. Many authors have pointed out that there is some correlation between the activity or the activation energy and the degree of occupation of the *d* band. According to BOND [1], the correlation can be explained by a change in the bond strength of chemisorption.

KARPOVA and TVERDOVSKII [2] used a galvanostatic method to investigate hydrogen sorption in 1 N sulfuric acid on electrolytically deposited Pd—Cu alloys. They found that Cu decreases the dissolution of hydrogen and the metal–hydrogen bond energy. Above a Cu content of 26 at. %, hydrogen did not dissolve in the alloy.

SOKOLSKII *et al.* [3] investigated Pd—Cu catalysts in liquid-phase hydrogenation. In the hydrogenations of dimethylethynyl carbinol and maleic

acid the activity decreased only above 60 at. % Cu, whereas in the hydrogenation of phenylacetylene the activity was maximum at 10 at. % Cu, and subsequently decreased.

Many references are to be found with regard to the selectivity-enhancing effect of the Cu additive [3,4].

In the course of our investigations we attempted to establish what correlations exist between the composition and the hydrogen sorption, and also the liquid-phase catalytic activity, in the case of Pd–Cu powder catalysts. The hydrogen sorption was studied by galvanostatic and potentiodynamic methods. These investigations are closely connected with our earlier electrochemical measurements on Pd powder catalysts [5].

Experimental

Pd—Cu catalysts containing 0, 10, 20, 30 or 40 at. % Cu were prepared from alkaline medium by reduction with hydrogen. 200 ml aqueous solution of palladium chloride and copper sulfate (in appropriate proportions), containing 0.02 g-atom metal, was poured with stirring into 400-ml sodium hydrogen carbonate solution (30 g/l) at 60°. After stirring for 30 min at 60°, the jointly deposited metal hydroxides were hydrogenated at 1 atm at room temperature. Filtration and a 4-hour washing with distilled water were followed by drying of the catalyst to constant weight in vacuum at room temperature.

The galvanostatic measurements were carried out in 1 *N* sodium hydroxide at room temperature, with 10 mg catalyst and a current of 2 mA. The previously described [6] three-electrode cell was used in the examinations: the measuring and auxiliary electrodes were of smooth Pt sheet, while the reference electrode was platinized Pt/H_2. The catalyst was first saturated with hydrogen by cathodic polarization, and the anodic curve was then recorded.

The potentiodynamic investigations were made in 1 *N* sulfuric acid at room temperature. Prior to measurement, the sample was saturated with hydrogen by shaking in distilled water, and was then transferred onto the measuring electrode under the liquid. The above-mentioned cell was employed for the measurement.

The (apparent) activities of the catalysts were measured in liquid-phase hydrogenation at 1 atm and 25 °C. 100 mg catalyst was saturated with hydrogen while being shaken in 7 ml 90% ethanol, and then 2 ml of an ethanolic solution containing 0.002 mol acetophenone or sugenol was injected into the flask. The activity was regarded as the consumption of hydrogen in unit time, extrapolated to the initial time, referred to 1 g catalyst or 1 g Pd.

Results and discussion

In the course of the galvanostatic measurements, primarily hydrogen sorption was examined, in 1 *N* sodium hydroxide. The approximate value of the resistance polarization (determined by the current-interruption method) was taken into consideration in the plotting of the curves.

The amount of hydrogen adsorbed was determined by the method of BURSHTEIN [7], according to which adsorption is negligible compared with the large amount of hydrogen dissolved in the palladium between 0 and 90 mV, whereas dissolution is negligible in comparison to adsorption from 90 to 300—400 mV. In our measurements, therefore, the first 'step' of the charge curve was taken as proportional to dissolved hydrogen, and the second 'step' to

adsorbed hydrogen. Subsequently too the hydrogen range was divided into two parts with this approximation, but this does not mean that there is no adsorption in the dissolved hydrogen range, and vice versa.

Table I

Hydrogen contents of Pd–Cu catalysts, determined by galvanostatic method

Copper content (at. %)	Total hydrogen (ml/g)	Adsorbed hydrogen (ml/g)	Dissolved hydrogen (ml/g)
0	99.8	12.9	86.9
10	62.0	13.6	48.5
20	20.4	13.3	7.1
30	11.0	5.9	5.1
40	8.8	4.3	4.5

Table I gives the amounts of adsorbed, dissolved and total hydrogen, determined from the charge curve, as functions of the composition. With the incorporation of copper the amount of adsorbed hydrogen did not change initially, while the much larger amount of dissolved hydrogen underwent an almost linear decrease. Above a copper content of 20 at. % hydrogen adsorption decreased, whereas there was barely any change in the amount of dissovled hydrogen, and the adsorbed and absorbed hydrogen contents of the catalyst became nearly the same. This can also be well seen in the sorption isotherms constructed from the galvanostatic curves (Fig. 1).

The potentiodynamic measurements were made with 1—5 mg catalyst by the method developed for Pd powder catalysts [5]. Samples with low copper

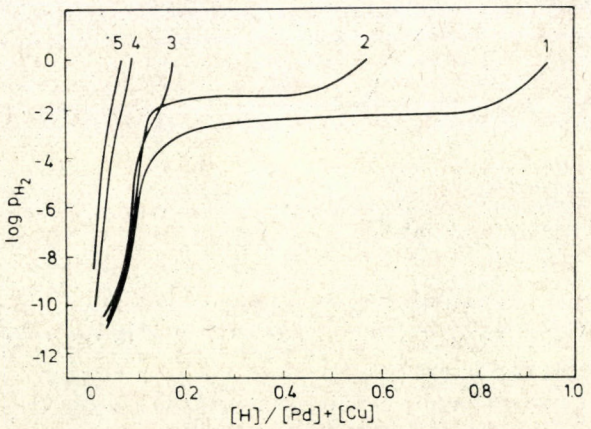

Fig. 1. Sorption isotherms of hydrogen on Pd–Cu catalysts, in 1 *N* sodium hydroxide. 1. 0 at. % Cu; 2. 10 at. % Cu; 3. 20 at. % Cu; 4. 30 at. % Cu; 5. 40 at. % Cu

contents were polarized in two steps: the measurement was commenced by changing the potential at a rate of 2—10 mV/min, and then, after removal of the bulk of dissolved hydrogen, the rate was increased to 10—100 mV/min. By this means the adsorbed hydrogen was magnified compared to the dissolved hydrogen.

The potentiodynamic curves for fresh catalysts containing 0—40 at. % copper can be seen in Figs 2—6. A total of six different hydrogen forms could be deduced in freshly prepared, unalloyed palladium (Fig. 2), but one month

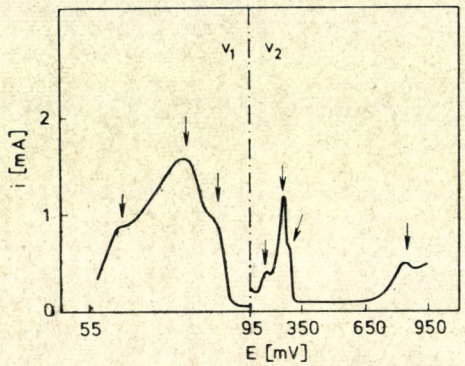

Fig. 2. Potentiodynamic curve of Pd catalyst in 1 *N* sulfuric acid. $v_1 = 10$ mV/min; $v_2 = 100$ mV/min; $m \approx 1$ mg

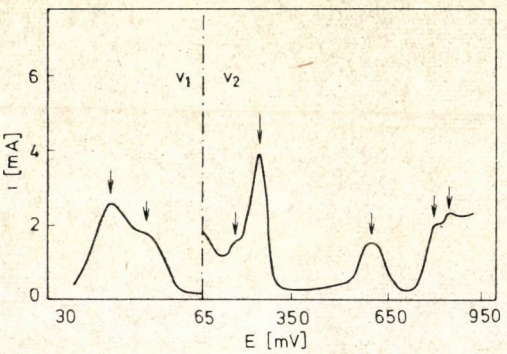

Fig. 3. Potentiodynamic curve of a Pd–Cu catalyst containing 10 at. % copper, in 1 *N* sulfuric acid. $v_1 = 2$ mV/min; $v_2 = 50$ mV/min; $m \approx 4$ mg

after preparation of the catalyst only a single maximum could be detected below 100 mV. A similar phenomenon was observed in the samples containing 10 and 20 at. % copper.

For the determination of the potentials relating to the individual maxima of the *i vs. V* curves, the rate of change of potential was decreased until the position of the peak no longer varied [5]. The positions of the hydrogen maxima

are listed in Table II. It should be noted that on the addition of further catalyst these values could be reproduced within $\pm$ 3 mV. These data refer to 1-month-old catalysts. (The curves in Figs 2—6 were not plotted with this 'limiting rate'.)

On the incorporation of copper, the maxima were shifted towards negative potentials, *i. e.* the metal–hydrogen bond energy decreased and the sorbed hydrogen became energetically more homogeneous: from 20 at. % only

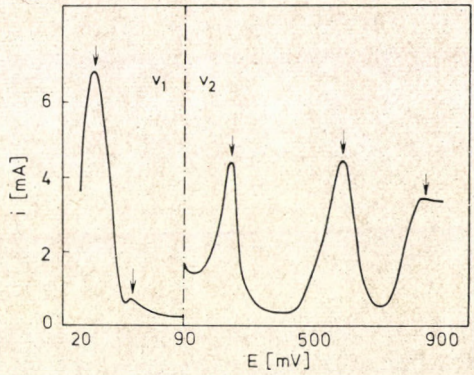

Fig. 4. Potentiodynamic curve of a Pd–Cu catalyst containing 20 at. % copper, in 1 *N* sulfuric acid. $v_1 = 10$ mV/min; $v_2 = 50$ mV/min; $m \approx 4$ mg

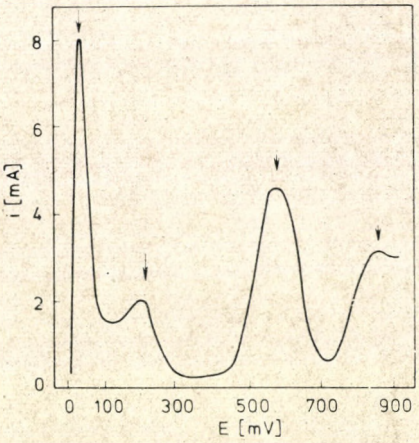

Fig. 5. Potentiodynamic curve of a Pd–Cu catalyst containing 30 at. % copper, in 1 *N* sulfuric acid. $v = 50$ mV/min; $m \approx 4$ mg

a single type of adsorbed hydrogen was found and from 30 at. % the dissolved hydrogen in the fresh catalyst was also homogeneous.

The potential of the peak of dissolved hydrogen underwent practically no change above 20 at. %. Since the quantity of dissolved hydrogen decreased to only a slight extent in this same interval, it may be assumed that 20 at. %

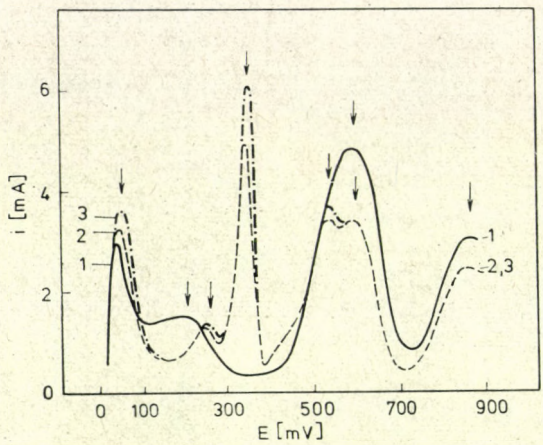

Fig. 6. Potentiodynamic curve of a Pd–Cu catalyst containing 40 at. % copper, in 1 *N* sulfuric acid. $v = 50$ mV/min; $m \approx 4$ mg; 1. cycle 1; 2. cycle 2; 3. cycle 3

Table II

Potentiodynamic study of hydrogen sorption on Pd–Cu catalysts, in **1** *N sulfuric acid (one month after preparation)*

Copper content (at. %)	Positions of maxima in hydrogen range (mV)	
	dissolved	adsorbed
0	60	170, 255, 265*
10	42	170*, 250
20	26	233
30	26	217
40	28	195

* shoulder, rather than a separate maximum

Cu is the concentration above which the alloy no longer dissolves, but only adsorbs hydrogen. The tabulated copper contents are average values; it is probable that even in the sample containing 40 at. % copper there are low copper-containing phases which dissolve the hydrogen, and because of this the changes occurring on the increase of the copper content become somewhat indistinct.

The position of the anodic oxygen peak for pure palladium is at ca. 850 mV, and this did not change as a result of alloying.

The potentiodynamic curves of the copper-containing samples exhibit a characteristic maximum at 575—600 mV. The area under the peak increased

with increase of the copper content. The peak is situated between the potentials corresponding to anodic dissolution of copper and palladium ($E^{\circ}_{Cu/Cu^{2+}} = 0.34$ V; $E^{\circ}_{Pd/Pd^{2+}} = 0.83$ V). Accordingly, it is probable that at this potential the copper in some Pd–Cu alloy undergoes oxidation.

The phase diagram indicates that up to a copper content of 40 at. % the Pd—Cu alloy is homogeneous, but above this the formation of two intermetallic compounds of definite composition (PdCu and $PdCu_3$, or Pd_3Cu_5 and $PdCu_5$) can be observed, the cubic lattice then becoming tetragonal [8]. Since the potential corresponding to the above-mentioned maxima (575—600 mV) is practically the same for all the copper-containing samples, it may be assumed that when the palladium was alloyed with 10—40 at. % copper, in every case some intermetallic compound of definite composition was formed on the surface, its amount increasing with increase of the copper content.

Figure 6 shows curves obtained by cyclic potentiodynamic polarization of the catalyst containing 40 at. % copper. In the course of anodic polarization of the hydrogen-containing sample for the first time a single large peak can be found between 450 and 700 mV. When the measurement was repeated with the same sample (cathodic, and then again anodic polarization), a new peak appeared at 300—350 mV, and the maximum at ca. 585 mV split into two readily distinguishable maxima at ca. 520 and 595 mV. At the same time, the curve also changed in the hydrogen range, as a consequence of anodic dissolution and cathodic deposition.

The peak at 300—350 mV corresponds to oxidation of copper in a Cu–Cu bond. The splitting of the maximum at ca. 585 mV indicates that in fact the dissolution of two intermetallic palladium—copper compounds of definite composition is taking place here. The maximum at 520 mV, which is the nearer to the normal potential of the Cu/Cu^{2+} process, corresponds to a chemical compound richer in copper, while the other maximum corresponds to a chemical compound poorer in copper. The areas under the 300—350 and 520 mV peaks increased with the number of cycles, for an increasing amount of copper was dissolved anodically and was deposited on polarization, thereby increasing the quantity of the phases richest in copper. (For this it must be assumed that the copper deposited from the Cu^{2+} ions on cathodic polarization is partially alloyed with the palladium.) The extended, sloping 'section' appearing at 400—450 mV in cycles 2 and 3 (the area corresponding to the difference of the curves for cycles 2 and 1) can be explained by the oxidation of a copper-rich phase of indefinite composition, containing more copper than the compound phases.

On this basis it may be assumed that the peaks between 450 and 700 mV in the potentiodynamic curves of the samples containing 10—40 at. % copper (Figs 3—6) are also the sum of two maxima. The potentials corresponding to the maxima of the peaks and to the completion of the peaks are

the same in all four cases, whereas the potential corresponding to the commencement of the peak decreases by ca. 100 mV on increase of the copper content from 10 to 40 at. %. This, together with the relatively large half-width of the peak for the higher copper-containing samples, permits the conclusion that even in the first anodic curve this peak is the sum of two unresolved peaks. With the increase of the copper content, the amount of the intermetallic com-

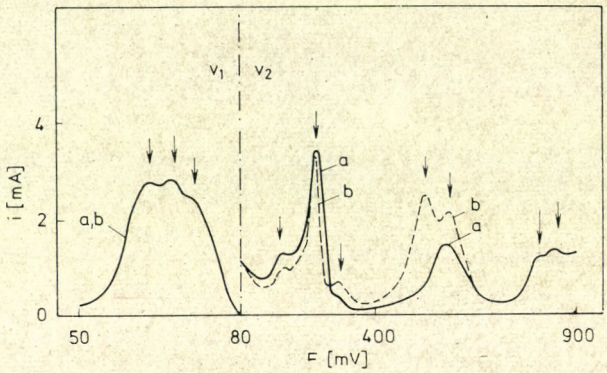

Fig. 7. Potentiodynamic curves of Pd catalyst containing copper deposited on its surface by hydrogenation, in 1 *N* sulfuric acid. $v_1 = 2$ mV/min; $v_2 = 50$ mV/min; $m \approx 4$ mg; 1. Cu/Pd = 0.014; 2. Cu/Pd = 0.065

pound richer in copper increases, and therefore the peak commences from ever lower potentials.

In the potentiodynamic curve for pure Pd (Fig. 2), the current is minimal and almost constant between 350 and 700 mV, corresponding to the fact that only the double layer is charged in this section. In the potentiodynamic curves of the copper-containing samples (Figs 3—6), with the increase of the copper content the value of the current at around 700 mV (the minimum) becomes continuously larger compared with that measured at 350 mV. This probably indicates oxidation of the copper dissolved in the palladium. For an exact evaluation, it would be necessary to depict the potentiodynamic curves for all of the samples in a single diagram and then to compare them in the range between 600 and 900 mV, but because of the ignorance of the exact weight of catalyst this is not possible.

In Fig. 6 the difference at around 700 mV in the anodic curves for cycles 1 and 2 is again presumably connected with the copper dissolved in the palladium: because of the high-surface Cu/Pd ratio on cathodic deposition after anodic dissolution of the surface of the sample, predominantly copper-rich phases were formed, and copper did not dissolve in palladium.

Experiments were also carried out in which a $CuSO_4$ solution was added to a Pd catalyst not containing copper, and copper was deposited onto the surface of the Pd catalyst by hydrogenation during shaking.

The Cu/Pd atomic ratios were (a) 0.014 and (b) 0.065. It can readily be seen in the potentiodynamic curves (Fig. 7) that copper was predominantly alloyed with palladium: both curves are very similar to the polarization curves of Pd–Cu alloy catalysts. When more copper was deposited onto the surface, the amounts of the copper-rich or pure copper phases increased, while at the same time the quantity of hydrogen adsorbed decreased. In the range of dissolved hydrogen the curve did not change perceptibly. All this indicates that under these conditions too copper is alloyed with palladium, but alloy formation proceeds only on the surface.

SZABÓ [9] also demonstrated alloy formation during copper adsorption, on a Pt electrode coated with palladium black.

The shoulder appearing at ca. 800 mV, which can be distinguished only with difficulty, can probably be explained by dissolution of some low copper-containing Pd–Cu phase.

From the results listed so far it may be concluded that on preparation, no homogeneous solid solution corresponding to the phase diagram was formed on the surface. Instead, copper partially dissolved in palladium and partially gave rise to new intermetallic compound phases. (The dissolution of hydrogen is characteristic for the entire volume, but the anodic dissolution of copper occurs only in the outermost surface layers under potentiodynamic conditions.)

Table III

Apparent activities of Pd–Cu catalysts in the hydrogenation of eugenol and acetophenone

Copper content (at. %)	Activity on eugenol		Activity on acetophenone	
	$\left(\frac{\text{ml } H_2}{\text{min } g_{cat}}\right)$	$\left(\frac{\text{ml } H_2}{\text{min } g_{Pd}}\right)$	$\left(\frac{\text{ml } H_2}{\text{min } g_{cat}}\right)$	$\left(\frac{\text{ml } H_2}{\text{min } g_{Pd}}\right)$
0	92.0	92.0	10.5	10.5
10	37.5	40.0	22.5	24.5
20	46.0	53.0	28.0	32.0
30	59.5	75.0	36.0	45.0
40	57.5	81.0	36.0	50.5

The apparent activities of the Pd–Cu catalysts in the liquid-phase hydrogenations of acetophenone and eugenol are given in Table III, and the variation of the apparent activities as a function of the atomic percentage of copper can be seen in Fig. 8. The apparent activity in the hydrogenation of acetophenone increases monotonously with the increase of the overall copper content, whereas in the hydrogenation of eugenol the activity is decreased significantly by 10 at. % copper, but further increase of the copper content subsequently increases the activity.

Both activity curves are at variance with the long-prevailing view that the catalytic activities of transition metals in two-component alloys decrease almost monotonously as a result of the *s* electrons of the I—B group metals. Some years ago, however, DOWDEN [10] and SACHTLER *et al.* (in several publications, *e. g.* [11]) demonstrated that this is not always the case, even if the two alloying metals form a homogeneous solid solution. A monotonous

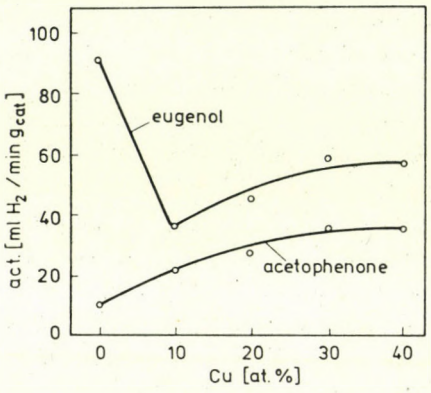

Fig. 8. Apparent activities of Pd–Cu catalysts as a function of the composition, in the hydrogenation of eugenol and acetophenone

decrease of the catalytic activity is not to be expected mainly when the two metals cannot form a solid solution in a certain composition interval, or this cannot be formed under the conditions of preparation of the catalyst. In this case the phases of various compositions may separate, and the composition of the surface phase may differ significantly from the overall composition of the alloy.

On the basis of the conditions of catalyst preparation already described in the Experimental section (reduction of a mixture of palladium and copper hydroxides at room temperature), it is very likely that a completely homogeneous solid solution was not formed from palladium and copper in the catalysts. (Our aim was to investigate catalytic activities are higher than those of palladium–copper catalysts in which a nearly homogeneous solid solution is formed from the two metals.) Our potentiodynamic studies clearly proved that copper dissolved only partially in palladium, also partially forming intermetallic compound phases with the palladium on the surface of the catalysts.

The variation of the activities may be correlated with at least two factors: the bond strength of hydrogen on the surface of the catalyst, and the nature of adsorption of the substance to be hydrogenated. The apparent activity in the hydrogenation of acetophenone increases almost linearly with

the decrease of the potentials relating to the hydrogen maxima (Table II). The adsorption of acetophenone also probably changes and becomes more favourable with the increase of the copper content. A similar phenomenon was observed by SOMA-NOTO and SACHTLER [12], who, in an IR spectroscopic study of CO sorbed on Pd—Ag alloys, demonstrated that the nature of CO adsorption is changed by increase of the Ag content. In the hydrogenation of eugenol, variations in the adsorption of the molecule and in the bond stength of the sorbed hydrogen may to a certain extent act in opposing directions as regards the hydrogenating activity, and this may bring about the rapid decrease up to a copper content of 10 at. %, while the subsequent increase may be explained by the decrease in the bond strength of adsorbed hydrogen becoming predominant. Based on our investigations to date, the effects of these factors can naturally only be suggested as a possibility. A deeper understanding will probably become possible as a result of further studies now under way (a wider composition range, and determination of selectivity).

Conclusion

Palladium–copper powder catalysts containing 0—40 at. % copper, prepared by hydrogenation, were studied by galvanostatic and potentiodynamic methods, and the liquid-phase catalytic activities were measured in the hydrogenation of model compounds. The following were the most important results:

1. For copper contents of 0—20 at. % the amount of hydrogen adsorbed did not change, but that of the dissolved hydrogen decreased considerably and almost linearly. The situation was the reverse for copper contents of 20—40 at. %: the amount of adsorbed hydrogen decreased relatively significantly, while that of the dissolved hydrogen barely changed. A copper content of around 20. at. % is probably the concentration above which the alloy no longer dissolves, but only adsorbs hydrogen.

2. The potentiodynamic measurements indicated that with the incorporation of copper the bond energy of sorbed hydrogen decreased, and the distribution of the bond energy became more homogeneous. On preparation of the catalyst no homogeneous solid solution was formed on the surface of the grains, but part of the copper dissolved in the palladium, and part formed new intermetallic compound phases. The quantity of the latter increased with increase of the copper content.

3. The apparent activity in the hydrogenation of acetophenone increases monotonously with increase of the overall copper content, whereas in the hydrogenation of eugenol 10 at. % copper decreases the activity considerably, while further increase of the copper content leads to an increase of

the activity. Such changes in the activities can probably be explained by the decrease of the metal–hydrogen bond energy and the change in adsorption strength of the reactants.

REFERENCES

[1] Bond, G. C.: Catalysis by Metals. Academic Press, London, New York 1962
[2] Karpova, R. A., Tverdovskii, I. P.: Zh. Fiz. Khim., **33,** 1393 (1959)
[3] Bizhanova, N. B., Erzhanova, M. S., Sokolskii, D. V.: Iz. Akad. Nauk. Kaz. SSR, Ser. Khim., **19,** 15 (1949)
[4] Mokroushav, P. V., Naumov, A. I.: Catalytic reactions in liquid phase. Tr. Vses. Konf. Alma-Ata, Kaz. SSR, p. 10 1966. (Publ. 1967).
[5] Petró, J., Mallát, T., Polyánszky, É.: (In press)
[6] Petró, J., Polyánszky, É., Csűrös, Z.: J. Catal., **35,** 289 (1974)
[7] Burshtein, R. H., Tarasevich, M. R., Vilinskaya, V. S.: Elektrokhimiya, **3,** 349 (1967)
[8] Savitskii, E. M., Plyakova, V. P., Tylkina, M. A.: Splavy palladiya. Izd. Nauka, Moscow 1967
[9] Szabó, S.: Magy. Kém. Folyóirat **81,** 528 (1975)
[10] Dowden, D. A.: Catalysis. Ed.: G. W. Hightower, Vol. 41, p. 621. Proc. 5th Int. Congr. Catalysis, Florida 1972
[11] Sachtler, W. M. H., Vander Plank, P.: Surface Sci., **18,** 62 (1969)
[12] Soma-Noto, Y., Sachtler, W. M. H.: J. Catal., **32,** 315 (1974)

Tamás Mallát
József Petró
Éva Polyánszky
Tibor Máthé

H-1111 Budapest Műegyetem rkp. 3—9.

Acta Chimica Academiae Scientiarum Hungaricae, Tomus 90 (4), pp. 345—354 (1976)

CATALYTIC DEUTERIUM EXCHANGE OF CYCLOPENTANE AND CYCLOHEXANE, AND DEHYDROGENATION OF CYCLOHEXANE ON Rh BLACK

A. SÁRKÁNY, L. GUCZI and P. TÉTÉNYI

(Institute of Isotopes of the Hungarian Academy of Sciences)

Received November 2, 1975

Results on deuterium exchange of cyclopentane, cyclohexane and dehydrogenation of cyclohexane in the presence of deuterium on Rh black are reported. Between 273 and 373 K the sole reaction is deuterium exchange with apparent activation energies of 51 and 63 kJ mol^{-1} for cyclopentane and cyclohexane, respectively. The deuterium distribution can be explained by assuming $\alpha\alpha$ and $\alpha\beta$ surface species. The appearance of tetradeuterated products at elevated temperatures can be attributed to $\alpha\alpha\beta\beta$ doubly-bonded intermediates which are assumed to be responsible for poisoning. Dehydrogenation of cyclohexane was studied in the temperature range 473—573 K. The rate of benzene formation is commensurable with the desorption of deuterated cyclohexane. However, the fact that deuterium appears in a nearly equilibrium distribution both in benzene and cyclohexane suggests that the interconversion steps yielding deuterated surface species are fast compared either with cyclohexane desorption or with benzene formation.

Introduction

Catalytic transformations of saturated hydrocarbons in the presence of hydrogen have been extensively investigated in our laboratory on Ni [1—3] and Pt [4] blacks. It was found [3] that different reaction routes such as hydrogenolysis and deuterium exchange can be satisfactorily explained by assuming 'weak' and 'strong' interactions on the surface. On applying this concept to characterize Ni and Pt, it was concluded [5] that the weak—strong conversion takes place easily on Ni, while a relatively 'hydrogen-rich' species exists on Pt. These phenomena have been confirmed [6] by correlating chemisorption measurements and deuterium exchange of methane, ethane and hydrogenolysis of ethane on Co, Ni and Pt catalysts.

Recently, we focused our attention on the catalytic properties of rhodium black. Rhodium films, supported rhodium catalysts [7] show high catalytic activities, as compared with other transition metals of group VIIIb in deuterium exchange and hydrogenolysis of saturated hydrocarbons. In the present work we report on the H–D exchange of cyclopentane and cyclohexane and on the dehydrogenation of cyclohexane in the presence of deuterium. The experimental results are compared with earlier data obtained on [8] Ni and Pt.

Table I

Deuterium distribution of

	T/K	d_0	d_1	d_2	d_3	d_4	d_5
Cyclopentane	265	obs. 93.31	5.1	1.5	0.1	0.00	
		calc. 93.31	6.4	0.2	0.0		
	297		16.7	28.9	12.6	4.4	24.1
	306		21.9	25.2	5.4	8.7	16.4
	328		10.5	10.1	7.6	8.5	7.3
	341		12.0	10.2	4.21	5.4	9.6
	378		4.3	2.5	1.2	12.0	3.1
Cyclohexane	265	obs. 80.2	18.2	1.5	0.1	0.00	
		calc. 80.2	17.8	1.8	0.1	0.00	
	294		34.6	8.6	7.9	7.2	8.3
	311		25.6	11.7	5.8	7.1	8.2
	328		18.1	13.2	8.7	4.5	5.8
	347		10.0	4.2	5.8	7.8	8.2
	369		12.5	6.6	4.1	5.2	5.8
	381		5.0	2.5	1.5	2.0	1.1

Experimental

All experiments were performed in an all-glass circulation apparatus with a total volume of 120.1 cm^3. The reaction vessel was connected through fine capillary to an AEI MS lOC 2 mass spectrometer, so that the reactions could be followed continuously. The correction procedure which was used in the determination of deuterium distribution has been described earlier [1]; the product distribution patterns were determined from the initial rate of formation of individual deuterated hydrocarbons. The mean deuterium number is

$$\overline{M} = \sum_{i=1} iW_i^0 / \sum_{i=1} W_i^0 \quad i.e. \quad W_\varnothing^0 / \sum_1 wt$$

The rhodium powder catalysts were prepared from $RhCl_3 \cdot 3\ H_2O$ solution by reduction with formaldehyde in an alkaline medium. The surface area of the catalyst, after hydrogen treatment at 300 °C, was 7.1 $m^2\ g^{-1}$ (BET method using N_2).

Deuterium was purified before use by passing it through a heated silver-palladium thimble. Hydrocarbons (supplied by Merck) and deuterium were always mixed in a 1 : 10 ratio at a total pressure of 29.33 kN m^{-2} unless otherwise stated. In each of the experiments 0.045 g rhodium was used.

CH and CP on Rh black

d_6	d_7	d_8	d_9	d_{10}	d_{11}	d_{12}	$\bar{M}$	E (kJ mol^{-1})
1.4	2.2	3.3	2.6	3.3			3.56	
1.0	2.1	7.6	8.7	9.9			4.60	
5.4	8.9	11.7	10.9	18.6			5.88	
4.8	4.2	11.4	18.6	19.2			6.23	
6.4	7.3	14.2	20.2	28.4			6.69	
								51
								63
19.0	0.7	1.3	2.4	2.7	3.1	3.8	4.03	
14.8	3.5	2.5	3.0	4.3	5.8	6.9	4.85	
10.9	5.3	4.1	7.8	8.9	11.4	14.5	7.11	
7.7	6.9	6.6	6.0	7.1	11.7	17.4	7.23	
6.8	5.3	5.1	8.3	8.6	11.6	19.7	7.31	
2.5	1.5	4.5	8.5	14.6	26.7	29.2	9.55	

Results

On a freshly prepared catalyst the rate of deuterium exchange of cyclopentane was rapid even at 196 K. The rate of exchange at 265 K and a total pressure of 13.32 kN m^{-2} was 4.73×10^{-8} mol m^{-2} s^{-1}.

Even at this temperature, the catalyst was poisoned rapidly and subsequent hydrogen treatment could not restore the original activity. In order to obtain reliable kinetic data to be considered as a steady-state characteristic of the sample, repeated runs were performed at 328 K on the same sample. The results are summarized in Fig. 1.

The initial deuterium distributions on this aged catalyst (Type I) are summarized in Table I. At 265 K the values measured relatively well to the points calculated from a binomial distribution. With increasing temperature 'one-side' exchange is predominant, *i. e.* the exchange of the first five or six hydrogen atoms in CP and CH, respectively, occurs easily. Above 353 K the intensity of CP—d_5 and CH—d_6 isomers drop and the distribution is shifted towards perdeuterated species. The apparent activation energy is 51 kJ mol^{-1} for cyclopentane and 63 kJ mol^{-1} for cyclohexane between 293 and 353 K. In this temperature range exchange with cyclopentane is about seven

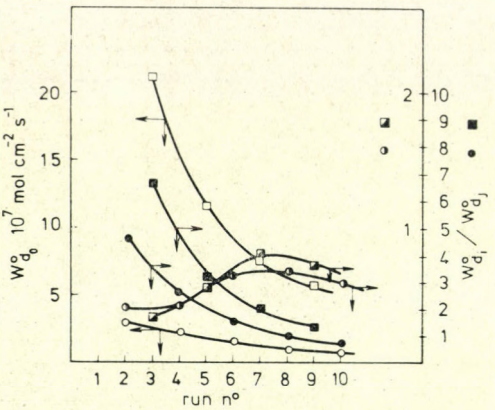

Fig. 1. Effect of catalyst self poisoning on the rate of deuterium exchange of cyclohexane (○) and cyclopentane (□) and the variation of the w^0_{di}/w^0_{dj} ratio for CP-d_5 and CP-d_2 (◪), CH-d_6 and CH-d_1 (◑) (left-hand scale); CP-d_{10} and CP-d_2 (■), CH-d_{12} and CH-d_1 (●) (right-hand scale).

times faster than that with cyclohexane. However, on increasing the temperature above 353 K, this ratio, as well as the apparent activation energy decrease.

Table II

Effect of catalyst deactivation on the dehydrogenation of CH at 520 K

No. of subsequent runs	w^0_H	S_{nH}	$w^0_{ex.CH}$	w^0_B	$\overline{M}_{CH}$	$\overline{M}_B$
1	77.1	0.007	—	1.03	—	—
2	1.12	0.012	—	2.21	—	—
3	0.81	0.23	—	—	—	—
4	—	—	3.11	5.41	7.09	4.71
5	—	—	4.03	5.37	6.73	4.38
6	—	—	5.71	4.68	6.25	4.47
7	—	—	5.43	4.41	6.12	4.28
8	—	—	4.61	4.32	6.03	4.17
9	—	—	4.71	—	5.95	4.12
10	—	—	4.43	4.12	5.95	4.06

w^0_H — rate of CH hydrogenolysis (10^8 mol m^{-2} s^{-1})

S_{nH} — selectivity to *n*-hexane formation

$w^0_{ex.CH}$ — rate of CH exchange = $\sum_{i\neq 0} w^0_{CH-d_i}$ (10^8 mol m^{-2} s^{-1})

w^0_B — rate of benzene formation = $\sum_{i=0} w^0_{B-d_i}$ (10^8 mol m^{-2} s^{-1})

$\overline{M}_{CH}$ and $\overline{M}_B$ — mean deuterium number in CH and B, respectively

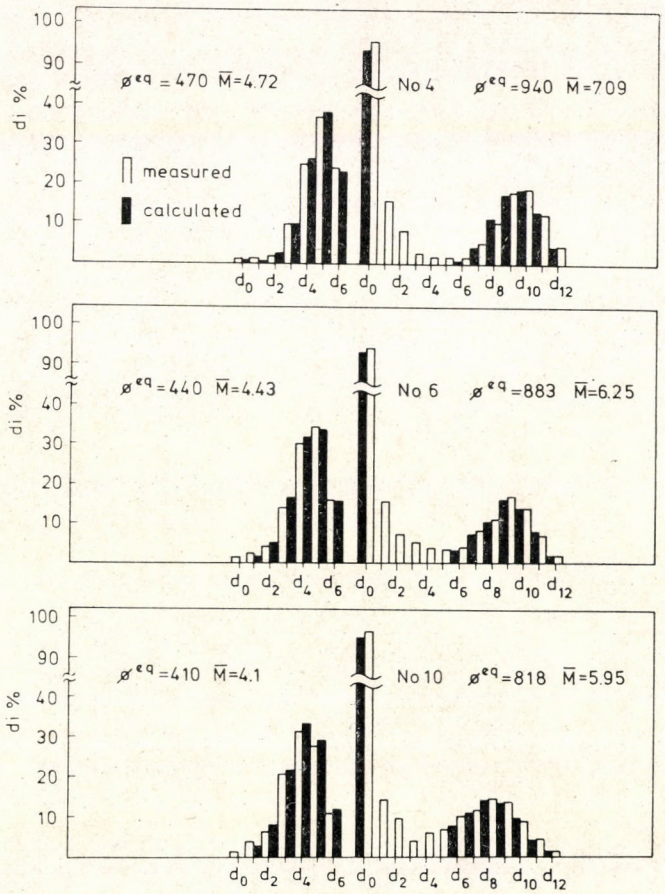

Fig. 2. Comparison of theoretical and measured spectra of deuterated cyclohexane and benzene (see Table II).

Above 393 K the deuterium exchange of cyclopentane was accompanied by multiple fragmentation of the cyclopentane ring. This is clearly seen from the low selectivity value of *n*-pentane formation, $S_{nP} = 0.17$, as measured with hydrogen at 420 K under otherwise identical conditions. Further attention was not paid to this reaction.

Dehydrogenation of cyclohexane in the presence of deuterium was measured in the temperature range between 474 and 573 K. In Table II we have summarized the effect of catalyst self-poisoning at 520 K for the Type I catalyst. The first three runs were performed in the presence of hydrogen. It was found that there is a great difference between the initial and subsequent rates. Between runs, the catalyst was treated with hydrogen only. During the first three runs the 'deep hydrogenolysis' of cyclohexane is the sole reaction

apart from the formation of a small amount of benzene. The rate of benzene formation therefore passed through a maximum due to the fast decrease in the rate of hydrogenolysis. The rate of deuterium exchange of cyclohexane was characterized by $\sum_{i\neq 0} w_{d_i}$. The initial deuterium distribution in cyclohexane and in the benzene* formed is shown in Fig. 2. From the deuterium distribution of cyclohexane one can conclude that the adsorbed species reaches equi-

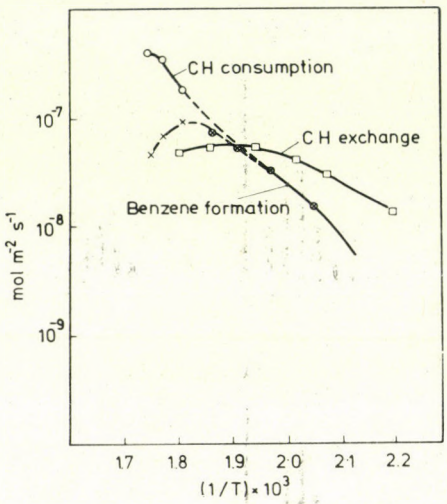

Fig. 3. Arrhenius plots for deuterium exchange of CH (□), benzene formation (X) and CH consumption (○).

librium distribution before it can leave the surface. (This distribution can be characterized by Θ_D/Θ_{CH} rather than by p_{D2}/p_{CH}.) With the aging of the catalyst the mean deuterium number of deuterated CH decreased due to the increased proportion of single deuterated isomers. On the other hand, the assumed equilibrium distribution of d_7-d_{12} isomers shifted toward smaller $\varnothing^{eq.}$.

On comparing $\sum w_{d_i}$—CH with the rate of benzene formation, it is apparent that the rate of desorption of CH is commensurable with the rate of the surface reaction.

* The separation of CH-d_0 and benzene-d_6 ($m/e = 84$) is based on the assumption that both CH and benzene contain the deuterium atoms in near equilibrium distribution, that is, $\varnothing^{eq.}_{benzene} \simeq 1/2\,\varnothing^{eq.}_{CH}$. Details of this calculation are in Ref. [8]. $\varnothing^{eq.}_{CH}$ was determined by a simple direct search method from the intensity of d_7-d_{12} isomers rather than from the ratio of p_{D2}/p_{CH}. It is of interest with respect to surface coverage that, according to $\varnothing^{eq.}$ the value of Θ_D is commensurable with Θ_{CH} ($\Theta_D \geq \Theta_{CH}$), suggesting that the chemisorption ability of the two compounds at this temperature is similar.

After completing these experiments the effect of temperature was investigated with reference to this carbonized (Type II) sample. The results are shown by Arrhenius plots in Fig. 3. The apparent activation energies are 78 kJ mol^{-1} and 52 kJ mol^{-1} for cyclohexane consumption and deuterium exchange (calculated from $\sum_{i \neq 0} w_{d_i}$), respectively. The rate of deuterium exchange above 533 K dropped and a similar trend was observed for benzene formation at 553 K. This effect cannot be explained by catalyst poisoning because the exchange rate at 473 K (after cooling the sample) was within the experimental error (4%). At this temperature, hydrogenolysis as a side reaction is dominant, leading mainly to CD_4.

Discussion

The experimental results concerning deuterium exchange of cyclopentane and cyclohexane can be explained by dissociative chemisorption. Besides the single exchange intermediate (resulting in a d_1 isomer) one has to assume at least two other intermediates responsible for multiple exchange. The maximum appeared at the CP—d_2 isomer, providing evidence that two-point adsorption may take place easily. Further maxima were found at CP—d_5 and, in the case of CH, at CH—d_6.

On the basis of the similar activation energy of the formation of CP—d_2 and CP—d_5 isomers, it can be concluded that this process involves the same intermediate, *i. e.* deuterium exchange on one side of the ring takes place through the α—β process [10]. It is known that the formation of a π-allylic type intermediate [9] leads to deuterium exchange on both sides of the ring, therefore, one cannot expect any maxima at CP—d_5 or at CH—d_6. In fact this is the case on Ni and Pt for cyclohexane exchange. Ruling out the possibility of 'roll-over' mechanisms [11, 12], in the absence of CP—d_8 and CH—d_{10} isomers, we were tempted to assume that the turning over of the ring involves $\alpha\alpha$ interactions as originally proposed by KEMBALL [10]. This assumption seems to be confirmed also by the fact that the apparent activation energy for the formation of d_6—d_{10} isomers of CP is by about 12—16 kJ mol^{-1} greater than that for CP—d_2. At elevated temperatures the distribution shifted toward multiple exchange, *i. e.* the proportion of multiply deuterated species grew at the expense of d_5 and d_6 isomers in CP and CH, respectively. Although one cannot rule out the possibility of a π-allylic type interaction in this temperature range, the strong poisoning effect suggests a rather localized chemisorption. This seems to be supported by the fact that CP—d_4 and CP—d_6 are always greater than CP—d_5, suggesting a $\alpha\alpha$—$\beta\beta$ type interaction.

The CP—D_2 exchange is about seven times faster than that with CH between 297 and 353 K. There is no significant difference between the disso-

ciation energies of C—H bonds in these hydrocarbons (389 and 393 kJ mol^{-1}) for CP and CH, respectively [13] therefore, the higher reactivity of CP can be attributed to the 'rigid' structure of this molecule. It is well-known that the CP ring is nearly planar and the hydrogen atoms are fixed in eclipsed conformation affording a favourable spatial arrangement for $\alpha\beta$ adsorption. This explains the ease of a two-point adsorption and the greater rate compared with CH.

The rate of CP exchange decreased to a greater extent than that of CH in successive runs (see Fig. 1). During this aging the formation of perdeuterated species is supressed by the formation of single deuterated products, as can be seen in Fig. 1. With reference to the surface state of the catalyst it is of interest that, while the CH d_{12}/d_1 or CP d_{10}/d_2 ratio continuously decreased due to the increased proportion of poisoned surface sites, the initial rate of CH d_6/d_1 and CP d_5/d_2 passed through a broad maximum in the same process. The rapid decrease in the formation of multiply deuterated species proves the importance of coordination of active sites being responsible either for the 'turnover' of the molecule or the formation of a π-allylic-type intermediate. On the other hand, we are prepared to accept that the poisoning of the surface by carbon may change not only the short-range surface geometry of active sites but also their energy levels.

Above 200 °C the dehydrogenation of cyclohexane represents the main reaction route. In order to explain the experimental results, we assume that both the H–D exchange of CH and benzene formation can be considered as 'weak' interactions [5]. Furthermore, the chemisorption steps yielding either multiply deuterated CH or the benzene precursor are common. The following tentative model can be proposed

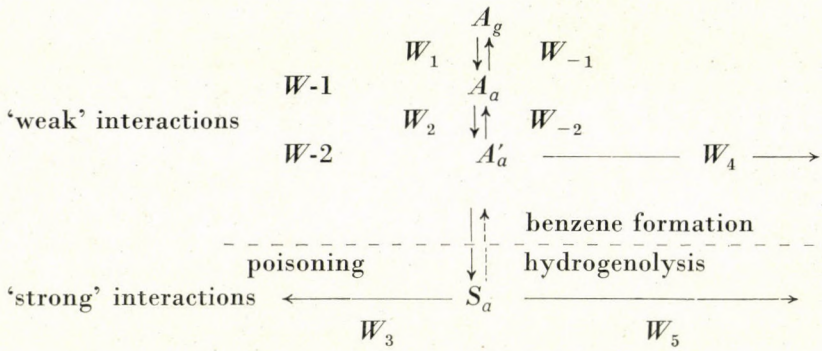

W-1 interaction is responsible for the formation of monodeuterated cyclohexane while W-2 interactions lead either to multiply deuterated species or to the benzene precursor.

For the sake of simplicity we have not taken into account the detailed mechanism of deuterium exchange. The steps between A_g and A'_a can therefore be related to α, $\alpha\beta$, π-allyl and π-olefin interactions and the rates W_2 and W_{-2} were considered as referring to interconversion steps between the species mentioned above. At low temperatures on a catalyst of steady-state activity, *i. e.* if $W_3 = W_4 = 0$, the equilibrium is between A_g and A'_a. In this temperature range the only reaction is H–D exchange; its rate is limited by W_1 as accepted generally. At elevated temperatures this adsorption–desorption equilibrium in the deuterium exchange of CH ceases to exist and the main reaction is benzene formation. It is generally accepted that the rate of dehydrogenation is controlled by the surface reaction [13]. Actually, in this temperature range *(cf.* Table II and Fig. 2) the rates of formation of deuterated CH and of benzene are commensurable. The fact, however, that the CH desorbed contains deuterium in near equilibrium distribution suggests that the interconversion steps (W_2 and W_{-2}) leading to deuterated species are extremely fast compared either with the desorption of CH or with the formation of benzene, therefore, $W_{-1} \ll W_2$, W_{-2} and $W_1 \approx W_4$. Although the adsorbed species reaches an equilibrium concentration of deuterium, this is not the overall equilibrium of the whole system.

With increasing temperature both the rate of CH exchange and that of benzene formation decreased and simultaneously hydrogenolysis prevailed. This means that the reversibility of interconversion steps partly ceased due to the formation of strongly bonded species whose fragmentation enters into competition with benzene formation; thus, in this case, $W_2 \gg W_{-2}$ and $W_5 \gg 0$.

Finally, we give a brief comparison between the experimental results observed on Ni and Pt [8]. The rate of H–D exchange of CH is greater than that over Pt or Ni; the activity sequence, is Rh > Pt > Ni. (The same reaction order was observed with respect to the rate of ethane-D_2 exchange [14]). The activation energies are nearly the same, being 63, 67 and 79 kJ mol^{-1} for CH exchange on Rh, Pt and Ni, respectively. A different activity sequence was observed, however, when benzene formation was compared, *i. e.* Pt > Rh > Ni. In order to explain this change in the activity sequence we have to remember that both Ni and Rh may cleave the C–H bond to a relatively large extent. The ease of weak—strong interactions on both catalysts explains the rapid poisoning of the surface. This also seems to be confirmed by the fact that on Rh and Ni the hydrogenolysis of CH predominates above 573 K. Both Ni and Rh may therefore be heavily contaminated by carbonaceous residues owing to the ease of formation of multiply bonded species. The greater number of working active sites together with the ease of formation of π-allyl or π-olefin intermediates might provide an explanation for the greater reactivity of Pt in benzene formation.

REFERENCES

[1] GUCZI, L., SHARAN, K. M., TÉTÉNYI, P.: Monatsh. Chem. **102,** 187 (1971)
[2] GUCZI, L., SÁRKÁNY, A., TÉTÉNYI, P.: Dokl. Bolg. Akad. Nauk, **6,** 349 (1973)
[3] GUCZI, L., SÁRKÁNY, A., TÉTÉNYI, P.: Proc. Vth Congress on Catalysis, Vol. 2, p. 1111 (1973)
[4] GUCZI, L., SÁRKÁNY, A., TÉTÉNYI, P.: J. Chem. Soc. Faraday Trans I, **70,** 1971 (1974)
[5] GUCZI, L., TÉTÉNYI, P.: Ann. N. Y. Acad. Sci., **213,** 173 (1973)
[6] BABERNICS, L., GUCZI, L., MATUSEK, K., SÁRKÁNY, A., TÉTÉNYI, P.: Paper A36 presented an the VIth Intern. Congr. on Catalysis, London 12-16 July 1976
[7] SINFELT, J. H.: Advances in Catalysis, Vol. 23, p. 91 Academic Press 1973
[8] SÁRKÁNY, A., GUCZI, L., TÉTÉNYI, P.: J. Catal. **39,** 181 (1975)
[9] GAULT, F. G., ROONEY, J. J., KEMBALL, C.: J. Catal. **1,** 255 (1962)
[10] KEMBALL, C.: Proc. Chem. Soc., **264** (1960)
[11] BURWELL, Jr., R. L., SCHRAGE, K.: Disc. Faraday Soc., **41,** 215 (1966)
[12] BURWELL, Jr., R. L.: Accounts Chem. Res., **2,** 289 (1969)
[13] KERR, J. A.: Chem. Rev., **66,** 465 (1966)
[14] SÁRKÁNY, A.: unpublished results
[15] TÉTÉNYI, P.: Acta. Chim. (Budapest) **82,** 459 (1974)

Antal SÁRKÁNY
László GUCZI
Pál TÉTÉNYI
H-1525 Budapest Pf. 77.

Acta Chimica Academiae Scientiarum Hungaricae, Tomus 90 (4), pp. 355–364 (1976)

FORCE FIELD CALCULATIONS FOR MALONONITRILE MOLECULES

B. VIZI and A. SEBESTYÉN

(Veszprém University of Chemical Engineering, Department of General and Inorganic Chemistry H-8200 Veszprém)

Received November 14, 1975

Harmonic force fields were developed for malononitrile molecules, based on uncorrected observed frequencies from literature. Also the potential energy distribution was calculated for each of the molecules.

Introduction

In a systematized study of the mean amplitudes of malononitrile molecules we have developed force fields for the models $X_2C(CN)_2$, X = H, D, F, Cl, Br, and $HXC(CN)_2$, X = D, Br.

Although normal coordinate analyses of these molecules have been carried out by a few investigators [1, 2, 3], a comprehensive force field has not yet been developed. Therefore, we have started our work with systematized force field study after adopting the spectroscopic and structural data from those papers. We have made a slight rectification on the spectrum of $HBrC(CN)_2$ published by VAN HAVERBEKE *et al.* [3]. This was an interchange of two frequencies (ν_9 with ν_{16} in Table II of [3]) in accordance with VAN HAVERBEKE and his coworkers' statement [3] that the A_1 and B_1 species of the C_{2v} become A' vibrations and A_2, B_2, species of C_{2v} symmetry class are reduced to A'' vibrations in C_s. Also the orthogonality of G matrix proves the competence of the interchange of frequencies.

Normal coordinate analysis

We have constructed the following set of symmetry coordinates for molecules $X_2C(CN)_2$ from the valence coordinates in Fig 1.:

$$
\begin{aligned}
A_1 \quad S_1 &= 1/\sqrt{2}\,(t_1 + t_2) \\
S_2 &= 1/\sqrt{2}\,(r_1 + r_2) \\
S_3^* &= \sqrt{ST}/2\,(\beta_1 + \beta_2 + \beta_3 + \beta_4) \\
S_4 &= 1/\sqrt{2}\,(s_1 + s_2) \\
S_5 &= \sqrt{ST/2}\,(\delta - \gamma) \qquad S_R = a\,S_3^* + b \cdot S_3^{**} \equiv 0
\end{aligned}
$$

$$S_6 = \sqrt{RS}/2\ (\vartheta_1 + \vartheta_2) \qquad S_3 = a\ S_3^* - b \cdot S_3^{**}$$
$$S_3^{**} = \sqrt{ST}/2\ (\delta + \gamma)$$

A_2
$$S_7 = \sqrt{ST}/2\ (\beta_1 - \beta_2 + \beta_3 - \beta_4)$$
$$S_8 = \sqrt{RS}/2\ (\vartheta'_1 + \vartheta'_2)$$

B_1
$$S_9 = 1/\sqrt{2}\ (t_1 - t_2)$$
$$S_{10} = \sqrt{ST}/2\ (\beta_1 - \beta_2 - \beta_3 + \beta_4)$$
$$S_{11} = \sqrt{RS}/2\ (\vartheta'_1 - \vartheta'_2)$$

B_2
$$S_{12} = 1/\sqrt{2}\ (r_1 - r_2)$$
$$S_{13} = \sqrt{ST}/2\ (\beta_1 + \beta_2 - \beta_3 - \beta_4)$$
$$S_{14} = 1/\sqrt{2}\ (s_1 - s_2)$$
$$S_{15} = \sqrt{RS}/2\ (\vartheta_1 - \vartheta_2)$$

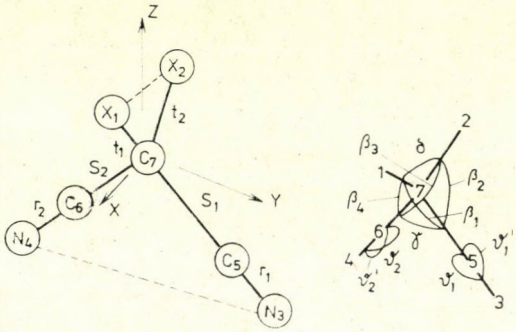

Fig. 1

Neglecting the valence coordinate δ in Fig. 1, we could avoid redundancy in species A_1. The calculation can be carried out with very similar results in both cases, we still publish the results according to this set of symmetry coordinates with redundancy to attach to earlier works on these molecules.

In Fig. 2 the valence coordinates are given for model $XHC(CN)_2$, symmetry C_s. As it can be recognized at once, we have kept all the valence coordinates from model $X_2C(CN)_2$ if it has been possible. Therefore, a bit unusual

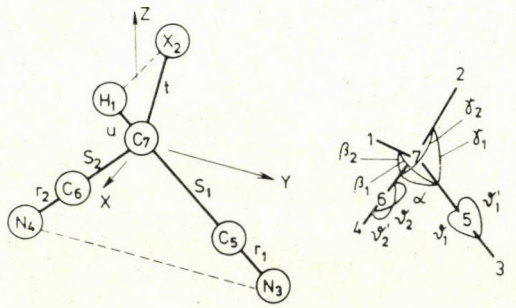

Fig. 2

Table I

Observed frequencies (cm^{-1}) and structural data of $X_2C(CN)_2$ molecules (X=H,D,F,Cl,Br)

Species	Assignation	$H_2C(CN)_2$ [1]	$D_2C(CN)_2$ [1]	$F_2C(CN)_2$ [2]	$Cl_2C(CN)_2$ [3]	$Br_2C(CN)_2$ [3]
	ν_1 C—X str.	2935	2146	1170	793	717
	ν_2 C≡N str.	2275	2272	2260	2258	2250
	ν_3 XCX bend.	1395	1037	465	504	384
A_1	ν_4 C—C str.	893	858	733	930	915
	ν_5 CCC bend.	582	577	559	569	572
	ν_6 CCN i. p. bend.	167	163	153	176	173
	ν_7 XCX bend.	1225	892	488	469	462
A_2	ν_8 CCN o. p. bend.	371	356	190	155	154
	ν_9 C—X str.	2968	2230	1144	793	717
B_1	ν_{10} XCX bend.	936	795	638	440	437
	ν_{11} CCN o. p. bend.	337	302	133	137	131
	ν_{12} C≡N str.	2275	2272	2259	2258	2250
	ν_{13} XCX bend.	1320	1153	521	266	284
B_2	ν_{14} C—C str.	985	829	804	1085	1080
	ν_{15} CCN i. p. bend.	366	356	255	233	209
R (C≡N)		1.17	1.17	1.17	1.17	1.17 Å
S (C—C)		1.47	1.47	1.47	1.47	1.47 Å
T (C—X)		1.10	1.10	1.35	1.70	1.86 Å
B (XCC) = Γ (CCC) = Δ (XCX)		109.47°	109.47°	109.47°	109.47°	109.47°
Θ (CCN)		180.00°	180.00°	180.00°	180.00°	180.00°

combinations emerged in S_9, S_{15}, because of the opposite side orientation of ϑ_1', and ϑ_2' to CCC plane. Symmetry coordinates are as follows:

$$
\begin{aligned}
\text{A'}\quad S_1 &= u \\
S_2 &= 1/\sqrt{2}\ (r_1 + r_2) \\
S_3 &= t \\
S_4 &= \sqrt{SU/2}\ (\beta_1 + \beta_2) \\
S_5 &= 1/\sqrt{2}\ (s_1 + s_2) \\
S_6 &= \sqrt{ST/2}\ (\gamma_1 + \gamma_2) \\
S_7 &= S \cdot \alpha \\
S_8 &= \sqrt{RS/2}\ (\vartheta_1 + \vartheta_2) \\
S_9 &= \sqrt{RS/2}\ (\vartheta_1' - \vartheta_2') \\
\text{A''}\quad S_{10} &= 1/\sqrt{2}\ (r_1 - r_2) \\
S_{11} &= \sqrt{SU/2}\ (\beta_1 - \beta_2)
\end{aligned}
$$

$$S_{12} = 1/\sqrt{2}\ (s_1 - s_2)$$
$$S_{13} = \sqrt{ST/2}\ (\gamma_1 - \gamma_2)$$
$$S_{14} = \sqrt{RS/2}\ (\vartheta_1 - \vartheta_2)$$
$$S_{15} = \sqrt{RS/2}\ (\vartheta'_1 + \vartheta'_2)$$

Force field

The force field calculations for each of the molecules studied started by the construction of starting F_0 matrices $F_{ii} \neq 0$, $F_{ij} = 0$ $(i \neq j)$. These F_0 matrices were constructed to give the best approach in terms of the eigenvalues λ_0 to the observed frequencies λ_{obs}. Then these initial F_0 matrices have been used to calculate the eigenvector matrices L_0 for each of the studied

Table II

Observed frequencies (cm^{-1}) and structural data of HXC $(CN)_2$ molecules ($X = D$, Br)

Species	Assignation	HDC $(CN)_2$ [1]	HBrC $(CN)_2$ [3]
	ν_1 C—H str.	2948	2946
	ν_2 C≡N str.	2272	2263
	ν_3 C—X str.	2194	690
	ν_4 HCC bend.	1247	1145
	ν_5 C—C str.	937	900
A'	ν_6 XCC bend.	816	429
	ν_7 CCC bend.	582	583
	ν_8 CCN o.p. bend.	320	200
	ν_9 CCN i. p. bend.	150	153
	ν_{10} C≡N str.	2272	2263
A''	ν_{11} HCC bend.	1282	1285
	ν_{12} C—C str.	1063	1020
	ν_{13} XCC bend.	856	460
	ν_{14} CCN o. p. bend.	374	363
	ν_{15} CCN i. p. bend.	357	153
R (C≡N)		1.17	1.17 Å
S (C—C)		1.47	1.47 Å
T (C—X)		1.10	1.86 Å
U (C—H)		1.10	1.10 Å
A (CCC) = B (XCC) = Γ (HCC)		109.47°	109.47°
Θ (CCN)		180.00°	180.00°

Table III

Elements of F matrices for $X_2C(CN)_2$ molecules (mdyne/Å)

	X =						X =						X =					
	H	4.80					H	0.42					H	4.68				
	D	4.80					D	0.42					D	4.75				
	F	3.24					F	0.43					F	3.73				
	Cl	5.79					Cl	0.38					Cl	1.96				
	Br	7.36					Br	0.42					Br	1.87				
							A_2											
	H	0.00	18.04				H	0.00	0.20				H	0.00	0.44			
	D	−0.06	17.95				D	0.00	0.19				D	0.00	0.45			
	F	0.07	17.67				F	0.03	0.15				F	0.47	0.96			
	Cl	0.54	17.07				Cl	0.00	0.17				Cl	0.23	0.42			
	Br	1.14	16.96				Br	−0.05	0.21				Br	0.17	0.30			
	H	0.01	0.00	0.33									H	0.00	0.00	0.17		
	D	0.02	0.05	0.34									D	0.00	0.00	0.17		
	F	0.00	−0.07	0.70									F	0.08	0.06	0.06		
	Cl	−0.15	−0.02	1.37									Cl	0.10	0.02	0.11		
	Br	−0.47	0.06	1.69									Br	0.17	0.00	0.20		
A_1																		
	H	−0.02	0.14	−0.02	5.34								H	17.83				
	D	−0.00	0.30	0.06	5.56								D	17.50				
	F	0.04	0.19	−0.14	5.90								F	18.66				
	Cl	0.39	−0.20	0.00	5.46								Cl	17.72				
	Br	1.42	−0.10	0.25	5.67								Br	17.49				
	H	−0.01	−0.07	0.06	−0.10	0.42							H	0.10	0.33			
	D	−0.03	−0.09	0.06	−0.13	0.40							D	0.23	0.37			
	F	0.12	−0.13	0.00	−0.26	0.69							F	0.16	0.43			
	Cl	0.98	−0.62	−0.27	−0.75	1.11							Cl	−0.02	0.29			
	Br	1.15	−0.56	−0.55	−0.66	1.20							B_2 Br	0.02	0.29			
	H	−0.00	−0.03	0.00	−0.06	0.00	0.30						H	0.45	0.16	6.12		
	D	−0.00	−0.02	0.01	−0.04	0.00	0.29						D	0.16	0.35	5.83		
	F	0.04	−0.12	0.09	−0.16	0.06	0.27						F	0.00	0.26	2.34		
	Cl	0.10	−0.07	0.04	−0.10	−0.02	0.24						Cl	−0.12	−0.04	4.15		
	Br	0.12	−0.04	−0.03	−0.02	−0.03	0.22						Br	−0.08	0.03	4.45		
													H	−0.00	−0.00	−0.00	0.19	
													D	0.01	0.00	0.01	0.18	
													F	0.12	0.06	0.21	0.23	
													Cl	−0.08	−0.07	−0.15	0.12	
													Br	−0.06	−0.07	−0.11	0.12	

Table IV

Elements of F matrices for $HXC(CN)_2$ molecules

X =									
D	4.70								
Br	4.70								
D	−0.00	18.38							
Br	−0.00	18.41							
D	0.00	−0.00	4.81						
Br	0.00	0.23	4.95						
D	−0.00	0.02	0.01	0.96					
Br	−0.04	−0.09	−0.20	0.76					
D	−0.00	0.17	−0.02	0.04	4.16				
Br	−0.01	0.18	0.36	−0.15	3.96				
D	0.00	0.02	−0.00	0.00	0.05	0.78			
Br	0.01	−0.08	0.11	0.14	−0.13	1.20			
D	0.01	0.12	0.02	0.01	0.22	0.02	0.98		
Br	0.01	0.16	−0.30	0.08	0.25	−0.05	0.87		
D	−0.00	−0.05	−0.00	−0.00	−0.06	−0.00	−0.03	0.14	
Br	−0.00	−0.03	0.04	−0.01	−0.06	−0.01	0.01	0.17	
D	0.00	−0.00	−0.00	−0.00	−0.00	0.01	−0.00	0.00	0.16
Br	−0.00	−0.01	−0.05	−0.02	−0.03	−0.03	−0.01	−0.01	0.14

X =									
D	17.73								
Br	17.56								
D	0.02	0.27							
Br	0.13	0.47							
D	0.10	0.02	5.19						
Br	0.03	0.21	4.97						
D	0.12	−0.03	0.18	0.62					
Br	−0.05	−0.07	−0.09	1.00					
D	0.00	−0.00	0.00	−0.00	0.19				
Br	−0.02	−0.01	−0.03	−0.05	0.20				
D	−0.00	0.00	−0.00	0.00	−0.00	0.18			
Br	0.00	0.01	0.00	−0.02	0.02	0.08			

Table V

Potential energy distribution ($Y_{ik} = 100 \cdot F_{ii}L_{ik}^2/\lambda_k$) for $X_2C(CN)_2$ molecules ($X = H,D,F,Cl,Br$)

	X =	S_1	S_2	S_3	S_4	S_5	S_6	S_7	S_8
	H	98.8							
ν_1	D	89.4							
	F	26.9			40.3	39.6			
	Cl			47.7	10.0		17.1		
	Br	13.1		65.4	24.3		15.7		
	H		89.8		10.7				
	D		82.2		12.7				
ν_2	F		88.1		13.0				
	Cl		85.0		12.6				
	Br		85.0		13.2				
	H			52.3		63.4			
	D			30.2	23.5	63.8			
ν_3	F	10.8		40.8		35.8			
	Cl			29.7		28.4			
	Br	21.3		14.6		25.0			
	H			16.4	67.4				
	D			36.4	45.3				
ν_4	F			25.5	11.2		26.9		
	Cl	69.8	14.7		50.1	105.6			
	Br	74.9	15.2	16.9	50.5	125.3	10.2		
	H			10.1	17.6	11.7	48.8		
	D			10.3	18.3	11.5	48.9		
ν_5	F	61.8				31.2			
	Cl	44.2			44.0				
	Br	32.4			36.6				
	H			23.9		25.8	42.5		
	D			26.4		24.7	42.3		
ν_6	F			36.2		20.2	74.8		
	Cl			22.6			78.4		
	Br			17.0			77.1		
	H							99.6	
	D							98.2	
ν_7	F							54.4	35.6
	Cl							47.7	49.9
	Br							52.1	67.2
	H								99.6
	D								98.3
	F							46.9	65.7
ν_8	Cl							52.4	50.2
	Br							50.6	35.6

Table V — *continued*

	X =	S_9	S_{10}	S_{11}	S_{12}	S_{13}	S_{14}	S_{15}
	H	99.5						
	D	98.4						
ν_9	F	67.2	61.5					
	Cl	60.9	67.2					
	Br	63.4	62.4	21.7				
	H		93.8					
	D		86.5	10.9				
ν_{10}	F		38.8	30.3				
	Cl	41.2	12.6	18.7				
	Br	32.6		39.2				
	H			94.3				
	D		12.1	88.4				
ν_{11}	F		18.6	100.4				
	Cl		27.3	78.4				
	Br	18.0	39.7	47.3				
	H				86.4		16.6	
	D				85.2		15.2	
ν_{12}	F				95.5			
	Cl				89.0		10.0	
	Br				88.2		11.1	
	H					56.7	44.4	
	D				14.4	37.0	76.1	
ν_{13}	F					10.7	18.6	38.1
	Cl					51.7	19.9	105.8
	Br					47.6	11.1	97.0
	H					44.0	39.8	
	D					68.1	13.7	
ν_{14}						57.8	74.7	
	Cl					15.2	71.4	
	Br				10.8	13.8	76.7	
	H							99.4
	D							98.4
ν_{15}	F					41.7	17.1	67.8
	Cl					51.7		17.4
	Br					52.5		18.7

molecules. After these preparatory steps the force field refinements have been carried out in one step according to the formula [4]:

$$F = \tilde{L}_0^{-1} \lambda_{obs} L_0^{-1}$$

These F matrices are consistent exactly with the given assignments λ_{obs}. although the diagonal form of initial force field matrices F_0 will be destroyed this way and interaction constants are introduced in F.

Table VI

Potential energy distribution ($Y_{ik} = 100 \cdot F_{ii}L^2_{ik}/\lambda_k$) for $HXC(CN)_2$ molecules ($X = D$, Br)

X =	S_1	S_2	S_3	S_4	S_5	S_6	S_7	S_8	S_9
ν_1 D	98.3								
Br	98.8								
ν_2 D		85.3							
Br		93.4							
ν_3 D			89.0						
Br				16.1	30.5	23.5			
ν_4 D				84.9		10.4			
Br			43.3	43.6		25.1			
ν_5 D					39.0		59.0		
Br			10.0	30.6	35.9		48.1		
ν_6 D				11.8		82.4			
Br			14.4		21.9	23.4		18.9	
ν_7 D					48.2		20.9		
Br			31.8	10.8			25.9	12.4	
ν_8 D									95.2
Br						25.1			73.2
ν_9 D							20.3	85.4	
Br							15.8	70.7	

	S_{10}	S_{11}	S_{12}	S_{13}	S_{14}	S_{15}			
ν_{10} D	86.9		13.6						
Br	86.8		13.2						
ν_{11} D		13.2	38.5	55.7					
Br	10.3	19.8	54.5	26.4					
ν_{12} D		51.1		31.8					
Br		82.1							
ν_{13} D		35.9	42.8	13.6					
Br		27.9	57.6	17.0					
ν_{14} D					98.6				
Br					76.1				
ν_{15} D						99.3			
Br				11.1		86.9			

Observed frequencies and structural data are summarized in Tables I—II, elements of refined force field matrices are collected in Tables III—IV.

Potential energy distribution

Neglecting the figures less than 10, calculated potential energy distribution terms for malononitrile molecules are shown in Tables V—VI. According to these calculations the description of normal modes are compatible

only in part with the assignments of frequencies done by the authors of cited papers [1, 2, 3]. Considerable mixing between different vibrational types is indicated in many cases. The C–C and C–X stretching modes contain in almost all of the cases significant contributions from CCX, CCC or XCX valence angle bending modes.

REFERENCES

[1] Fujiyama, T., Shimanouchi, T.: Spectrochim. Acta **20,** 829 (1964)
[2] Perettie, D. J., Wait, S. C. Jr.: J. Mol. Spectroscopy **32,** 222 (1969)
[3] Van Haverbeke, L., Desseyn, H. O., Van Der Veken, B. J.: Bull. Soc. Chim. Belg. **82,** 133 (1973)
[4] Cyvin, S. J.: Molecular Vibrations and Mean Square Amplitudes, Universitetsforlaget, Oslo, and Elsevier, Amsterdam, 1968

Béla Vizi
Attila Sebestyén } H-8200 Veszprém, Schőnherz Z. u. 12.

Acta Chimica Academiae Scientiarum Hungaricae, Tomus 90 (4), pp. 365—369 (1976)

ZUR EXTRAKTION DES NB(V) MIT POLYPHENOLEN

A. I. Busev, S. P. Karjakina und P. Nenning*

(Chemische Fakultät der Lomonossov-Universität, Moskau, und Sektion Chemie der Karl-Marx-Universität, Leipzig)

Eingegangen am 1. December, 1975

Untersucht wurden die Bedingungen der Bildung und Extraktion von Verbindungen des Niob(V) mit Pyrokatechin, Pyrogallol, Tetrabrompyrokatechin und Tribrompyrogallol in Anwesenheit von Diphenylguanidin.

Charakteristisch für das Niob ist seine Wechselwirkung mit verschiedenen hydroxylhaltigen organischen Reagenzien. Mit Phenolen, die zwei oder mehr Hydroxylgruppen in *ortho-* oder *meta*-Stellung tragen — Pyrogallol, Pyrokatechin, Tiron, Gallussäure, Tribrompyrogallol, Pyrokatechinsulfonsäure u. a. — bildet Niob farbige Verbindungen, die zu seiner fotometrischen Bestimmung Verwendung finden. So wird Pyrokatechin zur extraktiven Abtrennung und nachfolgenden fotometrischen Bestimmung von Niob, Tantal und Titan verwendet [1]. Vorgeschlagen wurde eine extraktionsfotometrische Bestimmungsmethode für das Niob in Form seines ternären Komplexes mit α, β-Dipyridil und Pyrokatechin [2]. Für die Niobbestimmung ist auch Pyrogallol [3, 4] schon verwendet worden. Die Selektivität der Methode wird durch Extraktion erhöht [5]. Beschrieben ist eine Niobbestimmung mit Tiron [6], Tribrompyrogallol [7], Gallussäure [8].

Das Ziel der vorliegenden Arbeit ist die Untersuchung der Extraktion von Niobverbindungen mit einigen Polyphenolen in Anwesenheit des relativ großen organischen Kations vom Diphenylguanidin.

Experimenteller Teil

Reagenzien und Geräte. Die Niobstandardlösung stellen wir durch Schmelzen von Nb(V)-oxyd mit Kaliumpyrosulfat und nachfolgendem Auslaugen der Schmelze mit Ammoniumoxalat her. Verwendet wird eine $5 \cdot 10^{-4}$ *M* Nioblösung in 1%igem Ammoniumoxalat.

Pyrokatechin und Pyrogallol werden durch Destillation gereinigt. Tribrompyrogallol wird durch Bromieren von Pyrogallol nach [9] erhalten. Umkristallisieren aus Chloroform und Trocknen bei 105 °C führt zu einem Produkt mit Fp 168 °C (Lit. [10]: 168—171 °C). Tetrabrompyrokatechin wird durch Bromieren von Pyrokatechin nach [11] hergestellt.

Eine $4 \cdot 10^{-2}$ *M*-Lösung von Diphenylguanidiniumchlorid erhalten wir durch Lösen einer genauen Einwaage von gereinigtem Diphenylguanidin in Salzsäure. Der pH-Wert der

* Postadresse: Dr Peter Nenning, Karl-Marx-Universität Leipzig, Sektion Chemie, 701 Leipzig, Liebigstraße 18. DDR

Lösung soll 4 betragen. Die Extinktion der Lösung wird am Spektrofotometer SF-4 gemessen in Küvetten mit 1 cm Schichtdicke, der pH der Lösung wird mit Glaselektrode und pH-Meter LP-58 kontrolliert.

Als Extraktionsmittel wird ein Gemisch von Chloroform und Isoamylalkohol 1 : 1 verwendet, z. T. auch Äthylacetat. Der Isoamylalkohol wird nach WEISBERGER [12] gereinigt, das Äthylacetat durch Destillation.

Fotometrische Charakteristik der entstehenden Verbindungen

In Abb. 1 sind die Absorptionskurven für die Extrakte des Niob mit Pyrokatechin (Kurve 1), Pyrogallol (Kurve 2), Tribrompyrogallol (Kurve 3), Tetrabrompyrokatechin (Kurve 4 und Kurve 5) mit einem Chloroform/Isoamylal-

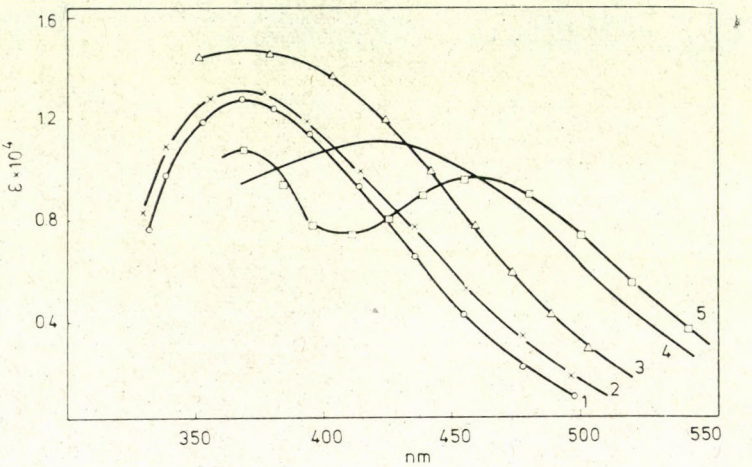

Abb. 1. Lichtabsorption der Extrakte der Niob(V)-polyphenolverbindungen: 1. Pyrokatechin; $5 \cdot 10^{-5}$ *M* Nb, 0.02 M Pyrokatechin, $4 \cdot 10^{-2}$ *M* Diphenylguanidin, pH der wäßrigen Phase nach der Extraktion 6,1; 2. Pyrogallol; $5 \cdot 10^{-5}$ *M* Nb, 0,2 *M* Pyrogallol, 10^{-2} *M* Diphenylguanidin, pH der wäßrigen Phase nach der Extraktion 6,2; 3. Tribrompyrogallol: $5 \cdot 10^{-5}$ *M* Nb, $2 \cdot 10^{-2}$ *M* Tribrompyrogallol, $4 \cdot 10^{-2}$ *M* Diphenylguanidin, pH der wäßrigen Phase nach der Extraktion 4,0; 4. Tetrabrompyrokatechin; $5 \cdot 10^{-5}$ *M* Nb, $4 \cdot 10^{-2}$ *M* Tetrabrompyrokatechin, $4 \cdot 10^{-2}$ *M* Diphenylguanidin, pH der wäßrigen Phase nach der Extraktion 2.5; 5. Tetrabrompyrokatechin: $5 \cdot 10^{-5}$ *M* Nb, $2 \cdot 10^{-2}$ *M* Tetrabrompyrokatechin, $4 \cdot 10^{-2}$ *M* Diphenylguanidin, pH der wäßrigen Phase nach der Extraktion 4,2

kohol-Gemisch 1 : 1 angegeben. Die Absorptionskurven für die Niobextrakte werden auf folgende Weise erhalten: In einen Scheidetrichter gibt man 1 ml $5 \cdot 10^{-4}$ *M* Nioblösung in 1%igem Ammoniumoxalat, dazu die gleiche Menge destilliertes Wasser, 2 Tropfen NH_4OH 1 : 10 verdünnt, 2 ml frischbereitete 1 *M*-Lösung eines der genannten Polyphenole in 1%igem Kaliummetabisulfit und schließlich Diphenylguanidinlösung; das Volumen der wäßrigen Phase beträgt ca 10 ml. Extrahiert wird mit 10 ml Chloroform/Isoamylalkohol 1 : 1, der pH der wäßrigen Phase ist nach der Extraktion ca 6,2. Die Extinktion der Extrakte, die gelb gefärbt sind, wird in Relation zu einer Leerprobe gemessen.

Das Absorptionsmaximum für die Niob-pyrokatechin-, Niob-pyrogallol- und Niob-tribrompyrogallolverbindungen liegt bei 370 nm. Für das Niob-tetrabrompyrokatechin ist das Maximum in das langwellige Gebiet verschoben (430 nm bei pH = 2,5); die sich bei pH = 4,2 bildende Verbindung hat 2 Maxima: bei 370 nm und 460 nm (Kurven 4 und 5 in Abb. 1). Der Charakter der Absorptionskurven des Niob-tetrabrompyrokatechins ändert sich nicht bei Extraktion mit Äthylacetat.

Der gelbe Komplex des Niob(V) mit Pyrokatechin läßt sich in Anwesenheit von Diphenylguanidin mit Dichloräthan, Isoamylalkohol, Amylalkohol, Äthylacetat, Cyclohexanon, Methylisobutylketon, Benzol, Chlorbenzol und Chloroform extrahieren. Tetrachlormethan flotiert die sich bildende Verbindung. Wir haben aus 10 ml wäßriger Lösung extrahiert, die Niobkonzentration ist $5 \cdot 10^{-5}$ *M*, des Pyrokatechins 0,2 *M*, des Diphenylguanidins $4 \cdot 10^{-2}$ *M*. Wir verwenden eines der folgenden Lösungsmittel:

1 — Chloroform
2 — Isoamylalkohol
3 — Chloroform/Isoamylalkohol 1 : 1
4 — Methylisobutylketon
5 — Benzol

Die geringste Extinktion hat der Benzolextrakt. Das Chloroform/Isoamylalkohol-Gemisch 1 : 1 extrahiert so gut wie Methylisobutylketon und besser als Chloroform und Isoamylalkohol allein. Die Absorptionskurven der Niobverbindung in verschiedenen Lösungsmitteln sind praktisch identisch, das Maximum liegt bei 370 nm.

Extraktionsbedingungen. In Abb. 2 ist das pH-Intervall angegeben, in dem die Niobverbindungen beständig sind. Kurve 1 zeigt die Bildung der gefärbten Niob-pyrokatechinverbindung, Kurve 2 die mit Pyrogallol, Kurve 3 die mit Tribrompyrogallol. Die Verbindung des Niob mit Tetrabrompyrokatechin (Kurve 4) ist auch im stärker sauren stabil (von pH 0 bis pH = 3,5). Zur Extraktion des Niob mit Tetrabrompyrokatechin verwenden wir Äthylacetat, zur Extraktion der übrigen Verbindungen ein Chloroform/Isoamylalkohol-Gemisch 1 : 1. Zum Erzielen einer konstanten Extinktion empfehlen wir für die Niobextraktion eine Pyrokatechinkonzentration von 0,2 *M* und eine Diphenylguanidinkonzentration von $2 \cdot 10^{-2}$ *M* bzw. eine Pyrogallolkonzentration von 0,2 *M* und eine Diphenylguanidinkonzentration von 10^{-2} *M* in der wäßrigen Phase.

Die scheinbaren molaren Absorptionskoeffizienten der Verbindung mit Pyrokatechin $\varepsilon_{370} = 12\,700 \pm 800$ und der Verbindung mit Pyrogallol $\varepsilon_{370} = 13\,600 \pm 800$.

Bei Verwendung eines Chloroform/Isoamylalkohol-Gemisches 1 : 1 zur Extraktion der Niob-tetrabrompyrokatechinverbindung wird in Anwesenheit von Diphenylguanidin ein konstanter Wert der Extinktion auch bei $6 \cdot 10^{-2}$ *M* Tetrabrompyrokatechinkonzentration in der organischen Phase nicht erreicht. Außerdem scheidet sich aus dem Extrakt ein weißer Niederschlag des

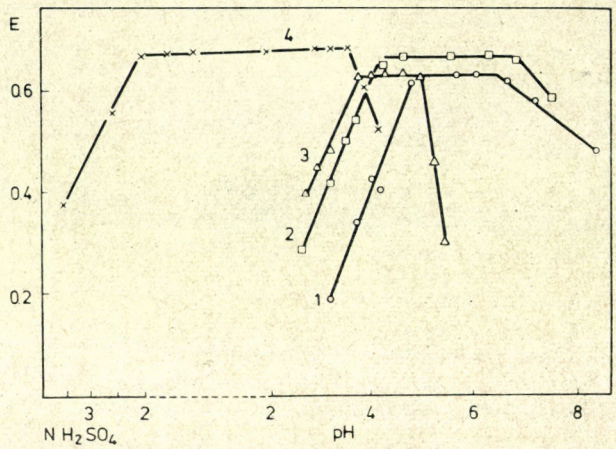

Abb. 2. Die Abhängigkeit der Extinktion vom pH Wert der Extrakte der Niob(V)-polyphenolverbindungen: 1. Pyrokatechin; $5 \cdot 10^{-6}$ *M* Nb, 0,2 *M* Pyrokatechin, $4 \cdot 10^{-2}$ *M* Diphenylguanidin; 2. Pyrogallol; $5 \cdot 10^{-5}$ *M* Nb, 0,2 *M* Pyrogallol, 10^{-2} *M* Diphenylguanidin; 3. Tribrompyrogallol; $5 \cdot 10^{-5}$ *M* Nb, $5 \cdot 10^{-3}$ *M* Tribrompyrogallol, $2 \cdot 10^{-2}$ *M* Diphenylguanidin; 4. Tetrabrompyrokatechin; $5 \cdot 10^{-5}$ *M* Nb, 0,1 *M* Tetrabrompyrokatechin, $4 \cdot 10^{-2}$ *M* Diphenylguanidin. Extraktionsmittel für 1, 2 und 3: Chloroform/Isoamylalkohol 1 : 1; Extraktionsmittel für 4: Äthylacetat

Reagenzes ab, der die Extinktionsmessung beeinträchtigt. Äthylacetat ist in diesem Falle günstiger zu verwenden. Eine konstante Extinktion bei pH > 3 wird erreicht bei einer Tetrabrompyrokatechinkonzentration von $5 \cdot 10^{-2}$ *M*, bei pH < 3 bei 0,1 *M* Konzentration. Das Extraktionsgleichgewicht hat sich nach ~ 3 min eingestellt. Im stark sauren Gebiet erhält man bisweilen nicht reproduzierbare Ergebnisse, da die Komplexbildung offenbar nicht vollständig verläuft.

Ist im Chloroform/Isoamylalkohol-Gemisch 1 : 1 die Tribrompyrogallolkonzentration $2 \cdot 10^{2}$ *M*, erhält man keine Konstanz der Extinktion für eine bestimmte Niobkonzentration, ungeachtet der Anwesenheit von Diphenylguanidin.

Was die Extrakte der Verbindungen des Nb(V) mit Pyrokatechin und Pyrogallol betrifft, so findet man eine direkte Proportionalität zwischen der Extinktion und der Niobkonzentration in den Grenzen 0.5—14 μg/ml. Die Eichkurven für die Extrakte der Verbindungen des Niob mit Pyrokatechin und Pyrogallol fallen praktisch zusammen.

Zusammensetzung der sich bildenden Verbindungen. Zur Feststellung des molaren Verhältnisses Niob-Diphenylguanidin in seiner Verbindung mit Pyrokatechin wurde die Methode der molaren Verhältnisse verwendet, für das Feststellen des molaren Verhältnisses Niob zu Diphenylguanidin in der Verbindung mit Pyrogallol die Methode der Verschiebung der Gleichgewichte. In beiden Fällen wurde das molare Verhältnis Niob zu Diphenylguanidin zu 1 : 2 gefunden. Bei Versuchen zur Bestimmung des molaren Verhältnisses des Niob zu Pyrokatechin und Pyrogallol durch die Methode der Gleichgewichtsverschiebung haben wir keine eindeutigen Ergebnisse erhalten.

LITERATUR

[1] SAIKOVSKIJ, F. V.: J. analyt. Chem. (UdSSR) **11 (13)**, 269 (1956)
[2] TALIPOV, S. T., DSHIJANBAJEVA, R. Ch.: Usbek. chem. J. (UdSSR) **5**, 26 (1963)
[3] PLATONOV, N. S., KRIVOSCHLYKOV, N. F.: Ber. Allunionskonfer. anal. Chem. (UdSSR) **2**, 359 (1943)
[4] ALIMARIN, I. P., FRID, V. I.: *ibid.* **2**, 333 (1943)
[5] CATOGGIO, J. A., ROGERS, L. B.: Talanta **9**, 377 (1962)
[6] FLASCHKA, H., LASSNER, E.: Mikrochim. Acta **4—6**, 778 (1956)
[7] ACKERMANN, G., KOCH, S.: Talanta **9**, 1015 (1962)
[8] MADHAVA MENON, V. P., MAHADEVAN, N., SRINIVASULU, K., Ch. VENKATESVARLU: J. Sci. Ind. Res. (India) **21** B, 20 (1962) C. A. **57**, 34 g (1962)
[9] HLASIWETZ, H.: Lieb. Ann. **142**, 250 (1867)
[10] KOHN, M., GRÜN, S.: Monatsh. **46**, 83 (1925)
[11] ZINCKE, Th.: Ber. dtsch. chem. Ges. **20**, 1776 (1887)
[12] WEISBERGER, A., PROSKAUER, E., RIDDIK, J., TUPE, E.: Organische Lösungsmittel (russ.), Moskau 1958

A. I. BUSEV
S. P. KARJAKINA } Lomonossov-Univ., Moskau UdSSR

P. NENNING Karl-Marx-Univ. Leipzig, Sektion Chemie, 701 Leipzig, Liebigstraße 18. DDR

Acta Chimica Academiae Scientiarum Hungaricae, Tomus 90 (4), pp. 371—374 (1976)

SPECTRAL AND MAGNETIC STUDIES OF COPPER(II) CHELATES OF L-ASPARAGINE AND L-GLUTAMINE

(SHORT COMMUNICATION)

R. C. TEWARI and M. N. SRIVASTAVA*

(Chemical Laboratories, University of Allahabad, Allahabad, India)

Received December 5, 1975

In revised form March 10, 1976

Copper (II) chelates of L-asparagine and L-glutamine have been studied using reflectance, u. v. absorption spectra, magnetic and e. s. r. measurements. On this basis a distorted octahedral structure is suggested for these complexes.

Introduction

Copper (II) chelates of L-asparagine and L-glutamine were investigated in solution by ALBERT [1], RITSMA *et al.* [2] and TEWARI and SRIVASTAVA [3]. Recently FUJIMOTO [4] and MISHRA [5] *et al.* made an e. s. r. study of copper (II) asparagine complex. In the present work an attempt has been made to study these complexes using reflectance and u. v. absorption spectra, magnetic and e. s. r. measurements. Their preparation and characterization from analytical and i. r. data were reported in an earlier paper [6]. The complexes are: bis (L-asparagino) copper (II) $[Cu(OOC \cdot CH \cdot NH_2 \cdot CH_2 \cdot CONH_2)_2]$ and bis (L-glutamino) copper (II) $[Cu(OOC \cdot CH \cdot NH_2 \cdot CH_2 \cdot CH_2 \cdot CONH_2)_2]$.

Experimental

Magnetic measurements at room temperature (304 °K) were made on powder samples of the complexes employing Gouy's method. A semimicro Sartorius balance was employed and mercury(II) tetrathiocyanatocobaltate(II) ($\chi_g = 16.44 \times 10^{-6}$ c. g. s. units) was used as calibrant. Both complexes were found to be paramagnetic. The data are presented in Table I.

Reflectance spectra of the solid complexes were recorded on a 'C ∅ — 10' recording spectrophotometer (Russian) in the range 400—700 m μ. Both complexes showed one asymmetric band, λ_{max} being observed at $\sim$ 620 m. μ (16 100 cm^{-1}) in the copper (II) L-asparagine chelate and at $\sim$ 610 m. μ (16 400 cm^{-1}) in the copper(II) L-glutamine chelate.

* Postal address: Dr. M. N. SRIVASTAVA, 266 (near distillery) Mumfordganj, Allahabad 211 002, U. P. India

Table I

Magnetic susceptibility measurements on Cu(II) chelates

Compound	T°K	$\chi_g \times 10^6$ (c. g. s. units)	$\chi_M \times 10^6$ (c. g. s. units)	$\chi_{M'} \times 10^6$ (c. g. s. units)	μ_{eff} (B. M.)
Cu $(Aspn)_2$	304	4.12	1341	1477	1.90
Cu $(Glun)_2$	304	3.82	1350	1509	1.92

U. V. absorption spectra were recorded on aqueous solution on a Cary-14 recording spectrophotometer, using 1 cm quartz cells. The absorption bands are listed in Table II.

Table II

U. V. spectra of Cu(II) chelates

Compound	Band (cm^{-1})	Compound	Band (cm^{-1})
	42 330 b. s.		42 190 b. s.
Cu $(Aspn)_2$	50 760 s	Cu $(Glun)_2$	51 280 s
	51 680 w		
	52 230 m		52 230 m

b = broad, s = strong, m = medium, w = weak

Electron spin resonance spectra of solid complexes were taken on a Bruker model B—ER 402 × band, ESR spectrophotometer and polycrystalline DPPH was used as a reference. The data on electronic '*g*' factors are given in Table III. These values tally well with those reported by other workers for copper(II) amino acid complexes [4, 5, 7].

Table III

'g' values of the Cu(II) chelates

Compound	$g_\perp$	$g_{\parallel}$	g_{av}
Cu $(Aspn)_2$	2.050	2.253	2.12
Cu $(Glun)_2$	2.046	2.212	2.10

Discussion

The ground state of the cubic octahedrally coordinated Cu(II) is ^2E_g, and the only excited state is $^2T_{2g}$, the energy difference being 10 Dq [8]. But tetragonal distortion splits the E_g and T_{2g} levels so that as many as three *d–d* transitions are possible [9].

$$d_{xy} \leftarrow d_{x^2-y^2};\ d_{z^2} \leftarrow d_{x^2-y^2};\ (d_{xz},\ d_{yz}) \leftarrow d_{x^2-y^2}$$

Thus the observed band envelope may not be due to a single transition, but may be made of two or three symmetrical absorption bands.

The expressions [10] derived for '*g*' values in a tetragonally distorted copper(II) molecule, which is stretched along the symmetry axis (Z axis) are $g_{||} = 2-8\lambda/(E_2-E_0)$ and $g_{\perp} = 2-2\lambda/(E_3-E_0)$ where E_0, E_2 and E_3 are the energies corresponding to $^2B_{1g}$, $^2B_{2g}$ and ^2E_g levels. Under such conditions $g_{||}$ values ≈ 2.2 are obtained, whereas if d_{z^2} σ is lowest orbital, $g_{\perp}$ values approach a value of 2.0. Thus, the observed results support the contention that in copper(II) chelates $d_{x^2-y^2}$ is the lowest energy orbital and tetragonal distortion occurs along φ axis.

The bands observed in the u. v. spectra of the copper chelates can be attributed to charge transfer transitions. Earlier, in the case of bis (phenylglycino) copper(II) HARE [11] ascribed the band observed at 39 000 cm^{-1} to an apparent charge transfer from the carboxylic group to the metal, and that observed at 52 000 cm^{-1} to a charge transfer from amino group to metal with a possible contribution from the $\pi \rightarrow \pi^*$ transition of the COO^- group. Thus, in the present case the strong broad bands observed at 42 330 cm^{-1} in $Cu(Aspn)_2$ and at 42 190 cm^{-1} in $Cu(glun)_2$ correspond to a charge transfer from carboxylic group to the metal, whereas the bands observed at 50 760 cm^{-1} and 51 280 cm^{-1}, respectively, in the two chelates may be ascribed to charge transfer from the amino group to the metal. Other bands at $\sim$ 52 000 cm^{-1} may correspond to carboxyl $\pi \rightarrow \pi^*$ transitions.

Thus the present evidences indicate a tetragonally, distorted octahedral structure for the two copper(II) L-asparagine and L-glutamine chelates.

*

Authors are grateful to the C. S. I. R. New Delhi for providing financial assistance in the form of Senior Fellowship to one of the authors (R. C. TEWARI).

REFERENCES

[1] ALBERT, A.: Biochem. J., **47,** 531 (1950); **50,** 690 (1962)
[2] RITSMA, J. H., WIEGERS, W. A., JELLINECK, F.: Rec. tran. Chim. **84,** 1577 (1973)
[3] TEWARI, R. C., SRIVASTAVA, M. N.: J. Inorg. Nucl. Chem., **35,** 2441 (1973)
[4] FUJIMOTO, M.: Bioinorganic Chem., **3,** 295 (1974)
[5] MISHRA, B. N., SHARMA, S. D., GUPTA, S. K.: J. Magn. Res. **16,** 193 (1974)
[6] TEWARI, R. C., SRIVASTAVA, M. N.: Ind. J. Chem., **12,** 527 (1974)
[7] TAMINAGA, I., Thesis, M. S.: The University of Tokyo (1967)
[8] BALLHAUSEN, C. J.: 'Introduction to Ligand Field Theory', McGraw Hill, N. Y. (1962)
[9] COTTON, F. A., WILKINSON, G.: 'Advanced Inorganic Chemistry', Interscience, N. Y. II Edn. p. 902 (1966)
[10] DRAGO, R. S.: 'Physical Methods in Inorganic Chemistry', Reinhold, N. Y., p. 340 (1965)
[11] HARE, R. C.: 'Visible and ultraviolet spectroscopy', in "Spectroscopy and structure of metal chelate compounds", NAKAMOTO, K., MCCARTHY, P. J., S. J. Eds. John Wiley and Sons, p. 74 (1968)

R. C. TEWARI
M. N. SRIVASTEVA
266 (near distillery) Mumfordganj Allahabad 211 002, U. P. India.

Acta Chimica Academiae Scientiarum Hungaricae, Tomus 90 (4), pp. 375—380 (1976)

ANALYTISCHE ANWENDUNG VON PT(II)-KOMPLEXEN MIT PYRAZOLONDERIVATEN

V. K. AKIMOV, A. I. BUSEV, K. V. KODUA und P. NENNING*

(Chemische Fakultät der Lomonossov-Universität, Moskau und Sektion Chemie der Karl-Marx-Universität, Leipzig)

Eingegangen an 5. Dezember 1975

Untersucht wurde die Wechselwirkung von Pt(II) in HBr-Lösung mit Pyrazolonderivaten. Die Tetrabromplatinate von Diantipyril-, Diantipyrilmethyl-, Diantipyrilpropylmethyl und Diantipyrilphenylmethan $(RH)_2\ PtBr_4$ wurden hergestellt, ihr Bildungsmechanismus, ihre Säure—Basen-Eigenschaften und die Löslichkeit der Verbindungen untersucht. Eine Methode zur gravimetrischen Bestimmung von 5—30 mg Pt durch Ausfällen und Wägen von $(C_{26}H_{30}N_4O_2H)_2\ PtBr_4$ wurde ausgearbeitet. Der maximale relative Fehler ist 0,91%. Es stören nicht: Mg, Al, Mn(II), Fe(II), Co, Ni, Ru (III), Rh(III).

Komplexe von Pt(IV)-halogeniden mit Pyrazolonderivaten wurden bereits früher untersucht [1]. Fotometrische und gravimetrische Platinbestimmungsmethoden mit diesen Komplexbildnern wurden ausgearbeitet [1, 2]. Die Halogenidkomplexe des Pt(II) mit Pyrazolonderivaten sind bisher nicht beschrieben. Es ist zu erwarten, daß auch sie günstige analytische Eigenschaften aufweisen, die man zur Ausarbeitung neuer Methoden der Platinbestimmung nutzen kann.

Wir haben Zusammensetzung und Eigenschaften von Pt(II)-bromidkomplexen studiert und ihre Eignung zur gravimetrischen Platinbestimmung festgestellt.

Experimenteller Teil

Reagenzien und Geräte. K_2PtBr_4 wird hergestellt durch Erwärmen einer K_2PtCl_4-Lösung in HBr 1 : 1 auf dem Wasserbad und anschließendes Verdünnen bis zu einer HBr-Konzentration 1 *N*. Verwendet werden weiterhin Diantipyrilmethan (DAM) der Reinheit p. a., Diantipyrilmethylmethan (DAMM) rein, Diantipyrilpropylmethan (DAPM) p. a., Diantipyrilphenylmethan (DAFM) p. a., ein Spektralfotometer UR 20, ein Potentiometer pH 340.

Darstellung, Zusammensetzung und Eigenschaften der Verbindungen. Beim Zufügen einer Lösung von DAM, DAMM, DAPM oder DAFM in Essigsäure 1 : 1 zu einer Lösung von Pt(II) in HBr fällt sofort ein Niederschlag aus. Die Niederschlagsbildung und der Niederschlag selbst werden wie folgt untersucht.

Eine Lösung von K_2PtBr_4 in 1 *N* HBr wird auf 70—80 °C erwärmt, unter Rühren werden langsam 5—7 ml einer 5%igen Lösung von DAM oder DAMM oder eine 2%ige Lösung von DAPM oder DAFM in Essigsäure 1 : 1 zugefügt. Es wird abgekühlt, der sich dabei (außer bei der Verbindung mit DAFM) abscheidende kristalline Niederschlag wird abfiltriert, 3 mal mit Wasser gewaschen und über P_2O_5 getrocknet. Im Niederschlag werden Pt und Stick-

* Postadresse: Dr. Peter NENNING, Karl-Marx-Universität Leipzig, Sektion Chemie, 701 Leipzig, Liebigstraße 18. DDR

stoff quantitativ bestimmt: Pt durch Verglühen einer Probe bei 700—800 °C und Auswiegen des metallischen Pt, Stickstoff nach Dumas. Die Summenformeln der Verbindungen sind in Übereinstimmung mit den Analysenwerten neben einigen Eigenschaften der Stoffe in Tabelle I aufgeführt.

Tabelle I

Zusammensetzung und Eigenschaften der Komplexe von Tetrabromplatinaten mit Pyrazolonderivaten

Summenformel	Fp °C	Farbe und Form des Niederschlags	Löslichkeit in 0,5 *N* HBr $M \cdot 10^{-5}$
$(C_{23}H_{24}N_4O_2H)_2PtBr_4$	180—190	hellbraune Platten	7,0
$(C_{24}H_{26}N_4O_2H)_2PtBr_4$	160—170	hellbraune Platten	1,35
$(C_{26}H_{30}N_4O_2H)_2PtBr_4$	200—210	hellbraune Platten	2,2
$(C_{29}H_{28}N_4O_2H)_2PtBr_4$	190—200	gelbes Pulver	1,0

So erhält man die Tetrabromplatinate von Diantipyrilmethan, Diantipyrilmethylmethan, Diantipyrilpropylmethan und Diantipyrilphenylmethan. Ihre Zusammensetzung entspricht der Formel $(RH)_2PtBr_4$, die Bildungsreaktion der Gleichung

$$2\,R + PtBr_4^{--} + 2\,H^+ \longrightarrow (RH)_2\,PtBr_4$$

Alle Verbindungen sind in Wasser wenig löslich, lösen sich gut in Dimethylformamid, weniger gut in Aceton, nicht in Methanol, Äthanol, Benzol, Tetra, Äther.

Die Infrarotsprektren

Die Infrarotsprektren der Verbindungen sind von den kristallinen Verbindungen (KBr-Tabletten) im Gebiet zwischen 9 000 und 400 cm^{-1} aufgenommen worden. In den Spektren aller Verbindungen fehlt die charakteristische Frequenz der Valenzschwingung der C = O-Gruppe eines Pyrazolonderivates bei 1656—1680 cm^{-1}. Das bestätigt, wie früher bei der Untersuchung der Komplexe von Pyrazolonderivaten mit anderen Metallen gezeigt wurde [3], daß bei der Bildung von Kationen $(RH)^+$ eine Protonisierung der C = O-Gruppe des Reagenzmoleküls erfolgt; die zweite C = O-Gruppe ist beteiligt an der Bildung einer festen innermolekularen Wasserstoffbrückenbindung.

Die sauren Eigenschaften

Die Verbindungen lösen sich gut in Dimethylformamid und in einem Gemisch Dimethylformamid/Aceton 2 : 1. In Lösung liegen sie als zweibasige Säuren vor und können potentiometrisch titriert werden unter Verwendung

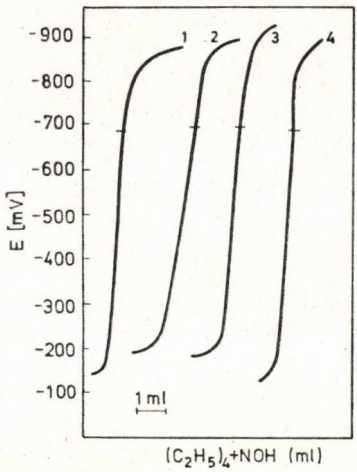

Abb. 1. Titration der jeweiligen Tetrabromplatinate mit 0,1 *N* Lösung von Tetraäthylammoniumhydroxid in Dimethylformamid/Aceton. 2 : 1 1 — $(C_{23}H_{24}N_4O_2H)_2PtBr_4$; 2 — $(C_{24}H_{26}N_4O_2H)_2PtBr_4$; 3 — $(C_{26}H_{30}N_4O_2H)_2PtBr_4$; 4 — $(C_{29}H_{28}N_4O_2H)_2PtBr_4$

einer Glas- oder einer ionensensitiven Elektrode. Die Titrationskurven (Abb. 1) zeigen einen scharf ausgeprägten Sprung, der die Neutralisation des Kations $(RH)^+$ anzeigt:

$$(RH)_2\ PtBr_4 + 2\ (C_2H_5)_4N\ OH \dashrightarrow$$
$$2\ R + [(C_2H_5)_4N]_2\ PtBr_4 + 2\ H_2O$$

Der Titrationssprung entspricht dem Äquivalenzpunkt; das Äquivalentgewicht, ausgerechnet nach den Resultaten der Titration, ist praktisch gleich dem nach den Formeln der Verbindung errechneten. Die Komplexeigenschaften können benutzt werden zur Ausarbeitung von titrimetrischen Methoden der Platinbestimmung.

Löslichkeit der Verbindungen

Bestimmt wurde die Löslichkeit der Komplexe in 0,5 N HBr. Die Löslichkeit in Wasser wurde nicht bestimmt wegen der möglichen Hydrolyse der Komplexe.

Frischgefällte Niederschläge, sorgfältig mit 0,5 *N* HBr gewaschen, werden in ein Gefäß überführt, das 50—60 ml 0,5 *N* HBr enthält. Die Lösung sättigt sich in 2—3 Stunden bei 25 ± 0,2 °C. Die gesättigte Lösung wird schnell durch ein Papierfilter filtriert, wobei die ersten Milliliter des Filtrats verworfen werden. Im klaren Filtrat wird der Platingehalt fotometrisch mit $SnCl_2$

bestimmt [4]. Die Zusammensetzung des Niederschlags verändert sich beim Sättigen der Lösung nicht. Wie aus den erhaltenen und in Tabelle 2 aufgeführten Werten ersichtlich ist, ist die Löslichkeit der Verbindungen mit DAMM, DAPM und DAFM hinreichend klein, um auch eine gravimetrische Platinbestimmung zu ermöglichen.

Gravimetrische Platinbestimmung

Am wenigsten löslich ist das Tetrabromplatinat des DAFM. Weil aber das bromwasserstoffsaure Salz des Reagenz' selbst auch schwerlöslich ist, erscheint es unzweckmäßig, dieses Reagenz zur gravimetrischen Platinbestimmung zu verwenden. Als günstiger erweisen sich die Reagenzien DAPM

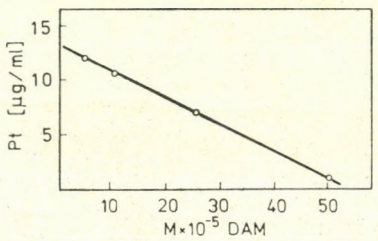

Abb. 2. Einfluß eines Reagenzüberschusses auf die Löslichkeit des Tetrabromplatinats des Diantipyrilmethans

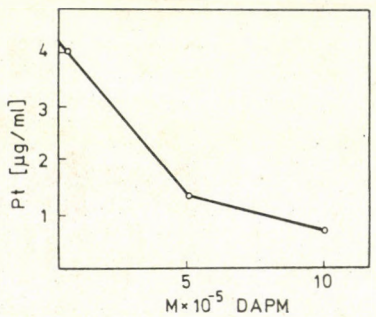

Abb. 3. Einfluß eines Reagenzüberschusses auf die Löslichkeit des Tetrabromplatinats des Diantipyrilpropylmethans

und DAM. Zur Auswahl der optimalen Fällungsbedingungen für das Platin ist der Einfluß eines Reagenzüberschusses auf die Löslichkeit untersucht worden. Die Ergebnisse sind aus den Abbildungen 2 und 3 ersichtlich.

Die Löslichkeit der Verbindungen verringert sich sehr stark in Anwesenheit

Tabelle II

Gravimetrische Bestimmung des Pt(II) mit Diantipyrilpropylmethan in Anwesenheit anderer Elemente

Eingesetzt sind jeweils **10,0** *mg Pt.*

mg Fremdion	Fehler der Pt-bestimmung in %	mg Fremdion	Fehler der Pt-best. in %
400 Al	−0,3	300 Ni	−1,0
500 Al	+0,2	400 Ni	±0,0
200 Mg	−0,1	300 Fe(II)	−1,0
300 Mg	+0,8	400 Fe(II)	−0,9
300 Mg(II)	+1,9	500 Fe(II)	+0,5
300 Mn(II)	+1,9	500 Fe(II)	+0,5
400 Mn(II)	+1,0	300 Co	+0,2
500 Mn(II)	−2,0	400 Co	+1,2
		500 Co	+0,5

eines auch kleinen Reagenzüberschusses: die Löslichkeit der entsprechenden Verbindung in 0,02%iger DAM-Lösung ist $3{,}7 \cdot 10^{-5}$ *M*, in 0,004%iger DAPM-Lösung $0{,}31 \cdot 10^{-5}$ *M*. Die Niederschläge haben eine gut definierte Zusammensetzung, die den Formeln $(C_{23}H_{24}O_2N_4H)_2\ PtBr_4$ und $(C_{26}H_{30}N_4O_2H)_2\ PtBr_4$ entsprechen, sind gut filtrierbar, lassen sich gut auswaschen und können ohne Zersetzung bei 100—110°C getrocknet werden. Im folgenden wird die Methodik der Platinbestimmung mit Diantipyrilpropylmethan DAPM angegeben.

Zu 50—60 ml einer Lösung Pt(II) in 1 *N* HBr (Pt(IV) wird vorher nach der in (5) beschriebenen Methode zu Pt(II) reduziert), die 5—30 mg Pt enthält, gibt man 2—7 ml einer 2%igen Lösung von DAPM in Essigsäure 1 : 1. Die Lösung mit Niederschlag wird zum Kochen erhitzt, abgekühlt auf 40—50 °C und auf die totale Platinausfällung geprüft. Der ausgefallene kristalline Niederschlag wird durch einen Filter G 3 filtriert, mit 10 ml kaltem Wasser gewaschen, bei 100—110 °C getrocknet und ausgewogen als $(C_{26}H_{30}N_4O_2H)_2\ PtBr_4$. Der Umrechnungsfaktor für Pt beträgt 0,1416.

Bei der statistischen Aufarbeitung der Ergebnisse werden folgende Werte erhalten: ($n = 5$; $\alpha = 0{,}95$): arithmetisches Mittel aus n Messungen $\bar{x} = 10{,}19$; mittlere quadratische Abweichung vom arithmetischen Mittel $S = 0{,}0753$; Vertrauensintervall 0,0934, Variationskoeffizient $V = 0{,}91\%$. Die Bestimmung wird nicht gestört durch Alkali und Erdalkalimetalle, Mg, Al, Mn(II), Fe(II), Co, Ni. Ruthenium, das unter diesen Bedingungen zu Ru(III) reduziert wird und Rh(III) bilden mit den Pyrazolonderivaten keine schwerlöslichen Verbindungen und werden auch mit dem Platinniederschlag nicht mitgefällt. [6] Pd und Os stören.

LITERATUR

[1] AKIMOV, V. K., JEMELJANOVA, I. A., BUSEV, A. I.: J. analyt. Chem. (UdSSR) **26**, 2416 (1971)
[2] AKIMOV, V. K., JEMELJANOVA, I. A., BUSEV, A. I.: J. analyt. Chem. (UdSSR) **26**, 1793 (1971)
[3] AKIMOV, V. K., BUSEV, A. I.: J. analyt. Chem. (UdSSR) **26**, (1971), 136
[4] BIMISCH, F. E.: Analytische Chemie der Edelmetalle, Teil 2, Verlag Mir, Moskau 1969, Seite 247
[5] Autorenkollektiv: Synthese von Komplexverbindungen der Metalle der Platingruppe, Verlag Nauka, Moskau 1964, Seite 9
[6] BUSEV, A. I., AKIMOV, V. K.: Vestnik MGU, serija chimija, No. 1, (1963), 43

V. K. AKIMOV
A. I. BUSEV
K. V. KODUA
} Chem. Fakultät der Lomonossov—Univ., Moskau

P. NENNING Karl-Marx-Universität Leipzig, Sektion Chemie, 701 Leipzig, Liebigstraße 18. DDR

Acta Chimica Academiae Scientiarum Hungaricae, Tomus 90 (4), pp. 381—393 (1976)

REDUCTIVE CONVERSIONS OF CHROMANOIDS, I

CATALYTIC HYDROGENATION OF ISOFLAVONE (3-PHENYLCHROMONE)*

V. SZABÓ and E. ANTAL

(Department of Applied Chemistry, Kossuth Lajos University, Debrecen)

Received June 11, 1974; in revised form October 8, 1975

Depending upon the solvent, the pH of the solution and the activity of the Pd/C catalyst isoflavone (3-phenylchromone) is reduced at various rates to isoflavanone (II), isoflavan-4-ol (III) and isoflavan (IV), or — in dilute solutions of alkali — to 2-hydroxy-α-methyldeoxybenzoin (IX). Appropriate choice of the conditions results in selective reductions; the formation of compounds II, III, IV and IX can be rendered the dominant process.

Isoflavanoid derivatives with different states of oxidation play an important part in the vegetable and animal kingdom, several of them possessing considerable biological actions. Therefore, their isolation, synthesis and conversions are of interest not only from the organic chemical, but also from the biological and pharmacological points of view.

Apart from the reductions of isoflavones, no other methods are known, or practically used [1—4], for the preparation of isoflavonids of lower oxidation number, in spite of the importance of these compounds. This is why the reduction processes of isoflavones have been so thoroughly studied. Usually, this reduction is effected with catalytically activated hydrogen [5—14], with complex metal hydrides [15—18], or by some other chemical method of reduction [13, 18, 19]. Among the reduction reactions, only catalytic hydrogenation is suitable for the preparation of all isoflavonoids with lower oxidation states than that of isoflavone; the other methods of reduction give only one product of a given oxidation number. Specifically, for the preparation of isoflavanones from isoflavones catalytic hydrogenation is the exclusively suitable method.

However, catalytic hydrogenation of isoflavones is in the majority of cases non-selective; the desired product of lower oxidation number is thus obtained in poor yields [5—14]. No report was found in the literature on any specific endeavour to achieve the selective hydrogenation of isoflavones to isoflavanones, isoflavan-4-ols, or isoflavans.

In this paper we discuss our attempts and experiments at selective hydrogenations of unsubstituted isoflavone. The hydrogenation experiments

* Preliminary communication published in Tetrahedron Letters **1973** (19) 1659.

were carried out in ethanol, dioxan, aqueous alcoholic buffers and in aqueous sodium hydroxide solutions, in the presence of palladium catalysts of different activities. The experimental finding [20] that the polarity of the solvent and the hydrogen ion concentration generally influence the rate and the product of hydrogenation was taken into account, and also the fact [21] was considered that in strongly alkaline media the structure of the isoflavone molecule is affected. The object of our work was to find experimental conditions conducive to the conversion of isoflavone, in the presence of palladium metal and hydrogen, into a definite product of a lower state of oxidation.

In preliminary experiments various commercial palladium catalysts (Fluka, Merck, Chinoin) were tested; then palladium catalysts on different carriers were tried (activated carbon, barium sulfate, aluminium oxide), the Pd content being 10% in each case.

The results have shown that selective reduction can only be achieved with a catalyst of medium activity* on activated carbon carrier. Catalysts on barium sulfate or aluminium oxide have low activities (3.2 and 8.3 mmole H_2/min.,) respectively, and poor selectivity. Consequently, the main experiments were carried out with Catalyst 'A' (30 mmoles H_2/min., Pd/C, Fluka) and Catalyst 'B' (23 mmoles H_2/min., Pd/C, Merck-A). For the synthesis of isoflavan, a high-activity Pd/C catalyst (Catalyst 'C'; 122 mmoles H_2/min., Merck) was used.

There is a significant difference in the rates of hydrogenation of isoflavone in ethanol, and in dioxan, (Scheme 1). Hydrogenation in ethanol proceeds more rapidly: the absorption of two moles of hydrogen results in isoflavan-4-ol, (**III**) and there is no essential difference between the rates of addition of the two moles of hydrogen *(cf.* Fig. 1, Curve 1). This was supported also by the fact that when the reaction was stopped after one mole of hydrogen had been added, TLC tests showed that besides isoflavanone (**II**) a nearly equal quantity of **III** was already also present in the reaction mixture. The rate of hydrogenation is much lower in dioxan than in ethanol, and **II** formed is further reduced to **III** at a very low rate (Fig. 1, Curves 2,3). No great difference is seen between the hydrogenation curves for the moderately active Pd/C catalysts 'A' and 'B'. With these, the product of hydrogenation in dioxan is nearly pure **II**, and only trace quantities of **III** can be detected by TLC. Thus the reduction of isoflavone in dioxan, with a Pd/C catalyst of moderate activity can be recovered in nearly quantitative yield.

Hydrogenation with a catalyst of moderate activity in ethanolic solution can also be considered a selective reduction which gives isoflavan-4-ol (**III**) in nearly quantitative yield. However, this reduction process is not stereo-

* The relative activities [22] of the catalysts used were characterized by the rate of hydrogen consumption (mmole H_2/min.), starting with the point of time $t = 0$, in the hydrogenation of isoflavone in pure dioxan, under the experimental conditions given in Fig. 1.

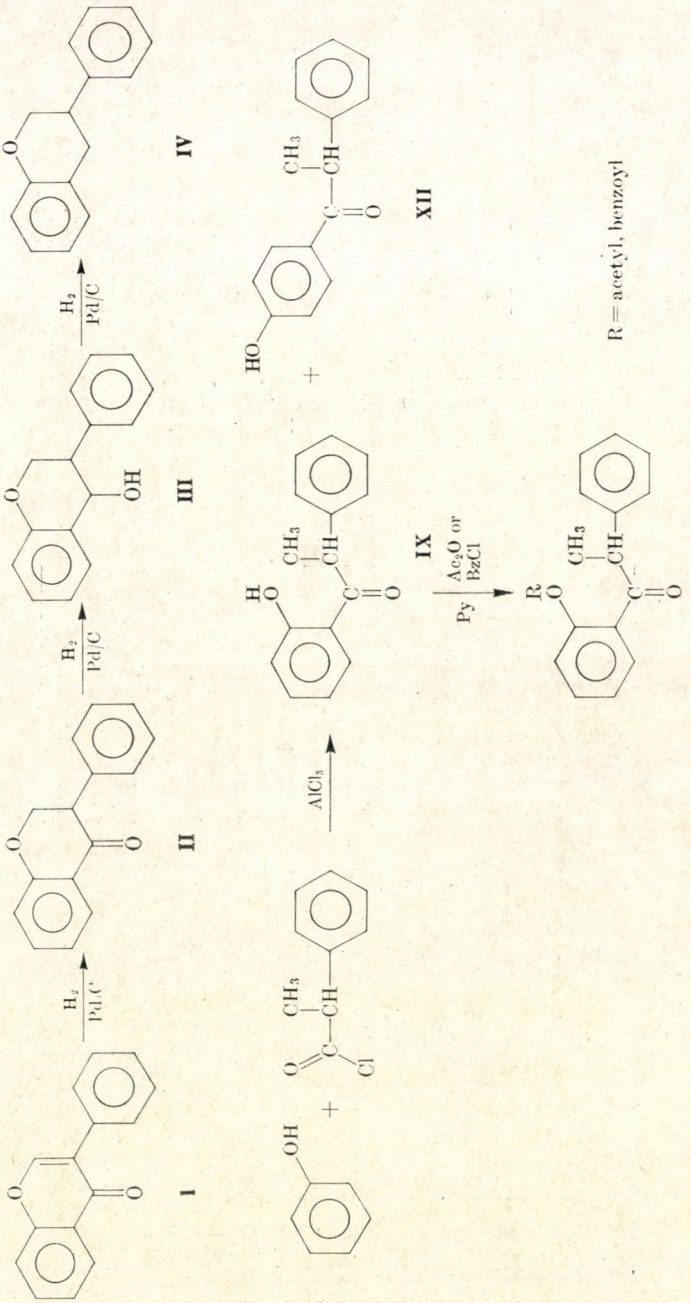
H2
Pd/C
I
II
III
IV
AlCl3
XII
IX
Py
Ac2O or
BzCl
R = acetyl, benzoyl

specific, unlike the reaction in a PtO_2/glacial acetic acid system [13]. Besides the *cis* (β) isomer, the recovered isoflavan-4-ol contains a substantial amount of the *trans* (α) isomer. These isomers can be detected by TLC and can be separated by fractional crystallization of their acetates.

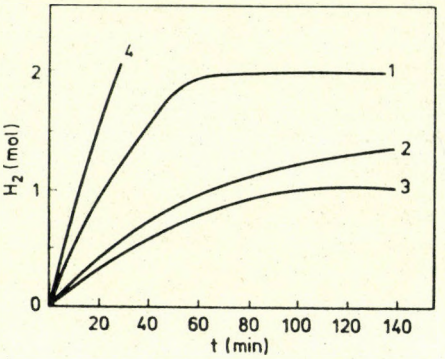

Fig. 1. Hydrogenation curves of isoflavone in dioxan and in ethanol, with various Pd/C catalysts. (200 mg isoflavone; 200 mg catalyst; 60 ml solvent; 20 °C). Curve 1, ethanol, Pd/C "A" Curve 2, dioxan; Pd/C "A"; Curve 3, dioxan, Pd/C "B"; Curve 4, dioxan, Pd/C "C"

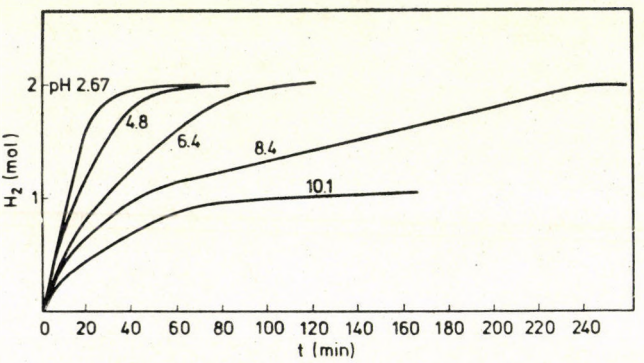

Fig. 2. Hydrogenation curves of isoflavone in aqueous ethanolic buffers of various pH values. (200 mg isoflavone; 200 mg Pd/C "A"; 60 ml solution; 20°C).

Isoflavone was reduced to isoflavane (**IV**) only in ethanol containing hydrochloric acid, or in acetic acid [13], when catalysts of moderate activity were used. The absorption of the first two moles of hydrogen is rapid, that of the third mole proceeds more slowly by one order of magnitude. Yet, in the presence of a highly active Pd/C Catalyst 'C' (*cf.* Fig. 1, Curve 4), the reduction to isoflavane proceeds rapidly also in dioxan.

With the purpose of improving the selectivity of the reduction method, we studied the reduction of isoflavone also in aqueous ethanolic Britton-Robinson buffer solutions [23]. As shown by the hydrogenation curves (Figs 2, 3), isoflavone absorbs two moles of hydrogen between pH 1 and 11.5. The

rate of hydrogenation by each of the two moles of hydrogen is differently affected by changes in the pH. The difference of the rates is insignificant in acidic medium, but above pH 3 this difference increases with increasing pH. The absolute value of the rate of reduction decreases in both processes up to

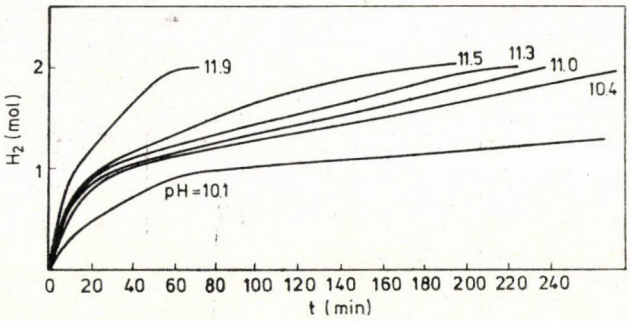

Fig. 3. Hydrogenation curves of isoflavone in aqueous ethanolic buffers of various pH values (200 mg isoflavone; 200 mg Pd/C "A" 60 ml solution; 20°C)

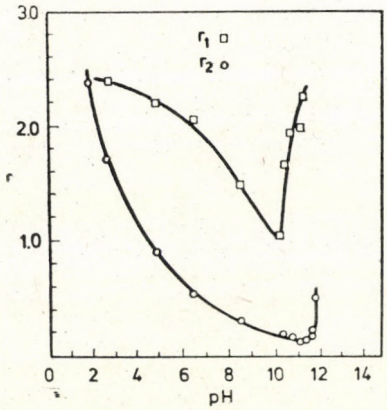

Fig. 4. Dependence of the hydrogenation rate, $r = \frac{\text{ml } H_2}{\text{min}}$, as a function of pH. r_1 is the rate of reduction **I** → **II**; r_2 that of **II** → **III**,

pH 10, but from this point on, the rates of both reduction stages will suddenly increase (Fig. 4). Between pH 9 and 10.5, the absorption of the first and second mole of hydrogen proceeds at very different rates (Fig. 5).

When the reaction is stopped after the addition of one mole of hydrogen, solely **II** can be recovered from the solution, and only traces of **III** are detected; thus also this reduction can be made selective for the preparation of isoflavanone. In alkaline media the activities of Catalysts 'A' and 'B' differ still less than indioxan, *i. e.* dependence of the hydrogenation on the catalyst decreases.

Therefore, selective transformation is practically better achieved in aqueous alkaline media, and a wider range of catalysts may be suitable.

When two hydrogens are added to the isoflavone molecule at a pH lower than 10.5, **III** will be formed exclusively; between pH 10.5 and 11.0, other products are also obtained besides **III**.

At pH 11.5 or higher, the course of the hydrogenation reaction is entirely different. As the hydroxide ion concentration is increased, the rate of hydrogenation becomes substantially higher, the amount of **III** gradually

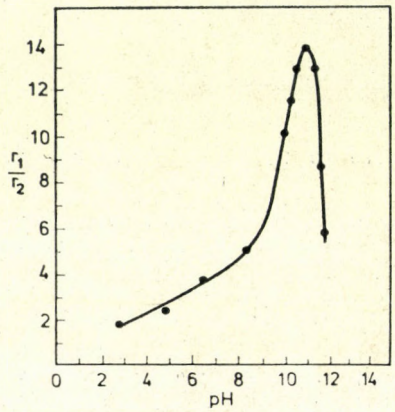

Fig. 5. The quotient of the rates of hydrogenation as a function of pH

decreases, and two new components appear in the reaction mixture; one of them is identifiable by TLC as 2-hydroxydeoxybenzoin (**X**) a product of the alkaline decomposition of isoflavone. The other product was, as shown by its chromatographic behaviour, reaction with $FeCl_3$, the UV, IR and NMR spectra of its acetate, 2-hydroxy-α-methyldeoxybenzoin (**IX**). Between pH 10.5 and 12 these two components are also accompanied by a small amount of an unidentified compound ('**X'**), which is presumably 1-(2-hydroxyphenyl)-2-phenylpropan-1-ol, possibly formed by the reduction of 2-hydroxy-α-methyldeoxybenzoin, since it appears in TLC as a faint pink spot with $FeCl_3$, and a sample isolated by preparative layer chromatography has characteristic UV spectrum as isoflavan-4-ol (a sharp double band between λ_{max} 275 and 280 nm). With the structure proof of this compound we intend to deal in a next communication.

Britton-Robinson buffers are unsuitable for adjusting pH values higher than 12, therefore further hydrogenations were carried out in variously composed aqueous ethanolic solutions of sodium hydroxide. In 0.1 *N* aqueous ethanolic NaOH solution, like in a buffer of pH 12, the principal product of reduction was 2-hydroxy-α-methyldeoxybenzoin (**IX**), together with about

20% of 2-hydroxydeoxybenzoin (**X**), slight quantities of isoflavanone (**II**) and compound 'x'. The change of product composition as a function of the hydroxide ion concentration is shown in Fig. 6.

Compound **IX** is difficult to isolate. The reaction product of the hydrogenation is an oil at room temperature, the purification of which could only be achieved by column chromatography on silica gel. From the purified oil the crystalline acetate and benzoate were prepared, and these were compared

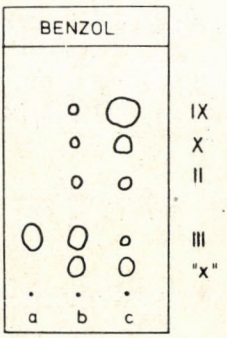

Fig. 6. Chromatogram of the product mixture of isoflavone hydrogenated up to the addition of two moles of hydrogen.

with samples of the corresponding derivatives synthesized from 2-hydroxy-α-methyldeoxybenzoin. The synthesis of **IX** was achieved as shown in Scheme 2.

Owing to their different solubilities, the *ortho and* the *para* isomers are readily separated; the *p*-hydroxy derivative (**XII**) is much less soluble in aliphatic hydrocarbons than the *o*-hydroxy compound (**IX**). **XII** can be crystallized from *n*-octane, wherein **IX** remains dissolved. After evaporation to dryness, the crystalline acetate (**XIII**) and benzoate (**XIV**) were prepared for identification.

In the course of the hydrogenation of isoflavone (**I**) in 0.1—0.5 *N* NaOH, an interesting phenomenon was noted. As a function of the alkalinity, the isoflavone solution — in an inverse proportion to this alkalinity — consumed greater or smaller quantities of hydrogen (Fig. 7) and, depending again on the hydroxide ion concentration but now in direct proportion to this, various amounts of isoflavone could be recovered after a given period (150 min.) of hydrogenation. When some time was allowed to elapse between the preparation of the solution and the beginning of its hydrogenation, similarly less hydrogen was absorbed. In normal or more concentrated solutions, isoflavone

cannot be hydrogenated, nor does it suffer decomposition. These findings suggest some fundamental change in the structure of isoflavone to occur in time, and leading to a state inaccessible to hydrogenation or decomposition [24]. However, in NaOH solutions of higher concentration than normal, this change or structural transformation is reversible, since, after the removal of the catalyst by filtration and on acidification of the solution, isoflavone can be recovered, as mentioned above.

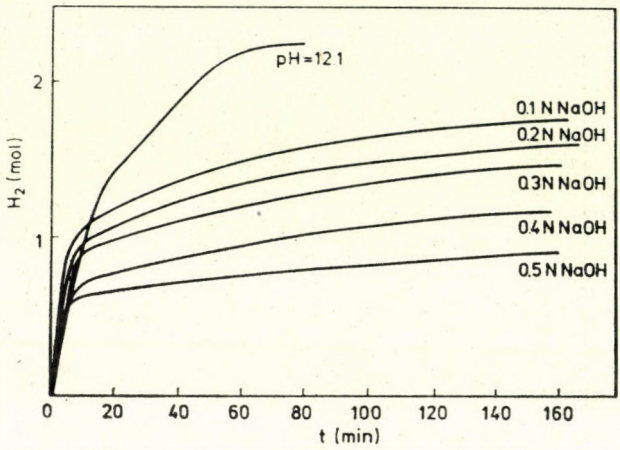

Fig. 7. Hydrogenation curves of isoflavone in aqueous ethanolic NaOH solutions of different concentrations (200 mg isoflavone; 200 mg Pd/C "A"; 60 ml solution, 20°C).

These experimental facts and a study [21] of the ring fission of isoflavone in alkaline medium suggest that isoflavone solutions at pH 11 and higher alkalinities must consist of a complicated equilibrium system. The hetero ring of isoflavone is opened to and extent determined by the hydrogen ion concentration; isoflavone is in equilibrium with the open structures (**V**, **VI**), and — supposedly — the components in equilibrium are hydrogenated as shown in Scheme 3. On the basis of equilibrium measurements [21], at pH 11.5 more than 50% of the isoflavone is converted into **V** and, following the pathway **V** → **VII** → **VIII**, the addition of hydrogen, water elimination and further hydrogenation produce **IX**, which is the principal product obtained under these conditions. The conversion of isoflavone into **IX** proceeds at the highest rate and to the greatest extent in a buffer of pH 12, or in 0.1 N sodium hydroxide solution.

The supposed intermediates **VII** and **VIII** could not be detected in the product mixture of hydrogenations in alkaline media. This suggests that elimination of water from **VII** and also the reduction of **VIII** proceed more rapidly than the hydrogenation of **V** $\rightleftharpoons$ **VI** to **VII**. Thus the last step of these consecutive reactions must be rate-determining, *i. e.* $v_3 < v_4 \leq v_5$. Obviously, above

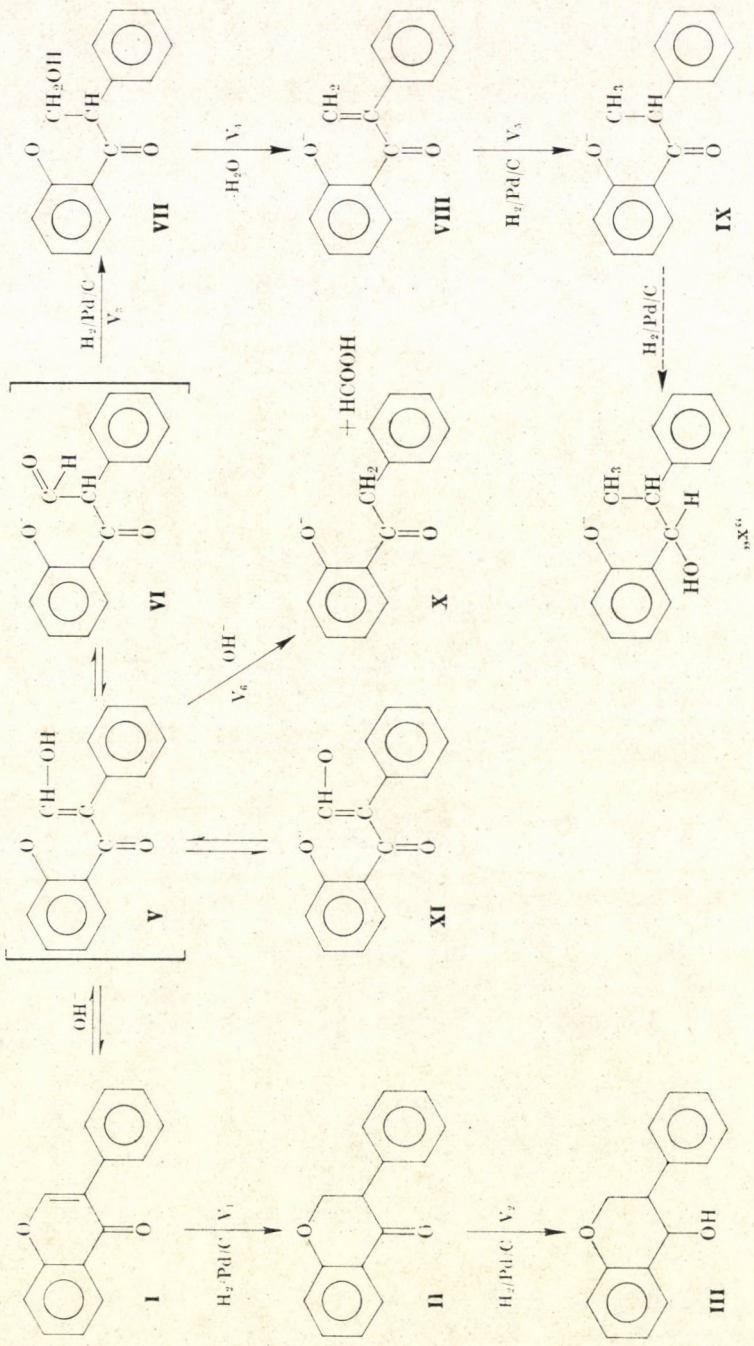

pH 11.5 the slowest step is the formation of **II** and **III** ($v_1 \ll v_3$), since, depending upon the hydroxide ion concentration, the equilibrium is shifted in the direction **I** → **V** ⇌ **VI** → **XI**, therefore the isoflavone concentration is low, giving rise only to trace quantities of **II** and **III**. However, decomposition to **X** (v_6) is quite significant under these conditions. We found that in a solution largely **X** is formed besides **IX**.

When the hydroxide ion concentration is increased further (in 0.1 to 0.5 *N* NaOH), the rate of decomposition to 2-hydroxydeoxybenzoin decreases

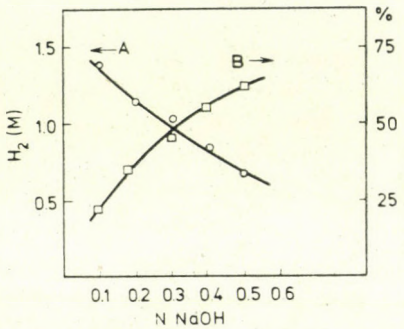

Fig. 8. Amounts of hydrogen absorbed and of isoflavone recovered, as functions of the NaOH concentration. Curve A. Moles of H_2 consumed in 10 min; Curve B. Percent of isoflavone recovered.

[24]; the amount and the rate of absorption of hydrogen also decrease (*cf.* Fig. 6). This finding also supports the notion that under such circumstances the dissociation process **V** ⇌ **XI** is predominating and that the enolate ion produced is neither hydrogenated nor decomposed. Also the amount of hydrogen absorbed during a given time is determined by the dissociation equilibrium **V** ⇌ **XI** [24], being a function of the hydroxide ion concentration (Fig. 8.)

Experimental

M. p.'s are uncorrected.

UV spectra were recorded with a UNICAM SP 800, and infrared spectra with a UNICAM SP 200 G instrument; for obtaining the NMR spectra a JEOL LNM-MH-100 instrument was used. TLC tests were made on Merck's DC-Alurolle Kieselgel F 254 plates; benzene, and benzene: ethanol mixture (95 : 5) were used as the developing solvent.

The hydrogenation apparatus consisted of a gas burette joined by ground glass fittings to a glass hydrogenating vessel; both were kept at 20° C with the help of an ultrathermostat; the hydrogenation mixture was vigorously agitated with a magnetic stirrer.

Catalytic hydrogenation (at 20 °C)

The Pd/C catalyst (0.2 g) was weighed into the reactor vessel and the solvent (30 ml; ethanol, dioxan, glacial acetic acid, or aqueous Britton-Robinson buffer) was added; the mixture was stirred until no more hydrogen was absorbed. Isoflavone (0.2 g) was dissolved in the appropriate solvent (30 ml; ethanol, dioxan, glacial acetic acid) previously saturated with

Table I

Product	Solvent	pH	Catalyst (a)	H_2 added, mole	Reaction time (min.)	Purification (recrystallization)	Yield, %	M. p., °C
Isoflavanone **II**	dioxane	—	A, B	1	100	80% ethanol	95	77
Isoflavanone **II**	buffer (b)	9—10	A, B	1	80	80% ethanol	90	77
Isoflavan-4-ol **III** (c)	ethanol	—	A, B	2	60	petroleum ether	90	86—89
Isoflavan-4-ol **III** (c)	buffer (b)	3—9	A, B	2	40—240	petroleum ether	90	85—89
Isoflavan **IV**	glacial acetic acid	—	A, B	3	600	ethanol	90	54—55
Isoflavan **IV**	ethanol + 2 ml cc. HCl	—	A, B	3	450	ethanol	95	55
Isoflavan **IV**	ethanol	—	C	3	80	ethanol	95	55
2-Hydroxy-α-methyl-deoxybenzoin **IX**	buffer (b)	11—12	A, B	2	60—220	column chromatography	60	oil
2-Hydroxy-α-methyl-deoxybenzoin **IX**	0.1—0.5*N* NaOH (d)	—	A, B	0.8—2	20—160	column chromatography	20—60	oil

(a) Catalysts: A, Fluka Pd/C, 10% Pd content
B, Merck "A" Pd/C, 10% Pd content
C, Merck Pd/C (active), 10% Pd content

(b) 50% aqueous ethanolic Britton-Robinson buffer

(c) mixture of the *cis-* and *trans* isomers

(d) 50% aqueous ethanolic NaOH solution

hydrogen, and this solution was transferred by suction into the hydrogenating vessel. The consumption of hydrogen was noted as a function of time.

After the hydrogenation had been completed, the catalyst was removed by filtration through a glass filter. In the case of aqueous ethanolic buffer solutions, the hydrogen ion activity of the solution was checked with a pH-meter, the acidic or alkaline solutions were neutralized, the catalyst collected on the filter was washed with two 10-ml portions of the solvent, and the combined filtrates were evaporated in vacuum. The crystalline product was collected by filtration and recrystallized. Oily products were extracted with three 30-ml portions of ether, the organic phase was dried over magnesium sulfate, and the ether was evaporated. The residual oil was crystallized, or purified by column chromatography. Table I shows the conditions and results of hydrogenations carried out under various experimental conditions.

Separation of the isomers of isoflavan-4-ol

(A) α-4-Acetoxyisoflavan

A sample (0.45 g) of the isoflavan-4-ol mixture obtained by hydrogenation was acetylated in a mixture of acetic anhydride (2 ml) and pyridine (2 ml). The acetate mixture (0.5 g; m. p. 66—69°C) obtained was dissolved in petroleum ether (b. p. 50—70°C). The crystals first separating (270 mg) consisted mainly of the α-isomer; two recrystallizations from petroleum ether gave 75 mg of α-4-acetoxyisoflavan, m. p. 73—74 °C (lit. [25] m. p. 73 °C).

(B) β-4-Acetoxyisoflavan

The mother liquor of the α-isomer was evaporated, and the crude residue was repeatedly recrystallized from petroleum ether until constant m. p. was attained. The chromatographically pure *cis*-4-acetoxyisoflavan (180 mg) had m. p. 92 °C (lit. [13] m. p. 93 °C).

Preparation of 2-hydroxy-α-methyldeoxybenzoin (IX)

(A) By catalytic hydrogenation of isoflavone

Isoflavone was dissolved in a NaOH solution of pH 11—12, or 0.1 to 0.5 *N*, and hydrogenated under the conditions shown in Table I. A sample (0.6 g) of the resulting oily product was dissolved in a small amount of benzene, the solution was poured on a column of Kieselgel PF 254 Merck (200 g), and elution was effected with a 1 : 1 mixture of benzene and heptane. The eluate fractions which gave a red-colour reaction with $FeCl_3$ were combined and evaporated to give **IX** (350 mg) in the form of a colourless oil. 250 mg of this product was acetylated with acetic anhydride in the presence of perchloric acid to obtain 2-acetoxy-α-methyldeoxybenzoin (**XIII**) (220 mg; m. p. 87—88 °C).

$C_{17}H_{16}O_3$ (268.3). Calcd. C 76.8; H 5.98; Ac 15.95. Found C 77.1; H 5.92; Ac 16.04%

UV (ethanol): λ_{max} 256 nm (log ε 3.98); λ_{max} 329 nm (log ε 3.58).

IR (KBr): $\nu_{C=O}$ (acetyl) 1755 cm^{-1}; $\nu_{C=O}$ 1683 cm^{-1}; ν_{CH_3} 1368, 2927, 2980 cm^{-1}.

NMR ($CDCl_3$): δ_{CCH_3} 1.50 d (3H); δ_{COCH_3} 2.26 s (3H); δ_{CH} 4.55 q (1H); $\delta_{arom.}$ 7—7.63 m 9H).

100 mg of the purified oil was treated with benzoyl chloride in pyridine to yield 2-benzoyloxy-α-methyl-deoxybenzoin (**XIV**), m. p. 73—74°C.

$C_{22}H_{18}O_3$ (330.40). Calcd. C 79.9; H 5.49; Bz 28.8. Found C 80.1; H 5.42; Bz 27.6%

(B) Friedel-Crafts acylation

In a three-necked flask fitted with a stirrer, and reflux condenser, phenol (3.5 g) was dissolved in dry *n*-octane (100 ml). Sublimed aluminium chloride (5.0 g) was added to the solution in portions and the mixture was stirred in an oil bath at 120 °C, whereupon a dark brown oil separated instantly. Slowly and dropwise α-methylphenylacetic acid chloride (6.3 g) was added, and the stirring was continued at this temperature for 16 hrs.; diluted hydrochloric acid (1 : 1) 100 ml) was then poured into the flask and the stirring was continued for 30 min. at the given oil bath temperature. The *n*-octane phase was separated and the warm aqueous phase was extracted with two 50-ml portions of octane. From the combined octane solution colourless crystal plates separated on cooling. The crystals were filtered off and recrystallized from aqueous ethanol to obtain a product (4.1 g; m. p. 133—134 °C) which, on the basis of its negative $FeCl_3$ reaction and the UV spectrum, proved to be 4-hydroxy-α-methyldeoxybenzoin (**XII**).

UV (ethanol): λ_{max} 284 nm (log ε 3.81); UV (ethanol-NaOEt): λ_{max} 332 nm (log ε 4.32).

The octane mother liquor was washed free from acid, dried, treated with charcoal, and evaporated. A red-brown oil (3.8 g) was obtained; according to its R_f value in TLC and $FeCl_3$

reaction, this was the same product as the one obtained by the hydrogenation of isoflavone in alkaline medium [method (A)], *viz.* 2-hydroxy-α-methyldeoxybenzoin. The acetate had m. p. 86—87 °C; mixed m. p. with **XIII** prepared according to (A): 86—87 °C.

UV (ethanol): λ_{max} 256 nm (log ε 3.98); λ_{max} 329 nm (log ε 3.48).

M. p. of the benzoate was 73—74 °C; m. p. in admixture with **XIV** made according to (A): 73—74 °C.

REFERENCES

[1] Da Re, P., Verlicchi, L.: Experientia **16,** 301 (1960)
[2] Saito, R., Izumi, T., Kasahara, A.: Bull. Chem. Soc. Japan **46,** 1776 (1973)
[3] Agarval, S. K., Grover, S. K., Seshadri, T. R.: Indian J. Chem. **7,** 1059 (1969)
[4] Arai, M., Kabuto, K., Horino, N., Inoue, N.: Chem. Lett. **1972,** 889
[5] Anderson, E. L., Marrian, G. F.: J. Biol. Chem. **127,** 649 (1939)
[6] Bradbury, R. B., White, D. E.: J. Chem. Soc. **1953,** 871
[7] Inoue, N.: Sci. Repts. Tohoku Univ., First Ser. XIV, 63 (1961)
[8] Wessely, F., Prillinger, F.: Ber. **82,** 629 (1939)
[9] King, F. E.: J. Chem. Soc. **1952,** 96
[10] Neill, K. G.: J. Chem. Soc. **1933,** 3454
[11] Suginome, H.: J. Org. Chem. **24,** 1955 (1959)
[12] Inoue, N., Ito, E.: Chem. Ind. **31,** 1382 (1956)
[13] Inoue, N.: Bull. Chem. Soc. Japan **37,** 601 (1964)
[14] Szabó, V.: Thesis (1958)
[15] Suginome, H., Iwadare, T.: Bull. Chem. Soc. Japan **33,** 567 (1960)
[16] Ramachandra Row L., Anyaneyulu, A. S. R., Sri Krishna, C.: Current Sci. **32,** 67 (1963)
[17] Thakar, G. P., Janak, N., Subba Rao, B. C.: Indian J. Chem. **3,** 74 (1964)
[18] Anirudhan, C. A., Whalley, W. B., Badran, M. M. E.: J. Chem. Soc. **1966,** 629
[19] Dudley, K. H. Miller, H. W., Corley, R. C., Wall, M. E.: J. Org. Chem. **32,** 2317 (1967)
[20] Rylander, P. N.: Catalytic Hydrogenation over Platinum Metals, p. 46. Academic Press, New York and London, 1967.
[21] Szabó, V., Zsuga, M.: Acta Chim. (Budapest) **85,** 179 (1975)
[22] (a) Szabó, Z. (ed): Kontakt-katalizis, p. 541. Akadémiai Kiadó, Budapest, 1966.
(b) Thomas, J. M., Thomas, W. J.: Introduction to the Principles of Heterogeneous Catalysis, p. 298. Academic Press, London, New York, 1967.
[23] Proszt, J., Győrbiró, K., Cieleszky, V.: Polarográfia, p. 501. Akadémiai Kiadó, Budapest, 1964
[24] Szabó, V., Zsuga, M.: Acta Chim. (Budapest) **85,** 191 (1975)
[25] Yamaguchi, S., Ito, S., Suzuki, I., Inoue, N.: Bull. Chem. Soc. Japan **41,** 2073 (1968)

Vince Szabó
Ernő Antal
H-4010 Debrecen 10.

Acta Chimica Academiae Scientiarum Hungaricae, Tomus 90 (4), pp. 395–397 (1976)

CONDENSED *AS*-TRIAZINES, III*

SYNTHESIS OF A NEW HETEROCYCLIC SYSTEM, THE DERIVATIVES OF *AS*-TRIAZINO [6,5-C] QUINOLINE

E. BERÉNYI, P. BENKÓ and L. PALLOS

(EGyT Pharmacochemical Works, Budapest)

Received August 22, 1975

The first derivative of a new heteroaromatic ring system has been synthesized. The reversible crystal dimorphism occurring in the synthesis of the intermediates was studied. The compounds prepared have remarkable biological activity.

The base-catalyzed cyclization of aromatic compounds carrying guanidino and nitro groups in *ortho* position was first investigated by ARNDT [1], who synthesized 3-aminobenzo-*as*-triazine in this way. This method has now been extended to quinoline derivatives, and thus the first representative of a new heteroaromatic ring system, *as*-triazino[6,5-c]quinoline has been prepared. The compound has anti-inflammatory and antimicrobial action.

In the first step of the synthesis, 4-chloro-3-nitroquinoline [2] was allowed to react with guanidine, yielding 4-guanidino-3-nitroquinoline, in the presence of excess guanidine acting as an acid-binding agent. The crystals of the new quinoline derivative are lemon-yellow or orange in colour, depending on the conditions of crystallization.

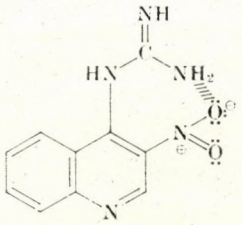

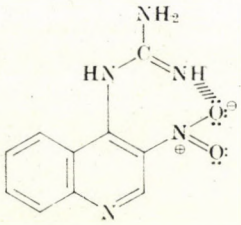

On the basis of analytical and spectroscopic evidence, it is highly probable that the modification consisting of yellow crystals — crystallized from non-polar organic solvents — has intramolecular hydrogen bonds between the NH_2 or = NH group of the guanidino radical and the oxygen atom of the NO_2 group.

The orange-red modification — which separates as prisms from polar solvents — contains 1/2 mole water of crystallization. This water is built in the crystal lattice and stabilizes the molecule as guanidinum nitronate, by

* Part II: A. GELLÉRI, A. MESSMER, P. BENKÓ, L. PALLOS: Acta Chim. (Budapest) **90**, 301 (1976)

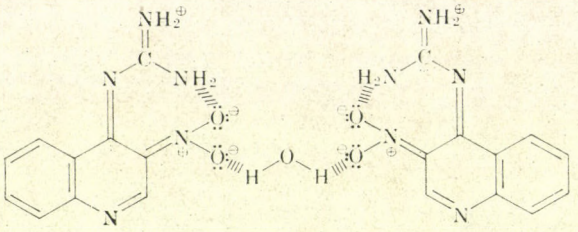

forming intermolecular hydrogen bridges. The two modifications can be reversibly converted into each other by crystallization.

The derivatogram of the guanidino compound shows about 8% weight loss in a strongly exothermic process between 226 and 260 °C, which indicates the release of 1 mole of water from the molecule. Indeed, 4-guanidino-3-nitroquinoline loses water and undergoes cyclization in alkaline medium yielding 2-amino-*as*-triazino[6,5-c]-quinoline-4-oxide.

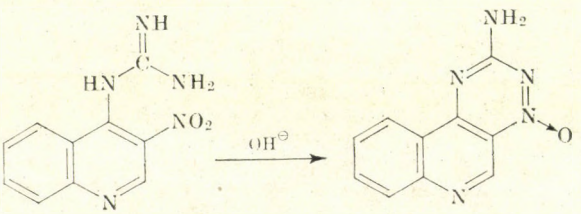

The N-oxide can be reduced with sodium dithionite as well as by catalytic hydrogenation. The first step is the formation of 2-amino-3,4-dihydro-*as*-triazino[6,5-c]quinoline, which is stable in the salt form only, and can readily be converted into 2-amino-*as*-triazino[6,5-c]quinoline by aromatization with potassium hexacyanoferrate.

The experiments aiming at the preparation of new derivatives having biological activity, are continued.

Experimental

4-Guanidino-3-nitroquinoline

The alkoxide was prepared from metallic sodium (6.9 g; 0.3 g-atom) and absolute ethanol (300 ml), then guanidine hydrochloride (28.65 g; 0.3 mole) was added, and the mixture was refluxed for 30 min. The sodium chloride which precipitated was filtered off and the alcohol solution of the guanidine base was allowed to react with 4-chloro-3-nitroquinoline (31.3 g; 0.15 mole) while keeping the temperature below 50 °C. A deep-red solution was obtained, from which the separation of 4-guanidino-3-nitroquinoline started immediately. 33.0 g (95%) of the product was obtained.

The crude 4-guanidino-3-nitroquinoline (0.2 g) was dissolved in chloroform (750 ml) in a Soxhlet extractor. The product separated quantitatively on cooling as yellow crystals, m. p. 230 °C.

$C_{10}H_9N_5O_2$ (231.22). Calcd. C 51.94; H 3.92; N 30.30. Found C 51.81; H 4.05; N 30.40%.
IR (KBr): νNH 3465 cm^{-1}; νNH_2 3430, 3360 cm^{-1}.
UV (water): 336 (3.96); (DMF): 340 (4.18).

Recrystallization of the crude 4-guanidino-3-nitroquinoline (1.0 g) from water (175 ml) gave orange-red crystals (0.9 g), which became yellow at 110—130 °C and after the loss of water, melted at 230 °C.

$C_{10}H_9N_5O_2$. 1/2 H_2O (240.23). Calcd. C 49.99; H 4.19; N 29.17. Found 49.91; H 4.39; N 28.94%.
IR (KBr): νNH 3490; νNH_2 3450, 3360 cm^{-1}.
UV (H_2O): 370 (3.47); (DMF) 440 (3.65).

2-Amino-as-triazino [6,5-c] quinoline-4-oxide

A solution of 4-guanidino-3-nitroquinoline (23.1 g; 0.1 mole) was refluxed with a solution of potassium carbonate (69.5 g; 0.5 mole) in water (500 ml) for 5 hrs, whereupon the initial orange colour of the reaction mixture turned into lemon-yellow. 2-Amino-*as*-triazino [6,5-c]quinoline-4-oxide separated from the mixture (20.0 g; 94%), m. p. 309—311 °C (from methyl cellosolve).

$C_{10}H_7N_5O$ (213.21). Calcd. C 56.35; H 3.31; N 32.85. Found C 56.13; H 3.48; N 32.59%.
IR (KBr): νNH_2 3420, 3340 cm^{-1}; $\nu N \rightarrow O$ 1360 cm^{-1}.
UV (EtOH): 219 (4.34), 236 (4.20), 271 (4.47).

2-Amino-as-triazino [6,5-c] quinoline

2-Amino-*as*-triazino[6,5-c]quinoline-4-oxide (10.65 g; 0.05 mole) was hydrogenated in ethanol in the presence of palladium catalyst at room temperature and atmospheric pressure. When no more hydrogen was absorbed the catalyst was removed by filtration and the solution was evaporated to dryness. The residual yellow crystals were treated with a solution of $K_3Fe(CN)_6$ (33.0 g; 0.1 mole) in water (500 ml) after adjusting its pH to 9 with ammonium hydroxide. Yellow-coloured 2-amino-*as*-triazino(6,5-c)quinoline was obtained (7.4 g; 75%), m. p. 290—291 °C (i-PrOH).

$C_{10}H_7N_5$ (197.21). Calcd. C 60.91; H 3.58; N 35.51. Found C 60.75; H 3.67; N 35.64%.
IR(KBr): νNH_2 3305, 3145 cm^{-1}; ν C = C (aromatic) 1605, 1585, 1564 cm^{-1}.
IR($CHCl_3$): νNH_2 3520, 3405 cm^{-1}.
UV(EtOH): 271 (4.52), 382 (3.72).
NMR(DMSO-d_6): 7.6—8.1 δ (m 3, *H* 5, *H* 6, *H* 7); 8.4 δ (s 2, NH_2); 8.81 δ (m 1, *H* 8); 9.48 δ (s 1, *H* 10).

*

The authors' thanks are due to Dr. L. BUDA (EGyT Pharmacochemical Works, Budapest) and to Dr. G. TÓTH (Pharmaceutical Chemical Institute of the Semmelweis Medical University, Budapest) for the spectroscopic investigations.

REFERENCES

[1] ARNDT, F.: Chem. Ber. **46,** 3522 (1913)
[2] SURREY, A. R., CUTLER, R. A.: J. Am. Chem. Soc. **73,** 2414 (1951)

Edit BERÉNYI
Pál BENKÓ
László PALLOS
H-1106 Budapest 10. Pf. 100.

Acta Chimica Academiae Scientiarum Hungaricae, Tomus 90 (4), pp. 399–404 (1976)

CONDENSED *AS*-TRIAZINES, IV*

SYNTHESIS OF *AS*-TRIAZINO[5,6-c]QUINOLINE AND ITS DERIVATIVES

E. BERÉNYI, P. BENKÓ L. PALLOS

(EGyT Pharmacochemical Works, Budapest)

Received July 7, 1975

The new syntheses of *as*-triazino[5,6-c]quinoline and its derivatives are reported.

In a previous communication [1] we described the results obtained in the synthesis of the first representative of a new heterocyclic system, 2-amino-*as*-triazino[6,5-c]quinoline and its derivatives. In the present paper the preparation of the isomeric *as*-triazino[5,6-c]quinoline and its derivatives is reported. Simultaneously, WRIGHT, GRAY and YU [2] also achieved the synthesis of this ring system and several derivatives in another, independent way, through the reduction of 4-(carbetoxyhydrazino)-3-nitroquinoline and subsequent cyclization of the product in the presence of a basic catalyst.

In the course of the procedure elaborated by us, 4-chloro-3-nitroquinoline (**I**) [3] was made to react with acylhydrazines (**II**), yielding 4-(acylhydrazino)-3-nitroquinolines (**V**). The compounds **V** could also be prepared by the reaction of 4-hydrazino-3-nitroquinoline (**III**) [4] and the appropriate acid chloride (**IV**).

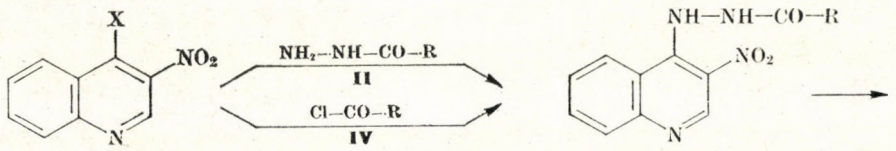

I X=Cl
III X=NH–NH$_2$

V

The reduction of the derivatives **V** yielded 4-(acylhydrazino)-3-aminoquinolines (**VI**) which readily could be cyclized to 1,2-dihydro-*as*-triazino-[5,6-c]-quinolines (**VII**) when acted upon by an acid. Compounds of type **VII** are stable only as their salts; they can easily be aromatized into *as*-triazino-[5,6-c]quinoline derivatives (**VIII**).

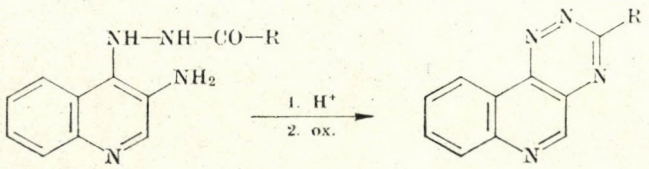

VI **VIII**

* Part III: E. BERÉNYI, P. BENKÓ, L. PALLOS: Acta Chim. (Budapest) **90**, 395 (1976)

In the preparation of the individual derivatives, very high yields could be achieved when the synthesis was accomplished in the following way: 4-hydrazino-3-nitroquinoline (**III**) was made to react with ortho acid esters (**IX**) to obtain 4-(alkoxymethylenehydrazino)-3-nitroquinolines (**X**), which were then converted into 1,2-dihydro-*as*-triazino[5,6-c]quinolines (**VII**) by means of reductive cyclization. The aromatization of these compounds was accomplished in the same way as in the first method, to yield the *as*-triazino-[5,6-c]quinoline derivatives (**VIII**).

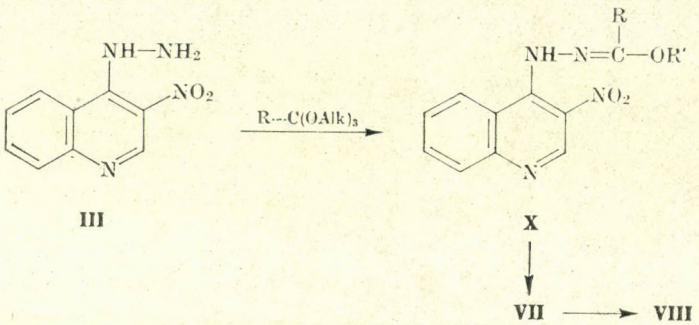

III **X**

VII → **VIII**

The structures of the compounds prepared were verified by means of microanalytical and spectroscopic investigations, for which the authors' acknowledgement is due to Dr. L. BUDA (EGyT Pharmacochemical Works) and to Dr. G. TÓTH (Pharmaceutical Chemical Institute of the Semmelweis Medical University, Budapest).

The excellent anti-imflammatory and antimicrobial action of this group of compounds, and the investigations and results in this field will be reported elsewhere.

Experimental

4-(Acylhydrazino)-3-nitroquinoline (V)

Method A

The appropriate acid hydrazide (0.1 mole) was dissolved (or suspended) in ethanol (200 ml) and 4-chloro-3-nitroquinoline (20.8 g; 0.1 mole) was added to the mixture, with stirring. The latter compound gradually dissolved, but the separation of the product from the reaction mixture usually started before complete dissolution. The reaction was accompanied by a colour change of the suspension to red, and a slight temperature increase (35—45°C). After 2 hrs stirring, the colour became paler, and a yellowish or pink crystal mass was obtained. This colour is characteristic of the hydrochlorides of acylhydrazinonitroquinolines.

The salt was suspended in tenfold amount of water and the base was liberated with equivalent sodium hydrogen carbonate. The colour of the free base was deep red, cherry-red or violet-red.

Method B

4-Hydrazino-3-nitroquinoline (2.04 g; 0.01 mole) was dissolved in pyridine (20 ml) with slight heating, then the acid chloride (0.01 mole) was added, with stirring. The reaction mixture was refluxed for 1 hr then cooled and poured into water. The precipitate that solidified was washed with water and dried. (Table I).

Table I

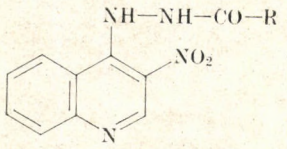

R	Formula	M. W.	M. p. °C	Calcd.			Found			Yield, %	Method
				C	H	N	C	H	N		
H	$C_{10}H_8N_4O_3$	232.21	190—191	51.74	3.47	24.11	51.43	3.86	24.11	92%	A
methyl	$C_{11}H_{10}N_4O_3$	246.23	194—195	53.65	4.09	22.76	53.64	4.13	22.62	88%	A
ethyl	$C_{12}H_{12}N_4O_3$	260.26	179—181	55.38	4.65	21.53	55.66	4.41	21.34	88%	A
n-propyl	$C_{13}H_{14}N_4O_3$	274.29	167—169	56.92	5.15	20.43	56.46	5.42	20.36	86%	A
i-propyl	$C_{13}H_{14}N_4O_3$	274.29	167—168	56.92	5.15	20.43	57.02	5.19	20.26	85%	A
t-butyl	$C_{14}H_{16}N_4O_3$	288.31	180—182	58.32	5.59	19.44	58.03	5.92	19.46	74%	B
phenyl	$C_{16}H_{12}N_4O_3$	308.30	202—203	62.33	3.92	18.57	62.09	3.59	18.09	98%	A, B
benzyl	$C_{17}H_{14}N_4O_3$	322.33	199—200	63.34	4.38	17.38	63.36	4.13	17.29	93%	A
4-hydroxyphenyl	$C_{16}H_{12}N_4O_4$	324.30	186—187	59.23	3.65	17.28	58.99	3.44	17.00	96%	A
2-hydroxyphenyl	$C_{16}H_{12}N_4O_4$	324.30	206—208	59.23	3.65	17.28	58.89	4.01	17.30	95%	A
4-aminophenyl	$C_{16}H_{13}N_5O_3$	323.32	246—248	59.43	4.06	21.66	59.72	4.06	21.59	96%	A
4-bromophenyl*	$C_{16}H_{11}N_4O_3Br$	387.21	219—221	49.63	2.86	14.47	49.40	3.05	14.21	91%	A
4-methylphenyl	$C_{17}H_{14}N_4O_3$	322.33	209—210	63.34	4.38	17.38	63.39	4.67	17.11	92%	A
3,4,5-trimethoxyphenyl	$C_{19}H_{18}N_4O_6$	398.38	213—215	57.28	4.55	14.07	57.46	4.22	14.35	82%	A, B
3,4-dimethoxybenzyl	$C_{19}H_{18}N_4O_5$	382.38	168—170	59.68	4.74	14.65	59.79	5.03	14.74	95%	A
4-pyridyl	$C_{15}H_{11}N_5O_3$	309.29	243—245	58.24	3.59	22.65	58.23	3.52	22.85	98%	A
3-pyridyl	$C_{15}H_{11}N_5O_3$	309.29	212—214	58.24	3.59	22.65	58.31	3.72	22.58	97%	A
2-pyridyl	$C_{15}H_{11}N_5O_3$	309.29	232—234	58.24	3.59	22.65	58.26	3.76	22.34	96.5%	A
2-phenylethyl	$C_{18}H_{16}N_4O_3$	336.36	202—204	64.27	4.80	16.66	64.27	4.92	16.90	96%	A

*Calcd. Br: 20,64; Found Br: 20;64

4-(β-ethoxy-substituted methylenehydrazino)-3-nitroquinoline (X)

4-Hydrazino-3-nitroquinoline (20.4 g, 0.1 mole) and *p*-toluenesulfonic acid (0.05 g) were suspended in the appropriate ortho acid ester (200 ml) and the temperature of the reaction mixture was kept for 4 hrs between the boliling point of ethanol and the ortho ester used (usually this was 120—130 °C); the ethanol formed during the reaction was continously removed by distillation. When the reaction was completed, the formation of ethanol ceased, and the temperature of the vapour space decreased. The product separated from the solution on cooling (Table II).

Table II

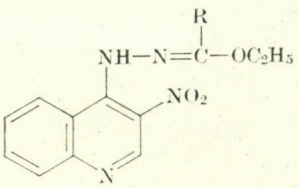

R	Formula	M. W.	M. p., °C	Calcd.			Found			Yield, %
				C	H	N	C	H	N	
H	$C_{12}H_{12}N_4O_3$	260.26	153—154	55.38	4.65	21.53	55.63	4.64	21.07	86
CH_3	$C_{13}H_{14}N_4O_3$	274.29	131—133	56.92	5.15	20.43	56.60	5.20	20.38	88
ethyl	$C_{14}H_{16}N_4O_3$	288.31	170—172	58.32	5.60	19.43	58.04	5.70	19.79	62
phenyl	$C_{18}H_{16}N_4O_3$	336.36	127—128	64.27	4.80	16.66	64.19	4.78	16.56	42

C—3-substituted as-triazino [5,6-c] quinoline (VIII)

(a) 4-(Acylhydrazino)-3-nitroquinoline (0.1 mole) was suspended in 15 parts of ethanol and hydrogenated in the presence of Pd/C catalyst at room temperature and atmospheric pressure until hydrogen absorption was no longer observed. The catalyst was removed by filtration, and the filtrate directly mixed with ethanol containing 10—15% hydrochloric acid (50 ml). Cherry-red or bright red crystals of the hydrochloride of C-3 substituted 1,2-dihydro-*as*-triazino[5,6-c]quinoline separated. The crystals were filtered off and washed with ethyl acetate. (Concentration of the mother liquor may be advisable.)

Potassium-[hexacyanoferrate(III)] (66.0 g; 0.2 mole) was dissolved in water (300 ml) and the pH of the solution was adjusted to 10 with conc. ammonium hydroxide solution. The hydrochloride of the C-3 substituted 1,2-dihydro-*as*-triazino[5,6-c]quinoline was added to this solution while stirring and maintaining the temperature below 10° C. A yellow or orange-coloured suspension was obtained, which was stirred further for 1—2 hrs then filtered. The solid was washed with water and recrystallized from chloroform or alcohol.

(b) 4-(Acylhydrazino)-3-nitroquinoline (0.1 mole) or its hydrochloride was added to a solution of tin(II) chloride (67.5 g; 0.3 mole) in water (600 ml). Conc. HCl (500 ml) was added dropwise with stirring, and the reaction mixture was refluxed for 1 hr. The crystal mass was filtered off and washed with water. Liberation of the base and oxidation were carried out as described under *(a)*.

(c) 4-(β-ethoxy-substituted methylenehydrazino)-3-nitroquinoline (0.1 mole) was suspended in ethanol and hydrogenated until the end of hydrogen absorption at room temperature and atmospheric pressure. The dark-brown solution obtained contained C-3-substituted 1,2-dihydro-*as*-triazino[5,6-c]quinoline. After removing the catalyst, the solution was evaporated while letting air bubble through the solution. C-3-substituted *as*-triazino[5,6-c] quinoline was obtained (Table III).

Table III

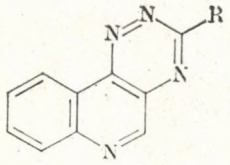

R	Formula	M. W.	M. p., °C	Calcd.			Found			Yield, %	Solvent	Method
				C	H	N	C	H	N			
H	$C_{10}H_6N_4$	182.19	161—163	65.92	3.32	30.76	65.81	3.26	30.83	85%	EtOH	A, C
methyl	$C_{11}H_8N_4$	196.22	137—138	67.33	4.11	28.56	67.50	4.23	28.32	83%	EtOH	A, C
ethyl	$C_{12}H_{10}N_4$	210.24	106—108	68.55	4.80	26.65	69.00	4.91	26.77	84,5%	EtOH	A, C
n-propyl	$C_{13}H_{12}N_4$	224.27	84—85	69.62	5.40	24.98	69.87	5.51	24.90	87%	Gasoline	A
i-propyl	$C_{13}H_{12}N_4$	224.27	71—72	69.62	5.40	24.98	69.77	5.46	24.88	79%	Gasoline	A
t-butyl	$C_{14}H_{14}N_4$	238.30	78—81	70.56	5.92	23.52	70.39	5.72	23.21	69%	Gasoline	A
phenyl	$C_{16}H_{10}N_4$	258.29	201—202	74.40	3.90	21.70	74.65	4.06	21.66	90%	$CHCl_3$	A, B, C
benzyl	$C_{17}H_{12}N_4$	272.31	150—152	74.98	4.44	20.58	74.65	4.48	20.34	72%	$CHCl_3$	A, B
4-hydroxyphenyl	$C_{16}H_{10}N_4O$	274.29	323—326	70.06	3.68	20.43	69.97	3.76	20.34	85%	DMF	B
2-hydroxyphenyl	$C_{16}H_{10}N_4O$	274.29	243—245	70.06	3.68	20.43	70.17	3.89	20.36	82%	$CHCl_3$	A, B
4-aminophenyl	$C_{16}H_{11}N_5$	273.30	268—270	70.30	4.06	25.64	70.45	4.08	25.60	62%	$CHCl_3$	B
4-bromophenyl*	$C_{16}H_9N_4Br$	337.19	248—250	56.99	2.69	16.62	56.94	2.66	16.37	71%	$CHCl_3$	B
4-methylphenyl	$C_{17}H_{12}N_4$	272.31	183—184	74.98	4.44	20.58	74.62	4.58	20.47	88%	$CHCl_3$	B
3,4,5-trimethoxyphenyl	$C_{19}H_{16}N_4O_3$	348.37	182—183	65.51	4.63	16.08	65.79	4.69	15.94	78%	$CHCl_3$	A, B
3,4-dimethoxybenzyl	$C_{19}H_{16}N_4O_2$	332.37	150—152	68.66	4.85	16.86	68.58	5.16	16.89	78.5%	$CHCl_3$	A
4-pyridyl	$C_{15}H_9N_5$	259.28	213—214	69.48	3.50	27.02	69.72	3.67	27.00	81%	$CHCl_3$	A, B
3-pyridyl	$C_{15}H_9N_5$	259.28	190—193	69.48	3.50	27.02	69.66	3.46	26.97	84%	$CHCl_3$	B
2-pyridyl	$C_{15}H_9N_5$	259.28	162—164	69.48	3.50	27.02	69.34	3.43	27.13	82%	$CHCl_3$	B
2-phenylethyl	$C_{18}H_{14}N_4$	286.34	96—97	75.50	4.93	19.57	75.15	4.91	19.64	84%	EtOH	A

*Calcd. Br. 23,7; Found Br 23,6

REFERENCES

[1] BERÉNYI, E., BENKÓ, P., PALLOS, L.: Acta Chim. (Budapest) (In press)
[2] WRIGT, G. C., GRAY, J. E., YU, C. N.: J. Med. Chem. **17,** 244 (1974)
[3] SURREY, A. R., CUTLER, R. A.: J. Am. Chem. Soc. **73,** 2414 (1951)
[4] FLEET, G. W. J., FLEMING, I.: J. Chem. Soc. (C) **1969,** 1758

Edit BERÉNYI
Pál BENKÓ
László PALLOS
H-1106 Budapest 10. Pf. 100.

Acta Chimica Academiae Scientiarum Hungaricae, Tomus 90 (4), pp. 405–410 (1976)

CONDENSED *AS*-TRIAZINES, V*

PYRIDO[4,3-e]-*AS*-TRIAZINES

P. BENKÓ, E. BERÉNYI, A. MESSMER**, Gy. HAJÓS** and L. PALLOS

*(EGyT Pharmacochemical Works, Budapest, and ** Central Research Institute for Chemistry of the Hungarian Academy of Sciences, Budapest)*

Received July 7, 1975

A one-apparatus procedure has been developed for the synthesis of 3-aminopyrido[4,3-e]-*as*-triazine-1-oxides (**III**). Base-catalyzed rearrangement of these compounds yielded 1H-v-triazolo[4,5-c]pyridine-1-carboxamide and 4-chloro-1H-v-triazolo[4,5-c] pyridine. Oxidation of **III** resulted in the 1,4-dioxide derivative, and the respective C-3 substituted amino derivatives were prepared with amines.

The ARNDT synthesis of benzo-*as*-triazine [1] has been successfully employed by LEWIS and SHEPHERD [2] for the preparation of pyrido[4,3-e]-*as*-triazine derivatives unsubstituted in the pyridine ring.

In the present paper a modified synthesis of 3-aminopyrido[4,3-e]-*as*-triazine-1-oxides, accomplished in one-apparatus, and the preparation of further C-3-substituted derivatives will be described.

The starting material was 4-methoxy-3-nitropyridine (**Ia**). It was allowed to react with guanidine in the presence of excess sodium alkoxide, at the boiling point of the solvent, to obtain 3-aminopyrido[4,3-e]-*as*-triazine-1-oxides (**III**) within a few hours, without isolating the intermediate **II**.

The method is based on the idea — not applied in the ARNDT synthesis [1] up to now — that *o*-nitroguanidinopyridines can be cyclodehydrated in the presence of an alkali alkoxide. The reaction is suitable for the preparation of the required derivatives (**III**) in one step, in high purity and good yields.

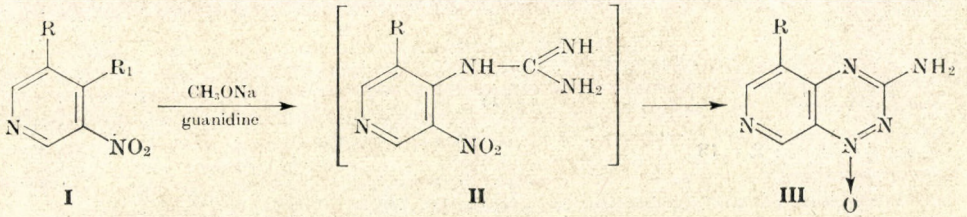

I II III

The structure of 3-aminopyrido[4,3-e]-*as*-triazine-1-oxide (**IIIa**) was confirmed by, among others, mass-spectrometric investigations. On this basis,

* Part IV: E. BERÉNYI, P. BENKÓ, L. PALLOS: Acta Chim. (Budapest) (In press)

its molecular weight proved to be 163. The most characteristic fragments are the following:

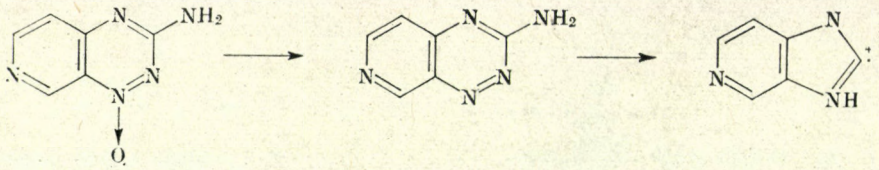

IIIa: *m/e* 163 *m/e* 147 *m/e* 119

Thus the band with $m/e = 147$ is also found (M-16); this has a diagnostic importance, being characteristic of heterocyclic N-oxides according to BRYCE and MAXWELL [4]. This is followed by the band with $m/e = 119$, brought about by the loss of N_2 [5] from heterocycles containing vicinal N-atoms, such as *as*-triazines. Interestingly, the H_2CN (M-28) fragment occurring in the case of C-amino compounds (aromatic primary amines) examined by GILLIS [6] does not appear at all; the next step here is the release of HCN resulting in decomposition of the triazine molecule, followed by complete destruction of the pyridine ring.

The base-catalyzed rearrangement of 3-aminobenzo-and 3-aminopyrido-[2,3-e]-*as*-triazine-l-oxides observed first by CARBON and TABATA [3,7] takes place with 3-aminopyrido[4,3-e]-*as*-triazine-l-oxide (**IIIa**) [2] in the same way.

In accordance with this, the rearrangement of the chloro derivative (**IIIb**) synthesized by us was also studied. The reaction with ring contraction was found to take place only at a temperature higher by about 20 °C than needed for **IIIa** (R = H).

Unexpectedly, no 4-chloro-1H-v-triazolo[4,5-c]pyridine-l-carboxamide (**IVb**) could be isolated, in spite of analogous conversions reported in the literature.

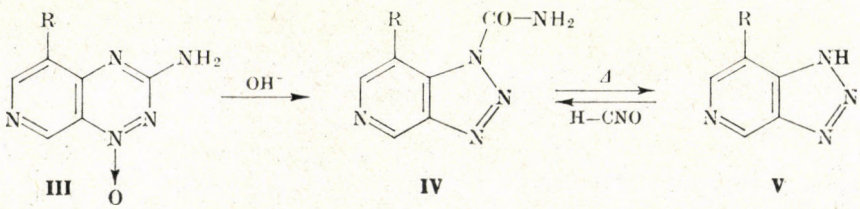

III **IV** **V**

a: R = H **b**: R = Cl

In order to get a deeper insight into the process, the rearrangement reaction of **IIIa** (R = H) described by LEWIS and SHEPHERD [2] was studied. The 3-amino-l-oxide derivative (**IIIa**) could be converted into 1H-v-triazolo-[4,5-c]pyridine (**Va**) with 10% sodium hydroxide solution at 80 °C during 30 min., in 85% yield. The product can only be isolated from the reaction mixture at pH 3.5—4, since in more acidic or in alkaline media it remains in solution.

This experimental result is in contradiction with the observation of the American researchers [2], as they described also the isolation of 1H-v-triazolo[4,5-c]pyridine-1-carboxamide (**IVa**), in the course of the rearrangement of **IIIa** into **Va**. No melting point was reported, only the appearance of the carbonyl band (1755 cm^{-1}) in the IR spectrum characteristic of compound **IVa** was given as evidence. Since in our experiments the carboxamide derivative (**IVa**) could not be isolated, it was prepared indirectly from v-triazolo-[4,5-c]pyridine (**Va**) in a reaction with potassium cyanate in acidic medium as suggested by CARBON [7]. It was found to be a compound consisting of white plates, its melting point being higher by almost 30 °C than that of **Va**; it transformed into triazolopyridine (**Va**) when fused at about 300 °C, or in solution (*e. g.*, during recrystallization from alcohol). The carbonyl band characteristic of carboxamide appears at 1790 cm^{-1} in the IR spectrum, together with bands characteristic of NH_2 groups (3385 and 3270 cm^{-1}). All spectral data were in good agreement with the corresponding values of authentic triazolo[4,5-b]pyridine-1-carboxamide prepared as described by CARBON and TABATA [3].

On the basis of our examinations it can be stated that in the course of the rearrangement of 3-aminopyrido[4,3-e]-*as*-triazine-1-oxides (**III**) the ring contraction may take place through carboxamides (**IV**), but the rearrangement reaction is faster in this system than in the case of pyrido[2,3-e]-*as*-triazines [3], therefore, the intermediates **IV** cannot be isolated.

3-Aminopyrido[4,3-e]-*as*-triazine-1-oxide (**IIIa**) was converted into the 1,4-dioxide with sodium tungstate and hydrogen peroxide [11] in a satisfactory yield. It was found that the methods using peracids [8] or hydrogen peroxide in glacial acetic acid [9], applied successfully in the preparation of heterocyclic N-oxides, are not advisable in the present case, owing to the low yields and the appearance of by-products.

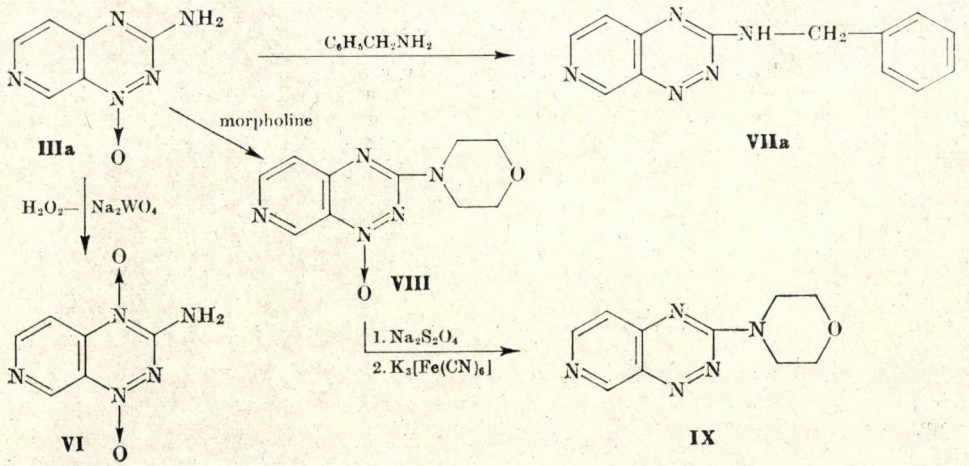

The C-3 amino group — which does not give the reactions characteristic of aromatic amines — can be converted into substituted amino derivatives (**VII**) of compound **III**, by means of the method suggested by WOLF *et al.* [12]. Thus, when compound **III** is heated with benzylamine for 2 hrs 3-benzylaminopyrido[4,3-e]-*as*-triazine (**VIIa**) is formed in about 45% yield. Chemical evidence for the deoxidation occurring during the reaction with benzylamine was provided by reacting the reduction product of **IIIa** with benzylamine, whereupon **VIIa** was obtained.

The reaction of morpholine with **III** yielded 3-morpholinopyrido[4,3-e]-*as*-triazine-l-oxide (**VIII**) in 50% yield. Oxidation after the reduction step with sodium dithionite resulted in 3-morpholinopyrido[4,3-e]-*as*-triazine (**IX**), as expected.

The experiments have shown that the above reactions with benzylamine and morpholine cannot be carried out when attempted with the corresponding derivatives of pyrido[2,3-e]-*as*-triazine. This can probably be explained by the fact that 7-bromo-3-aminobenzo-as-triazine employed in the reaction effected by Wolf [12] has the electron-attracting group in the same position where the pyrido[4,3-e]-*as*-triazine system (**IIIa**) contains the similarly electron-attracting nitrogen atom; thus, this latter can be regarded as the 7-aza analogue of the benzene series. These facts all suggest that successful nucleophilic exchange of the C-3 substituent of condensed *as*-triazines is primarily and particularly dependent on the electron-attracting effect of position C-7.

Experimental

Spectra were recorded with the following instruments:
IR: UR-10 (Carl Zeiss) spectrophotometer; UV: UNICAM SP 800; NMR: HA-60 Varian apparatus.

M. p.'s are uncorrected and were measured in capillary tubes.

4-Guanidino-3-nitro-5-chloropyridine (IIb)

Guanidine hydrochloride (6.9 g; 0.072 mole) was converted into guanidine with metallic sodium (4.55 g; 0.19 mole) dissolved in methanol (430 ml), then 4,5-dichloro-3-nitropyridine (**Ib**) (14.0 g; 0.072 mole) was added to the solution. The crystals which separated during 6 hrs at 30—40 °C were filtered off. The yellow bright crystalline product (12.4 g; 79.5%) had m. p. 232—233 °C (from i-PrOH).

$C_6H_6ClN_5O_2$ (215.61). Calcd. C 33.42; H 2.81; Cl 16.45; N 32.50. Found C 33.71; H 2.79; Cl 16.32; N 32.45%.

UV (EtOH): λ_{max} nm (log ε): 263 (4.00).

TLC ($CHCl_3$—MeOH, 80 : 20): $R_f = 0.528$.

3-Aminopyrido [4,3-e]-as-triazine-l-oxide (IIIa)

(a) The guanidine derivative **IIa** (3.1 g; 0.017 mole) was heated in 3% sodium hydroxide (60 ml) for 5 min. at 70—80 °C. First, a suspension was obtained, which dissolved for some time, then became thicker. The product was filtered off and washed to obtain ochre-yellow crystals (1.45 g; 84.5%), m. p. 304 °C (from EtOH) (lit. [2] m. p. 298 °C).

$C_6H_5N_5O$ (163.15). Calcd. C 44.20; H 3.09; N 42.90. Found C 43.95; H 3.07; N 42.45%
UV (EtOH): λ_{max} nm (log ε): 385 (3.51); 302 (4.20); 285 (3.48).
NMR (DMSO): δ ppm: 7.38 (d; 5-*H*); 8.58 (d; 6-*H*); 9.24 (s; 8-*H*);
TLC ($CHCl_3$—MeOH, 20 : 80): $R_f = 0.58$.

(b) Guanidine hydrochloride (81.5 g; 0.857 mole) was converted to a solution of the guanidine base with metallic sodium (20.9 g; 0.908 mole) in ethanol (1820 ml). 4-Methoxy-3-nitropyridine (**Ia**) (114 g; 0.734 mole) was added to this solution. The reaction mixture was refluxed for 3 hrs, and the yellow precipitate which separated was filtered off and washed with water. 90 g (75.3%) of the product was obtained, m. p. 302 °C (from EtOH). On the basis of elemental analysis and the UV spectrum, it is identical with the product prepared according to *(a)*.

3-Amino-5-chloropyrido [4,3-e]-as-triazine-1-oxide (IIIb)

3-Nitro-4-guanidino-5-chloropyridine (**IIb**) (4.3 g; 0.02 mole) was heated with 2% sodium hydroxide solution (60 ml) at 80 °C for 5 min., when the light-brown colour of the starting material turned into yellow. The precipitate was filtered off; yellow crystals were obtained (2.35 g; 59.7%), m. p. 325°C (from DMF).

$C_6H_4ClN_5O$ (197.59). Calcd. C 36.45; H 2.04; Cl 17.95; N 33.45. Found C 36.40; H 2.00; Cl 17.92; N 35.31%.

UV (0.1 *N* HCl): λ_{max} nm (log ε); 268 (3.45). 312 (4.00), 3.94 (3.50).

1H-v-Triazolo [4,5-c] pyridine-1-carboxamide (IVa)

1H-v-Triazolo[4,5-c]pyridine (6.0 g; 0.05 mole) was dissolved in a mixture of conc. hydrochloric acid (12.5 ml) and water (60 ml), and potassium cyanate (6.1 g; 0.075 mole) was added in small portions, with stirring, during 25 min. After about 15 min., the precipitation of a white substance started. The reaction was continued for about one and a half hour; the product was then filtered off to obtain white plates (3.4 g; 41.7%), m. p. 273—274 °C.

$C_6H_5N_5O$ (163.15). Calcd. C 44.20; H 3.09; N 42.90. Found C 44.62; H 3.14; N 43.10%.

UV (0.1 *N* HCl): λ_{max} nm (log ε): 263 (369).

IR (KBr): 3385, 3270 cm^{-1} (ν NH_2); 1790 cm^{-1} (ν CO).

When recrystallized from ethanol, the m. p. decreased to 246—247 °C.

IR (KBr): The characteristic bands of **IVa** disappeared and those characteristic of **V** appeared.

1H-v-Triazolo [4,5-c] pyridine (Va)

(a) The N-oxide of **IIIa** (1.63 g; 0.01 mole) was kept in 10% sodium hydroxide (20 ml) at 80—85°C for 30 min. A cherry-red solution was first obtained, which became pale yellow during the 30 min. It was filtered and adjusted to pH 4 with acetic acid. The crystals which separated were filtered off (1.02 g; 85%), m. p. 246—247 °C (from EtOH). No m. p. depression was observed in admixture with an authentic sample.

$C_5H_4N_4$ (120.12). Calcd. C 50.00; H 3.36; N 46.65. Found C 50.05; H 3.29; N 46.95%.

UV (EtOH): λ_{max} nm (log ε): 258 (3.66).

(b) The carboxamide **IVa** (1.63 g; 0.01 mole) was recrystallized from 38 volumes of ethanol to obtain white plates of **Va** in 95% yield; m. p. 244—245 °C.

UV (EtOH): λ_{max} nm (log ε); 258 (3.65).

4-Chloro-1H-v-triazolo [4,5-c] pyridine (Vb)

The N-oxide **IIIb** (1 g; 0.0051 mole) was refluxed in 10% sodium hydroxide (15 ml) until the disappearance of the initial red colour and the formation of a yellow solution. This occurred in about half an hour. The solution was filtered (after having adjusted its pH to 4 with acetic acid); white needles were obtained (0.55 g; 70%), m. p. 252—253 °C (from EtOH).

$C_5H_3ClN_4$ (154.57). Calcd. C 38.80; H 1.95; Cl 22.95; N 36.30. Found C 38.75; H 1.90; Cl 22.85; N 36.10%.

IR (KBr): no carbonyl band

3-Aminopyrido [4,3-e]-as-triazine-1,4-dioxide (VI)

A solution of sodium tungstate dihydrate (2.0 g; 0.063 mole) in 30% hydrogen peroxide (20 ml) was added to **IIIa** (1.0 g; 0.063 mole) and the suspension was stirred continuously. Most of the solid substance dissolved in 4 hrs. The mixture was allowed to stand overnight, then cooled at 0 °C for 2—3 hrs. The precipitate was filtered off (0.7 g; 64%), m. p. 295 °C.

$C_6H_5N_5O_2$ (179.15). Calcd. C 40.20; H 2.82; N 39.10. Found C 40.44; H 2.84; N 39.02%.
IR (KBr): 3330; 3140 cm^{-1} (ν NH); 1645, 1545, 1535, 1500, 1470 cm^{-1} (aromatic skeletal vibrations); 1235 cm^{-1} (N—O).

3-Benzylaminopyrido [4,3-e]-as-triazine (VII)

A solution of **IIIa** (0.4 g; 0.024 mole) in benzylamine (4 ml) was refluxed for 2 hrs, a red solution was obtained from which bright crystals separated on cooling (0.2 g; 35%). m. p. 164—166 °C (from MeCN).
$C_{13}H_{11}N_5$ (237.27). Calcd. C 65.88; H 4.68; N 29.55. Found C 65.50; H 5.08; N 29.42%.
IR (KBr): 2800—3050 cm^{-1} (aliphatic and aromatic CH); 3150 cm^{-1} (secondary NH).

3-Morpholinopyrido [4,3-e]-as-triazine-1-oxide (VIII)

Compound **IIIa** (1.0 g; 0.062 mole)was refluxed in morpholine (10 ml) for 30 hrs, then evaporated to dryness. The residue was rubbed with chloroform to obtain the product (0.52 g; 36%), m. p. 177—179 °C (EtOH).
$C_{10}H_{11}N_5O_2$ (233.24). Calcd. C 51.55; H 4.76; N 30.06. Found C 51.49; H 4.73; N 29.77%.

3-Morpholinopyrido [4,3-e]-as-triazine (IX)

Compound **VIII** (1.8 g; 0.077 mole) was added to an aqueous solution (40 ml) of conc. ammonium hydroxide (1 ml) and sodium dithionite (5 g; 0.029 mole). The reaction mixture was stirred. A pale yellow suspension formed in about 15 min. The precipitate was filtered off, added to an aqueous solution (60 ml) of potassium ferricyanide (10 g) also containing conc. ammonium hydroxide (5 ml). After 15 min. the product was extracted with chloroform, evaporated to dryness, and the residue was crystallized from ethanol to give yellow crystals (0.4 g; 24%), m. p. 171—173°C.
$C_{10}H_{11}N_5$ (217.24). Calcd. C 55.35; H 5.11; N 32.27. Found C 55.15; H 5.00; N 32.65%.

*

The authors' thanks are due to Dr. R. HERZSCHUH and Dr. R. BORSDORF (Karl-Marx-Universität, Leipzig), as well as to Dr. L. BUDA (EGyT Pharmacochemical Works) for the instrumental and microanalyses, and to Miss M. LAKATOS for technical assistance.

REFERENCES

[1] ARNDT, F.: Ber. **46,** 3522 (1913)
[2] LEWIS, A., SHEPHERD, R. G.: J. Heterocycl. Chem. **8,** 47 (1971)
[3] CARBON, J. A., TABATA, S. H.: J. Org. Chem. **27,** 2504 (1962)
[4] BRYCE, T. A., MAXWELL, J. R.: Chem. Comm. **1965,** 206
[5] PAUDLER, W. W., HERBENER, R. E.: J. Heterocycl. Chem. **4,** 224 (1967)
[6] GILLIS, R. G.: Org. Mass Spectrom. **5,** 1107 (1971)
[7] CARBON, J. A.: J. Org. Chem. **27,** 185 (1962)
[8] KATRITZKY, A. R., LAGOWSKI, J. M.: Chemistry of the Heterocyclic N-Oxides. Academic Press, London, 1971
[9] CHIVERS, G. E., SUSCHITZKY, H. J.: J. Chem. Soc. (C) **1971,** 2867
[10] BREMER, O.: Ann. **518,** 274 (1935)
[11] FIESER and FIESER: Reagents for Organic Chemistry, Vol. 1, pp. 475. Wiley, New York, 1967
[12] WOLF, F. J., WILSON, R. M., Pfister, K., Tischler, M.: J. Am. Chem. Soc. **76,** 4611 (1954)

Pál BENKÓ, Edit BERÉNYI } H-1106 Budapest, Pf. 100.

András MESSMER, György HAJÓS } H-1025 Budapest, Pusztaszeri út 49—57.

László PALLOS H-1106 Budapest, Pf. 100.

Acta Chimica Academiae Scientiarum Hungaricae, Tomus 90 (4), pp. 411—417 (1976)

THERMAL TRANSCARBOXYLATION REACTIONS, VII*

THE RELATIVE ABILITY TO TRANSFER OF AROMATIC HYDROGENS

J. SZAMMER and L. NOSZKÓ**

(Central Research Institute for Chemistry of the Hungarian Academy of Sciences, Budapest)

Received August 18, 1975

An experimental method, useful under the conditions of the Henkel reaction, has been developed for the determination of the frequency of hydrogen abstractions from aromatic carboxylic acid salts. It has been found that the hydrogen atoms of aromatic potassium carboxylates are rather readily split off, except for the hydrogens of terephthalate; the readiness of hydrogen abstraction is independent of the thermal stability of the salts.

The low reactivity of the hydrogens in dipotassium terephthalate towards the reactive intermediates of the thermal conversion is in agreement with the experience that this compound is the main product of the Henkel reaction.

During the thermal transformations of the potassium salts of benzenecarboxylic acids [1], the formation of a number of carboxylic acid salts has been observed. The relative amounts of these salts have been found to change as the reactions proceed [2—5]. The main product of this process, mentioned in the literature often as the Henkel reaction, is dipotassium terephthalate, which appears and becomes predominant in the later stages of the reaction.

According to the intermolecular mechanism (Fig. 1) of the reaction [6—9],

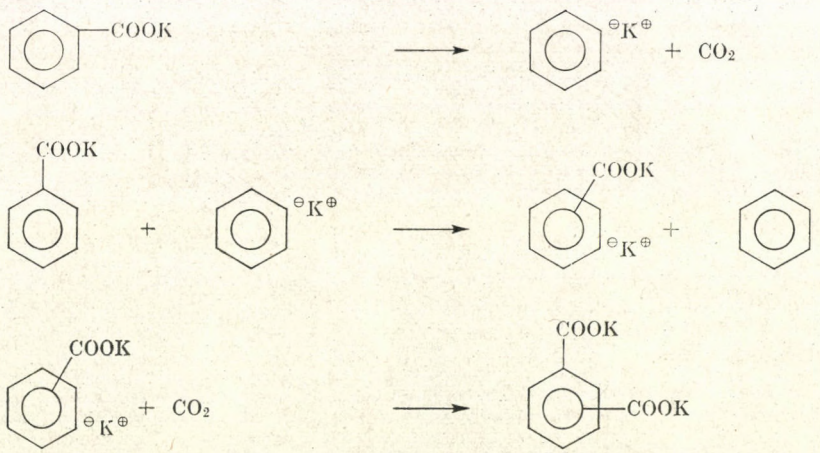

Fig. 1

* Part VI: Radiochem. Radioanal. Lett. **21**, 241 (1975)

** Present address: Budapesti Műszaki Egyetem Alkalmazott Kémiai Tanszék (Department of Applied Chemistry, Technical University, Budapest)

the reactive intermediates of the transformation are proton-deficient salt molecules [9]; these are formed by decarboxylation and the splitting off of hydrogen. This hydrogen abstraction by the reactive fragments is an individual stabilization and reproduction process (Fig. 2) resulting in intermolecular transprotonation [9, 10], which is the prerequisite of the repeated migration of the carboxyl group.



Fig. 2

The hydrogen abstraction steps shown in Figs 1 and 2 will undoubtedly also occur in the reaction products, affording the possibility of their further transformations, even in the case of otherwise thermally stable salt molecules. Obviously, the higher the relative frequency of the abstraction of hydrogen from a carboxylic acid salt present in the Henkel reaction, the more the stability of this salt decreases in the presence of reactive fragments. This relationship is expected to lead to a better understanding of the detected product composition.

For a study of the relative proneness to splitting off of aromatic hydrogens, an equimolecular mixture of perdeuterated potassium benzoate and a non-deuterated salt was thermally decomposed and the amount of benzenes formed in this reaction was determined by mass spectrometry.

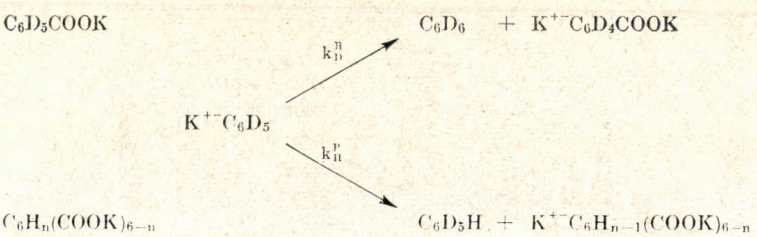

Fig. 3

As shown in Fig. 3, the produced fragment ($K^+ {}^-C_6D_5$) abstracts deuterium from the benzoate, and hydrogen from the carboxylate present to give the benzenes C_6D_6 and C_6D_5H, respectively. The ratio of the relative rates of the hydrogen- and deuterium abstractions is thus characterized by the ratio of the amounts of the C_6D_6 and C_6D_5H formed. This ratio can be determined by mass-spectrometric analysis.

From the experimental results in Table I, the relative hydrogen reactivity values referred to the hydrogens of potassium benzoate (k_H^P/k_H^B) were calculated on the basis of the following considerations.

Table I

Results of thermogravimetric and mass-spectrometric measurements

Salts[a]	Decompn., °C		Temp., °C	Time, min.	Y_5[b]	Y_6[b]
	Initial	DTG peak				
$KB-d_5$	430	520	450	20	0.008	0.992
K_2P + $KB-d_5$	460	540	430	10	0.660	0.340
K_2IP + $KB-d_5$	490	540	430	10	0.639	0.361
K_2TP			430	10	0.034	0.966
+	540	600	450	5	0.050	0.950
$KB-d_5$			410[c]	15	0.080	0.920
K_3TM + $KB-d_5$	470	520	430	10	0.631	0.369
K_3TS + $KB-d_5$	480	520	430	10	0.469	0.531
K_3HM + $KB-d_5$	470	530	430	10	0.550	0.450

[a] $KB\text{-}d_5$ = perdeuterated potassium benzoate; P = phthalate; IP = isophthalate; TP = terephthalate; TM = trimellitate; TS = trimesitate; HM = hemimellitate.

[b] mole fraction of benzene containing 5 or 6 atoms of deuterium

[c] Composition of the salt mixture, $K_2TP : KB-d_5 : KOCN = 1 : 1 : 15$

The rates of formation (W_6 and W_5) of the benzene molecules C_6D_6 and C_6D_5H, can be written as follows:

$$W_6 = 5\ k_D^B\ [C_6D_5^-]\ [C_6D_5COOK]$$
$$W_5 = n\ k_H^P\ [C_6D_5^-]\ [C_6Hn\ (COOK)_{6-n}] \qquad (1)$$

Division of W_5 by W_6 gives Eq. (2):

$$\frac{W_5}{W_6} = \frac{n}{5} \frac{k_H^P}{k_D^B} \frac{[C_6H_n(COOK)_{6-n}]}{[C_6D_5COOK]} . \tag{2}$$

The quotients of the corresponding rate constants were calculated from Eqs (1) and (2), by satisfying the following criteria and utilizing the simplifications below:

1. The tests were carried out on benzene samples removed in such an initial phase of the thermal transformation when intermolecular H–D exchange did not yet interfere.

2. The small material requirement of mass-spectrometric analysis permitted to make measurements at very low conversions. Therefore, in the above equations one may calculate with the starting molar ratios.

3. From the intensities corresponding to the mass numbers for the mole fractions Y_5, Y_6 we have

$Y_5 = \frac{B_5}{B_5 + B_6}$ and $Y_6 = \frac{B_6}{B_5 + B_6}$, where the numbers of benzene molecules with isotope composition C_6D_5H and C_6D_6 are denoted by B_5 and B_6, respectively.

In time t the amounts of B_5 and B_6 formed are

$$B_6 = \int_0^t W_6 \, dt = Y_6 \, (B_5 + B_6) \text{ and}$$

$$B_5 = \int_0^t W_5 \, dt = Y_5 \, (B_5 + B_6) .$$

Substitution of these in Eq. (2) gives

$$\frac{Y_5}{Y_6} = \frac{n}{5} \frac{k_H^P}{k_D^B} \frac{[C_6H_n(COOK)_{6-n}]}{[C_6D_5COOK]} . \tag{3}$$

4. The term for the quotient of the salt concentrations in Eq. (2) can be substituted by the ratio X_H^P/X_D^B, which is the number of moles of salt present in the salt mixture.

5. According to former studies [11, 12], in the reaction step of hydrogen- and deuterium abstraction from the benzoate molecule, the primary kinetic effect is:

$$\frac{k_H^B}{k_D^B} = 2.20, \text{ at } 430\,^\circ\text{C, and}$$

$$\frac{k_H^B}{k_D^B} = 2.15, \text{ at } 450\,^\circ\text{C}$$

If these conditions are fulfilled and, using the simplifications and the substitutions mentioned above, the relative hydrogen reactivity values at 430 °C, referred to the benzoate hydrogens, can be calculated.

$$\frac{k_H^P}{k_H^B} = \frac{5}{2.20\ n} \frac{Y_5}{Y_6} \frac{X_D^B}{X_H^D}$$

It is known [13] that the proneness of benzoate hydrogens to undergo splitting off considerably depends on their positions, thus the expression deduced above is merely an average value indicating the ratio of the average readiness of abstraction of the hydrogens from two different carboxylic acid salt molecules.

The tests for hydrogen mobility were carried out in 1 : 1 molar mixtures of the salts listed in Table I, at 430 °C. In the case of dipotassium terephthalate, measurements were also made at 450 °C, above the melting point of potassium benzoate, and at 420 °C, in a KOCN solution.

Table II

The relative reactivities of aromatic hydrogens in thermal transformation reactions

Salts [a]	Temp., °C	Time, min.	$\frac{k_H^P}{k_H^B}$	$\frac{n}{5}\frac{k_H^P}{k_H^B}$ [b]
KB	—	—	1	1
K_2P + KB-d_5	430	10	1.10	0.88
K_2IP + KB-d_5	430	10	0.95	0.76
K_2TP + KB-d_5	430	10	0.02	0.02
	450	5	0.03	0.02
in KOCN [c]	410	15	0.05[d]	0.05
K_3TM + KB-d_5	430	10	1.30	0.78
K_3TS + KB-d_5	430	10	0.67	0.40
K_3HM + KB-d_5	430	10	0.926	0.56

[a] KB-d_5 = perdeuterated potassium benzoate; P = phthalate; IP = isophthalate; TP = terephthalate; TM = trimellitate; TS = trimesitate; HM = hemimellitate.

[b] Frequency of carbanion formation, in an equimolar salt mixture, referred to the benzoate.

[c] Composition of the salt mixture, K_2TP : KB-d_5 : KOCN = 1 : 1 : 15.

[d] $\frac{k_H^B}{k_D^B} = 2.20$ was used in the calculations.

According to Table II, under the experimental conditions here prevailing, there is a significant difference between the readiness for abstraction of the hydrogens of the various potassium salts of benzenecarboxylic acids. Interestingly, under the conditions of the Henkel reaction practically no abstraction of hydrogen occurs from the dipotassium terephthalate molecule. This is in good agreement with the experience that dipotassium terephthalate is the end-product of the thermal transcarboxylation reaction. The low reactivity of the terephthalate hydrogens towards the reactive intermediates of the thermal transformation is a characteristic feature that qualitatively distinguishes the terephthalate molecule from the intermediary carboxylates observed in Henkel reactions. The experimental result also explains the reason why dipotassium isopthalate is not an end-product of this reaction, though it is produced at a much higher rate [2—5] in the thermal process and is, according to thermogravimetric measurements, stable under the given experimental conditions.

The results obtained by experiments in KOCN, and the fact that in most cases decomposition occurs at 430 °C in the solid phase, cast doubt on the suggestion that the transformation into terephthalate is due to its separation from the reaction mixture as a crystalline product. Hydrogen abstraction, *e. g.* from dipotassium isophthalate, takes place also in the solid phase, whereas from dipotassium terephthalate the splitting off of hydrogen is very slight even is KOCN solution.

In the literature [10] the possibility has been suggested that the first step of this thermal transformation is the dissociation of a proton; according to this, the transformation of potassium benzoate might be represented as shown in Fig. 4.

$$C_6H_5COOK \rightleftharpoons H^{\oplus} + {}^{\ominus}C_6H_4COOK$$

$$C_6H_5COOK + H^{\oplus} \longrightarrow C_6H_6 + CO_2 + K^{\oplus}$$

$${}^{\ominus}C_6H_4COOK + CO_2 + K^{\oplus} \longrightarrow C_6H_4(COOK)_2$$

Fig. 4.

Our experimental results seem to exclude this mechanism because

1. the catalytic effect of Cd and Zn is due to the formation of Cd- and Zn-carboxylates, and it is the low thermal stability of these compounds which accelerates the decarboxylation step [9, 14].

2. There is no intermolecular H–D exchange preceding [11] the thermal transformation of potassium benzoate.

3. According to the data in Tables I and II, in the case of the various carboxylic acid salts, there is no connection between the thermal stability and the mobility of the hydrogens, *i. e.* a relatively low thermal stability does not go together with a relatively high mobility of hydrogen, as one would expect it on the basis of the scheme in Fig. 4.

Experimental

Materials

The aqueous suspensions of the aromatic carboxylic acids were neutralized with an equivalent amount of KOH. The salt solutions were evaporated to dryness and dried in vacuum (1 torr) at 200°C. The purity of the salts was checked by the determination of potassium. The salt mixtures were prepared by weighing out the components in 1 : 1 molar ratio and dissolving them, followed by evaporation of the solution and the drying of the residue.

Benzoic-H_5^2-acid was prepared from commercially available highly deuterated benzene (deuterium content over 99.5) by bromination [15]. The bromobenzene-H_5^2 (b. p. 154—155 °C) was converted in abs. ether solution into phenylmagnesium bromide, and this was carboxylated with CO_2 [13]. The benzoic acid was recrystallized from water; m. p. 121 °C, yield 62% (calculated for benzene-H_6). For the determination of the deuterium content, a 0.5-g sample of the perdeuterated potassium benzoate, used in preparing the salt mixtures, was kept at 460 °C for 1 hr. According to the mass-spectrometric analysis of the resulting benzene, the deuterium purity was 99.7%.

Method

From the 1 : 1 molar salt mixtures a sample containing 10 millimoles of the two salts each was weighed into a quartz flask, which was connected to an evacuation system. After evacuation (1 torr) the flask was put into a metal bath thermostat which maintained the temperature given in Table I, within ± 1°C accuracy. Evacuation was continued for one more minute after thermostating, then the suction cock was closed and the benzene formed in the reaction was frozen with liquid air.

The samples of benzene were analyzed on an Ms-902 mass spectrometer. The accuracy of these determinations was ± 1%. After decomposition, a known amount of potassium benzoate 7-^{14}C was added to the aqueous solution of the salt mixtures, followed by acidification with HCl. The aromatic carboxylic acid which separated was filtered off, dried, and benzoic acid was extracted with chlorform. The chloroform solution was dried over $MgSO_4$, filtered, and concentrated. The residual benzoic acid was recrystallized from petroleum ether, and sublimed in vacuum. The radioacitivity of the benzoic acid thus prepared was determined in toluene solution, with a Packard Tri-Carb liquid scintillation spectrometer. From the radioactivity values the amount of potassium benzoate left was calculated according to the isotope dilution method. Under the experimental conditions shown in Table I, the conversion of perdeuterated potassium benzoate was less than 3% in every case.

REFERENCES

[1] Raecke, B.: Angew. Chem., **70,** 1 (1958)
[2] Kraus, M., Kochloefl, K., Setinek, K., Beránek, L., Sorm, F.: Chem. Ind., **1961,** 1060
[3] Ogata, Y., Nakajima, K.: Tetrahedron, **21,** 2393 (1965)
[4] Ratusky, J., Sorm, F.: Chem. Ind., **1966,** 1798
[5] Ratusky, J.: Coll. Czechoslov. Chem. Commun., **33,** 2356 (1968)
[6] Ratusky, J., Sorm, F.: Coll. Czechoslov. Chem. Commun., **24,** 2533 (1959)
[7] Riedel, O., Kienitz, H.: Angew. Chem., **72,** 738 (1960)
[8] McNelis, E.: J. Org. Chem., **30,** 1209 (1965)
[9] Furuyama, S.: Bull. Chem. Soc. Japan, **40,** 1212 (1967)
[10] Ratusky, J.: J. Lab. Comp., **6,** 124 (1970)
[11] Szammer, J., Noszkó, L.: Chem. Ind., **1970,** 1540
[12] Szammer, J. *et al.:* Unpublished results
[13] Szammer, J.: Acta Chim. (Budapest), **85,** 97 (1975)
[14] Szammer, J., Noszkó, L.: J. Thermal. Anal., **3,** 149 (1971)
[15] Erlenmeyer, H., Lobeck, H., Eppecht, A.: Helv. Chim. Acta, **19,** 793 (1936)

János Szammer
László Noszkó
H-1525 Budapest Pf. 17.

Acta Chimica Academiae Scientiarum Hungaricae, Tomus 90 (4), pp. 419—424 (1976)

A NOVEL ALDEHYDE SYNTHESIS BASED ON THE REDUCTION OF *s*-TRIAZOLO[2,3-*c*]QUINAZOLIN-4-IUM DERIVATIVES

G. DOLESCHALL

(Research Group for Alkaloid Chemistry of the Hungarian Academy of Sciences, Budapest)

Received November 12, 1975

A method has been developed which permits the transformation of carboxylic into carbaldehyde groups in the presence of ester groups.

Owing to their exceptional and manifold reactivity, aldehydes occupy a central position in organic synthesis. The development of simple and, possibly, selective methods for the introduction of the aldehyde function is therefore highly desirable. Methods for the synthesis of aldehydes based on the reduction of suitable heterocyclic compounds have been recently described in a series of papers by MEYERS *et al.* (see, *e. g.* [1, 2]). By replacing the dihydro-1,3-oxazine, 2-oxazoline rings, etc. of the starting compounds in the MEYERS syntheses by the *s*-traizolo-[2,3-*c*]quinazolin-4-ium ring, a novel and useful variant of this procedure has now been developed which has several advantages over the original method.

The starting point of our studies was the observation that $NaBH_4$ reduction of the oxo-*as*-triazinoquinazolium salt **1**, obtained in a three-step process starting with benzoyl chloride and the *as*-triazinone **2**, and careful alkaline hydrolysis of the resulting product furnishes benzaldehyde [3]. In order to develop this reaction into a useful method for the conversion of the carboxyl group (or its modified forms) into the aldehyde group, the reagent **2** and the intermediate **1** had to be replaced by simpler ones.

The *s*-triazolinethione **3** and the *s*-triazol **4** [4] were first tested as starting substances for the preparation of quaternary heterocyclic compounds related to **1**. Treatment of the thione **3** with triethyl orthoformate, Ac_2O/HCl and benzoyl chloride, followed by ring closure with Ac_2O/HCl, and benzoyl chloride, followed by ring closure with Ac_2O/HCl furnished the *s*-triazoloquinazoliniumthiolates **5a-c**; methylation of the latter with methyl iodide gave the *S*-methyl derivatives **6a-c**. Alternatively, compounds **6b** and **6c** were obtained by successive treatment of the *amino-N*-acetyl and *amino-N*-benzoyl derivatives of **4** with Ac_2O/HCl and aqueous KI. The best method for the preparation of the type **6** compounds, however, was successive treatment of compound **4** with the appropriate carboxylic acid in the presence of $POCl_3$ and pyridine, and with aqueous alkali iodide.

Compound **6b** was reconverted by acid hydrolysis into compound **4**, while alkaline treatment furnished the quinazolinone **7**. In the presence of aqueous methanolic NaOH an *O*-methyl derivative (**8** or **9**) of **7** was formed which, when treated with KI/AcOH, was reconverted into **6b**.

$NaBH_4$ reduction of compounds **6b-e** furnished the type **10** tetrahydro-*s*-triazoloquinazolines* whose isolation proved difficult and which, therefore, were in general immediately hydrolyzed to the corresponding aldehydes; the latter were isolated as their condensation products **12** [3, 5] formed with the triazinone **2**. The only type **10** compound which has been isolated (**10b**) is shown by its NMR spectrum to exist as a mixture of two diastereomeric racemic pairs.*

The efficiency of the new method may be rated on the basis of the overall yields (64% and 53%, respectively) of the conversions of methyl hydrogen succinate and methyl hydrogen terephthalate *via* **6** and **10** into methyl succinaldehydate and terephthalaldehydate, respectively, isolated in the form of their type **12** condensation product. These two examples serve also to demonstrate the selectivity of the new method which permits to reduce carboxylic into carbaldehyde groups in the presence of ester groups.

The disadvantage of our method is the rather difficult accessibility of the required reagents (**3** or **4**). Presently, attempts are made to replace the latter by more readily accessible ones.

Experimental

1-Phenyl-s-triazolo [2,3-c] quinazolin-4-ium-2-thiolates (5)

(a) A mixture of the thione **3** [4] (2.0 g; 7.45 mmoles), triethyl orthoformate (10 ml) and AcOH (2 ml) was refluxed for 10 min. A clear solution resulted temporarily, but the product soon started to precipitate from the hot solution. The mixture was allowed to cool to yield 1.9 g (92%) of **5a**, m. p. 331—333°C (DMF).

$C_{15}H_{10}N_4S$ (278.33). Calcd. C 64.73; H 3.62; N 20.13; S 11.52. Found C 65.00; H 3.71; N 20.51; S 11.55%.

(b) Dry HCl was introduced for 10 min. into a boiling mixture of the thione **3** [4] (30 g; 0.112 mole) and Ac_2O (100 ml). The mixture was allowed to cool. Anhydrous ether (300 ml) was added to precipitate 26 g (79%) of **5b** (which was triturated with 5% aqueous $NaHCO_3$ to remove traces of HCl), m. p. 348—349 °C (d.).

$C_{16}H_{12}N_4S$ (292.36). Calcd. S 10.96. Found S 10.57%.

(c) A mixture of the thione **3** [4] (2.0 g; 7.45 mmoles), PhCOCl (0.93 ml; 8 mmoles) and dry dioxane (15 ml) was refluxed for 30 min. 5% aqueous $NaHCO_3$ (50 ml) was then added to the clear yellow solution to precipitate an oil which gradually solidified. 2.7 g (98%) of *amino-N*-benzoyl-**3**, m. p. 254—255 °C (nitromethane), was obtained.

$C_{21}H_{16}N_4OS$ (372.44). Calcd. C 67.72; H. 4.33; S 8.61. Found C 68.01; H 4.17; S 8.70%.

IR (KBr): 1680 cm^{-1}.

Dry HCl gas was introduced for 10 min. into a boiling mixture of the crude benzoyl derivative (2.7 g; 7.25 mmoles) in Ac_2O (10 ml). The mixture remained heterogeneous throughout. It was allowed to cool, and ether (30 ml) was added. The crystalline product was triturated with 5% aqueous $NaHCO_3$ to yield 2.1 g (82%) of **5c**, m. p. 284—285 °C (DMF–ether).

$C_{21}H_{14}N_4S$ (354.42). Calcd. N 15.81; S 9.05. Found N 15.92; S 8.88%.

* The isomeric Schiff base structures **11** cannot be ruled out for these compounds.

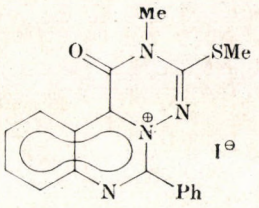

1

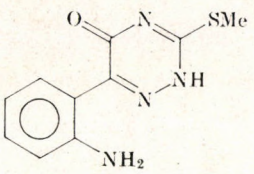

2

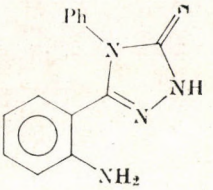

3

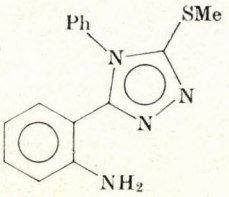

4

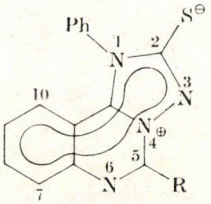

5 (a—c)

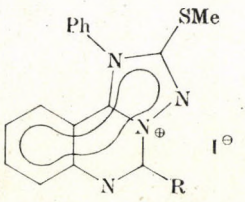

6 (a—f)

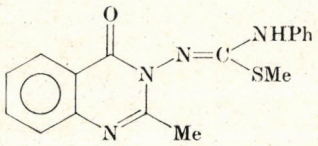

7*

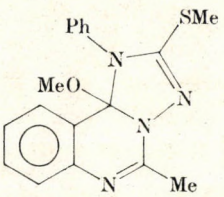

8

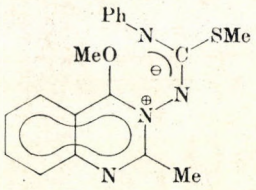

9

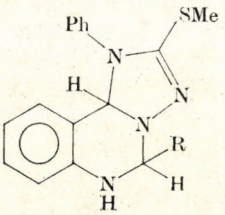

10 (b)

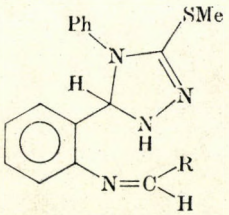

11

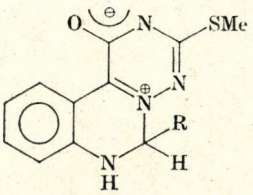

12 (b—e)

*Tautomeric structure unknown

5, 6, 10—12

	R
a	H—
b	Me—
c	Ph—
d	Ph—CH_2—
e	MeOOC—C_2H_4—
f	*p*-MeOOC—C_6H_4—

2-Methylthio-1-phenyl-s-triazolo [2,3-c] quinazolin-4-ium iodides (6)

(a) A mixture of **5a** (0.6 g; 2.15 mmoles), dry DMF (6 ml) and MeI (2 ml) was allowed to stand overnight (the mixture remained heterogeneous throughout) to yield 0.7 g (77%) of **6a**, m. p. 315—318°C (anhydrous EtOH).

$C_{16}H_{13}IN_4S$ (420.28). Calcd. I 30.20; S 7.65. Found I 30.24; S 7.85%.

(b) Methylation of **5b** (26 g; 89 mmoles) and of **5c** (1.5 g; 4.2 mmoles) were carried out similarly and furnished 36 g (93%) of **6b** and 1.9 g (90%) of **6c**, respectively, identical according to m. p.'s, mixed m. p.'s and IR spectra with the samples obtained according to *(d)* and *(f)*, respectively.

(c) Compound **4** [4] (2.0 g; 7.1 mmoles) was boiled up with Ac_2O (10 ml) to yield a clear yellow solution which, on cooling, deposited 1.7 g (74%) of the *amino-N*-acetyl derivative of **4**, m. p. 219—220 °C (EtOH).

$C_{17}H_{16}N_4OS$ (324.40). Calcd. C 62.94; H 4.97; N 17.27; S 9.88. Found C 62.57; H 4.94; N 17.11; S 9.84%.

IR (KBr): 1700 cm^{-1}.

NMR ($CDCl_3$): δ 11.0, bs, 1H, NH; 8.6, dd, $J \approx 8$ and 1.5 Hz, 1 H, 7-H; 7.7—6.75, m, 8 H, other ArH's; 2.8 and 2.3, both s, 3 H, each, *S*-Me and Ac.

(d) Dry HCl gas was introduced for 10 min. into a boiling mixture of compound **4** (6.0 g; 21.3 mmoles) and Ac_2O (40 ml). The mixture was allowed to cool and ether (100 ml) was added to yield the crystalline chloride **6b** (with $Cl^{\ominus}$ replacing $I^{\ominus}$). The latter was dissolved in water (20 ml), and 20% aqueous KI (40 ml) was added to precipitate 8.5 g (92%) of **6b**, m. p. 347—349 °C (anhydrous MeOH).

$C_{17}H_{15}IN_4S$ (434.31). Calcd. I 29.22; N 12.90; S 7.38%. Found I 29.57; N 13.05; S 7.40%.

IR (KBr): 1635, 1560, 1535 cm^{-1}.

(e) Treatment of the aqueous solution of the above chloride with 20% aqueous $NaBF_4$ furnished 90% of the tetrafluoroborate, m. p.318—320 °C (d.; after conversion into needles above 220 °C). The IR spectrum of this product was — apart from the intense $BF_4^{\ominus}$ band — identical with that of **6b**.

(f) A mixture of compound **4** [4] (10 g; 35.4 mmoles), PhCOCl (4.2 ml; 45 mmoles) and anhydrous dioxane (80 ml) was refluxed for 30 min. After cooling, 5% aqueous $NaHCO_3$ (200 ml) was added to precipitate an oily product which gradually solidified (13.5 g). Recrystallization from EtOH (100 ml) furnished 8.9 g (65%) of the *amino-N*-benzoyl derivative of **4**, m. p. 172 °C.

$C_{22}H_{18}N_4OS$ (386.46). Calcd. C 68.37; H 4.69; S 8.30. Found C 68.40; H 4.69; S 8.28%.

IR (KBr): 1670 cm^{-1}.

NMR ($CDCl_3$): δ 11.9, bs, 1 H, NH; 8.85, dd, $J \approx 8$ and 1.5 Hz, 1 H, 7-H; 8.3—8.15, m, 2 H, PhCO, *o*-H's; 7.7—6.75, m, 11 H, other ArH's; 2.75, s, 3 H, *S*—Me.

Dry HCl gas was introduced for 10 min. into the refluxing mixture of the above product and Ac_2O (30 ml). After cooling, ether (250 ml) was added to the resulting solution to precipitate an oily product which gradually solidified. The latter was dissolved in MeOH (60 ml), and 20% aqueous KI (60 ml) was added to precipitate 10.75 g (94%) of **6c**, m. p. 296—297 °C (d.; DMF).

$C_{22}H_{17}IN_4S$ (496.38). Calcd. C 53.23; H 3.45; I 26.32; S 6.46. Found C 53.62; H 3.42; I 26.32; S 6.90%.

IR (KBr): 1620, 1560, 1530 cm^{-1}.

(g) $POCl_3$ (5.6 ml; 60 mmoles) was added, with stirring, to a mixture of **4** [4] (10 g; 35.4 mmoles), phenylacetic acid (4.8 g; 35.4 mmoles) and anhydrous pyridine (30 ml) by drops at such a rate that the mixture came to boiling. The excess $POCl_3$ was decomposed with anhydrous MeOH (30 ml), and an aqueous (40 ml) solution of NaI (25 g) was added to the warm solution. The mixture was chilled at 0 °C to yield 10.7 g (60%) of **6d**, m. p. 318—320 °C (d.; EtOH).

$C_{23}H_{15}IN_4S$ (510.40). Calcd. C 54.12; H 3.75; I 24.87; N 10.98. Found C 54.93; H 3.59; I 24.96; N 10.75%.

IR (KBr): 1630, 1560 (w), 1530 cm^{-1}.

(h) **6e** (16.5 g; 92%), m. p. 282—284 °C (d.; MeOH) was obtained similarly by reacting **4** (10 g; 35.4 mmoles) and methyl hydrogen succinate (4.8 g; 36 mmoles) with $POCl_3$ (4.8 ml; 50 mmoles) in anhydrous pyridine (30 ml).

$C_{20}H_{19}IN_4O_2S$ (506.37) Calcd. C 47.44; H 3.78; I 25.07; N 11.06; S 6.33. Found C 47.98; H 4.25; I 25.16; N 11.30; S 7.09%.

IR (KBr): 1735, 1635, 1565, 1535 cm^{-1}.

(i) **6f** (19 g; 97%), m. p. 190 °C (d.; MeOH) was obtained similarly by reacting **4** (10

g; 35.4 mmoles) and methyl hydrogen terephthalate (6.5 g; 36 mmoles) with $POCl_3$ (4.8 ml; 50 mmoles) in anhydrous pyridine (40 ml).

$C_{24}H_{19}IN_4O_2S$ (554.41). Calcd. I 22.89; N 10.11; S 5.78. Found I 23.21; N 10.25; S 6.37%.

IR (KBr): 1720, 1620, 1560, 1530, 1280, 1110 cm^{-1}.

Hydrolysis of 6b

(a) A mixture of **6b** (2.0 g; 4.6 mmoles) and 20% aqueous HCl (20 ml) was refluxed for 5 hrs and evaporated to dryness in vacuum. The residue was dissolved in a mixture of 5% aqueous $NaHCO_3$ (40 ml) and DMF (20 ml) to yield, on cooling, 1.15 g (88%) of compound **4**, identical according to m. p. (142—143°C, i-PrOH), mixed m. p. and IR spectra with an authentic sample [4].

(b) 4 *N* NaOH (8 ml) was added at 0 °C, with stirring, to a mixture of **6b** (5.0 g; 11.1 mmoles) and dioxane (25 ml). Stirring was continued at room temperature until a clear solution resulted. Water (75 ml) was added to precipitate 2.6 g (72%) of the quinazoline compound **7**, identical according to m. p. (207 °C; EtOH), mixed m. p. and IR spectra with an authentic sample, prepared as described below.

The same product was obtained when compound **6b** was refluxed with 5% aqueous $NaHCO_3$.

Methanolysis of compound 6b

4 N aqueous NaOH (3 ml) was added at 0 °C, with stirring, to a mixture of **6b** (5.0 g; 11.1 mmoles) and MeOH (25 ml). Stirring was continued at room temperature until a clear solution resulted. Water (75 ml) was added to precipitate a partly crystalline gummy product which was taken up in two 50-ml portions of ether. The combined ethereal solutions were washed with water and dried over $MgSO_4$. Evaporation of the solvent in vacuum furnished 2.5 g (66%) of compound **8** (or **9**), m. p. 137 °C (benzene–pentane).

$C_{18}H_{18}N_4OS$ (338.42). Calcd. C 63.88; H 5.36; N 16. 56; S 9.47. Found C 63.30; H 4.79; N 16.48; S 9.83%.

NMR ($CDCl_3$): δ 3.6, 2.75 and 1.6, all s, 3 H, each, OMe, SMe, $\geqslant$C—Me, 7.5—6.65, m, 11 H, ArH's.

The above product (0.3 g; 0.9 mmole) was dissolved in a mixture of MeOH and 20% aqueous KI (3 ml, each), and the mixture was acidified with AcOH. Water (10 ml) was added to give 0.35 g (91%) of **6b**, identical according to m. p. (346—348 °C, d.), mixed m. p. and IR spectra with an authentic sample.

3-(1-Anilino-1-methylthiomethyleneamino)-2-methyl-4(3H)-quinazolihone (7).

A mixture of 3-amino-2-methyl-4(3 *H*)-quinazolinone [6] (5.0 g; 33 mmoles), PhNCS (4.8 ml; 40 mmoles) and anhydrous EtOH (30 ml) was refluxed for 1 hr to yield 5.0 g (49%) of 2-methyl-3-(3-phenylthioureido)-4(3 *H*)-quinazolinone, m. p. 201—202 °C (EtOH).

$C_{16}H_{14}N_4OS$ (310.37). Calcd. S 10.33. Found S 10.52%.

A solution of the above product (1.0 g; 3.2 mmoles) in DMF (5 ml) was treated with MeI (0.31 ml; 5 mmoles) and 5% aqueous $NaHCO_3$ (5 ml); the resulting product was recrystallized from EtOH (90 ml) to yield 0.7 g (69%) of compound **7**, m. p. 207°C.

$C_{17}H_{16}N_4OS$ (324.40). Calcd. C 62.94; H 4.97; N 17.27; S 9.98. Found C 63.28; H 5.25; N 17.36; S 9.92%.

IR (KBr): 3200, 1655, 1600, 1550 cm^{-1}.

$NaBH_4$ reductions of the s-triazoloquinazolinium iodides 6

(a) An aqueous (20 ml) solution of $NaBH_4$ (1.6 g; 42 mmoles) was made alkaline by the addition of a few drops of 10% aqueous NaOH, then it was added by drops, with stirring and ice-salt cooling, to a mixture of **6b** (15 g; 33.3 mmoles) and MeOH (50 ml) at such a rate that the temperature did not exceed 3—5 °C*. 8.75 g (85%) of **10b** was obtained, colourless needles, m. p. 145—146 °C (nitromethane).

$C_{17}H_{18}N_4S$ (310.41) Calcd. N 18.05; S 10.33. Found N 17.92; S 10.41%.

* At 20 °C, overreduction, *i. e* saturation of the exocyclic N = C bond of **11b** took place.

NMR ($CDCl_3$): δ 7.5—6.5, m, 9 H, ArH's; 4.4—3.8, m, 3 H, 5-H + 6-H + 10 bH; 2.43, weak s, + 2.38, s, total intensity 3 H, S—Me; 1.34, d, $J = 7.2$ Hz + 1.18, weak d, $J = 6$ Hz, 5-Me (two diastereomeric racemic pairs?).

(b) A mixture of crude **10b** (5.0 g; 16.1 mmoles), water (50 ml) and conc. H_2SO_4 (10 ml) was subjected to steam distillation. The recipient, into which a solution of the triazinone **2** (3.76 g; 16.1 mmoles) in a mixture of MeOH (40 ml) and AcOH (5 ml) had been placed, was cooled in ice-water. 2.43 g (58%) of the *as*-triazinoquinazoliumolate **12b** was obtained which, according to m. p. (244—246°C, DMF), mixed m. p. and IR spectra proved identical with an authentic sample [3,5].

(c) An aqueous (10 ml) solution of $NaBH_4$ (0.67 g; 18 mmoles) was made slightly alkaline with 10% aqueous NaOH and added by drops, with stirring and ice-salt cooling, to a mixture of **6c** (7.0 g; 14 mmoles), DMF and MeOH (20 ml, each) at such a rate that the temperature did never exceed 3—5 °C. Water (100 ml) and conc. HCl (10 ml) were added. The mixture was boiled up, allowed to cool and extracted with three 50-ml portions of ether. The combined ethereal solutions were washed with 5% HCl, water, 5% aqueous $NaHCO_3$ and water, and dried over $MgSO_4$. Fractional distillation furnished 1.2 g (80%) of PhCHO, b. p. 70—72° C (20 torr), identified as its condensation product **12c** [3,5] formed with the triazinone **2**.

(d) Compound **6d** (5.0 g; 9.8 mmoles) was reduced with $NaBH_4$ (0.46 g; 12.5 mmoles), essentially as described under *(c)*. AcOH (10 ml) and **2** (2.3 g; 9.8 mmoles) were added. The mixture was stirred for 30 min. and heated to the b. p. Water (50 ml) was added to the hot solution from which 1.7 g (52%) of **12d**, m. p. 226—227°C (DMF), separated on cooling.

$C_{18}H_{16}N_4OS$ (336.41). Calcd. N 16.66; S 9.53. Found N 16.48; S 9.80%.

(e) Compound **6e** (16.5 g; 32.7 mmoles), suspended in MeOH (70 ml), was reduced with $NaBH_4$ (1.3 g; 35 mmoles) as described under *(c)*. AcOH (15 ml) and **2** (7.0 g; 30 mmoles) were added, and the mixture was stirred for 30 min. to yield 7.6 g (70%) of **12e**, m. p. 241 °C (DMF).

$C_{15}H_{16}N_4O_3S$ (332.38). Calcd. C 54.20; H 4.85; N 16.86; S 9.65. Found C 54. 26; H 5.33; N 16.48; S 9.95%.

(f) Compound **6f** (4.0 g; 7.2 mmoles) was similarly reduced. The resulting mixture was acidified with AcOH. Water was added to precipitate a yellow product (2.7 g). This was refluxed for 5 min. in a mixture of AcOH (10 ml) and water (20 ml).

Water (40 ml) was added, and the resulting methyl terephthalaldehydate was extracted with three 20-ml portions of ether. The solvent was evaporated and the residue treated with compound **2** (1.2 g; 5 mmoles) in hot MeOH (15 ml) to yield 1.5 g (55%) of **12f**, m. p. 255—256 °C (DMF)

$C_{19}H_{16}NO_3S_4$ (380.42). Calcd. N 14.73; S 8.43. Found N 14.55; S 8.27%.

REFERENCES

[1] MEYERS, A. I., NAZARENKO, N.: J. Am. Chem. Soc. **94,** 3243 (1972)
[2] MEYERS, A. I., NABEYA, A., ADICKES, H. W., POLITZER, I. R., MALONE, G. R. KOVELEVSKY, A. C., NOLEN, R. L., PORTNOY, R. C.: J. Org. Chem. **38,** 36 (1973)
[3] MEYERS, A. I., DURANDETTA, J. C.: J. Org. **40,** 2021 (1975)
[4] DOLESCHALL, G., LEMPERT, K.: Unpublished results
[5] VERESHCHAGINA, N. N., POSTOVSKII, I. Ya, MERTSALOV, S. L.: Zh. Organ. Khim. **1,** 1154 (1965); Chem. Abstr. **63,** 13 256 g (1965)
[6] DOLESCHALL, G., LEMPERT, K.: Tetrahedron **29,** 639 (1973)
[7] DOLESCHALL, G., LEMPERT, K.: Acta Chim. (Budapest) **77,** 345 (1973)
[8] LEONARD, N. J., RUYLE, W. V.: J. Org. Chem. **13,** 903 (1948)

Gábor DOLESCHALL H-1521 Budapest, Gellért tér 4.

RECENSIONES

Methodicum Chimicum. Band 5. C—O-Verbindungen

Herausgegeben von J. Falbe, Georg Thieme Verlag, Stuttgart, 1975

Academic Press New York, San Francisco, London

Methodicum Chimicum gibt eine kritische Übersicht bewährter Arbeitsmethoden und ihrer Anwendung in Chemie, Naturwissenschaften und Medizin.

Band 5 des Methodicum Chimicum beschreibt bewährte und aussichtsreich erscheinende Methoden zur Herstellung von Kohlenstoff—Sauerstoff-Verbindungen. Altbewährte Synthesen sind nur kurz umrissen, während moderneren Verfahren breiter Raum gewidmet wird. Dieses Werk berücksichtigt nicht nur wissenschaftliche Aspekte, sondern bietet auch den in der Industrie tätigen Chemikern wertvolle Ideen. Viele der beschriebenen Verfahren besitzen erhebliche wirtschaftliche Bedeutung und haben in großem Umfang industrielle Anwendung gefunden. Methoden, denen sich in absehbarer Zeit Möglichkeiten für eine technische Realisierung eröffnen, werden besonders ausführlich behandelt.

Band 5 des Methodicum Chimicum wurde wegen der Fülle des zu bewältigenden Stoffes von insgesamt 40 Autoren bearbeitet. Dieses Handbuch gibt keine Rezepte für die Herstellung der einzelnen Verbindungen. Die vorhandenen Methoden sind im allgemeinen beschrieben und gegeneinander kritisch abgewogen. Die ausführlichen Inhaltsverzeichnisse, zahlreiche Formelbilder, die Übersichtstabellen und der klare Aufbau der einzelnen Kapitel erleichtern die Suche nach den gewünschten Informationen.

Die Originalliteratur wurde bis 1972 berücksichtigt (über achttausend Literaturangaben), in Einzelfällen bis 1974. Zur detaillierten und ausführlichen Information werden auch ausgewählte Übersichtsartikel zitiert.

Die ersten zwei Kapitel sind der Herstellung von Alkoholen und Phenolen gewidmet. Die Äther und Epoxide schließen sich an. Die Synthesen der Aldehyde sind im nächsten Kapitel beschrieben. Wegen ihrer Verwandschaft zu den Aldehyden werden anschließend die Ketone behandelt. Die Ketene beschreibt Kapitel 6 ausführlich. Kapitel 7 ist den Acetalen gewidmet. Die Synthesen der Carbonsäuren, Carbonsäureanhydride und Carbonsäureester sind in den folgenden drei Kapiteln beschrieben. Die Lactone werden in Kapitel 11 recht ausführlich behandelt. Die letzten zwei Kapitel umfassen die Oxyde des Kohlenstoffes sowie Kohlensäureester und die Perverbindungen.

Band 5 des Methodicum Chimicum ist ein ausgezeichnetes und modernes Nachschlagewerk, wertvoll für den in der theoretischen und industriellen Forschung tätigen Chemiker.

B. BORDÁS

J. D. DUNITZ, P. HEMMEYICH, R. H. HOLM, J. A. IBERS, C. K. JÖRGENSEN, J. NEILANDS, D. REINEN and R. J. P. SILLIAMS (editors): *Structure and Bonding, Volume* **23** — *Biochemistry*

Springer-Verlag Berlin, Heidelberg, New York, 1975. 193 pages; Index to Vol. 1—23

The series "Structure and Bonding" issued at irregular intervals, is a collection of highest-level review articles on diverse aspects of the central theme pointed out by the title. Some of the papers published in former volumes were written by authors doing substantial research work on the very frontier of modern structural-theoretical chemistry.

The present 23rd volume, published in 1975, has the subtitle „Biochemistry". Judged by the index containing all papers of the 23 volumes published, truely biochemical questions were dealt with in roughly half of the studies. Of the four papers making up the present volume, two (J. A. FEE's study on Copper Proteins and M. F. DUNN's paper on Zinc Ion Catalysis) deal with really biochemical topics. The two others (SCHNEIDER's paper on Metalloporphyrin Formation and M. ORCHIN and D. M. BOLLINGER's work on Hydrogen-Deuterium Exchange in Aromatic Compounds) are less directly related to biological macromolecules.

Both metallo-enzyme topics are dealt with consciously from the point of view of molecular mechanisms only, the physiological aspects being neglected. Both are excellent synthetising surveys made with all the rigours of modern structural and physical chemistry. The two other studies of the volume are written similarly with the high level of concentration and depth of treatment, well in line with the high standards of the editing house. The quality of printing and illustrations is also of the traditional Springer level.

E. BIRÓ

Nicholas B. PETERSON: *Edible Starches and Starch-derived Syrups*,

Noyes Data Corporation, Park Ridge, New Jersey, U. S. A., London, England, 1975 (427 pages, 27 figures, list of inventors and U. S. A. Patents)

Endeavours towards enlarging the choice of food-products, as well as the diverse possibilities of utilization of starch and the great development in the production of starch derivatives have resulted in a very marked increase in the use of starch and its derivatives in the food industry. PETERSON gives a comprehensive survey of this field in this book, published as the 24th volume of the series Food Technology Review. Actually the subject-matter of the present book is the review of U. S. Patents granted since 1968 concerning edible starch and its derivatives. More than two hundred processes are surveyed which are grouped according to the types of products.

The first two chapters following the Introduction are devoted to the production of starch and to the procedures suitable for the removal of foreign substances from crude starch. Besides the patents providing improvement of the conventional techniques, the author also reviews the possibilities of direct utilization of starch in the food industry. In the third chapter the advancement achieved in the technique of production of gelatinised starches and related starch products is described. Fields of utilization like in puffed products and easily digested nutriments, etc., are also discussed.

The most important derivatives, starch esters and ethers are treated in the next two chapters. Although the use of starch esters and ethers in the food industry is rather restricted by the respective food acts, the ample material presented in these chapters is very interesting. It clearly illustrates how different substituents provide possibilities for changing the physical and chemical properties of starch in a way favourable for the consumers. The sixth and seventh chapters deal with the new procedures available for the preperation of components of starch (amylose and amylopectin) and of its decomposition products. The author emphasizes the increasing use of enzyme preparations and the prospects of further development provided by them.

The last four chapters of the book are concerned with the production of starch syrup, starch sugar, maltose and other oligosaccharides, as well as fructose from starch hydrolysates. The abundance of patents in this field clearly reflects that the increase in sugar prices opened up new possibilities for the utilization of starch hydrolysates.

The book written by PETERSEN gives valuable information primarily for experts in the given field, for production engineers and those working on the development of new products, by surveying the literature on patents which are often hardly accessible and less studied. At the same time, it may also be useful for those working on food research and in education; the volume may be of assistance in choosing the directions of further research projects, too.

R. LÁSZTITY

Delbert J. EATOUGH, James J. CHRISTENSEN and Reed M. IZATT: *Experiments in Thermometric Titrimetry and Titration Calorimetry*

Brigham Young University Press, Provo, Utah, USA

In the middle of the fifties, the technique of measuring temperature reached such an advanced state that analytical methods based on enthalpy changes became comparable with other instrumental techniques in respect of simplicity and speed; thus they have gained growing application in analytical laboratories. This situation is reflected by the increasing number of papers and monographs dealing with these methods. Another supplement to the several monographs published since the sixties is the present book. It was edited first in 1973 and the revised edition was published in 1974.

In the monograph the authors give a concise survey of the theory of thermometric titration.

Within the subject, particular attention has been paid to the exact determination of the end-point of the titration and to the possibilities of increasing the sharpness of end-point detection. Along with the theoretical considerations, practical problems have also been treated, such as measuring techniques and the evaluation of the results.

A separate chapter is devoted to the calibration of the apparatus. This is of decisive importance particularly when thermometric titrations are used for the determination of reaction heats, heats of complex formation and other molar enthalpy changes. Several practical examples are presented in order to demonstrate the analytical applications of thermometric titration, like the titration of sodium hydroxide, carbonate or acetate solutions with hydrochloric acid; of boric acid or hydrochloric acid solutions by means of sodium hydroxide; and of cerium(IV) ions by iron (II) standard solutions.

Other possibilities of the widespread practical applications of thermometric titration are illustrated on several further examples. Using pyridine as the model compound, the Δ H values and log K values of its reactions with hydrochloric acid and acetic acid are determined from calorimetric data.

Another example presented to point out the applicability of the technique in reaction kinetic studies is the determination of the rate of hydrolysis of ethyl acetate in alkaline medium.

When mercury(II) perchlorate solution is titrated with sodium chloride solution, the formation of $HgCl_2$ can clearly be distinguished from the formation of the complex taking place under the effect of excess reagent involving incorporation of chloride ions as ligands into the molecule. The two processes can be separated by the appearance of a break on the enthalpofram at the end-point of the thermometric titration.

Finally, some examples are given for titrations in non-aqueous media, such as the titration of phenol with pyridine in cyclohexane, yielding the ΔH and log K values for the reaction between a donor and an acceptor. In another case, dilution of a phenol solution in carbon tetrachloride is utilized for the determination of the log K value belonging to the dissociation constant and the ΔH value, that is, the change in enthalpy due to dissociation.

The carefully selected examples give a comprehensive picture of the present possibilities of practical applications of thermometric titration. Detailed description of the experimental technique and of the method of calculating the results affords great help to the users of the book in solving related problems in this field.

I. SAJÓ

Irradiation in Chemical Processes. Recent Developments.

(Ed.: M. W. RANNEY). Noyes Data Corporation, Park Ridge, New Jersey, London, England 1975.

This is the 50th volume in the recent Chemical Technology Review series. Like the earlier members of the series, this volume contains extracts of practical use to the chemist from American patents related to the topic indicated in the title. 207 patents are cited, covering the period from 1970 to the end of 1974. From a practical aspect, the patented material can be classified into the following main groups:

(a) organic synthetic photochemistry;
(b) photochemistry of polymers, including adhesives, printing inks and polymer mixtures employed for various purposes;
(c) photochemistry of polyolefins, a separate chapter dealing with the special applications of photo- and radiochemistry.

The material within these individual groups is extremely ramified. Besides special synthetic and polymerization methods, one can find accounts of photochemical reactors with various purposes, sensitizers and photostabilizers, together with the utilization of special photochemical methods in tyre manufacture; similarly, although this is mentioned only as an interesting feature, an account is also given of a patented preparation of tube systems used in space ships to repair damage by means of ultraviolet radiation, without human intervention.

In addition to the extremely useful practical information, the volume provides an excellent illustration of the fact that the practical application of photo- and radiochemical reactions is becoming increasingly more widespread and is now established in the most varied fields of chemistry, including some where this would not have been thought feasible even 1—2 years ago. The explanation of this is to be found in the introduction to the volume, where it is stated that the spreading of photo- and radiochemical methods increases in parallel with the decrease of the costs of producing the radiation energy. In the view of the author, the cost of producing 1 megarad/pound in the U. S. A. is 1 cent or less. If one takes into account the special syntheses (the selective preparation of optically active compounds, photoresolution, polymerization reactions without initiators, *i. e.* without the addition of foreign substances, or the variation of the properties of various polymers by grafting, to mention only a few examples), it is readily understandable that photochemistry is one of the preparative chemical methods of the future.

B. LOSONCZI

M. G. HALPERN: *Paper Manufacture*

Chemical Technology Review No. 47. Noyes Data Corp., New Jersey, London, 1975, 379 + 8 pages.

The book reviews 176 patents issued in the USA since 1970 in connection with the paper industry, providing detailed technical information covering the entire technology of paper manufacture at the same time. It naturally assumes a knowledge of the classical procedures, and discusses the innovations based on these.

Patents are generally reported in the literature only as abstracts, and since the book goes into the details of the individual patents it is unique in its kind. The author does not deal with a review of the patents, and does not discuss whether the patents have proved fruitful. The aim of the compilation was to stimulate further research and development work with the new conceptions described in the patents.

The book covers the following topics:
Refining and sheet-formation
Sizing
Use of retention aids
Dry-strength-increasing additives
Improvement of wet strength with additives
Improvement of the optical properties of paper
Other modifications of paper
Slime, foam and pitch control

Utilization of the book is facilitated by the fact that the patents are listed according to manufacturing company, inventor and number too. Published in 1975, the book includes patents issued up to the middle of 1974. Its rapid publication was ensured by special printing and binding procedures.

The same publishing company has also issued reviews of patents on other subjects and other branches of industry.

P. LENGYEL

R. Bryan MILLER and LOUIS S. HEGEDÜS (editors): *Annual Reports on Organic Synthesis—1973*

Academic Press, New York 1974. 423 pages

The object of the book, appearing now for the fourth year, has remained the same: to help organic chemists finding their way in a sea of publications, *i. e.* "to keep up with the literature". This task is particularly difficult for synthetic organic chemists, as the information of interest to them is often published scattered in many different journals. Theilheimer, offering the complete solution of this problem, is hardly available to private persons, owing to its high price. "Annual Reports . ." intending to cover this gap is therefore wittily and aptly called by the reviewer in J. Am. Chem. Soc. "the poor man's Theilheimer". In accordance with the established practice, reactions of synthetic value are presented succintly by equation with adjacent reference, and are organized in seven chapters covering broad categories, such as "Carbon-carbon bond forming reactions", "Oxidations", "Reductions", "Synthesis of Heterocycles", "Protecting groups", "Useful synthetic prep rations", plus a six-page list of reviews of synthetic processes. In producing the book, the authors have abstracted 47 primary chemistry journals, selecting useful synthetic advances. They have exercised selectivity in choosing which papers to abstract. Each entry is comprised primarily of structures accompanied by very few comments.

This book can be recommended for personal purchase.

GY. DEÁK

BORIS WEINSTEIN *(editor): Chemistry and Biochemistry of Amino Acids Peptides and Proteins. A Survey of Recent Developments. Vol. 2*

Marcel Dekker, New York, 1974. 380 pages

The first volume of this monograph series was published in 1971. The purpose of the series is to present periodically a collection of review papers surveying recent developments in the closely intertwining and inseparable fields of the chemistry and biochemistry of amino acids, peptides and proteins. Though countless reviews and books have been published in the last 15 years in this domain, the editor deems repeated survey of certain topics important, particularly when connections between the various branches of science can be pointed out. The most significant common characteristic of the papers is the organic chemical concept, which is indispensable for an understanding and interpretation of the molecular mechanism of vital processes.

The first volume was followed by the second with a relatively great delay, in 1974. This was evidently due to difficulties in printing, because the papers published in the volume were received till summer 1972, so that they cover, in general, the scientific literature up to the end of 1970.

The volume consists of five chapters. The first (38 pages), discussing the chemistry and biochemistry of gramicidine S and related compounds on the basis of 117 references, was written by TETSUO KATO and NOBUO IZUMIYA, researchers at the Japanese Kyushu University. After a brief treatment of the biosynthesis and chemical preparation of gramicidine S, they discuss in detail the synthesis and biological action of those derivatives and analogues, which were made primarily for a study of the relationship between structure and action. They report briefly also on the conformational analysis of gramicidine S, and describe the research work, which led to the recognition of the relationship between conformation and biological action.

The second chapter, dealing with the adrenocorticotropic hormone and the synthesis of ACTH-active peptides, is almost three times as long as the first chapter, and contains 282 references. The authors are HARUAKI YAJIMA and HIROKI KAWATANI working in the scientific staff of the Kyoto University. The survey describes the methods of testing ACTH, the isolation and structural analysis of the hormone, its synthesis and that of biologically active fragments; further, as the indubitably most interesting chapter, indispensable today in sum-

maries, the relationship between the chemical structure and the biological action of the hormone is discussed. Experiments aimed at clarifying the mode of action of ACTH, and the difficulties in identifying the ACTH releasing hormone are briefly mentioned. In accordance with his own scientific research for over a decade, YAJIMA treats the chemical synthesis of the fragments in the greatest detail, summarizing them, instead of chronological order, in a novel grouping, according to the method of removal of the protecting groups.

Perhaps the farthest removed from what the reader would expect in a work on the chemistry of amino acids, peptides and proteins, is the third chapter, which reviews the reactions of small-ring (three- and four-membered) heterocyclic compounds with amino acids. Emphasis is actually laid here on the chemical properties of the heterocyclic compounds *(e. g.* epoxides aziridines, β-lactones), so that the paper by K. JANKOWSKI (University of Moncton, New Brunswick, Canada) will be of primary interest to others than peptide- and protein chemists. The summary of sixty pages illustrates the most characteristic reactions by detailed experimental prescriptions in addition to 100 references.

The fourth chapter is concerned with the new coupling method introduced in peptide chemistry by WOODWARD *et al.* in 1961: the use of isoxazolium salts. This process, in the course of which the isoxazolium cation reacts with carboxylate ions to give activated enol esters, was known as early as the beginning of the century, but like in many other cases, only the discovery of a possible practical application made it important, after sixty years. "WOODWARD's reagent", N-ethyl-5-phenylisoxazolium-3'-sulfonate, is today a widely used condensing agent. D. J. WOODMAN (University of Washington, Seattle) gives a summary of 90 pages on the use of this compound and its derivatives in peptide synthesis, describing the reaction mechanism, the by-products to be expected, and the possibilities of racemization.

The last chapter testifies again the varied interests considered when compiling this volume. KAOURU HARADA (Institute for Molecular and Cellular Evolution, University of Miami) discusses the possibilities of amino acid and peptide synthesis under conditions when no organic life could have existed on the Earth ("prebiotic conditions"). In gas mixtures containing the appropriate elements, amino acids are actually formed, besides several other low-molecular organic compounds, when exposed to energy of various kinds (electric discharge, ultraviolet radiation, ionizing radiation, thermal energy, etc.). This reaction has been known since the beginning of the century; however, its complex character could only be elucidated by the modern refined separation techniques. The amino acids formed also undergo polycondensation reactions, mainly when acted upon by thermal energy. Thus the synthesis of polyamino acids and by heating several kinds of amino acids together, also the formation of "proteinoids" could be realized. By the co-polymerization of certain amino acids, even a substance with hormonal effect was successfully prepared. The review deals only with the possibilities of the prebiotic formation of these compounds, and does not touch upon the much debated question whether the origin of life on the Earth can be explained with the aid of such simple physical and chemical reactions.

K. MEDZIHRADSZKY

BORIS WEINSTEIN *(editor): Chemistry and Biochemistry of Amino Acids. Peptides and Proteins. A Survey of Recent Developments. Vol. 3*

Marcel Dekker, New York, 1974. 324 pages

In contrast with the great delay in publishing the second volume, the third followed it very shortly, almost simultaneously.

The first chapter of the volume, entitled "Conformation of Peptides in Solution as Dererermined by NMR Spectroscopy and Other Physical Methods", comprises almost 200 pages, written by V. J. HRUBY (University of Arizona, Tucson). It is an excellent survey of this field, which recently has become very important. Intensive research work has been in progress for a long time to elucidate the relationship between chemical structure (primary structure) and biological action; however, the theory attaching at least the same importance to conformation in the mechanism of action, has suddenly increased the volume of pertinent physical-chemical research. High-molecular weight peptides and proteins have long been known to possess higher levels of structure, but it was only recently shown for peptides of low molecular

weight (2—12 amino acid units) that these compounds in solution do not necessarily consist of a mixture of a large number of conformers, which are easily convertible into each other, but often a single, well characterizable conformation can only be detected. This discovery is important because this conformation presumably corresponds to a reactive structure also in biological environment, furthermore, the energetic conditions of its formation, which are relatively easy to elucidate, can be utilized in the study of the steric structures of much more complex molecules.

The physical methods of determining the conformation are partly spectroscopic techniques, such as nuclear magnetic resonance spectroscopy, optical rotatory dispersion, circular dichroism and infrared spectroscopy. These are often complemented by X-ray diffraction studies and theoretical calculations. Among non-spectroscopic methods, primarily hydrogen exchange studies, thin-film dialysis, dipole moment measurements and partition chromatography are to be mentioned.

In the review the author discusses the conformational analysis of dipeptides, diketopiperazines, higher linear peptides and cyclopeptides, and a separate chapter is devoted to the conformation of biologically active cyclopeptides. The survey, being very lucidly composed and starting from the fundamentals up to a high level, will be readily understood also by the reader not specializing in this field. The volume of the work is characterized by the great number of references (800) which cover the literature on the recent results of conformational analysis up to the middle of 1973.

In the second chapter of the volume, J. P. SCANELL and D. L. PRUESS (Hoffmann — la Roche, Nutley, New Jersey) review naturally occurring antimetabolites with amino acid and peptide character. After some definitions and theoretical considerations, the antimetabolites known so far and belonging to this group are listed lexically, and their occurrence, formula, synthesis, as well as the metabolite which they antagonize are given. The chapter of nearly 50 pages is concluded with 217 references.

The last and shortest chapter deals with the chemistry of an interesting group of enzymes, dioxygenases. These enzymes oxidize a substrate by introducing both atoms of an oxygen molecule. The most characteristic example of this reaction is the oxidative cleavage of an aromatic ring; this reaction is catalyzed by the dioxygenase enzyme of soil microorganisms. The author of the chapter, D. G. BROW (University of Idaho, Moscow, Idaho) gives a survey of all the known dioxygenases, including such important enzymes as those splitting chlorinated hydrocarbons. The chapter is a valuable source of information for those engaged in the development of pesticides and concerned with the aspects of environmental protection, who are thus interested in natural metabolic processes, *i. e.* in the degradation of these very efficient and hazardous substances by the catalytic action of the enzymes of soil microorganisms.

The subject-matter of the series edited by Boris WEINSTEIN has proved sor far varied and highly readable. Further volumes are expected with interest, because the series can be used to good advantage by researchers working in the field of organic chemistry, biochemistry or physical chemistry, as well as by those who wish to solve practical, therapeutic or agricultural problems.

K. MEDZIHRADSZKY

M. J. SATRIANA: *Large-scale Composting*

Noyes Data Corporation, Park Ridge, New Jersey—London, England, 1974, 269 pages

The book has been written on a topic which is cultivated very intensively all over the world, due to its importance in pollution control, economy of soil fertility, as well as soil erosion. Three methods are known for treating city wastes formed in ever increasing amounts (3 million cubic meters per year in Budapest); these are: controlled disposal, composting and incineration. The book is Volume 12 of the series Pollution Technology Review. As listed at the end of the present work, this series contains several other important books on subjects, such as controlled deposition, energy recovery by waste burning, pollution caused by organic chemical industry and pollution analysis.

Theory, technology, application and economy of composting are treated basically from the American point of view. In addition, a detailed description is given on the large Dutch, German, Swiss and French experience and technologies, their costs (both capital investment

and operation) and their marketing possibilities. Several features may be of interest from the Hungarian point of view, too, such as problems of soil erosion and pedological aspects of preventing soil washoff in hillside viticulture.

The operation of American composting plants is described in great detail, covering technological, chemical and microbiological aspects. A very interesting comparison is given between capital investment and operating costs of composting and waste incineration. Applications in agriculture and horticulture are discussed also with emphasis.

A separate chapter has been devoted to the disposal of waste sludge (which is a difficult problem also in Hungary); this describes the process which is, for the time being, the most favourable from both the economical and technical points of view: the combined composting of waste and sludge. The composting of leaves, animal wastes and industrial organic wastes may be combined by this process. Theoretical aspects (C/N ratio, the role of microorganisms, elimination of pathogenic microflora, etc.), as well as practical problems based on the experience of several plants, are discussed in detail.

In can be concluded that the entire book deals with an up-to-date problem, giving an appropriate, critical summary on its subject.

J. HOLLÓ

INDEX

PHYSICAL AND INORGANIC CHEMISTRY

Studies on Some Metal Complexes with Keto-Anils as Ligands, I (Short Communication), R. K. Upadhyay, V. P. Singh 325
Electrochemical Study of Palladium–Copper Catalysts, T. Mallát, J. Petró, É. Polyánszky, T. Máthé 333
Catalytic Deuterium Exchange of Cyclopentane and Cyclohexane, and Dehydrogenation of Cyclohexane on Rh Black, A. Sárkány, L. Guczi, P. Tétényi 345
Force Field Calculations for Malononitrile Molecules, B. Vizi, A. Sebestyén 355
On the Extraction of Nb (V) with Polyphenols (in German), A. I. Busev, S. P. Karjakina, P. Nenning 365
Spectral and Magnetic Studies of Copper (II) Chelates of L-Asparagine and L-Glutamine (Short Communication), R. C. Tewari, M. N. Srivastava 371
Analytical Use of Pt (II) Complexes with Pyrazolone Derivatives (in German), V. K. Akimov, A. I. Busev, K. V. Kodua, P. Nenning 375

ORGANIC CHEMISTRY

Reductive Conversions of Chromanoids, I. Catalytic Hydrogenation of Isoflavone (3-Phenylchromone), V. Szabó, E. Antal 381
Condensed *as*-Triazines, III. Synthesis of a New Heterocyclic System, the Derivatives of *as*-Triazino [6,5-C] Quinoline, E. Berényi, P. Benkó, L. Pallos 395
Condensed *as*-Triazines, IV. Synthesis of *as*-Triazino [5,6-c] Quinoline and its Derivatives, E. Berényi, P. Benkó, L. Pallos 399
Condensed *as*-Triazines, V. Pyrido [4,3-e]-*as*-Triazines, P. Benkó, E. Berényi, A. Messmer, Gy. Hajós, L. Pallos 405
Thermal Transcarboxylation Reactions, VII. The Relative Ability to Transfer of Aromatic Hydrogens, J. Szammer, L. Noszkó 411
A Novel Aldehyde Synthesis Based on the Reduction of *s*-Triazolo [2,3-*c*] Quinazolin-4-ium Derivatives, G. Doleschall 419

RECENSIONES 425

Printed in Hungary

A kiadásért felel az Akadémiai Kiadó igazgatója — Műszaki szerkesztő: Zacsik Annamária

A kézirat nyomdába érkezett: 1976. VI. 9. — Terjedelem: 9,8 (A/5) ív, 47 ábra

76.3264 Akadémiai Nyomda, Budapest — Felelős vezető: Bernát György

ACTA CHIMICA

ТОМ 90—ВЫП. 4

РЕЗЮМЕ

Электрохимическое исследование катализаторов палладий—медь

Т. МАЛЛАТ, Й. ПЕТРО, Е. ПОЛЯНСКИ и Т. МАТЕ

В щелочной среде, путем гидрирования были приготовлены порошкообразные катализаторы Pd/Cu с содержанием меди 0, 10, 20 30 и 40 ат.%. Были исследованы зависимости водородной сорбции и каталитической активности от состава катализатора.

Гальваностатические измерения проводились в растворе 1N NaOH, а потенциодинамические измерения — растворе 1N H_2SO_4 и при комнатной температуре. Активность катализаторов была измерена при 25°C, при давлении 1 атм и в условиях жидкофазного гидрирования.

Было установлено, что под влиянием меди сорбированный водород становится гомогеннее и его энергия связи уменьшается. В большой степени уменьшается и его количество: при содержании меди 0—20 ат.% оно совпадает с растворенным количеством, а в интервале 20—40 ат.% меди, в первую очередь, с адсорбированным. На основе исследования сорбции водорода можно заключить, что приблизительно при содержании 20 ат.% Cu происходит переход, т. е. сплав уже не растворяет, а адсорбирует водород.

Под влиянием меди изменяется активность палладиевого катализатора при гидрировании двойной связи и карбонильной группы.

На поверхности зерен катализатора Pd/Cu образуется негомогенный твердый раствор. Медь частично растворяется в палладии и частично образует с палладием новые фазы интерметаллических соединений.

Каталитический обмен дейтерия в циклопентане и циклогексане

Дегидрирование циклогексана на Rh черни

А. ШАРКАНЬ, Л. ГУЦИ и П. ТЕТЕНИ

Приводятся результаты по обмену циклопентана и циклогексана, а также дегидрирования циклогексана в присутствии дейтерия на Rh черни. В интервале температур 273 и 372°K основной реакцией является обмен дейтерия, с кажущейся энергией активации 51 и 63 кдж.моль$^{-1}$ для циклопентана и циклогексана, соотвественно. Распределение дейтерия объясняется, полагая существование $\alpha\alpha$ и $\alpha\beta$ поверхностных частиц. Появление тетрадейтерированных продуктов при повышенных температурах приписывается промежуточным продуктам с $\alpha\alpha\beta\beta$ двойными связями, которые считают ответственными за отравление. Дегидрирование циклогексана изучено в интервале температур 473—572°K. Скорость образования бензола соизмерима с десорбцией дейтерированного циклогексана. Тот факт, однако, что дейтерий появляется в почти равновесном распределении как в бензоле, так и в циклогексане, указывает на то, что ступени взаимопревращений, приводящие к дейтерированным поверхностным частицам, быстры по сравнению как с десорбцией циклогексана, так и с образованием бензола.

Расчеты силового поля малонитрилов

Б. ВИЗИ и А. ШЕБЕШТЕН

На основе немодицированных частот, взятых из литературы, было составлено гарбоническое силовое поле для производных малонитрила. Для каждой изученной молекулы ыло рассчитано распределение потенциальной энергии.

Об экстракции Nb(V) полифенолами

А. И. БУСЕВ, С. П. КАРЯКИНА и П. НЕННИНГ

Были исследованы условия образования и экстракции соединений ниобия(V) с пирокатехином, пирогаллолом, тетрабромпирокатехином и трибромпирогаллолом в присутствии дифенилгуанидина.

Аналитическое применение комплексов Pt(II) с производными пиразолона

В. К. АКИМОВ, А. И. БУСЕВ, К. В. КОДУА и П. НЕННИНГ

Было исследованию взаимодействие Pt(II) с производными пиразолона в растворе HBr. В случае диантипирил-, диантипирилметил-, диантипирилпропилметил- и диантипирилфенилметанов были получены тетрабромплатинаты типа $(RH)_2PtBr_4$, был исследован механизм их образования, а также их кислотно-щелочные свойства и растворимости. Был разработан метод для гравиметрического определения 5—30 мг Pt путем осаждения и взвешивания $(C_{26}H_{30}N_4O_2H)_2PtBr_4$. Максимальная относительная погрешность равна 0,91%. При определении ионы Mo, Al, Mn(II), Fe(II), Co, Ni, Ru(III) и Rh(III) не мешают

Восстановительные превращения хромоноидов, I

Каталитическое гидрирование изофлавона (3-фенилхромона)

В. САБО и Э. АНТАЛ

В зависимости от растворителя, pH раствора и активности катализатора Pd—C, изофлавон (3-фенилхромон) с различной скоростью превращается в изофлаван (II), изофлаван-4-ол (III), изофлаван (IV), а в разбавленных щелочных растворах в 2-гидрокси-α-метилдезоксибензоин (IX). При соответствующем выборе условий процесс восстановления протекает селективно, т. е. с доминирующим образованием соединений II, III, IV и IX.

Конденсированные асим-триазины, III

Новая гетероциклическая система. Синтез производных асим-триазино-[6,5-c]хинолина

Е. БЕРЕНИ, П. БЕНКО и Л. ПАЛЛОШ

Были получены первые производные новой гетероароматической кольцевой системы. Была исследована обратимая кристаллическая диморфия, имеющая место при синтезе промежуточных продуктов. Для соединений была обнаружена ценная биологическая активность.

Конденсированные асим-триазины, IV

Синтез аисм-триазино[5,6-c]хинолина и его производных

Е. БЕРЕНИ, П. БЕНКО и Л. ПАЛЛОШ

Были разработаны два новых синтеза *асим*-триазино[5,6-c]хинолина и его производных. Биологическая актвность соединений является отличной: хорошими с точки зрения терапевтической практики являются их как фармакологические, так и хемотерапевтические свойства.

Конденсированные асим-триазины, V

Исследования в области пиридо[4,3-e]-асим-триазинов

П. БЕНКО, Е. БЕРЕНИ, А. МЕССМЕР, ДЬ. ХАЙОШ и Л. ПАЛЛОШ

Был разработан одноаппаратурный метод синтеза 3-аминопиридо[4,3-e]-*асим*-триазин-1-оксидов (III). За счет основно-катализированной перегруппировки последнего были получены 1H-V-триазоло[4,5-c]пиридин-1-карбоксамид и 4-хлор-1H-V-триазоло-[4,5-c]пиридин. Окисление III приводит к 1,4-диоксидным производным, а с аминами были получены соответствующие 3-замещенные аминопроизводные.

Термические реакции перекарбоксилирования, VII

Исследование относительной способности отрыва ароматических водородов в реакции термопревращений

Я. САММЕР и Л. НОСКО

Был разработан метод определения вероятности отрыва водородов от солей ароматических карбоновых кислот, успешно применимый в условиях реакции Хенкеля. С помощью данного метода было установлено, что водороды калиевых солей бензокарбоновых кислот, за исключением водородов терефталата обладают значительной способностью отрыва, которую нельзя связать с термостабильностью этих солей. Низкая реактивность водородов дикалий терефталата по отношению к реактивным промежуточным продуктам термопревращений находится в согласии с тем фактом, что дикалий терефталат является основным продуктом реакции Хенкеля.

Новый синтез альдегидов, основанный на восстановлении производных S-триазоло[2,3-c]хиназолин-4-ия

Г. ДОЛЕШАЛ

Обрабатывая 5-(2-аминофенил)-4-фенил-3-метилтио-S-тиазол и пиридиновую смесь карбоновых кислот с помощью $POCl_3$ и затем водным KJ, были получены 5-замещенные йодиды 1-фенил-2-метилтио-S-триазоло[2,3-c]хиназолин-4-ия. Подобным образом вышеуказанные производные получаются из производных 5-(2-ациламинофенил)-4-фенил-3-метилтио-S-триазола после обработки ангидридом уксусной кислоты и газообразным хлористым водородом и под влиянием водного KJ Йодиды 3-триазоло[2,3-c]хиназолин-4-ия, подвергнутые кислому или щелочному гидролизу и алкоголизу, дают различные продукты. Простое восстановление за счет водного $NaBH_4$ с последующим кислотным гидролизом позволяет получить обратно карбоновую кислоту, использованную при построении молекулы, но уже в форме альдегида. Восстановление карбоновых кислот до альдегидов оказалось селективным.

The Acta Chimica publish papers on chemistry, in English, German, French and Russian.

The Acta Chimica appear in volumes consisting of four parts of varying size, 4 volumes being published a year.

Manuscripts should be addressed to

Acta Chimica
H-1521 Budapest, Hungary

Correspondence with the editors should be sent to the same address.

The rate of subscription in $ 32 00 a volume.

Orders may be placed with "*Kultúra*" Foreign Trade Company for Books and Newspapers (H-1389 Budapest 62, P. O. B. 149. Account No. 218 10990) or with representatives abroad.

Les Acta Chimica paraissent en français, allemand, anglais et russe et publient des mémoires du domaine des sciences chimiques.

Les Acta Chimica sont publiés sous forme de fascicules. Quatre fascicules seront réunis en un volume (4 volumes par an).

On est prié d'envoyer les manuscrits destinés à la rédaction à l'adresse suivante:

Acta Chimica
H-1521 Budapest, Hongrie

Toute correspondance doit être envoyée à cette même adresse.

Le prix de l'abonnement est de $ 32,00 par volume.

On peut s'abonner à l'Entreprise pour le Commerce Extérieur de Livres et Journaux "*Kultúra*" (1389 H-Budapest 62, P. O. B. 149 Compte-courant No. 218 10990) ou à l'étranger chez tous les représentants ou dépositaires.

«*Acta Chimica*» издают трактаты из области химической науки на русском, французском, английском и немецком языках.

«*Acta Chimica*» выходят отдельными выпусками разного объема, 4 выпуски составляют один том, 4 тома публикуются в год.

Предназначенные для публикации рукописи следует направлять по адресу:

Acta Chimica
H-1521 Budapest, BHP

По этому же адресу направлять всякую корреспонденцию для редакции.

Подписная цена — $ 32,00 за том.

Заказы принимает предпринятие по внешней торговле книг и газет "*Kultúra*" (138 H-Budapest 62, P. O. B. 149. Текущий счет № 218 10990) или его заграничные представительства и уполномоченные.

Reviews of the Hungarian Academy of sciences are obtainable at the following addresses:

AUSTRALIA

C. B. D. Library and Subscription Service
Box 4876, G. P. O.
Sydney N. S. W. 2001

Cosmos Bookshop
145 Acland St.
St. Kilda 3182

AUSTRIA

Globus
Höchstädtplatz 3
A—1200 Wien XX

BELGIUM

Office International de Librairie
30 Avenue Marnix
1050-Buxelles

Du Monde Entier
162 Rue du Midi
1000—Bruxelles

BULGARIA

Hemus
Bulvar Ruszki 6
Sofia

CANADA

Pannonia Books
P. O. Box 1017
Postal Station "B"
Toronto, Ont. M5T 2T8

CHINA

CNPICOR
Periodical Department
P. O. Box 50
Peking

CZECHOSLOVAKIA

Mad'arská Kultura
Národní třida 22
115 66 Praha

PNS Dovoz tisku
Vinohradská 46
Praha 2

PNS Dovoz tlače
Bratislava 2

DENMARK

Ejnar Munksgaard
Nörregade 6
DK—1165 Copenhagen K

FINLAND

Akateeminen Kirjakauppa
P. O. Box 128
SF-00101 Helsinki 10

FRANCE

Office International de Documentation et Librairie
48, Rue Gay-Lussac
Paris 5

Librairie Lavoisier
11 Rue Lavoisier
Paris 8

Européridiques S. A.
31 Avenue de Versailles
78170 La Celle St.-Cloud

GERMAN DEMOCRATIC REPUBLIC

Haus der Ungarischen Kultur
Karl-Liebknecht-Strasse 9
DDR—102 Berlin

Deutsche Post
Zeitungsvertriebsamt
Strasse der Pariser Kommüne 3—4
DDR—104 Berlin

GERMAN FEDERAL REPUBLIC

Kunst und Wissen
Erich Bieber
Postfach 46
7 Stuttgart 5

GREAT BRITAIN

Blackwell's Periodicals
P. O. Box 40
Hythe Bridge Street
Oxford OX1 2EU

Collet's Holdings Ltd.
Denington Estate
London Road
Wellingrough Northants NN8 2QT

Bumpus Haldane and Maxwell Ltd.
5 Fitzroy Square
London W1P 5AH

Dawson and Sons Ltd.
Cannon House
Park Farm Road
Folkestone, Kent

HOLLAND

Swets and Zeitlinger
Heereweg 347b
Lisse

Martinus Nijhoff
Lange Voorhout 9
The Hague

INDIA

Hind Book House
66 Babar Road
New Delhi 1

India Book House
Subscription Agency
249 Dr. D. N. Road
Bombay 1

ITALY

Santo Vanasia
Via M. Macchi 71
20124 Milano

Libreria Commissionaria Sansoni
Via Lamarmora 45
50121 Firenze

JAPAN

Kinokuniya Book-Store Co. Ltd.
826 Tsunohazu 1-chome
Shinjuku-ku
Tokyo 160—91

Maruzen and Co. Ltd.
P. O. Box 5050
Tokyo International 100—31

Nauka Ltd.-Export Department
2—2 Kanda
Jinbocho
Chiyoda-ku
Tokyo 101

KOREA

Chulpanmul
Phenjan

NORWAY

Tanum-Cammermayer
Karl Johansgatan 41—43
Oslo 1

POLAND

Węgierski Instytut Kultury
Marszalkowska 80
Warszawa

BKWZ Ruch
ul. Wronia 23
00—840 Warszawa

ROUMANIA

D. E. P.
Bucureşti

Romlibri
Str. Biserica Amzei 7
Bucureşti

SOVIET UNION

Sojuzpechatj — Impor t
Moscow

and the post offices in each town
Mezhdunarodnaya Kniga
Moscow G—200

SWEDEN

Almaqvist and Wiksell
Gamla Brogatan 26
S—101 20 Stockholm

A. B. Nordiska Bokhandeln
Kunstgatan 4
101 10 Stockholm 1 Fack

SWITZERLAND

Karger Libri AG.
Arnold-Böcklin-Str. 25
4000 Basel 11

USA

F. W. Faxon Co. Inc.
15 Southwest Park
Westwood, Mass. 02090

Stechert-Hafner Inc.
Serials Fulfillment
P. O. Box 900
Riverside N. J. 08075

Fam Book Service
69 Filth Avenue
New York N. Y. 1003

Maxwell Scientific International Inc.
Fairview Park
Elmsford N. Y. 10523

Read More Publications Inc.
140 Cedar Street
New York N. Y. 10006

VIETNAM

Xunhasaba
32, Hai Ba Trung
Hanoi

YUGOSLAVIA

Jugoslavenska Knjiga
Terazije 27
Beograd
Forum
Vojvode Mišića 1
21000 Novi Sad